REPORT DOCUMENTATION PAGE	1. REPORT NO. NSF/CEE-81061	2.	3. Recipient's Accession No. PB82 147794

4. Title and Subtitle
Structural Walls in Earthquake Resistant Buildings, Dynamic Analysis of Isolated Structural Walls, Development of Design Procedure, Design Force Levels, 1981 Final Report

5. Report Date
July 1981

6. 008201

7. Author(s)
W.G. Corley, A.T. Derecho, M. Igbal, S.K. Ghosh, M. Fintel,*

8. Performing Organization Rept. No.

9. Performing Organization Name and Address
Portland Cement Association
Construction Technology Laboratories
5420 Old Orchard Road
Skokie, IL 60077

10. Project/Task/Work Unit No.

11. Contract(C) or Grant(G) No.
(C)
(G) ENV7715333

12. Sponsoring Organization Name and Address
Directorate for Engineering (ENG)
National Science Foundation
1800 G Street, N.W.
Washington, DC 20550

13. Type of Report & Period Covered
Final

14.

15. Supplementary Notes
Submitted by: Communications Program (OPRM)
National Science Foundation
Washington, DC 20550
*A. Scanlon

16. Abstract (Limit: 200 words)

A procedure is used to establish estimates of stiffness, strength, and deformation demands of isolated structural walls subjected to ground motions of varying intensity. The investigaton characterizes earthquake ground motions to select critical input motions; identifies the most significant structural and ground motion parameters; and formulates a simple design procedure for correlating earthquake demands with structural capacities. The computer program that was used to analyze the variables, DRAIN-2D, is described. The compilation of maximum or near-maximum values of the significant response quantities is shown to be a major step in determining design force levels for earthquake-resistant structural walls. The procedure, which is based on fundamental period and flexural yield level, is illustrated for the case of twenty-story walls subjected to input motions.

17. Document Analysis a. Descriptors

Earthquakes
Hazards
Concrete structures
Walls
Isolated walls
Ductility
Earthquake resistant structures
Dynamic response
Structural analysis

b. Identifiers/Open-Ended Terms

Shear walls
Reinforced concrete
Ground motion
W.G. Corley, /PI

c. COSATI Field/Group

18. Availability Statement	19. Security Class (This Report)	21. No. of Pages
NTIS	20. Security Class (This Page)	22. Price

A Report on Research Sponsored by
NATIONAL SCIENCE FOUNDATION
(ASRA)
Grant No. ENV77-15333

STRUCTURAL WALLS IN EARTHQUAKE-RESISTANT BUILDINGS

DYNAMIC ANALYSIS OF ISOLATED STRUCTURAL WALLS

DEVELOPMENT OF DESIGN PROCEDURE - DESIGN FORCE LEVELS

by

Arnaldo T. Derecho
M. Iqbal
S. K. Ghosh
Mark Fintel
W. Gene Corley
Andrew Scanlon

Submitted by

Engineering Development Division
CONSTRUCTION TECHNOLOGY LABORATORIES
A Division of the Portland Cement Association
5420 Old Orchard Road
Skokie, Illinois 60077

July 1981

TABLE OF CONTENTS

TABLE OF CONTENTS

(Cont'd)

TABLE OF CONTENTS

(Cont'd)

SYNOPSIS

Although structural walls have a long history of satisfactory use in stiffening buildings against wind, there is insufficient information on their behavior under strong earthquakes. Observations of the performance of buildings during recent earthquakes have demonstrated the superior performance of buildings stiffened by properly proportioned and designed structural walls from the point of view of safety and especially from the standpoint of damage control.

This report describes an analytical investigation of isolated walls subjected to ground motions of varying intensity. Estimates of maximum forces and deformations that can reasonably be expected in critical regions of structural walls subjected to strong ground motion are obtained. Results of the analytical investigation are combined with data from a concurrent experimental program to develop a procedure for determining design force levels for isolated structural walls. These design forces can be used for proportioning earthquake-resistant structural walls using static analysis methods.

The procedure is based on the two major structural variables, fundamental period and yield level in flexure. Using this procedure, the minimum yield level and associated maximum dynamic shear force are determined for an assumed or available ductility and a particular value of ground motion intensity.

DYNAMIC ANALYSIS OF ISOLATED STRUCTURAL WALLS

DEVELOPMENT OF DESIGN PROCEDURE - DESIGN FORCE LEVELS

by

A. T. Derecho,[1] M. Iqbal,[2]
S. K. Ghosh,[3] M. Fintel,[4]
W. G. Corley,[5] and A. Scanlon[6]

BACKGROUND

Although structural walls (shear walls)* have a long history of satisfactory use in stiffening multistory buildings against wind, much less information is available on the behavior of such elements under strong earthquake.

Observations of the performance of buildings subjected to earthquakes during the past decade have focused attention on the need to minimize damage in addition to ensuring the general safety of buildings during strong earthquakes. The need to control damage to structural and nonstructural components during earthquakes becomes particularly important in hospitals and other facilities that must continue operation following a major

(1)Former Manager and (2) Former Senior Structural Engineer, Structural Analytical Section, Engineering Development Division; (3)Principal Structural Engineer and (4)Director, Advanced Engineering Services Department, (5)Divisional Director, Engineering Development Division, and (6)Manager, Analytical Design Section, Portland Cement Association, Skokie, Illinois.

*In conformity with the nomenclature adopted by the Applied Technology Council(1) and in the forthcoming revised edition of Appendix A to ACI 318-77, Building Code Requirements for Reinforced Concrete(2), the term "structural wall" is used in place of "shear wall."

disaster. Damage control, in addition to life safety, is also economically desirable in tall buildings designed for residential and commercial occupancy, since the nonstructural components in such buildings usually account for 60 to 80 percent of the total cost.

There is little doubt that structural walls offer an efficient way to stiffen a building against lateral loads. When proportioned so that they possess adequate lateral stiffness to reduce interstory distortions due to earthquake-induced motions, walls reduce the likelihood of damage to nonstructural elements in a building. When used with rigid frames, walls form a structural system that combines the gravity-load-carrying efficiency of the rigid frame with the lateral-load-resisting efficiency of the structural wall.

Observations of the comparative performance of rigid frame buildings and buildings stiffened by structural walls during recent earthquakes[3,4,5], have highlighted better performance of buildings stiffened by properly proportioned structural walls. Performance of these structural wall buildings was better both from the point of view of safety and from the standpoint of damage control. The need to minimize damage during strong earthquakes, in addition to the primary requirement of life safety (i.e., no collapse), clearly imposes more stringent requirements on the design of structures.

Among the more immediate questions to be answered before a rational design procedure can be developed are:

1. What magnitude of deformation and associated forces can reasonably be expected at critical regions of structural walls for specific combinations of structural and ground motion parameters? How many cycles of large deformations can be expected in critical regions of walls under earthquakes of expected duration?
2. What stiffness and strength should structural walls have relative to the expected ground motion in order to limit deformations to acceptable levels?

3. What design and detailing requirements must be met to provide walls with the strength and deformation capacities indicated by analysis?

The combined analytical and experimental investigation of which this study is a part was undertaken to provide answers to these questions. The objective of the overall investigation as indicated in Fig. 1(a) is the development of practical and reliable design procedures for earthquake-resistant structural walls and wall systems.

The program to accomplish the objectives of the analytical portion of the investigation consists of the following steps:

a. Characterization of input motions in terms of the significant parameters to enable calculation of critical or "near-maximum" response using a minimum number of input motions[6].

b. Determination of the relative influence of the various structural and ground motion parameters on dynamic structural response through parametric studies[7]. The purpose of this study is to identify the most significant variables.

c. Calculation of estimates of strength and deformation <u>demands</u> in critical regions of structural walls as affected by the significant parameters determined in Step (b). A number of input accelerograms chosen on the basis of information developed in Steps (a) and (b) are used[8].

d. Development of procedure for determining design force levels[8] by correlating the stiffness, strength, and deformation <u>demands</u> obtained in Step (c) with the corresponding <u>capacities</u> determined from the concurrent experimental program[9,10].

Another important result of the analytical investigation is the determination of a representative loading history that can be used in testing laboratory specimens under slowly reversing loads[11].

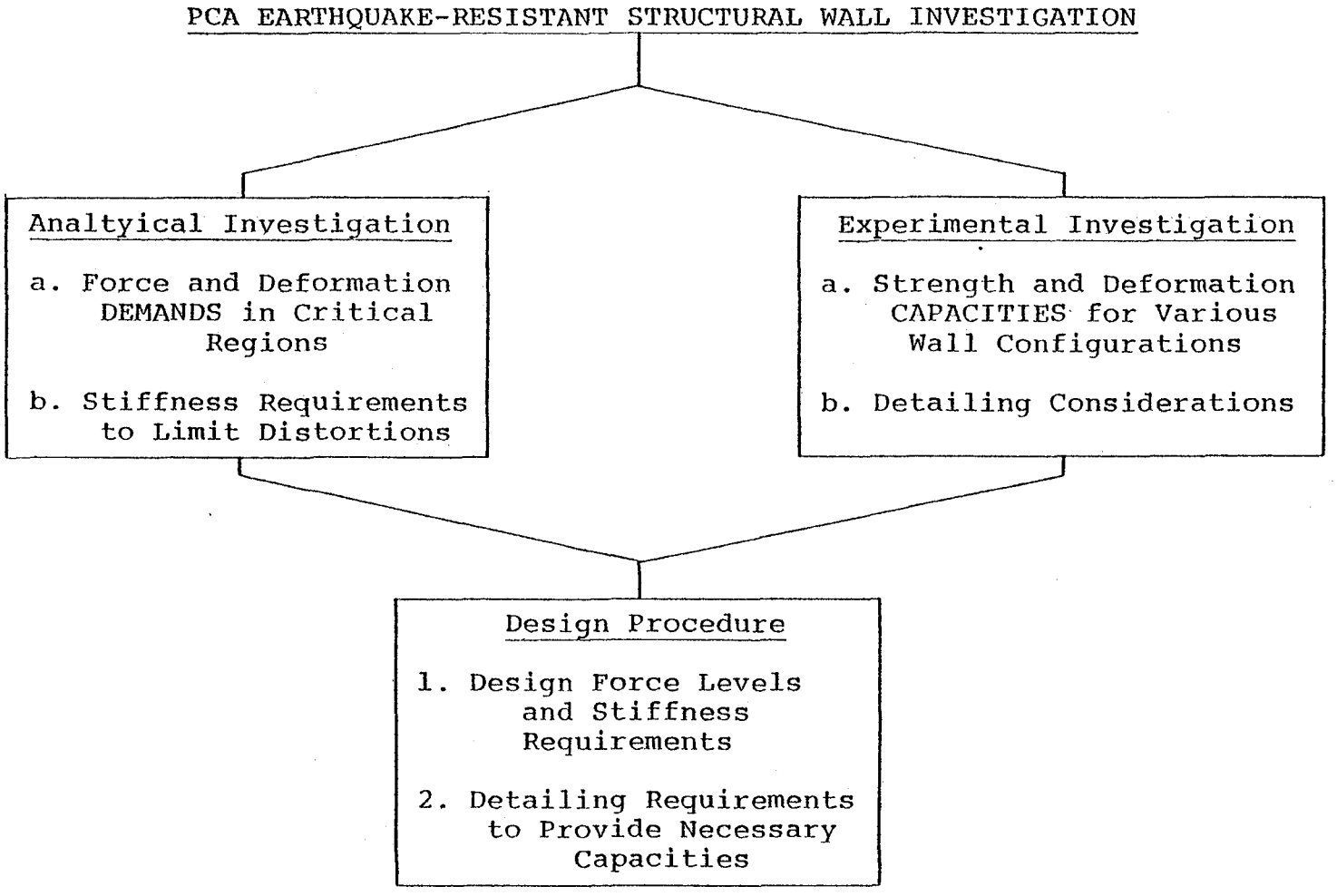

Fig. 1a Outline of Basic Functions and Objectives of Overall Investigation

1. CHARACTERIZATION OF INPUT MOTIONS

   Objective: To enable use of a selected few input motions in analyses to determine critical or near-maximum response.

2. PARAMETRIC STUDIES

   Objective: To identify the most significant structural and ground motion parameters affecting dynamic inelastic response - for use as basic variables in subsequent development of design procedure.

3. DEVELOPMENT OF DESIGN PROCEDURE - DESIGN FORCE LEVELS

   Objective: To provide estimates of force and deformation demands corresponding to various combinations of the significant structural and ground motion parameters.

4. CHARACTERIZATION OF REPRESENTATIVE LOADING HISTORY

   Objective: To define quantitatively a basis for selecting loading programs for use in testing large-size specimens under slowly reversing loads.

Fig. 1b Major Tasks Involved in Analytical Investigation of Isolated Structural Walls

Two previous reports[6,7] dealt with Steps (a) and (b) of the anaytical investigation. The first report[6] dealt mainly with the characterization of input motions in terms of duration, intensity, and frequency content, with particular regard to the effects of these parameters on dynamic inelastic response. The second report[7] presented results of parametric studies designed to isolate the most significant structural and ground motion parameters. A brief description of the major tasks involved in the analytical investigation of isolated structural walls is shown in Fig. 1b.

This report discusses the procedure used to establish estimates of stiffness, strength, and deformation demands in isolated structural walls subjected to ground motions of varying intensity. Results of some 300 cases are analyzed. The analytically derived information on demands is correlated with data on capacity obtained from the concurrent experimental program. A procedure for determining design force levels for earthquake-resistant structural walls is developed. A significant part of the material presented here first appeared in Ref. 8. This part of the analytical investigation corresponds to Steps (c) and (d) listed above.

INTRODUCTION

In developing design procedures for earthquake-resistant structures, information on demand as well as on capacity has to be developed. As indicated in Fig. 1a, this information relates mainly to stiffness, strength, and inelastic deformation capacity or ductility. Reasonable estimates of both demand and capacity are necessary to achieve economy in engineering design.

The relative infrequency of intense earthquakes and the dependence of the resulting forces and deformations on structural properties as well as ground motion characteristics, make systematic accumulation of field data on earthquake demands a difficult task. Furthermore, it is unlikely that a building exposed to an intense earthquake will be adequately instrumented to record its response.

In view of the difficulty of obtaining data on earthquake demands from field measurements, the best alternative is to obtain estimates of these demands through dynamic inelastic analysis. Estimates of capacity are usually obtained by testing large-size specimens under slowly reversed loading to simulate earthquake response.

Objective

The primary objective of this part of the investigation is the development of a procedure for determining design forces for earthquake-resistant structural walls. The intent is that these forces will be used in design assuming static loading conditions. The overall design objective is to provide structures capable of sustaining, without significant loss of strength, the dynamic forces and deformations associated with particular ground motion intensities. Based on results of the experimental program, recommendations have been made[9,10] for detailing wall sections to ensure adequate strength and deformation capacity.

Structure Considered

The basic structure considered in this phase of the investigation is an isolated structural wall. Such a structure may be thought of as being one of a series of parallel walls in a building having a plan configuration as shown in Fig. 2. The isolated wall was chosen not only to obtain dynamic response data for this basic element but also to establish a reference with which to compare response of more complex wall systems.

In certain cases, the frame in a frame-wall system or the coupling beams in a coupled wall system are relatively flexible compared to the structural wall. In these cases, the wall can be considered as acting essentially as an isolated structural element.

Basic Approach

The approach adopted in establishing design force levels for earthquake-resistant isolated structural walls involved compilation and analysis of comprehensive inelastic response data for a wide range of values of the significant structural and ground motion parameters. For simplicity it was necessary to base the procedure for determining design force levels on a few of the most important parameters.

Identification of the most important parameters for use in the design formulation was accomplished by means of a parametric investigation[7]. Included in the investigation was a study of the effects on dynamic inelastic response of the three major parameters characterizing earthquake ground motions. These parameters are intensity, duration, and frequency content. Other structural parameters considered were fundamental period, yield level in flexure, ratio of post-yield stiffness to initial elastic stiffness, parameters characterizing the moment-rotation hysteretic loop, damping, stiffness taper, strength taper, number of stories, and base fixity.

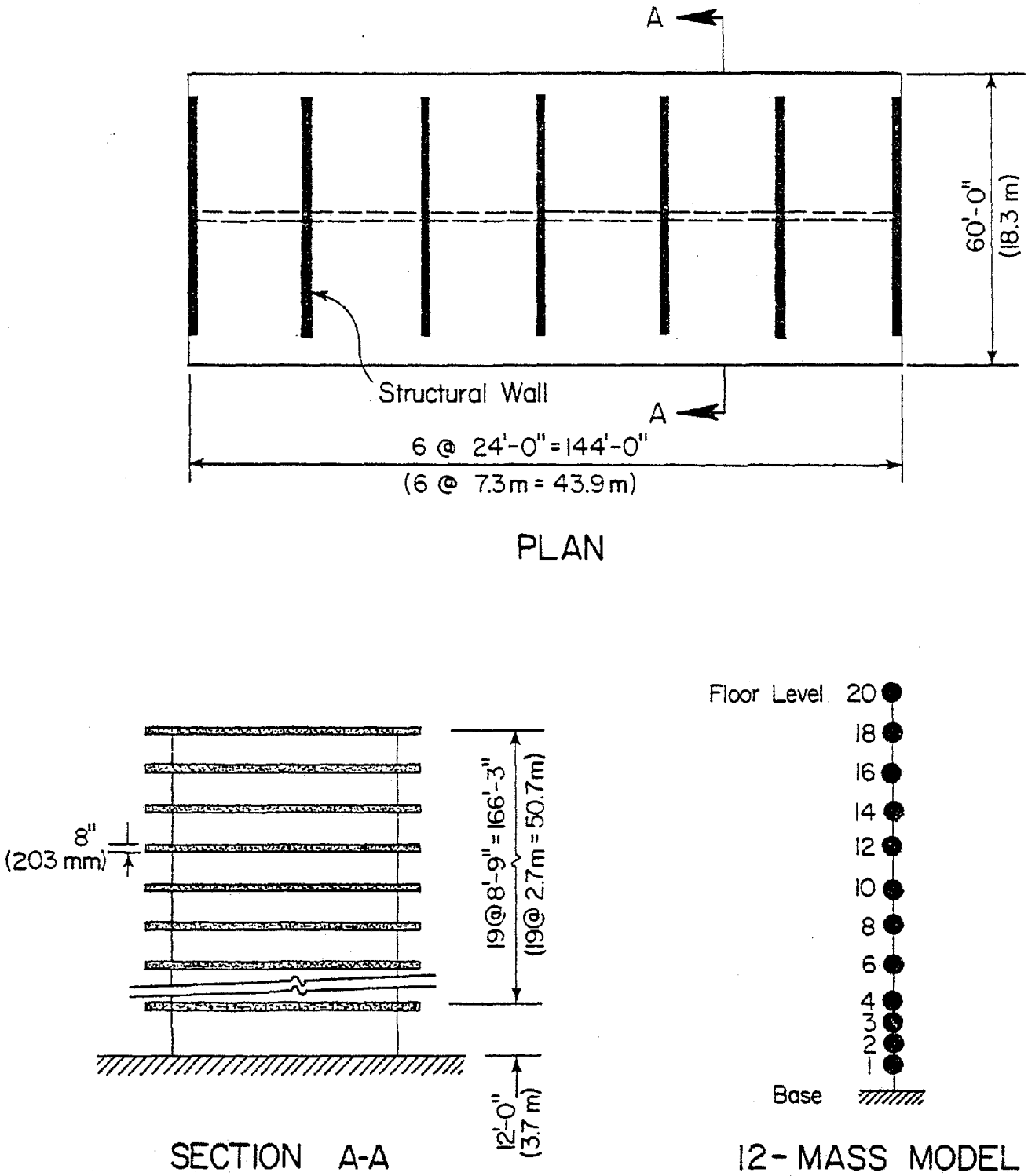

Fig. 2 Twenty Story Building with Isolated Structural Walls

The computer program DRAIN-2D[12], developed at the University of California, Berkeley, was used in the analyses. Results of the parametric study show that, within the practical range of values of the variables considered, the most significant structural parameters are fundamental period and yield level in flexure. The major ground motion parameter is intensity.

After the major variables affecting inelastic dynamic response were identified, an extensive series of analyses was carried out. Over 300 analyses were performed. The objective of the work was to compile response data corresponding to a wide range of values of the major variables. These data were then organized, evaluated, and correlated with relevant experimental data to develop a procedure for determining design force levels.

In developing a design procedure for earthquake-resistant structural walls, it was considered desirable to formulate the resulting recommendations in terms similar to those used in current practice. It is believed such an approach will make the results of the study of immediate value to design engineers and code-formulating bodies.

COMPUTER PROGRAM

Dynamic response analyses were carried out using the computer program DRAIN-2D[12] developed at the University of California, Berkeley. A number of modifications, designed mainly to allow more efficient extraction and plotting of output data, have been introduced into the program at the Portland Cement Association[13]. The program has been implemented on the computer facilities at Northwestern University, Evanston, Illinois.

Program DRAIN-2D - Basic Features

Features of the program, as implemented at Northwestern University, are as follows:

1. The program considers only plane structures.
2. A structure may consist of a combination of beam or beam-column elements, truss elements or infill panel elements. Moment-rotation characteristics for beam elements can be defined by a bilinear relationship. This relationship may be stable hysteretic or may exhibit "degrading stiffness" in deformation cycles subsequent to yielding. More recent modifications to the program relating to force-displacement characteristics are discussed in a subsequent paragraph.
3. Mass is assumed to be concentrated at nodal points.
4. Horizontal and vertical components of input (base) acceleration may be considered simultaneously. Input motions are assumed to be applied directly to the base of the structure. Soil-structure interaction effects are not considered.
5. Several types of damping may be specified, including mass-proportional and stiffness-proportional damping.
6. Elastic shear deformation and the P-Δ effect in frame elements can be taken into account.

7. Output options include printouts of response quantities and response envelopes at given time intervals. Envelopes of basic response quantities are automatically printed at the end of each computer run. Time histories of specified response quantities can also be presented in compact form. For structures consisting of beam and column elements, plots of a variety of response quantities can be obtained during each run.

The structural stiffness matrix is formulated by the direct stiffness method, with nodal displacements as unknowns. Dynamic response is determined using step-by-step integration assuming a constant response acceleration during each time step.

Element properties characterized by a progressive decrease in reloading stiffness with cycles of loading subsequent to yield are of particular interest in this study. In DRAIN-2D, both flexural and axial stiffnesses of these elements are considered. Variable cross sections may be taken into account by specifying appropriate stiffness coefficients. Inelasticity is allowed in the form of concentrated plastic hinges at the element ends. For beam-column elements, yielding resulting from interaction between axial force and moment is taken into account in an approximate manner.

Primary moment-rotation curves for inelastic hinges at ends of beam and beam-column elements are specified in terms of an initial stiffness, k, and a post-yield stiffness, $k_y = r_y k$ as shown in Fig. 3. The ratio $r_y = k_y/k$ is referred to as the yield stiffness ratio.

Two types of hysteresis loop can be specified for the moment-rotation curve characterizing inelastic point hinges at element ends. The first type is the more common stable loop, shown in Fig. 4a. For this case, the unloading and reloading stiffnesses are both equal to the initial stiffness. The program accounts for inelastic behavior of this type of element by assuming an equivalent element consisting of two parallel components, one elastic and the other elasto-plastic.

The second type of hysteresis loop is one that exhibits

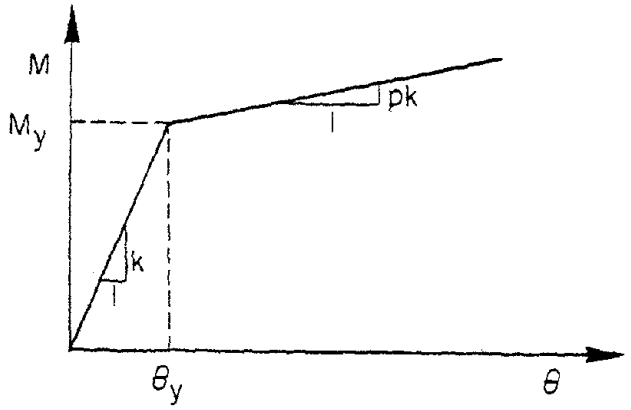

Fig. 3 Moment - Rotation Relationship

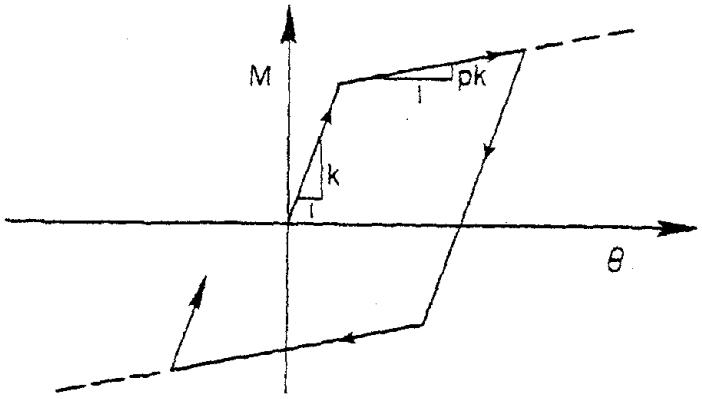

Fig. 4a Stable Hysteretic Loop

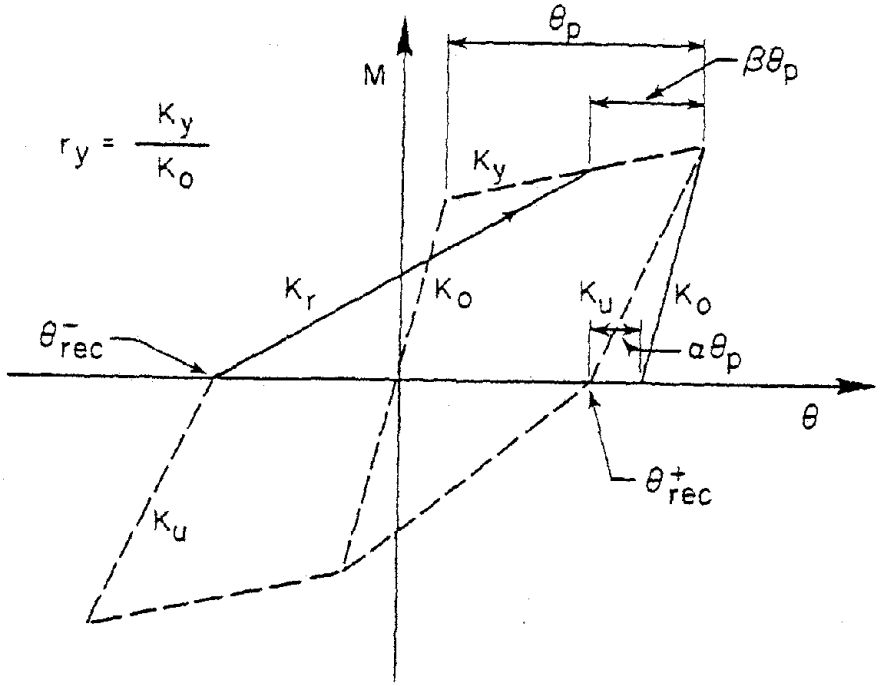

Fig. 4b Unloading and Reloading Parameters α and β Characterizing Hysteretic Loop of Decreasing Stiffness Model

decreasing stiffness for reloading cycles subsequent to yield as shown in Fig. 4(b).

After yielding occurs, the unloading and reloading branches exhibit decrease in slope (i.e., stiffness). This decrease in stiffness is assumed to be a function of maximum rotation attained during any previous cycle. Detailed behavior of inelastic point hinges, such as unloading and reloading from intermediate points within the primary envelope, is determined by a set of rules that are an extended version of those proposed by Takeda and Sozen[14].

Modifications To Program DRAIN-2D

Early runs using DRAIN-2D indicated the desirability of making several changes in the program. At the request of the Portland Cement Association, G. H. Powell and R. W. Litton at the University of California, Berkeley, introduced changes to enable the program to incorporate modifications to the basic Takeda model for the decreasing stiffness beam element.

The unloading and reloading parameters α and β shown in Fig. 4b allow the basic decreasing stiffness model to be varied to correspond more closely to experimental results. These modifications have been incorporated into the program. Powell and Litton also provided options for printing and storing on file the time histories of most response quantities in a compact and convenient form.

Plotting capabilities were incorporated in the program by the Portland Cement Association. Plots of time histories of forces and deformations, as well as response envelopes, can be obtained automatically with each run and may be stored for retrieval at a later date. Options to punch cards for both envelopes and time histories of response have also been incorporated.

All modifications to the program DRAIN-2D as used in the study of isolated walls, have been documented and are discussed in detail in Ref. 13.

COMPILATION OF CRITICAL RESPONSE VALUES

A major step in determining design force levels for earthquake-resistant structural walls was the compilation of maximum or near-maximum values of the significant response quantities. To do this, a comprehensive series of dynamic inelastic analyses was undertaken, using several accelerograms as input. Over 300 analyses were made to serve as basis for this part of the investigation. Of this number, about 45 represent analyses carried out in connection with the parametric studies reported in Ref. 7.

Summary of Results of Parametric Studies

Among the more important conclusions of the parametric studies[7] was the observation that when significant yielding in a structure can be expected, a "broad band" accelerogram tends to produce more severe deformations than a "peaking" accelerogram. Basic shapes for broad-band and peaking spectra are shown in Fig. 5. Definitions for peaking and broad-band accelerograms are given in Ref. 6.

Significant yielding may result from a relatively low structure yield level or a high earthquake intensity relative to the yield level. On the other hand, when only nominal yielding is expected, a peaking accelerogram represents the more critical excitation for the same duration and intensity of motion.

It was also observed, however, that in cases where significant yielding occurs, a broad band accelerogram that is critical with respect to deformations often produces relatively low maximum base shears. This behavior has been attributed mainly to the greater sensitivity of base shear to higher modes of response.

Conversely, cases arise in which an accelerogram that is critical with respect to shear produces relatively small deformations. Apparently the criticality of an accelerogram

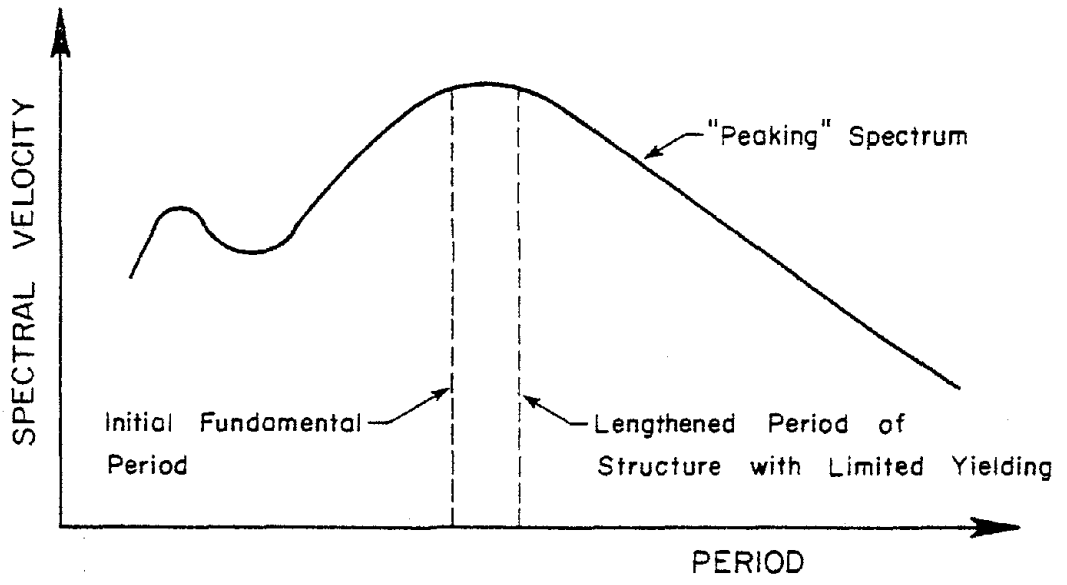

(a) Peaking Spectrum

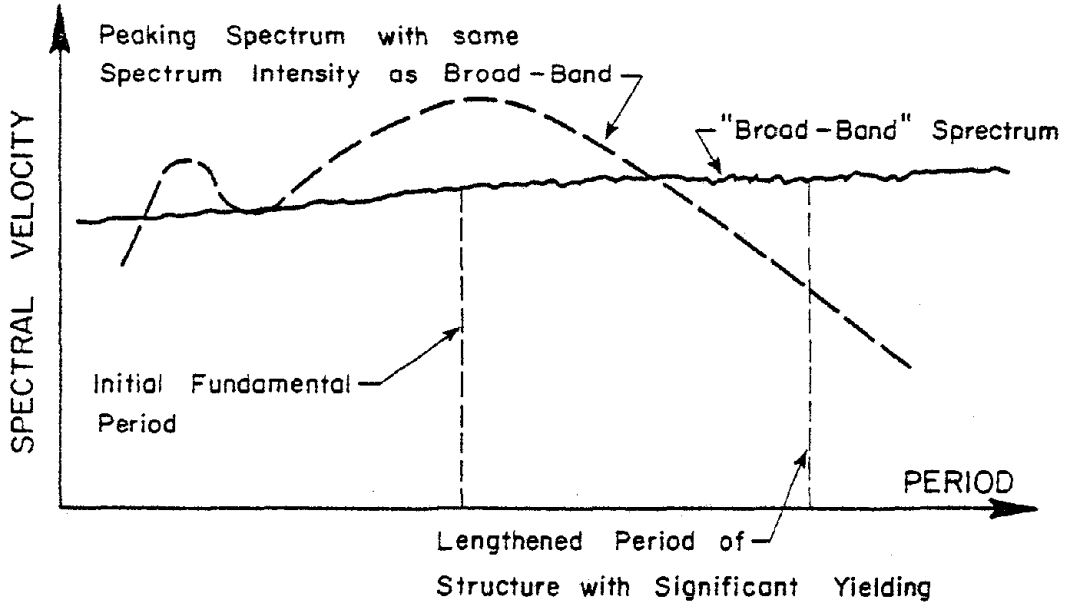

(b) Broad-Band Spectrum

Fig. 5 Typical Basic Shapes of Damped Velocity Response Spectra

with respect to shear depends on the character of its velocity response spectrum in frequency ranges where the significant effective higher frequencies of the yielded structure occur. Determination of critical base shears is important because of the significant effect that high shears can have on deformation capacity of hinging regions in reinforced concrete members.

Where yielding is not significant, the peaking accelerogram is more likely to be critical with respect to deformations and usually gives near-maximum values of the base shear. To cover a range of periods, different peaking input motions were used. A number of accelerograms were thus selected to span the period range of interest.

Use of several input motions also provides better estimates of critical base shears. As indicated above, the choice of input motions for producing maximum base shears is determined by factors other than those that apply to maximum deformations.

The parametric studies also indicated that, for a structure of given height, the most significant structural variables affecting forces and deformations are initial fundamental period, T_1, and yield level in flexure, M_y. If an input motion of reasonable duration is chosen with the appropriate frequency content to critically excite a particular structure then the only other ground motion parameter that need be varied is intensity. For a particular site, the estimated ground motion intensity can be related to seismic risk. This correlation is, however, not considered in this study.

Effects of shear yielding on dynamic response and associated design force levels were not considered in this phase of the investigation.

Ranges of Principal Structural Parameters

To compile data on maximum values of force and deformation demands in the hinging region of walls, a comprehensive series of analyses was undertaken. The analyses covered a wide range of values of the principal structural parameters and used six different accelerograms were used as input motions. The main

structural variables considered are initial fundamental period, T_1, and flexural yield level, M_y.

Fundamental period was assigned values ranging from 0.5 sec. to 2.4 sec. Yield level values from 150,000 in.kips (16,950 kN m) to 3,000,000 in.kips (339,000 kN m) were considered. For comparison, results were also obtained for the case of linearly elastic response, i.e., very high yield level. In addition to the basic 20-story wall considered in the parametric studies, responses of 10-, 30-, and 40-story structures were also analyzed.

The parameter combinations used in the 300 cases considered in this investigation are summarized in Table 1. Basic properties of the reference structure for each wall height category are listed in Table 2.

The largest number of analyses was carried out on 20-story structural walls using the reduced 12-mass model shown in Fig. 2. Analytical models for the other wall heights are shown in Fig. 6.

The basic moment-rotation relationship assumed for the hinging region in the walls is a bilinear idealization of the primary curve. The hysteresis loop, a modified version of the Takeda model[14], exhibits decreasing stiffness in unloading and reloading cycles subsequent to yield. The basic hysteresis loop is shown in Fig. 4b, where unloading and reloading parameters are denoted by α and β, respectively. An example of a calculated moment-rotation loop, for an isolated wall with fundamental period, T_1 = 1.4 sec., α = 0.10, and β = 0, is shown in Fig. 7.

Parameters Held Constant

Values of other structural parameters, assumed constant for all of the walls considered, were: yield stiffness ratio, r_y = 0.05; hysteretic loop unloading parameter, α = 0.10; reloading parameter, β = 0; damping coefficient = 0.05; stiffness uniform throughout height of wall; strength, M_y, uniform throughout height except for adjustments to reflect effect of

Table 1 - Summary of Cases Considered

No.	Number of Stories	Fundamental Period, T_1 (sec.)	Yield Level, (M_y) (in-kips)	Intensity (SI)	Duration (sec.)	Earthquake Input
1	10	0.5, 0.8 and 1.4	150,000, 500,000, 1,000,000 and Elastic	$1.5(SI_{ref})$	10	1971 Pacoima Dam, S16E 1971 Holiday Orion, E-W 1952 Taft, S69E 1940 El Centro, E-W S1 (Artificial Acc.) 1940 El Centro, N-S
2	20	0.8, 1.4, 2.0 and 2.4	750,000, 1,000,000, 1,500,000 and Elastic			
3	30	1.4, 2.0, and 2.4	1,000,000, 1,500,000, 2,000,000 and Elastic			
4	40	1.4, 2.0, 2.4 and	1,500,000, 2,000,000, 3,000,000 and Elastic			
5	20	0.8, 1.4, 2.0 and 2.4	250,000, 500,000 750,000, 1,000,000 1,500,000 and Elastic	0.75 and $1.0(SI)_{ref}$		
6	20	0.8, 1.4, 2.0 and 2.4	500,000, 1,000,000 and 1,500,000	$1.5(SI)_{ref}$	10 and 20	1940 El Centro, E-W 1940 El Centro, N-S 1971 Holiday Orion, E-W 1971 Pacomia Dam, S16E

Table 2 - Basic Properties of Reference Structures

Basic Properties	Number of Stories			
	10	20	30	40
Fundamental Period	0.8	1.4	2.0	2.4
Total Height	90.75 ft	178.25 ft	265.75 ft	353.25 ft
Total Weight/Wall (for mass computation)	2174 kips	4374 kips	6574 kips	8774 kips
Stiffness Parameter, EI (uniform throughout height of wall)	$.457 \times 10^{11}$ k-in.^{2}	2.05×10^{11} k-in.^{2}	4.72×10^{11} k-in.^{2}	10.11×10^{1} k-in.

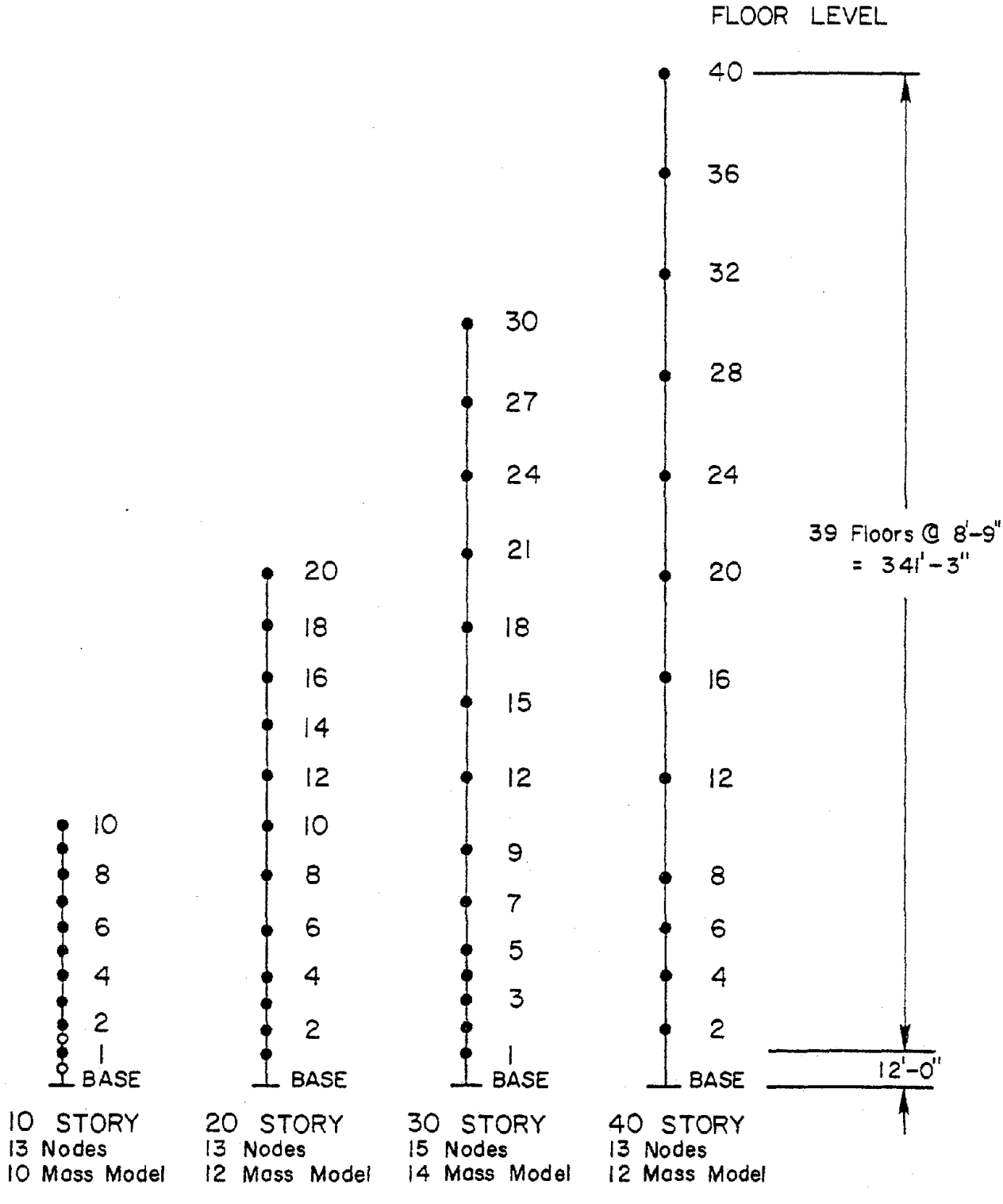

Fig. 6 Lumped-Mass Models of Isolated Walls Investigated

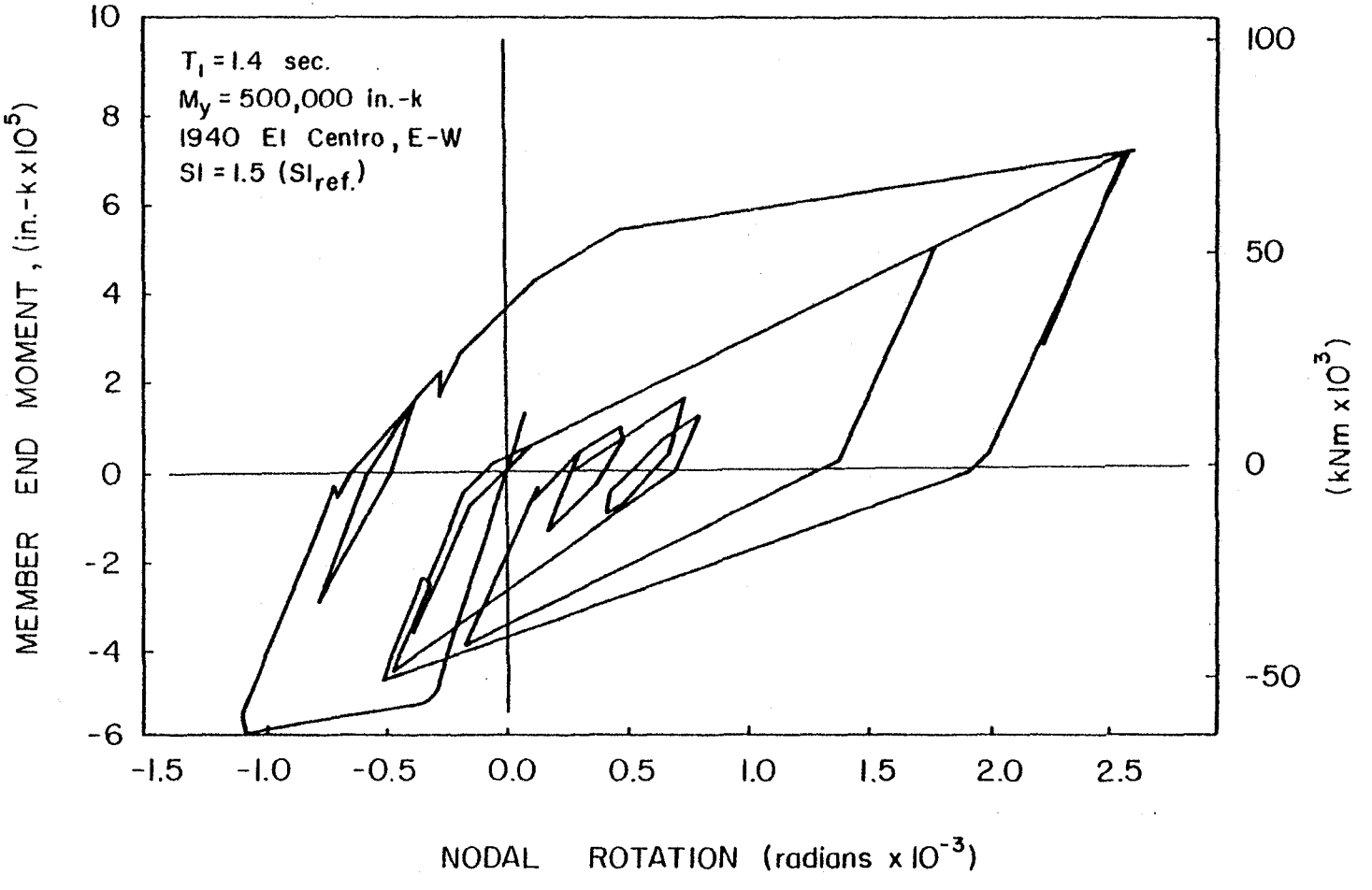

Fig. 7 Base Moment Versus Nodal Rotation at First Floor Level
20-Story Isolated Wall

axial load; and wall fully fixed at base with input motion assumed directly applied to the base. Figure 8 shows the distribution of mass, stiffness and strength over the wall height.

Input Motions Used

For most of the parameter combinations considered in the analyses of 20-story structural walls, the six accelerograms shown in Fig. 9[15] were used. These include the five accelerograms used in the parametric studies in addition to the S69E component of the record taken at the Taft Lincoln School Tunnel during the July 12, 1952, Kern County earthquake. The corresponding 5%-damped velocity response spectra are shown in Fig. 10. In subsequent analyses of structures of other heights, it was possible to use fewer input motions since a basis for selecting the critical input was available from analyses of 20-story structures.

Most analyses were carried out using a duration of 10 seconds and a spectrum intensity, SI*, equal to 1.5 ($SI_{ref.}$). To have a basis for adjusting design values for the "strong" ground motion intensity of 1.5 ($SI_{ref.}$) to values corresponding to lesser intensities, analyses were made using input motion intensities equal to 0.75 and 1.0 ($SI_{ref.}$). Also, to obtain estimates of cumulative deformation requirements corresponding to ground motion durations exceeding 10 seconds, a number of analyses were made using 20-sec.-duration input motions.

*Spectrum intensity (SI) is defined in this investigation as the area under the 5%-damped relative velocity response spectrum corresponding to the first 10 seconds of an accelerogram, between periods of 0.1 sec. and 3.0 sec. The spectrum intensity corresponding to the N-S component of the 1940 El Centro (Imperial Valley earthquake) record is used as the reference measure, $SI_{ref.}$. $SI_{ref.}$ = 70.15 inches (1,782 mm).

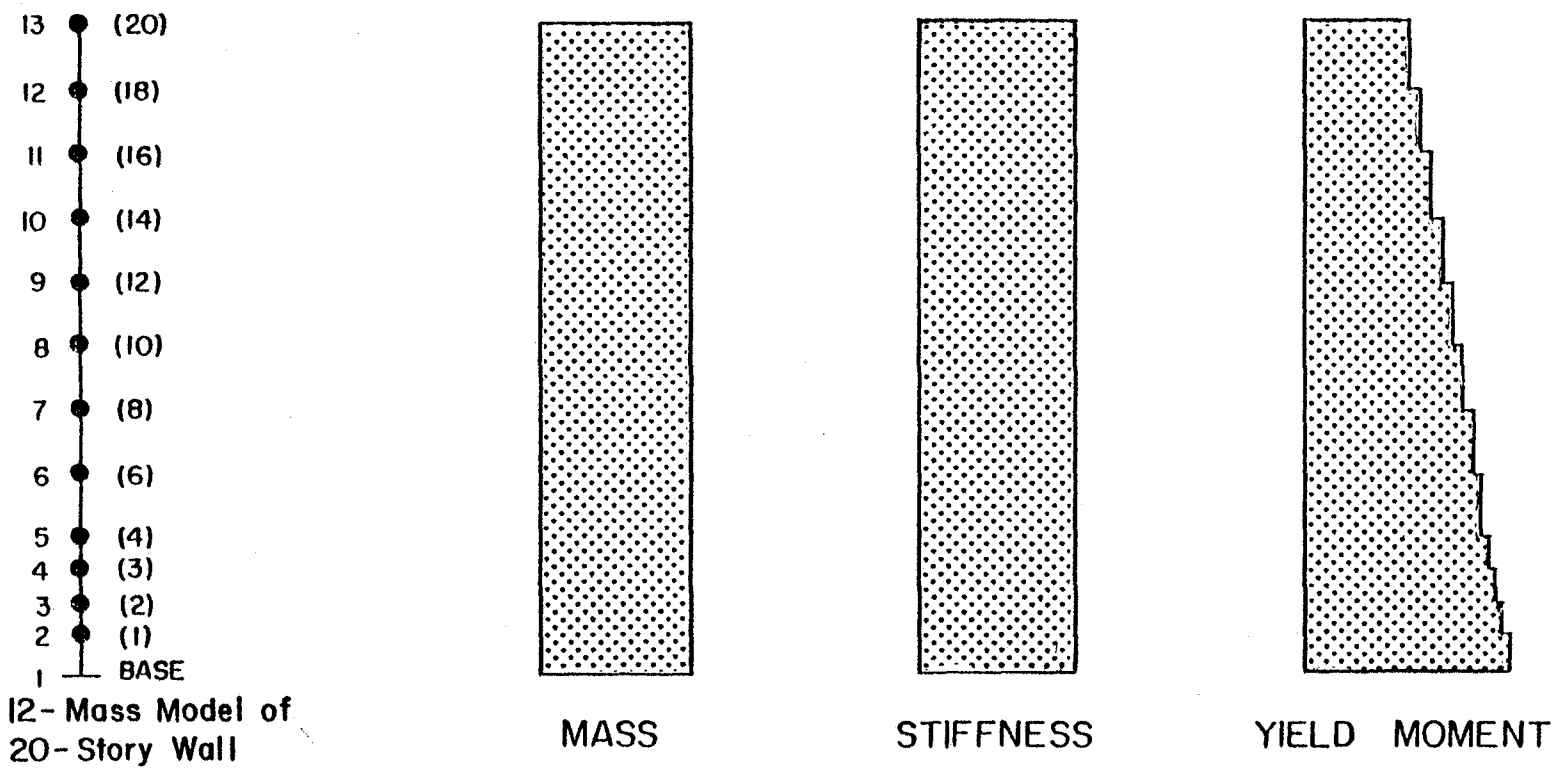

Fig. 8 Mass, Stiffness and Strength Distribution Over the Wall Height

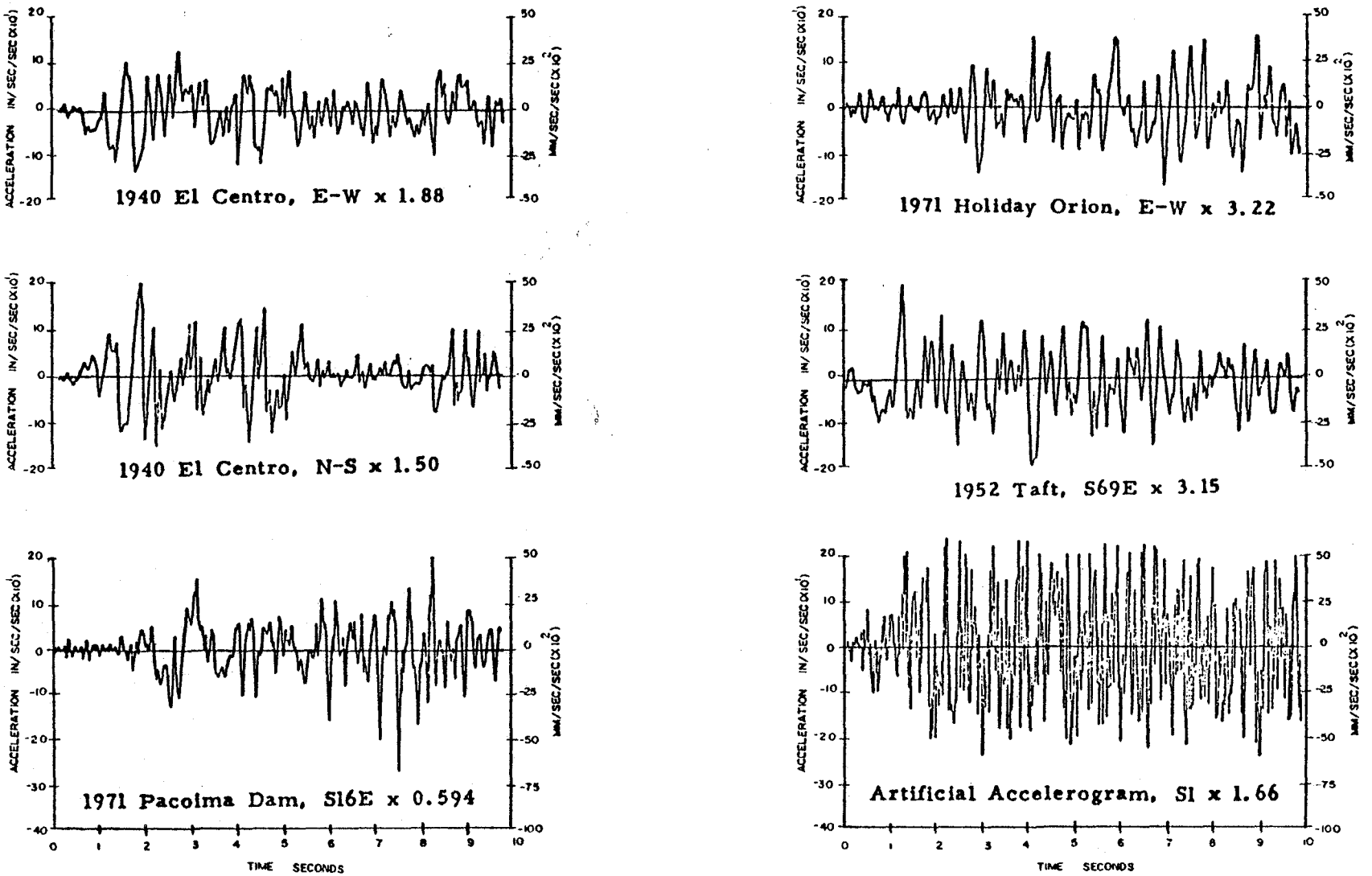

Fig. 9 Ten-Second Duration Normalized Accelerograms

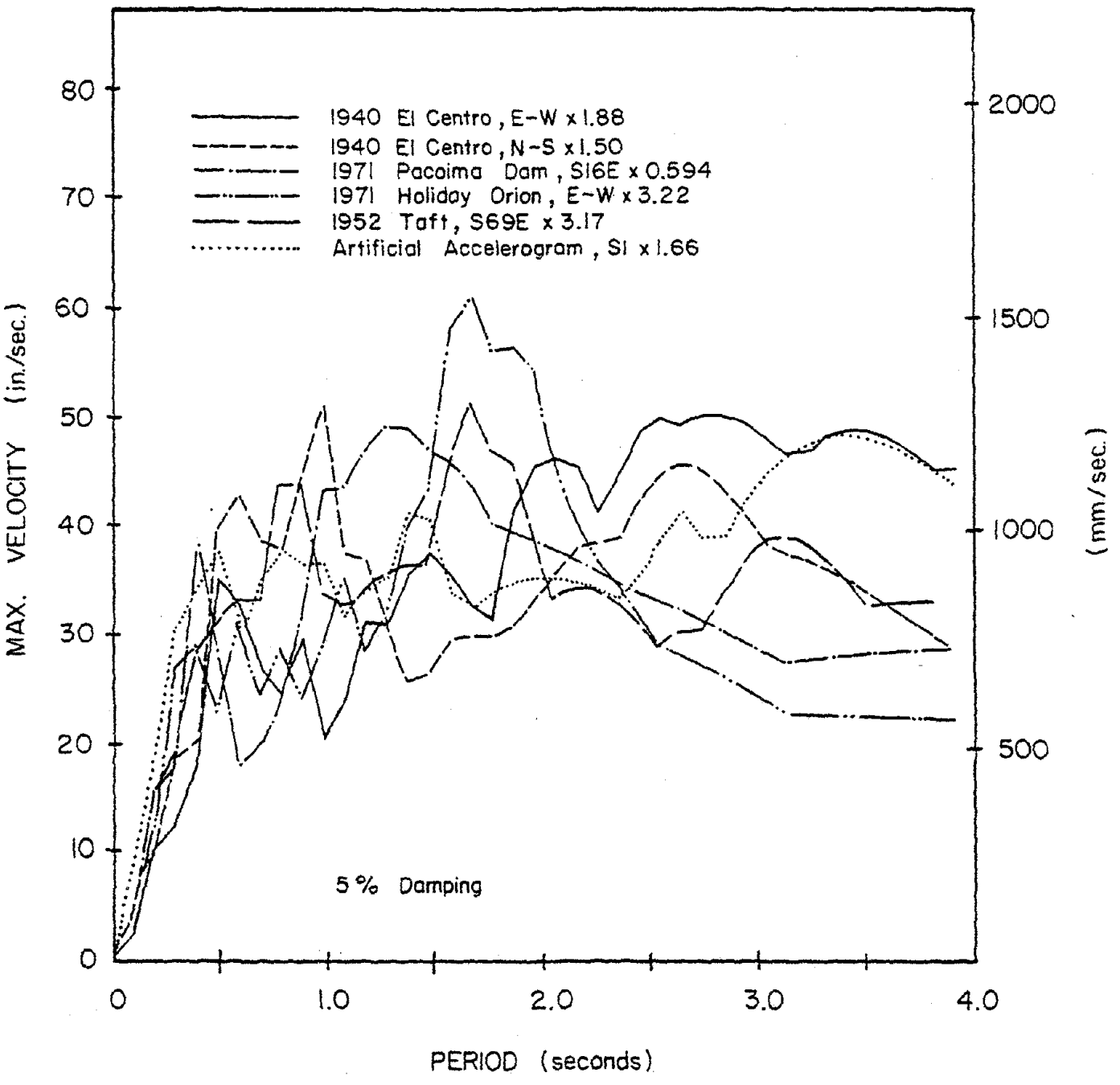

Fig. 10 Relative Velocity Response Spectra for First Ten-Seconds of Normalized Input Motions

Each of the 20-sec. composite accelerograms was synthesized by appending to the 10-sec. motions shown in Fig. 9, another 10 seconds of the strong-phase portion of the same accelerogram. It was suggested in Ref. 6 that 20 seconds of strong ground motion should provide an adequate basis for the design of most structures.

Maximum Response Values

The major effort in developing a design procedure involved compiling comprehensive data on the relevant dynamic response quantities as functions of the two principal structural parameters T_1 and M_y. Variations in level of response corresponding to changes in input motion intensity were also considered.

Plots were prepared showing maximum values of top displacement, interstory displacement, bending moment, shear, rotational ductility, and cumulative plastic hinge rotation at the base of the wall. Definitions for ductility measures are given under the heading "MEASURES OF DUCTILITY DEMAND IN HINGING REGION." Data for particular combinations of fundamental period, T_1, and yield level, M_y, were obtained for each input motion. Separate sets of data were compiled for different wall heights. Results for the case of 20-story structures with M_y = 750,000 in.-kips are shown in Fig. 11.

Plots summarizing results of analyses for the different structure heights and combinations of M_y and T_1 are included in Appendix A as Figs. A1 through A16. Numerical values of the maximum response quantities corresponding to Figs. A1 through A16 are also listed in Tables A1 through A14 of Appendix A. All of these results correspond to a ground motion intensity equal to 1.5 ($SI_{ref.}$) and a duration of 10 seconds.

It is significant to note in Fig. 11 that although the 1940 El Centro E-W and the 1971 Pacoima Dam S16E motions produce the largest displacements (Figs. 11a and 11b), moments (Fig. 11c)

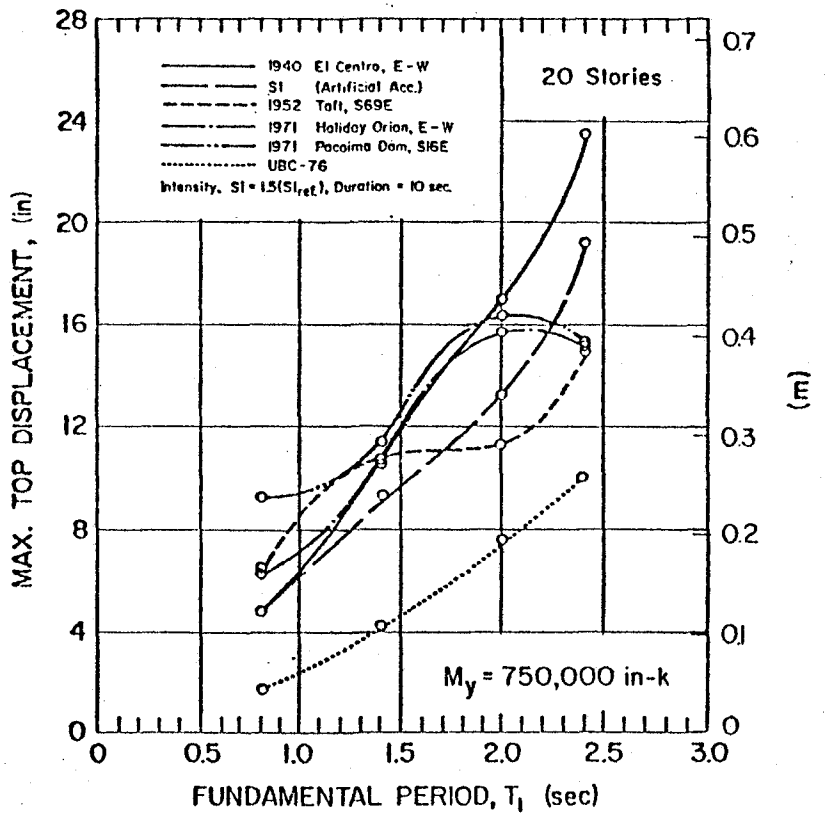

(a)

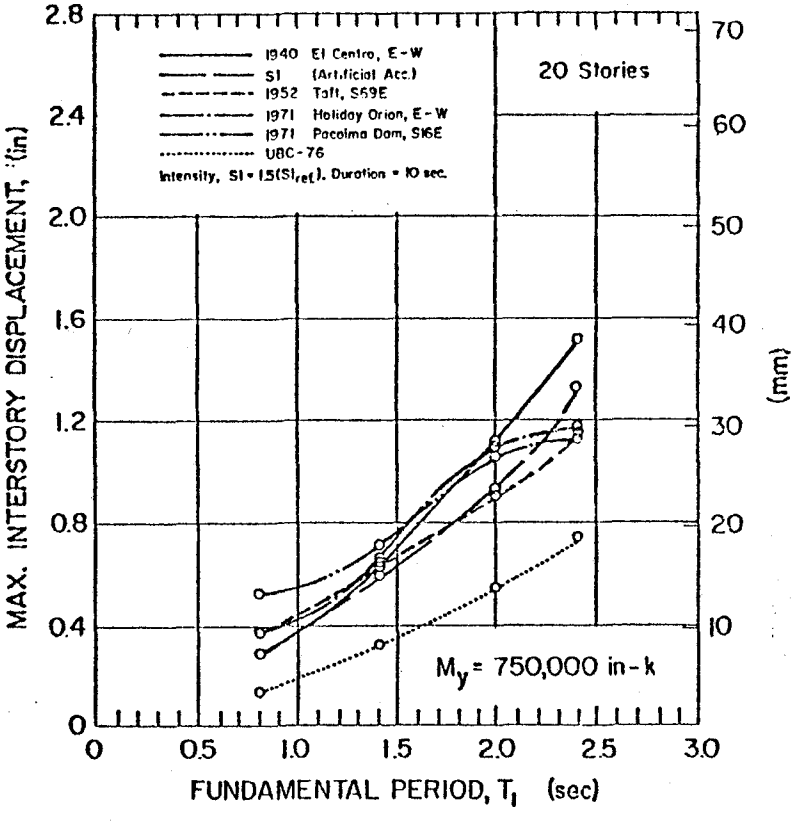

(b)

Fig. 11 Maximum Response Values for Different Input Motions
20-Story Isolated Structural Walls - M_y = 750,000 in.-k

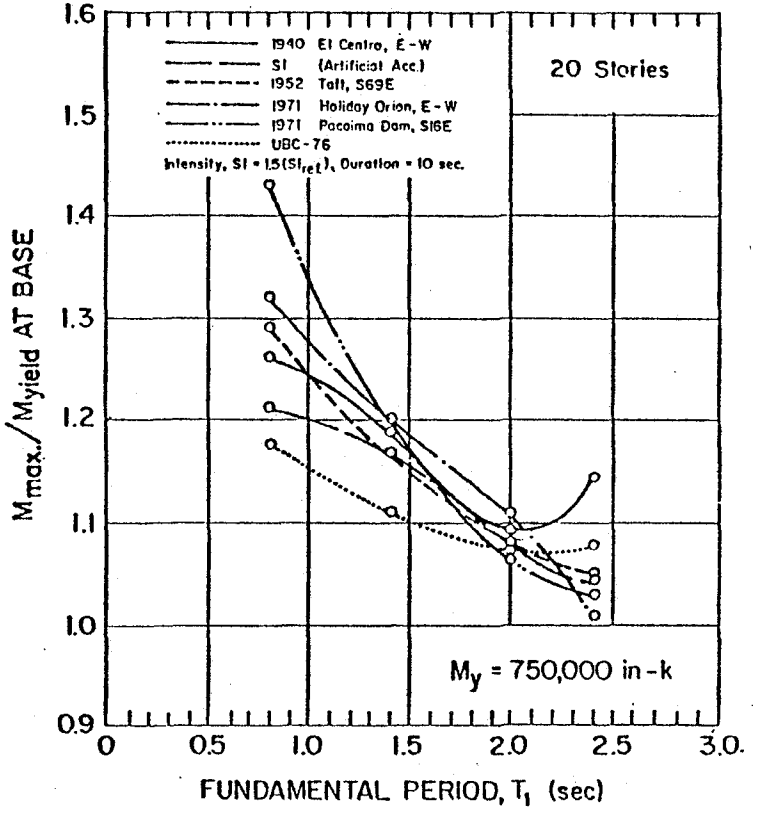

(c)

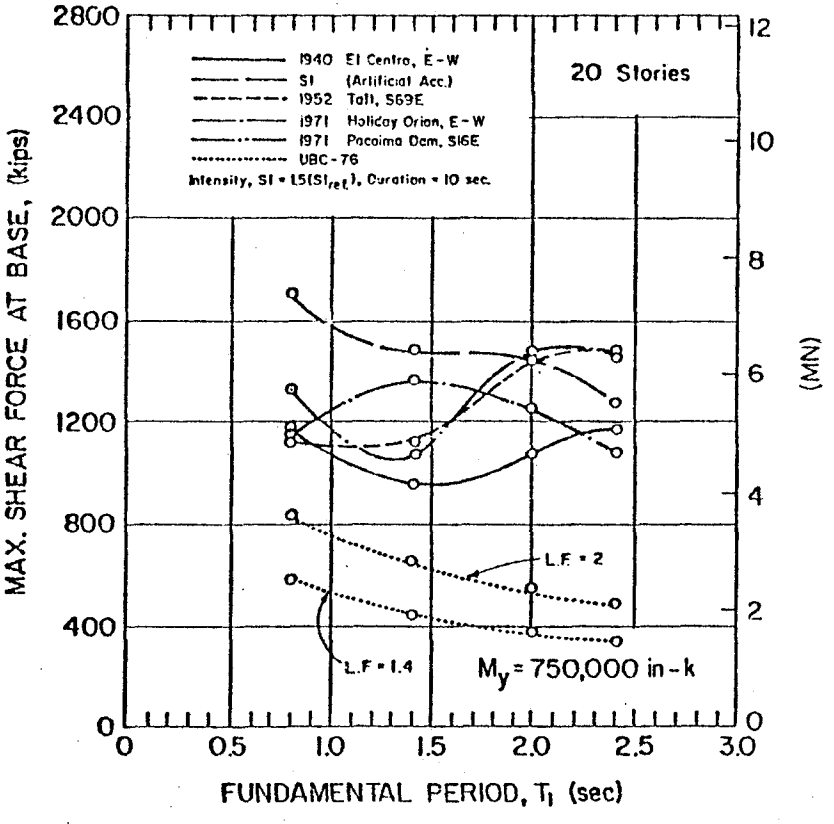

(d)

Fig. 11 (cont'd.) Maximum Response Values for Different Input Motions
20-Story Isolated Structural Walls - M_y = 750,000 in.-k

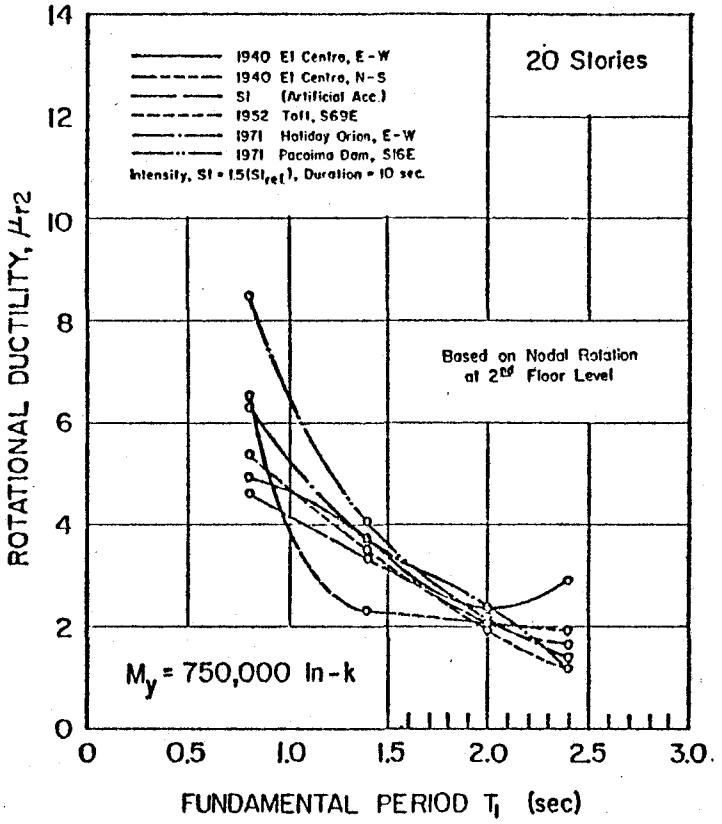

(e)

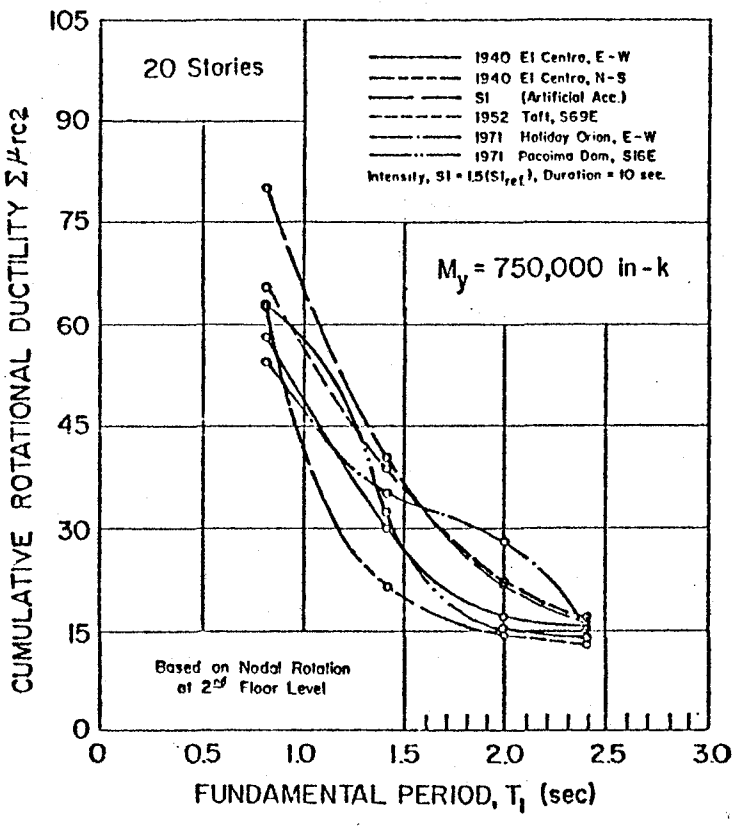

(f)

Fig. 11 (cont'd.) Maximum Response Values for Different Input Motions
20-Story Isolated Structural Walls - M_y = 750,000 in.-k

and rotational ductility (Fig. 11e), these motions produce relatively low maximum shears compared to the artificial accelerogram S1 (Fig. 11d). This difference in criticality of input motions with respect to moments and displacements on one hand and shears on the other is even more pronounced when significant yielding occurs. This effect is evident in Fig. 12 for the case of walls with M_y = 500,000 in.-kips (56,490 kN m). This behavior is attributed mainly to the greater sensitivity of maximum base shears to higher mode response.

Critical Response Values

From plots of maximum response values corresponding to different input motions, a second set of plots was prepared showing only the critical values of the response quantities. Figure 13 shows plots of critical response values for 20-story walls with different M_y-values.

A curve in Fig. 13 for a specific yield level, M_y, is defined by points representing the largest values of the response quantity indicated in the corresponding maximum response plot, such as shown in Fig. 11. Points on a curve in Fig. 13 can thus correspond to different input motions. An "e" beside a point in Figs. A1 through A16 in Appendix A indicates that the maximum bending moment associated with the response quantity plotted did not reach the assumed yield moment.

The use of critical response values for design assumes that an earthquake with the most unfavorable frequency characteristics with respect to a specific structure is possible. It was decided to take this approach in the absence of specific information concerning particular sites. It is recognized that for some locations, geological conditions and the distance from potential earthquake foci may make the occurrence of ground motions having dominant components over a particular frequency range unlikely. Thus, because high-frequency waves tend to be attenuated relatively rapidly with distance, it may be reasonable to assume that beyond a certain distance from

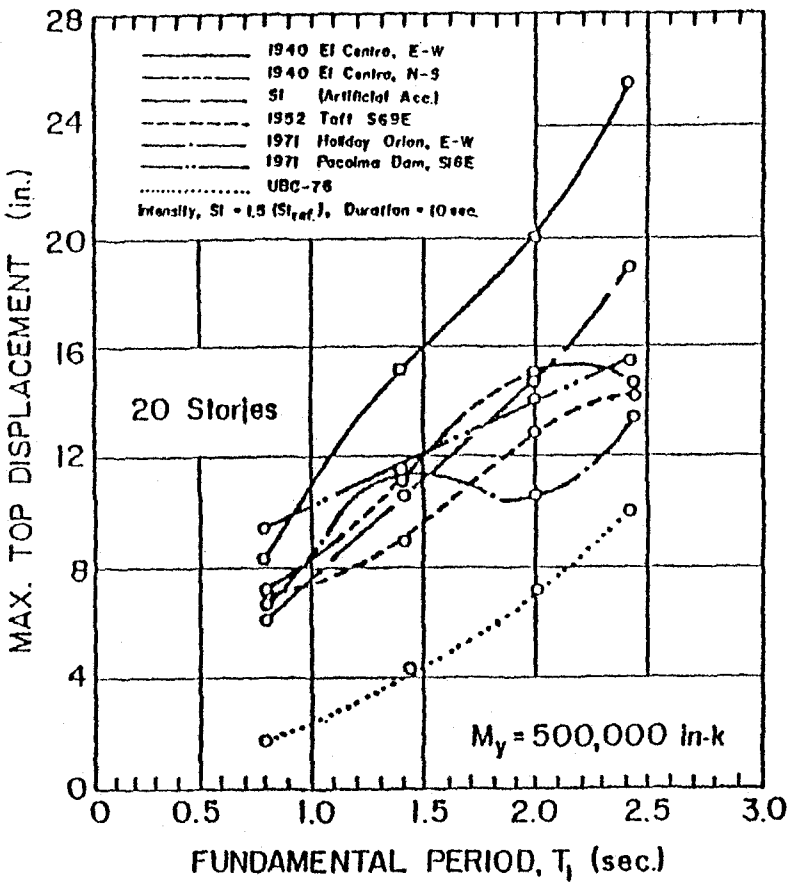

(a)

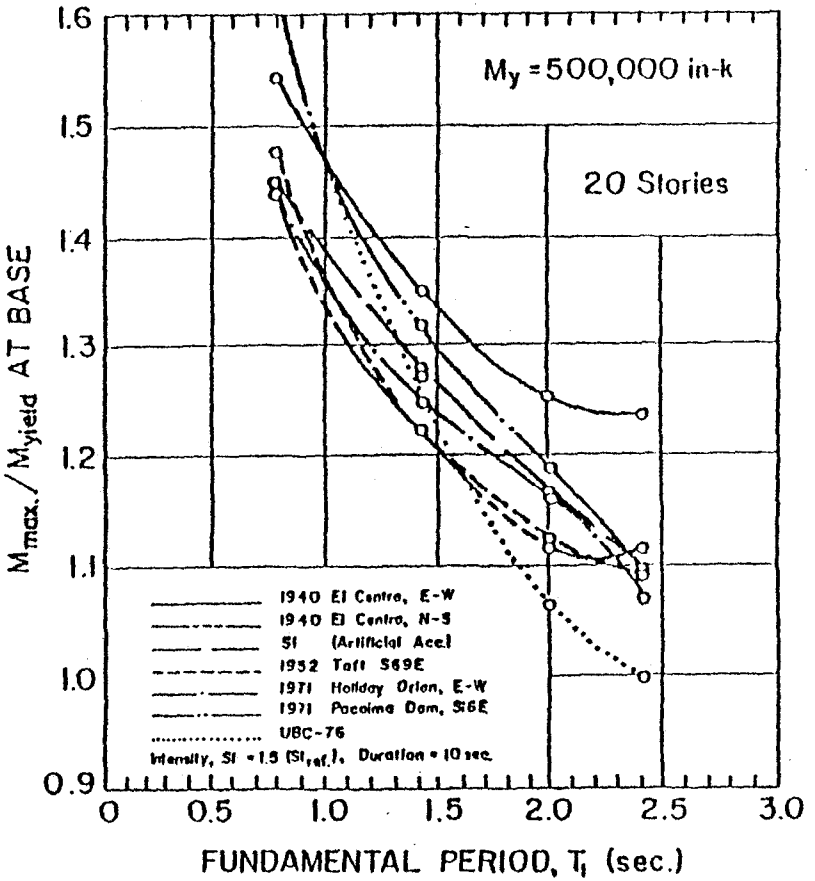

(b)

Fig. 12 Maximum Response Values for Different Input Motions
20-Story Isolated Structural Walls - M_y = 500,000 in-k

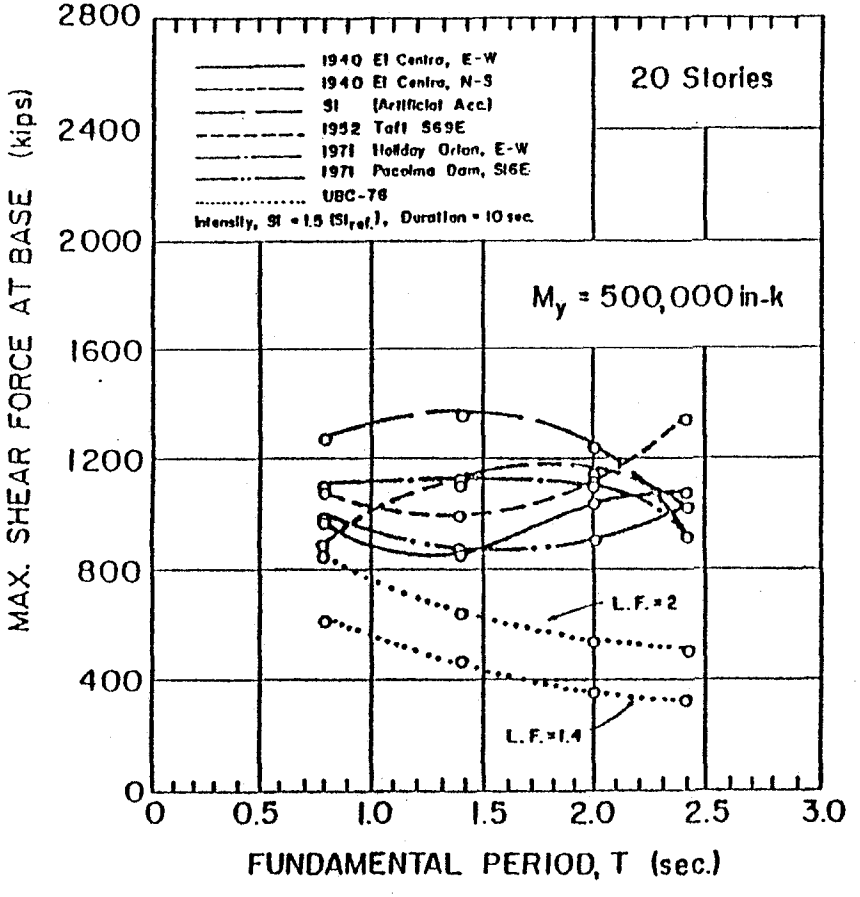

(c)

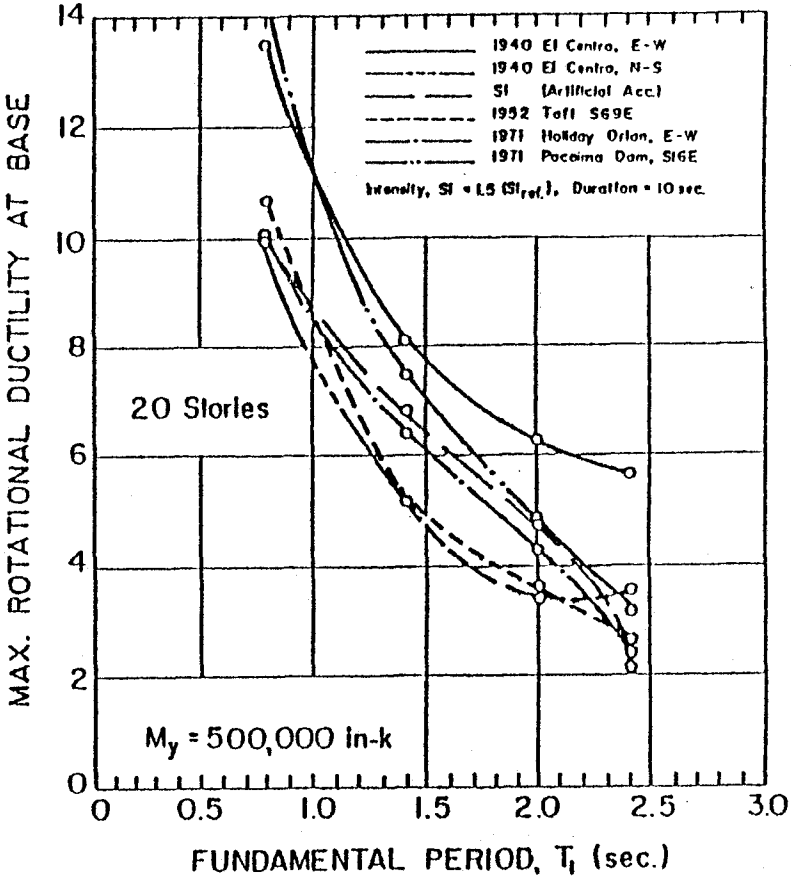

(d)

Fig. 12 (contd.) Maximum Response Values for Different Input Motions
20-Story Isolated Structural Walls - M_y = 500,000 in-k

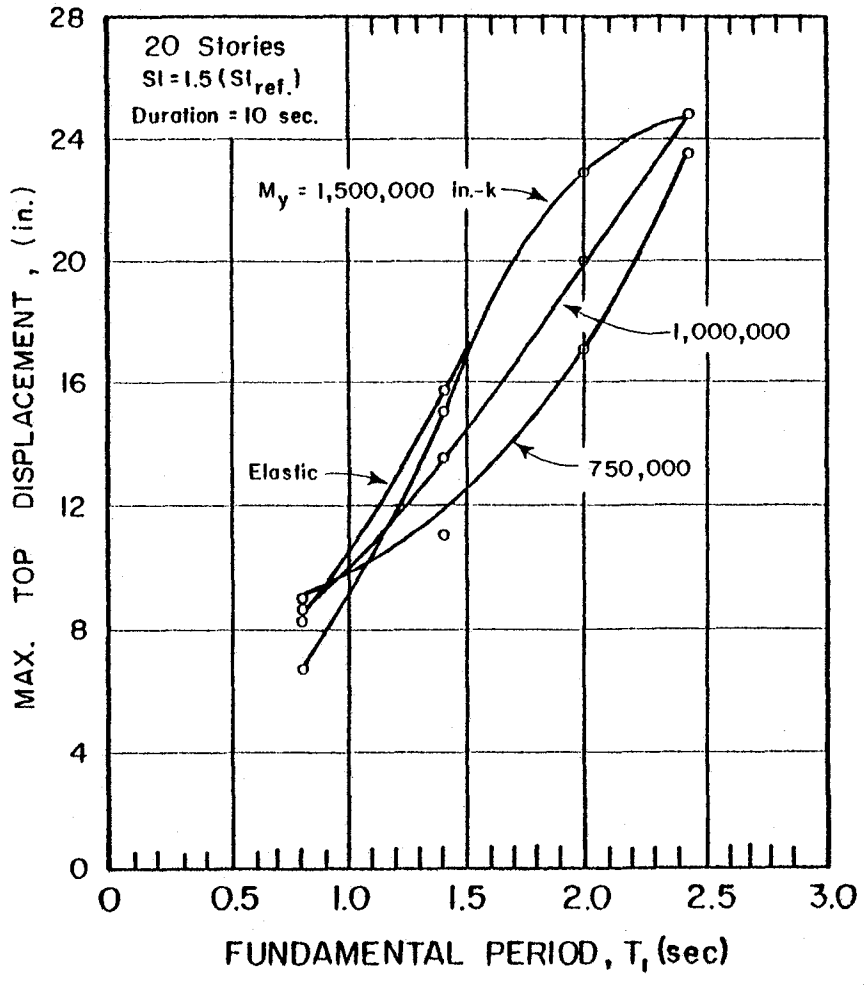

(a)

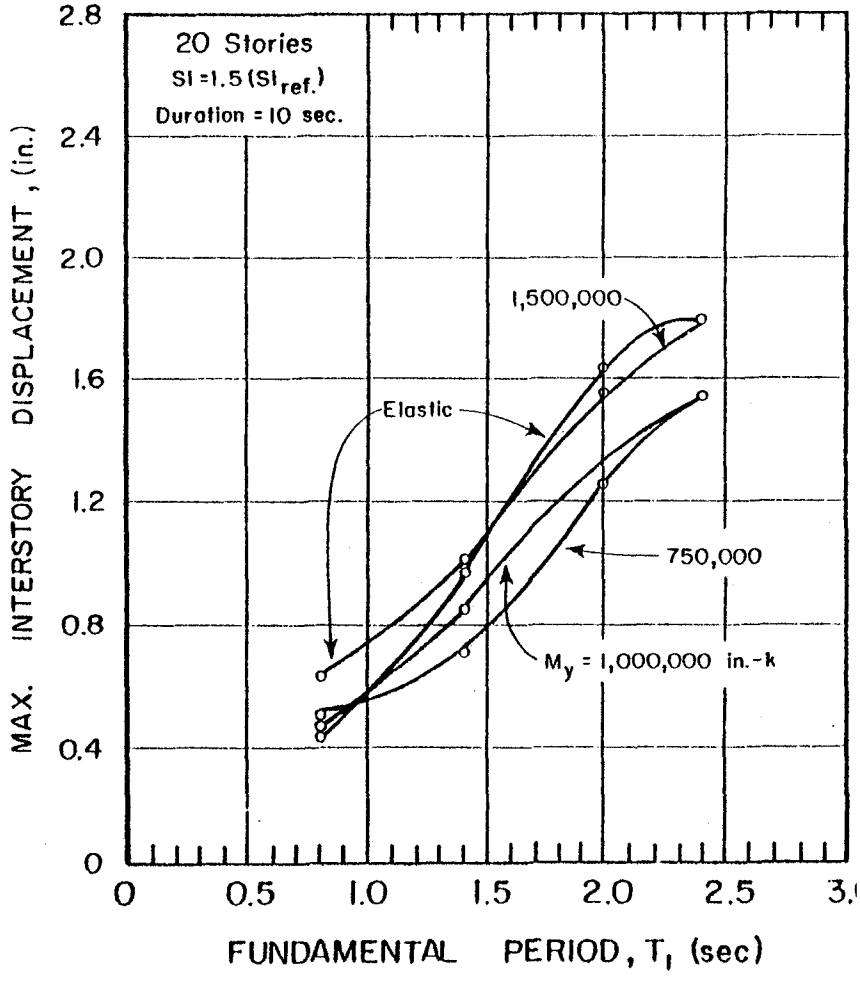

(b)

Fig. 13 Critical Response Values as Functions of Fundamental Period, T_1, and Yield Level, M_y, 20-Story Isolated Structural Walls

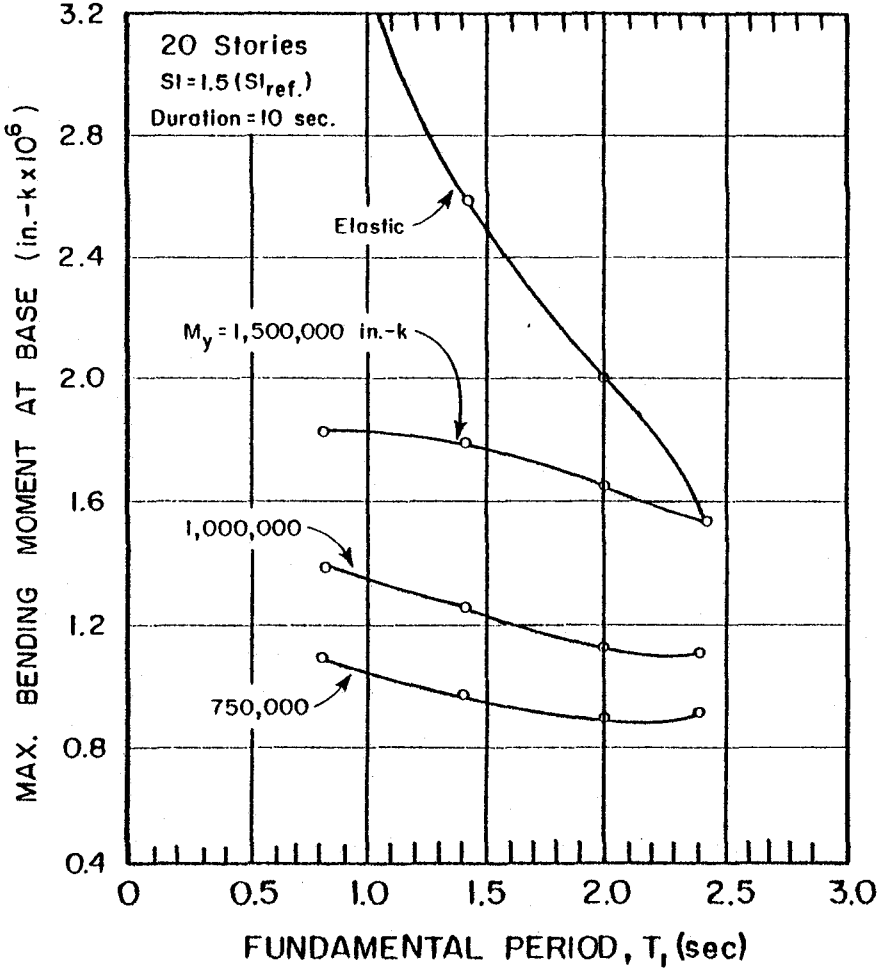

(c)

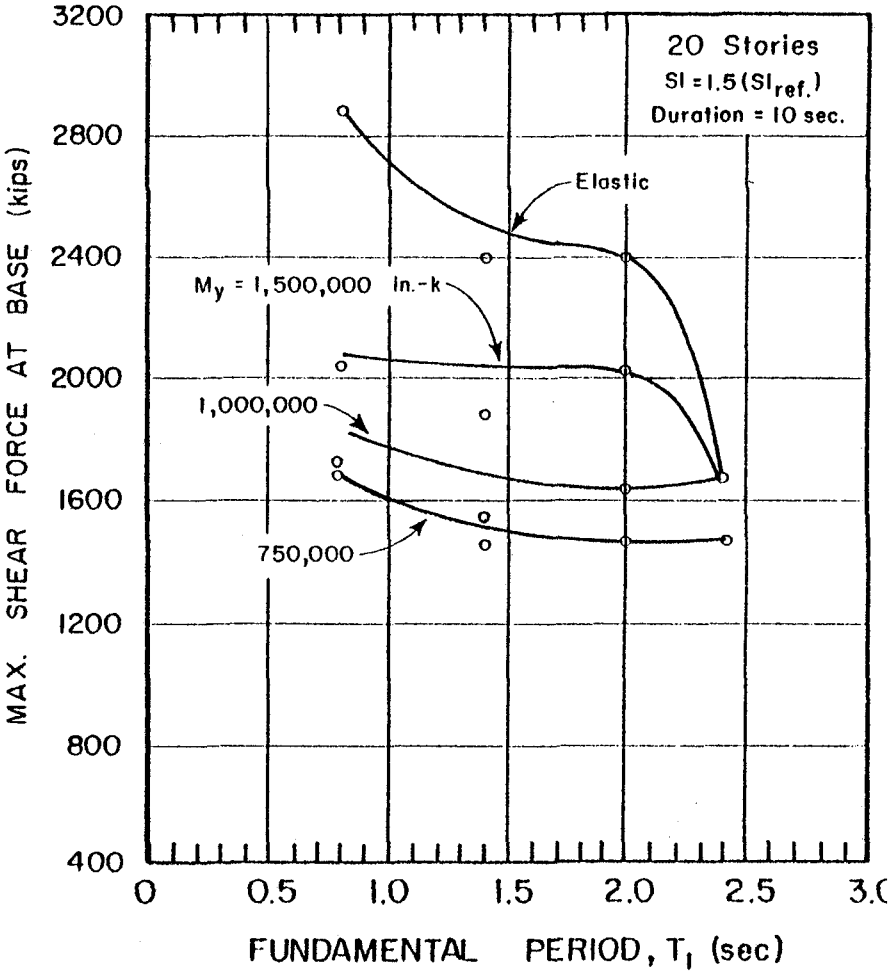

(d)

Fig. 13 (contd.) Critical Response Values as Functions of Fundamental Period, T_1, and Yield Level, M_y, 20-Story Isolated Structural Walls

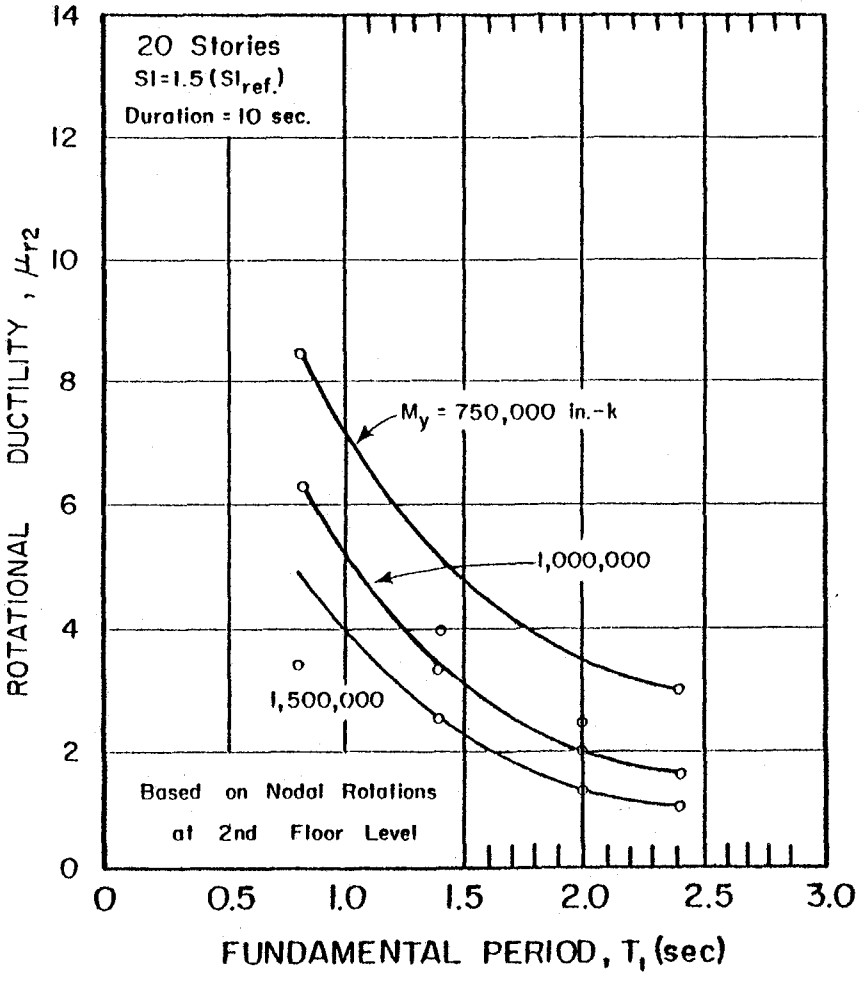

(e)

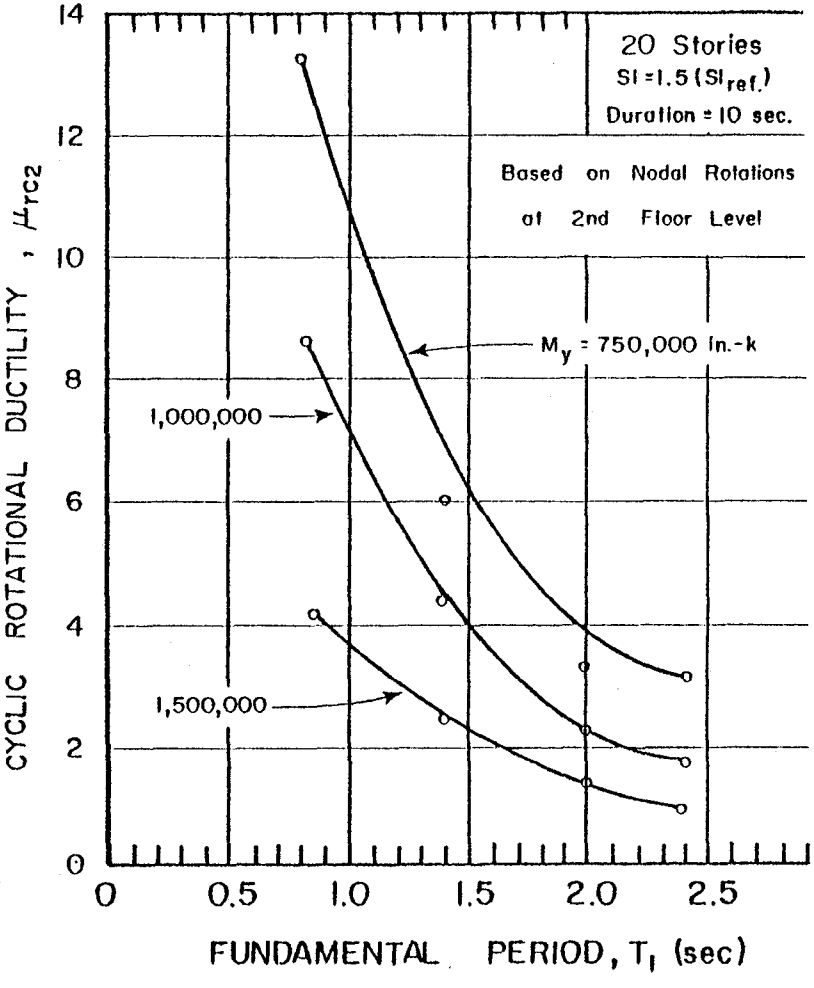

(f)

Fig. 13 (contd.) Critical Response Values as Functions of Fundamental Period, T_1, and Yield Level, M_y, 20-Story Isolated Structural Walls

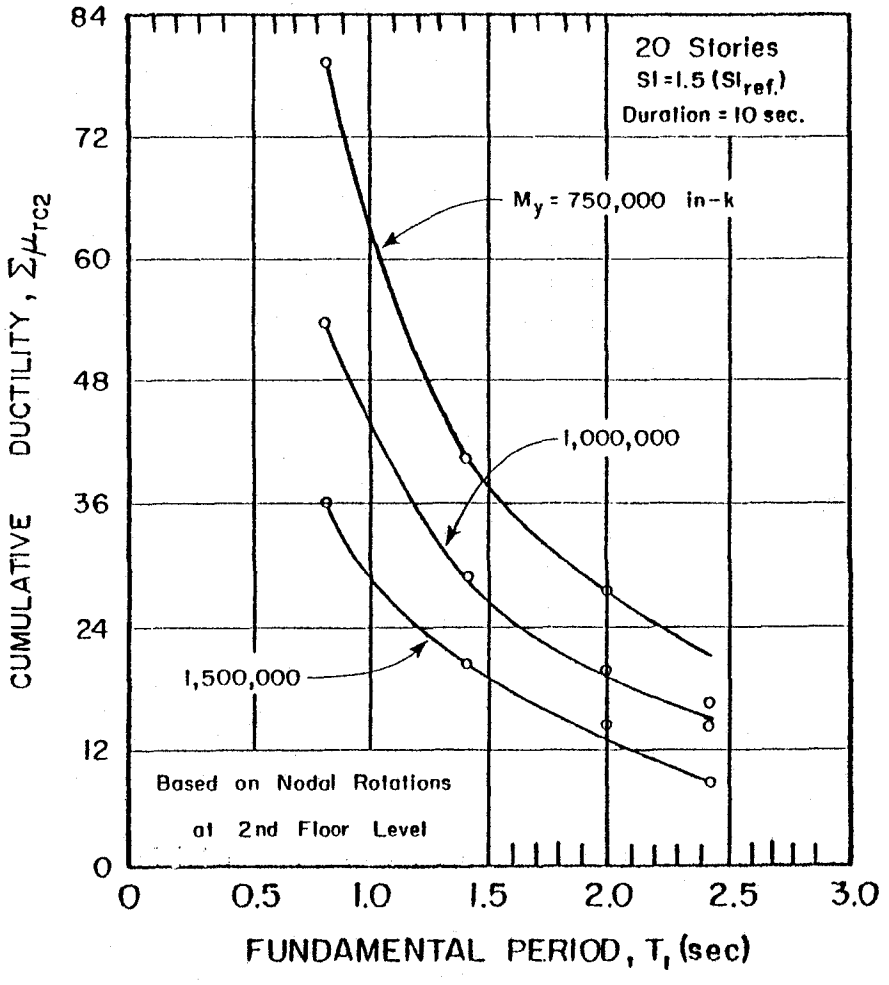

(g)

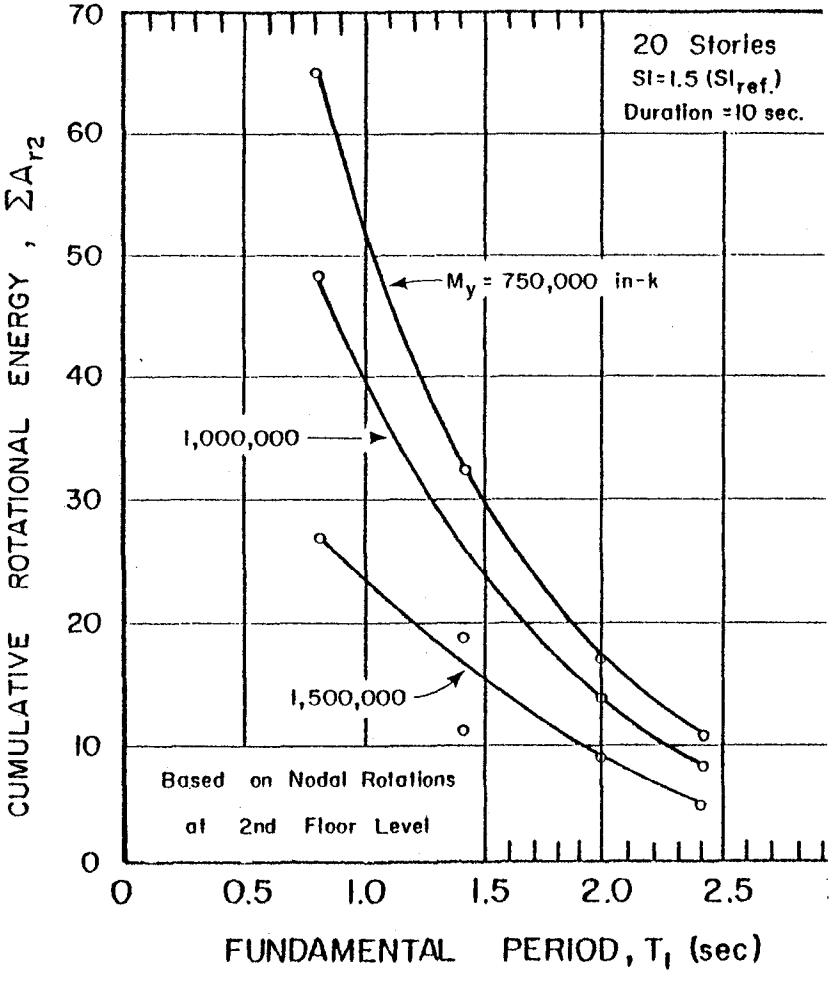

(h)

Fig. 13 (contd.) Critical Response Values as Functions of Fundamental Period, T_1, and Yield Level, M_y, 20-Story Isolated Structural Walls

a potential epicenter, component frequencies above a certain value are unlikely to occur.

The fact that an input motion that is critical with respect to moments and deformations is not necessarily critical with respect to shear made it necessary to use other accelerograms to obtain near-maximum values for shear. In view of this, the critical values of the moments and displacements shown in Fig. 13 are generally not concurrent with the maximum shear values. This aspect will be examined more closely later in the report.

Three-dimensional plots showing the maximum response quantities as functions of fundamental period, T_1, and yield level, M_y, are shown in Fig. 14. This figure presents in three dimensions, the data shown in Fig. 11. Also shown in Figs. 14a, 14c, and 14d are surfaces corresponding to the design forces specified under the Uniform Building Code, 1976 Edition (UBC-76)[16], for seismic Zone No. 4.

The forces used to calculate top displacement and base moment were obtained by multiplying the base shear, V, as given by Eq. (12-1) of the code by a factor of 1.4. The forces used to determine the base shear were obtained by using a factor of 2.0.

The coefficients I and S in the equation for V in UBC-76 were both taken equal to 1.0, with K = 1.33, in calculating the UBC values for Fig. 14. Values of the unfactored forces corresponding to the different wall heights as specified in UBC-76 are listed in Table 3.

Curve Fitting

In fitting curves to calculated data points for critical response values, it was decided to disregard some points in order to preserve the trends indicated by the majority of points. In some cases a data point is significantly detached from a curve representing the trend exhibited by other data points. This indicates that the criticality of the input motion relative to the structure for this case is not of the

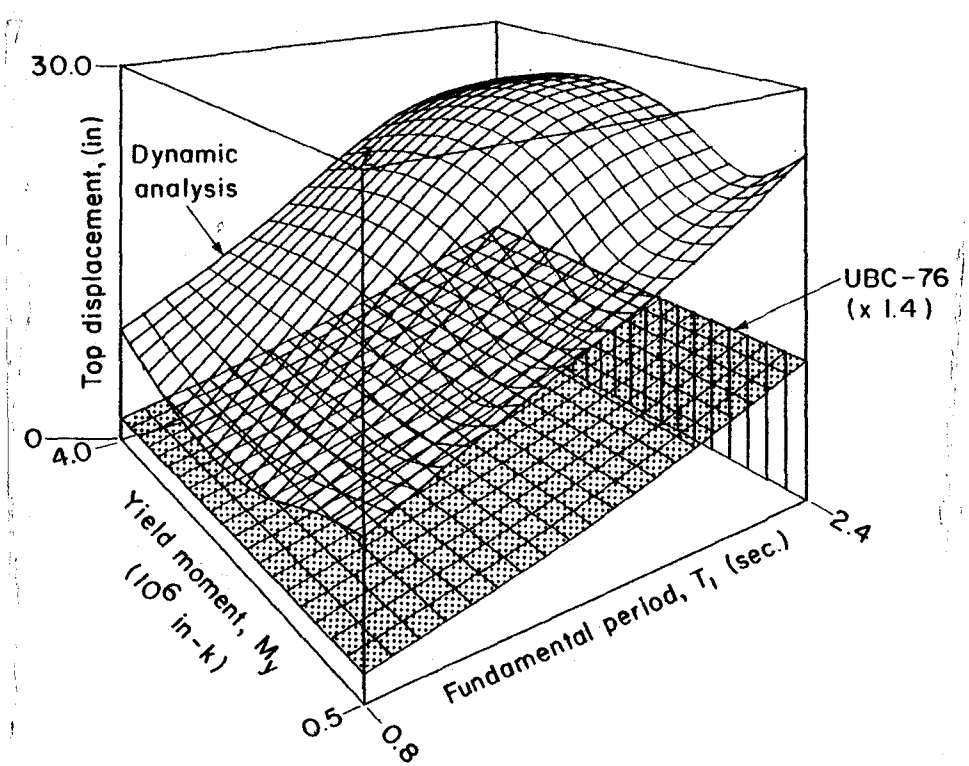

(a)

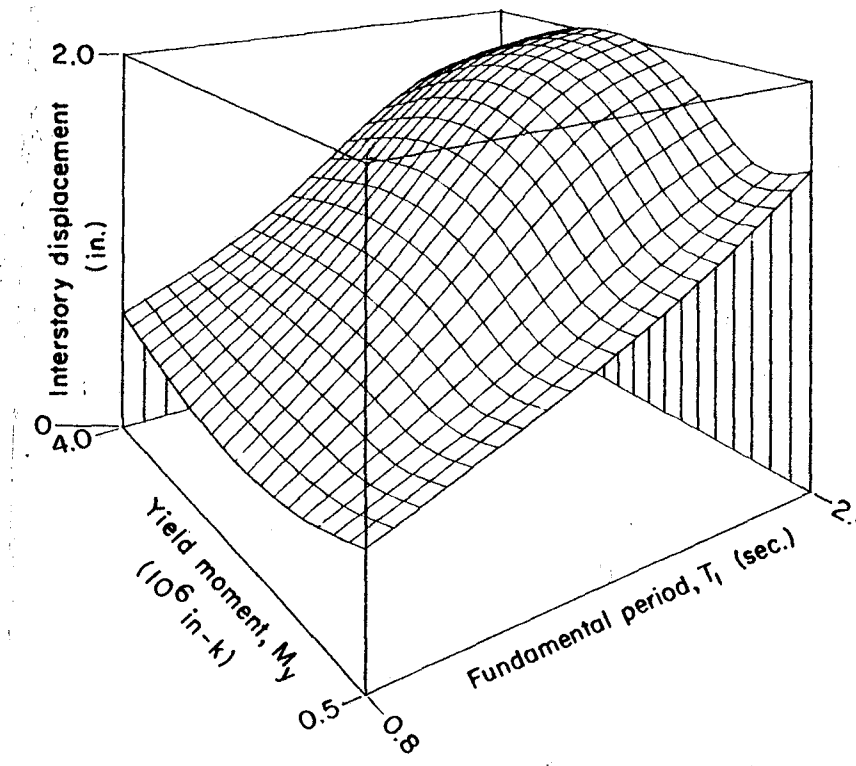

(b)

Fig. 14 Maximum Response as a Function of Fundamental Period, T_1, and Yield Level, M_y 20-Story Isolated Structural Walls - SI = $1.5(SI_{ref.})$, Duration = 10 sec.

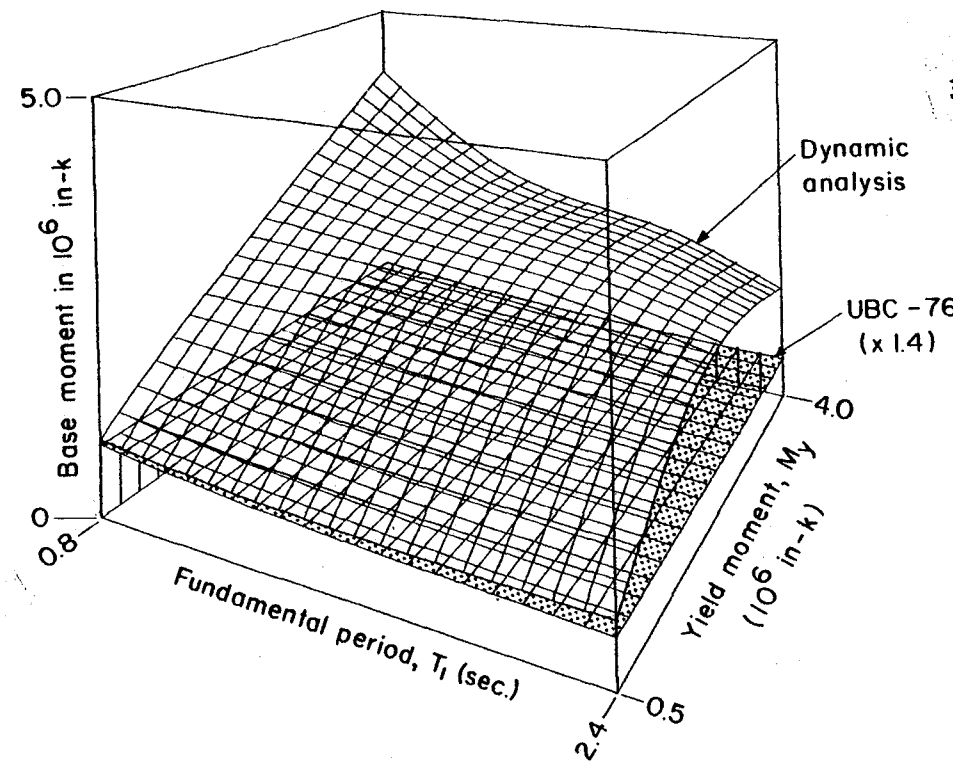

(c)

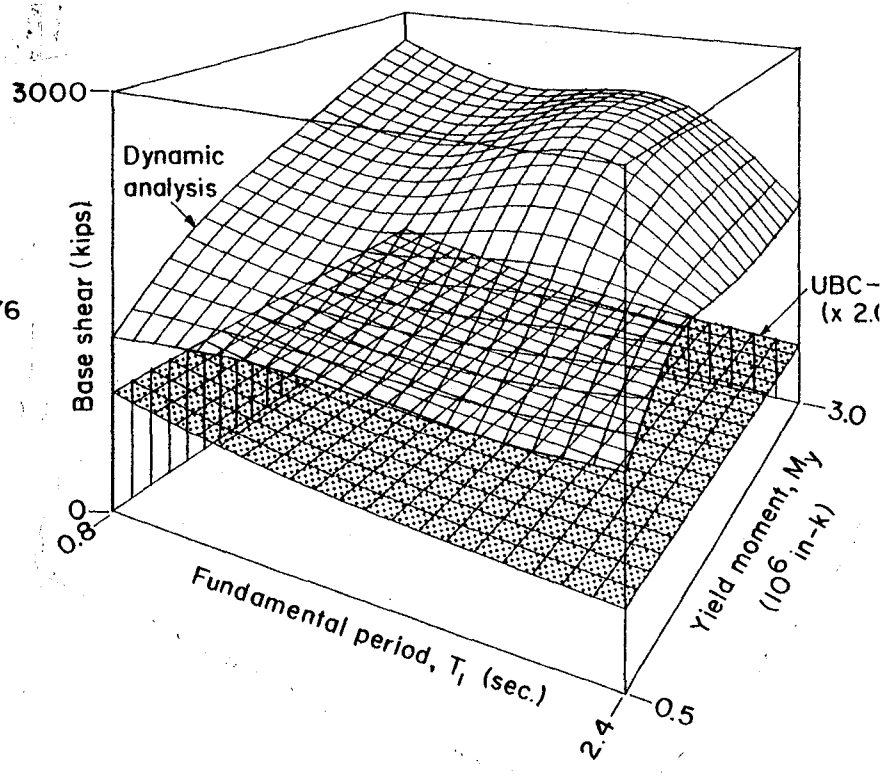

(d)

Fig. 14 (contd.) Maximum Response as a Function of Fundamental Period, T_1, and Yield Level, M_y 20-Story Isolated Structural Walls - SI = $1.5(SI_{ref.})$, Duration = 10 sec.

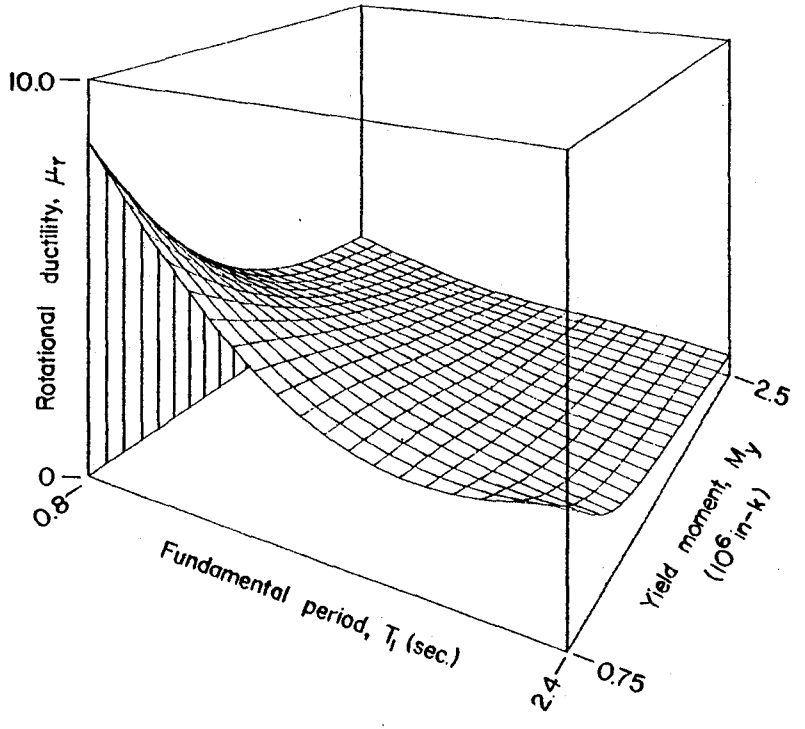

(e)

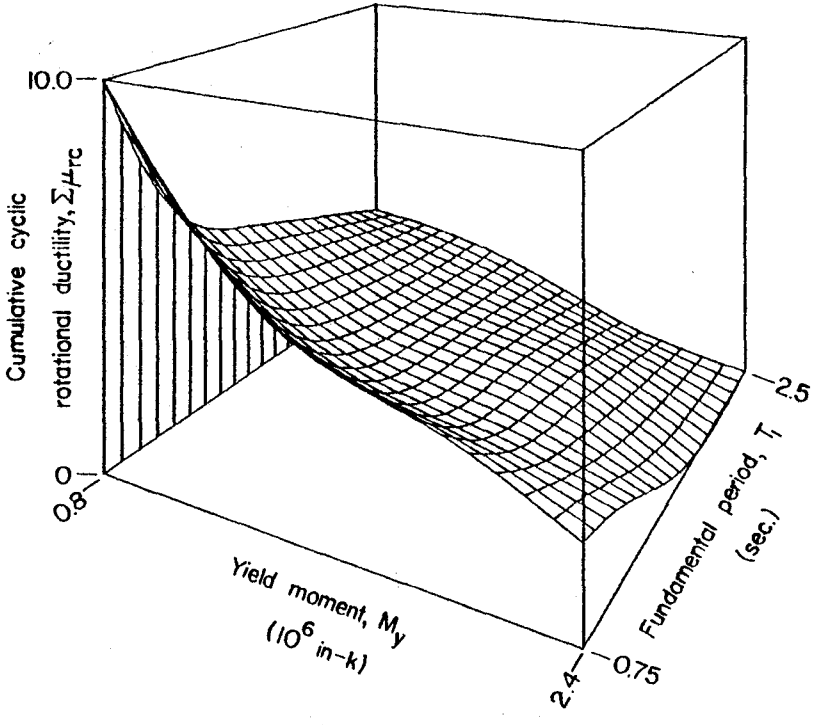

(f)

Fig. 14 (contd.) Maximum Response as a Function of Fundamental Period, T_1, and Yield Level, M_y 20-Story Isolated Structural Walls - SI = $1.5(SI_{ref.})$, Duration = 10 sec.

Parameters	Fundamental Period, T_1 (sec.)		
	0.5	0.8	1.4
10 Stories			
Height (ft)	90.75	90.75	90.75
Weight (k)	2,174	2,174	2,174
EI (10^{11} in^2-k)	1.21	.46	.15
Base Shear (kips)	273.3	215.5	163.3
Base Moment (10^6 in-k)	0.2	.16	.12
Top Displ. (in.)	0.54	1.17	2.76
Drift Ratio	1/2030	1/930	1/400

Parameters	Fundamental Period, T_1 (sec.)			
	0.8	1.4	2.0	2.4
20 Stories				
Height (ft)	178.25	178.25	178.25	178.25
Weight (k)	4,374	4,374	4,374	4,374
EI (10^{11} in^2-k)	6.44	2.05	.99	.68
Base Shear (kips)	435.0	329.0	275.0	252.0
Base Moment (10^6 in-k)	.64	.49	.42	.39
Top Displ. (in.)	1.26	3.10	5.57	7.46
Drift Ratio	1/1690	1/690	1/380	1/290

Parameters	Fundamental Period, T_1 (sec).		
	1.4	2.0	2.4
30 Stories			
Height (ft)	265.75	265.75	265.75
Weight (k)	6,574	6,574	6,574
EI (10^{11} in^2-k)	9.81	4.72	3.27
Base Shear (kips)	494.0	413.0	377.0
Base Moment (10^6 in-k)	1.10	.94	.87
Top Displ. (in.)	3.23	5.80	8.95
Drift Ratio	1/1000	1/550	1/360

Parameters	Fundamental Period, T_1 (sec.)			
	1.4	2.0	2.4	3.0
40 Stories				
Height (ft)	353.25	353.25	353.25	353.25
Weight (k)	8,774	8,774	8,774	8,774
EI (10^{11} in^2-k)	32.4	16.7	10.22	6.48
Base Shear (kips)	659.0	552.0	503.0	480.0
Base Moment (10^6 in-k)	1.96	1.67	1.54	1.41
Top Displ. (in.)	3.07	6.79	7.82	11.37
Drift Ratio	1/1380	1/730	1/540	1/370

same order as that corresponding to the other data points. In all cases, however, the data points are shown in the figures.

In practically all cases, the plotted curve was passed through the largest calculated values so that the curve represents an upper bound with respect to the calculated data. The only exceptions to this are a few cases where the artificial accelerogram S1 was the critical input motion with respect to shear. The accelerogram S1 is characterized by pulses of nearly uniform amplitude and a relatively larger number of zero-crossings when compared to most natural records. This can can be seen in Fig. 9. These features tend to give the artificial accelerogram stronger components in the low-period range than might be expected in most natural records. It was therefore decided to disregard data points corresponding to S1 when these departed appreciably from those for other input motions.

Plots of critical response values, similar to Fig. 13, for 10-, 30-, and 40-story isolated structural walls are shown in Figs. 15, 16, and 17. Plots of critical response values corresponding to the four heights of structural walls considered have also been reproduced in Appendix A as Figs. A17 through A23 for completeness of the set.

Discussion of Results

An examination of the charts shown in Fig. 13 leads to the following significant observations relating mainly to the effects of the two principal structural parameters T_1 and M_y on the different response quantities considered.

1. Critical horizontal and interstory displacements increase with increasing fundamental period of a structure. This follows from the greater flexibility of longer-period structures. However, displacements are not significantly different for different yield levels.*

*This result confirms the observation made by earlier investigators concerning the approximately equal maximum displacements of elastic and inelastic structures having the same initial fundamental period.

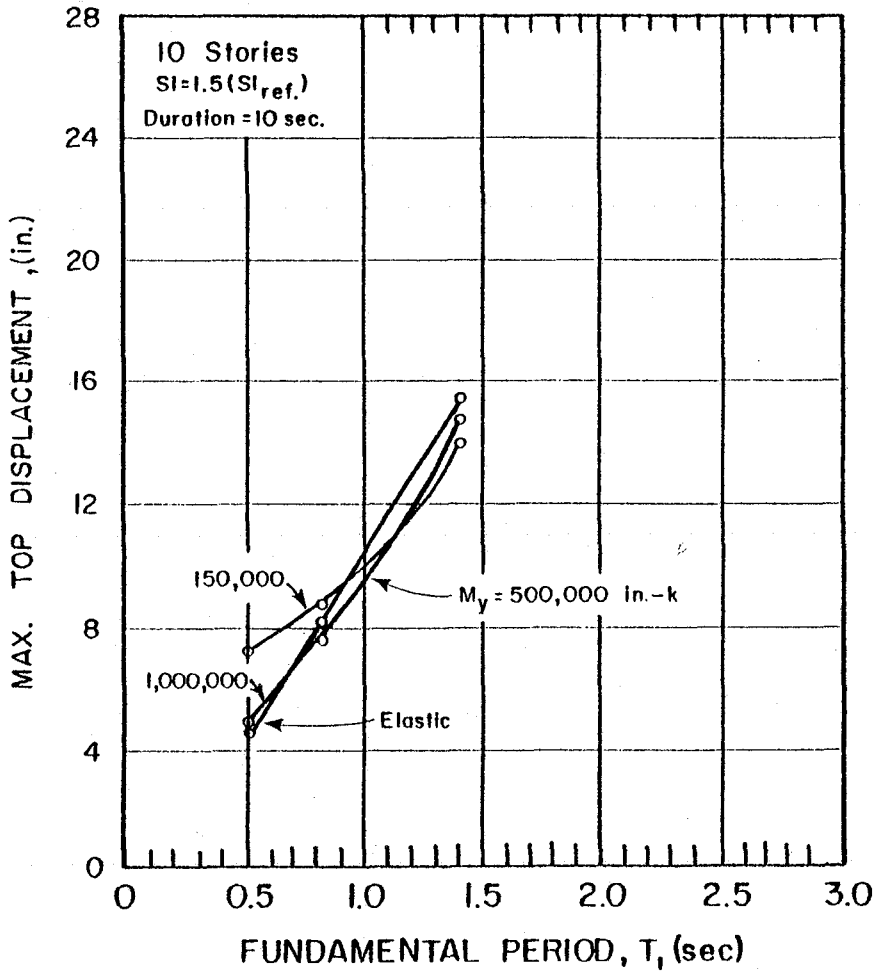

(a)

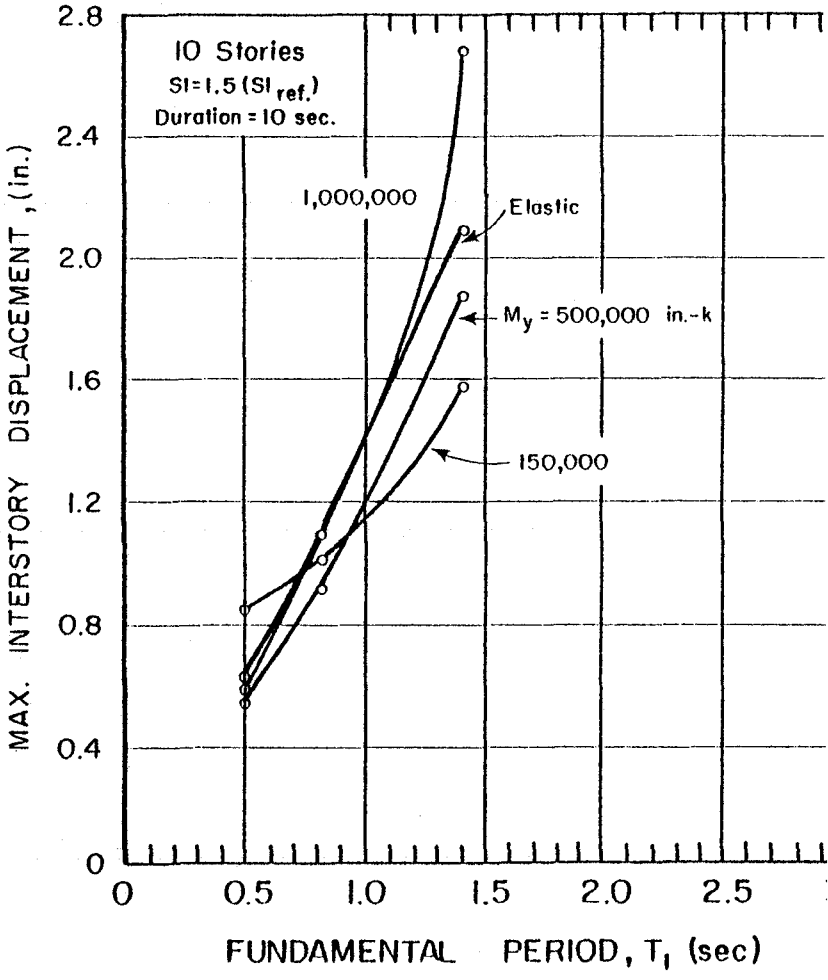

(b)

Fig. 15 Critical Response Values as Functions of Fundamental Period, T_1, and Yield Level, M_y, 10-Story Isolated Structural Walls

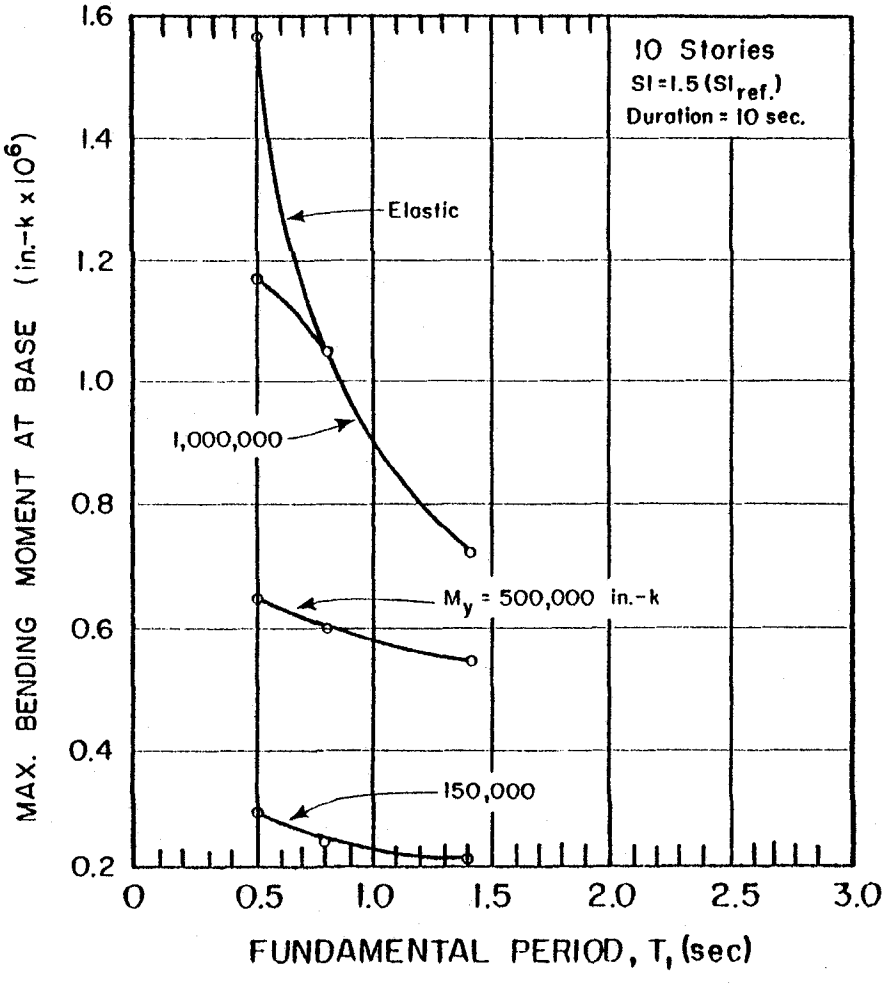

(c)

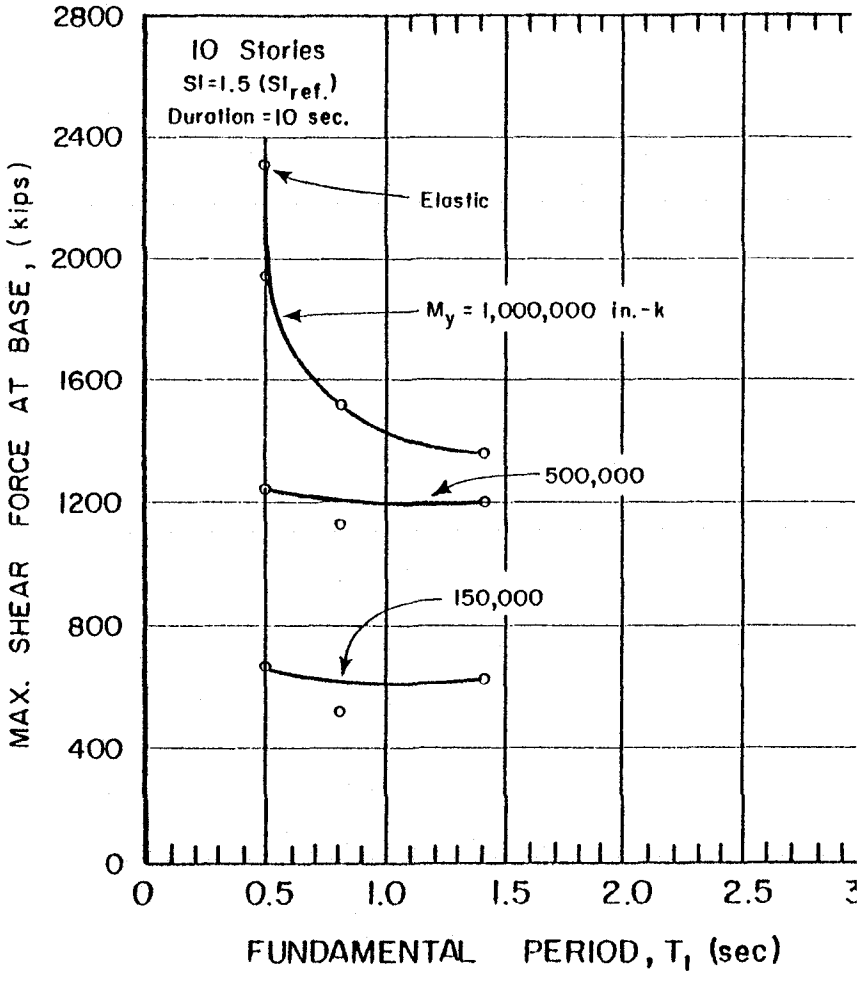

(d)

Fig. 15 (contd.) Critical Response Values as Functions of Fundamental Period, T_1, and Yield Level, M_y, 10-Story Isolated Structural Walls

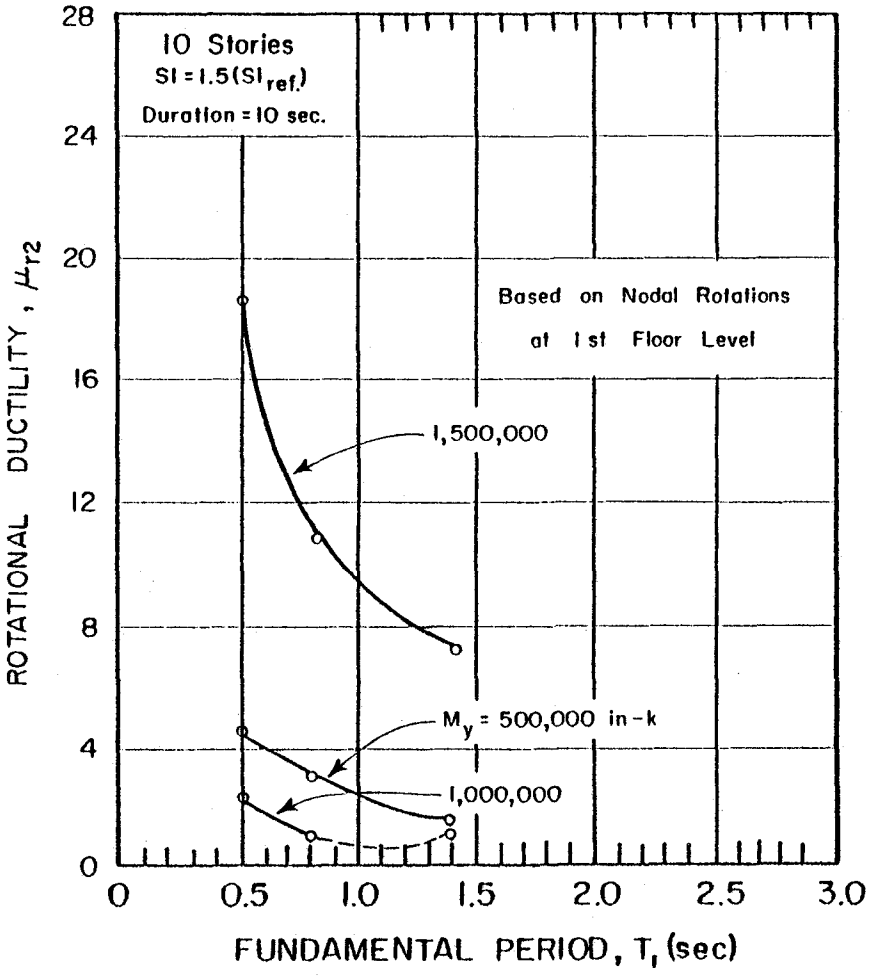

(e)

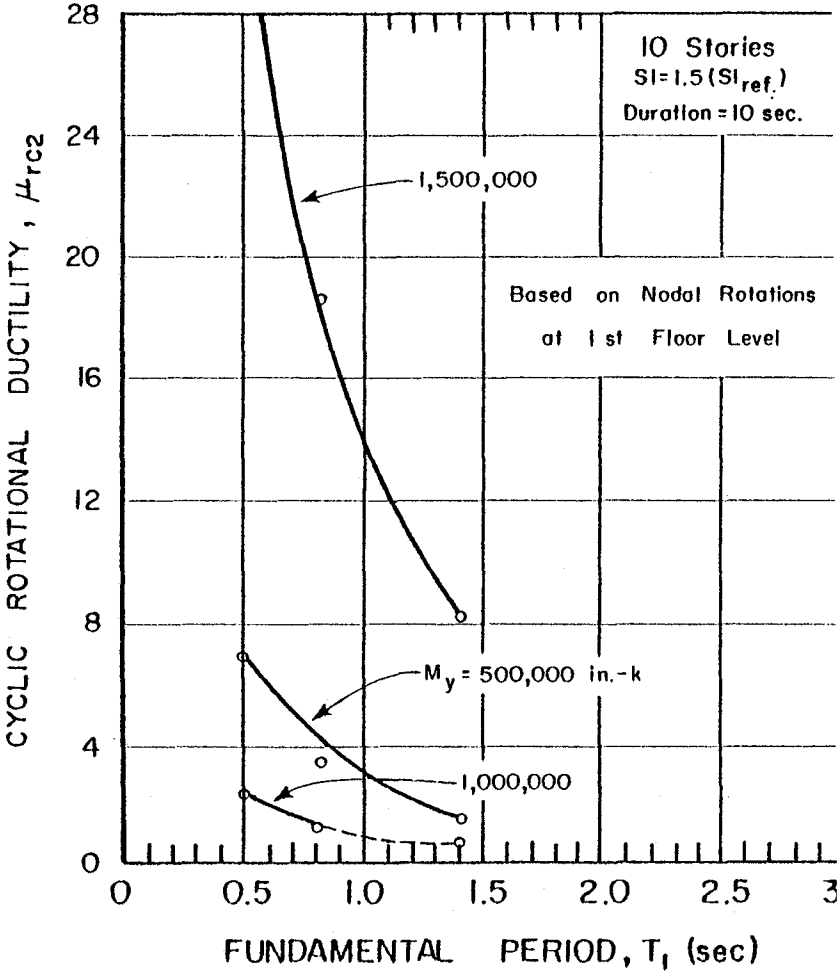

(f)

Fig. 15 (contd.) Critical Response Values as Functions of Fundamental Period, T_1, and Yield Level, M_y, 10-Story Isolated Structural Walls

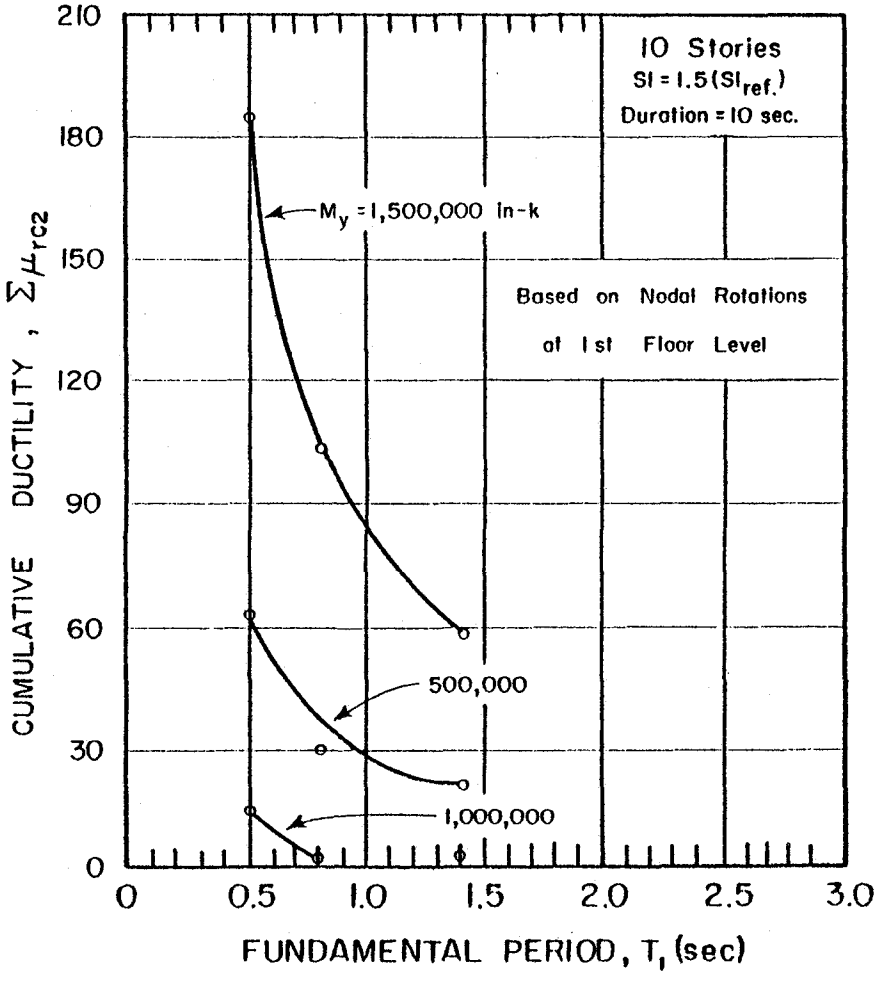

(g)

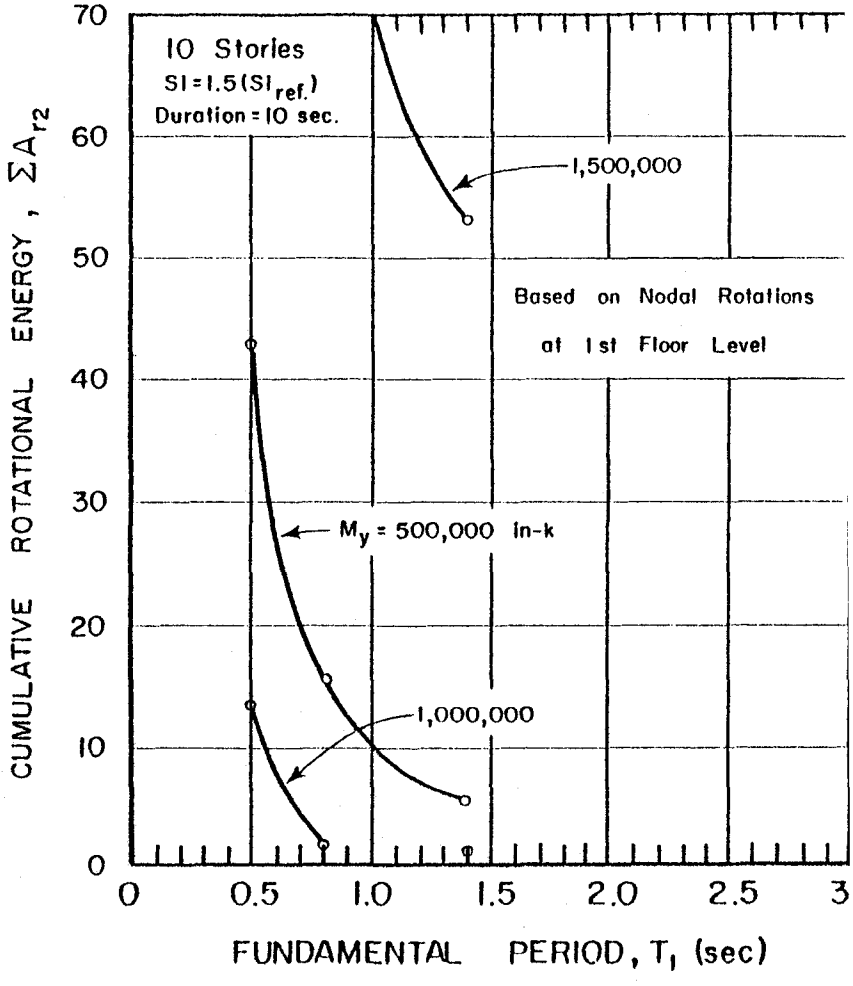

(h)

Fig. 15 (contd.) Critical Response Values as Functions of Fundamental Period, T_1, and Yield Level, M_y, 10-Story Isolated Structural Walls

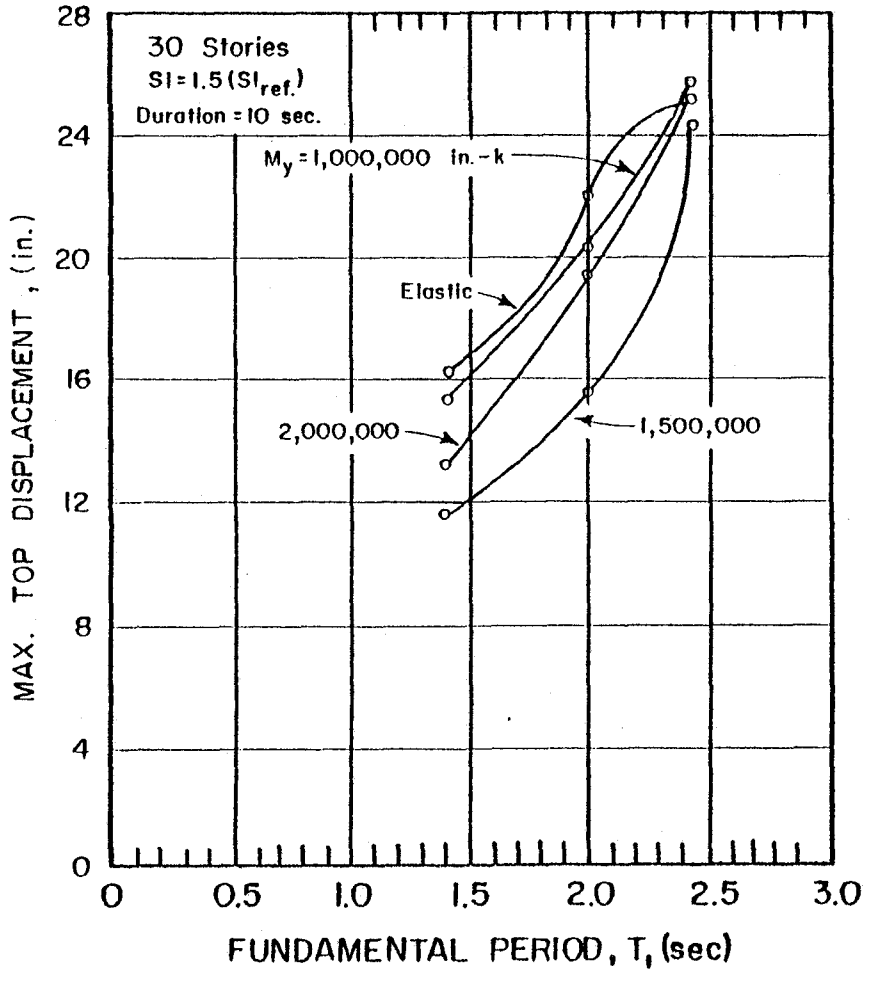

(a)

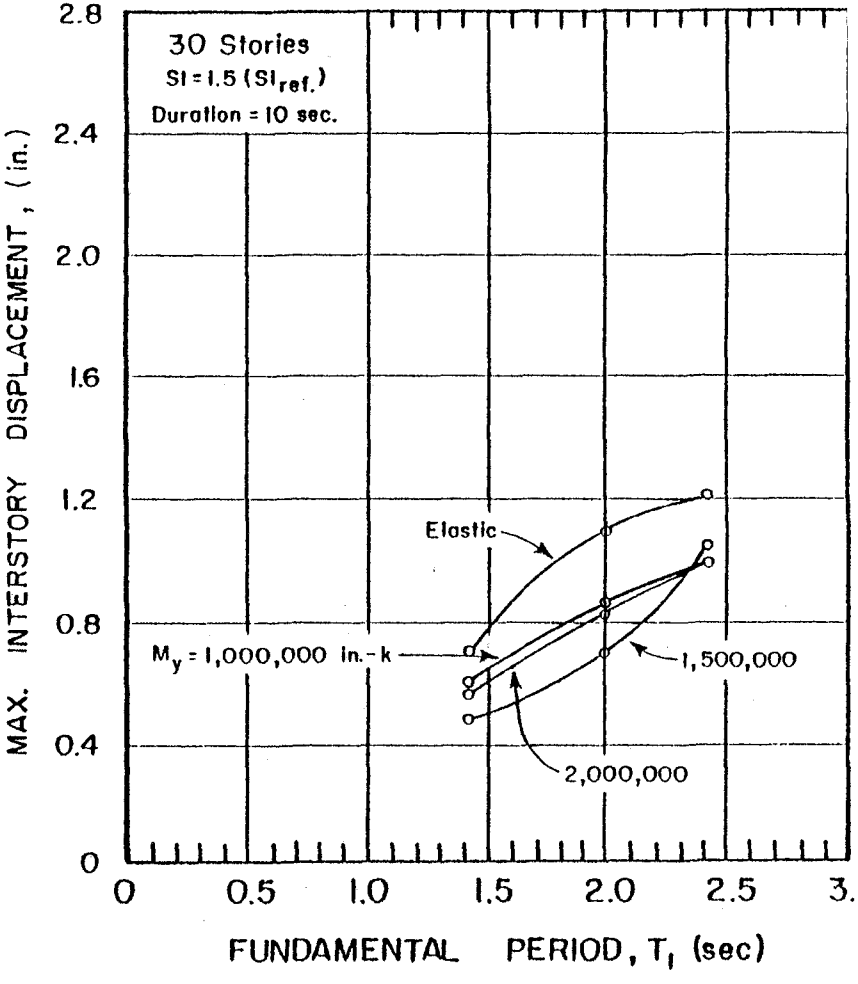

(b)

Fig. 16 Critical Response Values as Functions of Fundamental Period, T_1, and Yield Level, M_y, 30-Story Isolated Structural Walls

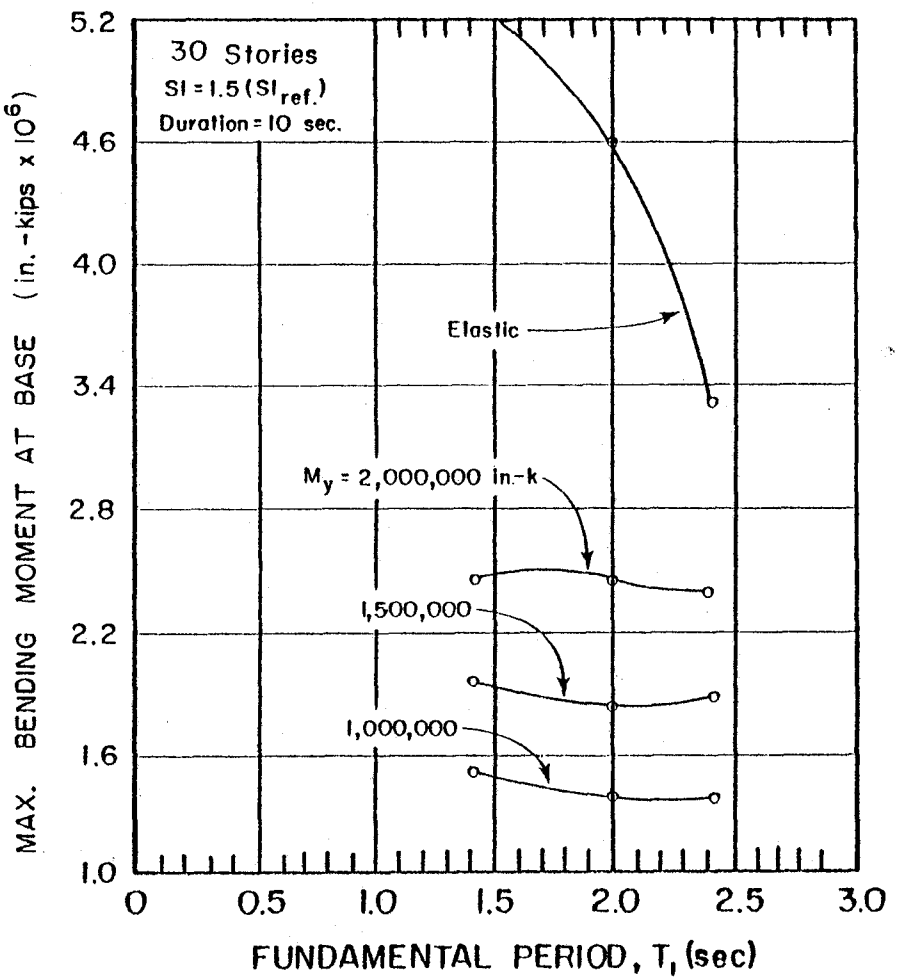

(c)

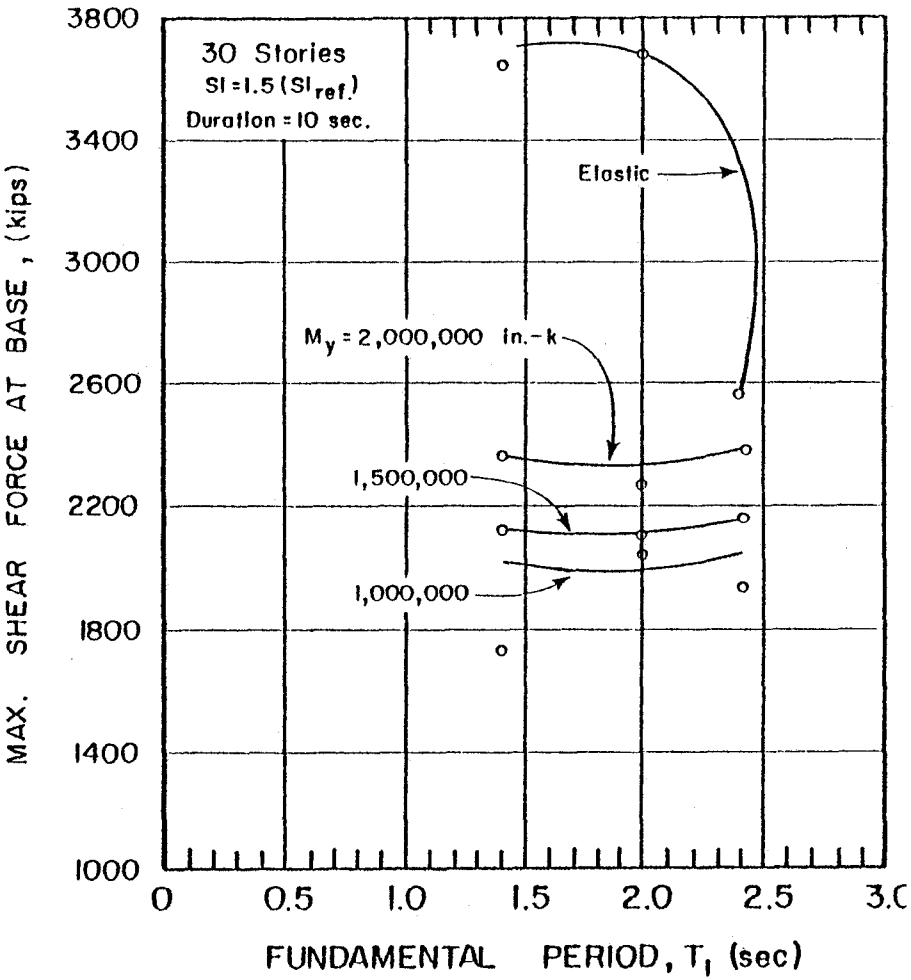

(d)

Fig. 16 (contd.) Critical Response Values as Functions of Fundamental Period, T_1, and Yield Level, M_y, 30-Story Isolated Structural Walls

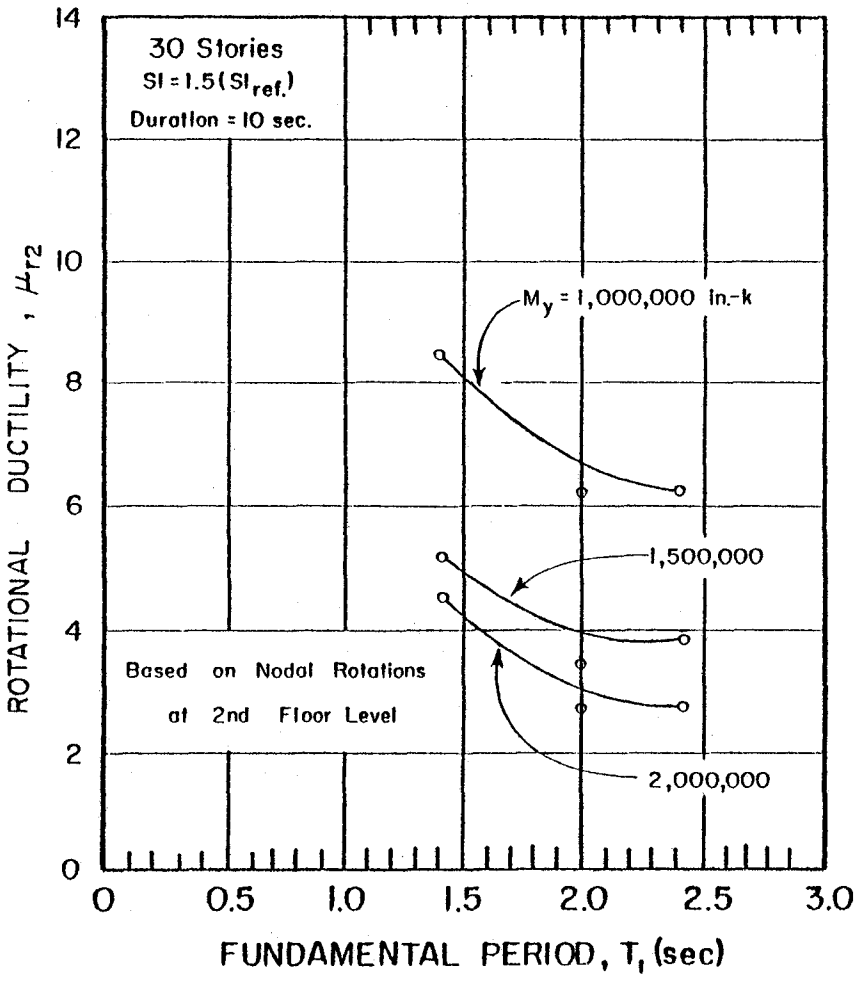

(e)

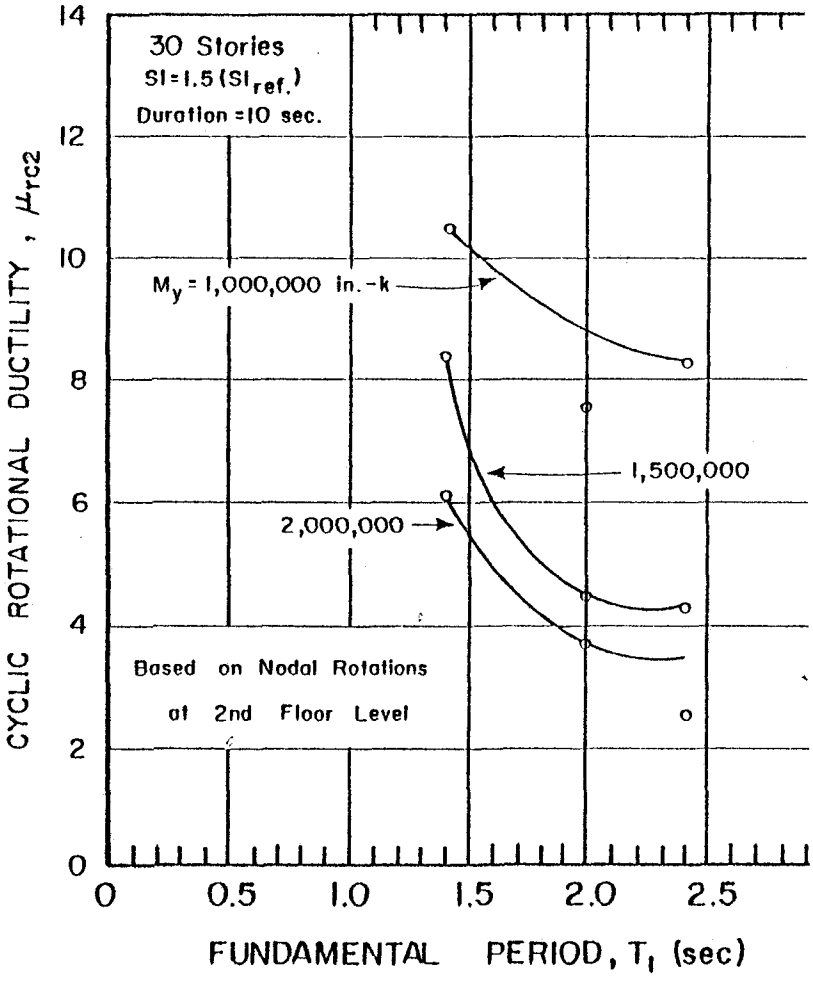

(f)

Fig. 16 (contd.) Critical Response Values as Functions of Fundamental Period, T_1, and Yield Level, M_y, 30-Story Isolated Structural Walls

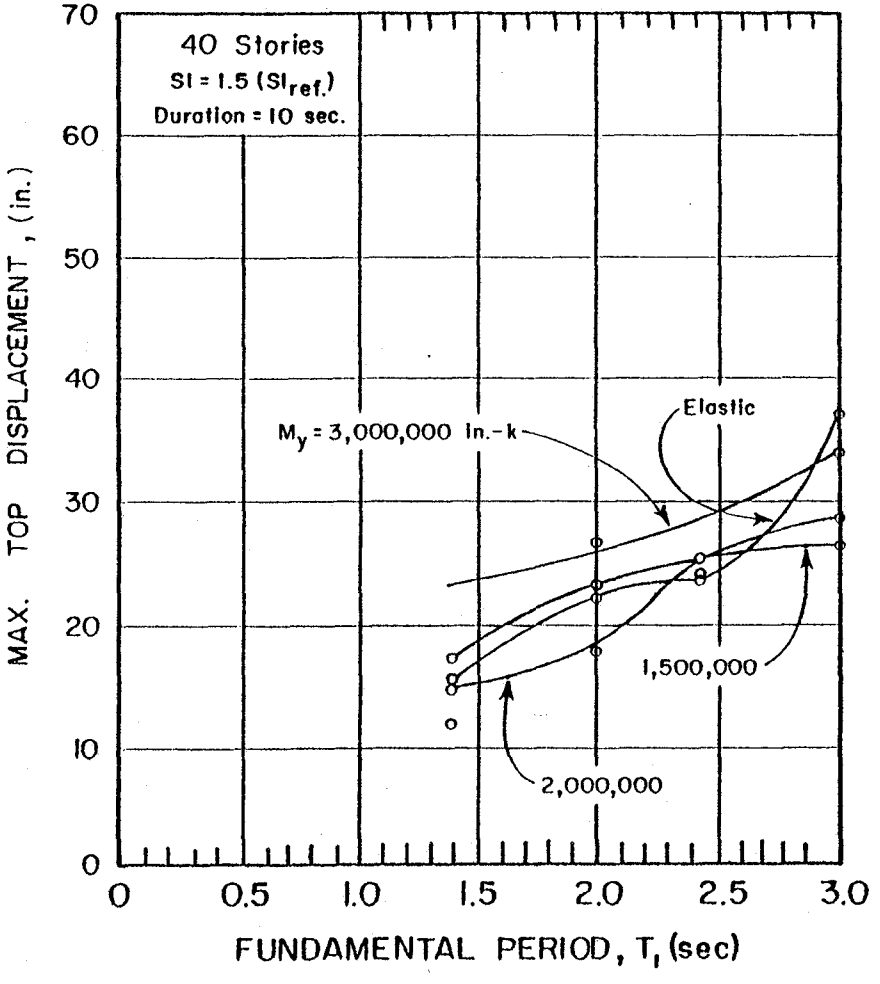

(a)

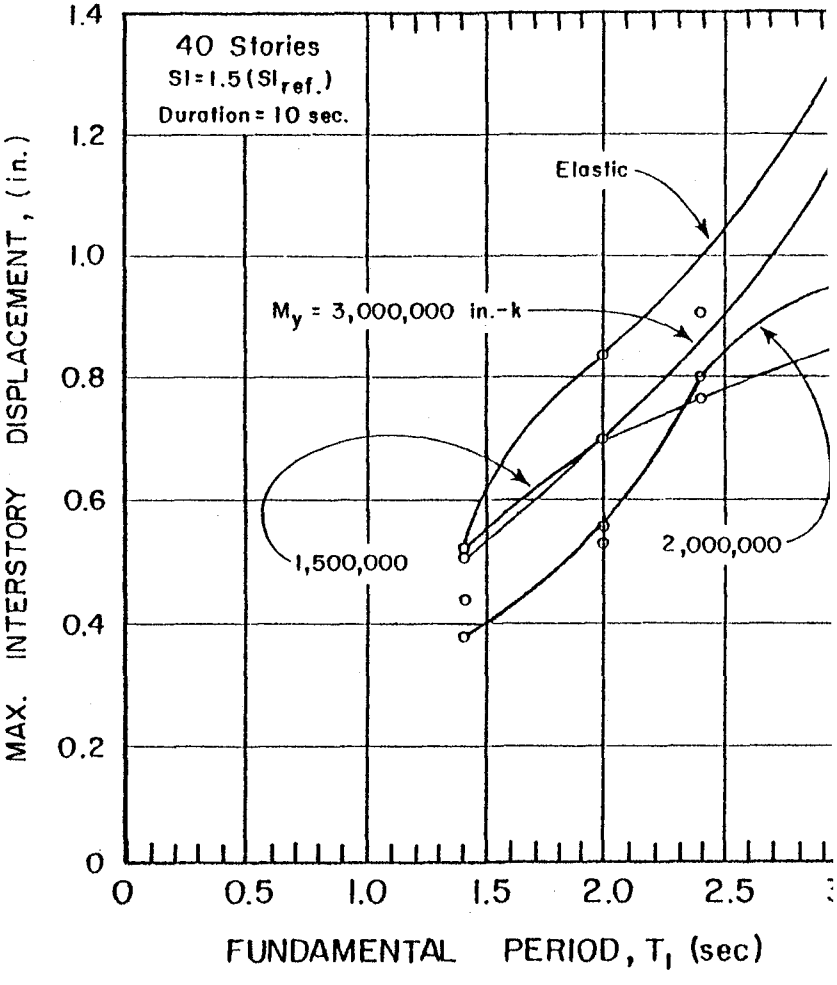

(b)

Fig. 17 Critical Response Values as Functions of Fundamental Period, T_1 and Yield Level, M_y, 40-Story Isolated Structural Walls

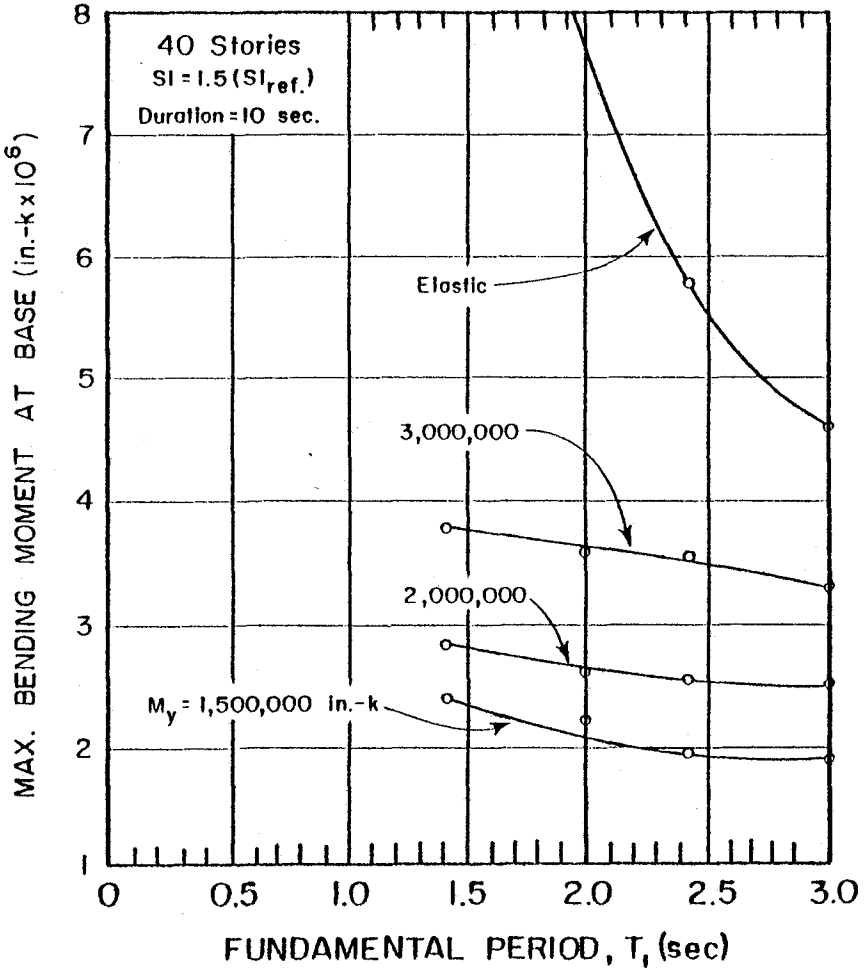

(c)

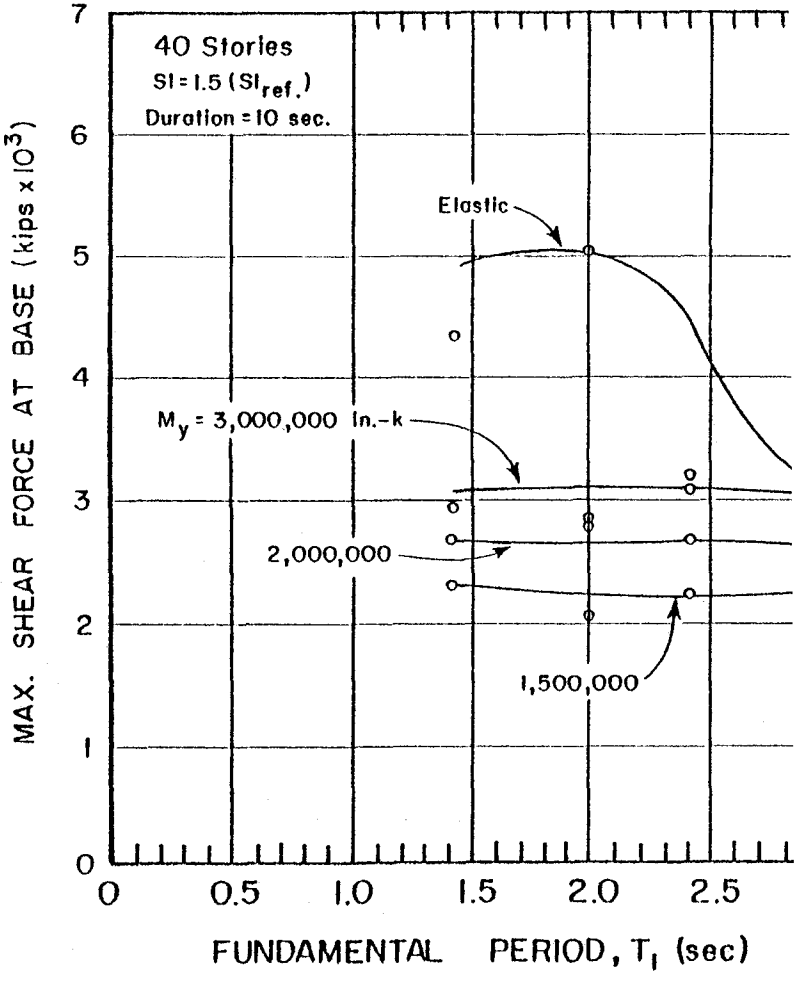

(d)

Fig. 17 (contd.) Critical Response Values as Functions of Fundamental Period, T_1, and Yield Level, M_y, 40-Story Structural Walls

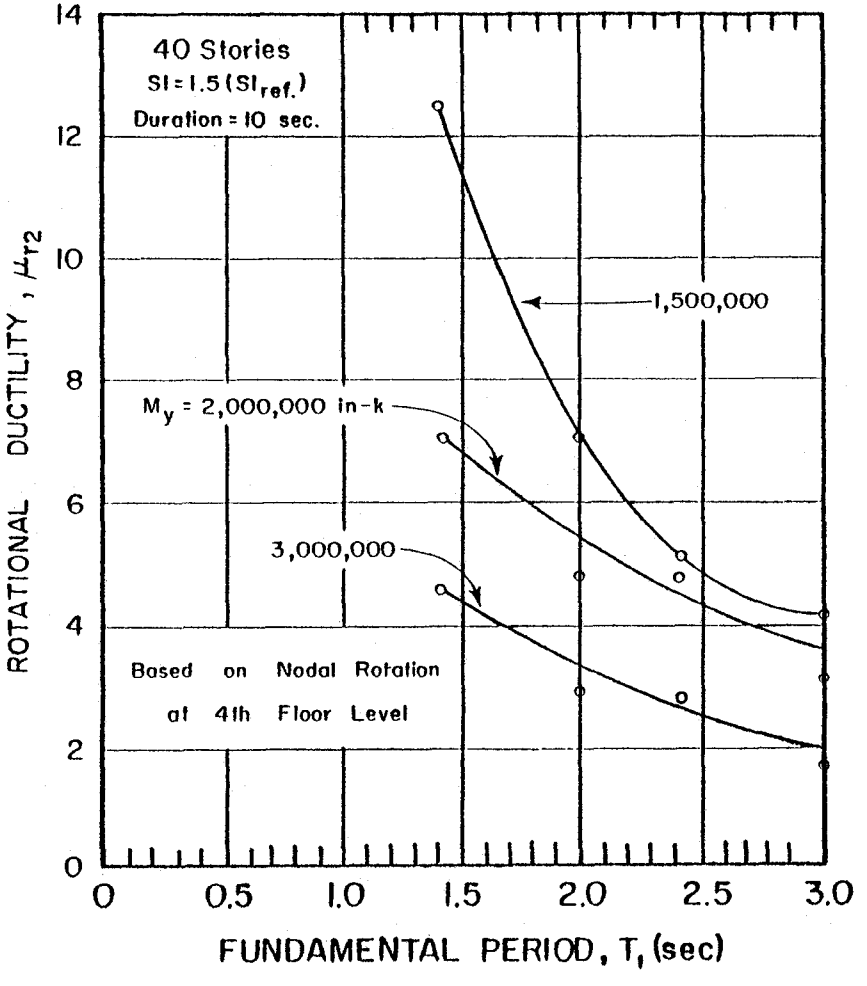

(e)

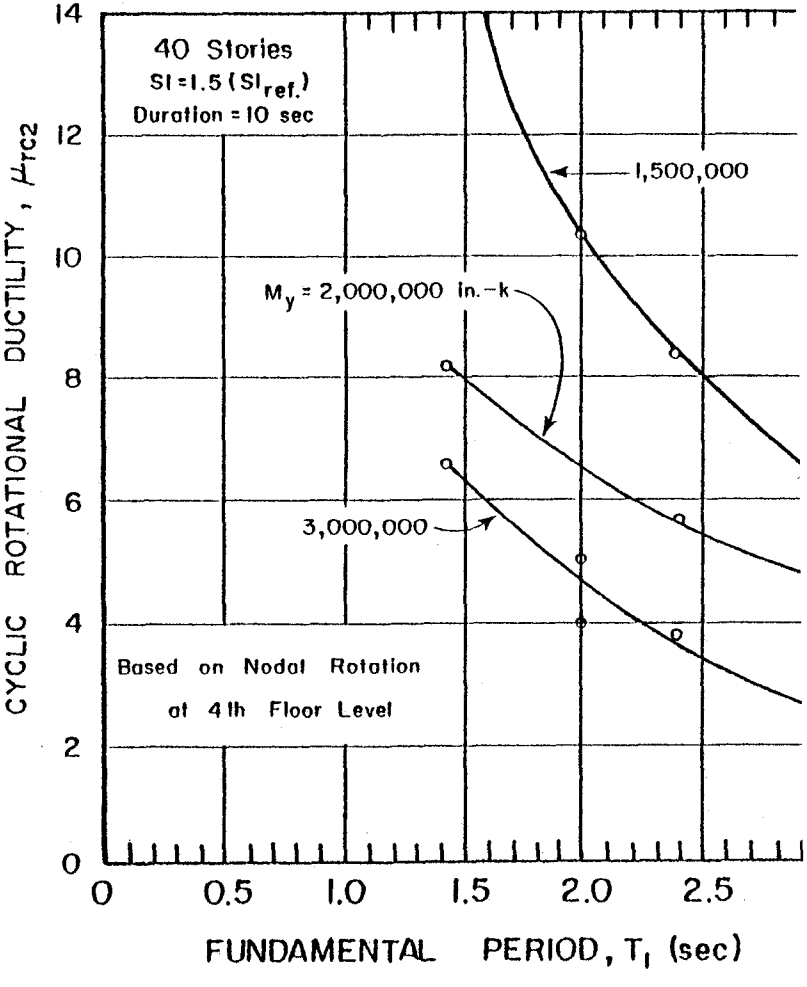

(f)

Fig. 17 (contd.) Critical Response Values as Functions of Fundamental Period, T_1, and Yield Level, M_y, 40-Story Structural Walls

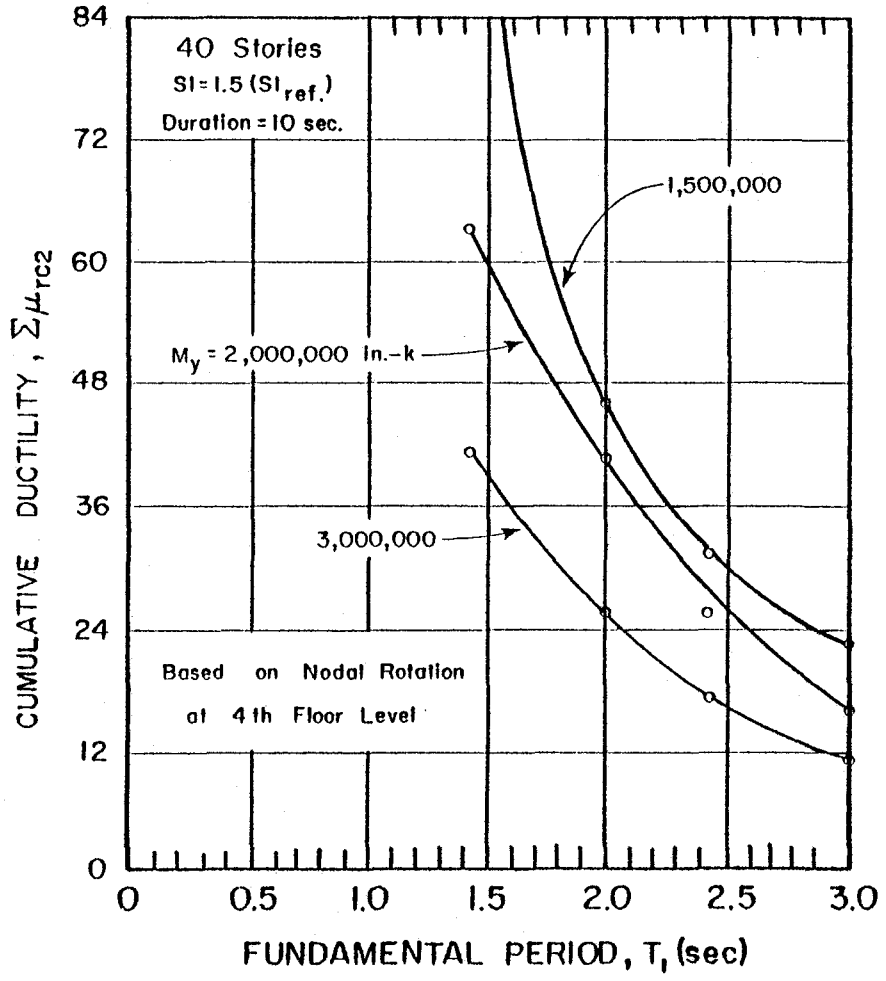

(g)

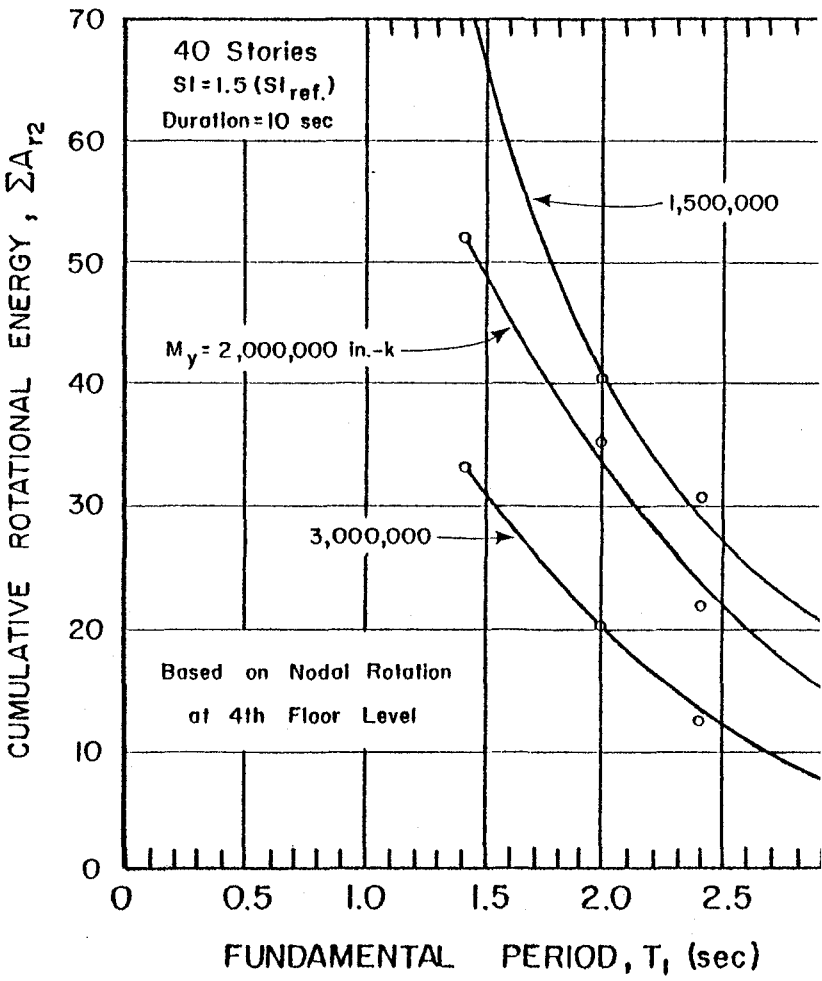

(h)

Fig. 17 (contd.) Critical Response Values as Functions of Fundamental Period, T_1, and Yield Level, M_y, 40-Story Structural Walls

2. Critical bending moments and shears at the base of the wall increase with increasing yield level. This would be expected where all structures yield under the specified ground motion intensity. These forces, however, do not vary significantly with fundamental period, except in the elastic case, where an increase in forces accompanies a decrease in period.

3. Rotational ductility demands increase with decreasing flexural yield level and fundamental period of a structure.

It is important to note the relationship between flexural yield level, rotational ductility demand, and critical base shear. An increase in flexural yield level results in a decrease in rotational ductility demand. However, it also increases the magnitude of shear in the critical hinging region at the base of the wall. Since the presence of high shear stresses tends to reduce the deformation capacity of the hinging region in reinforced concrete members, particularly under reversed loading, a balance between decreasing the ductility demand and increasing the shear must be worked out in determining the optimum level to use.

MEASURES OF DEFORMATION DEMAND IN HINGING REGION

Rotational ductility ratio was calculated from the maximum moment at the base of the wall using the relationship*

$$\mu_{ro} = \frac{\theta_{max}}{\theta_y} = 1 + \frac{(M_{max} - M_y)}{r_y M_y} , \qquad (1)$$

Other measures of deformation requirement near the base of the wall were considered. A major reason for considering other measures of deformation was to obtain estimates of the relative magnitudes of these measures. This information was obtained to determine the suitability and adequacy of each measure as an index of deformation demand, particularly in relation to deformation capacity. The intent was to determine relationships between these various measures of deformation demand as indicated by dynamic analysis and compare them with similar data from laboratory tests. The objective was to identify a readily determinable parameter that could be used in design for correlating deformation demand with capacity.

Definitions for Measures of Deformation

In the analytical model used, hinging is assumed to occur at a point. In actual walls, however, inelastic deformation occurs over a finite length. Measures of deformation considered are based on nodal rotations calculated at a nodal point located at the top of the assumed hinging length as shown in Fig. 18. The calculated nodal rotation represents total rotation of the assumed hinging length.

*Equation (1) above is based on an assumed moment-rotation (M-θ) curve for the "point hinge" at the base of the analytical model of the wall. Since the point hinge in the model represents an idealization of the hinging region in a member, the assumed M-θ curve implies a particular, yet unspecified, hinging length. In terms of the model itself, the above expression for the rotational ductility, μ_{ro}, accounts only for the rotation at the point hinge. Most experimental data indicate that the hinging length is primarily a function of the depth of a member.

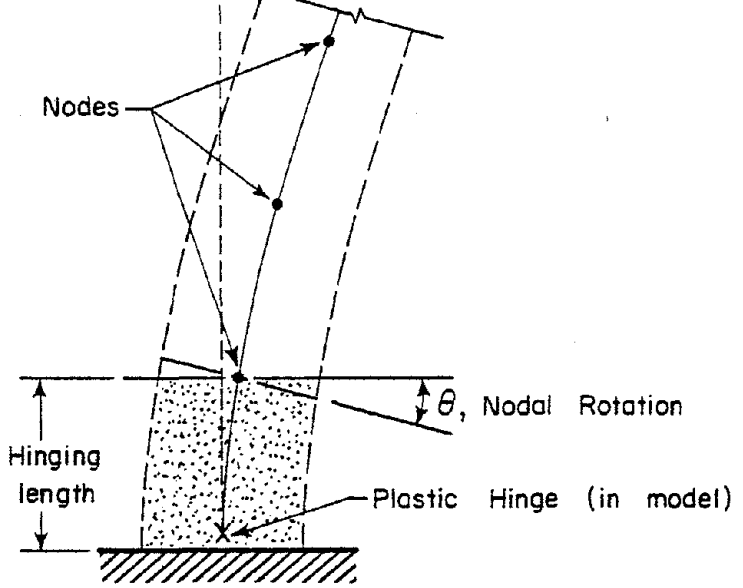

Fig. 18 Nodal Rotation as a Measure of Inelastic Deformation in Hinging Region

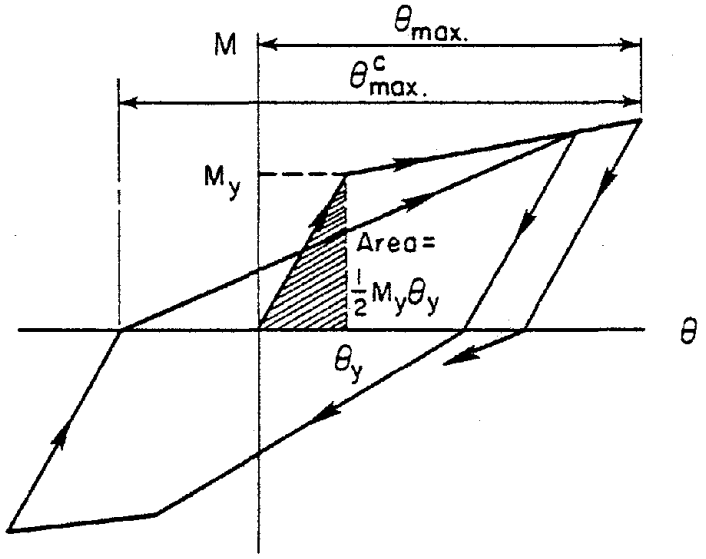

Rotational Ductility, $\mu_r = \dfrac{\theta_{max.}}{\theta_y}$

Cyclic Rotational Ductility, $\mu_{rc} = \dfrac{\theta^c_{max.}}{\theta_y}$

Cumulative Rotational Ductility, $\sum\mu_{rc} = \dfrac{\Sigma\theta^c_{max.}}{\theta_y}$

Cumulative Rotational Energy, $\sum A_r = \dfrac{\text{cumulative area under } M-\theta \text{ loops}}{\frac{1}{2}M_y\theta_y}$

Fig. 19 Measures of Inelastic Deformation in Hinging Region

Using moment-nodal rotation (M -θ) curves as shown in Fig. 19, the following measures of deformation requirement for the hinging region near the base of the wall were considered:

a. Rotational ductility ratio:

$$\mu_r = \frac{\theta_{max}}{\theta_y}$$

where θ_{max} is maximum nodal rotation and θ_y is rotation corresponding to moment M_y at first yield

b. Cyclic rotational ductility ratio:

$$\mu_r = \frac{\theta^c_{max}}{\theta_y}$$

where θ^c_{max} represents the maximum algebraic diference between maximum nodal rotation and point where M-θ curve intersects the zero-moment axis

c. Cumulative rotational ductility:

$$\Sigma\ \mu_{rc} = \frac{\Sigma\ \theta^c_{max}}{\theta_y}$$

where $\Sigma\ \theta^c_{max}$ represents the cumulative sum of the absolute values of the nodal rotations for the entire duration of the response

d. Cumulative rotational energy ratio:

$$\Sigma\ A_r = \frac{\Sigma\ A_{ri}}{A_y}$$

where $\Sigma\ A_{ri}$ represents the cumulative sum of the absolute values of the areas unde the M-θ hysteretic loops for the entire duration of the response and $A_y = M_y\theta_y/2$

Maximum deformation alone does not provide complete information on the deformation demand associated with dynamic response. Information on maximum deformation must be supplemented by data on the number of cycles of large-amplitude (comparable to the maximum) deformation. This is important since the behavior of structures loaded in the inelastic range

can be significantly affected by the number of large-amplitude cycles imposed.

Figures 20 and 21 show examples of the variation with time of cumulative nodal rotation and cumulative rotational energy, respectively. The structure considered in these figures has a fundamental period, T_1 = 1.4 sec. and yield level, M_y = 500,000 in.-kips (56,400 kN m). The base motion used was the E-W component of the 1940 El Centro record. The hysteretic M-θ loop for this case is shown in Fig. 7. These figures show the variation of the total cumulative quantities as well as the "primary" and "secondary" components, as defined in Fig. 22. In subsequent evaluation of data, the cumulative measures of deformation are nondimensionalized. Thus, the cumulative rotation is divided by the associated yield rotation and the cumulative rotational energy by one-half the product of the yield rotation and the yield moment.

Hinging Length at Base of Wall

To determine the effect of assumed hinging length on the different measures of deformation, analyses were performed for two assumed hinging lengths. Assumed hinging lengths for each analysis are listed in Table 4.

Figure 23 shows the variation of critical rotational ductility demand with fundamental period for the two values of assumed hinging length considered. The plot is for the case of 20-story walls with M_y = 750,000 in.-kips (84,740 kN m). Ductility demands μ_{r1} and μ_{r2} correspond to hinging lengths listed for Case Nos. 1 and 2 respectively in Table 4. Also shown is the rotational ductility μ_{ro} calculated from the moment at the base of the wall using Eq. (1). In relation to the curves based on nodal rotations at the first and second floor levels, the curve for μ_{ro} considers only the rotation at the hinge nearest the base. A slight decrease in calculated ductility demand with increase in assumed hinging length is

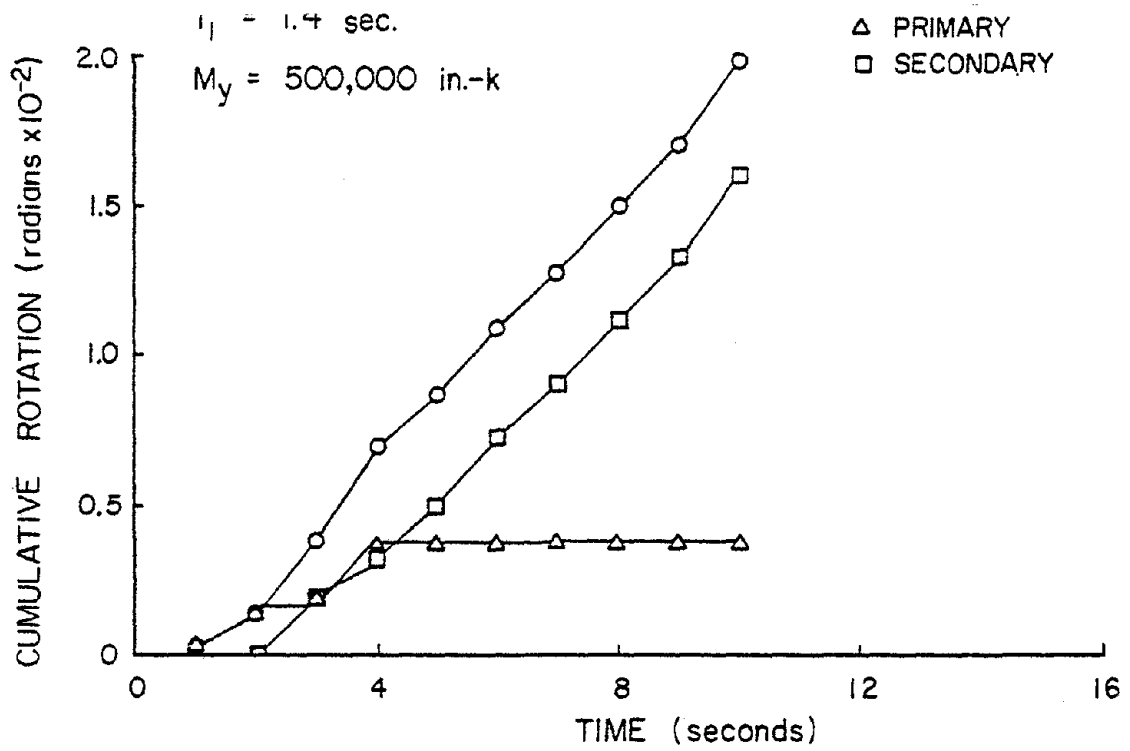

Fig. 20 Cumulative Nodal Rotations versus Time for Node at First Story Level

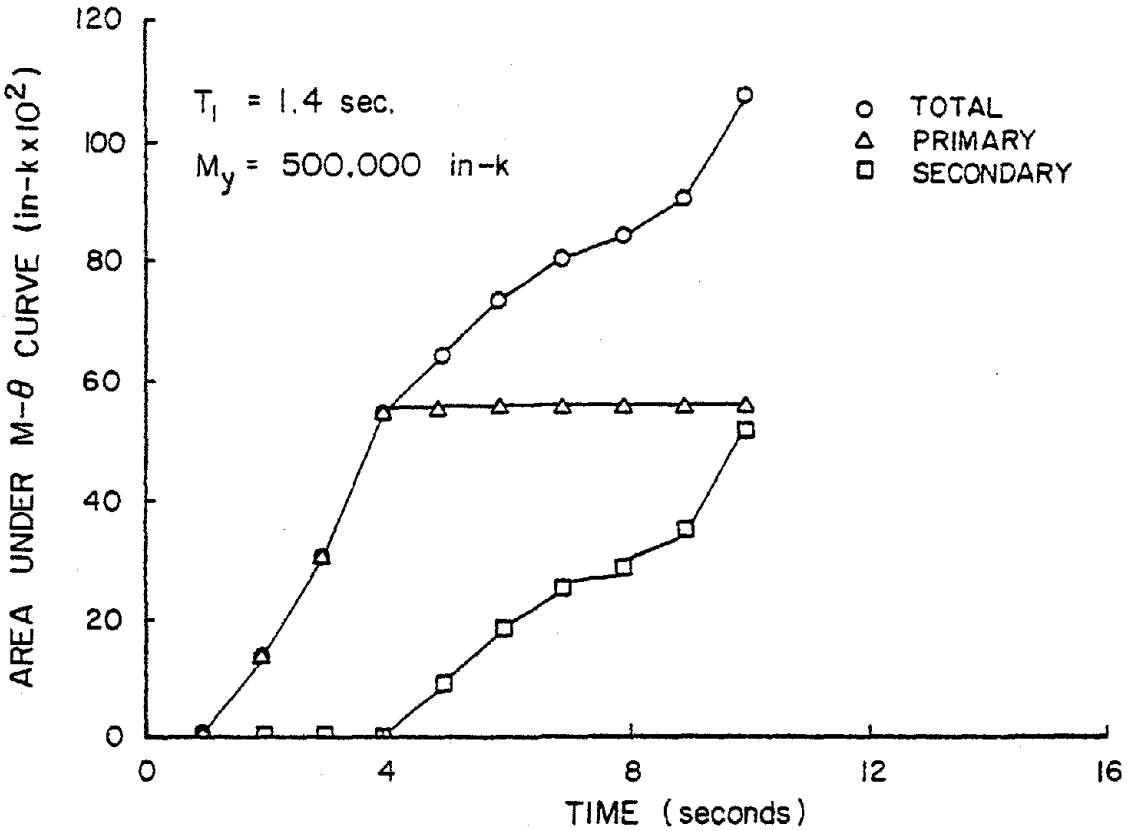

Fig. 21 Cumulative Rotational Energy versus Time for Node at First Floor Level

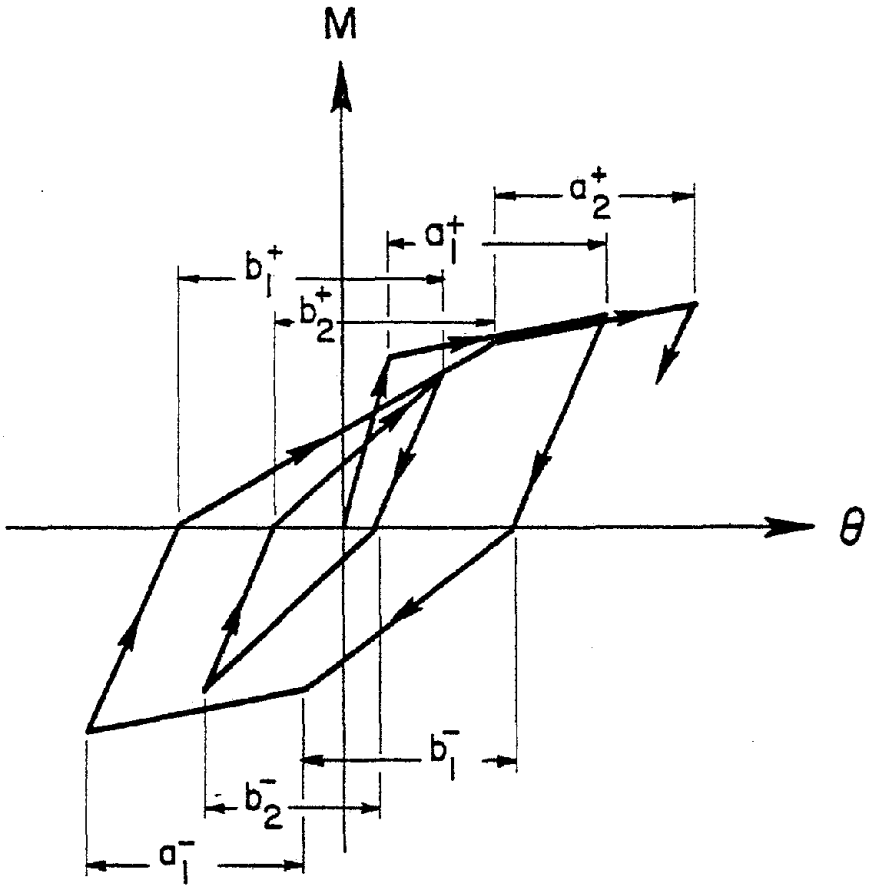

Accum. Primary Rotations = $\Sigma a^+, \Sigma a^-$
Accum. Secondary Rotations = $\Sigma b^+, \Sigma b^-$

Fig. 22 Components of Cumulative Plastic Rotations for Stiffness-Degrading Model

Table 4 - ASSUMED HINGING LENGTHS

No. of Stories	CASE 1		CASE 2	
	Hinging Length (ft)	No. of Stories in hinging length	Hinging Length (ft)	No. of Stories in hinging length
10	6.00	1/2	12.00	1
20	12.00	1	20.75	2
30	12.00	1	20.75	2
40	20.75	2	38.25	4

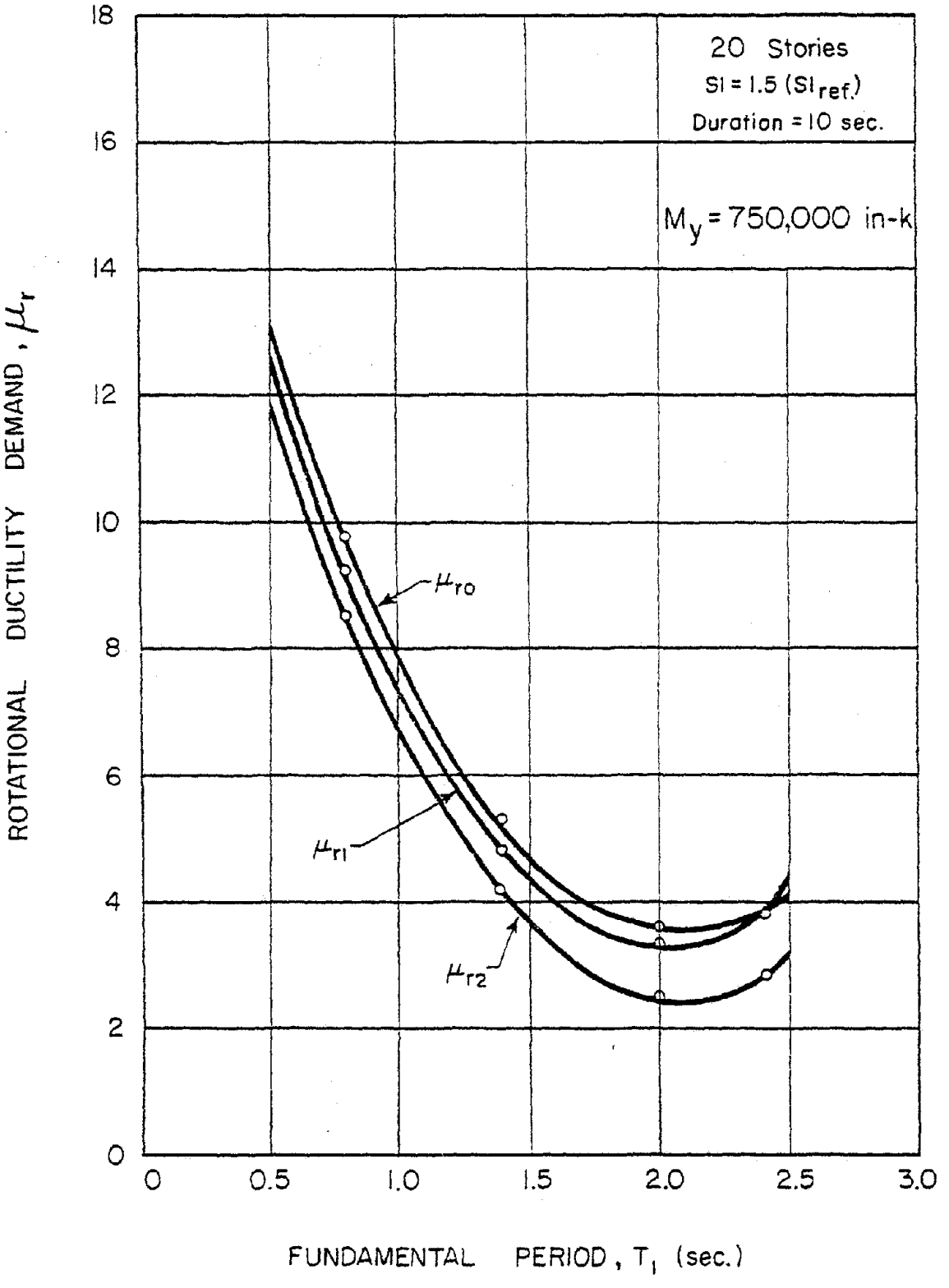

Fig. 23 Rotational Ductility Demand Based on Different Assumed Hinging Lengths

apparent in Fig. 23. This indicates that deformation requirements based on nodal rotations at lower floor levels provide slightly more conservative estimates of demand than those based on nodal rotations at higher floor levels.

Figure 24 shows the variation of critical rotational ductility demand with assumed hinging length for 20-story walls. The results shown represent a wide range of values of fundamental period (T_1 = 0.8 to 2.4 sec.) and yield level (M_y = 750,000 to 1,500,000 in.-kips). The ordinate in Fig. 24 represents the factor equal to f_μ the ratio of ductility demand for an assumed hinging length to ductility demand calculated for hinging length corresponding to the first two stories.

Observations of tests on walls[9] indicate that in most cases, inelastic deformation is concentrated within a length approximately equal to the width of the wall. On this basis, it is reasonable to assume a hinging length equal to the width of the wall. Thus, if the 10-story wall considered here is about 12-ft wide, the nodal rotation at the first floor level, 12 ft above the base, should provide a reasonable estimate of the deformation demand in the hinging region at the base of the wall. If the 10-story wall is significantly wider than 12 ft, the deformation demand based on nodal rotations at the 12-ft height (1st floor level) will give a conservative estimate of demand. Likewise, a reasonable estimate of rotational deformation demand in the 30-story walls considered here is provided by the nodal rotation at the 3rd floor level if the wall is about 30-ft wide. Similar remarks apply to 20- and 40-story walls if these are about 20-ft and 40-ft wide, respectively.

Critical values of the four measures of deformation demand for 10-, 20-, 30-, and 40-story walls are shown as plots (e), (f), (g), and (h) in Figs. 13, 15, 16, and 17. All values are based on nodal rotations at the second level discussed above for each wall height.

In the remainder of this report it is assumed that the wall widths are at least equal to the height from the base to the

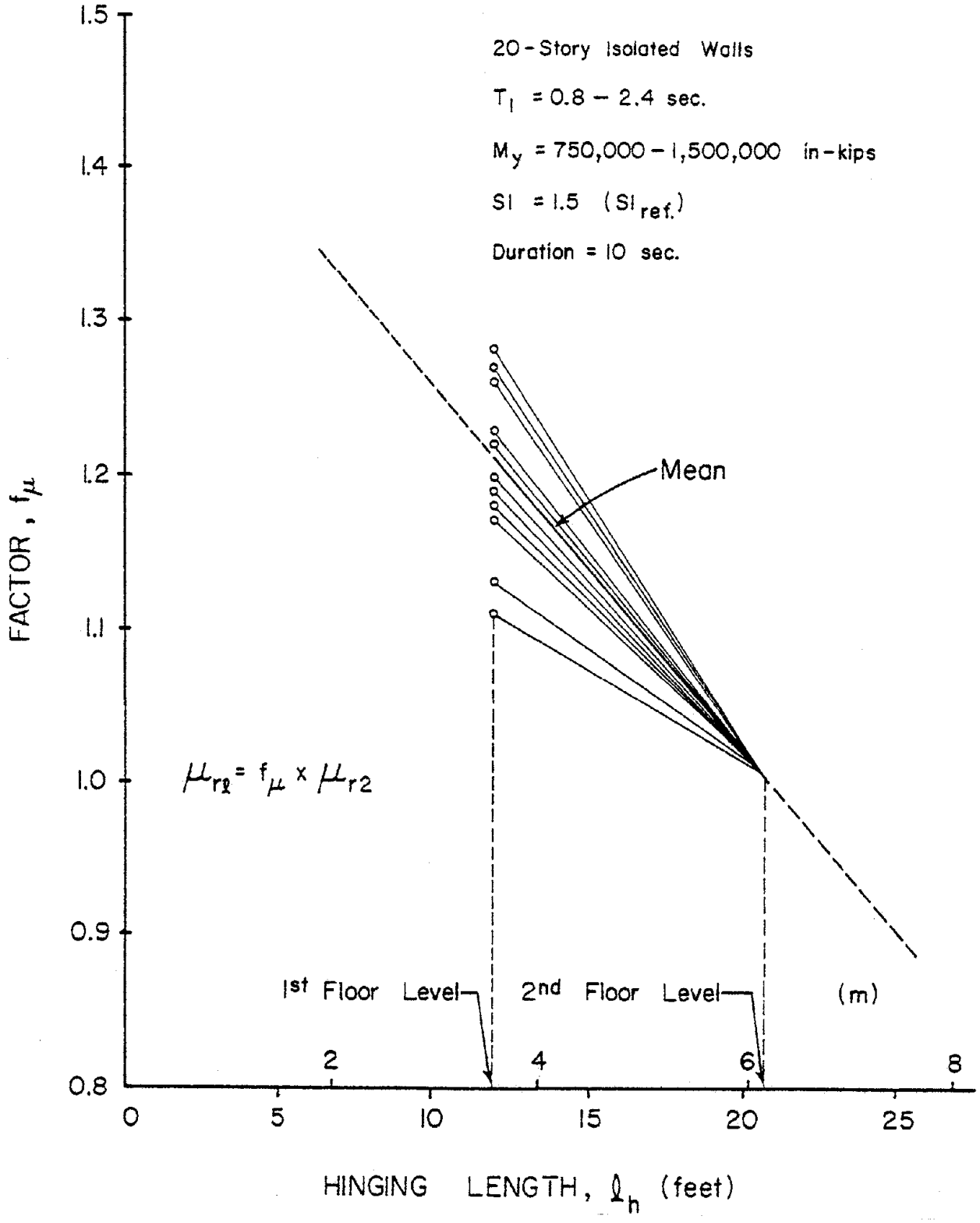

Fig. 24 Variation of Ductility Demand with Assumed Hinging Length

node at the second level* noted above for each wall height examined. Thus, only deformation requirements associated with nodal rotations at the second level, μ_{r2}, are considered.

For cumulative measures of deformation, which depend on duration of input motion, the values for 10-second input motions were adjusted, as described in the next section, to reflect a 20-second duration of strong ground motion.

Adjustment of 10-Second Cumulative Measures of Deformation to Reflect 20-Second Duration of Input Motion

In the parametric studies reported in Ref. 7, it was noted that the major effect of duration of strong ground motion is on cumulative deformation. This assumes not only that the short- and long-duration earthquakes have the same intensity, measured in terms of spectrum intensity, but also that the average amplitude of the input acceleration pulses is about the same for both cases.

The increase in cumulative deformation with longer duration of the input motion essentially reflects the greater number of cycles of oscillation that a structure undergoes under the longer-lasting excitation. It was further noted that for the same intensity and frequency characteristics of the input motion, maximum response values are not significantly changed by increasing the duration of the input motion.

*For the development of design charts, discussed in the subsequent sections, the measures of deformation demand for 30-story walls were based on the nodal rotation at the 3rd floor level. This is consistent with using the rotations at the 1st, 2nd and 4th floor levels for estimating the rotational ductility requirements for 10-, 20-, and 40-story walls, respectively. This approach is based on the assumption that the length of the hinging region is approximately equal to the width of the wall and further that the width of the wall is proportional to the height of the structure.

It was pointed out in the study of input motions reported in Ref. 6 that most recorded motions[15] have their strong phases lasting from 10 to 15 seconds. It was concluded, on the basis of several studies mentioned in Ref. 6, that a duration of 20 seconds for the strong motion excitation should provide an adequate basis for determining design requirements.

Twenty-Second Input Motions

To obtain a basis for adjusting the cumulative measures of deformation corresponding to 10 seconds, listed in Tables A1 through A14, a number of analyses were made using 20-second input motions. These 20-second motions were synthesized from the first 13 seconds of the same records from which the 10-second motions shown in Fig. 9 were obtained. The four 20-second accelerograms used are shown in Fig. 25. The corresponding 5%-damped velocity response spectra are shown in Fig. 26. The first 10 seconds of the accelerograms shown in Fig. 25 are identical to the respective records in Fig. 9. The portions of the records used to make up the second 10 seconds of the composite accelerograms are indicated in Table 5. The same intensity normalization factors used for the 10-second accelerograms in Fig. 9 were used for the corresponding 20-second motions of Fig. 25.

A total of 12 analyses, all for 20-story walls, were made. Fundamental period values considered ranged from 0.8 sec. to 2.4 sec. Yield level values ranged from 500,000 in.kips (56,400 kN m) to 1,500,000 in.kips (169,460 kN m). The input accelerogram used in each case was intended to produce near-maximum displacement response.

Results of 20-Second Analyses

Results of 20-second analyses are listed in Table A14, Appendix A. The last column in Table A14 indicates the ratios of response quantities for 20-second base motions to the corresponding quantities for 10-second base motions. The ratio

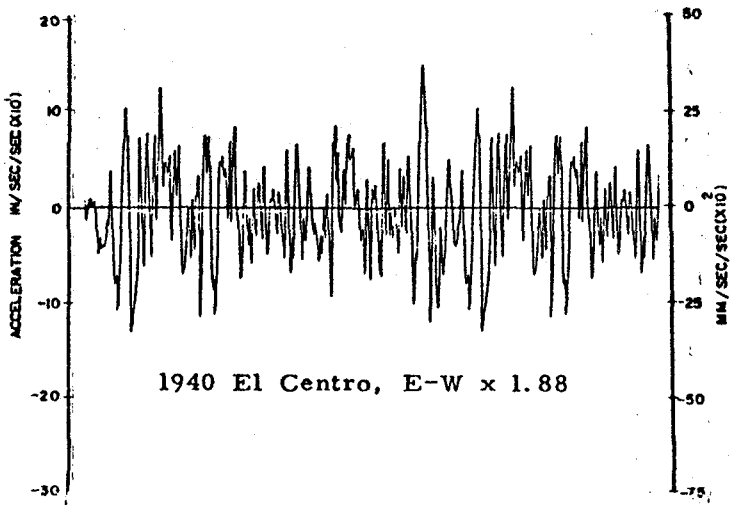

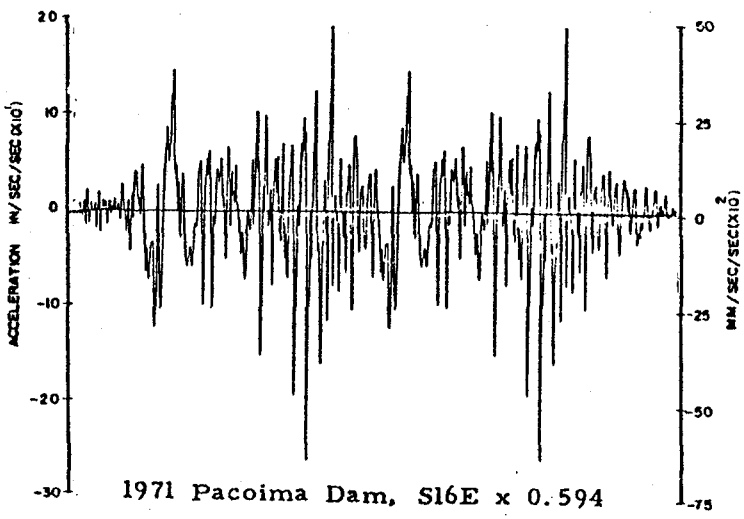

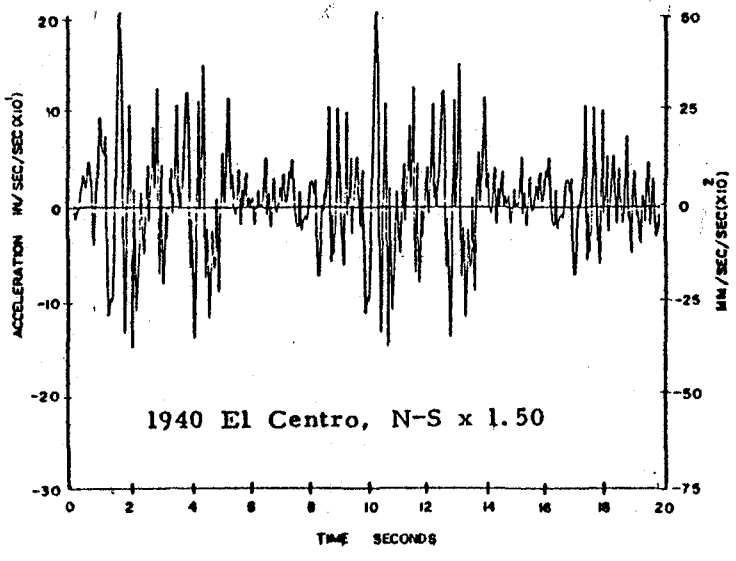

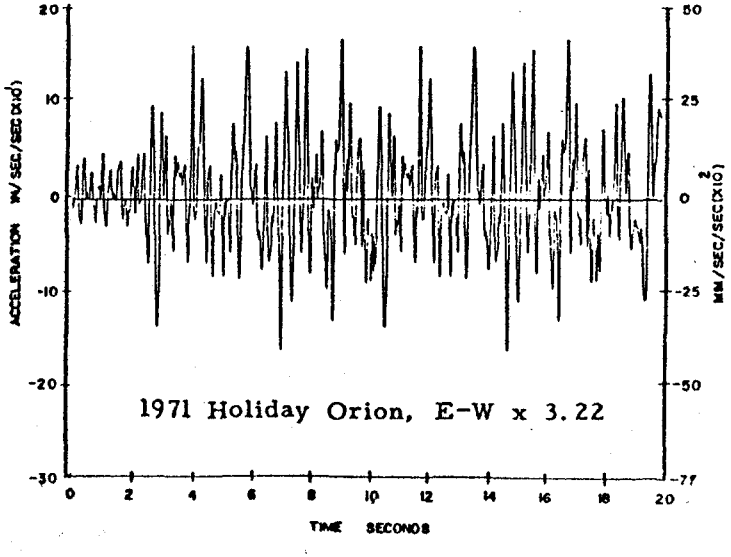

Fig. 25 Normalized 20-Second Duration Composite Accelerograms

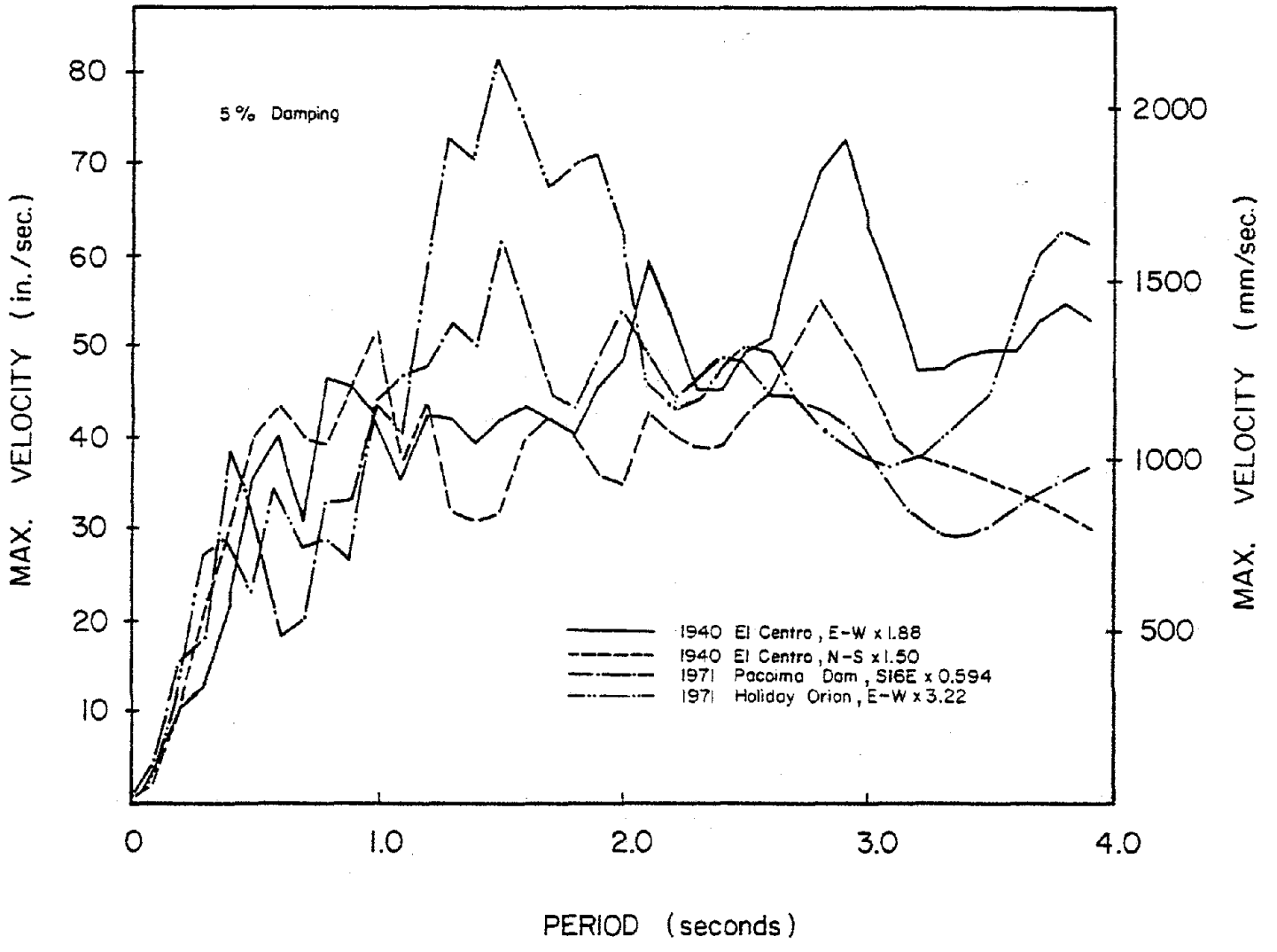

Fig. 26 Relative Velocity Response Spectra for Normalized 20-Second Composite Accelerograms

Table 5 - Composition and Intensity of 20-Second Composite Accelerograms

Basic Accelerogram	Composition		Spectrum Intensity, (in.)@		$\left(\frac{SI_{ref.}}{SI_{10}}\right)$+ x 1.50	$\left(\frac{SI_{ref.}}{SI_{20}}\right)$ x 1.50
	1st Part	2nd Part	First 10 Sec. SI_{10}	20-Second SI_{20}		
1940 El Centro, E-W	First 12.48 sec. as recorded*	From 0.98 to 8.5 sec. of record*	55.97	68.16	1.88	1.54
1940 El Centro, W-S	First 10.08 sec. as recorded*	From 2.90 sec. to 12.82 sec. of record*	70.15#	77.44	1.5	1.36
1971 Holiday Orion, E-W	First 10.08 sec. as recorded*	From 1.70 sec. to 11.62 sec. of record*	32.67	42.86	3.22	2.46
1971 Pacoima Dam, S16E	First 10.08 sec. as recorded*	From 2.42 sec. to 12.34 sec. of record*	177.25	206.07	0.594	0.511

*See Reference No. 15.

@Based on 5%-damped velocity spectrum, for period range 01 to 3.0 seconds.

#Reference spectrum intensity, $SI_{ref.}$

+Intensity normalization factors used in analyses corresponding to results listed in Tables 5 and A14.

varies from 1.0 to 1.4 for maximum response values and from 1.6 to 2.3 for cumulative measures of deformation. A summary of the data presented in Table A14, showing average ratios for each value of yield level (with fundamental period values ranging from 0.8 to 2.4 sec.) is given in Table 6. Table 6 indicates the average ratio for maximum responses ranging from about 1.0 to 1.2, and from about 1.8 to 2.2 for the cumulative measures of deformation.

An examination of Table A14 shows that the highest value of the ratio R_{20}/R_{10}, i.e., the ratio of the 20-second maximum to the corresponding 10-second maximum, of 1.4 is associated with the E-W component of the 1940 El Centro motion. A major reason for the significant increase in the calculated maximum response for this particular 20-second composite accelerogram is the fact that it represents a more intense motion than the corresponding 10-second accelerogram. Because the peak acceleration occurs after 10 seconds (at about 11.5 sec.), the 20-second composite accelerogram has a spectrum intensity (68.16 in.) that is 1.22 times greater than that of the 10-second motion (55.97 in.).

As mentioned, the same intensity normalization factor of 1.88 was used on the 20-second motion as on the 10-second motion. This makes the 20-second motion 1.22 times more intense than the corresponding 10-second motion. If the same value of the spectrum intensity were to be used for both 10- and 20-second accelerograms, a slightly lower intensity normalization factor (1.54 instead of 1.88) would have to be applied to the 20-second composite motion. This would result in correspondingly lower maximum response values and hence a lower R_{20}/R_{10} ratio for this particular input motion.

Table 6 indicates that similar reductions in maximum response can also be expected for the other input motions if the same spectrum intensity were used for both 10-second and 20-second accelerograms. For the 20-sec. motions to have the same spectrum intensity as the 10-sec. motions, the intensity

Table 6 - Average Ratios* of Maximum and Cumulative Response Quantities Corresponding to 20-Second and 10-Second Duration Input Motions
20-Story Isolated Structural Walls

Response Parameter	Average Ratio, R_{20}/R_{10}		
	Yield Level, M_y (in-kips)		
	500,000	1,000,000	1,500,000
Top Displacement	1.23	1.15	1.12
Interstory Displacement	1.25	1.16	1.10
Horizontal Shear at Base	1.06	1.07	1.04
Bending Moment at Base	1.06	1.03	1.02
Rotational Ductility Ratio, μ_{r0} (Based on Equation 1)	1.23	1.16	1.11
Deformation Measures Based on Nodal Rotations at 1st Floor Level			
Rotational Ductility, μ_{r1}	1.23	1.16	1.14
Cyclic Rotational Ductility, μ_{rc1}	1.17	1.15	1.03
Cum. Cyclic Rotational Ductility, $\Sigma\mu_{rc1}$	2.33	2.14	1.99
Cum. Rotational Energy, ΣA_{r1}	2.18	1.97	1.78
Deformation Measures Based on Nodal Rotations at 2nd Floor Level			
Rotational Ductility, μ_{r2}	1.18	1.17	1.20
Cyclic Rotational Ductility, μ_{rc2}	1.16	1.13	1.08
Cum. Cyclic rotational Ductility, $\Sigma\mu_{rc2}$	2.32	2.11	2.00
Cum. Rotational Energy, ΣA_{r2}	2.18	1.95	1.82

* Using four different accelerograms as input with SI = 1.5 (SI_{ref}). Fundamental period range: 0.8 to 2.4 sec. See Table A 14, Appendix A, for details.

normalization factor, i.e., the factor by which the as-recorded acceleration amplitudes are to be multiplied, should be equal to 1.5 $(SI_{ref.})/(SI_{20})$. This quantity is listed in the last column of Table 5.

In the case of the 1971 Holiday Orion, E-W motion, the ratio of the spectrum intensity for the 20-second composite motion to that of the 10-second motion is even slightly greater (1.31) than the corresponding value for the 1940 El Centro, E-W motion. However, Table A14 shows that the maximum increase in the 20-second response occurs only for structures with initial fundamental period of 1.4 sec.

Figure 26 shows that this particular accelerogram has a velocity spectrum that peaks near this period value. If allowance is made for reductions in maximum response values for the 20-second input motions to account for their greater effective intensity, as discussed above, a value of R_{20}/R_{10} closer to unity is obtained for the maximum response quantities.

In view of the above, it was decided to adopt, without change, the critical response values for displacements, moments, shears and ductility ratios obtained for the 10-second input motions as representative of 20-second response values. The cumulative measures of deformation, however, were adjusted to reflect the considerable increase due to the longer-duration input motions.

Figure 27 shows the variation of the ratio R_{20}/R_{10} with the yield moment, M_y, for the cumulative cyclic rotational ductility, $\Sigma\mu_{rc2}$, and the cumulative rotational energy, ΣA_{r2}, in 20-story structural walls. These deformation measures are based on the nodal rotation at the second floor level.

Although Fig. 27 appears to indicate a decrease in R_{20}/R_{10} for values of M_y greater than 1,000,000 in.-kips, there is a lack of consistency in the trends exhibited by the relatively few data points for the different fundamental period values. It was therefore decided to use a single correction factor for each parameter for all combinations of M_y and T_1. This correction factor was applied to the appropriate measure of

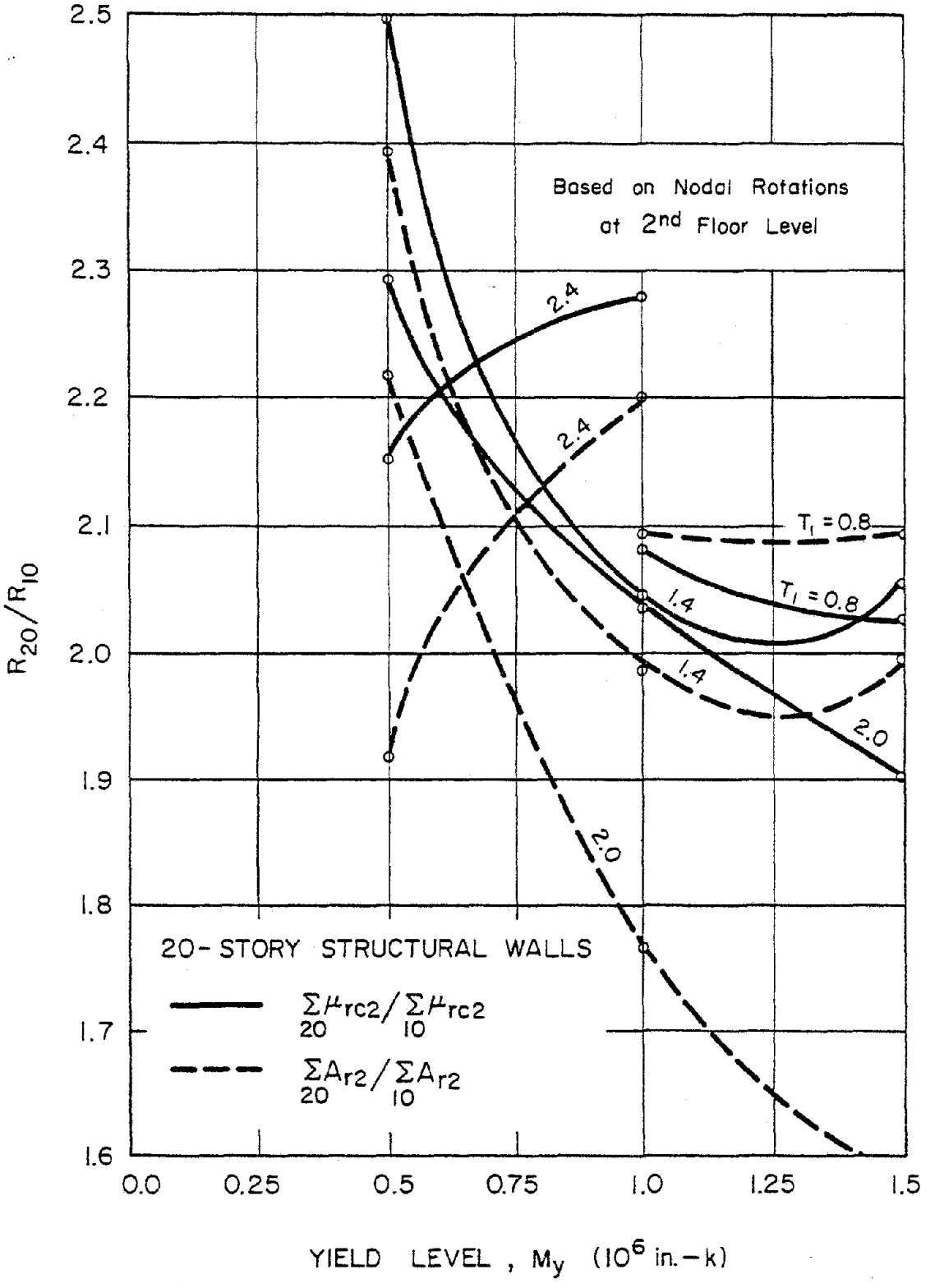

Fig. 27 Ratios of Cumulative Cyclic Rotational Ductility $\Sigma\mu_{rc}$, and Non-dimensionalized Cumulative Energy, ΣA_r, Corresponding to 20-Second and 10-Second Input Motions

cumulative deformation for 10-second input motions to obtain values corresponding to 20-second duration input motions.

On the basis of the tabulated values shown in Tables 5 and A14, and allowing for the greater effective intensities of the 20-second accelerograms used in obtaining these values, a factor of 2.0 was used for cumulative rotational ductility, $\Sigma\mu_{rc2}$, and 1.9 for cumulative rotational energy, ΣA_{r2}. It is pointed out that for the input motion intensity used (1.5 $SI_{ref.}$), the yield level value of 500,000 in.-kips appears to be too low for most cases and can, therefore, be considered impractical. The factors 2.0 and 1.9 are to be applied to the critical cumulative rotational ductility and the critical cumulative rotational energy for 10-second input motions to obtain estimates of the corresponding values for 20-second motions.

To assess the adequacy of each of the various measures of ductility as a representative index of deformation demand, a comparison with corresponding measures of capacity obtained from tests was undertaken.

The evaluation involves ratios of each of the various measures of deformation to a specific "reference measure." Rotational ductility is used as the reference measure. The check on adequacy then refers to rotational ductility. Ratios of deformation demands from the analytical investigation are compared with corresponding ratios of deformation capacity from tests. The experimental data considered are results from the concurrent experimental investigation[9,10].

Relative Magnitudes of Measures of Deformation Demand

Figures 28, 29, and 30 show relative magnitudes of the different measures of deformation demand representing critical dynamic response. These figures correspond to 20-story structural walls subjected to input motions with intensity SI = 1.5 ($SI_{ref.}$). Data for these figures are based on the critical response plots shown in Figs. 13e, f, g, and h.

Cumulative measures have been adjusted to reflect a 20-second duration of the input motion. In these figures, the ratio of each measure of deformation to μ_{r2} is plotted against fundamental period for different values of μ_{r2}. Solid lines in Figs. 28 to 30 represent the mean of the plotted points. Dashed lines represent upper bounds for the corresponding data. The distribution of the plotted points does not appear to indicate a dependence of the different ratios on the value of the reference measure μ_{r2}.

Figure 28 shows the average ratio of the critical cyclic rotational ductility to the critical rotational ductility, μ_{rc2}/μ_{r2}, to be 1.2. The ratio of the cumulative rotational

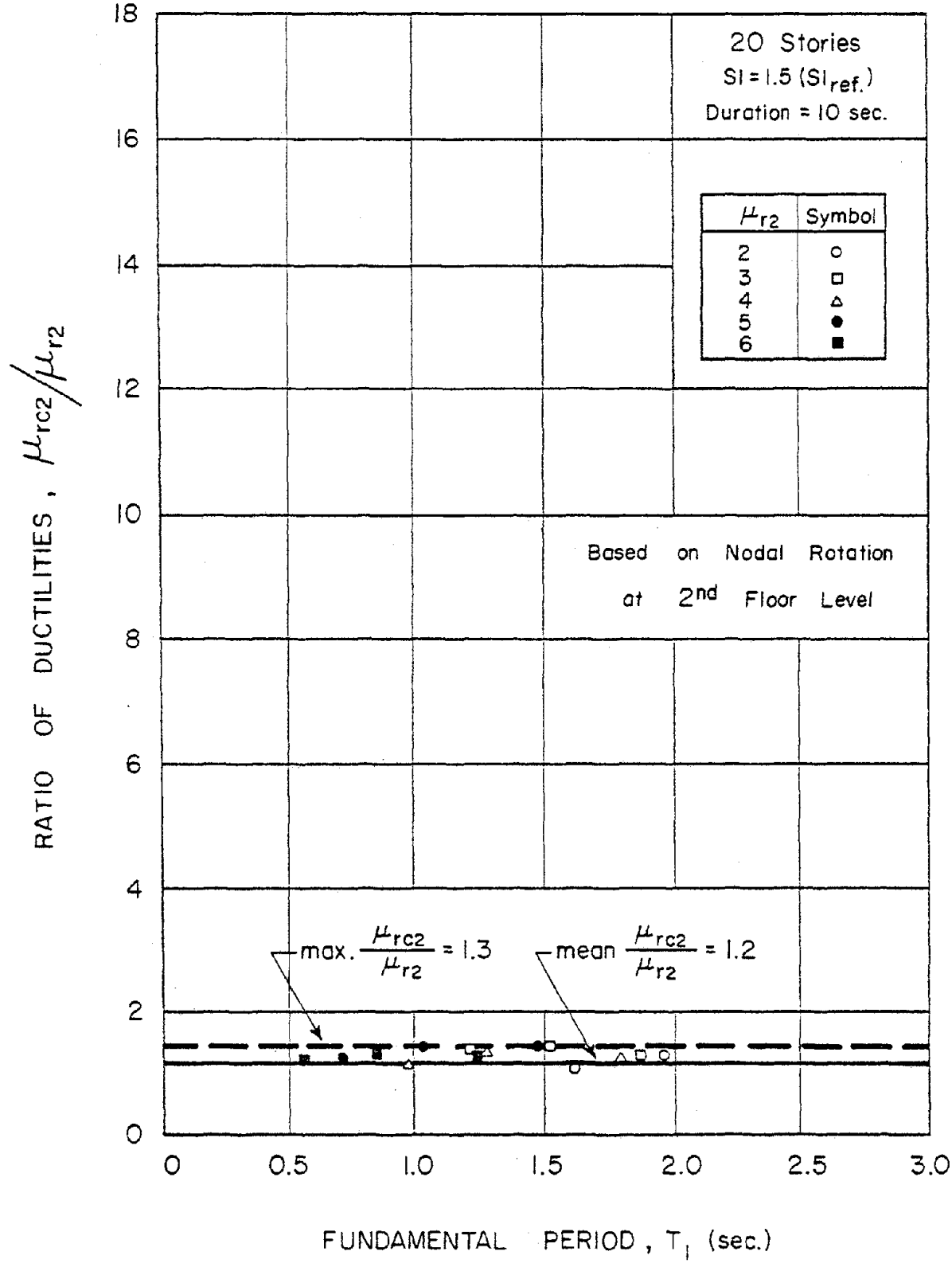

Fig. 28 Ratio of Cyclic Rotational Ductility, μ_{rc2}, to Rotational Ductility, μ_{r2}, for Different Values of T_1 and μ_{r2}

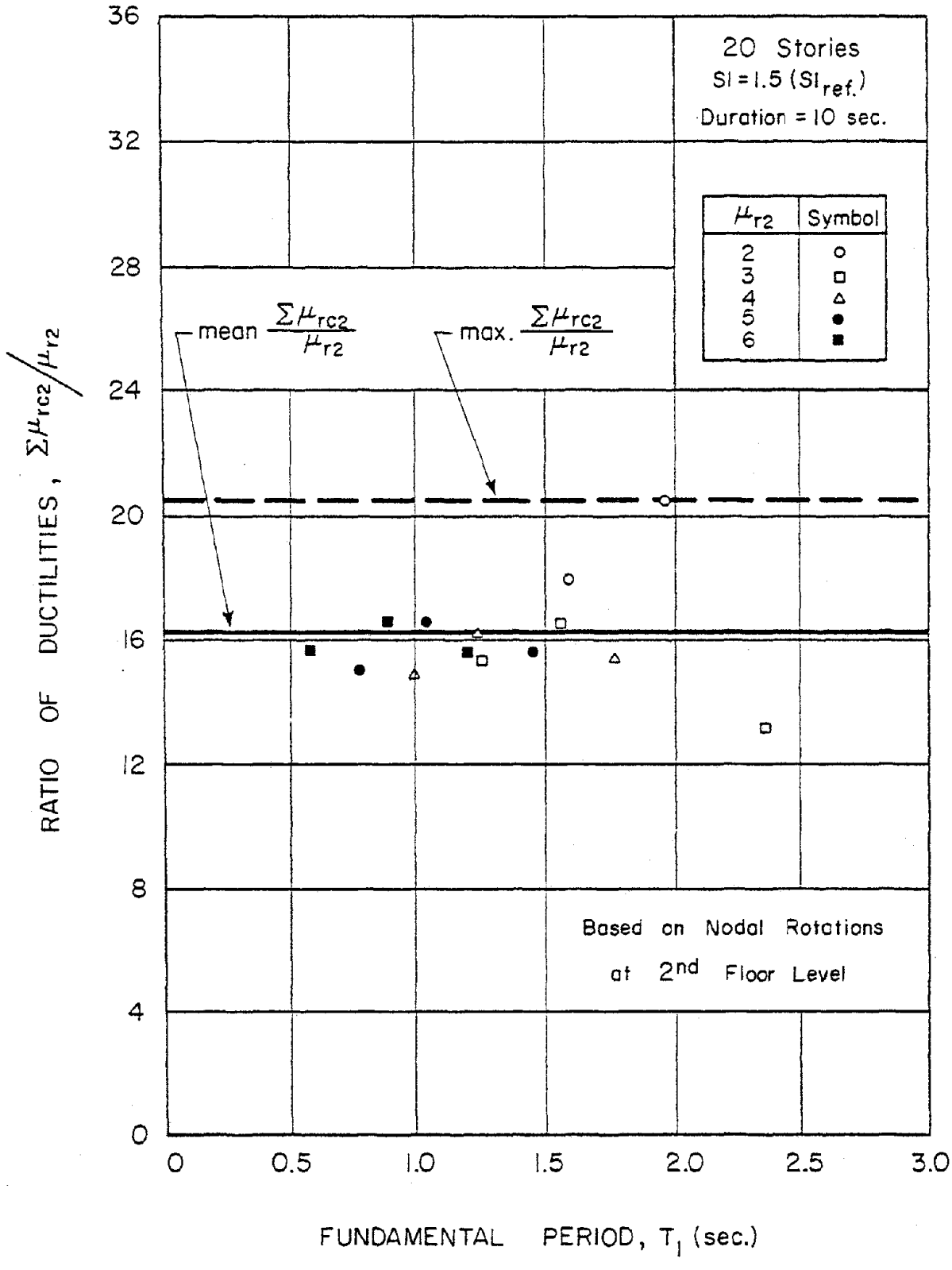

Fig. 29 Ratio of Cumulative Rotational Ductility, μ_{rc2}, to Rotational Ductility, μ_{r2}, for Different Values of T_1 and μ_{r2}

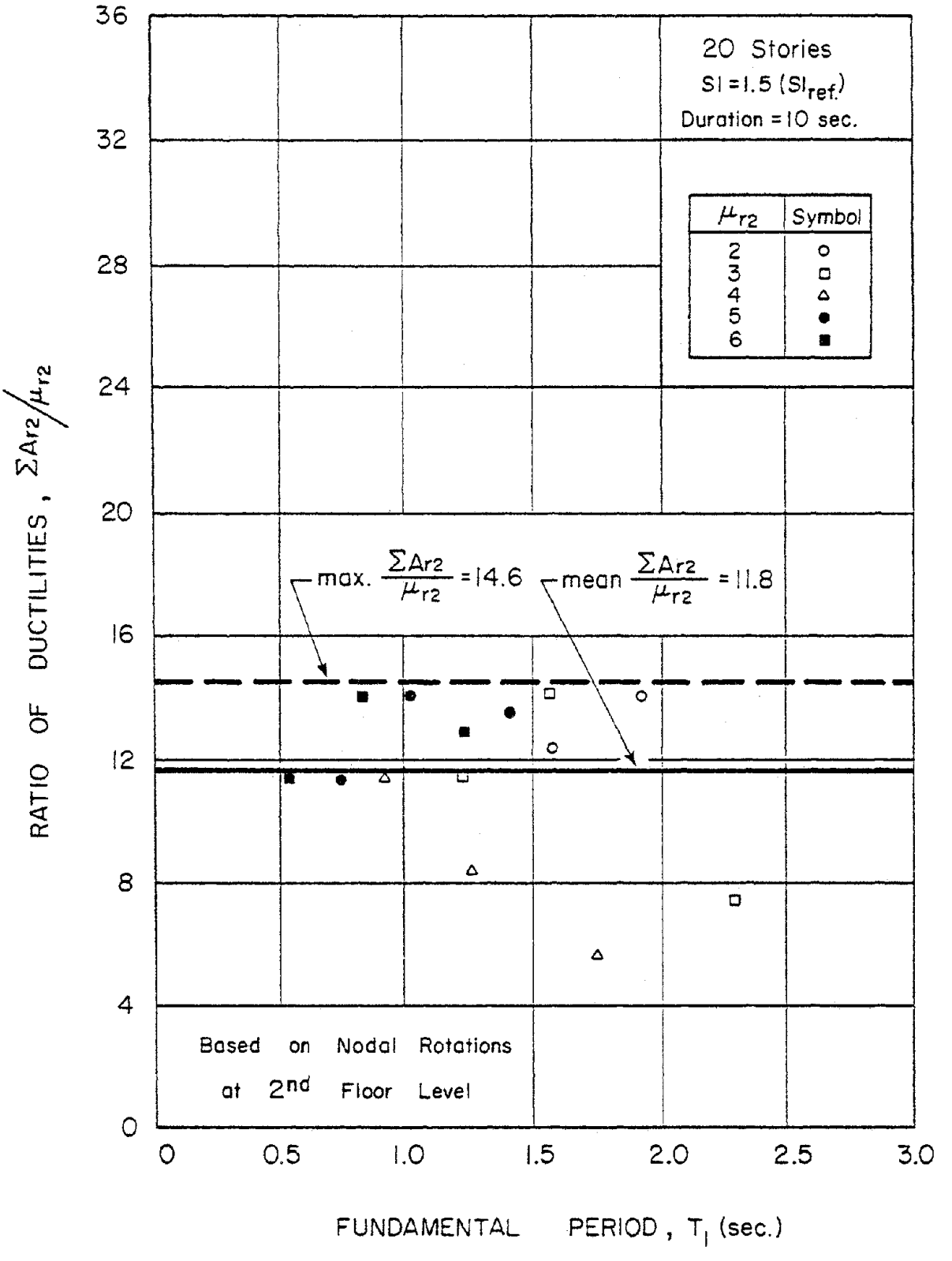

Fig. 30 Ratio of Cumulative Rotational Energy, ΣA_{r2}, to Rotational Ductility, μ_{r2}, for Different Values of T_1 and μ_{r2}

ductility to rotational ductility, μ_{rc2}/μ_{r2}, varies from about 12.5 to 20.5, with a mean value of 16.2. The ratio of cumulative rotational energy to rotational ductility, A_{r2}/μ_{r2} varies from about 5.0 to 14.6, with a mean value of 11.8.

A plot showing the mean of all three ratios discussed above is shown in Fig. 31. The mean values are plotted as solid lines. The dotted curves in Fig. 31 represent the upper bound envelopes of the corresponding data points in Figs. 28 through 30.

Experimental Investigation

The experimental investigation[9,10] is aimed at developing procedures for design of structural walls to provide the strength and deformation capacity indicated by dynamic response studies.

During the first phase of the experimental investigation, isolated structural walls with three different cross sectional configurations were constructed and tested. Summaries of observed results on strength and deformation have been reproduced from Refs. 9 and 10 as Tables 7 and 8, respectively. Out of the 16 tests reported, one was conducted under monotonic loading and 2 were retests of repaired specimens that had been tested earlier. Results of the 13 tests form the basis for the comparison discussed in this section.

For most of the tests, loading was applied in three increments until yielding occurred. At each load increment, three complete cycles of loading were applied. Subsequent to yielding, loading was controlled by deflections in 1-in. increments. The largest absolute value of deformation in which at least 80% of the maximum observed load was sustained was considered the "ultimate deformation" stage[9,10]. A typical loading program of this type is shown in Fig. 32a.

To determine the effect of loading history on the behavior of specimens subjected to reversed cyclic loading, three specimens, two virgin and one repaired, were tested using a loading

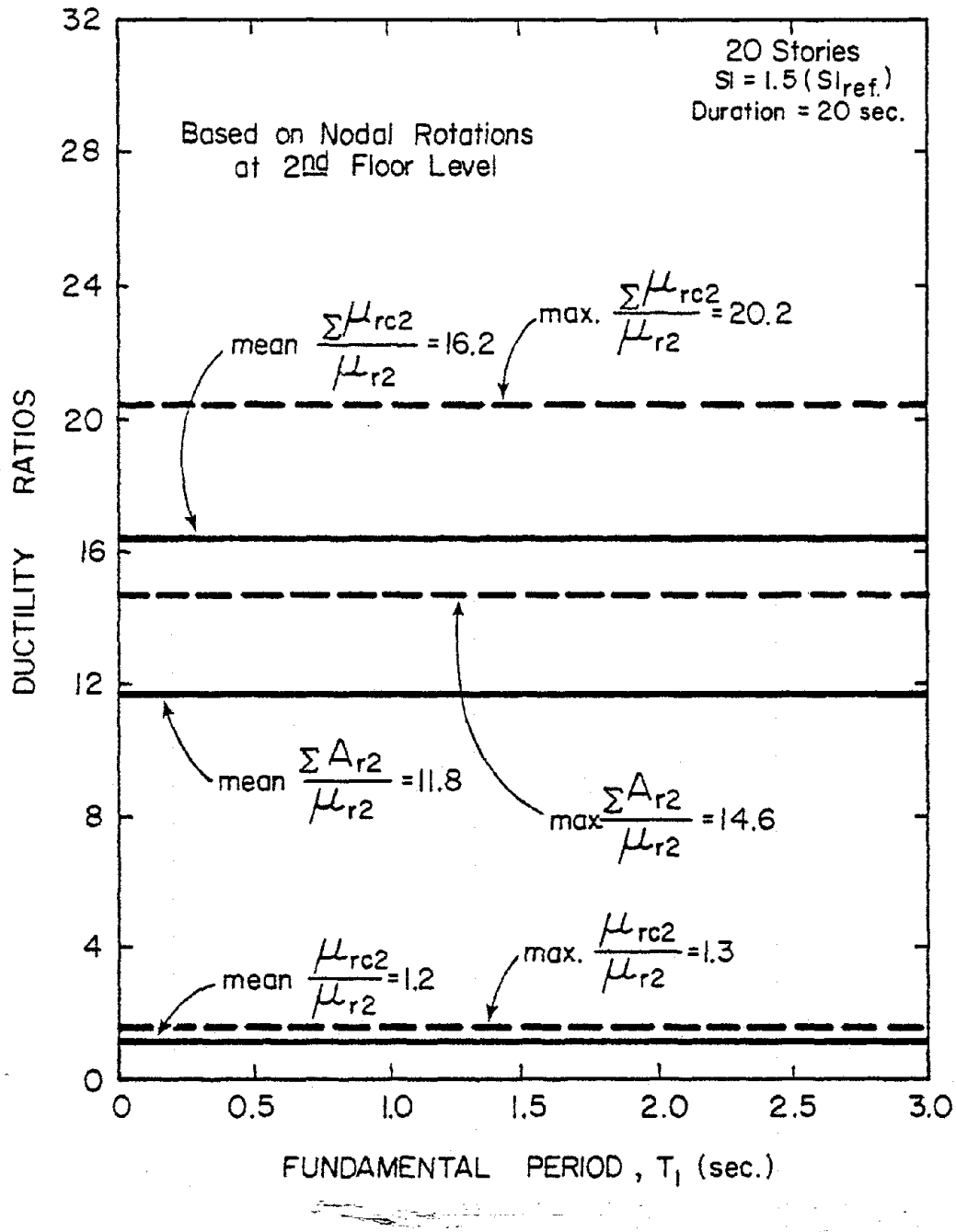

Fig. 31 Summary of Ductility Ratios Based on Rotational Ductility, μ_{r2}

Table 7 - Strength Results for Isolated Wall Specimens from Experimental Investigation

Specimen	Confined Boundary Element	Axial Load psi	ACI Design				Full Yield Load					Maximum Load						Failure Mode (5)
			Flexure		Shear		Calculated (3)		Observed		Obs.	Calculated (3)		Observed		Obs.	Obs.	
			kips	$\sqrt{f'_c}$ (1)	kips	$\sqrt{f'_c}$	kips	$\sqrt{f'_c}$	kips	$\sqrt{f'_c}$	Calc.	kips	$\sqrt{f'_c}$	kips	$\sqrt{f'_c}$	Calc.	ACI (4)	
R1	No	—	18	0.9	82 (2)	4.2	17.7	0.9	21.8	1.1	1.23	29.1	1.5	26.6	1.4	0.92	1.48	F
R2	Yes	—	35	1.8	82 (2)	4.2	33.2	1.7	41.8	2.1	1.26	57.3	2.9	48.7	2.5	0.85	1.39	F
B1	No	—	46	2.2	82 (2)	3.9	42.9	2.0	51.0	2.4	1.19	72.1	3.4	61.0	2.9	0.85	1.33	F
B3	Yes	—	46	2.3	82 (2)	4.1	41.9	2.1	51.5	2.6	1.23	73.4	3.7	62.0	3.1	0.84	1.35	F
B4	Yes	—	46	2.4	82 (2)	4.2	43.1	2.2	54.6	2.8	1.27	74.3	3.8	75.3	3.9	1.01	1.64	F
B2	No	—	129	6.1	127	6.0	115.6	5.5	128.0	6.0	1.11	170.9	8.1	152.8	7.2	0.89	1.18	WC
B5	Yes	—	129	6.6	127	6.5	123.1	6.3	138.0	7.1	1.12	213.7	11.0	171.3	8.8	0.80	1.33	WC
B5R	Yes	—	129	6.8	127	6.7	123.1	6.5	--	--	--	213.7	11.5	167.8	8.9	0.79	1.30	WC
B6	Yes	423	157	11.6	132	9.7	154.5	11.4	173.9	12.9	1.13	190.5	14.1	185.5	13.8	0.97	1.41	WC
B7	Yes	545	173	8.5	148	7.3	174.0	8.6	187.5	9.2	1.08	256.2	12.6	220.4	10.9	0.86	1.49	WC
B8	Yes	545	173	9.3	186 (6)	9.9	171.6	9.2	189.0	10.1	1.10	241.4	12.9	219.8	11.7	0.91	1.27	WC
B9	Yes	545	173	9.0	148	7.7	165.6	8.6	186.4	9.7	1.13	241.6	12.6	219.6	11.4	0.91	1.48	WC
B9R	Yes	451	173	5.6	162	5.2	165.6	5.3	--	--	--	241.6	7.7	218.7	7.0	0.91	1.35	WC
B10	Yes	545	121	6.2	148	7.6	116.1	5.9	139.7	7.2	1.20	168.0	8.7	159.0	8.2	0.95	1.32	BC
F1	No	—	145	8.1	140	7.8	148.1	8.3	150.6	8.4	1.02	242.6	13.5	187.9	10.5	0.77	1.30	WC
F2	Yes	482	170	8.7	148	7.6	164.4	8.4	180.3	9.2	1.10	240.8	12.3	199.5	10.2	0.82	1.34	WC

(1) Lateral load in terms of nominal shear stress $v = \dfrac{V}{0.8\,\ell_w\, b\sqrt{f'_c}}$ (psi)

(2) Shear reinforcement governed by maximum bar spacing

(3) Calculated monotonic flexural strength from analysis based on strain compatibility using measured material properties including strain hardening of reinforcement

(4) ACI taken as the lower of flexure or shear design strength

(5) F = Flexural Bar Fracture, WC = Web Crushing, BC = Boundary Element Crushing

(6) Maximum $v = 10\sqrt{f'_c}$ governs, ACI Desgin Shear for B8 would be 256 kips = $13.7\sqrt{f'_c}$ disregarding the maximum allowable

(7) 1 kip = 4.45 kN, $1.0\sqrt{f'_c}$ (psi) = $0.083\sqrt{f'_c}$ (MPa)

Table 8 - Deformation Results for Isolated Wall Specimens from Experimental Investigation

Specimen	Last Stable Top Deflection Increment (in.)	Top Deflection At Full Yield (in.)	No. of Stable Inelastic Cycles	Rotation, θ_3 [1] At Full Yield (rad.)	Max. Observed Rotation [2] θ_3 [1] (rad.)	Max. Observed Shear Distort. [2] γ_3, [3] (rad.)	Max. Slip At CJ1 [2] (in.)
R1	± 4	0.53	13	0.0030	-0.0240	-0.0130	-0.20
R2	± 5	0.85	14	0.0046	+0.0212	-0.0300	-0.38
B1	± 5	0.70	14	0.0042	-0.0269	-0.0235	-0.26
B3	± 7	0.70	21	0.0040	+0.0276	-0.0481	+0.10 [7]
B4 [5]	+12.5	0.80	--	0.0047	+0.0630	+0.0340	+0.15
B2	± 4	1.00	9	0.0052	+0.0161	-0.0224	+0.17
B5	± 5	1.10	10	0.0065	-0.0197	-0.0237	-0.13
B5R	± 5	2.50 [6]	9	0.0119 [6]	+0.0204	-0.0237	+0.19
B6	± 3	1.31	4	0.0049	-0.0136	-0.0085	-0.03
B7	± 5	1.38	12	0.0047	-0.0242	-0.0141	-0.11
B8	± 5	1.23	12	0.0049	-0.0255	-0.0123	-0.10
B9	± 5.4 [8]	1.36	1	0.0048	+0.0238	-0.0137	-0.07
B9R	± 6.8	2.99 [6]	8	0.0125 [6]	-0.0287	-0.0197	-0.10
B10	± 5 [8]	1.17	5	0.0048	-0.0243	-0.0112	-0.13
F1	± 2	1.00	6	0.0034	-0.0093	-0.0080	-0.10
F2	± 4	1.13	9	0.0037	-0.0179	-0.0124	-0.06

(1) θ_3 = Rotation of the horizontal section approximately 74 in. (1.88 m) above the base block
(2) Maximum measured during the last stable deflection increment
(3) γ_3 = Average shear distortion in a zone from the base to a level approximately 74 in. (1.88 m) above the base block
(4) CJ1 = Construction joint at the base of the wall
(5) Monotonic test
(6) Measured yield deformation at yield load level of original specimen
(7) Gage failed in cycle 31 at ±5 in. increment
(8) Specimen load capacity was not stable within the modified load history, deformation values listed are maximums from a stable cycle.
(9) 1 in. = 25.4 mm

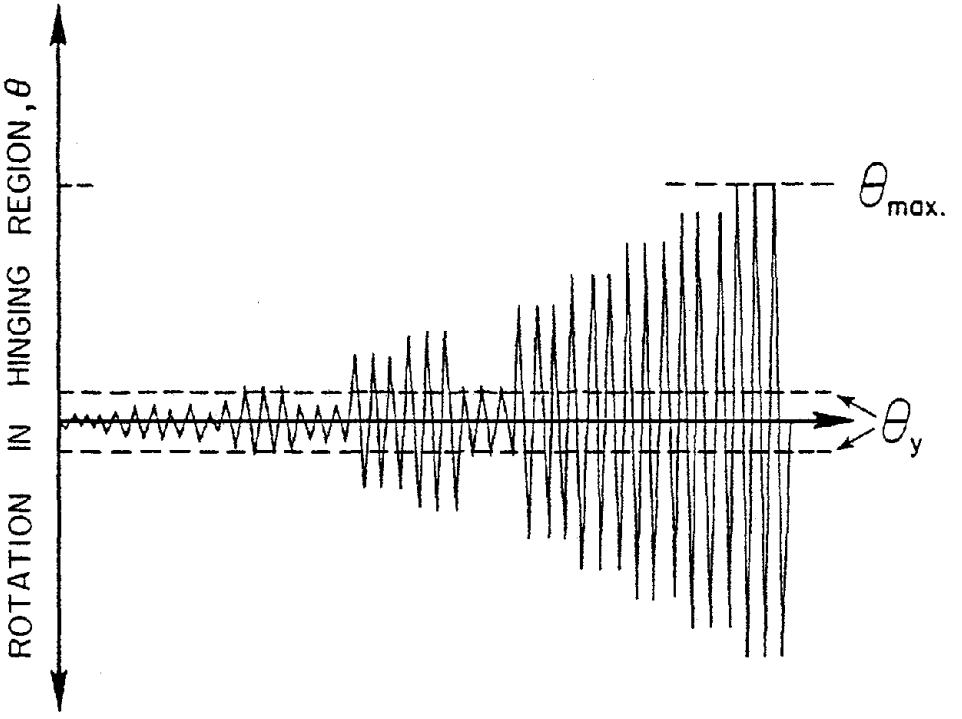

(a) Loading Program A

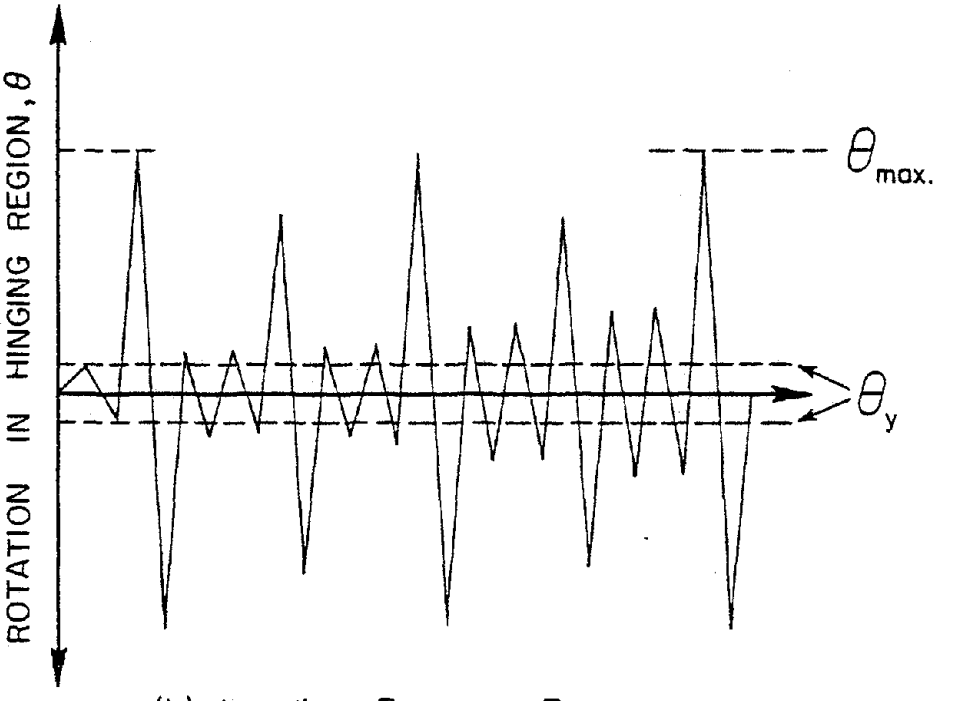

(b) Loading Program B

Fig. 32 Loading Programs Used in Experimental Investigation

program developed on the basis of dynamic response data[11]. This loading program is shown schematically in Fig. 32b. It is distinguished primarily by the occurrence of a loading cycle corresponding to the maximum expected deformation early in the test, with only one small inelastic cycle preceding it.

Ductilities of Test Specimens

The rotational ductility, μ_r, cyclic rotational ductility, μ_{rc}, cumulative rotational ductility, $\Sigma\mu_{rc}$, and cumulative rotational energy, ΣA_{rc}, were computed from digitized data for each of the test specimens considered. Values of these measures of deformation for each specimen are listed in Table 9. Listed values are based on the measured rotation of a section about 74 in. above the base. These correspond to moment-rotation curves such as are shown in Figs. B2 to B14 of Appendix B.

Most of the inelastic deformation in the walls tested was confined to the first 6 ft at the base of the walls. This segment of wall will be referred to as the hinging region. Calculated values of measures of deformation at various load stages are listed in Tables B1 to B13 for each specimen considered. Table 9 presents a summary of measures of ductility corresponding to the ultimate deformation stage.

Also listed in Table 9 are the observed yield moments, corresponding yield rotations and maximum observed shear forces. It should be noted that the yield rotations listed in Table 9 correspond to "full yield" or to yielding of all the tension reinforcement in the boundary element, rather than rotations "at first yield" corresponding to the onset of yielding in the extreme tension reinforcement. "Full yield" corresponds more closely to the definition of yielding (i.e., marked deviation of response from the initial linear elastic behavior) used in the dynamic analyses. Thus, the yield rotations corresponding to full yield as listed in Table 9 have been used in the computation of ductilities. The ratios of ductilities μ_{rc}/μ_r, $\Sigma\mu_{rc}/\mu_r$, and $\Sigma A_r/\mu_r$ are also listed in Table 9. These ratios are discussed later in this section.

Table 9 - Deformation Capacities of Isolated Wall Specimens by Various Definitions

Specimen	Confined Boundary Element	Compressive Axial Load, (~500 psi)	Observed Yield Moment, in-k	Yield Rotation, (rad.)	Max. Nominal Shear Stress $\sqrt{f'_c}$	At Ultimate Deformation Stage						
						Rotational Ductility, μ_r	Cyclic Rotational ductility, μ_{rc}	μ_{rc}/μ_r	Comulative Ductility, $\Sigma\mu_{rc}$	$\Sigma\mu_{rc}/\mu_r$	Cumulative Rotational Energy, ΣA_r	$\Sigma A_r/\mu_r$
R1	No	--	3,600	0.0030	1.4	7.93	12.9	1.63	134.9	17.01	111.3	14.04
R2	Yes	--	6,000	0.0046	2.5	4.39	7.5	1.71	118.7	27.04	126.0	28.70
B1	No	--	8,100	0.0042	2.9	6.26	10.1	1.61	159.6	25.5	156.9	25.10
B3	Yes	--	8,100	0.0040	3.1	6.02	10.2	1.69	290.2	48.21	296.8	49.30
B4*	Yes	--	9,800	0.0047	3.9	13.39	--	--	--	--	--	--
B2	No	--	21,500	0.0052	7.2	2.86	4.3	1.50	62.6	21.89	58.6	20.49
B5	Yes	--	20,000	0.0064	8.8	3.05	4.7	1.54	59.1	19.38	64.0	20.98
B5R	Yes	--	20,000	0.0119	8.9	--	--	--	--	--	--	--
B6	Yes	423	31,300	0.0049	13.8	2.78	4.1	1.47	20.3	7.30	14.5	5.22
B7	Yes	545	33,750	0.0047	10.9	5.06	7.6	1.50	118.4	23.40	142.9	28.24
B8	Yes	545	34,000	0.0049	11.7	5.19	8.3	1.60	123.2	23.74	133.2	25.66
B9 #	Yes	545	33,600	0.0048	11.4	5.00	8.2	1.64	29.7	5.94	36.7	7.35
B9R #	Yes	451	33,600	0.0125	7.0	--	--	--	--	--	--	--
B10 #	Yes	515	25,100	0.0048	8.2	5.1	3.6	2.77	86.7	66.69	75.0	57.69
F1	No	--	27,000	0.0034	10.5	2.6	3.2	1.23	25.8	9.92	14.5	5.58
F2	Yes	482	32,450	0.0037	10.2	4.75	7.3	1.54	90.2	18.99	83.3	17.54
Average								1.65		25.76		24.08

*monolithic test

Tested using loading program B, see Fig. 25. All other specimens tested using loading program A.

The rotational ductility, μ_r, of the "hinging region" at the ultimate deformation stage for the thirteen test specimens is plotted against the corresponding nominal shear stress in Fig. 33. The data "points" shown in this figure, as well as in Figs. 34 through 36, indicate the sectional shape of each specimen. A "c" appearing beside a data point in this figure indicates confined boundary elements in the corresponding specimen. An "a" beside a point indicates that an axial compressive load equivalent to approximately 500 psi was imposed on the specimen during the test. The rest of the specimens had no axial load. The dashed line drawn in this figure represents a lower bound to the plotted points. Any point on this line thus indicates the minimum rotational ductility which, according to test results, is available under the corresponding nominal shear stress.

Figures 34, 35, and 36 show similar plots of cyclic rotational ductility, μ_{rc}, cumulative rotational ductility, $\Sigma\mu_{rc}$, and cumulative rotational energy, ΣA_{rc}, respectively. These are plotted against the maximum applied nominal shear stress.

The dashed line in Fig. 34 represents a magnification of the values corresponding to the dashed line in Fig. 33 by a factor of 1.5. In other words, for the same value of the nominal shear stress, the dashed line of Fig. 34 yields a cyclic rotational ductility, μ_{rc}, equal to 1.5 times the corresponding rotational ductility, μ_r. It can be seen that the dashed line of Fig. 34 constitutes a lower bound to the plotted points. This means that for the same nominal shear stress, a minimum cyclic rotational ductility equal to 1.5 times the minimum available rotational ductility can be counted on.

The dashed lines in Figs. 35 and 36 similarly represent magnifications of the values corresponding to the dashed line in Fig. 33 by factors of 22.0 and 21.0, respectively. It may be seen that in each figure, all plotted points except that corresponding to Specimen F1 lie above the dashed line.

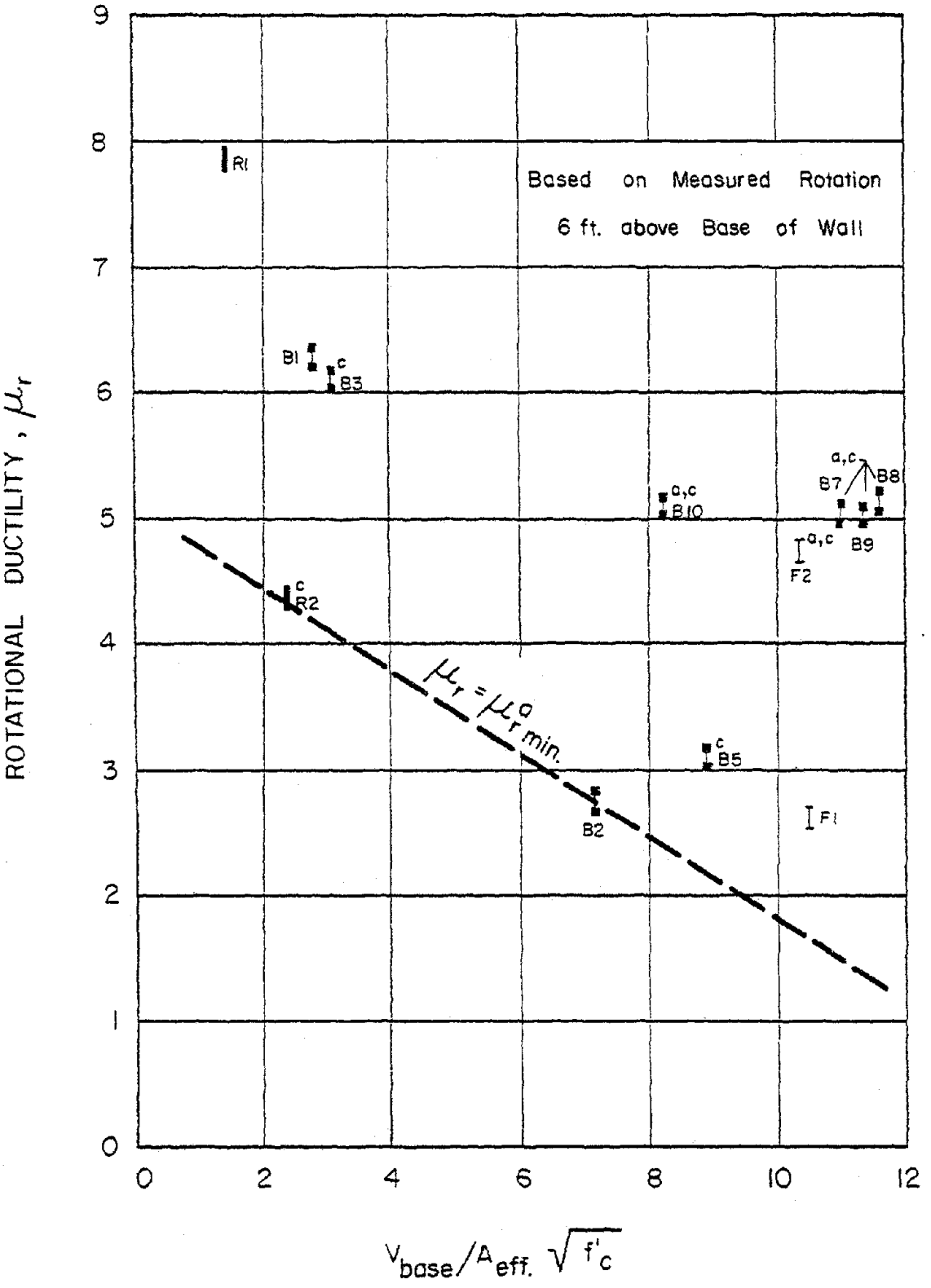

Fig. 33 Rotational Ductility Ratio, μ_r, as a Function of Maximum Nominal Shear Stress - Isolated Wall Specimens

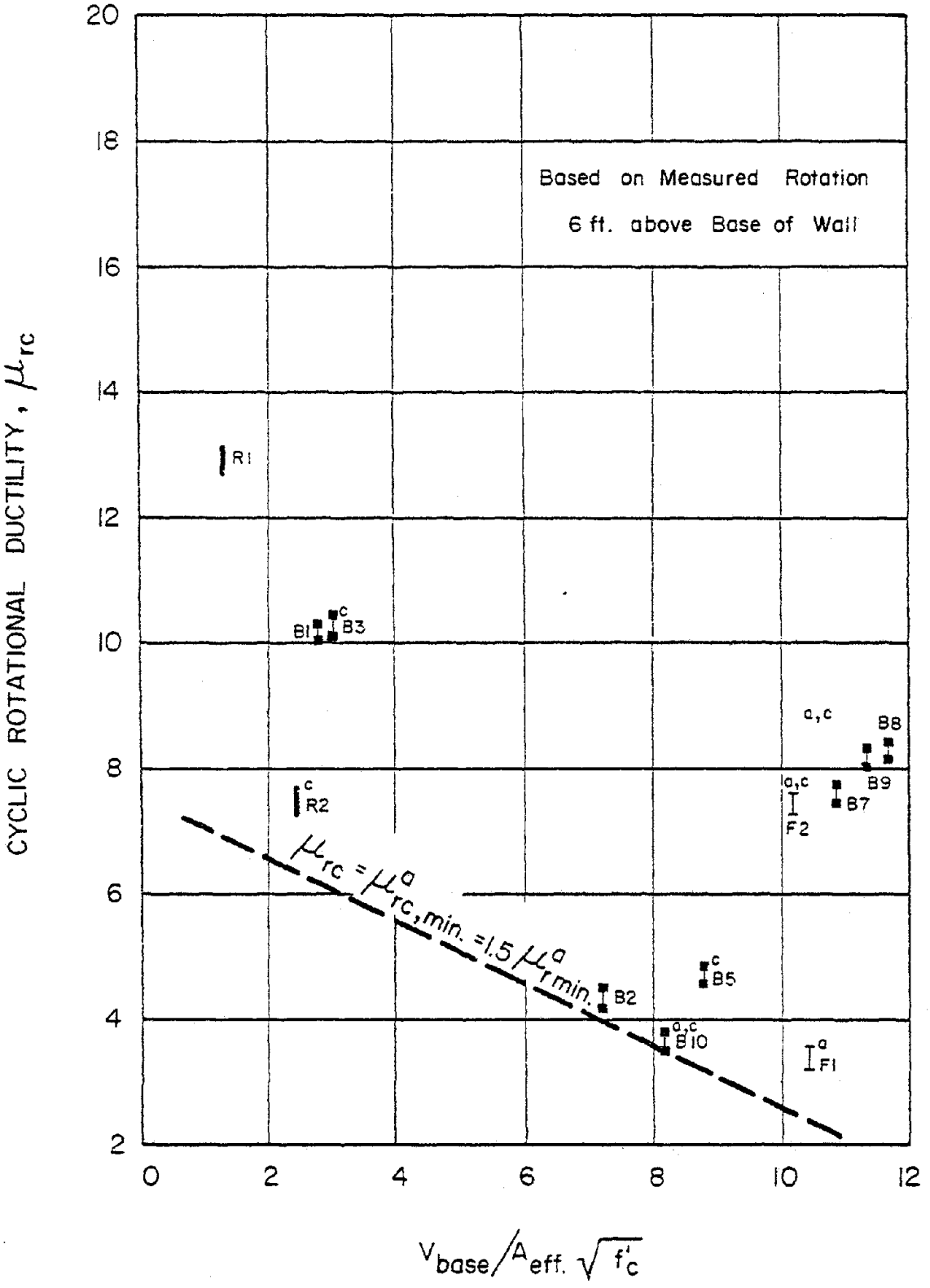

Fig. 34 Cyclic Rotational Ductility Ratio, μ_{rc}, as a Function of Maximum Nominal Shear Stress - Isolated Wall Specimens

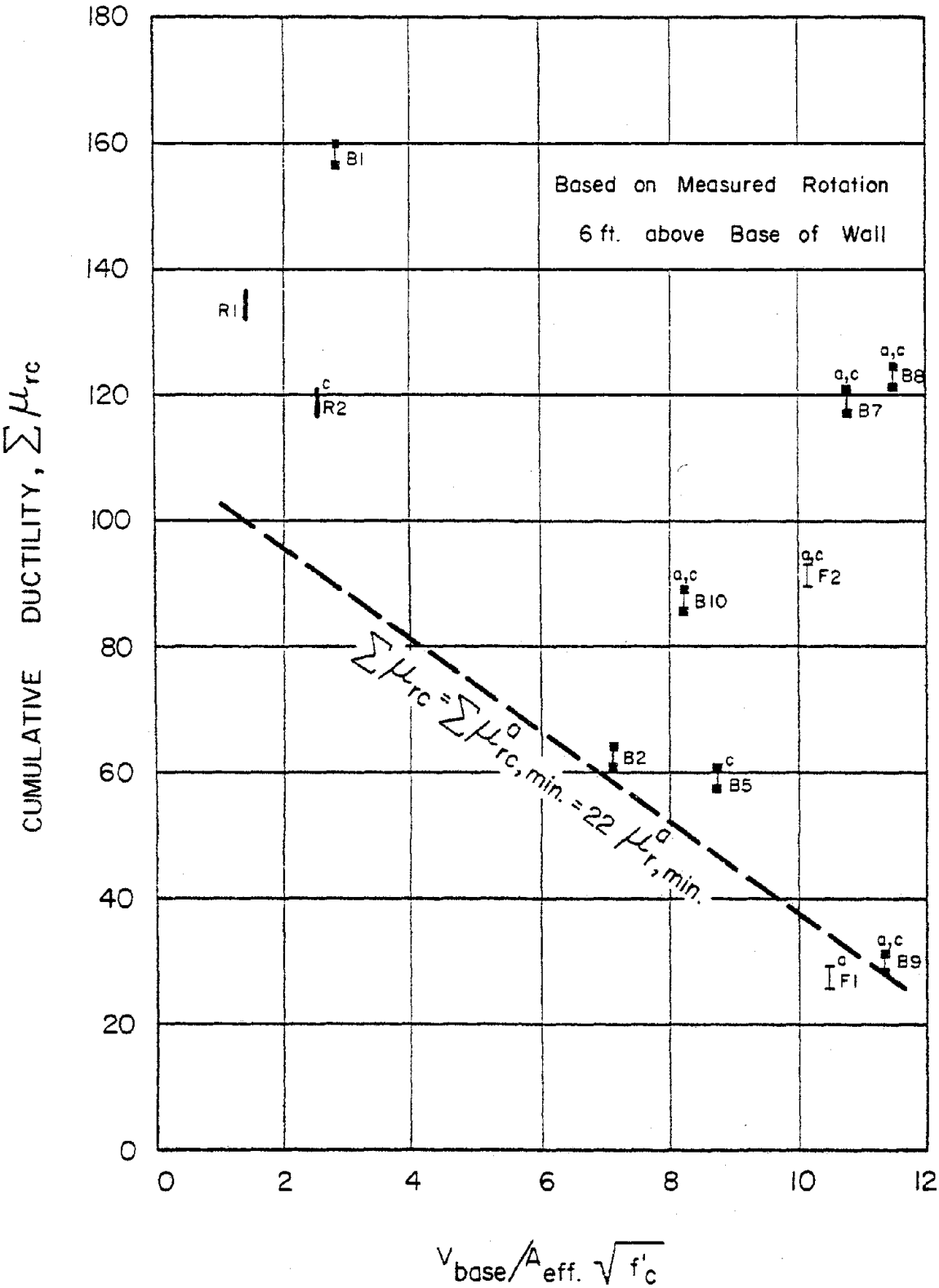

Fig. 35 Cumulative Rotational Ductility, $\Sigma\mu_{rc}$, as a Function of Maximum Nominal Shear Stress - Isolated Wall Specimens

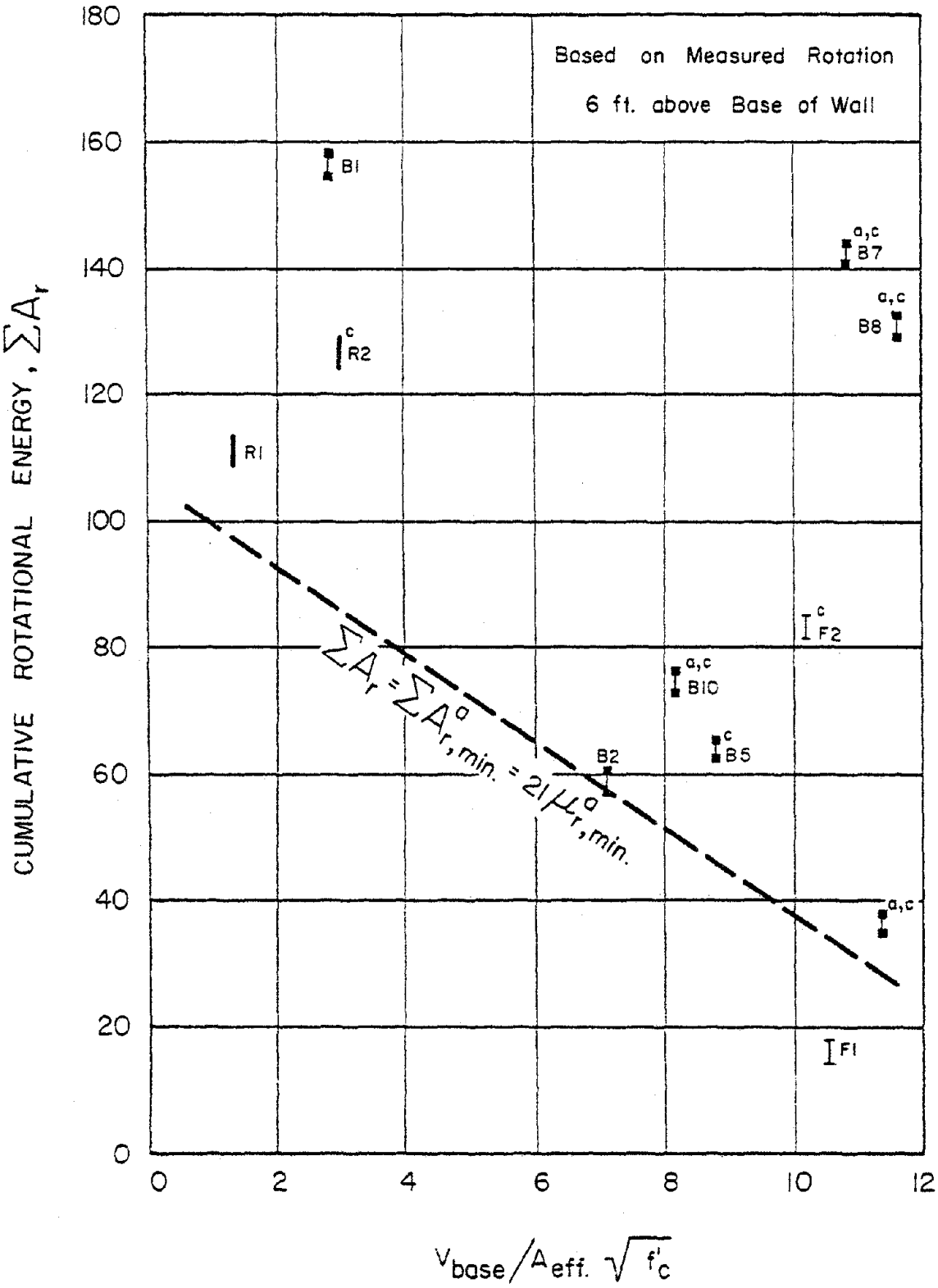

Fig. 36 Cumulative Rotational Energy, ΣA_r, as a Function of Maximum Nominal Shear Stress - Isolated Wall Specimens

Specimen F1 was the very first specimen tested. Subsequent to the yielding of this specimen, the top deflection was increased directly from 2 in. to 4 in. instead of three inelastic load cycles being applied at one-inch deflection increments as in other specimens. The first inelastic cycle at 4-in. deflection was stable; but the specimen then failed suddenly by web crushing. It appears very likely that the specimen would have easily withstood three inelastic load cycles at a top deflection of 3 in. If this had been the case, the cumulative ductility and the cumulative rotational energy of this particular specimen would very probably have been much larger than the values appearing in Figs. 35 and 36. The points representing Specimen F1 in Figs. 35 and 36 can thus be disregarded. Disregarding F1, the dashed line in each of these figures thus constitutes a lower bound to the plotted points.

The dashed lines in Figs. 34, 35, and 36 indicate that if a minimum rotational ductility, μ_r, of 3, say, is available under a particular nominal shear stress, a minimum cyclic ductility of 3 x 1.5 = 4.5, a minimum cumulative ductility of 3 x 22 = 66, and a minimum cumulative rotational energy of 3 x 21 = 63 are also available. It is of interest to compare the factors of 1.5, 22.0, and 21.0 with the corresponding ratios of ductilities in Table 9 (1.65, 25.76, and 24.88, respectively).

By noting the relative magnitudes of the different measures of available ductility in terms of a reference measure (in this case, μ_r), a comparison with the corresponding quantities representing ductility demands can conveniently be made.

Comparison of Measures of Demand and Capacity

Figure 37 shows a comparison of the different measures of deformation demand with corresponding measures of capacity. The ranges of the ratios representing demand shown in Fig. 37 are based on the Figs. 27 to 30 while those representing capacity are based on Figs. 33 to 36. In Fig. 30 and in the subsequent discussion, the subscript "2" attached to the symbols for

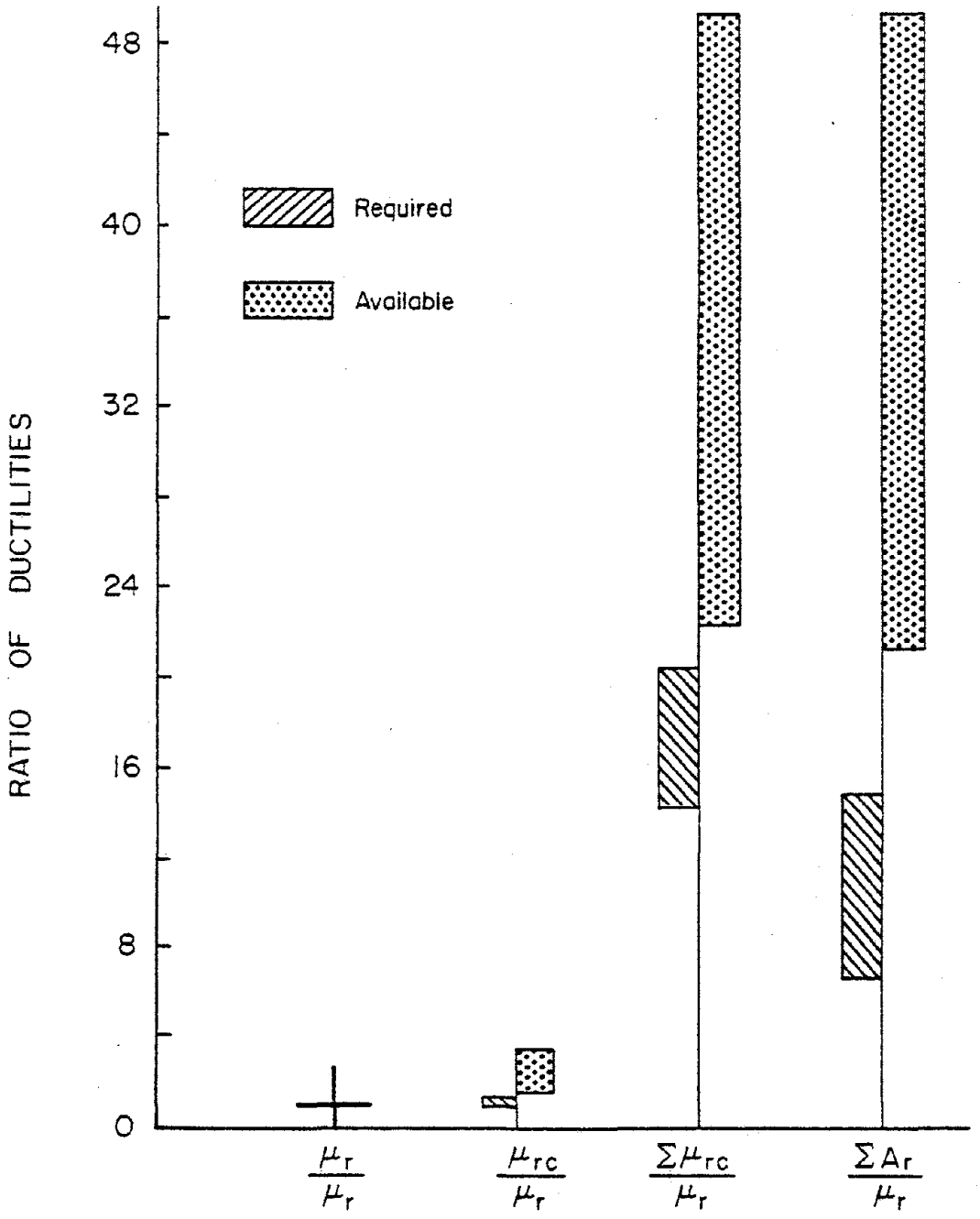

Fig. 37 Comparison of Ratios of Maximum Ductility Required with Corresponding Ratios of Available Ductilities - Using Rotational Ductility, μ_r, as the Reference Measure

measures of deformation demand has been dropped for convenience. Ductility demands are based on nodal rotations at a level above the base approximately equal to the width of the wall.

Ratios of ductilities relating to demand are relatively insensitive to changes in fundamental period. A horizontal line in each of Figs. 28 through 30 sufficiently describes the variation of the mean ratio with T_1. It is apparent from Fig. 37 that the demand in terms of the three ratios is less than the corresponding available capacity.

The test results as shown in Fig. 34 indicate that the minimum available ductility in terms of μ_{rc} is at least 1.5 times the available ductility in terms of μ_r. Figure 28 shows that the maximum ductility demand in terms of the ratio of μ_{rc} to μ_r is only 1.3. It follows that satisfaction of the ductility requirements in terms of μ_r automatically implies satisfaction of the same requirements in terms of μ_{rc}.

Similarly, the test data of Fig. 35 indicate that the minimum available ductility in terms of μ_{rc} is at least 22 times the available ductility in terms of μ_r. The analytical results in Fig. 29 show that the maximum ductility demand in terms of the ratio of μ_{rc} to μ_r is about 20.2. Thus, if the ductility requirements are satisfied in terms of μ_r, they will automatically be satisfied in terms of μ_{rc} also. The same observation can be made concerning the adequacy of μ_r as an index of the satisfaction of ductility requirements in terms of the cumulative rotational energy ΣA_r.

Although the data considered are limited, the above comparison provides a strong indication of the adequacy of rotational ductility, μ_r, as a measure of deformation demand and capacity, in the sense that satisfaction of ductility requirements in terms of μ_r automatically implies satisfaction of the same requirements in terms of the other three measures of ductility. Because μ_r is the most conveniently determined measure among the four measures considered, and one that has been widely used in the literature, it was decided to adopt it as the basic measure of deformation demand and capacity.

Assumptions Underlying Comparison

In comparing measures of deformation demand obtained from dynamic analysis with deformation capacity from laboratory tests, it was implicitly assumed that the test conditions corresponded to the response of isolated walls to 20-second input motions having an intensity equal to 1.5 ($SI_{ref.}$). It should be pointed out that a 20-second strong motion with a spectrum intensity of 1.5 ($SI_{ref.}$) represents a very severe earthquake.

Another important assumption made in carrying out the above comparisons is that the behavior of reinforced concrete walls is not significantly affected by differences between tests and analyses with respect to number of cycles of large-amplitude deformations or the sequence in which these large deformations are imposed. Thus, an equivalence in deformations from analytical and experimental results was assumed as indicating that specimens tested under the loading pattern used in the laboratory could sustain the same deformations under typical dynamic response conditions.

Whether the sequence of loading used for most of the test specimens (Fig. 32a) represents an equivalent or more severe loading than that which would typically occur under earthquake excitation is an important question. This question requires further investigation to more fully establish the validity of the preceding comparison.

A detailed study of deformation response histories for most of the cases considered in this investigation for the purpose of characterizing a representative loading history is discussed in Ref. 11.

DETERMINATION OF DESIGN FORCE LEVELS - BASE OF WALL

A procedure for determining design forces has been developed based on critical response quantities compiled and plotted for a wide range of values of the principal structural parameters, fundamental period, T_1, and yield level M_y. Design forces of major interest are those necessary for proportioning wall sections located in critical regions. For an isolated wall, the most critical region is located at the base of the wall.

The design procedure is presented in a form suitable for design office use. Dynamic response data are reduced to static design values. A comparison was made between design values obtained by the proposed procedure and by the Uniform Building Code[16] procedure.

Preparation of Design Charts

The basic steps involved in the preparation of charts for use in determining design force levels are illustrated in Fig. A on the following pages. The main objective of the procedure is to determine design moments and shears at the base of the wall corresponding to particular combinations of four basic parameters, namely, fundamental period, flexural yield level, expected earthquake intensity, and deformation capacity of the structure.

The basic steps for determining design force levels shown in Fig. A use rotational ductility factor, μ_r, as the measure of deformation. The schematic chart shown under Step (4) in Fig. A indicates how experimental data on capacity can be presented for correlation with analytical results on demand.

Steps indicated in Fig. A are concerned primarily with the forces and deformations in the critical region at the base of the wall.

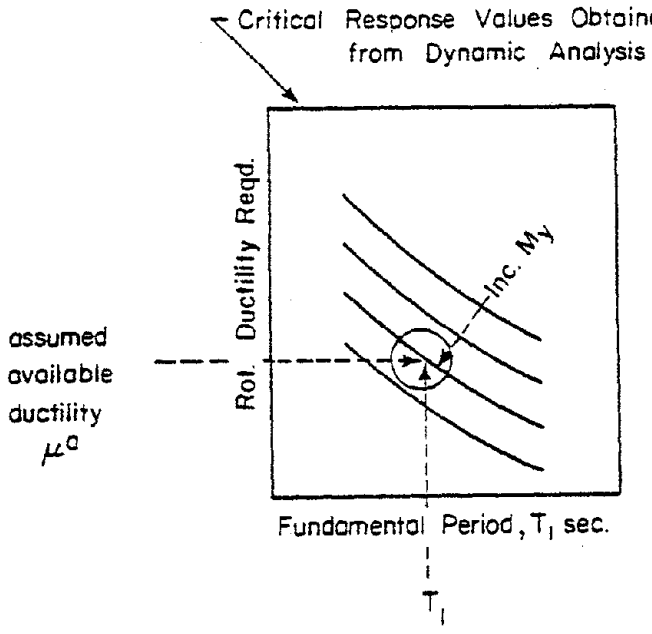

(1)

For a given height of wall and ground motion intensity

Obtain mimimum yield moment, M_y^{min} (at base) corresponding to assumed available rotational ductility, μ_r^a, and particular values of the initial fundamental period, T_1. (Any value of M_y less than this minimum can result in ductility requirements greater than avail...

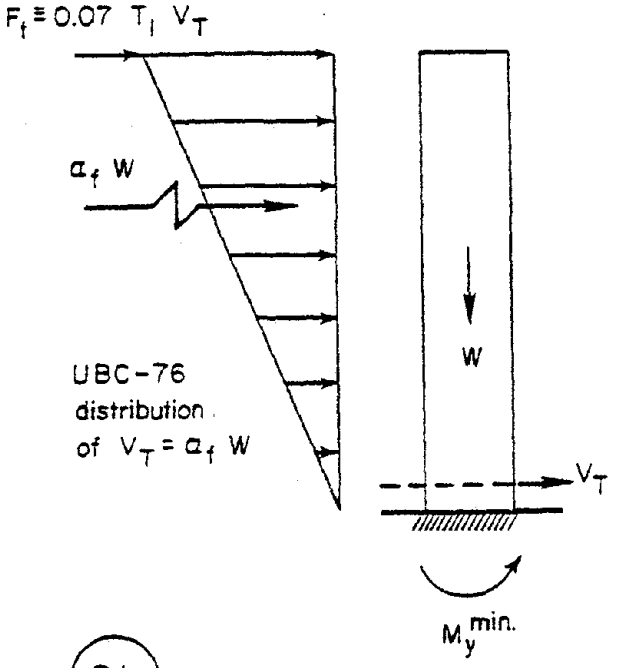

(2a)

Determine value of $\alpha_f = V_T/W$ which produces a moment at the base of the wall equal to M_y^{min}, using UBC-76 distribution of base shear. (This gives a static design force, $\alpha_f W$, similar to the UBC design base shear, for detemining the flexural reinforcement at the base of the wall. The minimum yield moment capacity, M_y^{min}, is needed to limit the required ductility under the design ground motion intensity to the assumed available ductility.)

(2b)

For different values of the fundamental period, T_1, and assumed available ductility, μ_r^a, a chart such as is shown at right is obtained.

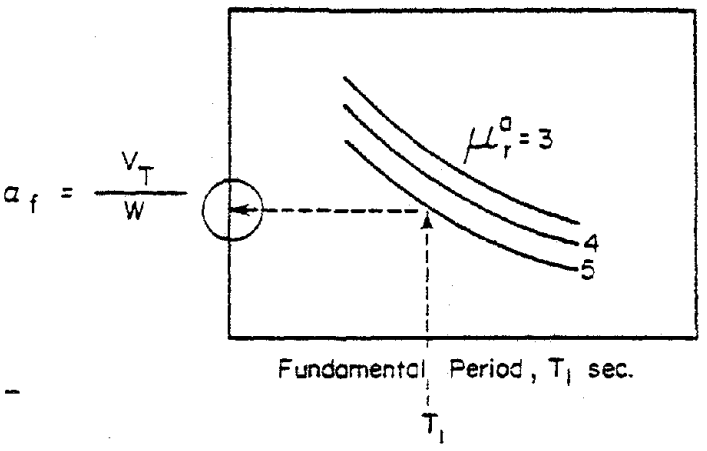

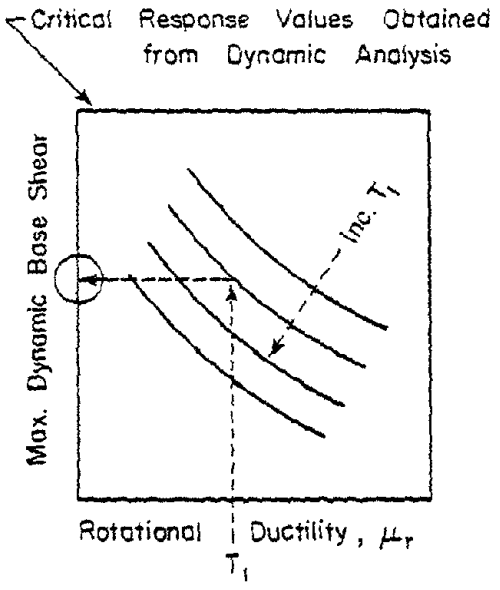

3a

Determine maximum dynamic base shear, V_T^{dyn}, corresponding to μ_t^a assumed in Step (1) and particular values of the fundamental period, T_1. Then calculate ratio $V_T^{dyn}/V_T = \bar{\alpha}_v$. The factor $\bar{\alpha}_v$ is generally greater than unity. (The force $\bar{\alpha}_v V_T = V_T^{dyn}$ provides a basis for the design of the shear reinforcement at the base of the wall.)

3b

For different values of available ductility, μ_t^a, and fundamental period T_1, a chart such as is shown at right is obtained.

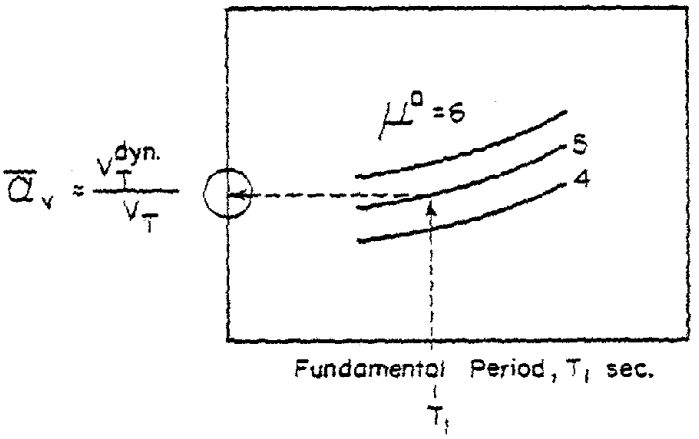

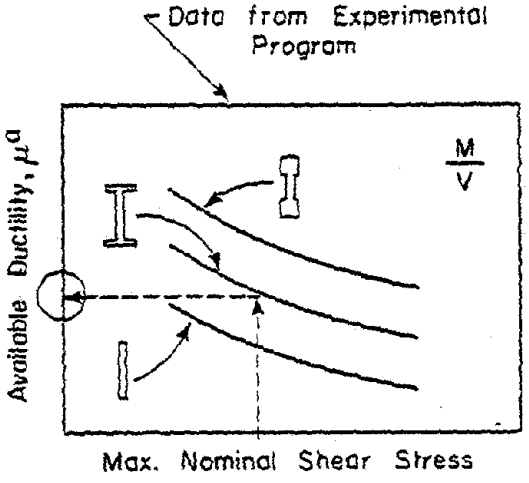

4

Results of laboratory tests on wall specimens subjected to reversed loading, such as indicated in the sketch at left, will serve as bases for estimating the available rotational ductility for any particular combination of wall cross-section and maximum applied nominal shear stress. (This chart will correspond to a more-or-less constant M/V ratio and a specified loading sequence).

Steps in Design Procedure Using Design Charts

The procedure for determining forces needed to design the critical region at the base of a structural wall, uses charts developed following Steps 2 and 3 in Fig. A.

The major steps in the design procedure are briefly described below:

a. Select a preliminary wall section, with associated initial fundamental period. The preliminary section could be based, for example, on gravity and wind load requirements.

b. Assume an available rotational ductility, μ_r^a. An estimate may be obtained by using a chart, based on experimental data, similar to the plot shown under Step (4) in Fig. A.

c. Determine the flexural design factor, α_f, from a chart similar to that shown under Step (2b) of Fig. A. Determine the corresponding required flexural reinforcement to provide M_y^{min}.

d. Determine $\bar{\alpha}_v$ and the "effective static nominal shear stress"* from a chart similar to that shown under Step (3b) of the outlined procedure.

e. Using a chart similar to that shown under Step (4) of the outlined procedure, check if the available ductility, μ_r^a, assumed in Step (a) above can be developed under the design shear stress determined in Step (c) above.

   If the assumed ductility can be developed, then determine the required shear reinforcement using

*This is an equivalent static design shear value obtained by applying a reduction factor to the calculated critical dynamic shears. The reduction is intended to account for the effect of a number of factors discussed under "Reduction in Critical Dynamic Shear Forces" and allows a comparison with capacity values obtained experimentally under slowly reversed loading.

design recommendations to be developed on the basis of the results of the experimental program.

If the assumed ductility cannot be developed under the calculated design shear, adjust the assumed ductility value accordingly and repeat Steps (a) through (d) until a reasonable agreement between assumed and developable ductilities is obtained.

Preparation of Design Charts for 20-Story Isolated Structural Walls

To illustrate the procedure, design charts were prepared for 20-story isolated walls. In this particular case, the walls were subjected to input motions having an intensity, SI, equal to 1.5 ($SI_{ref.}$).

On the assumption that the width of the walls is at least 20 ft,* rotational ductility ratio based on nodal rotation at the 2nd floor level was used as the measure of deformation in the critical region at the base of the wall.

Figure 38a, corresponding to the plot shown in Step (1) of the procedure outlined in Fig. A, shows the variation of rotational ductility demand with fundamental period, T_1, and yield level, M_y. (Figure 38a is identical, except for size, to Fig. 13e.) From this, another chart, Fig. 38b, was prepared, to allow a closer determination of M_y-values lying between curves in Fig 38a. Each plotted point in Fig. 38b, corresponding to a particular value of the fundamental period, T_1, represents the intersection of a vertical line through the period value with the corresponding M_y-curve in Fig. 38a. Here again the curves have been passed through as many points as would permit a fairly smooth upper-bound curve to be drawn.

By assuming available ductility ratios, μ_r^a, equal to 3, 4, 5, and 6, and using Fig. 38b, a set of values for the minimum

*A procedure for adjusting the ductility demand for cases where the width of the wall, and hence the length of the hinging region, is less than the minimum assumed in deriving the design charts, is given in Fig. 24.

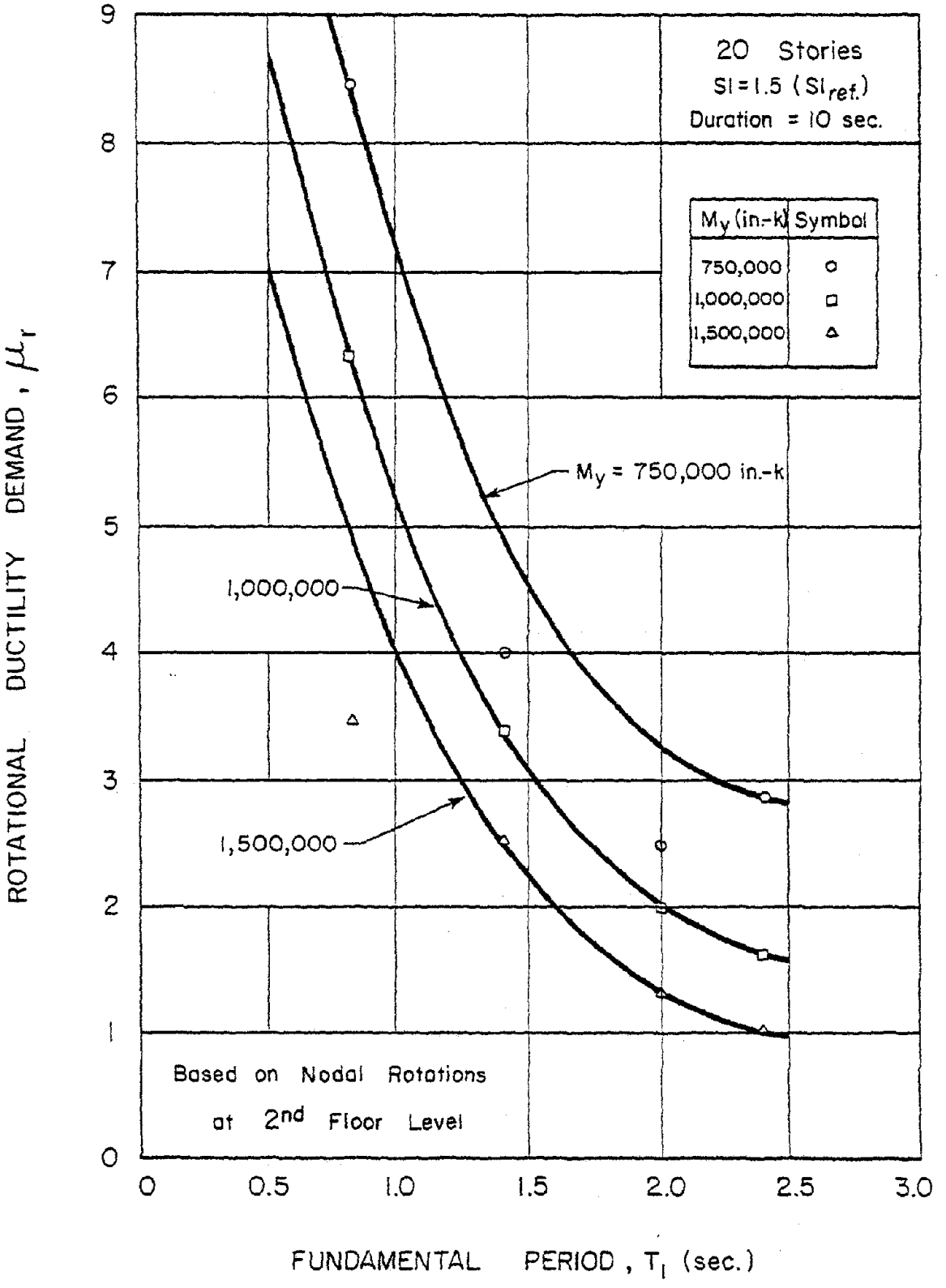

Fig. 38a Rotational Ductility Demand, μ_r, as a Function of Fundamental Period, T_1, and Flexural Yield Level, M_y - 20-Story Structural Walls - SI = 1.5 ($SI_{ref.}$)

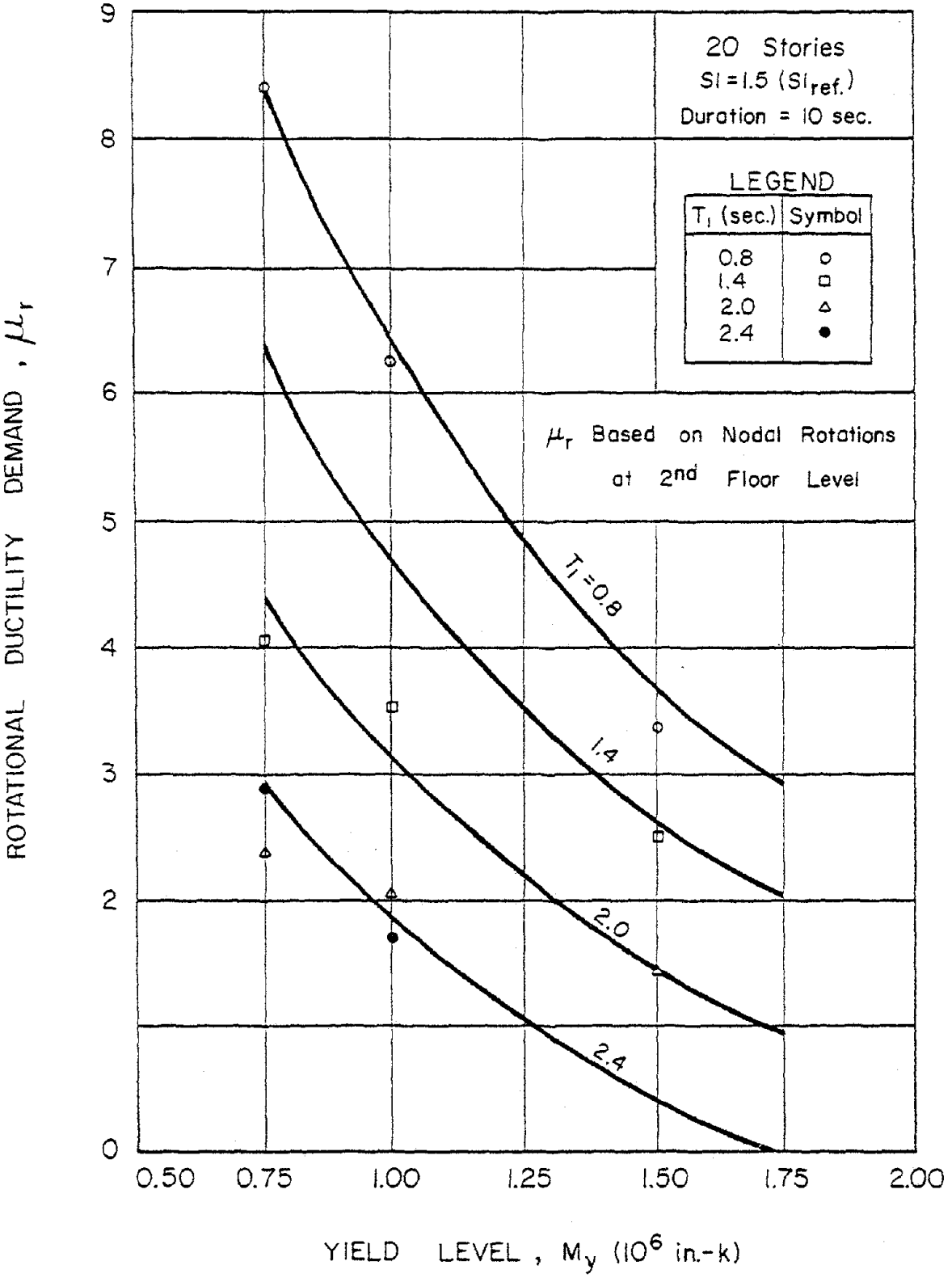

Fig. 38b Rotational Ductility Demand, α_r, as a Function of Fundamental Period, T_1, and Yield Level, M_y
20-Story Structural Walls - SI=1.5 ($SI_{ref.}$)
(A Replot of Fig. 38a with T_1 and M_y Interchanged)

yield level at the base, M_y^{min}, is obtained as a function of fundamental period, T_1, and available ductility. This relationship, as shown in Fig. 39, indicates that the minimum design yield level, M_y^{min}, increases with decreasing available ductility and fundamental period. M_y^{min} represents the minimum value of yield moment at the base needed to ensure that the ductility demand does not exceed the assumed available ductility. A higher value of M_y will result in a lower ductility demand, but a correspondingly higher shear force at the base. This will in turn tend to reduce the available ductility or deformation capacity of the wall.

Figure 40, corresponding to the figure in Step (2b) in Fig. A, shows the flexural design factor, α_f, as a function of the fundamental period, T_1, for different values of the available rotational ductility ratio, μ_r^a. The factor α_f is used to obtain the total design horizontal force, V_T (= $\alpha_f W$, where W is the total effective weight of the structure) for designing the flexural reinforcement at the base of the wall. Figure 40 is essentially a re-plot of Fig. 39, with the minimum yield level at the base, M_y^{min}, expressed in terms of the corresponding total lateral force, V_T. The total lateral force, V_T, is conveniently expressed as a fraction of the total effective weight of the structure, W, and is assumed to be distributed as prescribed in UBC-76[16] and indicated in Fig. 41.

Using a technique similar to that applied to the critical base moment in preparing Fig. 40 for the flexural design factor, α_f, Fig. 42b was prepared from the plot of critical base shears shown in Fig. 42a. (Figure 42a is identical, except for scale, to Fig. 13d.) Figure 43 shows the shear design factor $\bar{\alpha}_v$, as a function of the fundamental period, T_1, and the assumed available ductility, μ_r^a.

Figure 43 was prepared using Figs. 38b, 40 and 42b. To determine the ordinate, $\bar{\alpha}_v$, of a point on a curve in Fig. 43

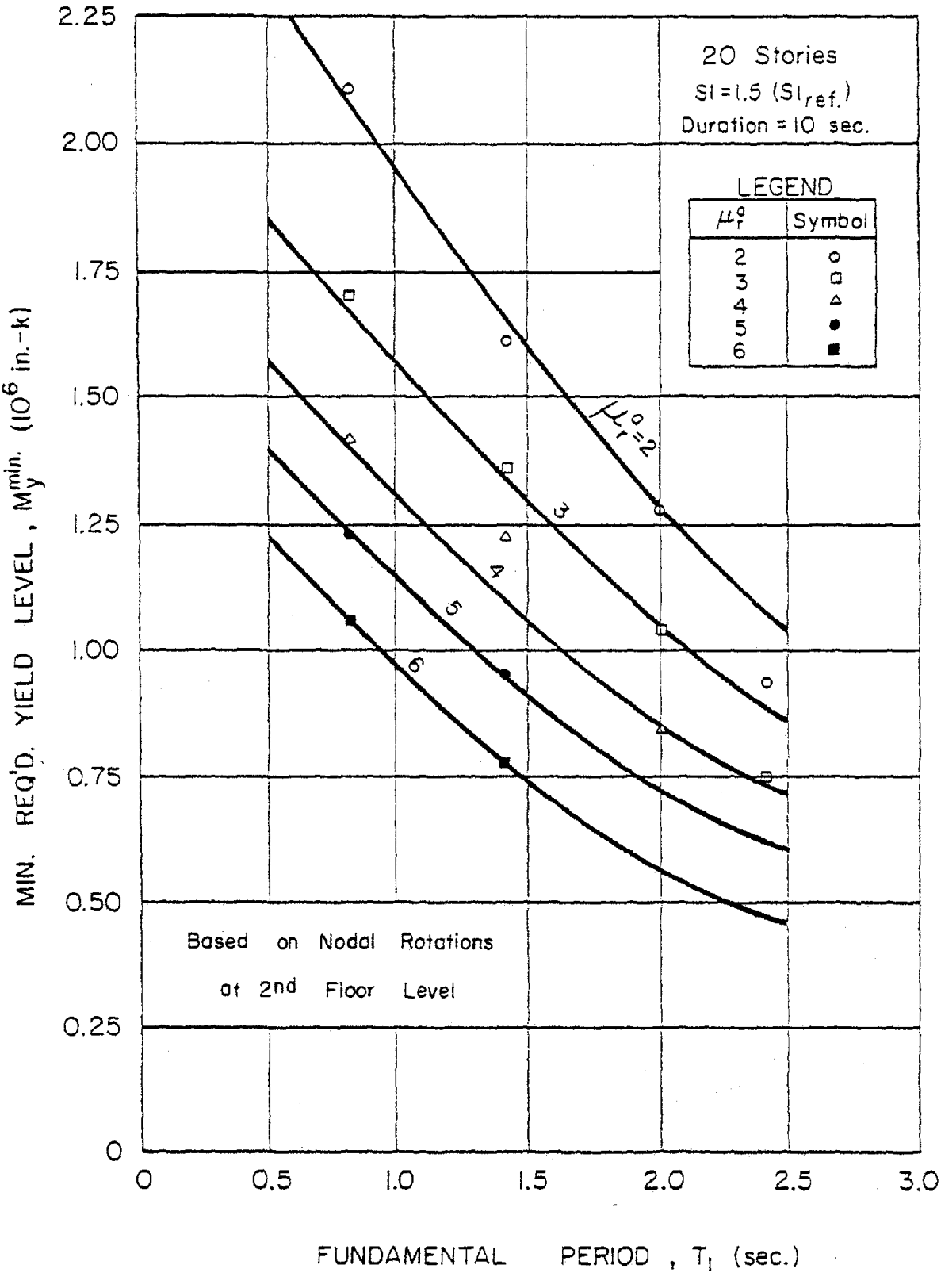

Fig. 39 Minimum Required Yield Level, M_y^{min}, Corresponding to Different Values of Fundamental Period, and Available Rotational Ductility, μ_r^a
20-Story Structural Walls -- SI = 1.5 ($SI_{ref.}$)

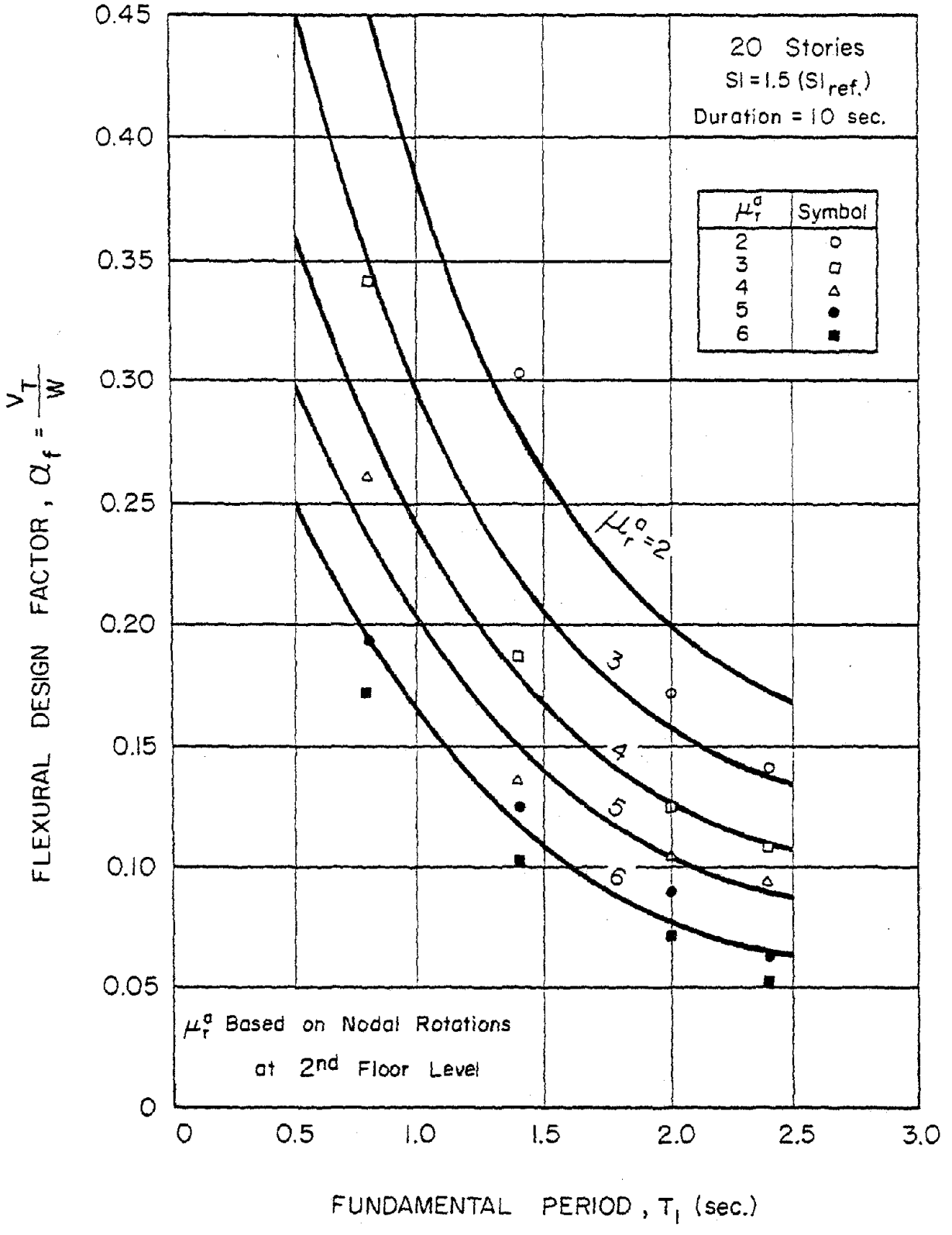

Fig. 40 Flexural Design Factor, α_f, as a Function of Fundamental Period, T_1, and Available Rotational Ductility, μ_r^a
20-Story Structural Walls

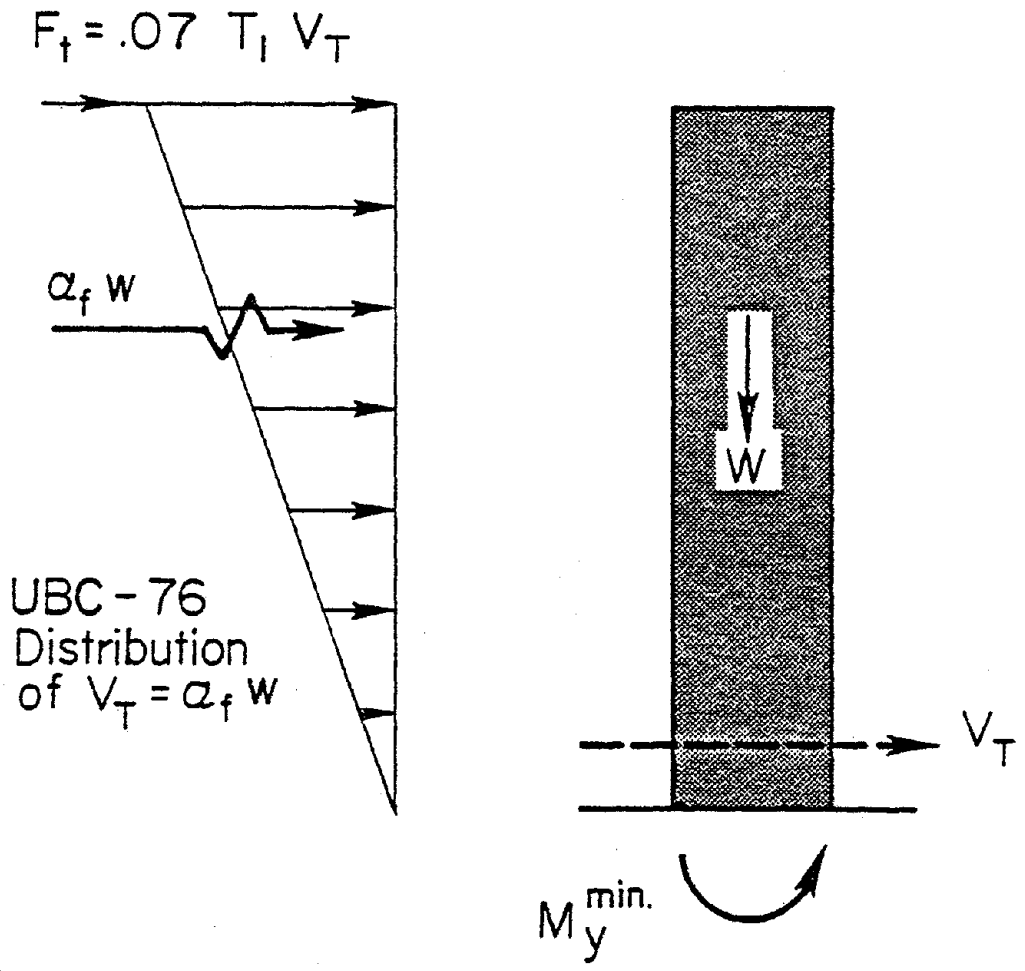

Fig. 41 Assumed Distribution of Lateral Load $\alpha_f W$, for Flexural Design of Base of Wall (Based on UBC-76 Provisions)

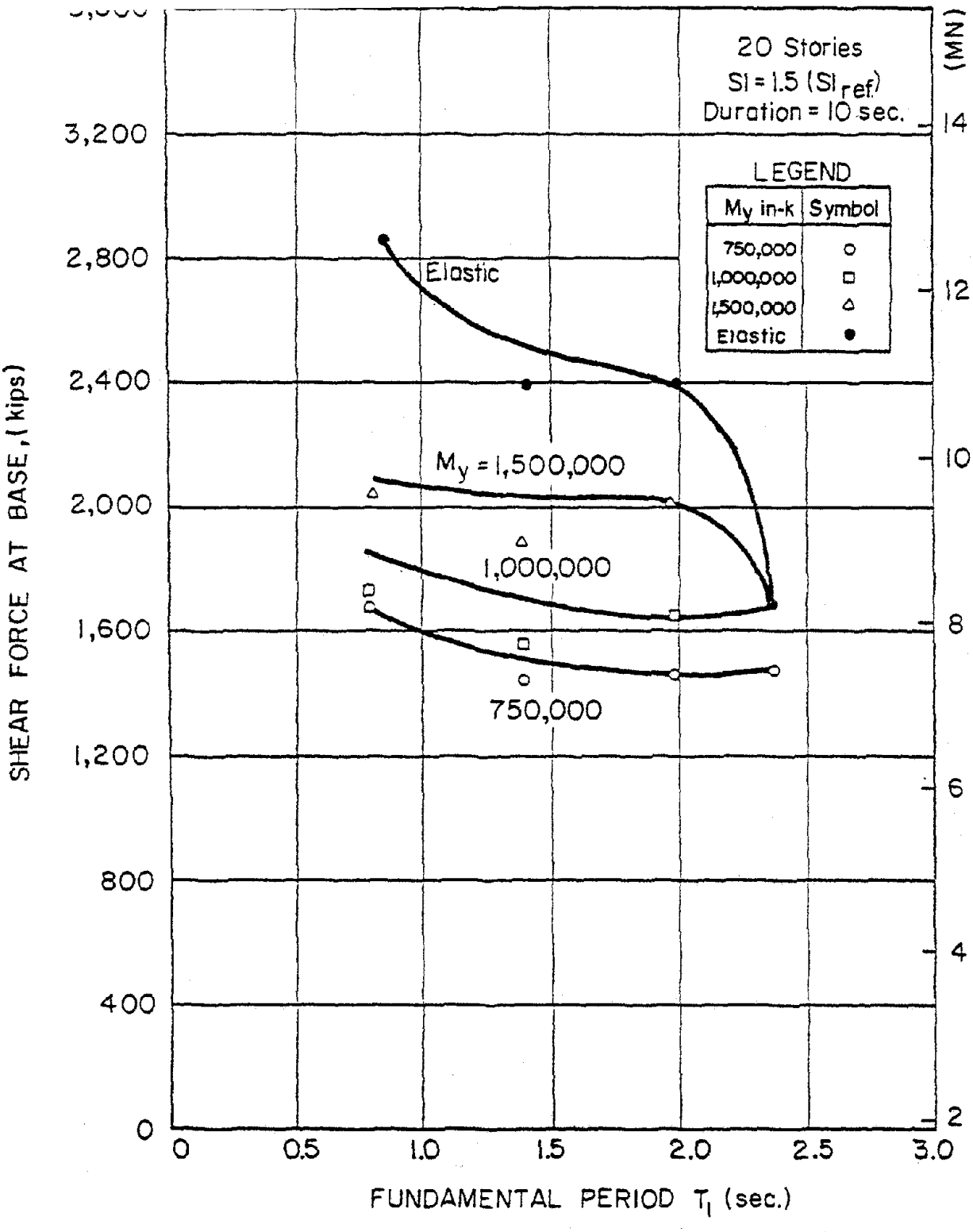

Fig. 42a Critical Base Shear as a Function of Fundamental Period, T_1, and Yield Level, M_y
20-Story Isolated Structural Walls

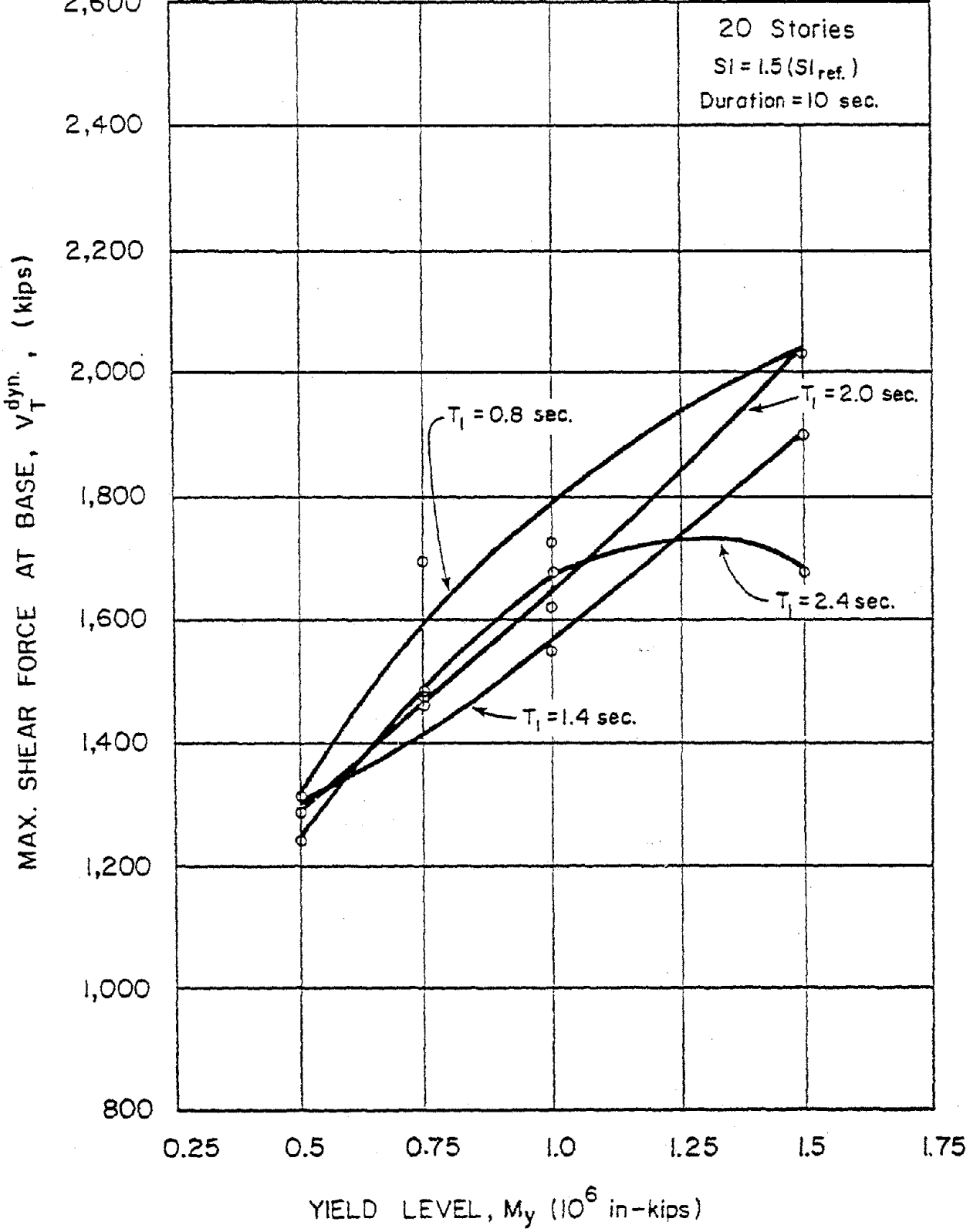

Fig. 42b Critical Base Shear as a Function of Fundamental Period, T_1, and Yield Level, M_y - 20-Story Isolated Structural Walls (a Replot of Fig. 42a with T_1 and M_y Interchanged)

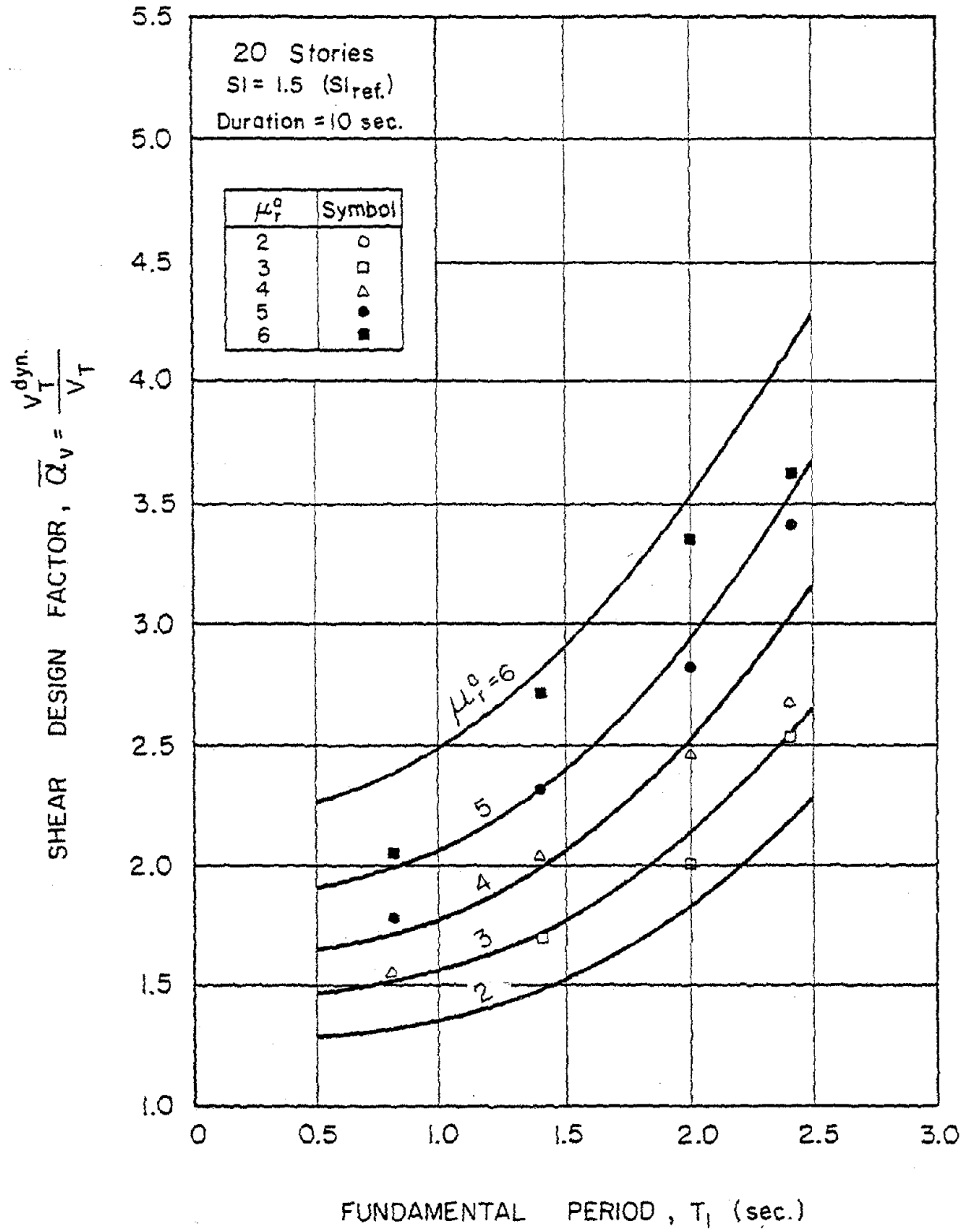

Fig. 43 Shear Design Factor, $\bar{\alpha}_v$, as a Function of Fundamental Period, T_1, and Available Rotational Ductility, μ_r^a
20-Story Structural Walls

corresponding to particular values of μ_r^a and T_1, use was made of Fig. 38b to determine the yield level, M_y, associated with μ_r^a and T_1. Using these values of M_y and T_1, the maximum dynamic base shear, V_T^{dyn}, is then obtained from Fig. 42b. The shear design factor, $\bar{\alpha}_v$ results from dividing V_T^{dyn}, by the base shear V_T corresponding to M_y and T_1. The value of $V_T = \alpha_f W$, where W is the total effective weight of the wall, is obtained using Fig. 40. As in previous plots, a major consideration in drawing curves for different values of μ_r^a in Fig. 43 was to obtain a reasonably conservative estimate of the variable concerned, in this case $\bar{\alpha}_v$.

The design shear factor, $\bar{\alpha}_v$, is the factor by which the calculated dynamic shear force at the base, V_T^{dyn}, exceeds the base shear, V_T, associated with the design yield moment, M_y, at the base. M_y is related to V_T by assuming the latter to be distributed along the height of the wall in accordance with UBC-76 provisions. It is significant to note that the factor $\bar{\alpha}_v$ has values that are generally greater than unity. Figure 43 shows $\bar{\alpha}_v$ increasing with increasing values of available ductility and fundamental period.

The variation of the ratio M_y^{min}/V_T^{dyn} with the fundamental period for different values of the ductility ratio, μ_r, is shown in Fig. 44. This ratio may be interpreted as the distance above the base of the wall of the equivalent resultant static horizontal force necessary to produce M_y^{min} and V_T^{dyn} simultaneously at the base. The ordinate on the right side of the figure shows this distance in terms of the total height of the wall. It will be noted that for all cases the equivalent resultant force lies below the 2/3 point associated with the triangular loading specified in codes. This is consistent with the observation that the shear design factor, $\bar{\alpha}_v$, is generally greater than unity.

Figures 45 and 46 show critical values of the top displacement and interstory displacement, respectively, as functions of fundamental period and the rotational ductility at the base of

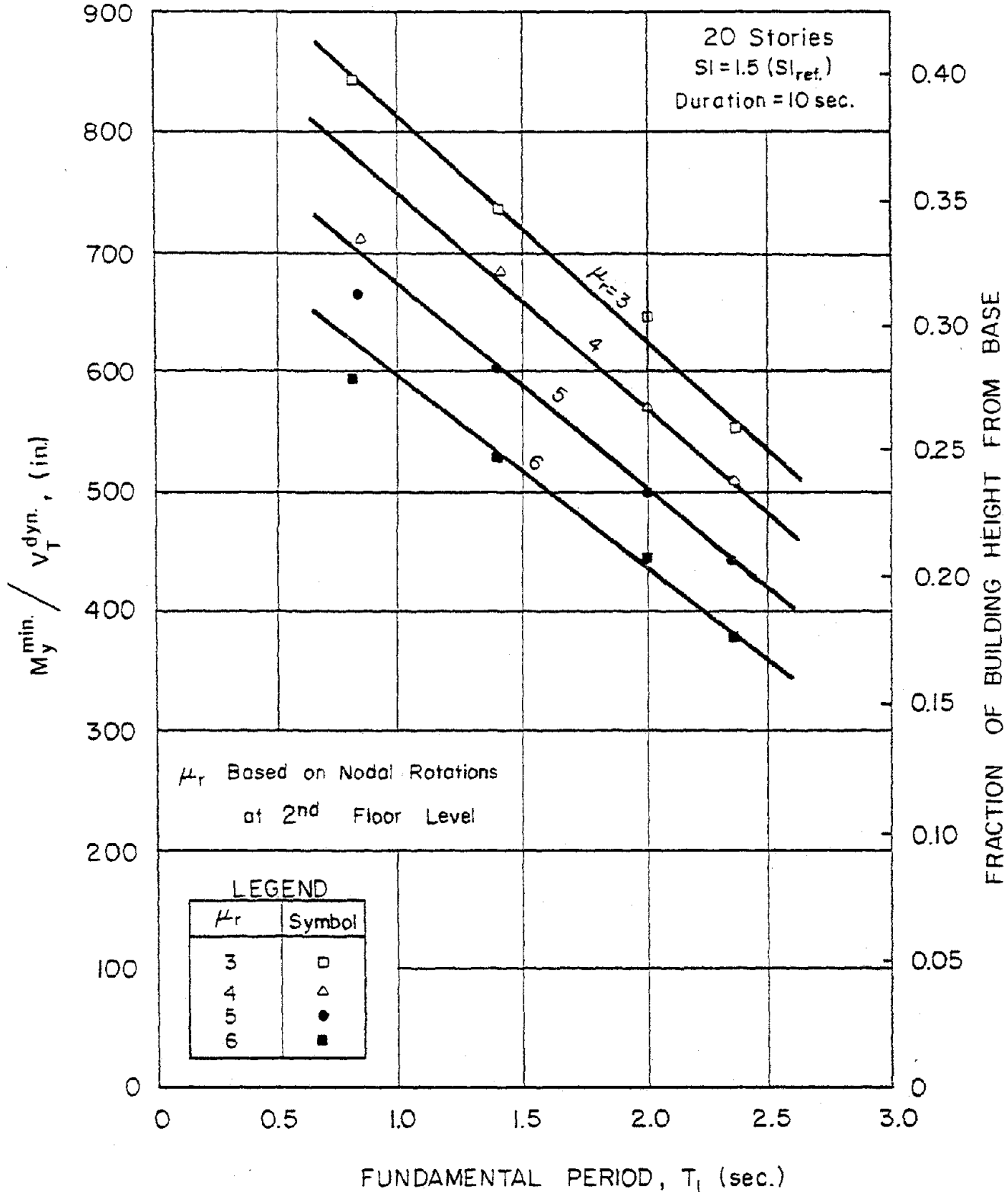

Fig. 44 Ratio of Required Yield Moment at Base, M_y^{min}, to Maximum Dynamic Base Shear, V_T^{dyn}, as a Function of T_1, and Available Ductility Ratio, μ_r

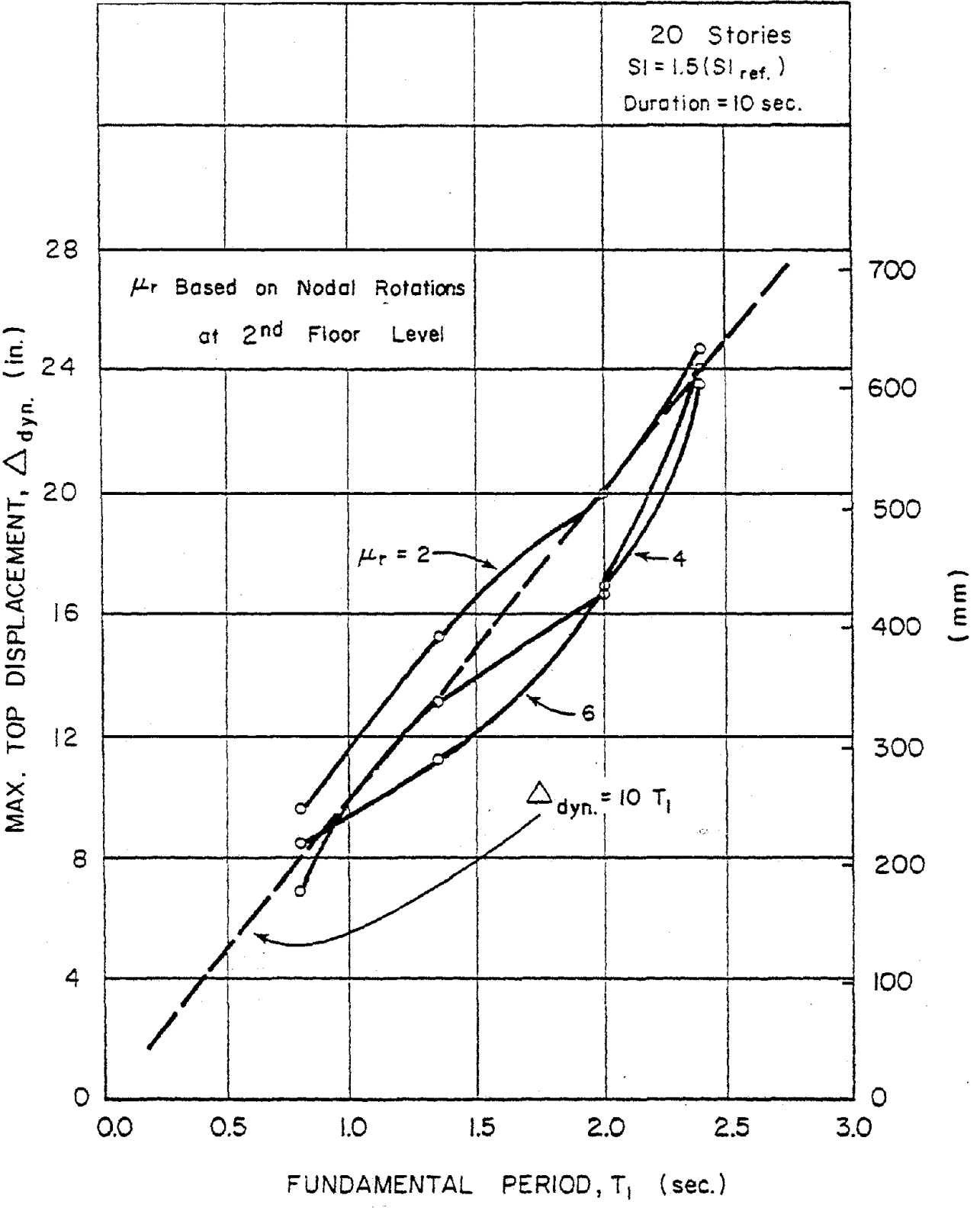

Fig. 45 Maximum Top Displacement as a Function of Fundamental Period, T_1, and Rotational Ductility at Base, μ_r

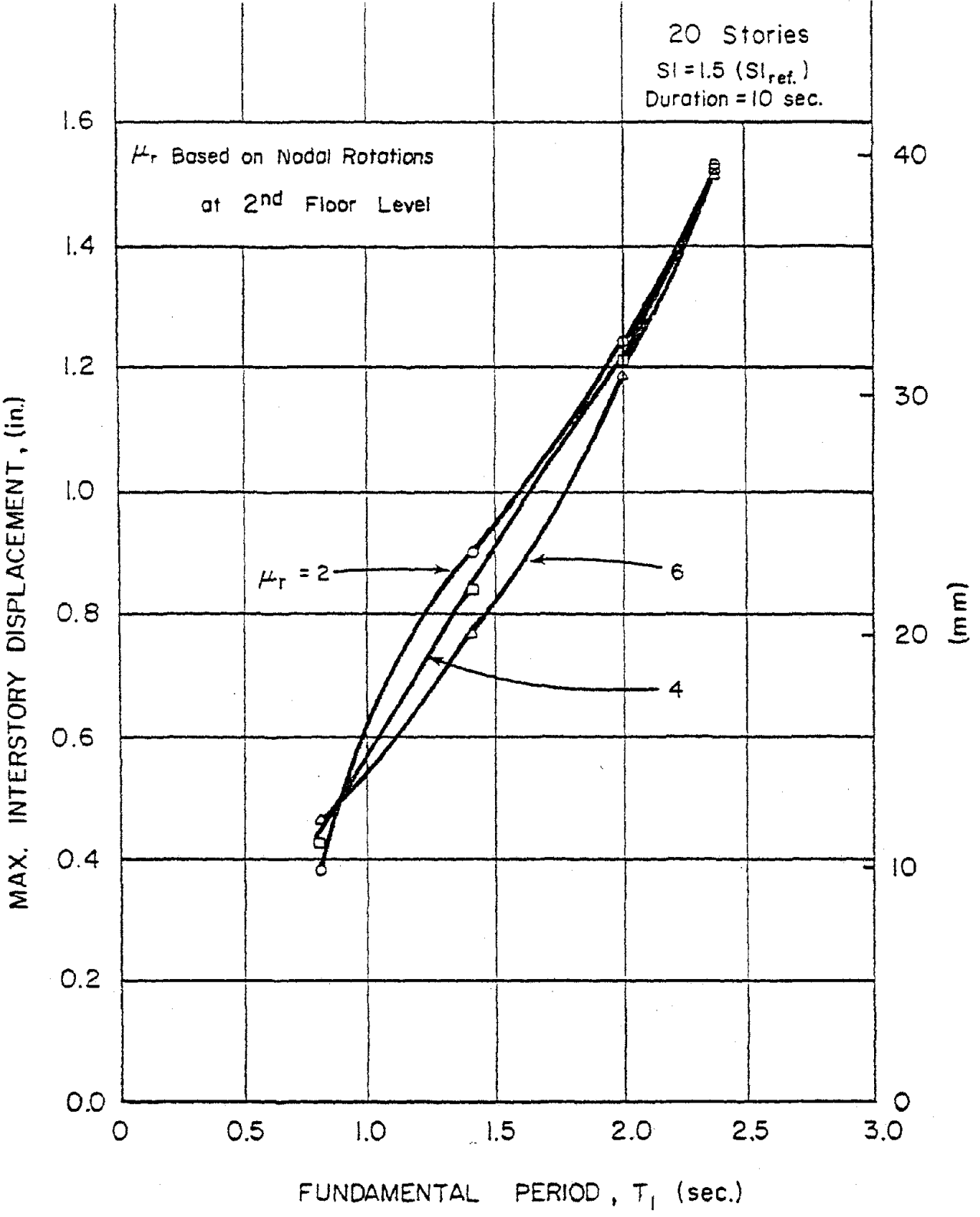

Fig. 46 Maximum Interstory Displacement as a Function of Fundamental Period, T_1, and Rotational Ductility at Base, μ_r

the wall. The figures are for 20-story walls subjected to input motions with intensity SI = 1.5 ($SI_{ref.}$). The clustering of the curves within a narrow band indicates the relative insensitivity of displacements to rotational ductility at the base. These figures and similar ones for other structure heights and earthquake intensities can be used as guides in selecting the appropriate fundamental period, and hence stiffness, of a wall once the tolerable maximum displacement has been selected.

Design Charts for 10-, 30, and 40-Story Walls

Following the same procedure described in the preceding section for 20-story structural walls, flexural and shear design factors were prepared for the other wall heights considered. Charts for these cases are shown in Figs. 47 and 48. The charts for 20-story walls have been reproduced in these figures for completeness.

Integration of Results for Walls of Different Height

Figures 49 and 50 were prepared to permit combining charts for walls of different heights. Each of the first five charts, (a) through (e), in these figures shows plots corresponding to a particular value of rotational ductility, for all wall heights considered. The smooth curves shown in these figures represent approximate averages of the plotted points. The last charts, Figs. 49f and 50f, show the curves for all five rotational ductility values.

Larger scale plots for the flexural and shear design factors, without the data points shown, are given in Figs. 51 and 52. The charts shown in Figs. 47 through 52 correspond to input motions with intensity SI = 1.5($SI_{ref.}$).

The charts of Figs. 51 and 52 show the flexural and shear design factors as functions of the initial fundamental period and the available rotational ductility factor. The latter is

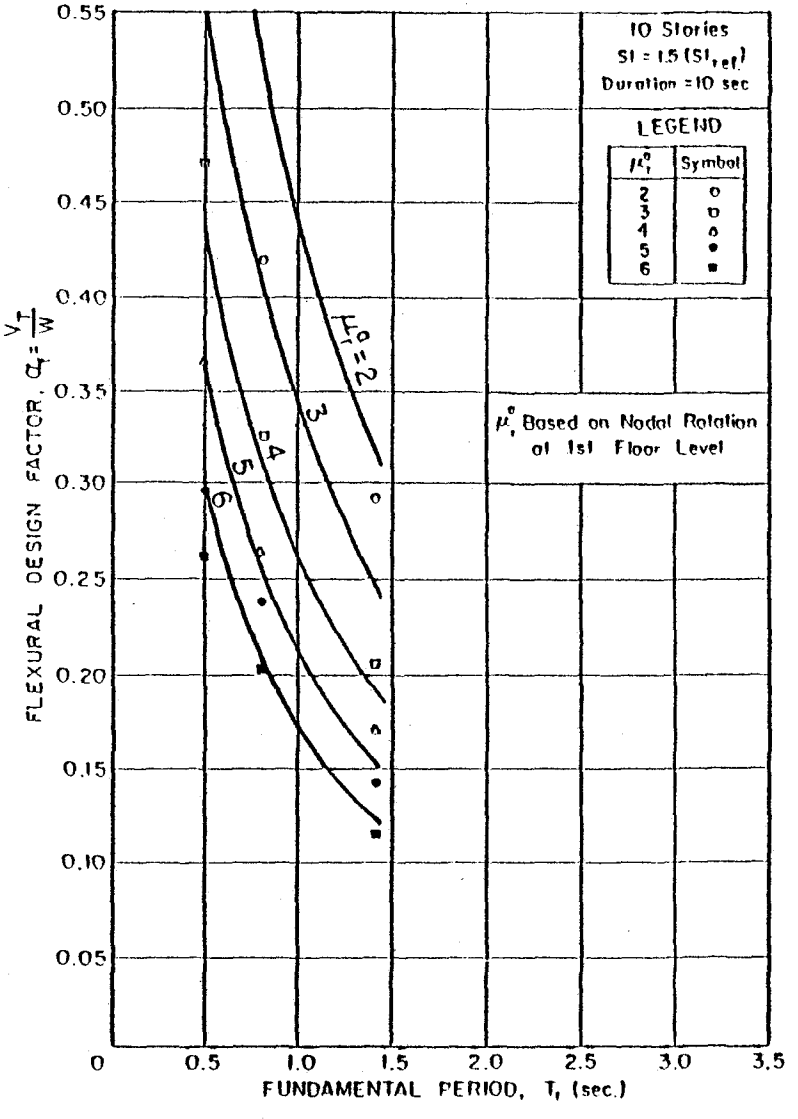

(a)

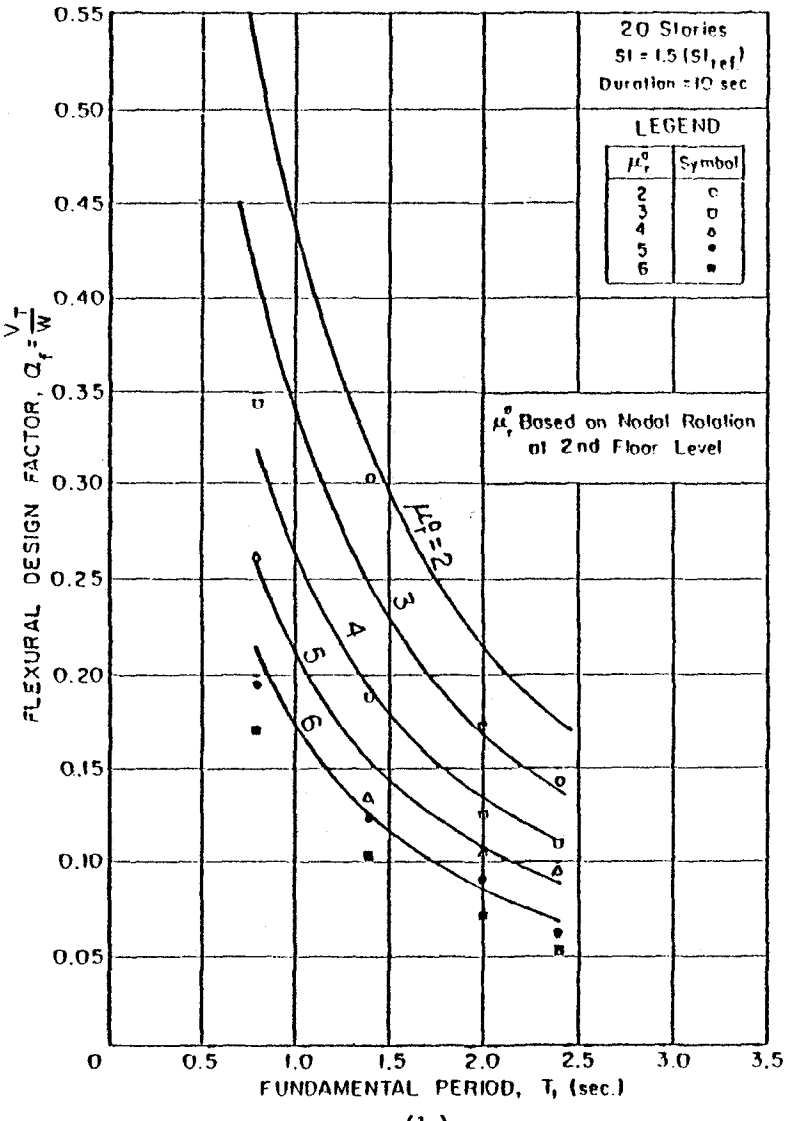

(b)

Fig. 47 Flexural Design Factor, α_f, for Walls of Different Heights

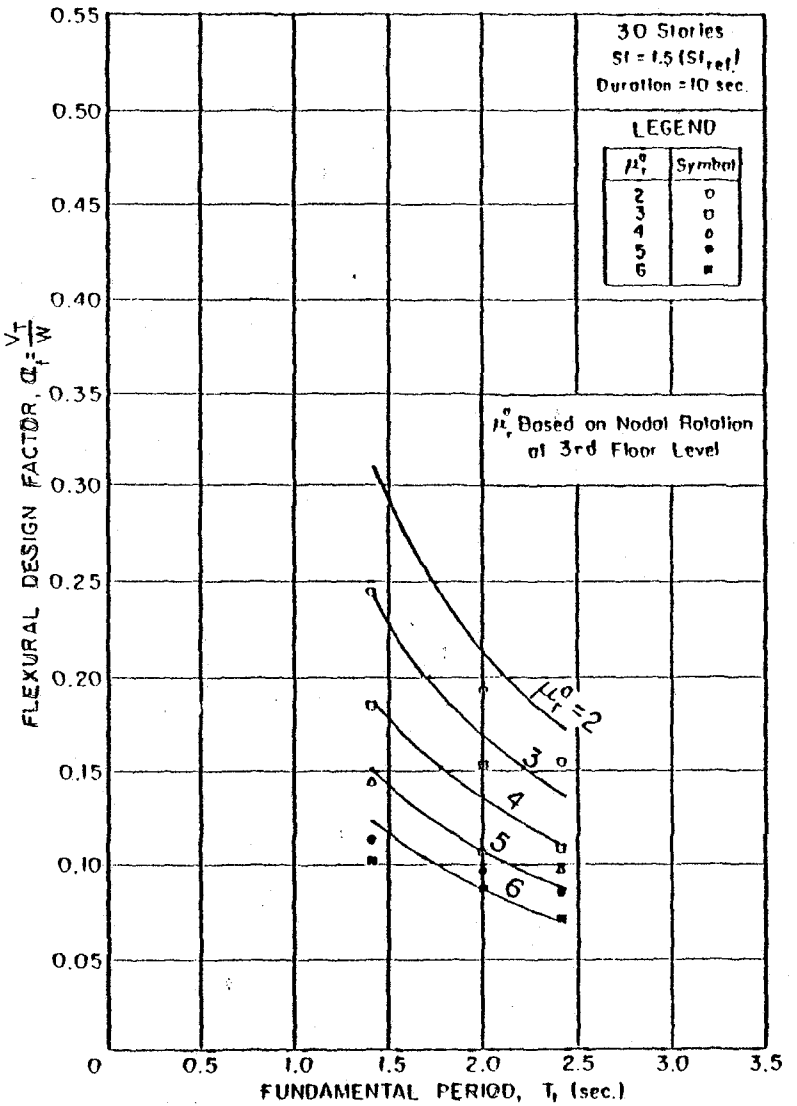

(c)

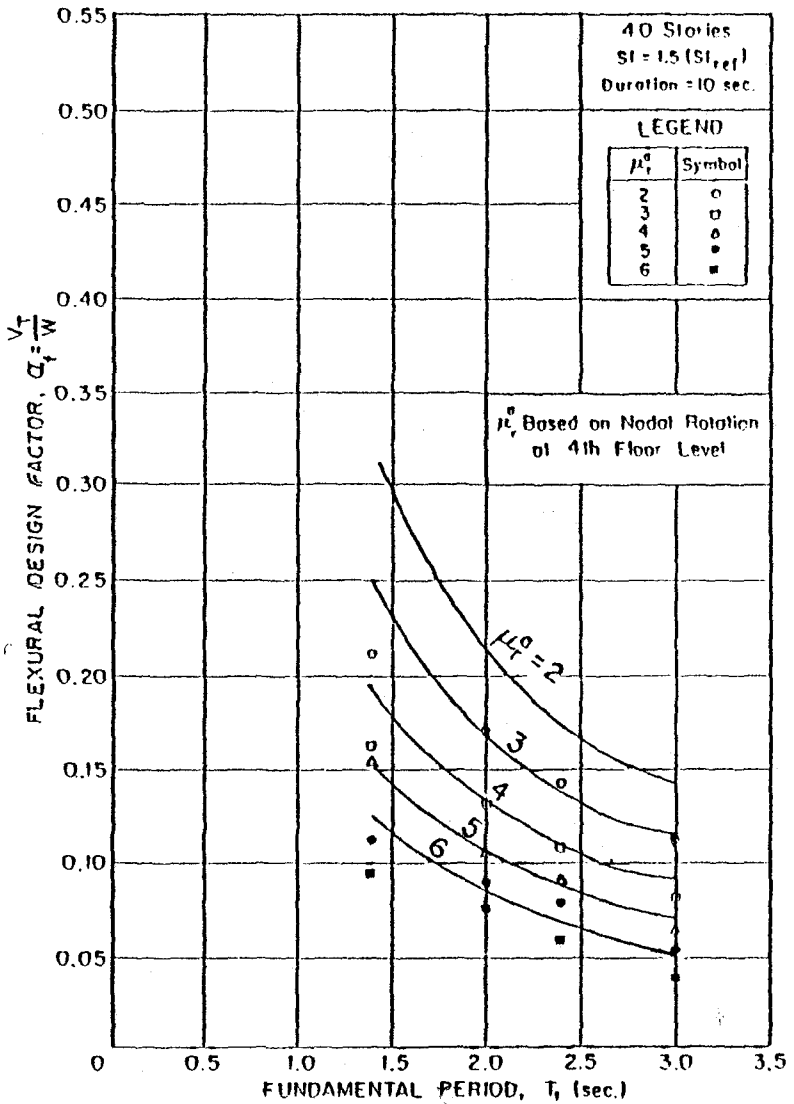

(d)

Fig. 47 (contd.) Flexural Design Factor, α_f, for Walls of Different Heights

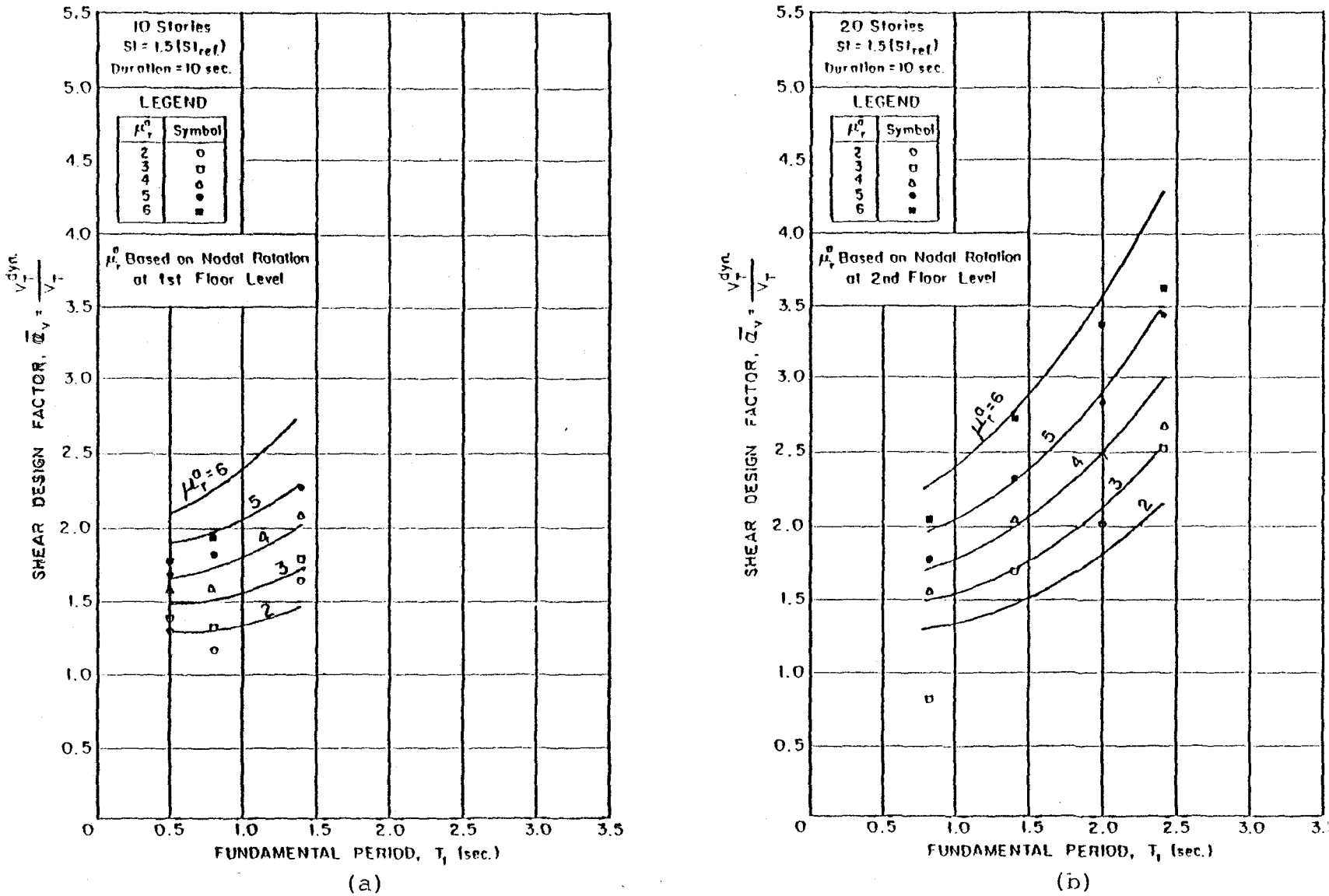

Fig. 48 Shear Design Factor, $\overline{\alpha}_v$, for Walls of Different Heights

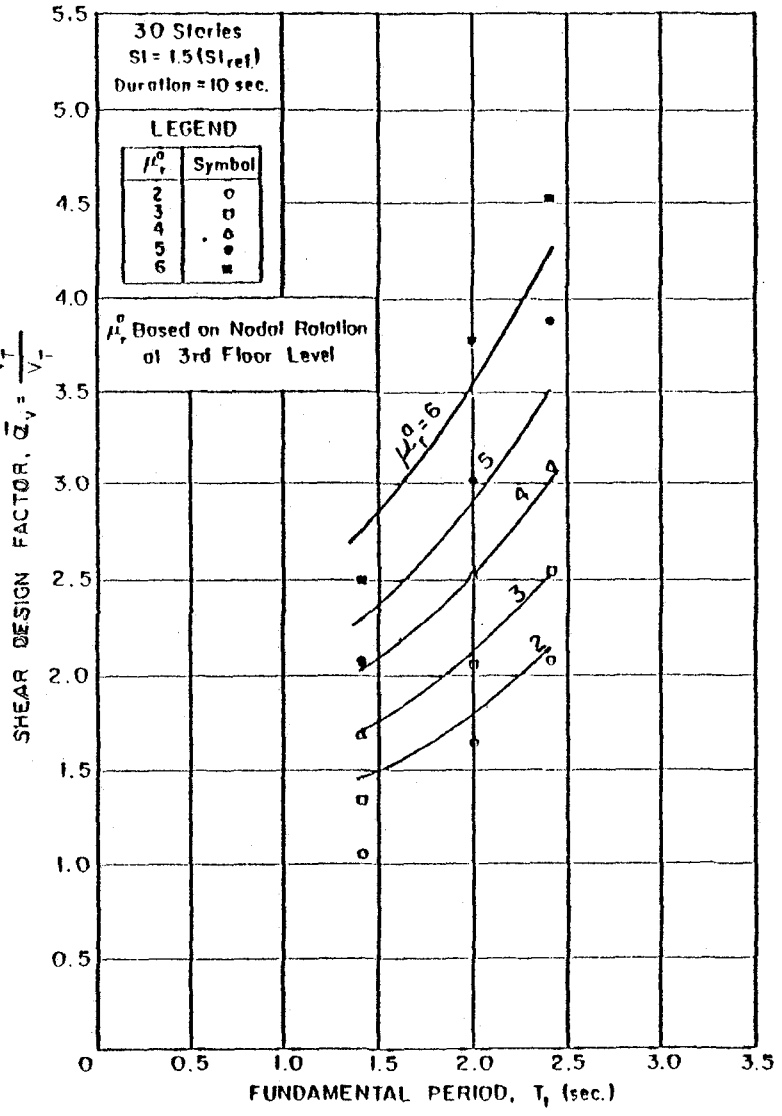

(c)

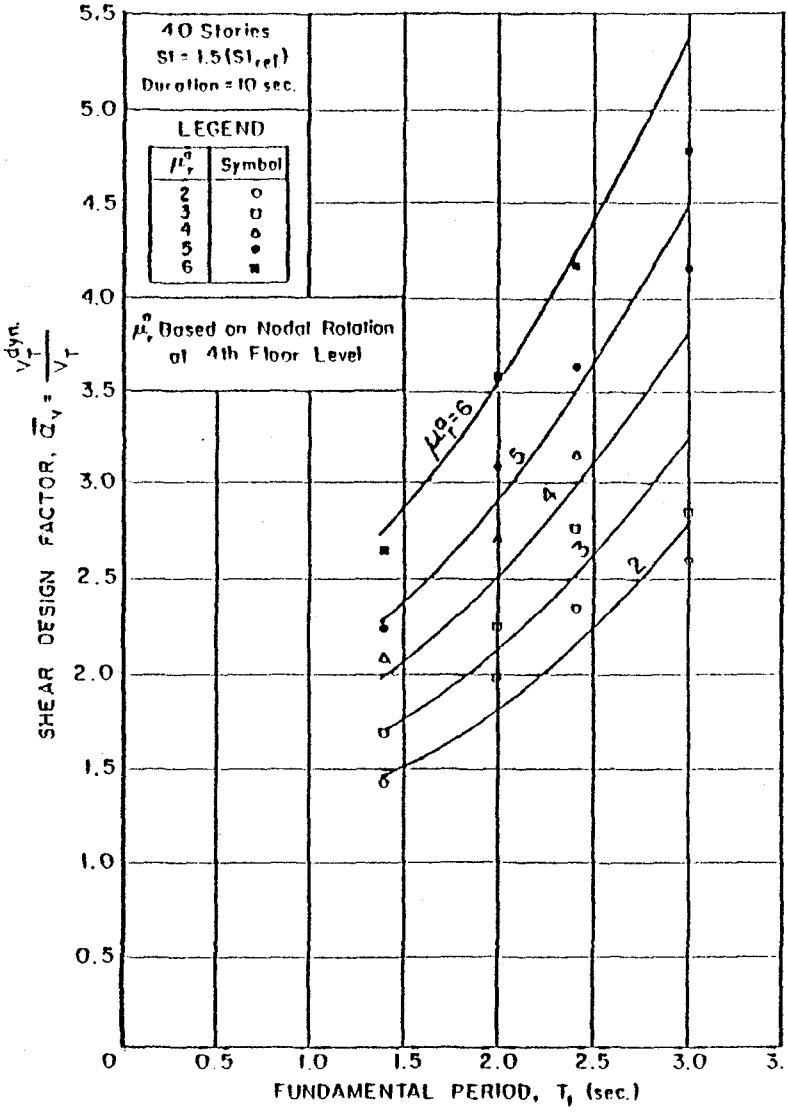

(d)

Fig. 48 (contd.) Shear Design Factor, $\bar{\alpha}_v$, for Walls of Different Heights

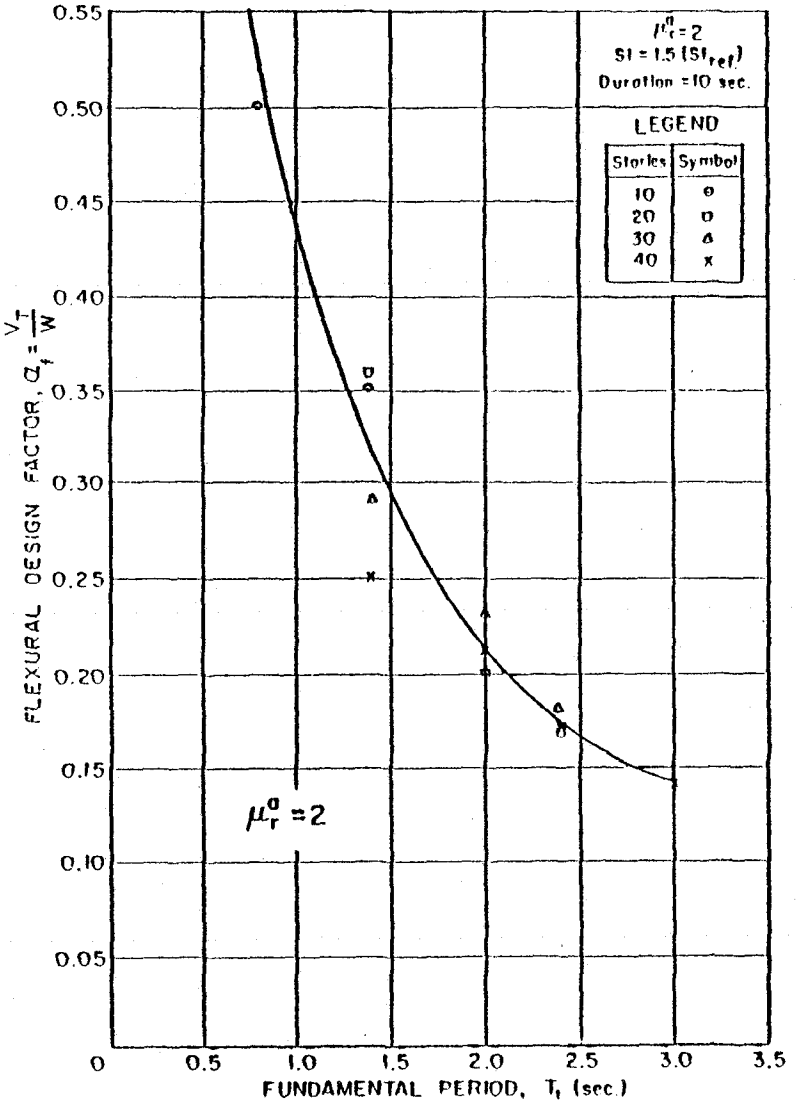

(a)

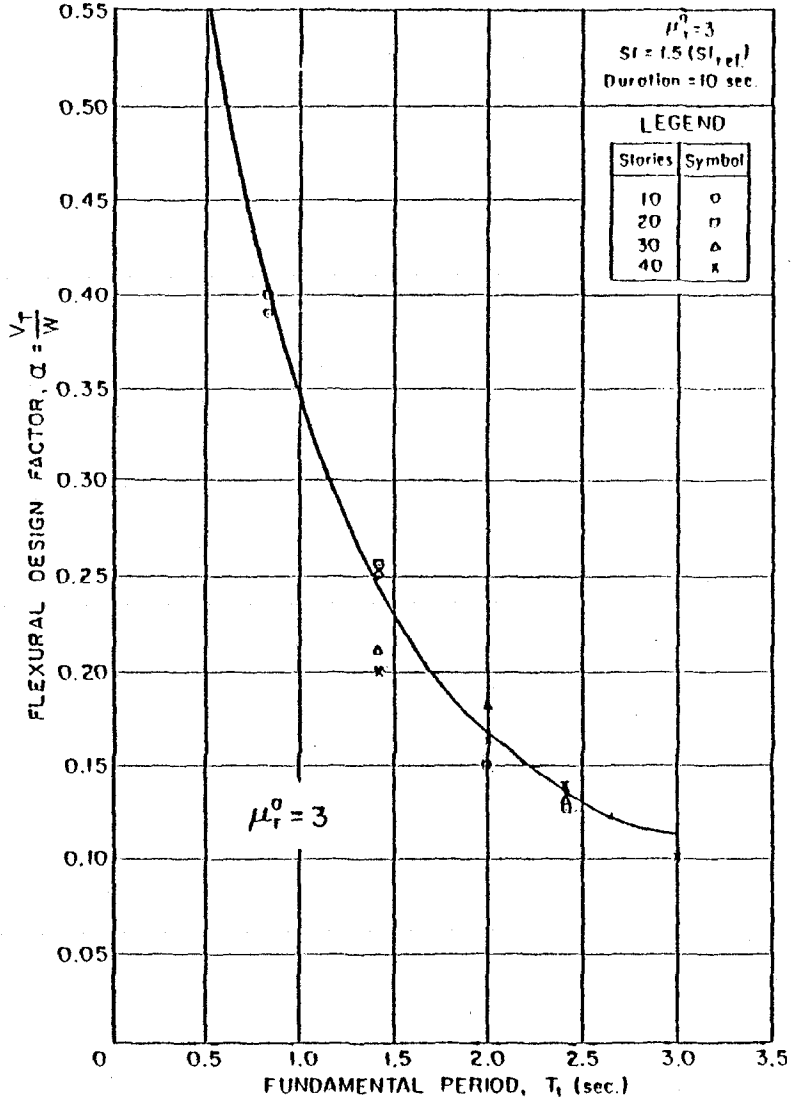

(b)

Fig. 49 Flexural Design Factor, α_f, for Specific Values of Available Rotational Ductility, μ_r^a - 10-40 Story Walls

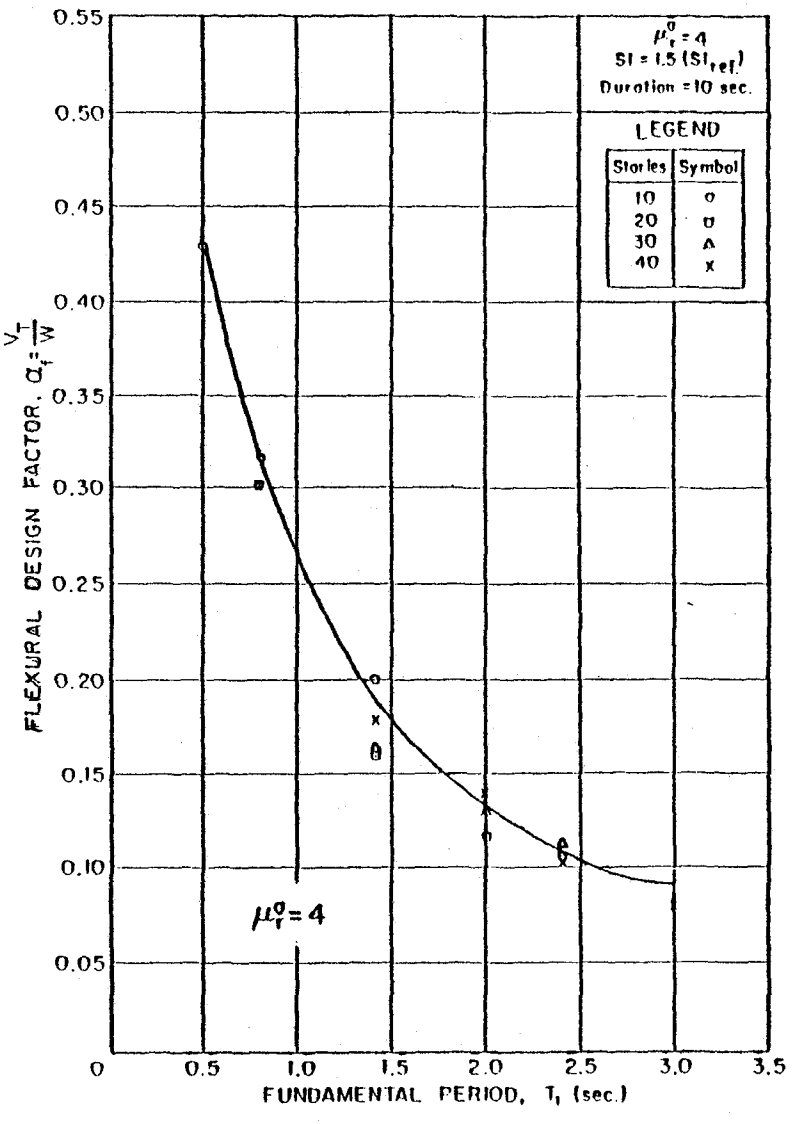

(c)

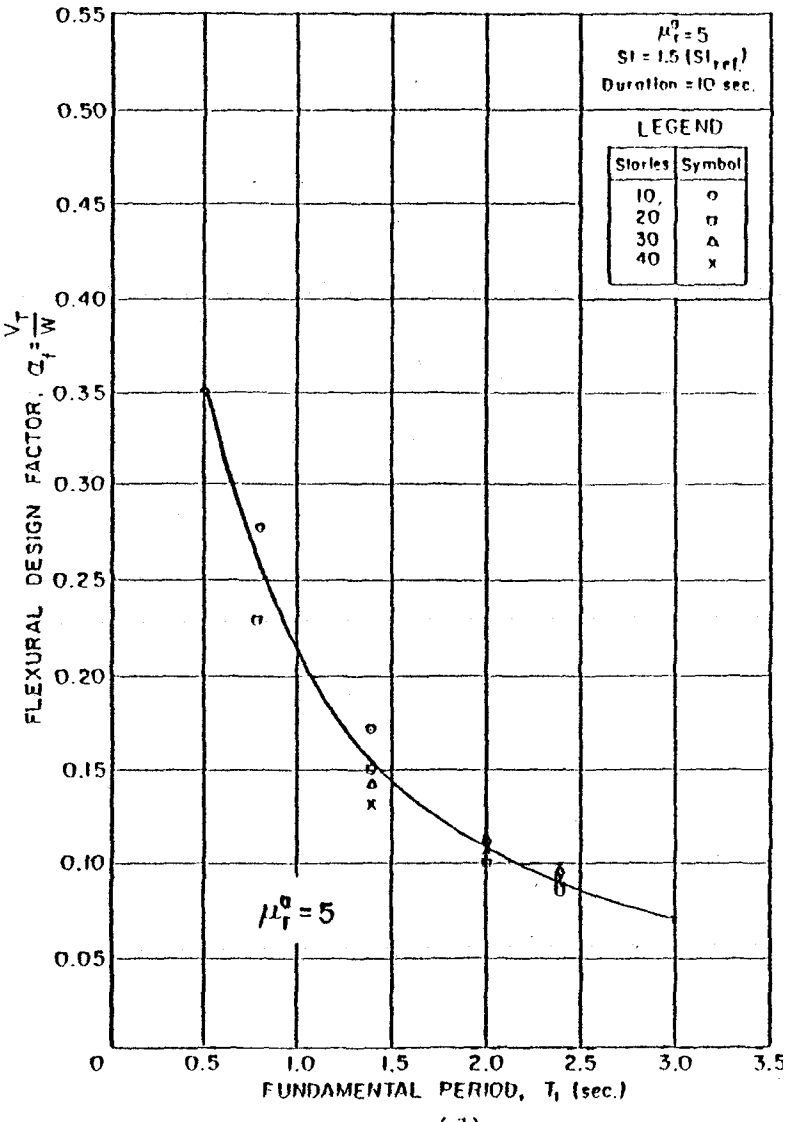

(d)

Fig. 49 (contd.) Flexural Design Factor, α_f, for Specific Values Available Rotational Ductility, μ_r^a - 10-40 Story Walls

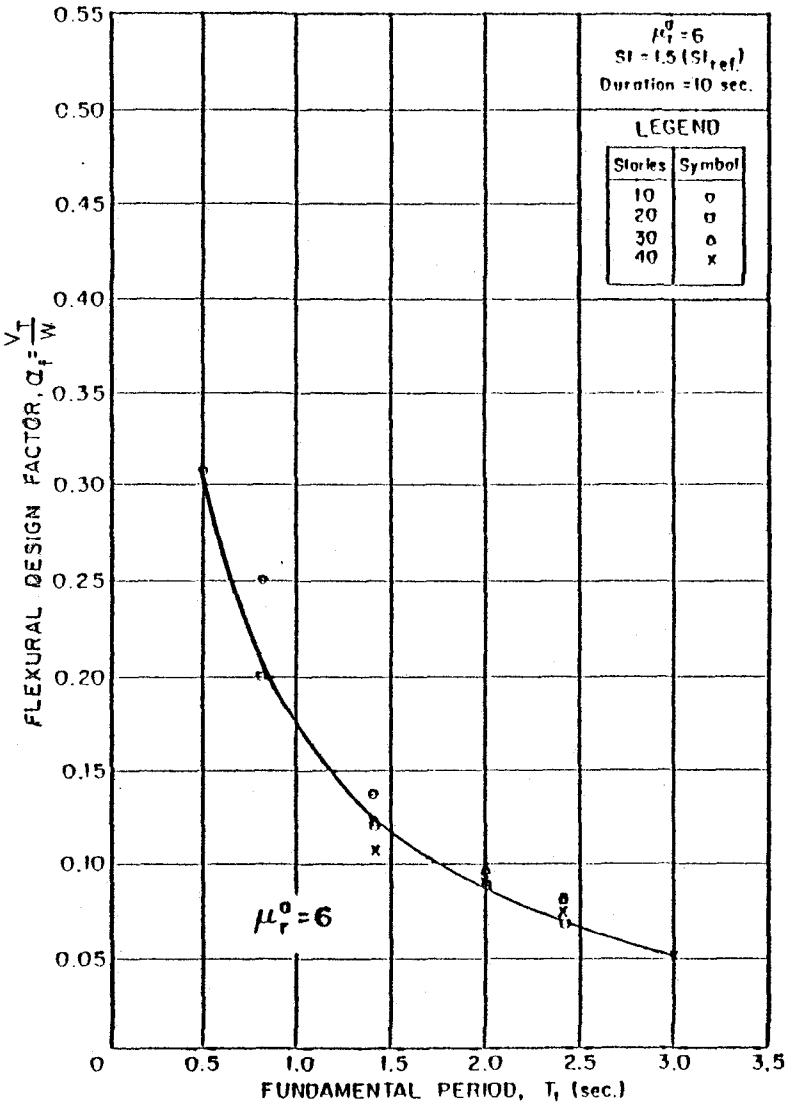

(e)

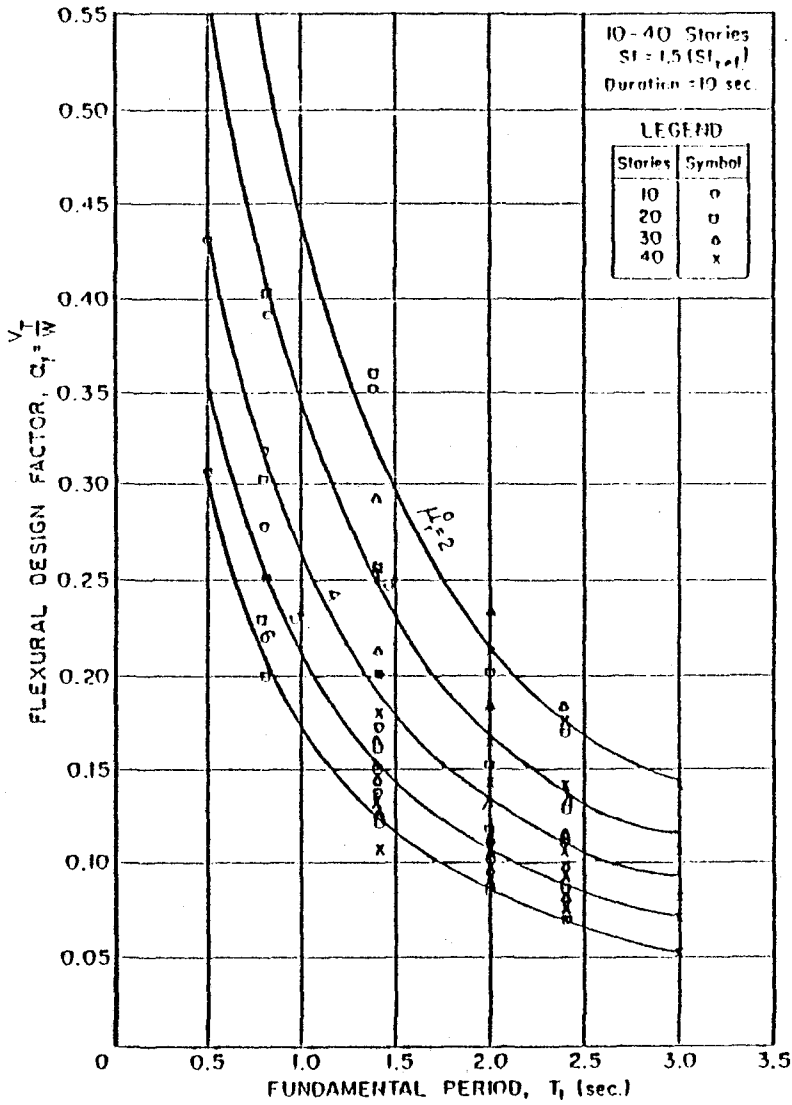

(f)

Fig. 49 (contd.) Flexural Design Factor, α_f, for Specific Value of Rotational Ductility, μ_r^a - 10-40 Story Walls

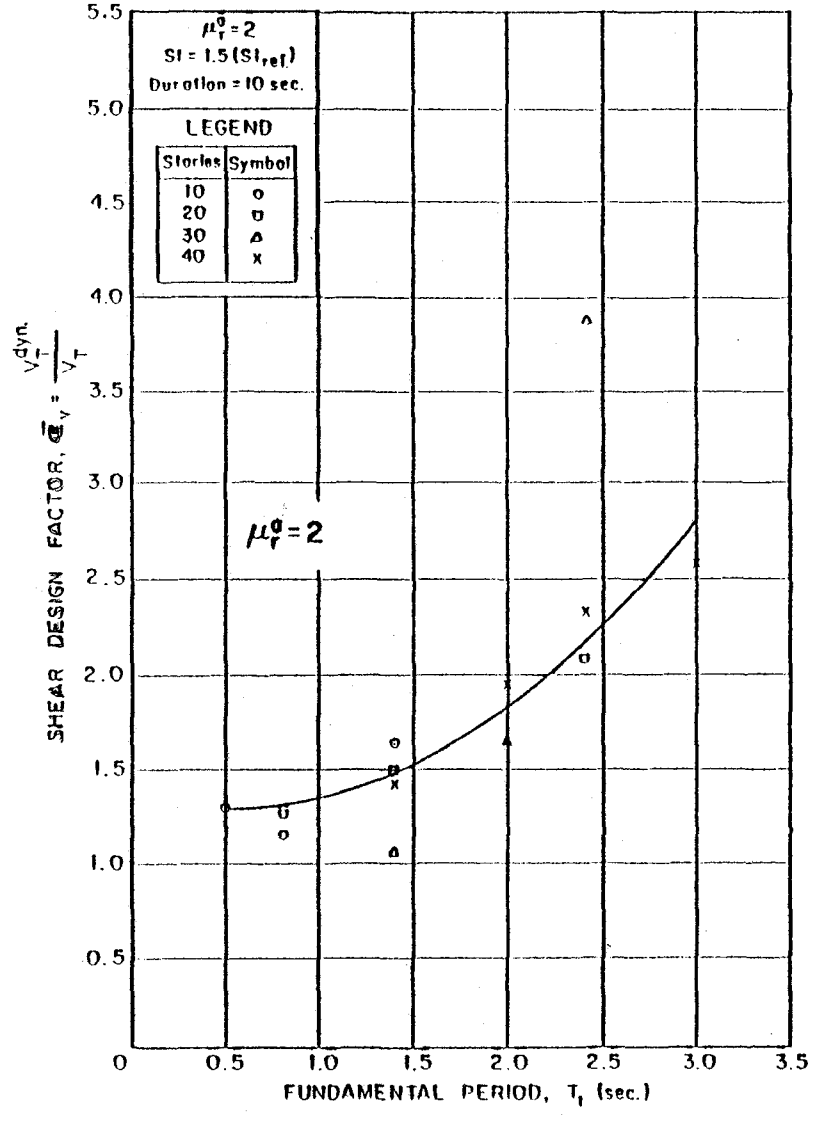

(a)

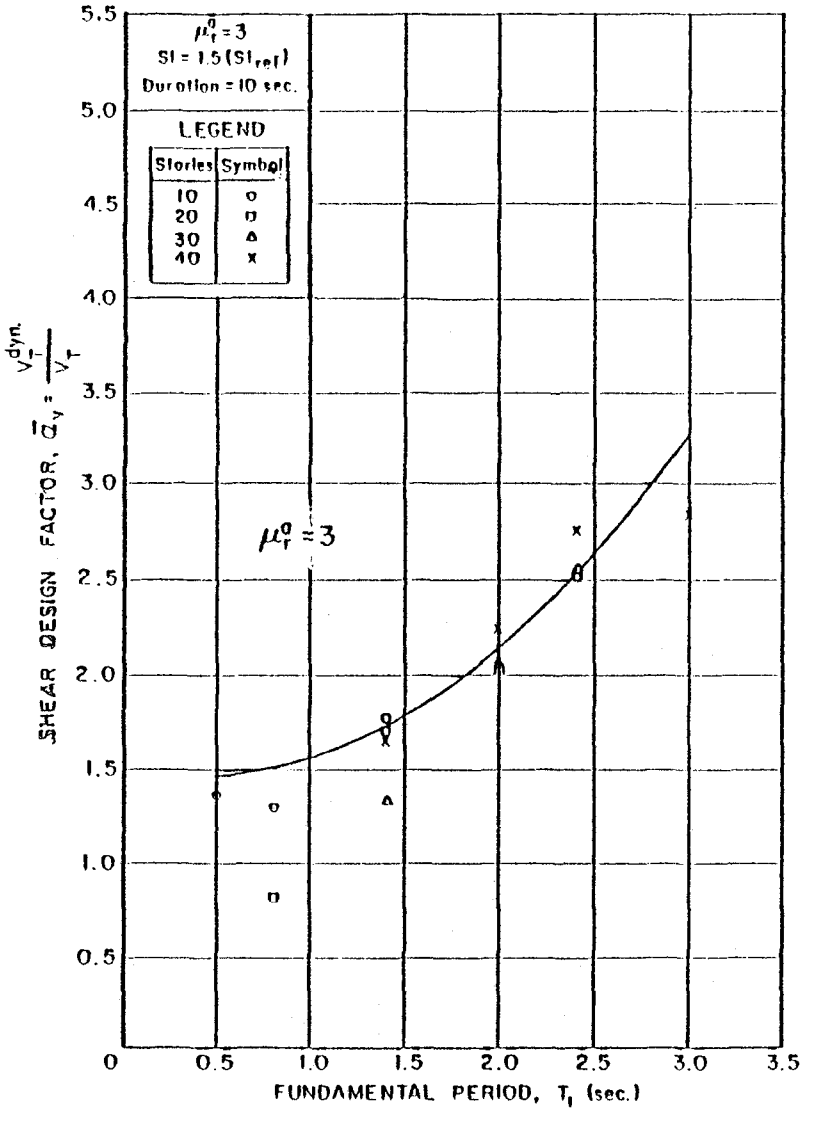

(b)

Fig. 50 Shear Design Factor, $\bar{\alpha}_v$, for Specific Values of Available Rotational Ductility, μ_r^a - 10-40 Story Walls

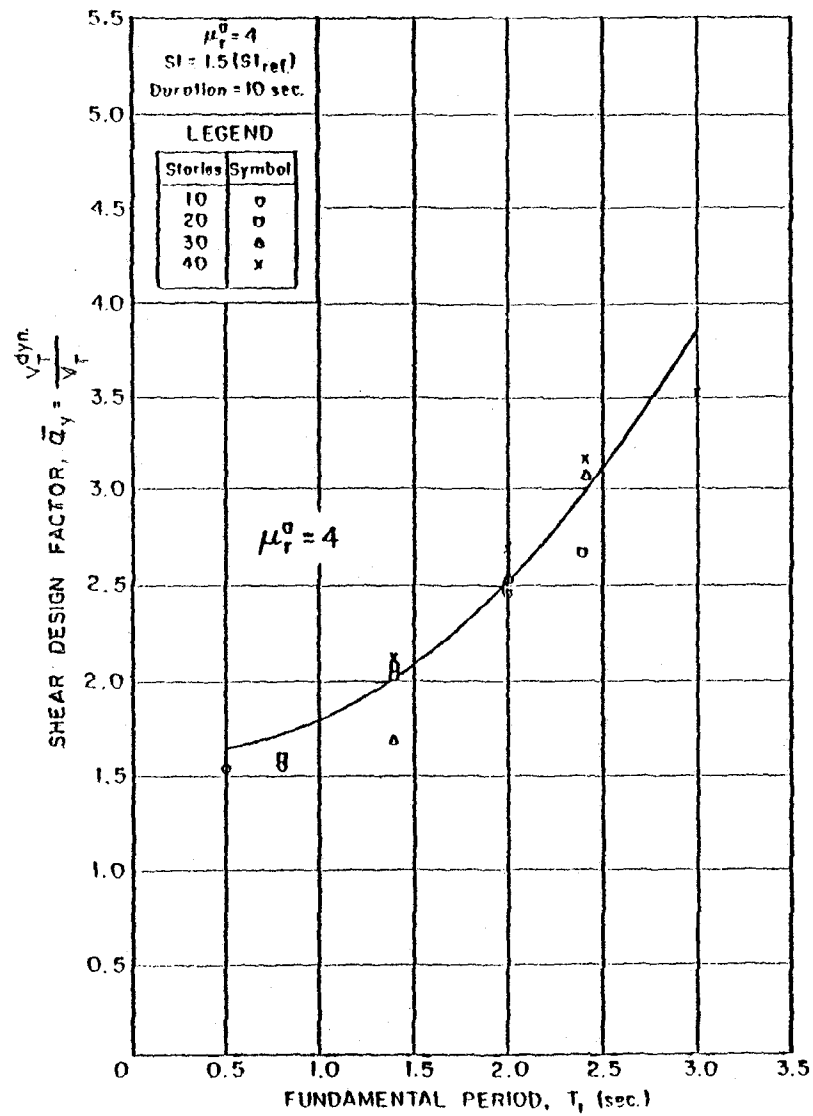

(c)

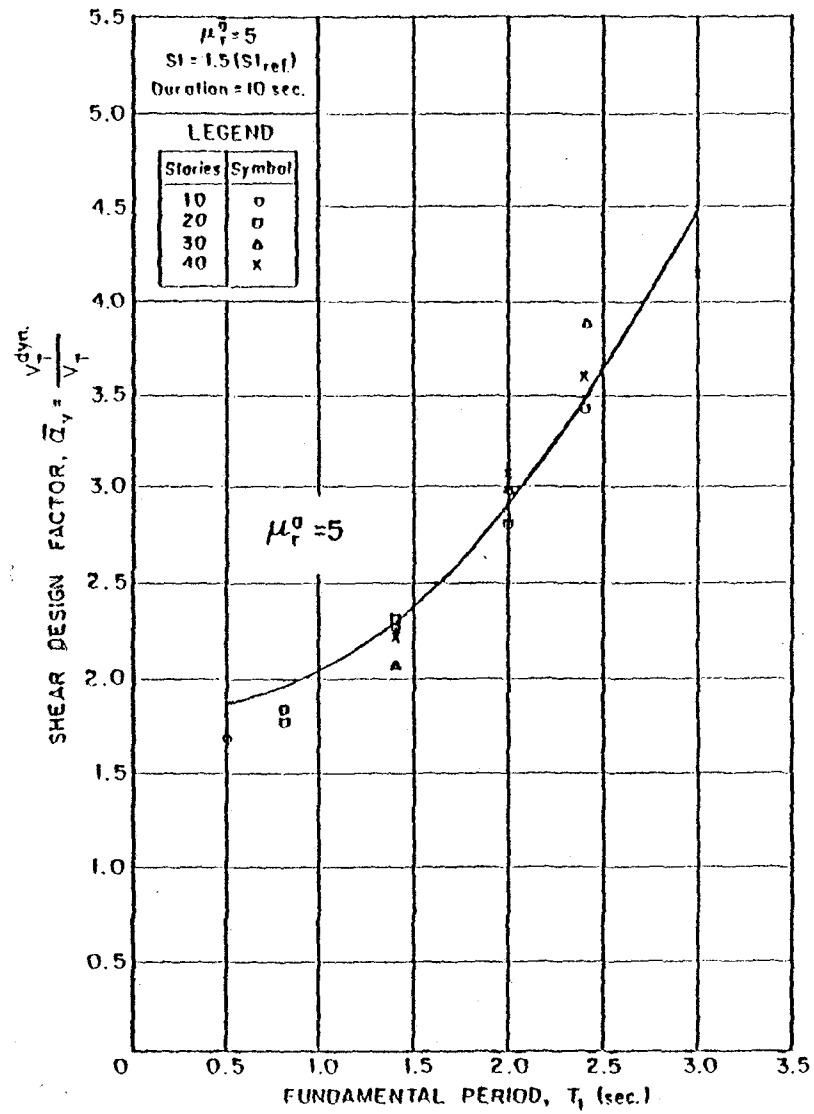

(d)

Fig. 50 (contd.) Shear Design Factor, $\bar{\alpha}_v$, for Specific Values of Available Rotational Ductility, μ_r^a - 10-40 Story Walls

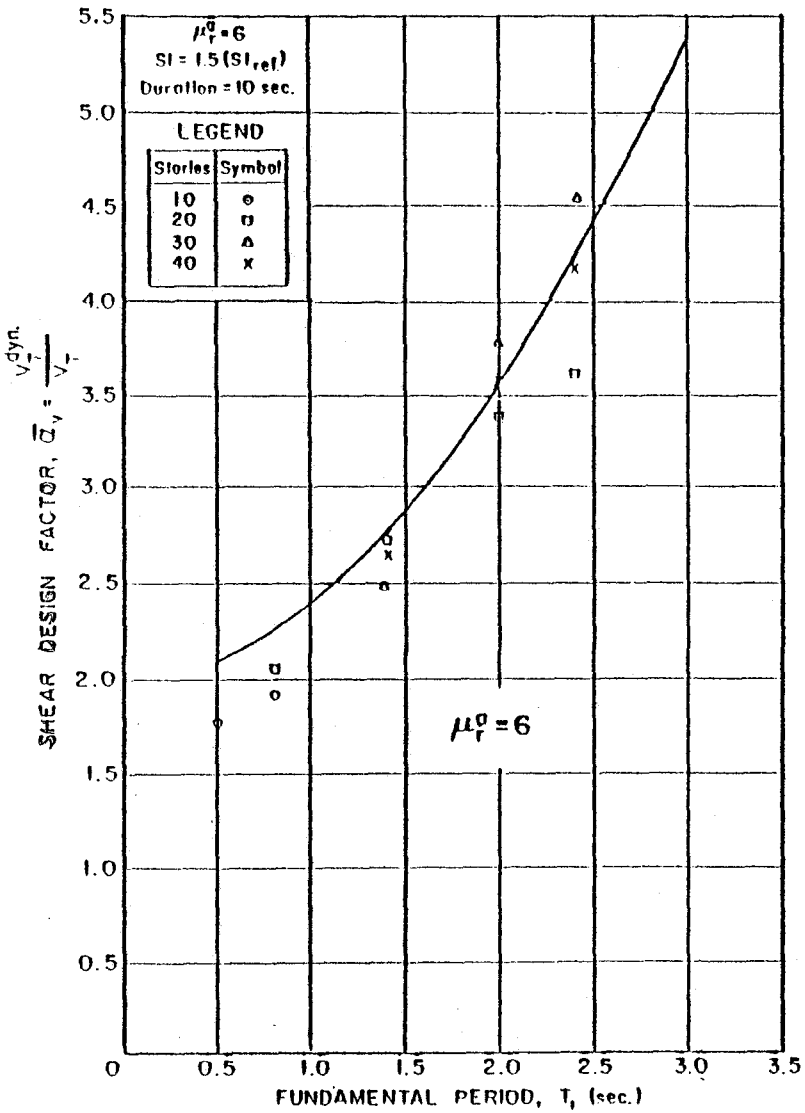

(e)

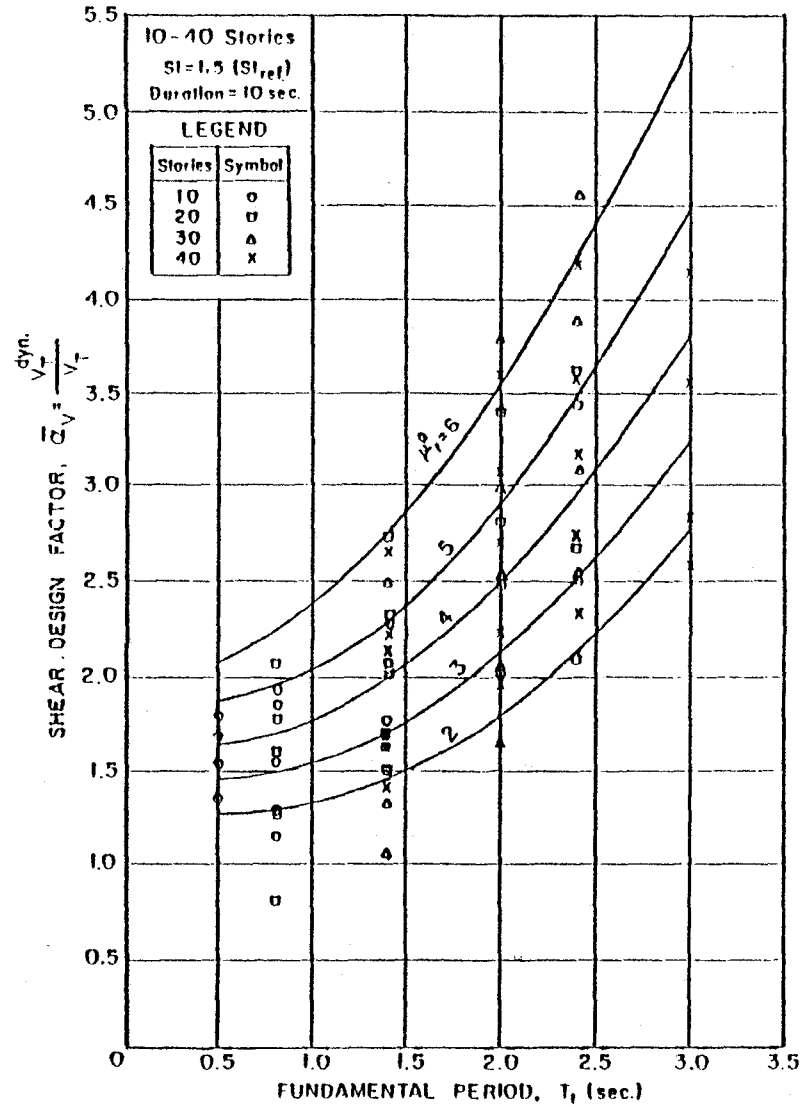

(f)

Fig. 50(contd.) Shear Design Factor, $\bar{\alpha}_v$, for Specific Values of Available Rotational Ductility, μ_r^a - 10-40 Story Walls

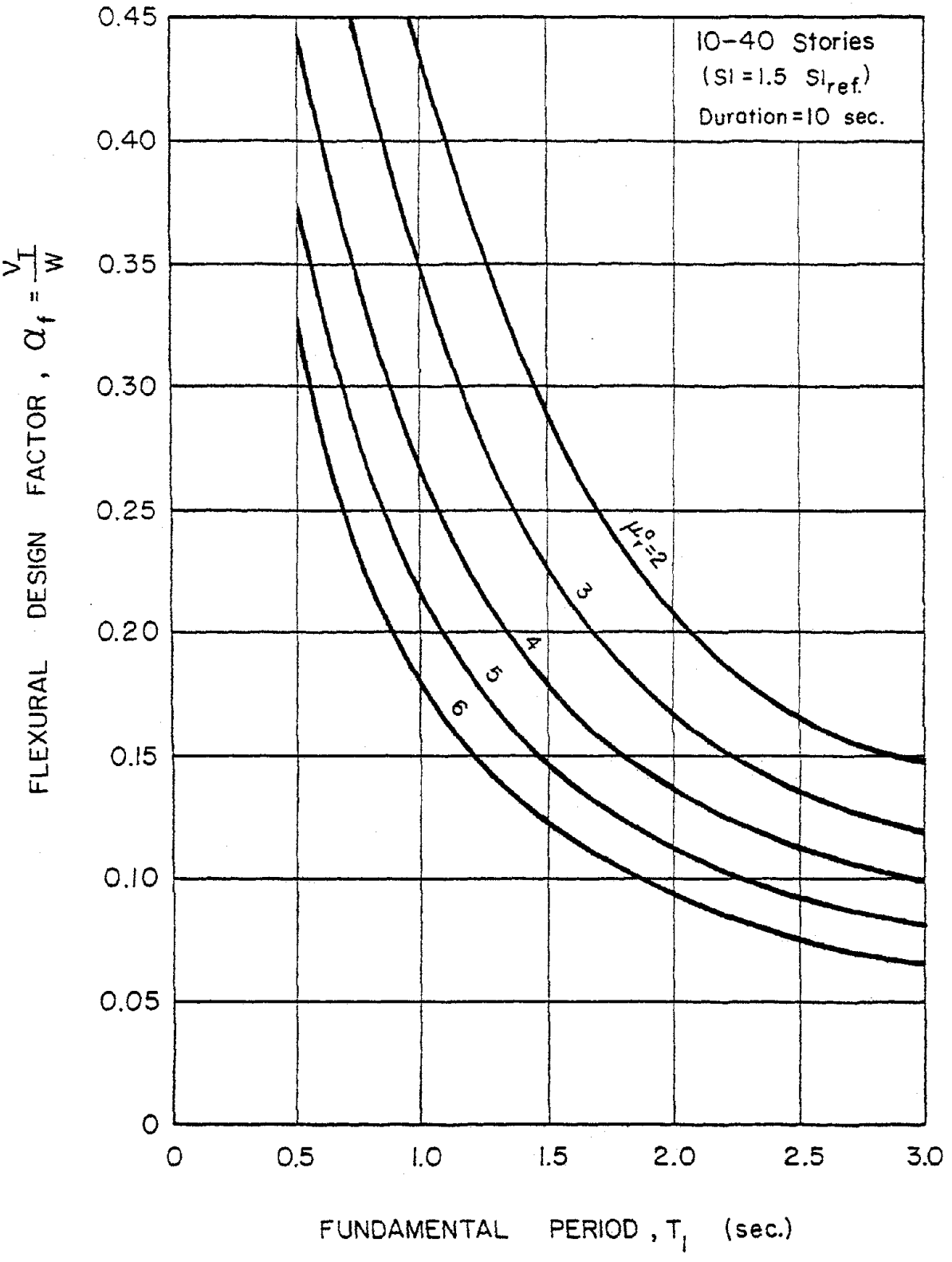

Fig. 51 Flexural Design Factor, α_f, as a Function of Fundamental Period, T_1, and Available Rotational Ductility, μ_r^a
10- 40 Story Walls

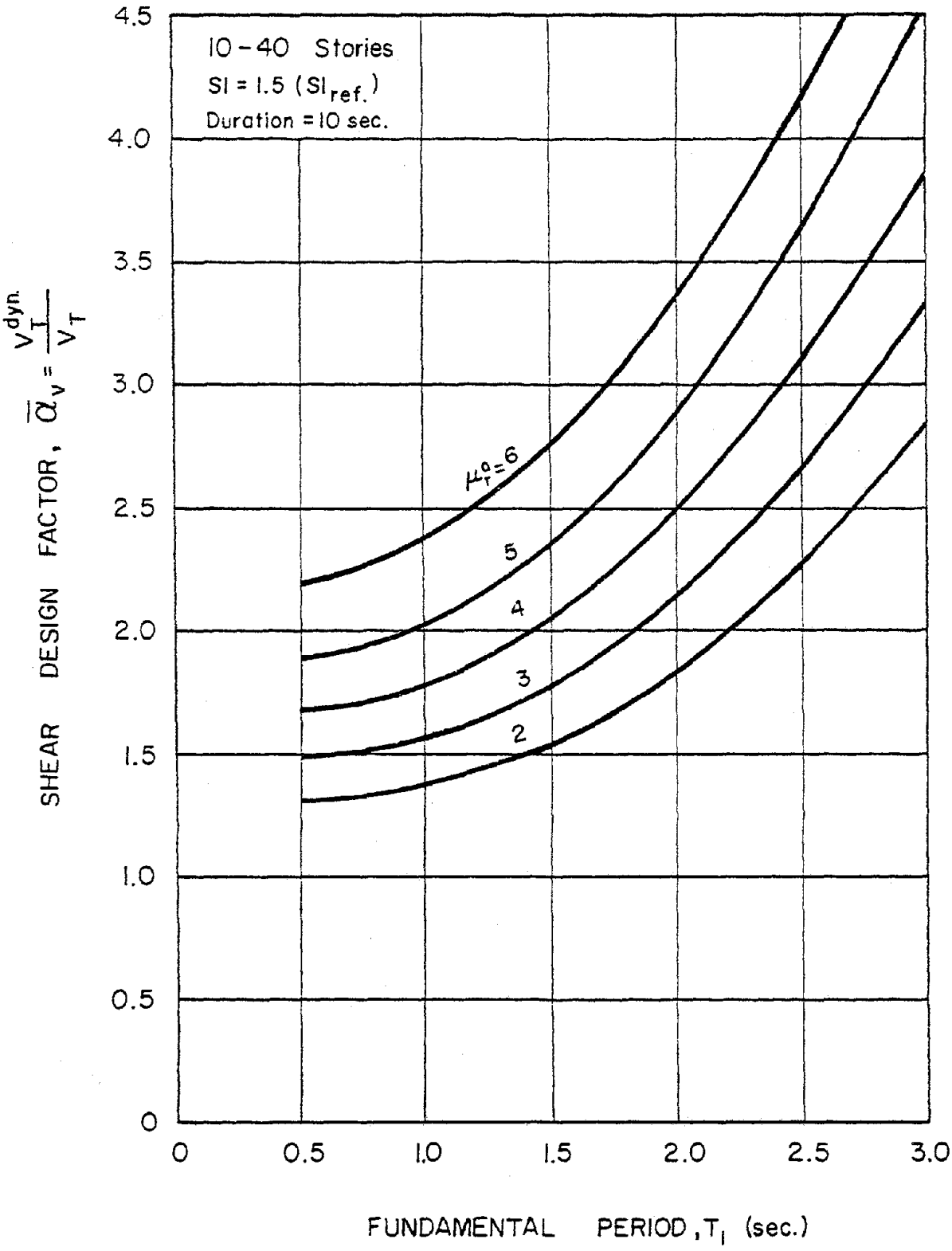

Fig. 52 Shear Design Factor, $\bar{\alpha}_v$, as a Function of Fundamental Period, T_1, and Available Rotational Ductility, μ_r^a 10-40 Story Walls

directly related to the flexural yield level of a structure. Both charts are for a ground motion intensity SI = 1.5 ($SI_{ref.}$), the reference intensity ($SI_{ref.}$) being that of the N-S component of the 1940 El Centro record. These charts reflect the effects on design force levels of the most significant structural parameters, for a specific ground motion intensity.

To complement the design information provided in Figs. 51 and 52, data on maximum interstory and top displacements for walls ranging in height from 10 to 40 stories are summarized in Figs. 53 and 54. The displacements are plotted against fundamental period. They are given in terms of absolute values and as ratios of displacement to total height (in the case of top displacement) or to story height (for interstory displacements).

Figure 53a gives the absolute value of the top displacement while Fig. 53b shows this in terms of its ratio to the wall height, Δ_t/H. A single least-squares-fit line appears to adequately represent the variation of the critical top displacement with fundamental period in 53a. When expressed as a ratio, Δ_t/H, however, a distinction between the top displacements corresponding to the different wall heights is indicated by the four least-squares-fit lines shown in Fig. 53b.

For the critical interstory displacement, distinct least-squares-fit lines correspond to each wall height. This occurs for both absolute interstory displacements as well as for the ratio of interstory displacement to story height, Δ_i/h, as shown in Figs. 54a and 54b.

In generating data for Figs. 51 through 54, other variables characterizing the structure were held constant. The constant values assumed for these other parameters were those considered as averages for the normal range of variation of each parameter. The values of these constant parameters are as follows:

Yield stiffness ratio, $r_y = 0.05$

Parameters characterizing hysteretic loop (see Fig. 4b):

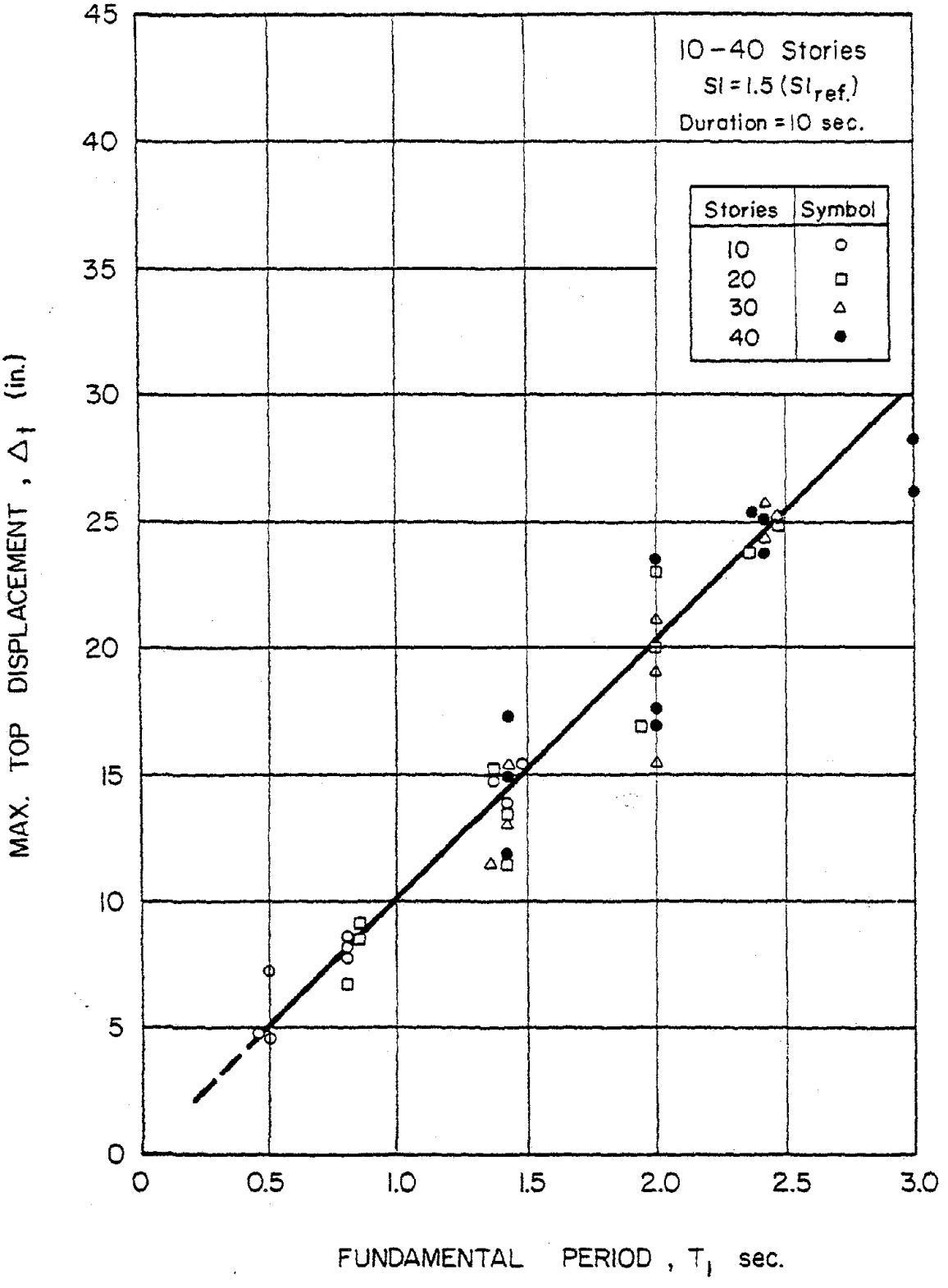

Fig. 53a Maximum Top Displacement, Δ_t, as a Function of Fundamental Period, T_1, - 10-40 Story Walls

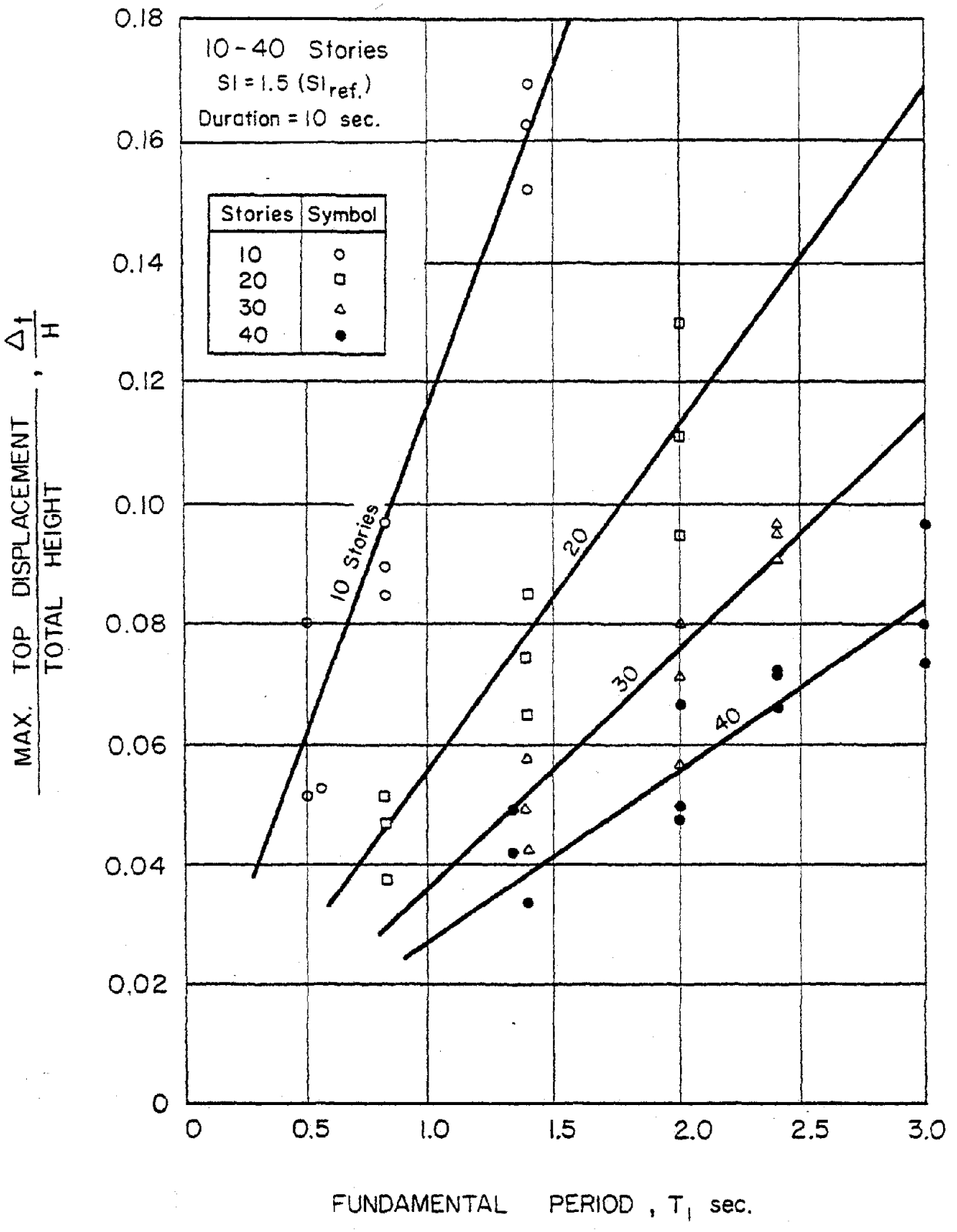

Fig. 53b Ratio Δ_t/H as a Function of Fundamental Period, T_1
10-40 Story Walls

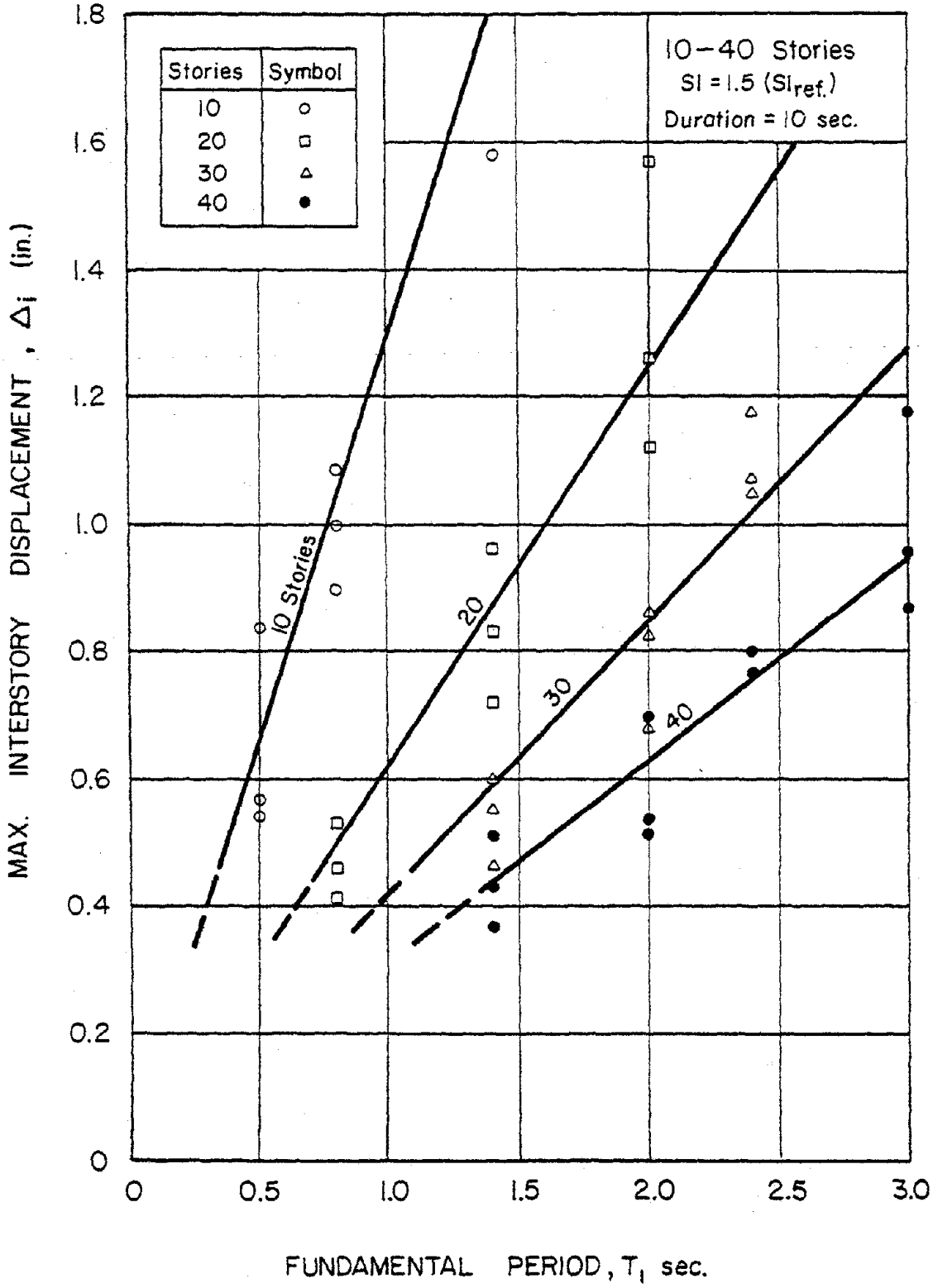

Fig. 54a Maximum Interstory Displacement, Δ_i, as a Function of of Fundamental Period, T_1, - 10-40 Story Walls

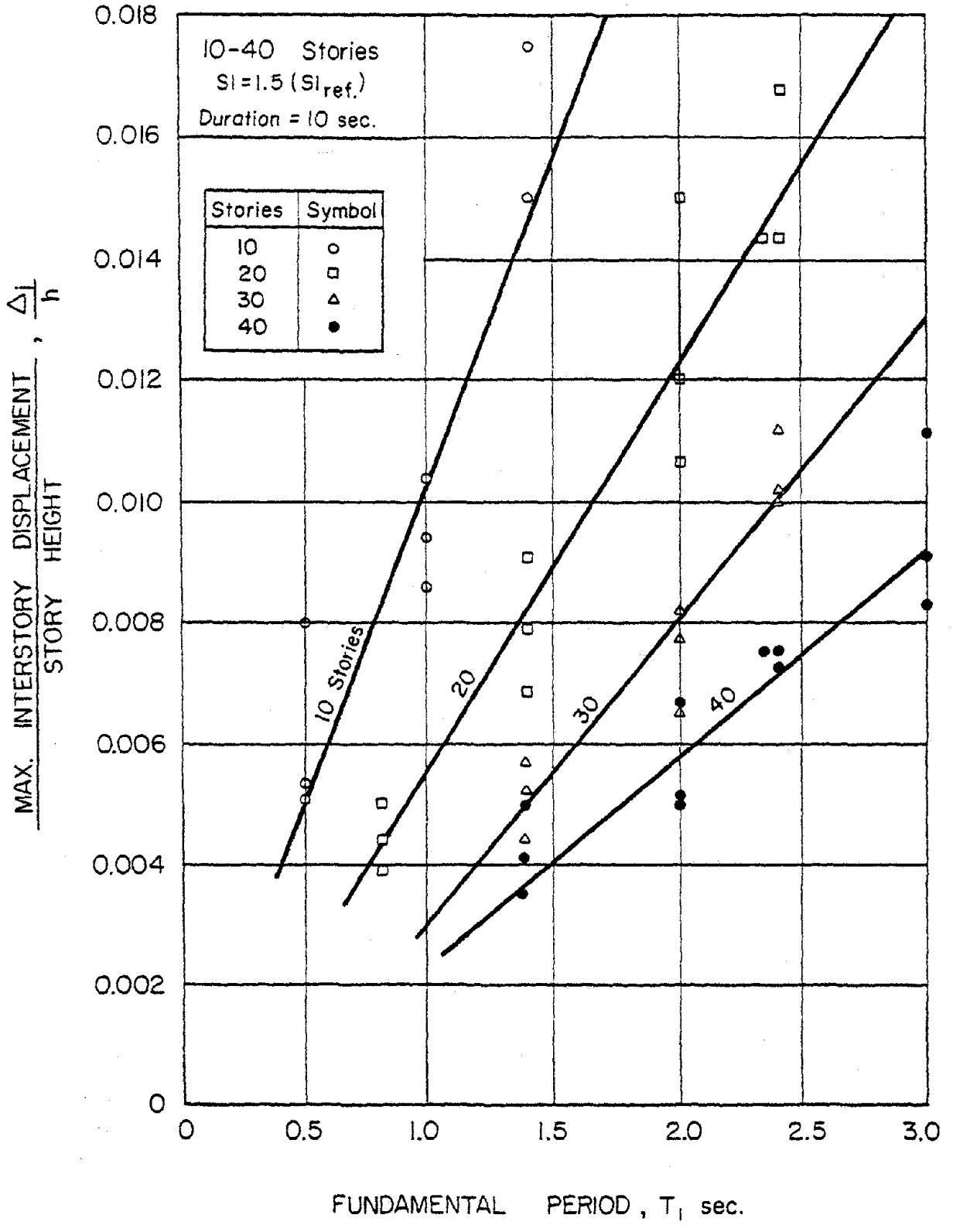

Fig. 54b Ratio Δ_i/h as a Function of Fundamental Period, T_1
10-40 Story Walls

Unloading parameter, α = 0.10
Reloading parameter, β = 0

Viscous damping coefficient
(for first and second modes) = 0.05

Uniform stiffness throughout height of wall

Strength (M_y) uniform throughout height
except for adjustments to reflect effect
of axial load due to dead weight

Wall fully fixed at base

Response of a structure characterized by parameters different from those indicated above, may differ from the calculated response used to prepare Figs. 51 and 52. However, based on results of the parametric studies reported in Ref. 7, it is believed that for most practical cases the values obtained from Fig. 51, 52 and similar charts will be conservative.

A method of adjusting for differences between mass of a particular structure and mass of the structures used for Figs. 51 and 52 is discussed in the following section.

Adjusting Flexural Design Factor for Difference in Mass

Variation in fundamental period of structures considered in preparing Figs. 51 and 52 was obtained by varying only the effective stiffness of the walls. For each wall height, the effective mass (corresponding to the weight that would be effective in the lateral motion of the wall) was kept constant. Thus, as shown in Table 3, total weights of 2174 kips, 4374 kips, 6574 kips, and 8774 kips were assumed for the 10-, 20-, 30-, and 40-story walls, respectively.

Where the effective mass of a given structure differs significantly from that of the corresponding structure of the same period considered in developing the data for Figs. 51 and 52 (hereafter referred to as "basic walls") an adjustment in the yield level is necessary. This is because an increase in the effective mass (assuming the same mass distribution along

the height of the wall) will require a corresponding increase in the effective stiffness of the wall to obtain the same fundamental period.

Two structures having the same fundamental period and yield level but with different stiffnesses can be expected to have about the same maximum displacement under a given base excitation. However, because the stiffer structure will have a smaller yield rotation it will register a higher ductility requirement than the more flexible structure for the same maximum displacement or rotation. This is shown in Fig. 55. In order for both structures to have about the same ductility requirement, the yield level and hence the yield rotation of the stiffer structure will have to be increased such that both structures yield at the same rotation.

As an example, if a 20-story wall has an effective mass twice that of the corresponding basic structure of the same period, this would imply that it also has twice the stiffness of the basic wall. If such a wall had the same yield level as the basic wall of the same period it would be expected to have twice the ductility demand associated with the basic wall. For such a wall to have the same required ductility as the basic wall, its strength or yield level would have to be twice that of the corresponding basic wall.

In using Fig. 51 for the above example, the value of α_f obtained from the figure would have to be multiplied by 2.0. This adjustment effectively doubles the strength or yield level of the wall resulting in the same rotational ductility as the basic wall. The flexural design factor would thus have to be multiplied by the ratio of the effective mass of the given wall to that of the corresponding basic wall having the same fundamental period. No adjustments need be made in the value of $\bar{\alpha}_v$.

The masses of 'basic walls' having heights between the four wall heights listed in Table 3 can be estimated by linear interpolation between the closest two basic cases for which masses are given in the table.

T_1 (Wall ①) = T_1 (Wall ②)

Mass (Wall ①) = ½ Mass (Wall ②)

Stiffness (Wall ①) = ½ Stiffness (Wall ②)

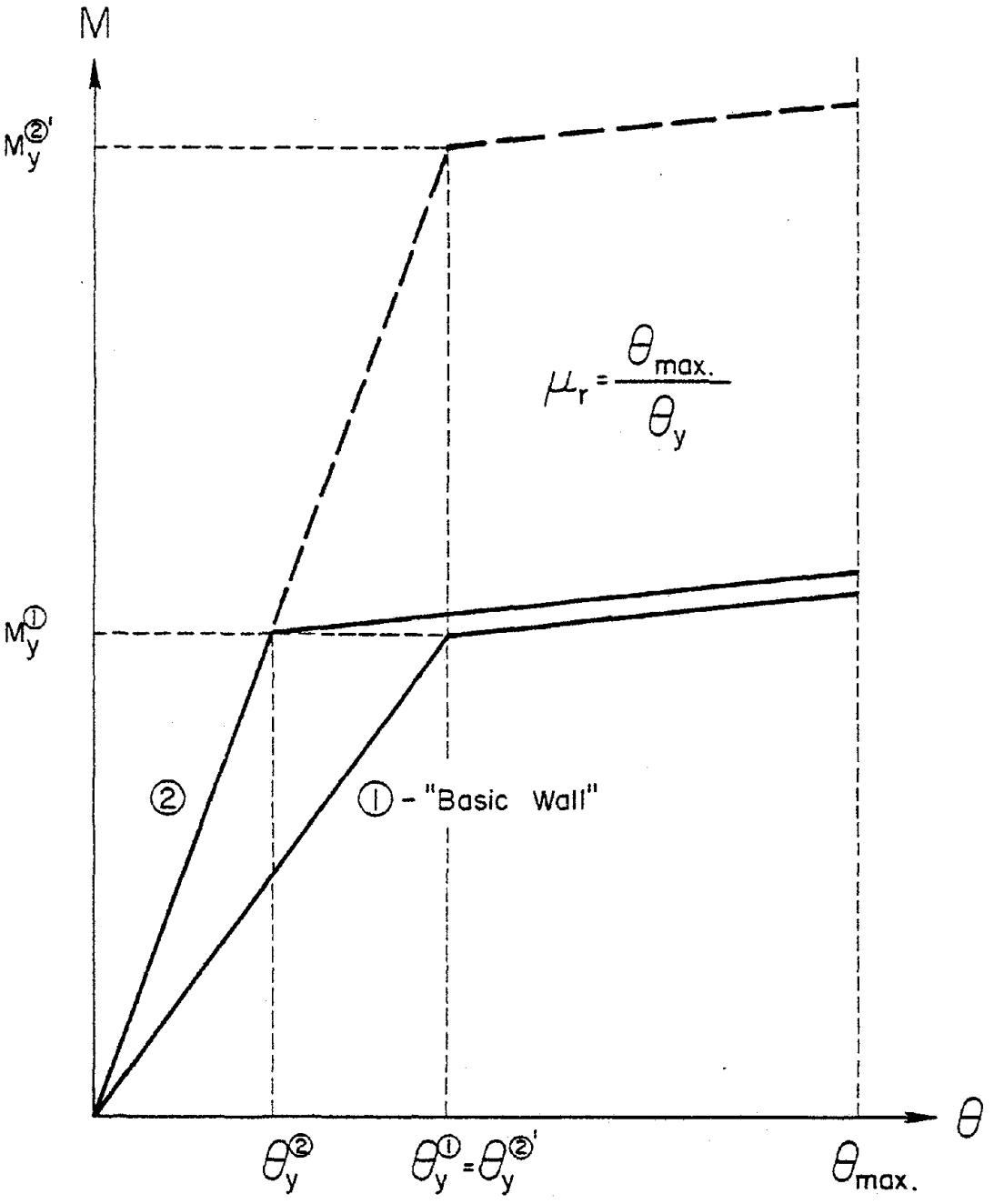

Fig. 55 Adjusting Yield Level of Wall (#2) with Twice the Mass and Stiffness But Same Period as "Basic Wall" (#1)

Critical Response Values for Different Earthquake Intensities

To extend the procedure developed in the preceding sections to a broader class of problems in terms of seismic exposure, analyses were carried out for input motion intensities equal to 0.75 and 1.0 times ($SI_{ref.}$). Results of these analyses, when combined with the extensive data for SI = 1.5($SI_{ref.}$), provide a basis for adjusting the design values developed for 1.5 ($SI_{ref.}$) to obtain values corresponding to a reasonably wide range of input motion intensities.

The additional analyses using input motion intensities other than 1.5 ($SI_{ref.}$) were done only for 20-story walls. Fundamental period values ranging from 0.8 sec. to 2.4 sec. and flexural yield levels from 250,000 in-kips (28,250 k N) to 1,000,000 in-kips (112,980 k N) were considered. Results of these analyses are listed in Tables A15 through A26 of Appendix A. Since the critical input motion corresponding to each parameter combination had already been indentified earlier, only a few of the six input motions considered earlier were used for these supplementary analyses.

Critical values of maximum top displacement, maximum bending moment, maximum base shear, and rotational ductility for walls with different yield levels are shown in Figs. 56 and 57. The curves in Fig. 56 correspond to an input motion intensity SI = 0.75($SI_{ref.}$), while those in Figs. 57 are for SI = 1.0($SI_{ref.}$).

Critical response values corresponding to the three input motion intensities considered, for the case of walls with yield level M_y = 750,000 in-kips (84,740 kN m), are shown in Fig. 58. The earthquake intensity ratio, $\overline{SI}$, in Fig. 58 represents the ratio of the spectrum intensity, SI, of a particular input motion to the reference spectrum intensity, $SI_{ref.}$. The curves for critical top displacement, base moment, shear, and rotational ductility for intensity ratios of 0.75 and 1.0 were obtained using the same procedure described for the case of $\overline{SI}$ = 1.5. An almost regular decrease in the magnitude of all response quantities occurs with a decrease in input motion intensity.

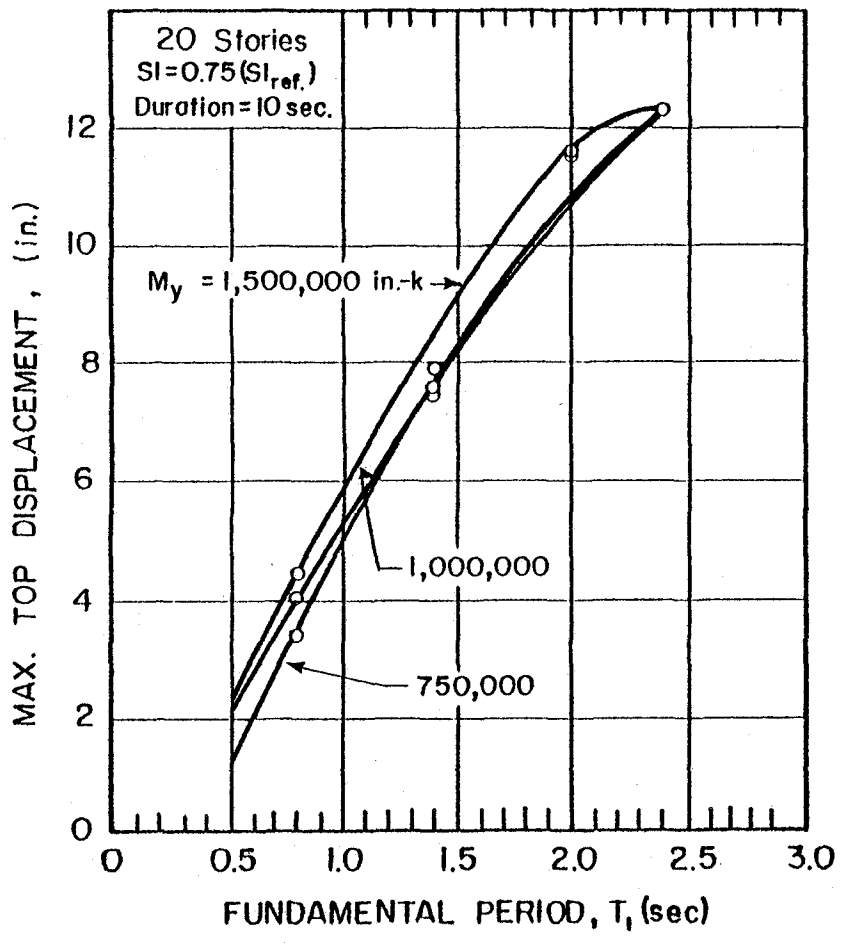

(a)

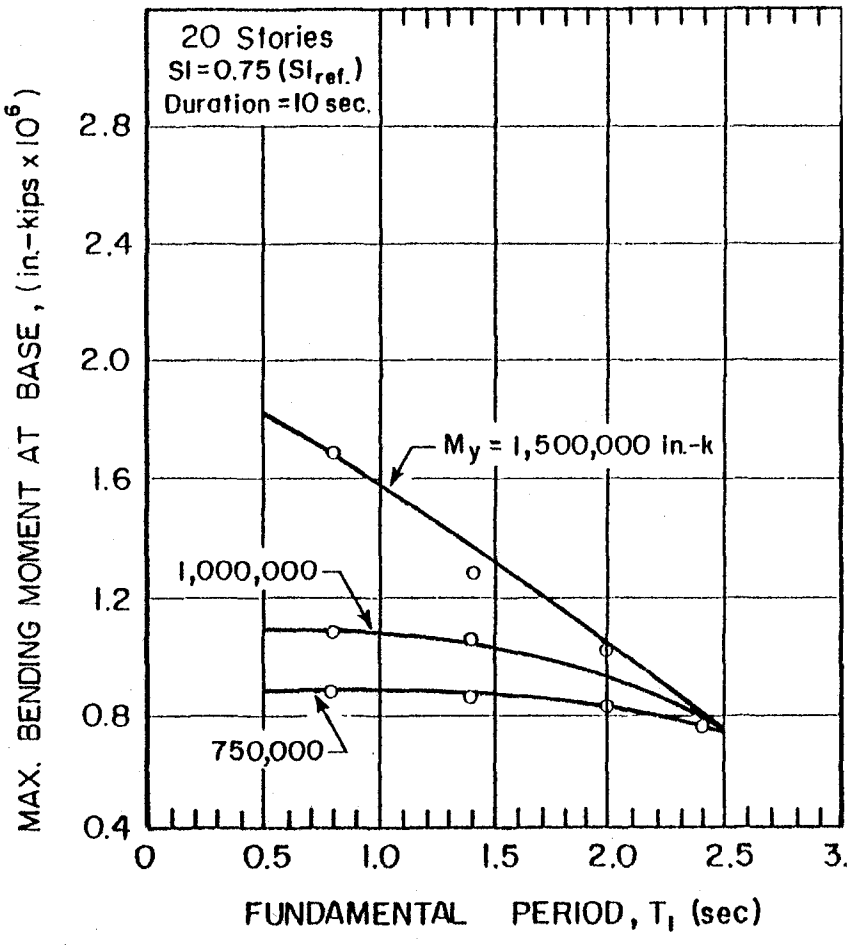

(b)

Fig. 56 Critical Response Values as Functions of Fundamental Period, T_1, and Yield Level, M_y, 20-Story Structural Walls - SI = $0.75(SI_{ref.})$

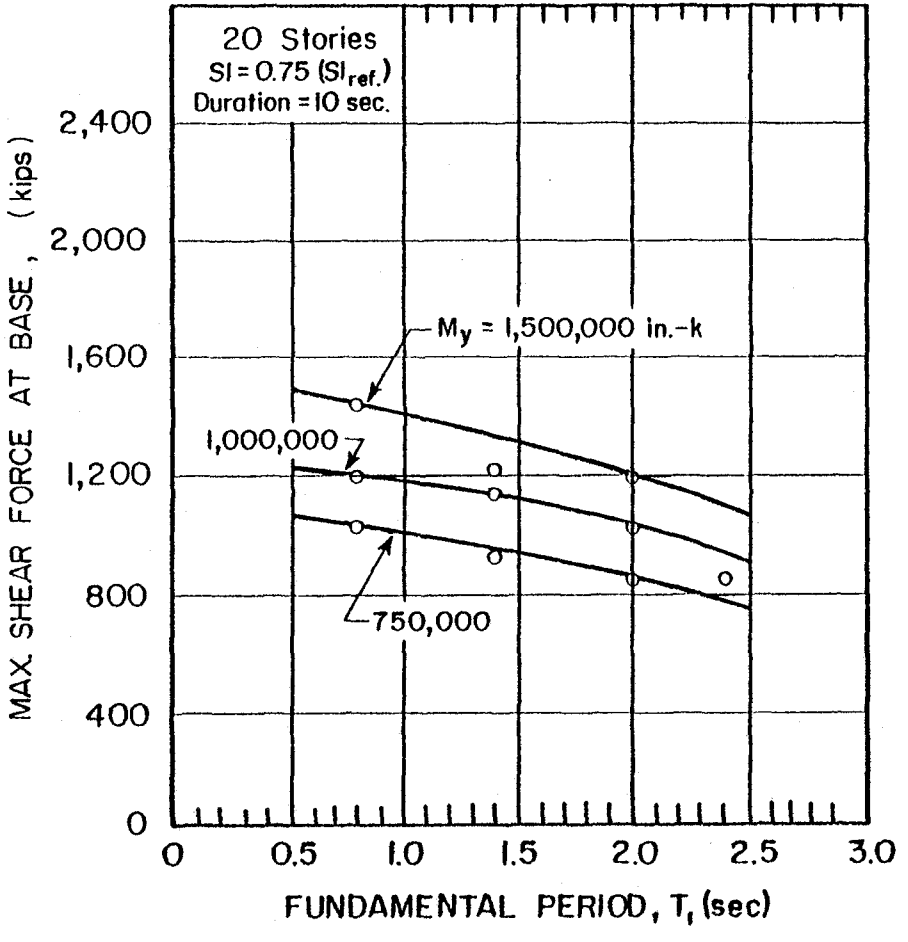

(c)

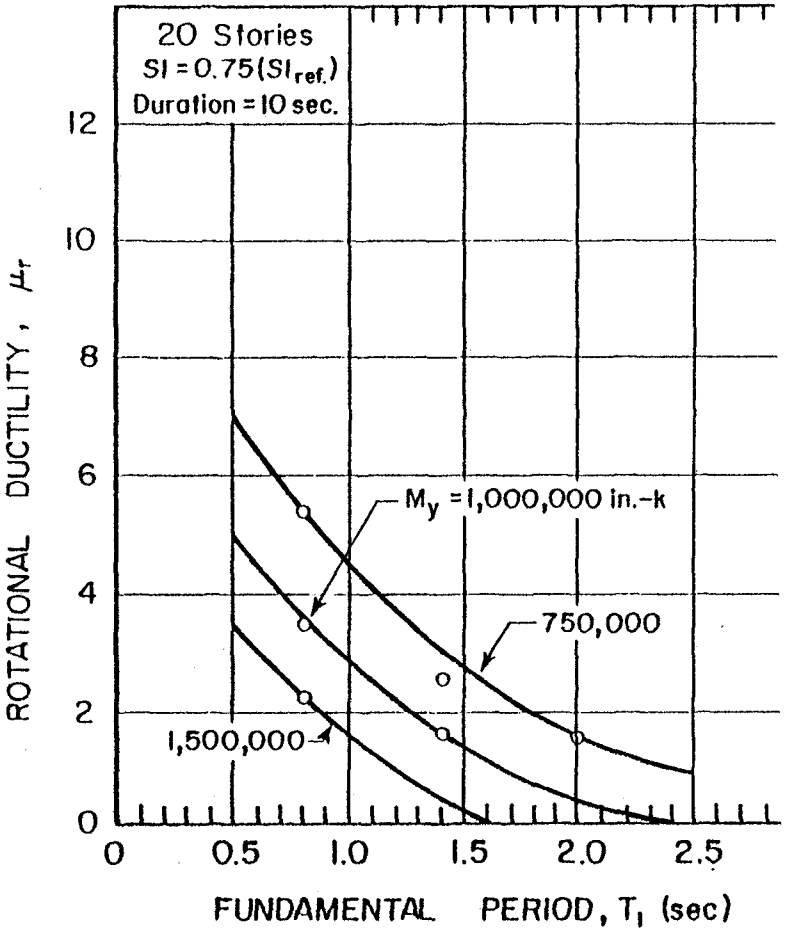

(d)

Fig. 56(contd.) Critical Response Values as Functions of Fundamental Period, T_1, and Yield Level, M_y, 20-Story Structural Walls - SI = $0.75(SI_{ref.})$

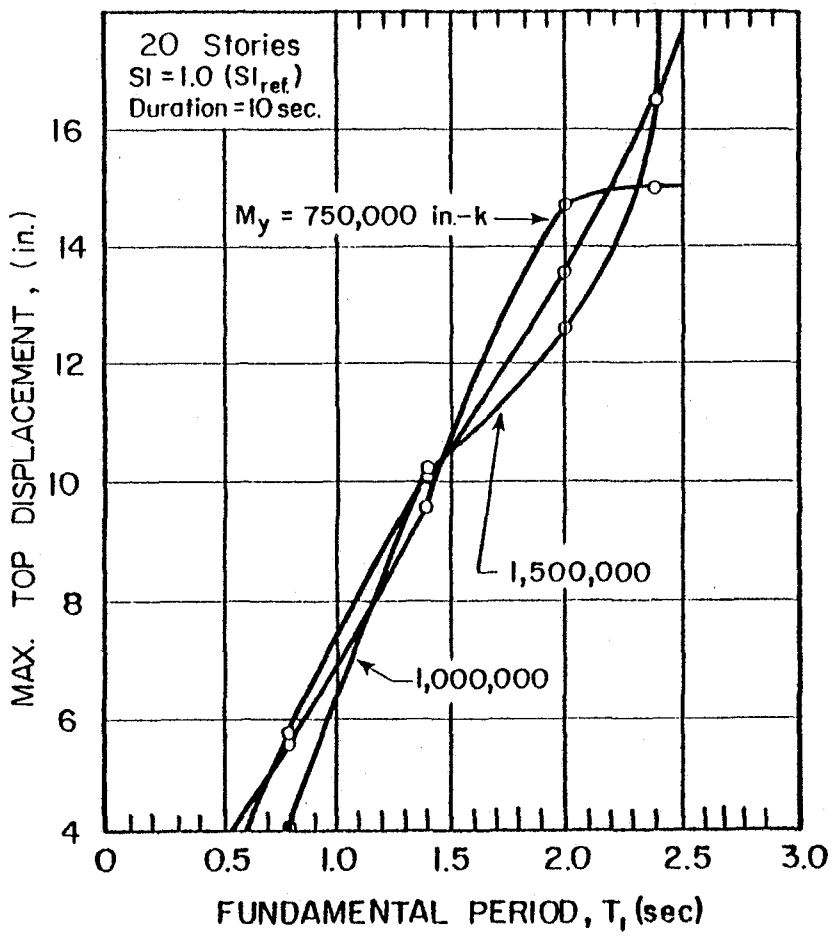

(a)

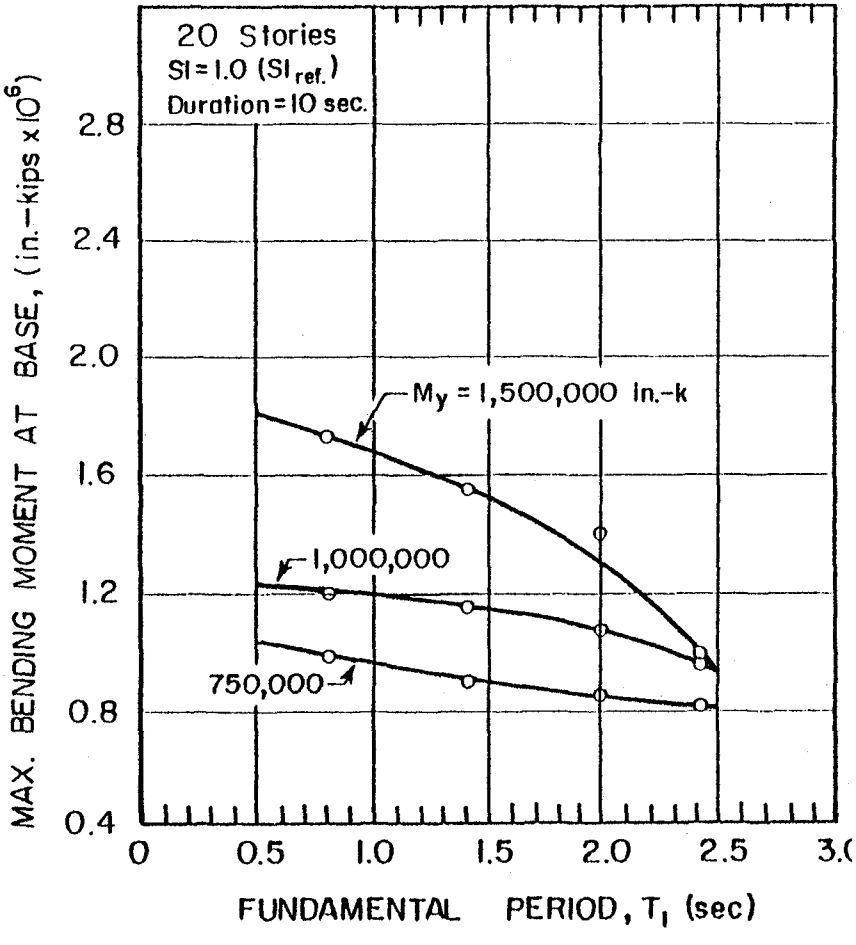

(b)

Fig. 57 Critical Response Values as Functions of Fundamental Period, T_1, and Yield Level, M_y, 20-Story Structural Walls - SI = $1.0(SI_{ref.})$

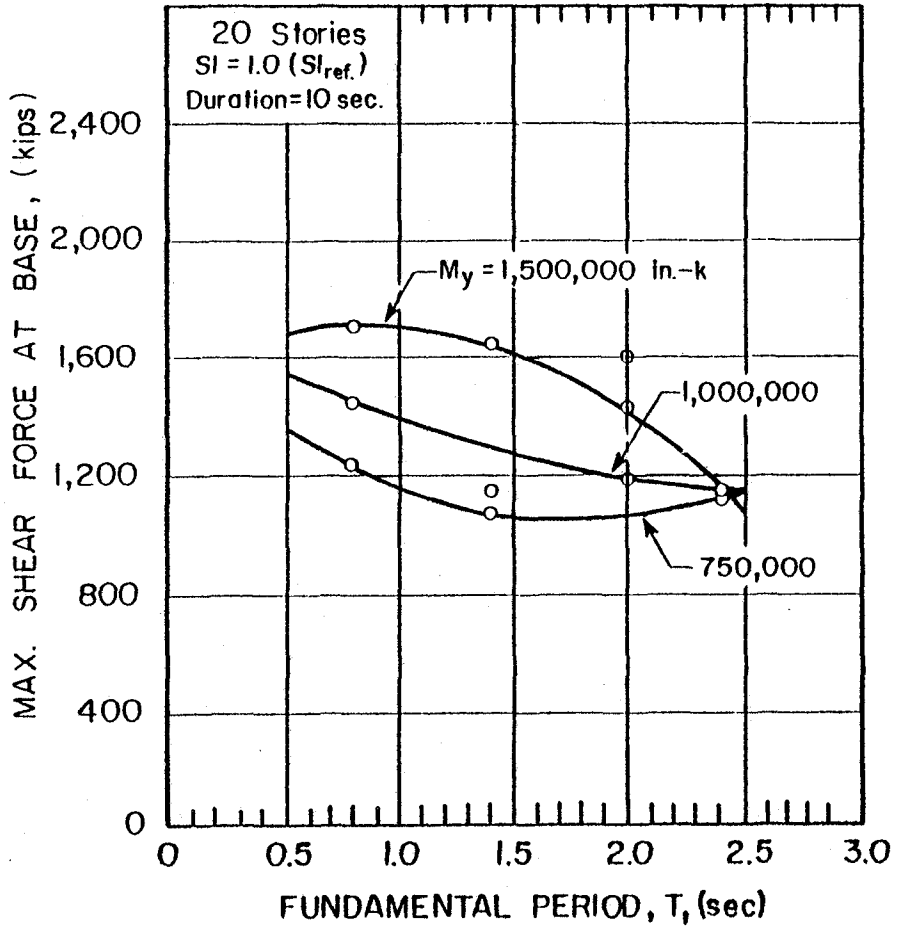

(c)

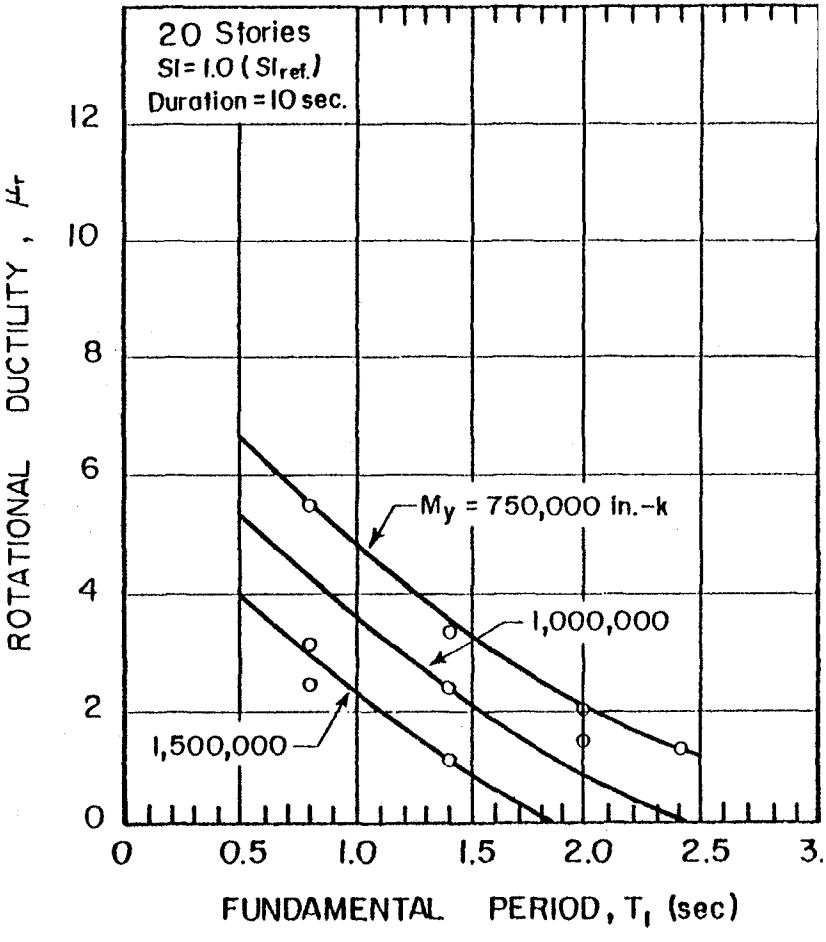

(d)

Fig. 57 (contd.) Critical Response Values as Functions of Fundamental Period, T_1, and Yield Level, M_y, 20-Story Isolated Structural Walls - SI = $1.0(SI_{ref.})$

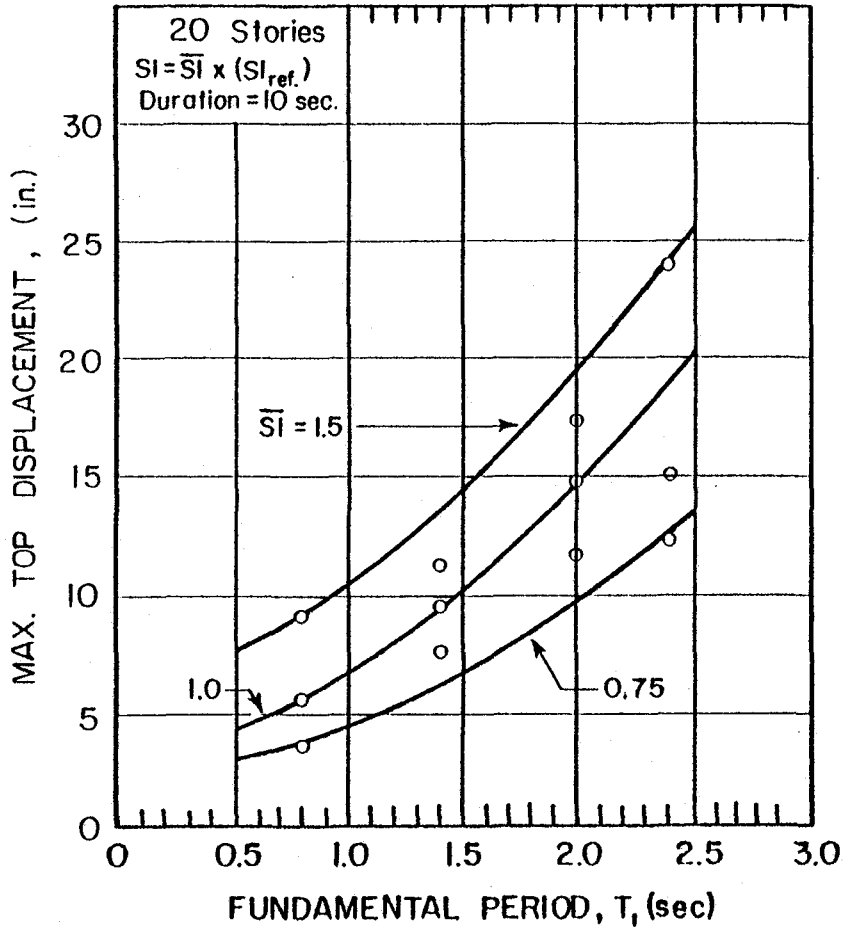

(a)

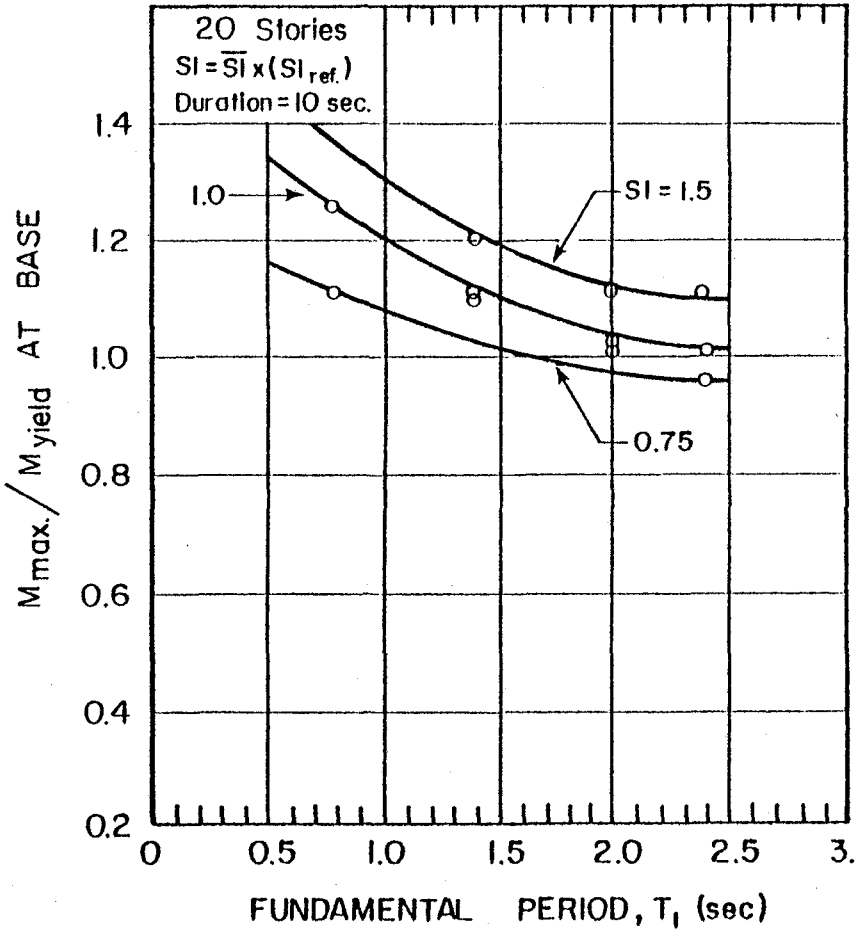

(b)

Fig. 58 Critical Response Values as Functions of Fundamental Period, T_1, and Earthquake Intensity, SI, 20-Story Isolated Structural Walls

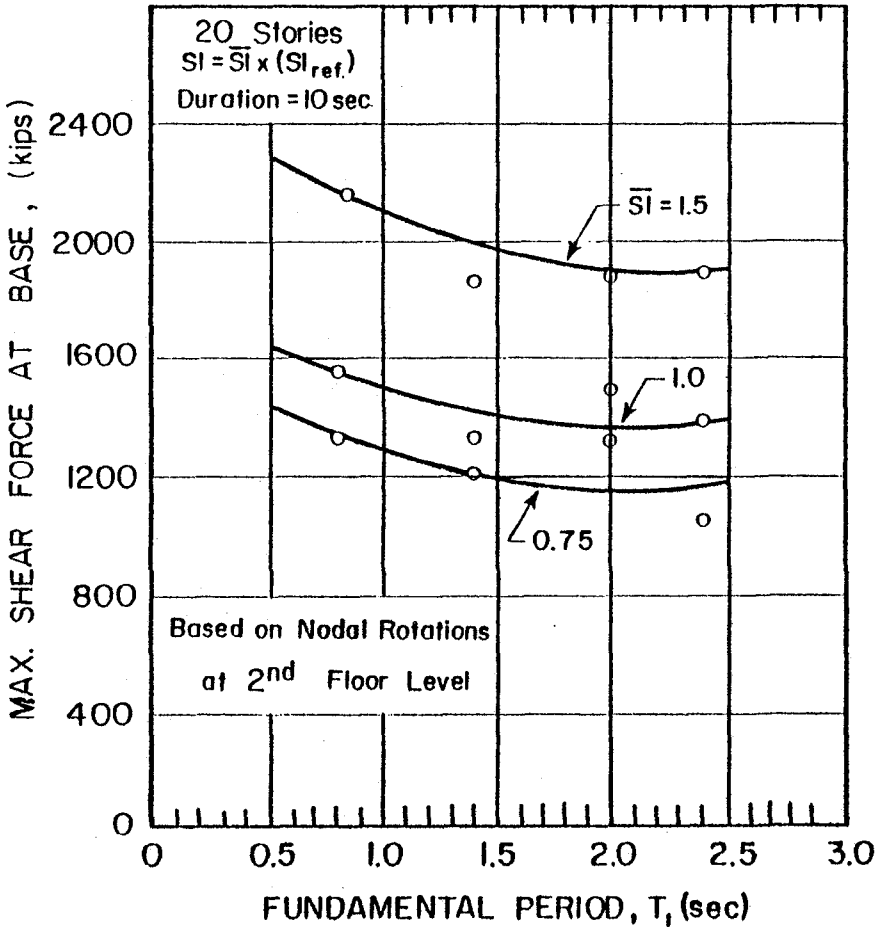

(c)

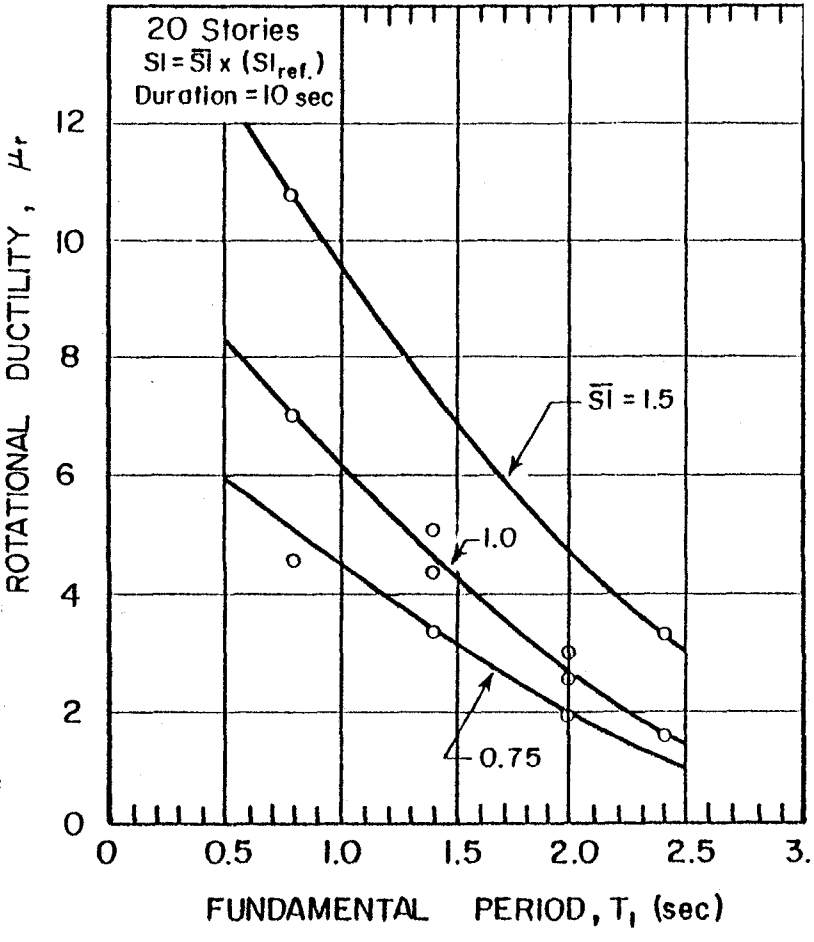

(d)

Fig. 58(contd.) Critical Response Values of Functions of Fundamental Period, T_1, and Earthquake Intensity, SI, 20-Story Isolated Structural Walls

Design Factors for Different Earthquake Intensities

Based on critical response plots such as shown in Fig. 58, flexural and shear design factors α_f and $\bar{\alpha}_v$ were determined for $\overline{SI}$ = 0.75 and 1.0. These are shown plotted in Figs. 59 and 60.

To allow use of the extensive response data for input motions with SI = 1.5 for other earthquake intensities, an approximate relationship was established between the design factors for $\overline{SI}$ = 1.5 and those for the lesser intensities. This was done by calculating the ratios of the flexural and shear design factors for SI = 0.75 and 1.0 to the corresponding factors for $\overline{SI}$ = 1.5. Plots of these ratios against $\overline{SI}$ are shown in Figs. 61 and 62.

Figures 61 and 62 show least-squares-fit lines for the respective data. The linear regression line in each case was obtained by assuming the value of the intensity factor of 1.0, corresponding to $\overline{SI}$ = 1.5, as representing 100 data points. It will be noted, from a comparison of the data points in Figs. 61 and 62, that the scatter of data for the shear intensity factor is wider than that for the flexural intensity factor.

To further simplify the expressions relating the flexural and shear intensity factors, I_{α_f} and $I_{\bar{\alpha}_v}$ with the earthquake intensity ratio, SI, lines passing through the points I_{α_x} = 1.0, $\overline{SI}$ = 1.5 (x = f, v) and closely parallel to the respective linear regression lines are proposed, as shown in Figs. 61 and 62. The algebraic expressions for the lines are as follows:

$$I_{\alpha_f} = 0.67\ \overline{SI} \quad \text{for the flexurual design factor,} \tag{2}$$

and

$$I_{\bar{\alpha}_v} = 1.6 - 0.4\ \overline{SI} \quad \text{for the shear design factor.} \tag{3}$$

The above relationships, when used in conjuction with Figs. 51 and 52, give design forces for the critical region at the base of isolated walls subjected to a range of earthquake intensities. Thus, the total base shear, V_T, required for the design of the flexural reinforcement at the base of walls

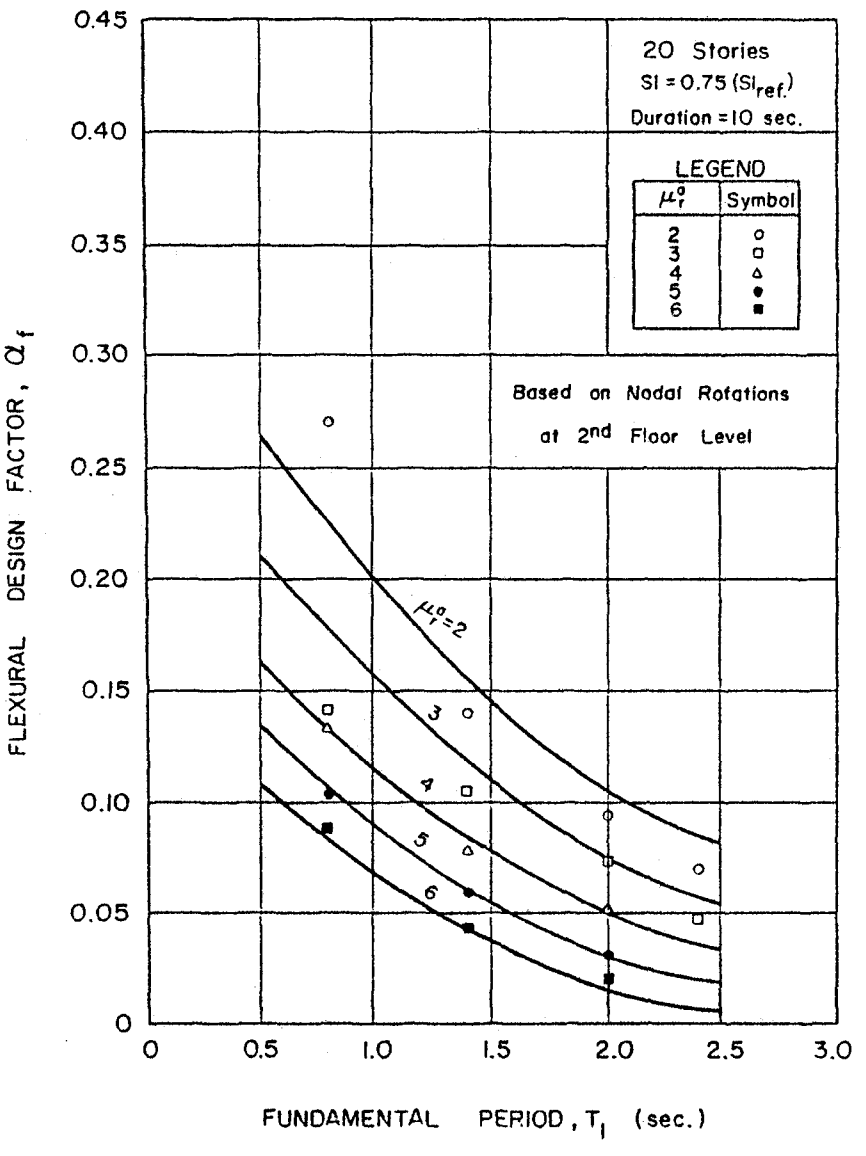

(a)

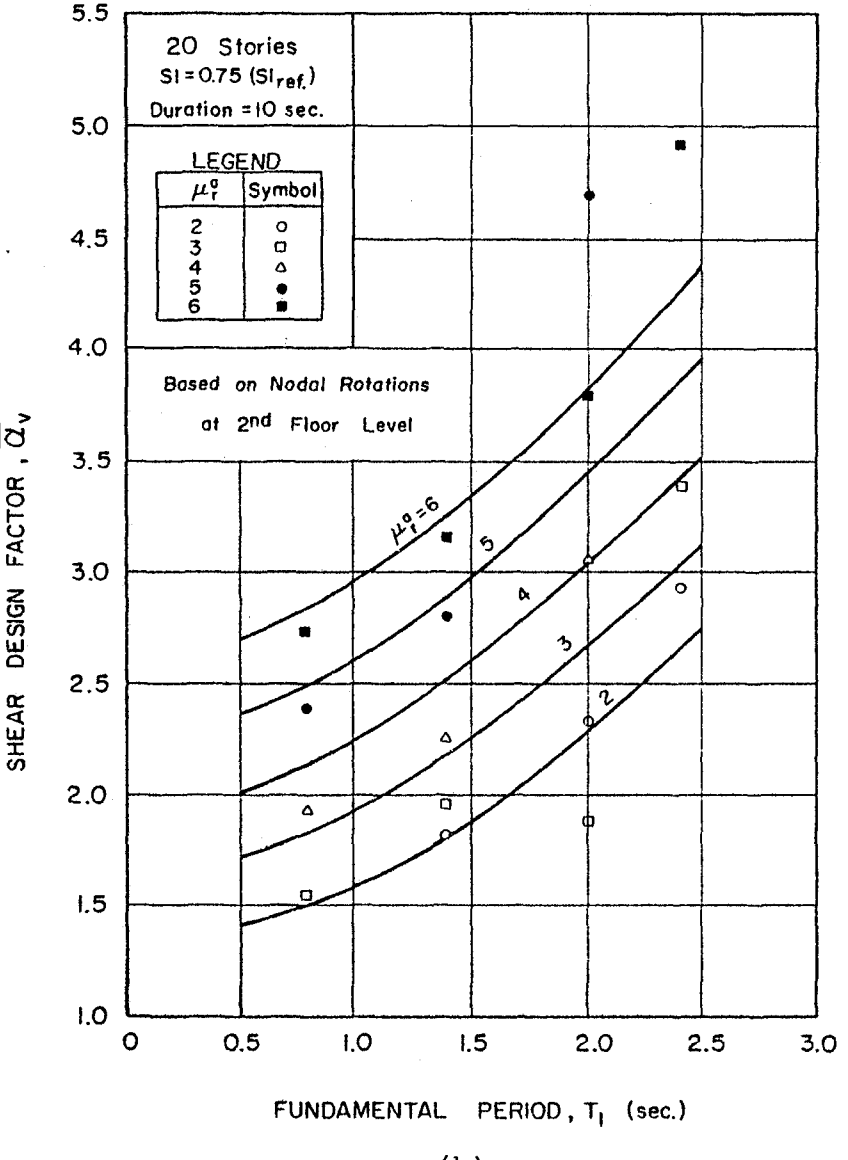

(b)

Fig. 59 Flexure and Shear Design Factors as Functions of Available Rotational Ductility, μ_r^a and Fundamental Period, T_1 20 Story Structural Walls - SI = 0.75(SI$_{ref.}$)

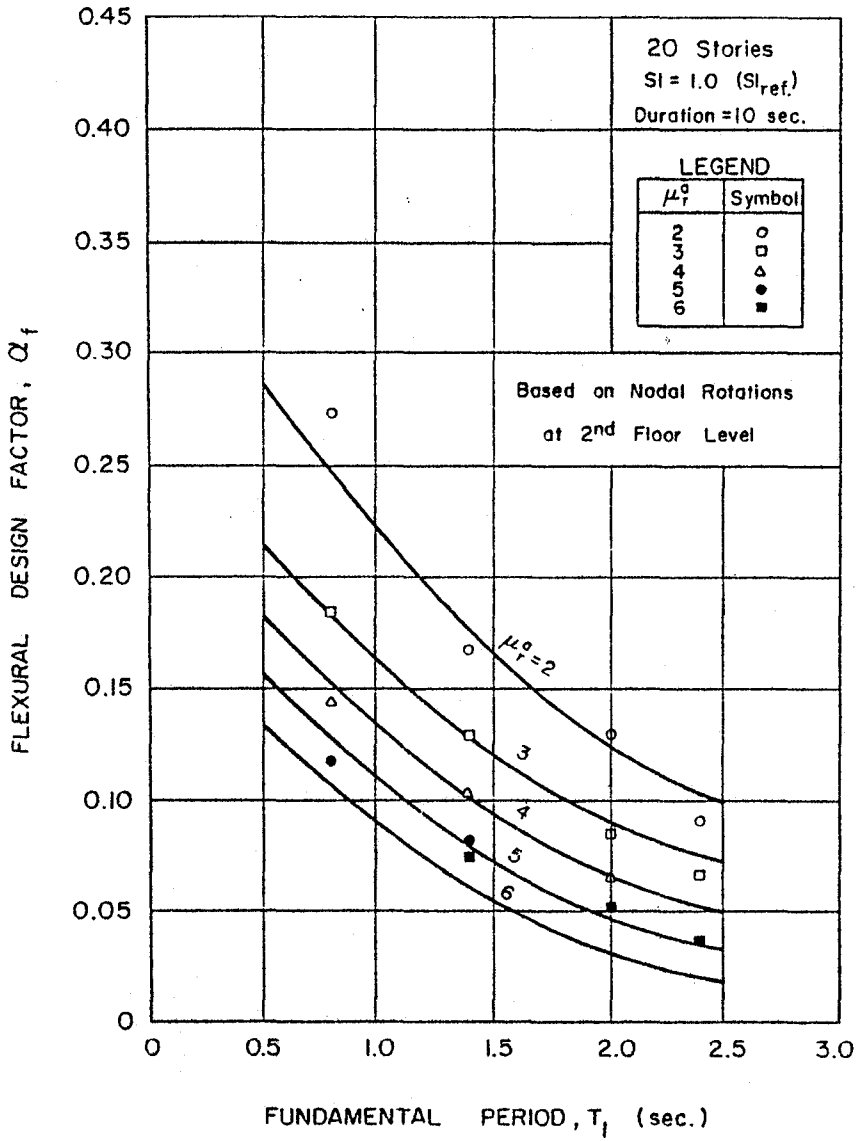

(a)

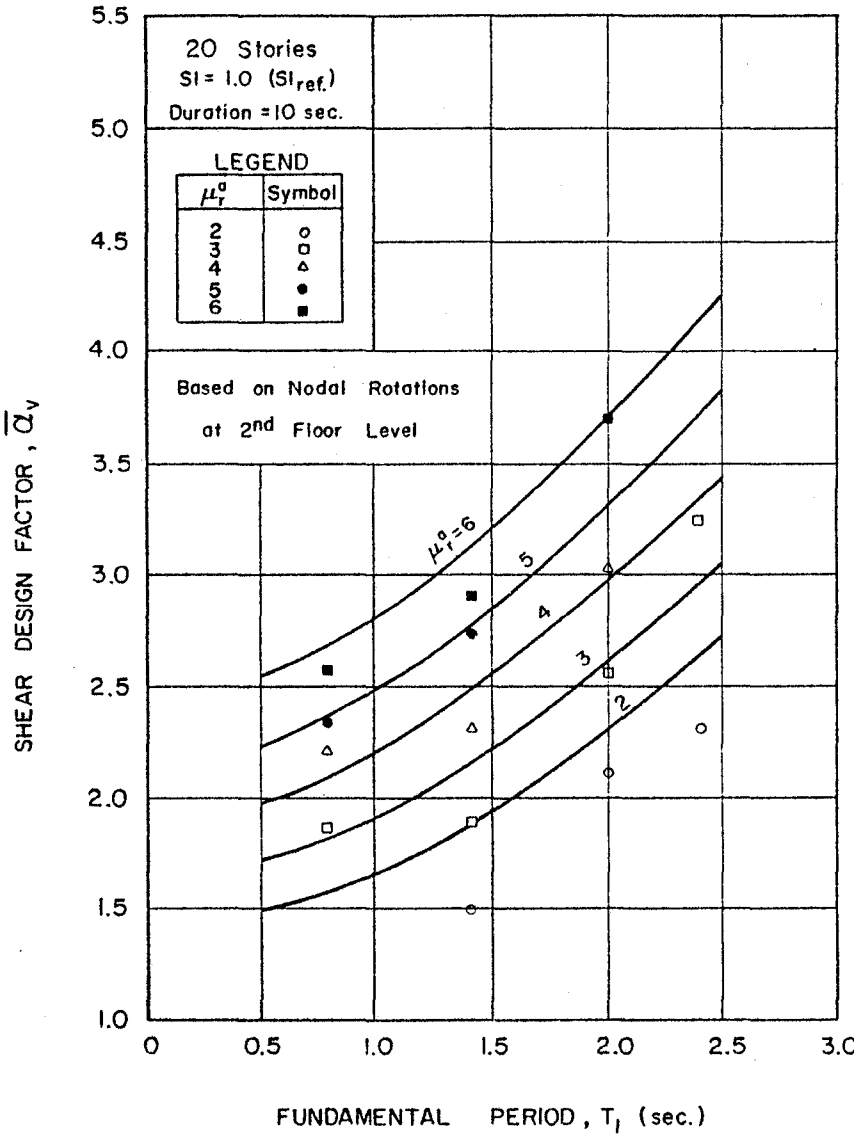

(b)

Fig. 60 Flexure and Shear Design Factors as Functions of Available Rotational Ductility, μ_r^a and Fundamental Period, T_1 20-Story Structural Walls SI = 1.0($SI_{ref.}$)

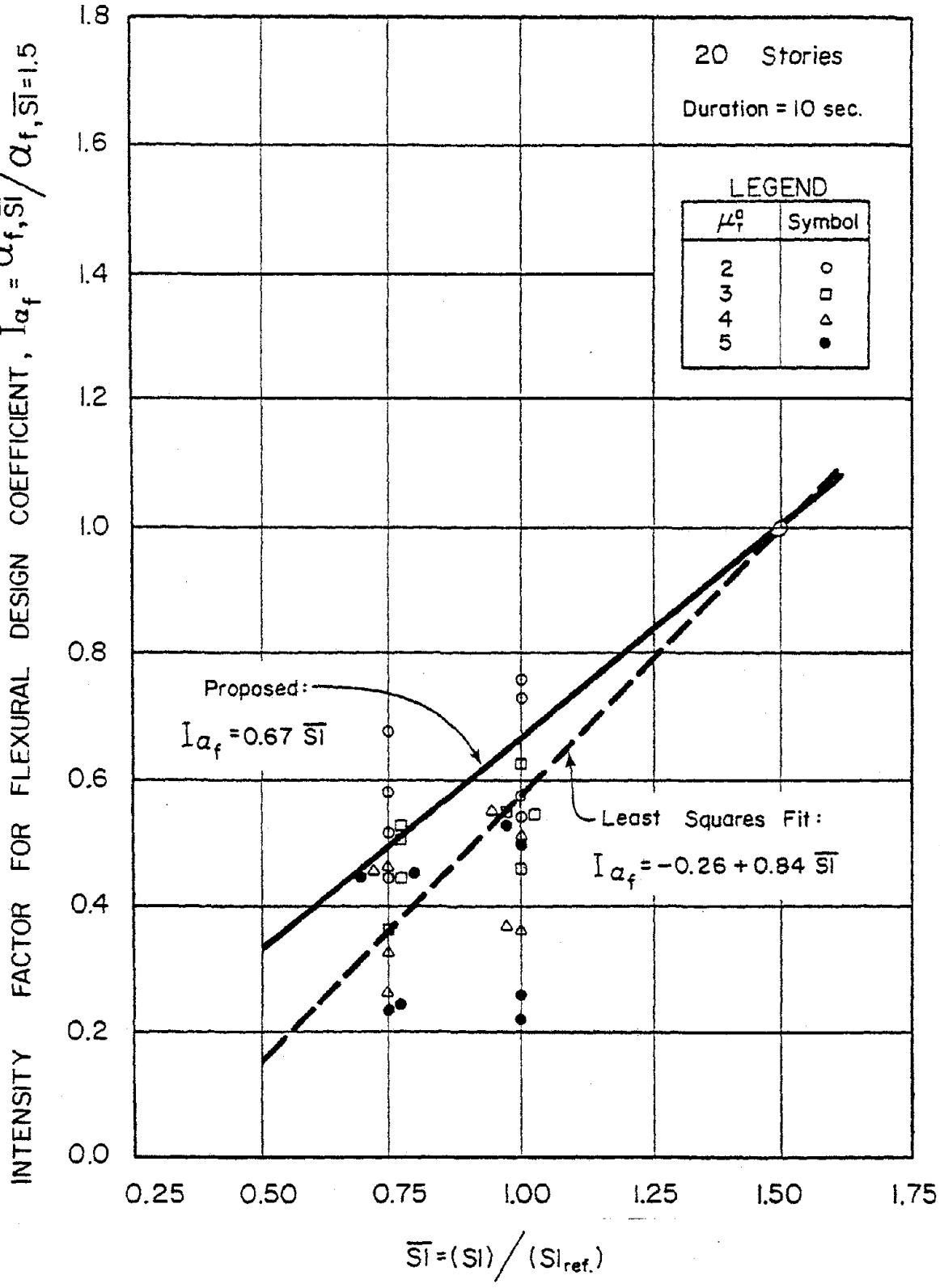

Fig. 61 Intensity Factor for Flexural Design Coefficient, I_{α_f} as a Function of Earthquake Intensity Ratio, SI - 20-Story Structural Walls

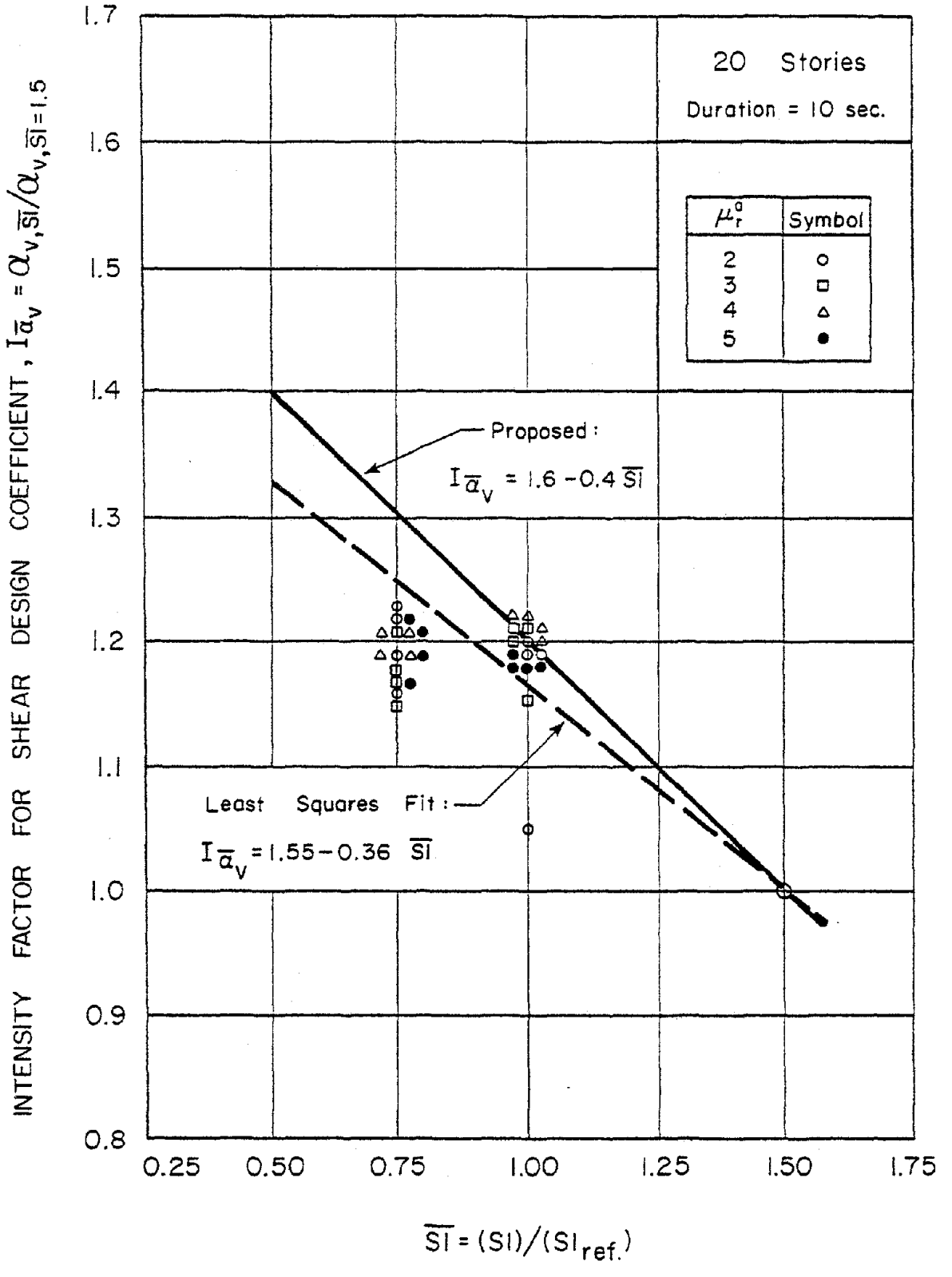

Fig. 62 Intensity Factor for Shear Design Coefficient, $I_{\bar{\alpha}_v}$, as a Function of Earthquake Intensity Ratio, $\overline{SI}$ - 20-Story Structural Walls

ranging in height from 10 to 40 stories subjected to a ground motion of intensity SI = $\overline{SI}$ x ($SI_{ref.}$) is given by

$$V_T = I_{\alpha_f} \alpha_f W, \tag{4}$$

where I_{α_f} is given by Eq. (2) above and α_f is obtained from Fig. 51. The corresponding expression for the total base shear for the shear design of the base is

$$\begin{aligned} V_{TS} &= I_{\bar{\alpha}_v} \bar{\alpha}_v V_T \\ &= I_{\bar{\alpha}_v} \bar{\alpha}_v \alpha_f W \end{aligned} \tag{5}$$

where $I_{\bar{\alpha}_v}$ is given by Eq. 3 above and $\bar{\alpha}_v$ is obtained from Fig. 52.

Figures 63 and 64, also based on data for 20-story walls subjected to different input motion intensities, provide guides for adjusting the maximum top and interstory displacements corresponding to $\overline{SI}$ = 1.5 given in Figs. 53 and 54.

Spectrum Intensity and Seismic Zones

No attempt has been made to relate the various levels of input motion intensity with the different seismic zones prescribed in seismic risk or regionalization maps of codes. This step is beyond the scope of the investigation.

However, it is hoped that, as more data on earthquakes are accumulated, seismic regionalization maps can be established defining seismic risk in terms of the expected maximum earthquake intensities and their corresponding return periods or recurrence intervals. With the availability of such maps, it will be possible to directly utilize the proposed design force levels developed in this study for different ground motion intensities. This assumes that earthquake intensity will be defined in terms of some measure with which spectrum intensity as used in this study can be correlated. In the absence of maps defining spectrum intensities and their

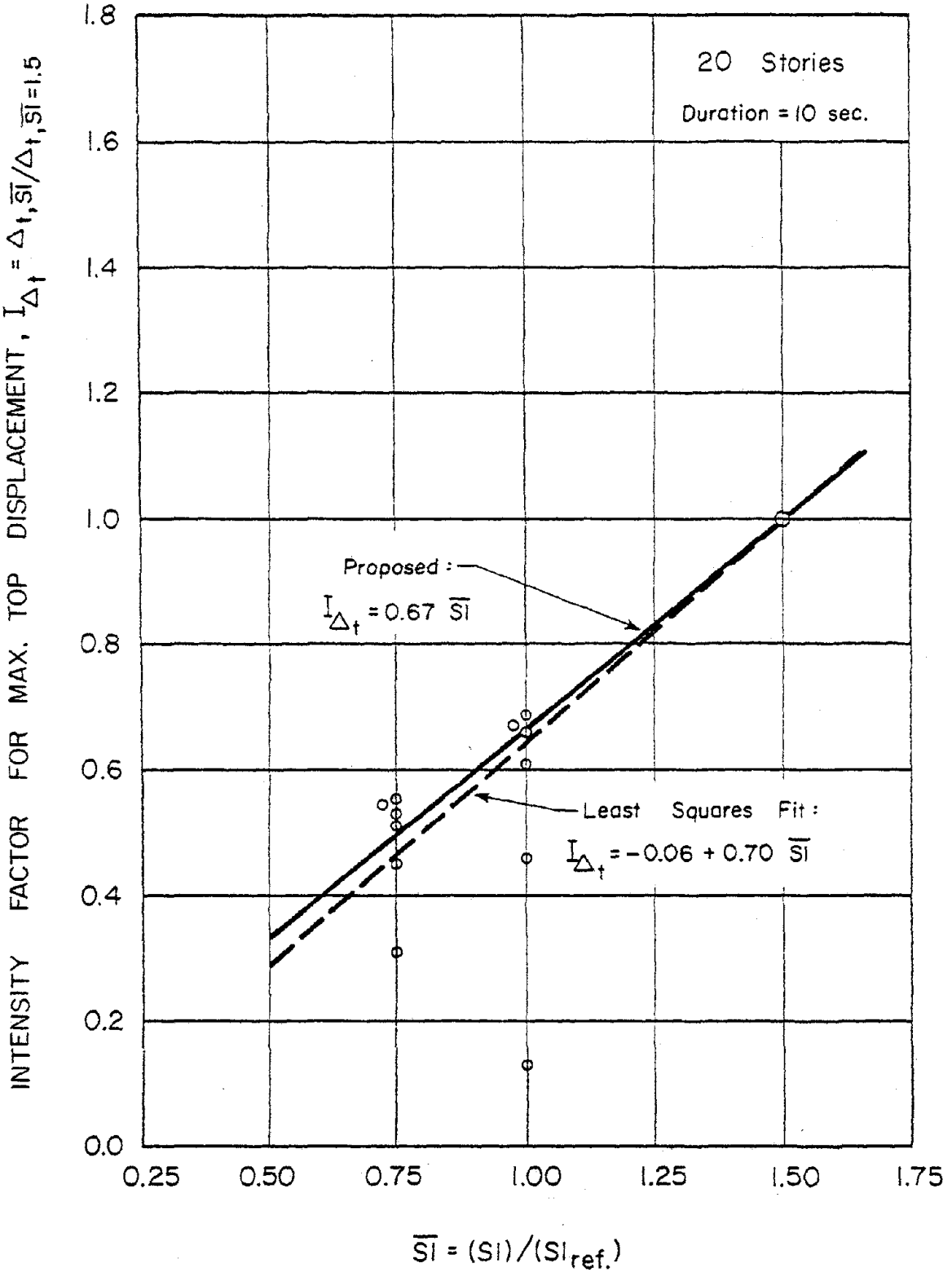

Fig. 63 Intensity Factor for Maximum Top Displacement

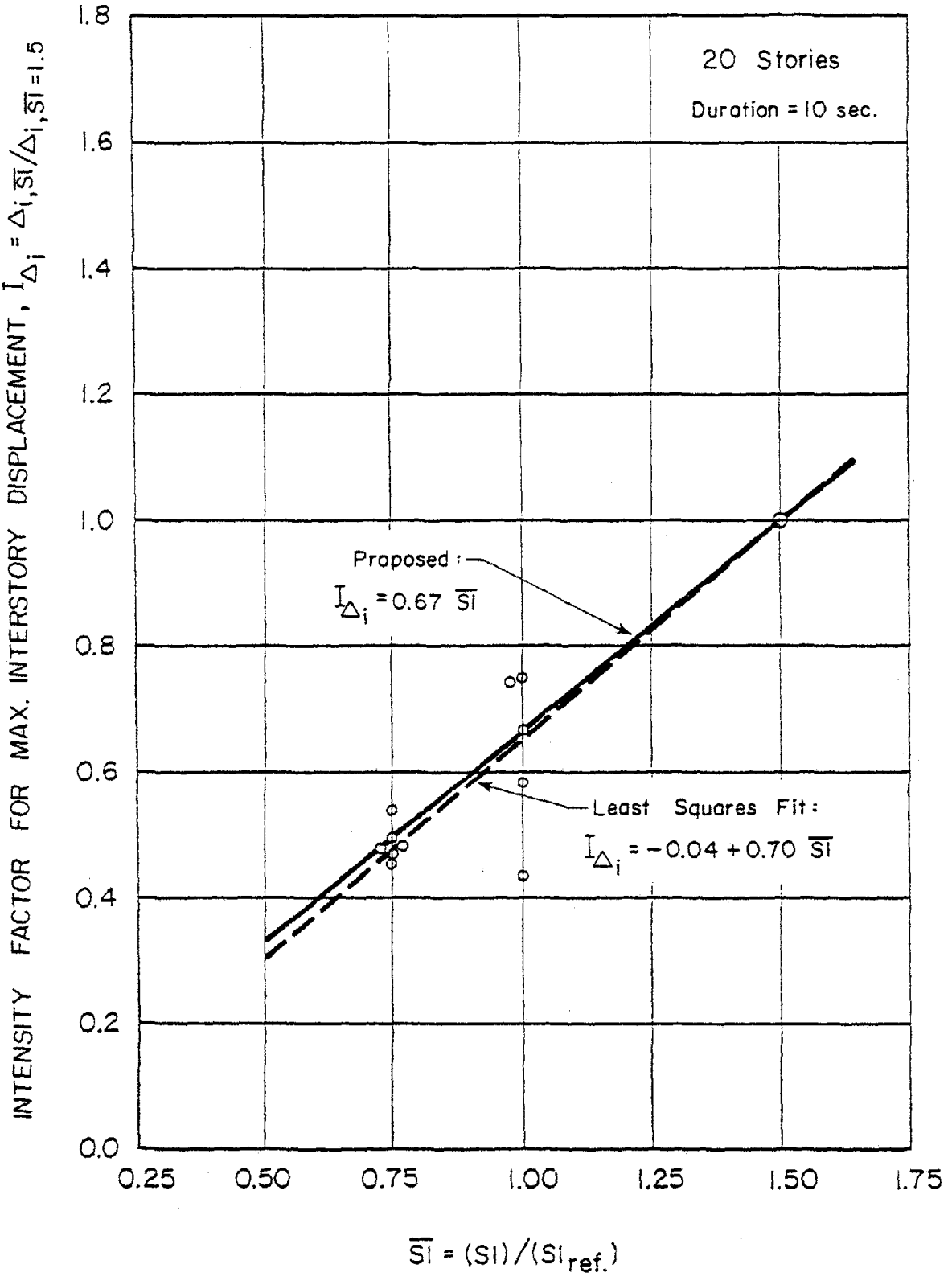

Fig. 64 Intensity Factor for Maximum Interstory Displacement

corresponding recurrence intervals for different regions, the design force levels presented here can still be utilized by estimating the spectrum intensity associated with particular seismic zones on the basis of available information.

In an effort to provide some guidance in this direction, a comparison was made of the velocity response spectra of the six accelerograms used in this study with the velocity spectrum associated with the "effective peak velocity" defined in the Applied Technology Council's "Tentative Provisions for the Development of Seismic Regulations for Buildings," (ATC 3-06)[1]. In the subsequent discussion, Ref. 1 will be referred to as "ATC-3".

In ATC-3, the maximum effective peak velocity (EPV) assigned to the most seismically active parts of California is 12 inches per sec. This corresponds to the contours labeled "0.4" in the effective peak-velocity-related acceleration (A_v) map shown in Fig. 65, which is taken from Ref. 1. As explained in Ref. 1, the spectral velocity, S_v, associated with EPV is obtained approximately from the relationship

$$S_v = 2.5 \text{ EPV} \tag{6}$$

Similarly, the spectral acceleration is obtained from

$$S_a = 2.5 \text{ EPA}, \tag{7}$$

where EPA is the "effective peak acceleration" as defined in Ref. 1.

With the maximum effective peak velocity, $(\text{EPV})_{max} = 12$ in./sec. the maximum spectral velocity

$$(S_v)_{max} = 2.5 \ (\text{EPV})_{max} = 2.5(12) = 30 \text{ in./sec.}$$

This value of the maximum spectral velocity, which is applicable to the period range from about 0.5 sec. to about 4.0 sec., corresponds to the most seismically active regions of California,

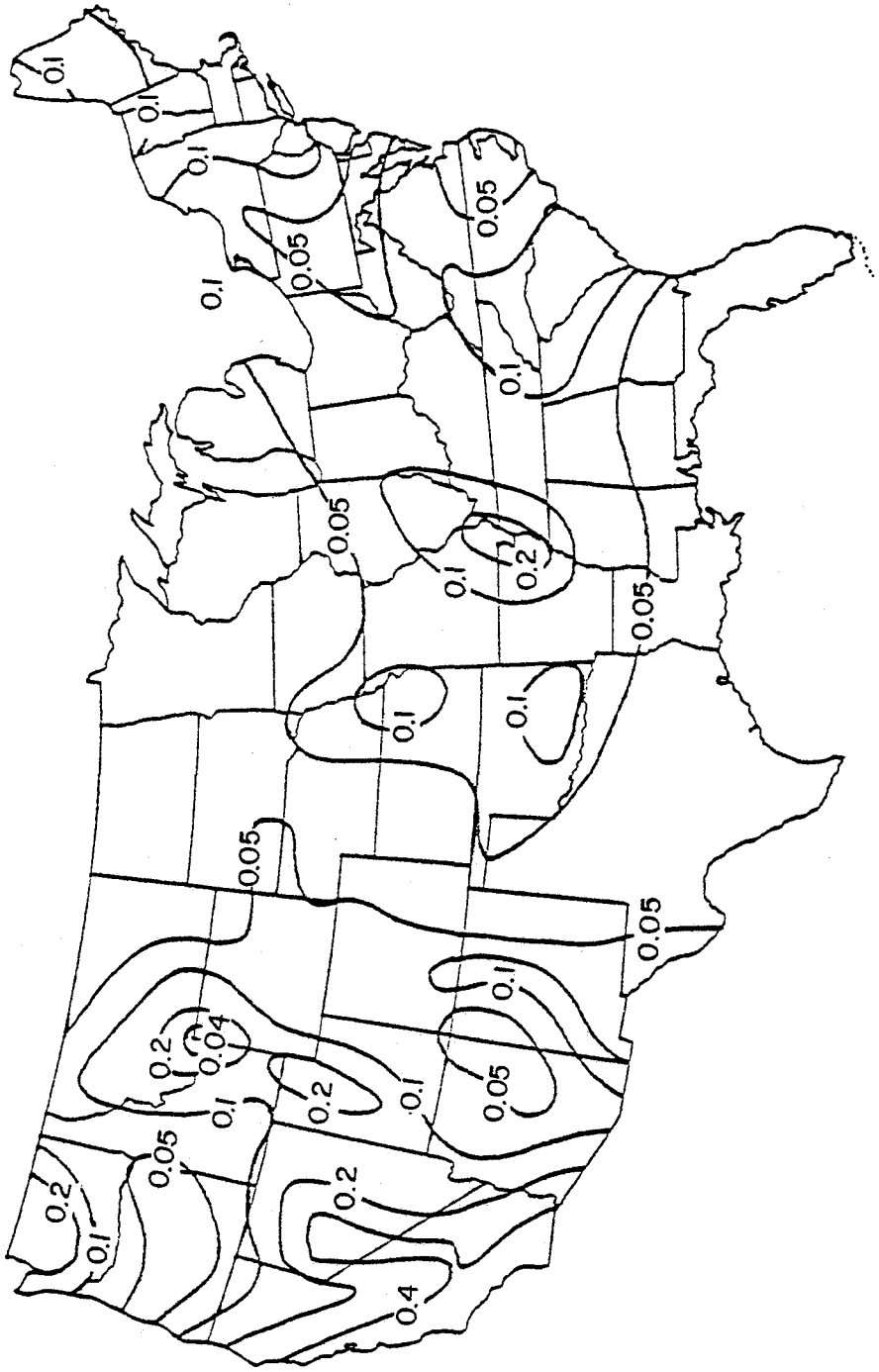

Fig. 65 Contour Map for Effective Peak Velocity-Related Acceleration Coefficient, A_v (from Ref. 1)

classified as Zone 4 under the Uniform Building Code (UBC-76).[16]

Similarly, with $(EPA)_{max}$ = 0.4g, the maximum spectral acceleration is given by

$$(S_a)_{max} = 2.5\ (EPA)_{max} = 2.5(0.4g) = 1.0g$$

This value of $(S_a)_{max}$ is applicable to the period range from about 0.1 sec. to 0.5 sec.

Figure 66 shows a tripartite, log-log plot of the 5%-damped velocity response spectra for the six accelerograms used in this study. All six accelerograms were normalized with respect to intensity such that their spectrum intensity was equal to 1.2 times the reference spectrum intensity, $(SI_{ref.})$.* The heavy dashed lines in the figure represent constant values of S_a = 1.0 g (for the period range 0.1-0.5 sec.) and S_v = 30 in./sec. (for the period range 0.5-3.0 sec.). In the period range 0.5 - 3.0 sec., which is of primary interest in this investigation, Fig. 66 shows that an intensity factor, SI, equal to about 1.2 or 1.25 yields spectral velocities for the six accelerograms considered averaging 30 in./sec.

The above comparison leads to the conclusion that, at least for the period range of interest, i.e., 0.5 to 3.0 sec., a design spectrum intensity equal to 1.2 or 1.25 $(SI_{ref.})$ would roughly correspond to the intensity recommended by ATC-3 for the most seismically active regions in California. Equivalent intensity ratios, SI, corresponding to the other contours in Fig. 65 can be obtained by direct proportion. Thus, if we take an SI of 1.2 as corresponding to S_v = 30 in./sec. the intensity ratio corresponding to the contour marked "0.2" in Fig. 65, would be

*Corresponding to the first 10 seconds of the N-S component of the 1940 El Centro record.

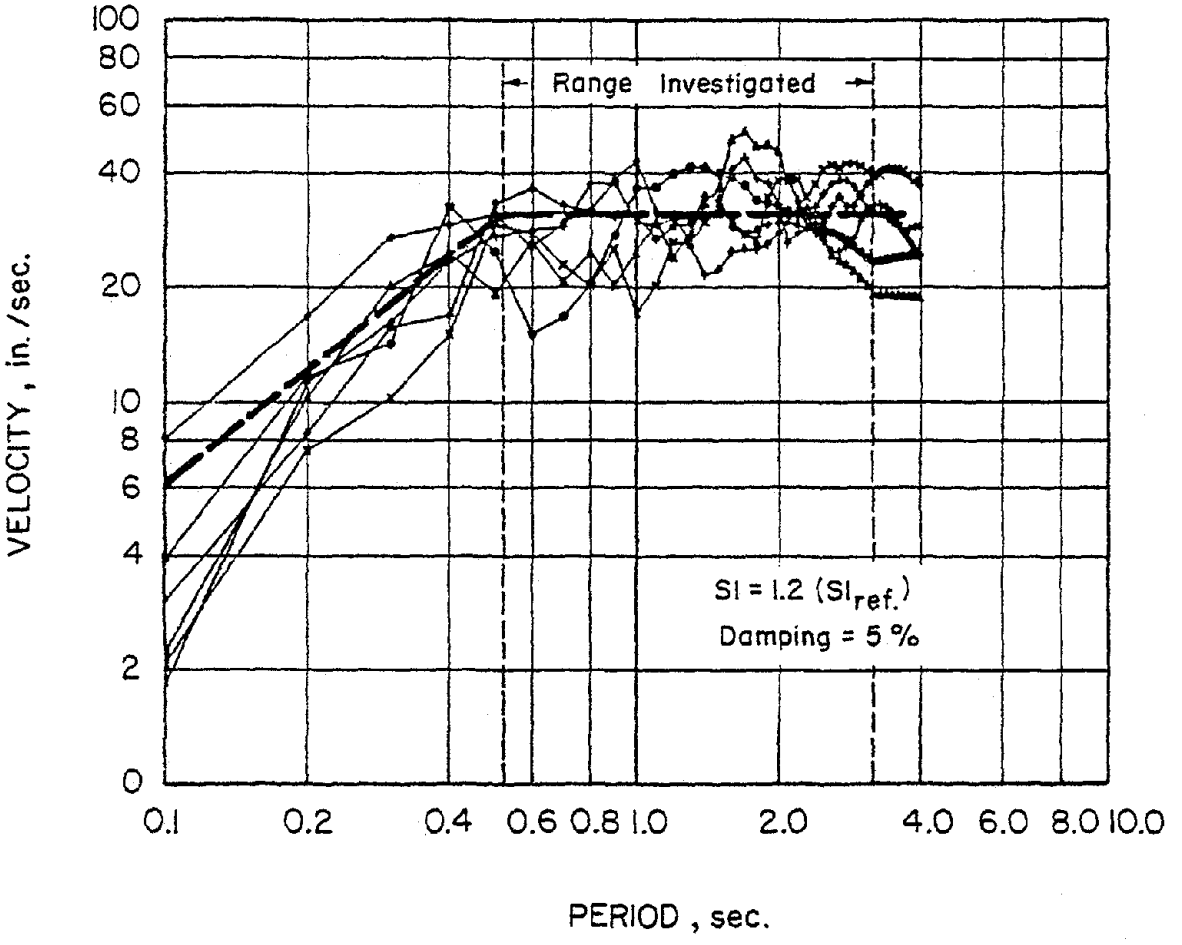

Fig. 66 Velocity Response Spectra for the Six Input Motions Used in Investigation

$$\overline{SI}_{0.2} = 1.2 \frac{0.2}{0.4} = 0.6$$

or, in general, for any value of A_v

$$\overline{SI}_{A_v} = 1.2 \frac{A_v}{0.4} .$$

Comparison of Proposed Design Force Levels with Calculated Response Values

The design force levels implied in Figs. 51 and 52, together with the flexural and shear intensity factors defined by Eqs. (2) and (3), essentially summarize the basic results of this investigation. These results were obtained by a procedure involving a number of approximations including curve fitting techniques. Because of the subjective nature of some of the procedures used, effects of these procedures on the final results were examined. Of particular interest was the degree of conservatism or unconservatism represented by the proposed design forces relative to the calculated dynamic response data from which they were developed.

Figures 67 and 68 provide a comparison between the proposed design forces and the corresponding dynamic response data. Figure 67a shows a histogram indicating the frequency distribution of the ratio of the maximum base moment calculated from dynamic analysis to the corresponding value indicated by Fig. 51 (and Eq. (3), where appropriate) for the same combination of T_1, μ_r and $\overline{SI}$. As indicated in the figure, this ratio was determined for a total of 175 cases representing fundamental period values ranging from 0.5 sec. to 3.0 sec., wall heights from 10 stories to 40 stories, ductility ratios from slightly less than 2.0 to slightly greater than 6.0, and earthquake intensity ratios of 0.75, 1.0 and 1.5. Six different input motions are included in the 175 cases considered.

Figure 67b shows a percentage exceedance plot, which is the complement of the cumulative frequency plot associated with

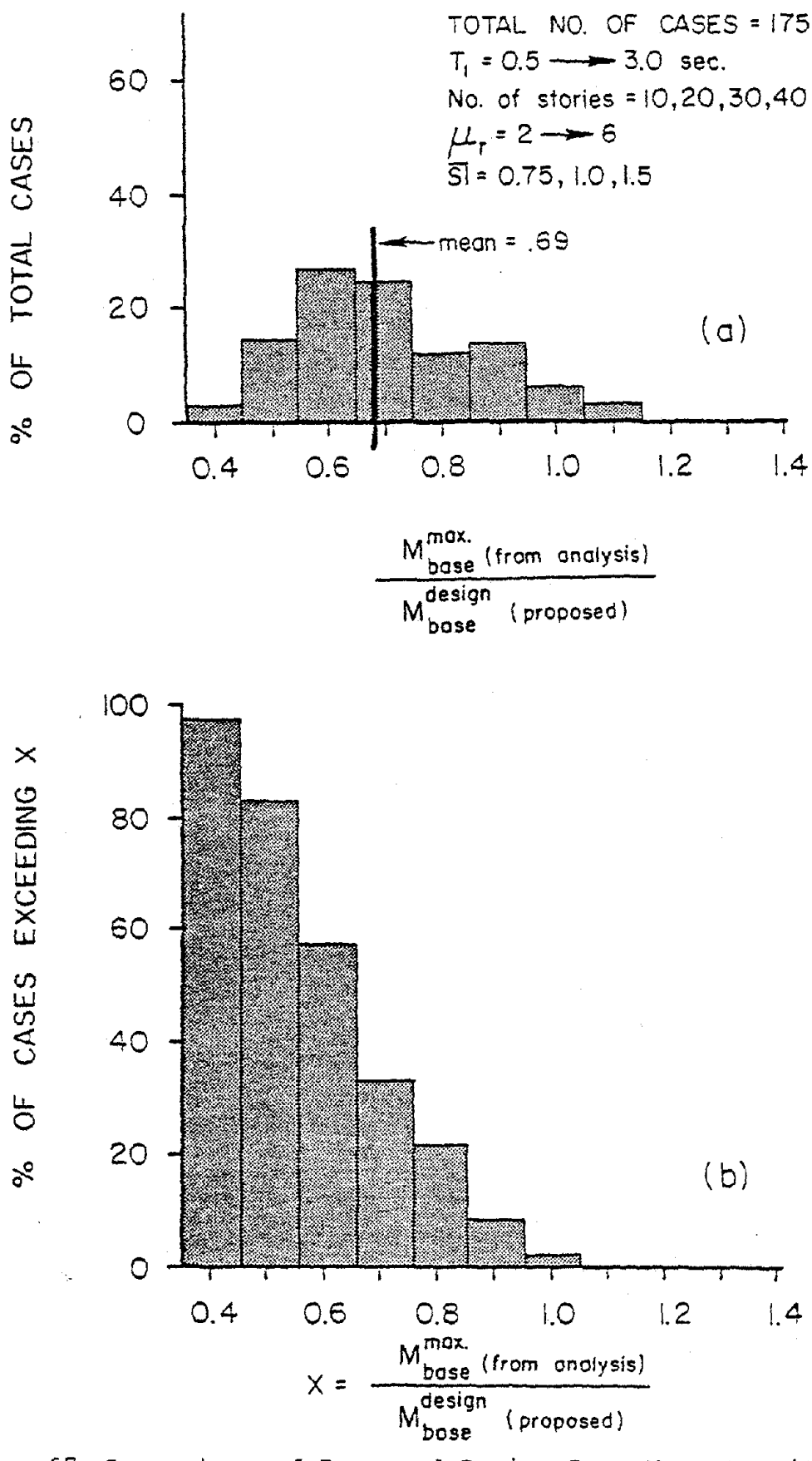

Fig. 67 Comparison of Proposed Design Base Moments with Corresponding Maximum Dynamic Base Moments

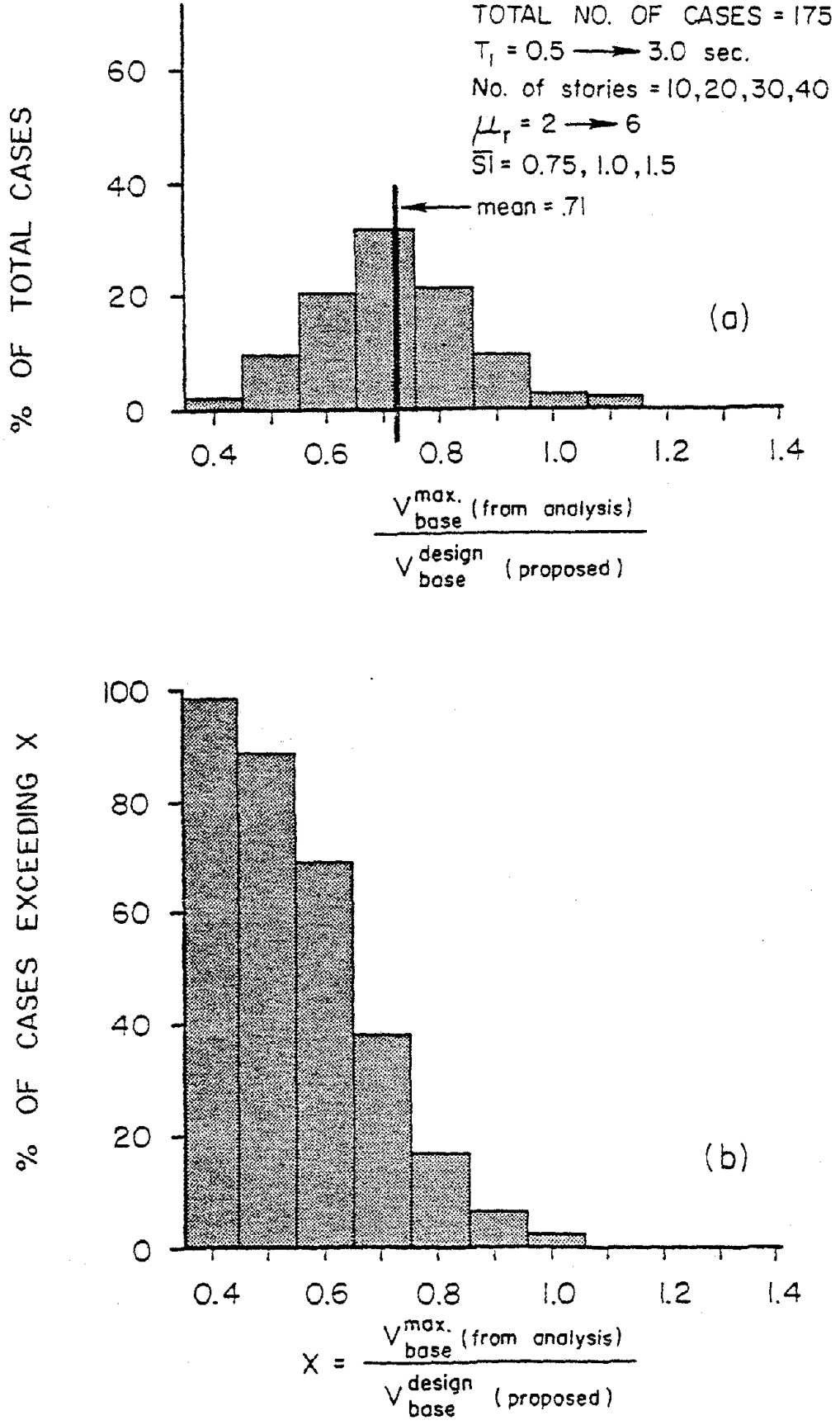

Fig. 68 Comparison of Proposed Design Base Shears with Corresponding Calculated Maximum Dynamic Base Shears

Fig. 67a. This plot gives the percentage of the total number of cases considered for which the moment ratio

$$\frac{M_{base}^{max} \text{ (from analysis)}}{M_{base}^{design} \text{ (proposed)}}$$

exceeds a specific value (as indicated on the horizontal scale in the figure). Figures 68a and 68b show similar figures for base shear.

Figure 67 indicates that of the 175 cases considered, the majority (70 percent) of these have moment ratios between 0.55 and 0.95. The mean for the entire set is 0.69. Figure 67 shows that the proposed design base moment underestimates the calculated maximum moment in 3 percent of the cases, the underestimate being as much as 15 percent.

The histogram for base shear shown in Fig. 68a shows that about 80 percent of all cases have values of shear ratio

$$\frac{V_{base}^{max} \text{ (from analysis)}}{V_{base}^{max} \text{ (proposed)}}$$

between 0.55 and 0.95. The mean for all cases is 0.71. Figure 68b indicates that the proposed design base shear underestimates the calculated maximum dynamic base shear in about 3 percent of all cases; the underestimate being as high as 15 percent.

Based on the above statistics and considering the uncertainties associated with earthquakes and earthquake-resistant design, it is believed that the proposed values for both flexure and shear at the base of isolated structural walls represent a reasonable basis for design.

Reduction in Critical Dynamic Base Shears for Design Use

In deriving values of the shear design factor, $\bar{\alpha}_v$, it was implicitly assumed that the critical dynamic shears on which

these were based represented reasonable upper-bound values for the combinations of structure and ground motion parameters considered. A comparison with the design shears corresponding to the provisions of UBC-76 for Seismic Zone 4 shows that the calculated critical shears at the base of the wall are significantly (about 2 to 3 times) greater than the UBC values.

The significant divergence from current UBC-76 specified values does not, in itself, constitute a valid argument for a reduction in the calculated critical dynamic shears for design purposes. The following reasons can, however, be put forward to support a reduction in $\bar{\alpha}_v$-values for design.

1. The model of the hinging region used in the analyses allowed for yielding in flexure only. The force-displacement relationship assumed for shear behavior was always linearly elastic. Although several investigators[17,18] have suggested that yielding of shear reinforcement should be minimized, if not completely avoided in design, the effect of reversed loading cycles of large amplitude tends to reduce the stiffness of the "flexural" hinging region with respect to transverse ("shear") displacements. Laboratory results[9,10] show that the contribution of the shearing component of displacement in the hinging region to the total displacement increases significantly with increasing amplitude of inelastic deformation.

   These observations indicate that under inelastic flexural deformation, the hinging region exhibits behavior corresponding to yielding in shear. Such shear yielding would increase the effective period of vibration and hence the maximum displacements of a structure. It would also set a practical upper limit on the magnitude of shear developed at the base of the wall. Thus, if a reasonable yield level in shear were assumed in the dynamic analysis model, the calculated maximum shear values would not be as high as in the linearly elastic shear model used in obtaining the critical shears reported above.

2. As pointed out in the section on "Maximum Response Values," the critical dynamic shears are generally not concurrent with the critical dynamic moments and ductility demands. Because of the reduced likelihood of the critical shears occurring simultaneously with the critical ductility demand, a reduction in the critical shears to reflect the relatively low probability of simultaneous occurrence with the critical (design) ductility appears warranted.

To provide an indication of the probability of the critical shear occurring simultaneously with the critical moment and ductility demand, Fig. 69 was prepared. This figure is based on data for isolated walls of different heights, periods, and yield levels. Results from 43 cases were considered. The abscissa in Fig. 69a represents the ratio of the maximum shear due to the same input motion that produced the critical ductility demand, to the critical shear as obtained from Fig. 42.

Figure 69a indicates that the ratio "maximum shear/critical shear"* ranges from 0.6 to 1.0 with a mean value of 0.81. An alternative way of presenting the data in Fig. 69a is given in the percentage exceedance plot of Fig. 69b, which is the complement of the associated cumulative frequency plot. Figure 69b gives the percentage of the total number of cases considered for which the ratio $V_{max}/V_{critical}$ exceeds a specific value, as indicated on the horizontal scale. Figure 69 shows that in only 20 percent of the total number of cases considered did the ratio $V_{max}/V_{critical}$ exceed 0.9.

It is important to note that the shears considered in Fig. 69 are the maxima that occur in the 10-second

*The "critical response value (e.g., shear, moment, etc.) is defined as the largest among the maximum response values produced by the six input motions considered, for a particular structure.

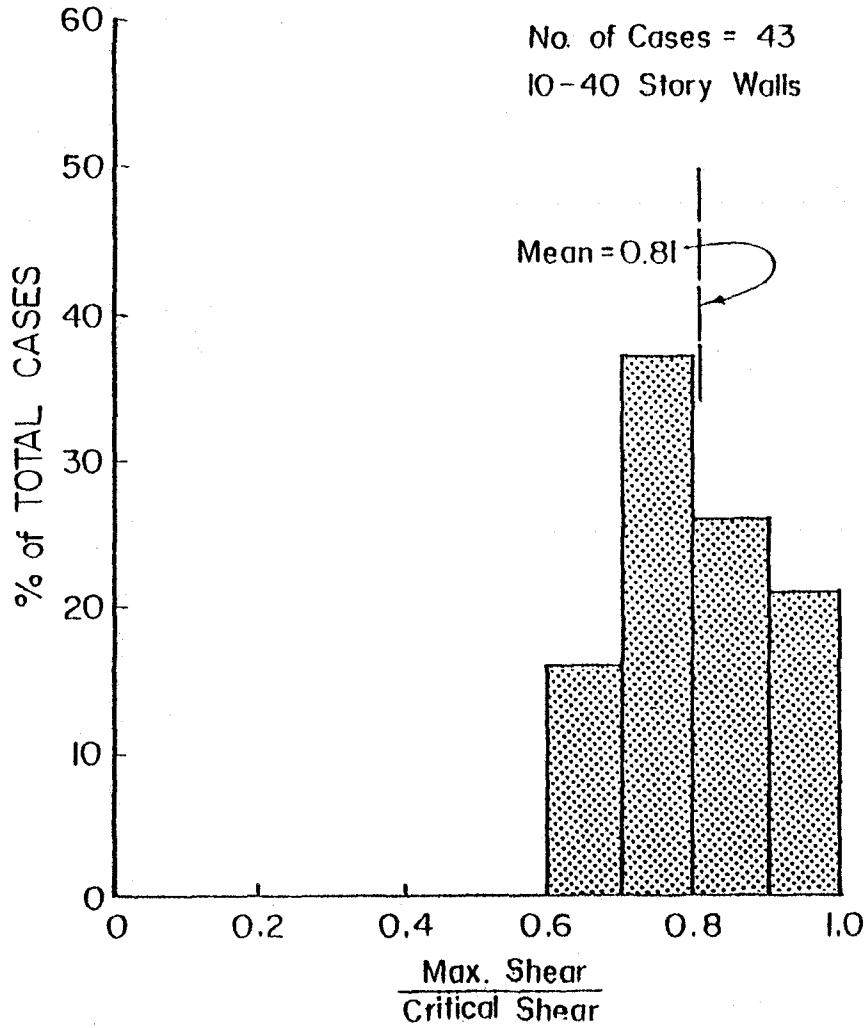

Fig. 69a Distribution of Ratio of Maximum Shear to Critical Shear

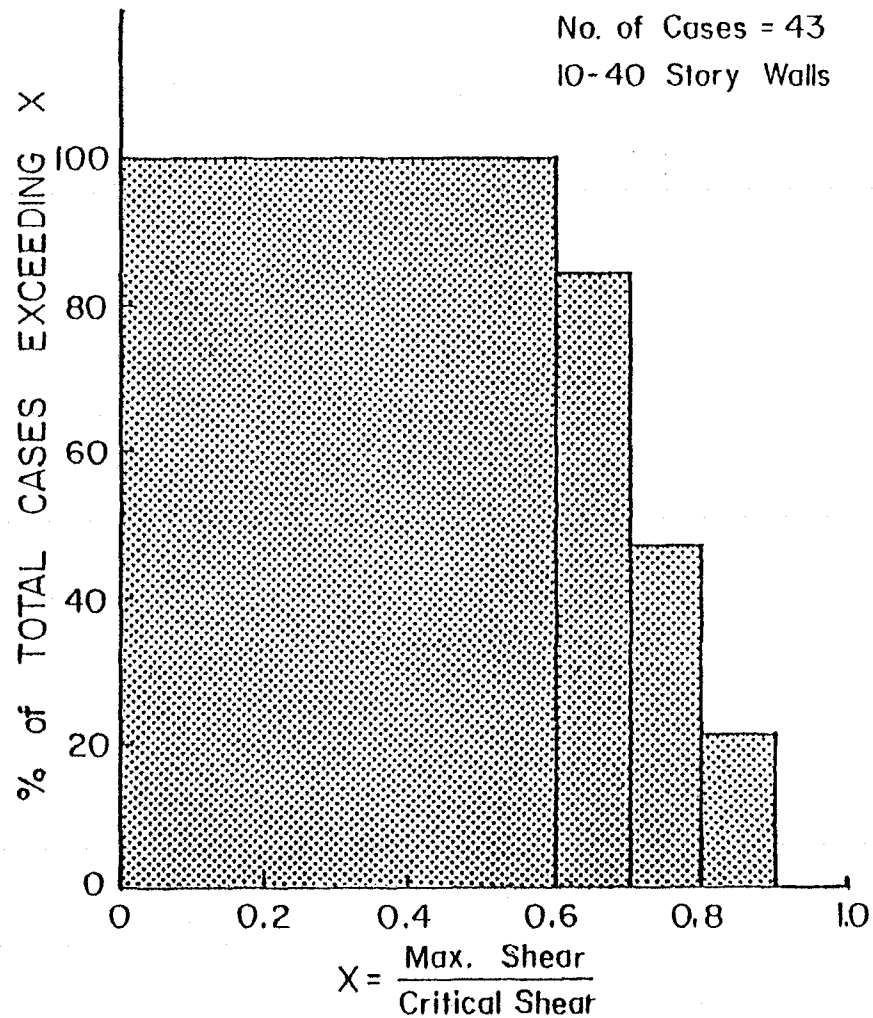

Fig. 69b Percentage Exceedance Plot Corresponding to Fig.

response period and are not necessarily the shears that are concurrent with the maximum moments and ductility demands.

Figure 70 illustrates the relationship between the maximum shear and the shear that is concurrent with the maximum moment and rotation. The "concurrent shear" is the base shear that occurs at about the same time as the critical moment and base rotation. It may be equal to or less than the "maximum shear". Both shears are produced by the same earthquake that produces the critical moment and ductility demand. Response histories for two cases are shown in Figs. 71a and 71b to illustrate the distinction between "maximum shear" and "concurrent shear".

Figure 70a shows the distribution of the ratio "concurrent shear/maximum shear" for the forty-three cases considered in Fig. 69. The ratio ranges from 0.30 to 1.0, with a mean value of 0.59. Figure 70b shows the corresponding percentage exceedance plot.

The above comparisons indicate that the simultaneous occurrence of critical dynamic shears, such as shown in Fig. 42, and critical rotational ductility, such as shown in Fig. 38, is unlikely.

3. In correlating force and deformation <u>demands</u> indicated by dynamic analyses with corresponding <u>capacities</u> obtained from tests of specimens under essentially static loading conditions, some adjustments have to be made in the values of either the demand or the capacity to reflect the difference in loading condition. This is essential if a valid comparison is to be made between demand and capacity.

If capacity values are determined from slowly-reversed loading tests in which the deformation, moment and shears are all in phase, then the critical dynamic response values must be adjusted in some manner to yield values comparable to these experimental results.

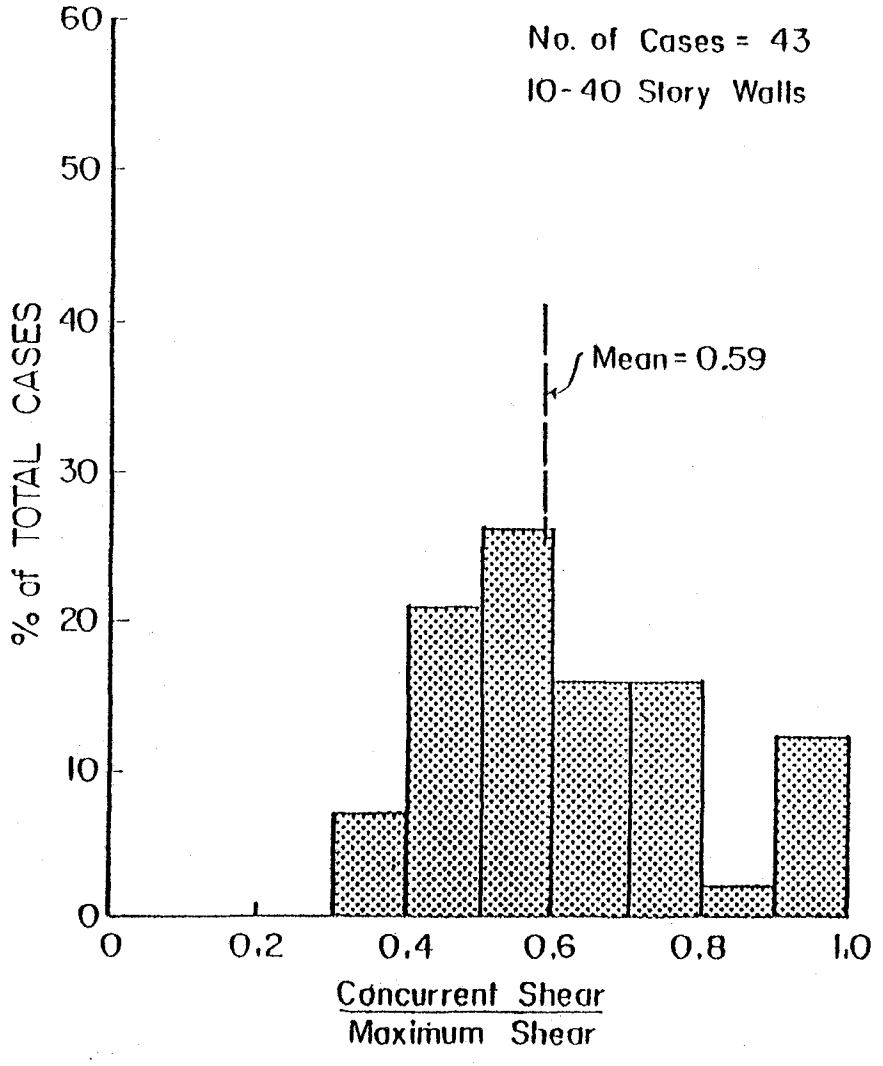

Fig. 70a Distribution of Ratio of Concurrent Shear to Maximum Shear

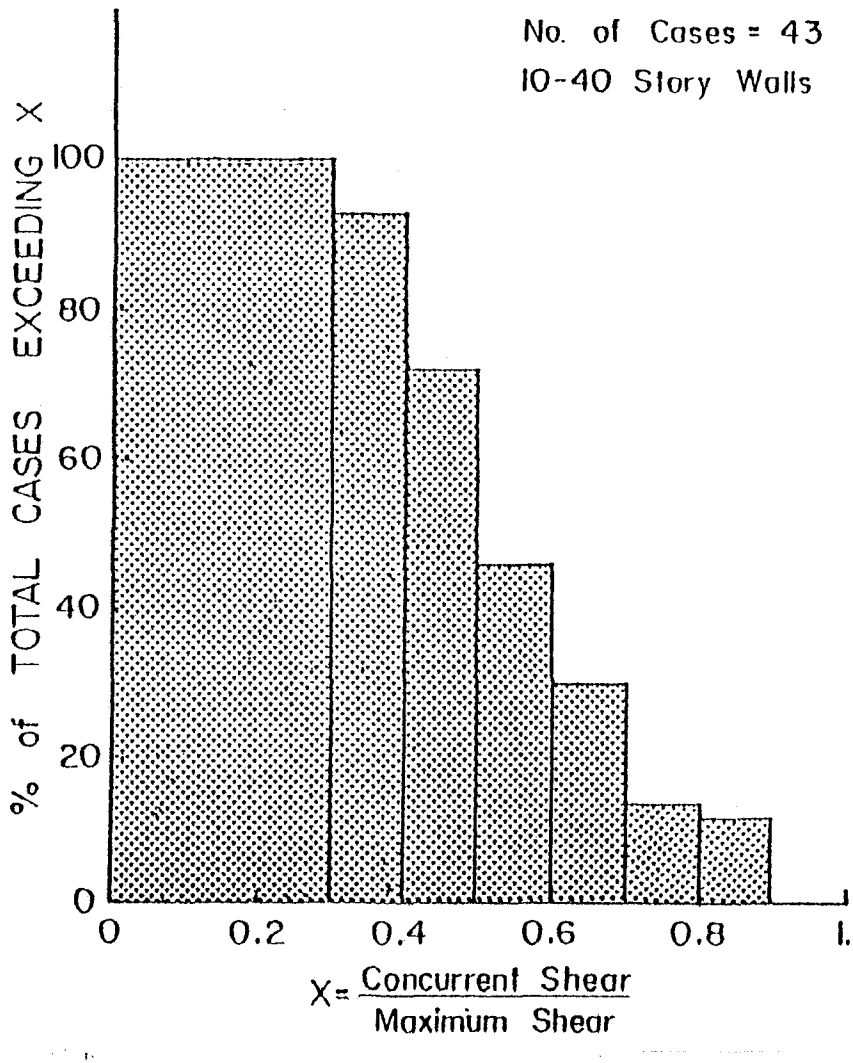

Fig. 70b Percentage Exceedance Plot Corresponding to Fig.

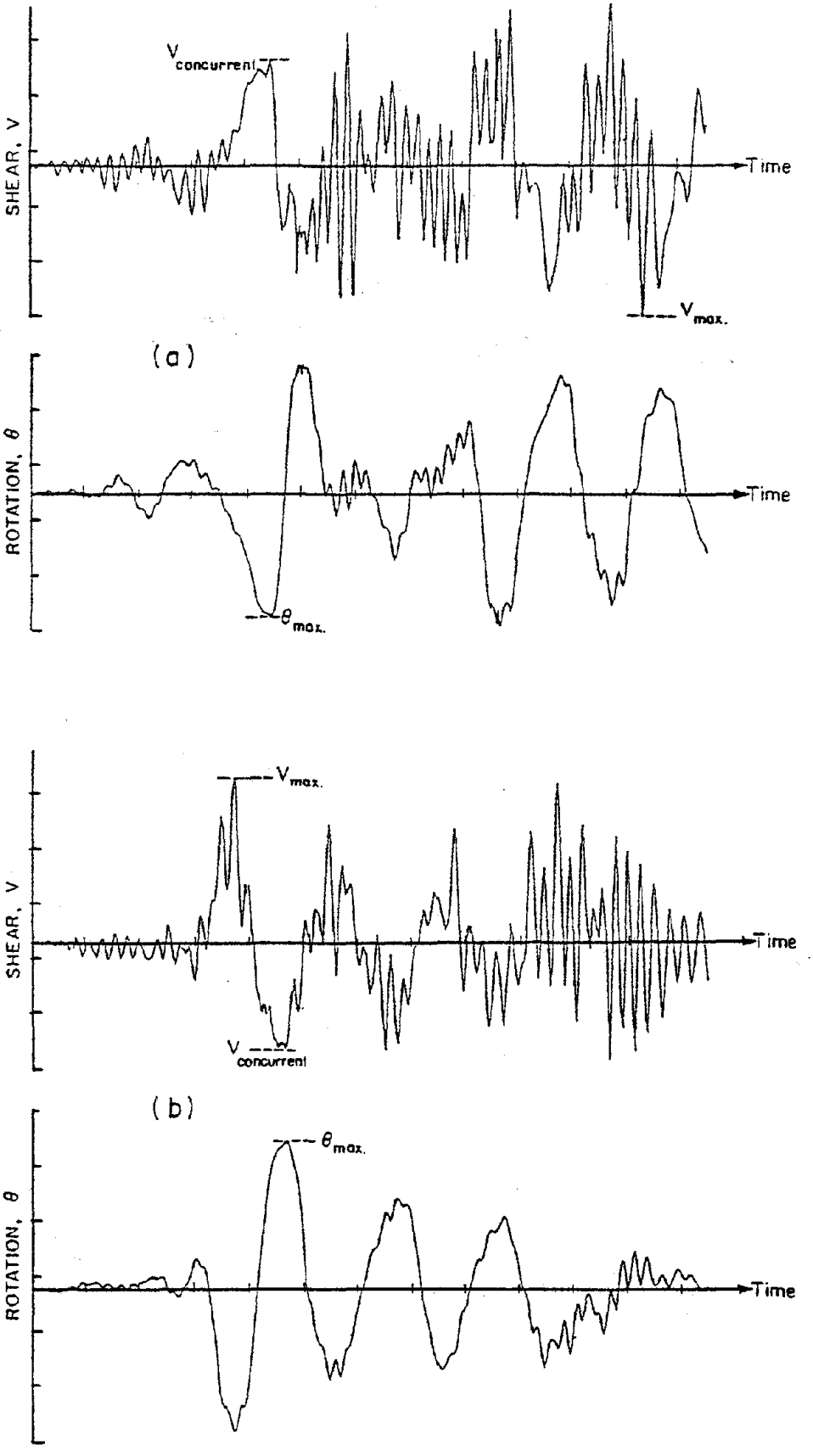

Fig. 71 Maximum Shear and Concurrent Shear Defined

A major difference between dynamic response shears and those obtained in laboratory tests under slowly reversing loads is the transitory character of the shear under dynamic conditions. Figures 72a through 72e, show the time variation of the base shear for 20-story walls subjected to different input motions. Also shown are the corresponding histories for base moment and nodal rotation at the first floor level. These figures indicate that the shear force generally changes more rapidly with time than the corresponding moment and rotation.

As previously mentioned, this is a reflection of the greater sensitivity of the base shear to higher modes of vibration. A loading condition in which the shear force fluctuates relatively rapidly with respect to moment and deformation, and reaches its peak value only for very short durations, represents a less severe loading than the usual slowly reversed loading test. In the slowly reversed loading test, the shear, moment, and deformation reach their peak values simultaneously and are sustained over a longer duration.

Although the need for an adjustment in critical dynamic shears is apparent if a comparison with results of slowly reversed loading tests is to be made, the magnitude of such an adjustment is not easily determinable on the basis of available data. A sound basis for determination of such an adjustment would involve tests of large-size specimens in earthquake simulators, i.e., shaking table tests.

On the basis of the above arguments, it is expected that a reduction factor, r_v, less than unity can be determined so that a shear design factor $\bar{\alpha}_v$, given by

$$\bar{\alpha}_v = r_v \bar{\alpha}_v \quad (r_v < 1.0)$$

is obtained. Although the magnitude of r_v cannot be determined from existing data, preliminary calculations given under the heading DESIGN EXAMPLE suggest that a value of r_v in the range of 0.4 to 0.6 may be appropriate for design purposes.

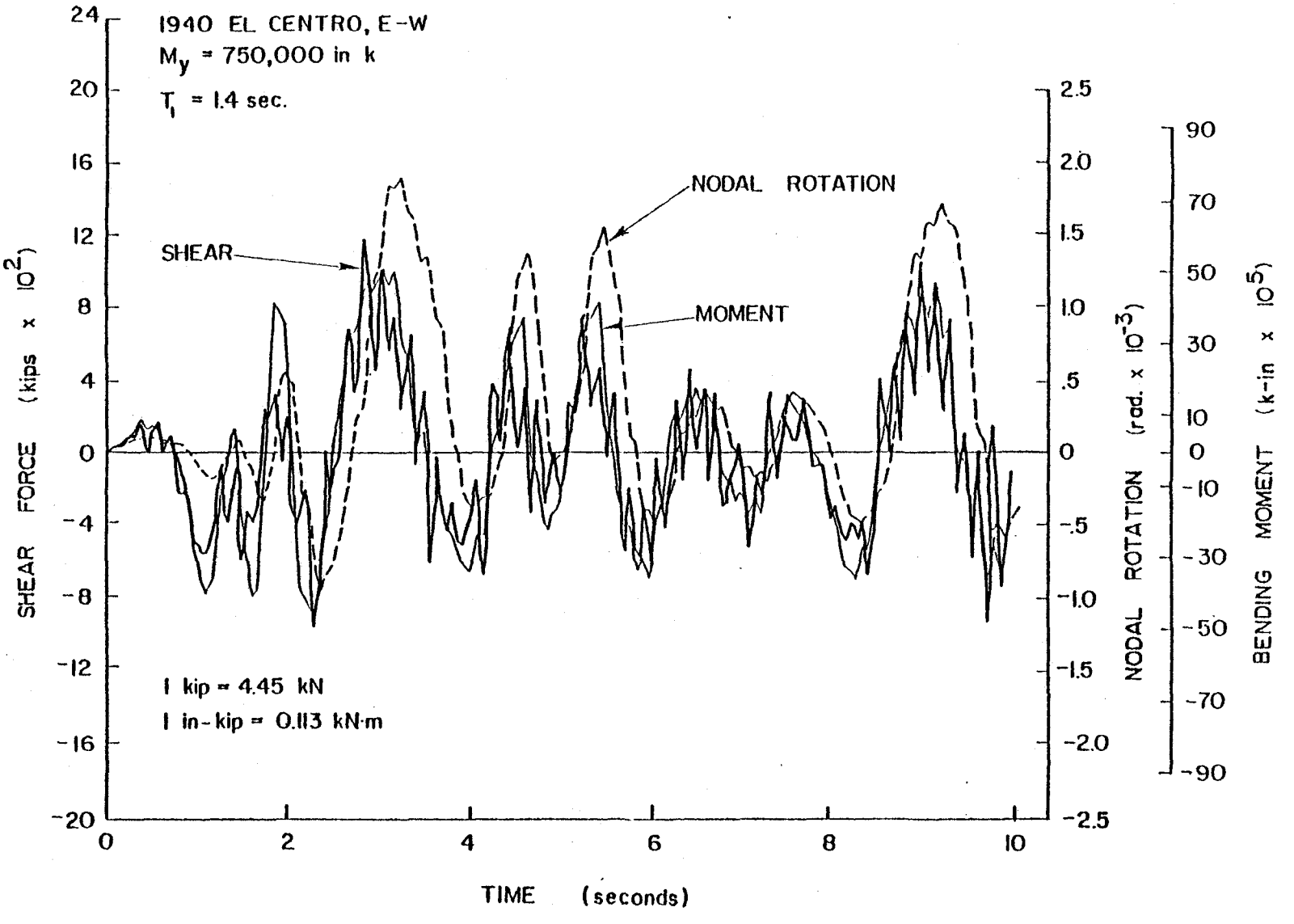

Fig. 72a Relative Variation with Time of Shear, Moment and Rotation in Hinging Region - 20-Story Isolated Wall

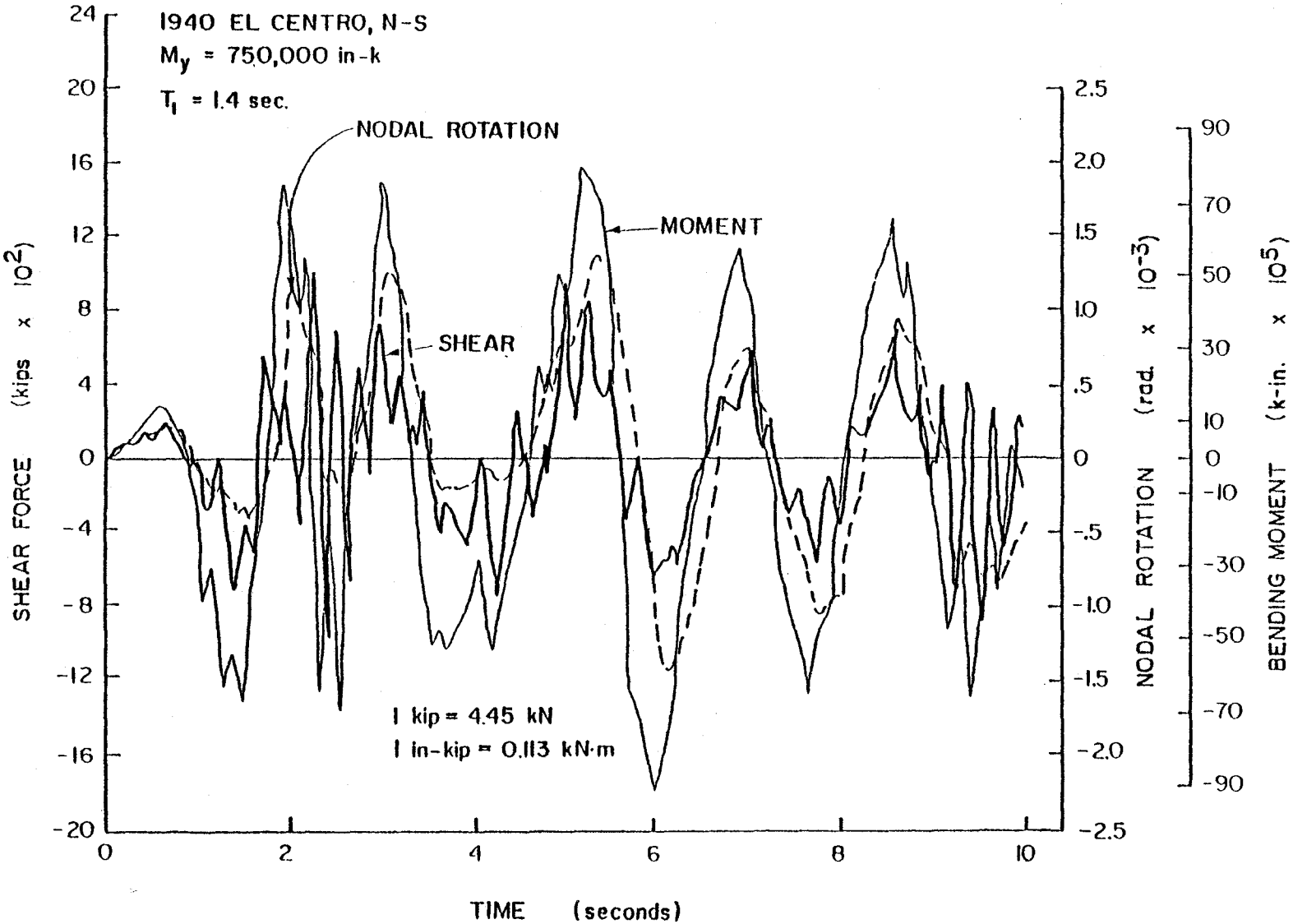

Fig. 72b Relative Variation with Time of Shear, Moment and Rotation in Hinging Region - 20-Story Isolated Wall

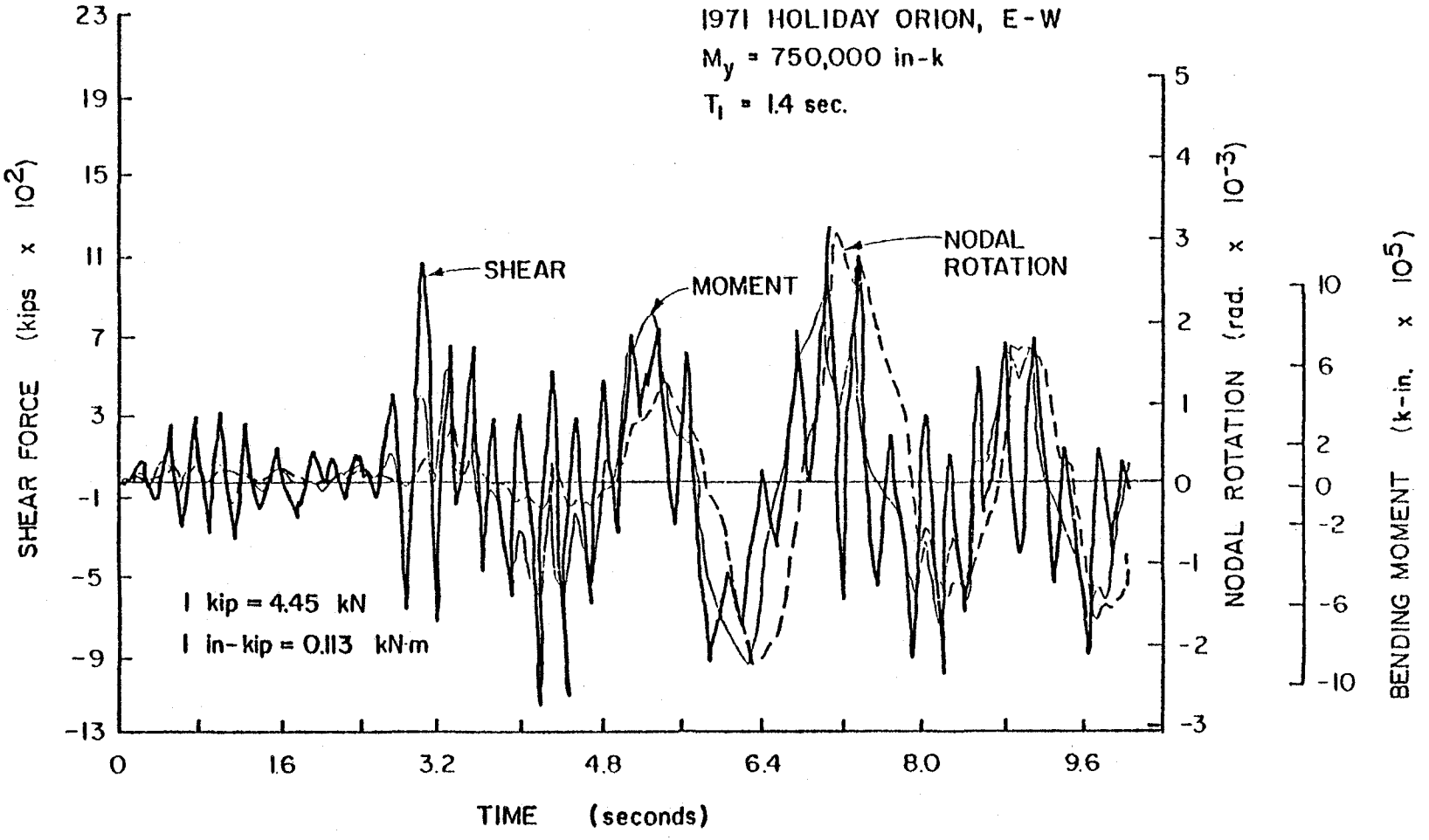

Fig. 72c Relative Variation with Time of Shear, Moment and Rotation in Hinging Region - 20-Story Isolated Wall

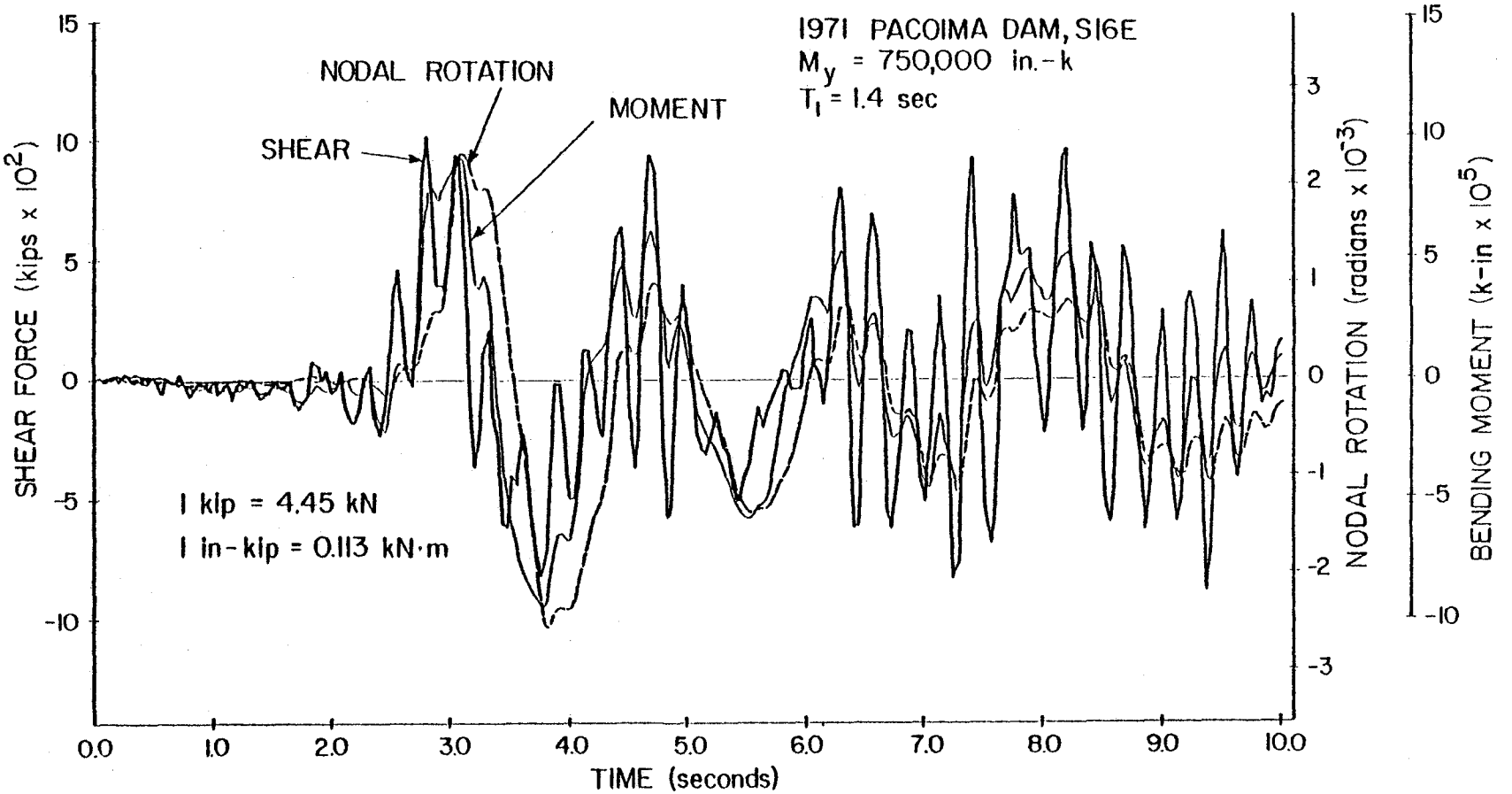

Fig. 72d Relative Variation with Time of Shear, Moment, and Rotation in Hinging Region - 20-Story Isolated Wall

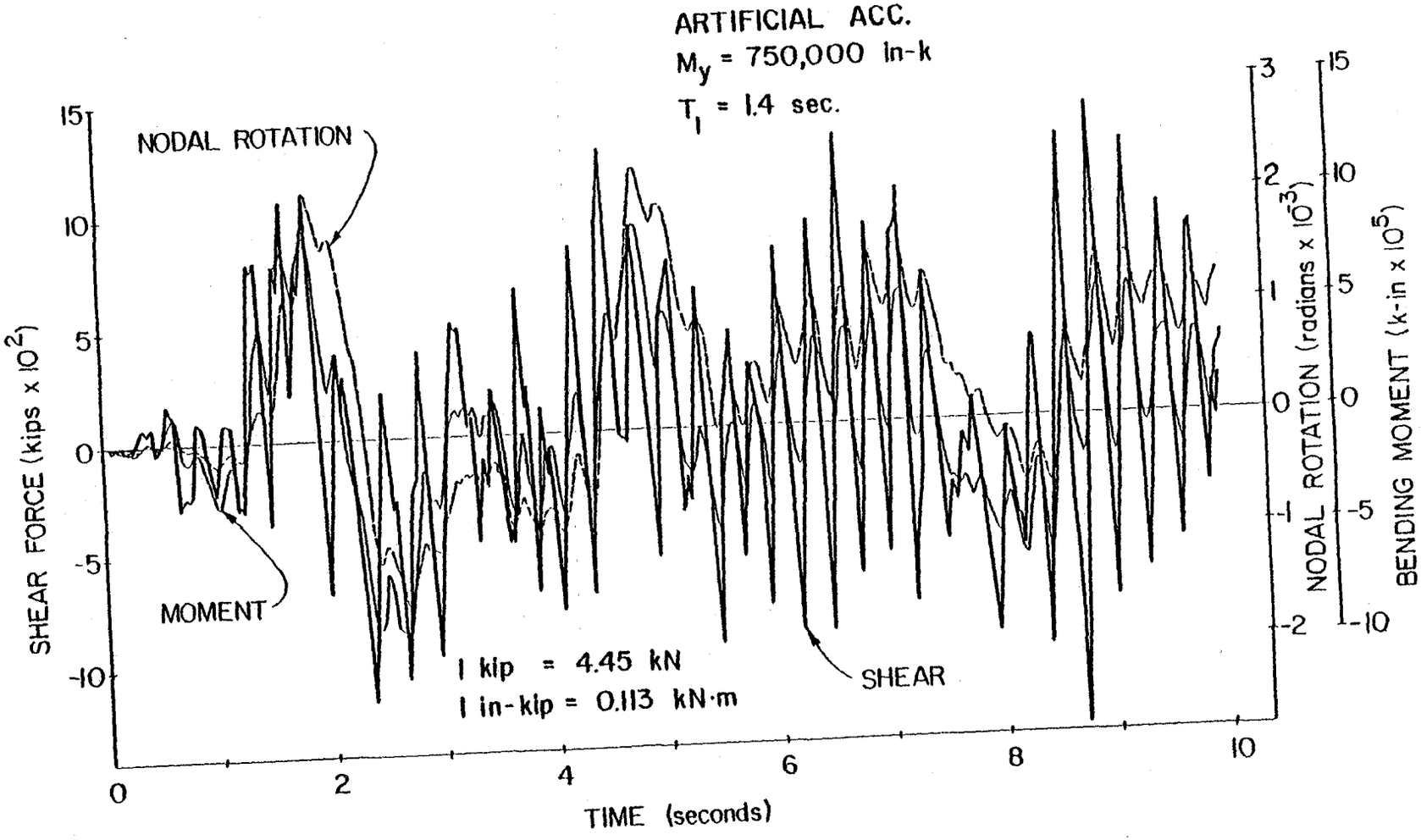

Fig. 72e Relative Variation with Time of Shear, Moment and Rotation in Hinging Region - 20-Story Isolated Wall

CHECK ON DISTRIBUTION OF DESIGN FORCES FOR UPPER PORTIONS OF WALL

Design forces developed in the preceding sections are intended for design of the potential hinging region at the base of a wall. The base of the wall is generally the most critical part in terms of the magnitude of force and deformation requirements. The tests of isolated walls, conducted as part of the overall project, were aimed primarily at determining the behavior of the hinging region near the base of the walls.

In determining design forces for flexural design of the base of the wall, total base shear, V_T was assumed to be distributed in accordance with UBC-76[16]. This distribution, i.e., an 'inverted triangular' distribution with a top force, F_t, as shown in Fig. 41, reflects the dominant effect of the fundamental mode on response. To verify the applicability of this distribution to the design of the upper portions of a wall, a comparison was made between distributions of maximum moments and shears associated with the assumed (UBC-76) distribution of forces and those obtained from analysis.

Normalized Maximum Force Distribution

An indication of the spread in the distribution of the maximum dynamic story shears along the height of isolated walls is given in Fig. 73. This figure is based on data from twenty-four 40-story walls with T_1 = 2.4 sec. and varying yield levels. The walls were subjected to five different input motions. The values of the maximum story shears plotted in Fig. 73 have been normalized by dividing the shear at each floor level by the corresponding calculated maximum base shear. Thus, at the base, where maximum shear occurs, the normalized base shears all equal unity. The length of the horizontal bars in the figure indicate the range of scatter of the data. For this particular set of data, the scatter is least near the base and largest near midheight.

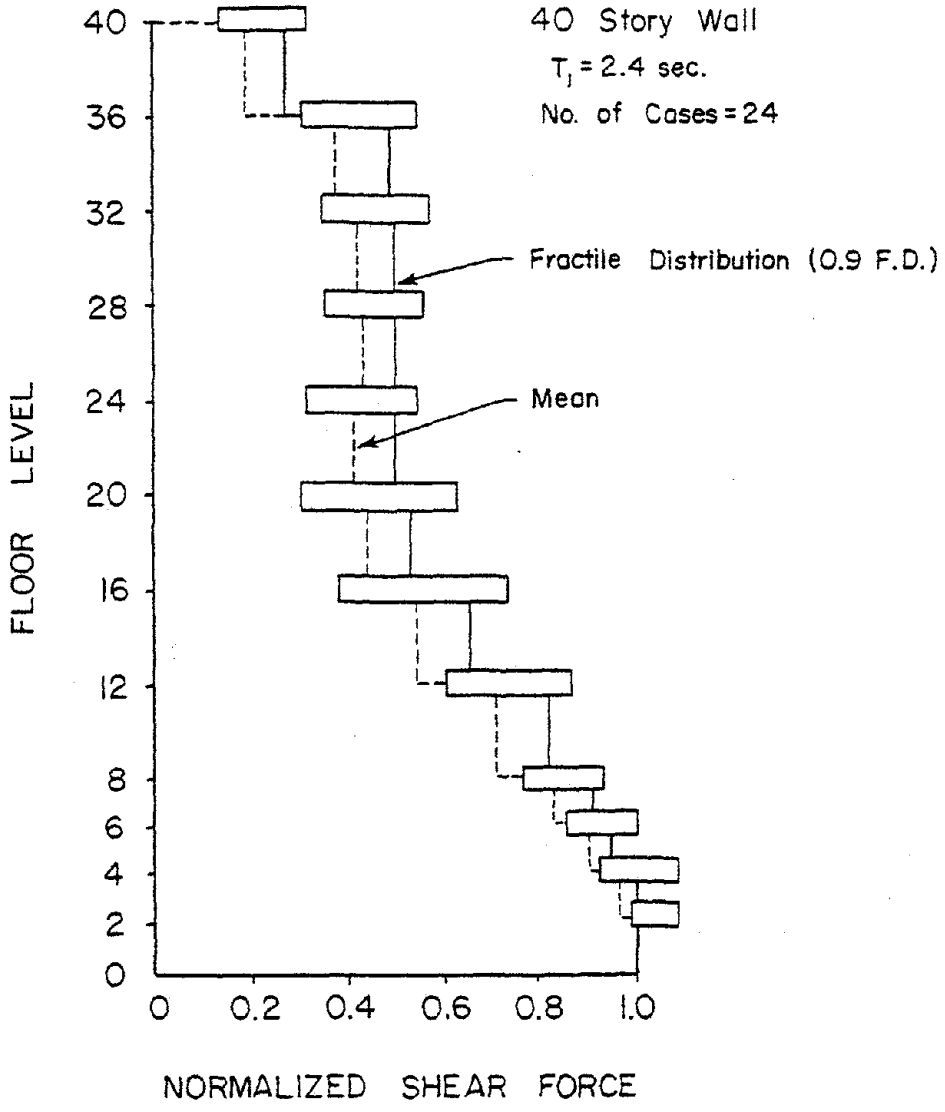

Fig. [73] Scatter Plot for Normalized Shear Force

Figure 74a shows the frequency distribution of the lateral force at the top, F_t, for the same set of twenty-four cases. The maximum top force, F_t, has also been normalized by dividing by the corresponding maximum calculated base shear. Figure 74b shows a percentage exceedance plot for the normalized top force.

Information such as shown in Figs. 73 and 74 can be used to determine a suitable design shear distribution over the wall height. From this the corresponding lateral force distribution can be obtained. In view of the scatter of the data, the question of what value to use as a basis for design naturally arises. A distribution based on average values cannot be justified since many cases fall outside such a distribution. On the other hand, a distribution encompassing all values appears unduly conservative.

In this study, a distribution covering at least 90% of all cases considered was adopted as a reasonable compromise between economy and safety. In statistical terms, such a distribution is called a 0.90 fractile distribution (0.9 F.D.). Figure 73 shows both the mean and the 0.9 fractile distribution of maximum story shears. Figure 74b indicates that the 0.9 fractile value of the normalized top force, F_t, for the data set considered is about $0.29(V_{base})_{max}$.

Comparison of Distribution of Maximum Dynamic Forces with Corresponding UBC-76 Distribution

For the purpose of comparing the distribution of maximum dynamic forces along the height of isolated walls with that recommended by UBC-76, the 0.9 fractile distribution of normalized maximum forces was used. The comparison was made using normalized story shears and moments along the height of the structure. These quantities were used instead of lateral forces since the former are more directly related to design. Normalization of the maximum dynamic forces serves to focus

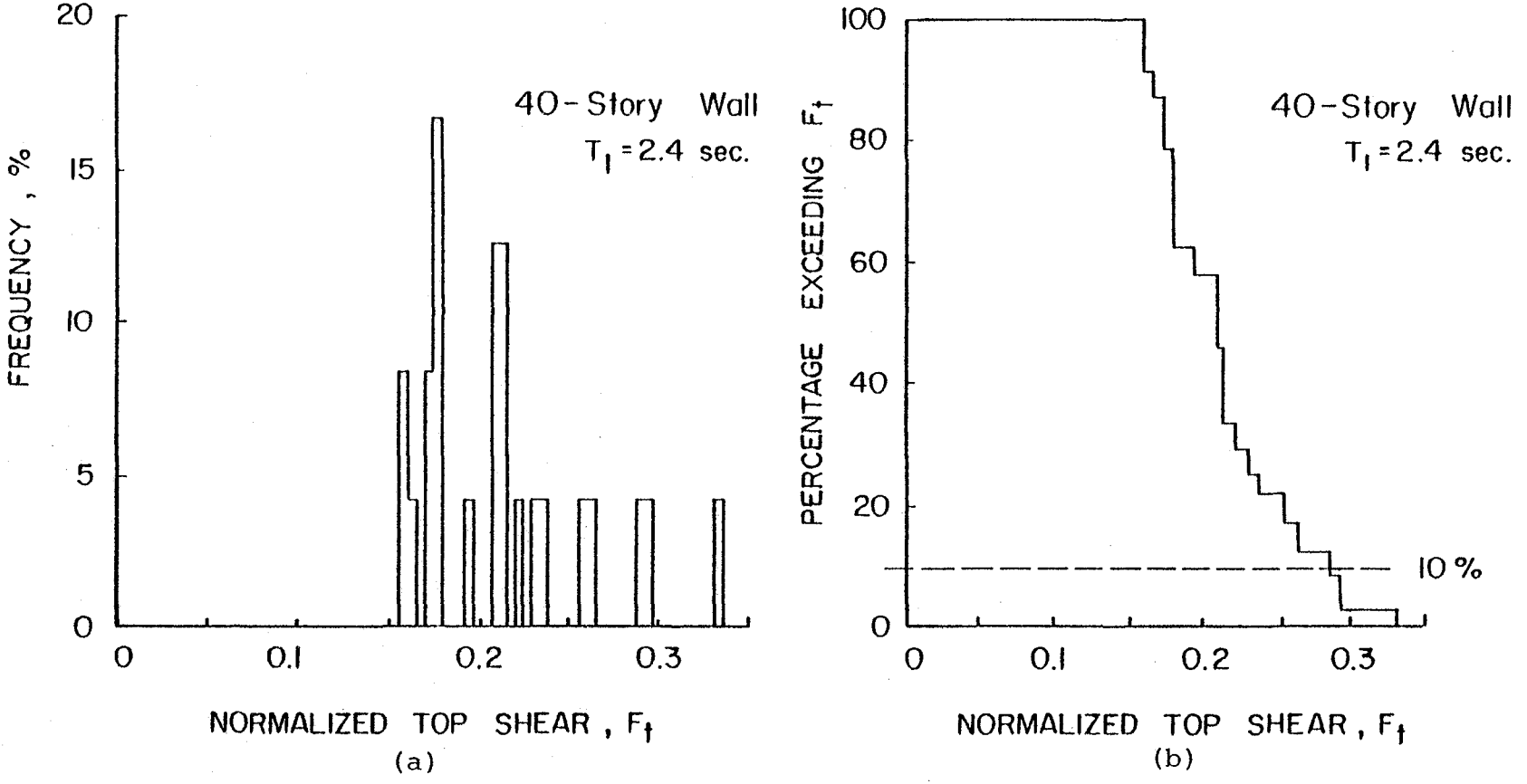

Fig. 74 Frequency Distribution of Top Shear Force, F_t

attention on the distribution or relative magnitudes of these forces rather than their absolute magnitudes.

The lateral forces specified by UBC-76 were determined by distributing the base shear, V, according to the expression

$$F_x = \frac{(V-F_t)\ w_x\ h_x}{\sum_{i=1}^{n} w_i\ h_i}$$

where

F_t (top force) = 0.07 T V

T = fundamental period of vibration

w_x = weight of mass of floor level "x"

h_x = distance of floor level "x" from base of wall

n = total number of floor levels.

After the story shears and moments were determined from the lateral forces, these were normalized by dividing by the base shear, and the total overturning moment, respectively.

Distribution of Normalized Maximum Story Shears

Figure 75 shows a comparison of the maximum normalized shear 0.9 F.D. with the corresponding normalized story shear distribution prescribed by UBC-76 for specific fundamental periods of walls ranging from 10 to 40 stories. The cases selected cover the entire range of wall properties investigated. A total of 18 cases were considered for each wall height, representing three different yield levels and six input motions.

Figure 75a shows that in terms of relative magnitude (or for the same total base shear) the UBC story shears exceed slightly the corresponding 0.9 fractile shears over the lower three-fourths of the wall height. However, the UBC distribution gives story shears that are less than the 0.9 fractile shears near the top of the wall. The same observation applies to Figs. 75b, c, and d for the other wall heights. The percentage difference between story shears at the top is greatest for the short-

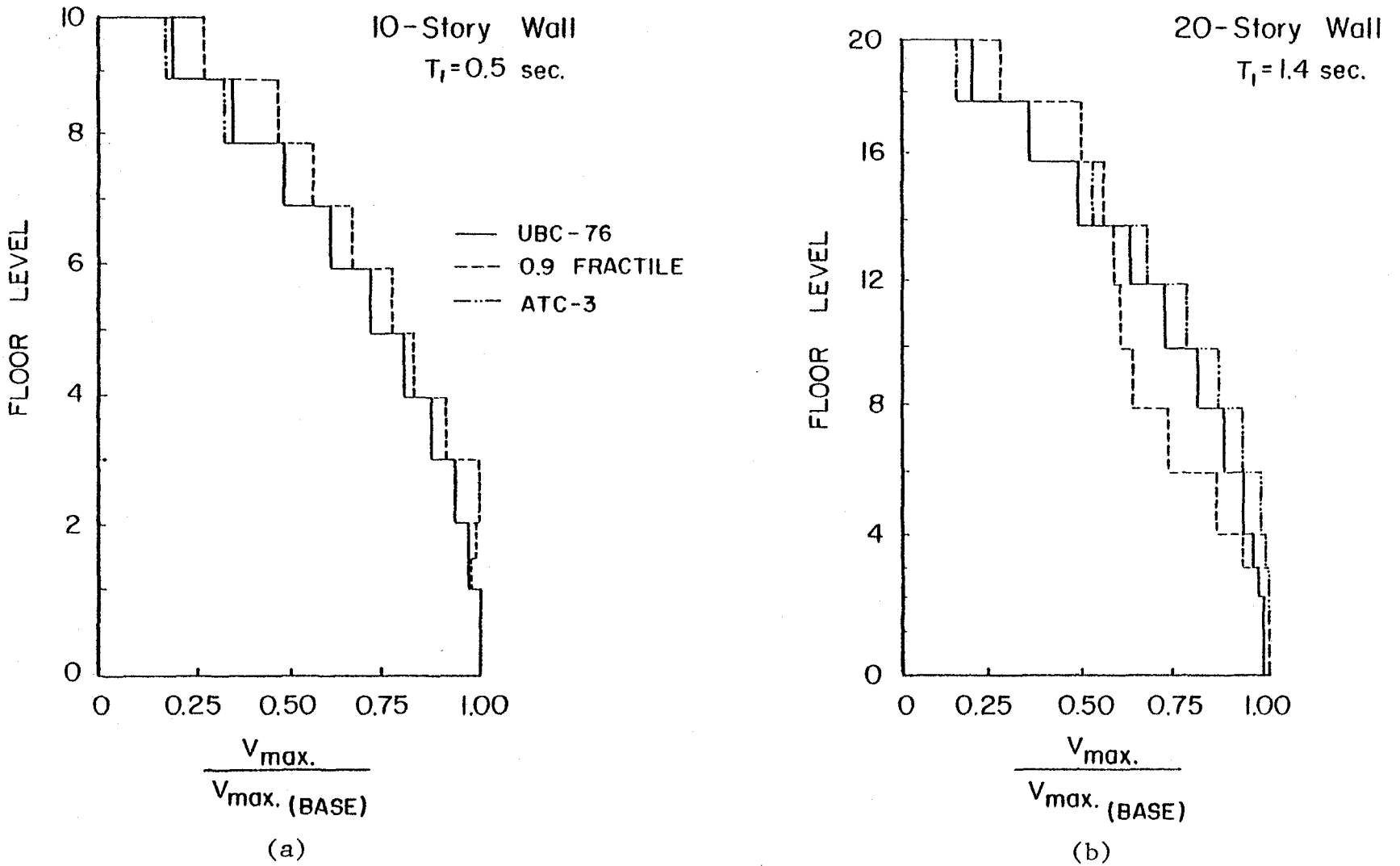

Fig. 75 Normalized Story Shear Distributions Over Height for Different Wall Heights

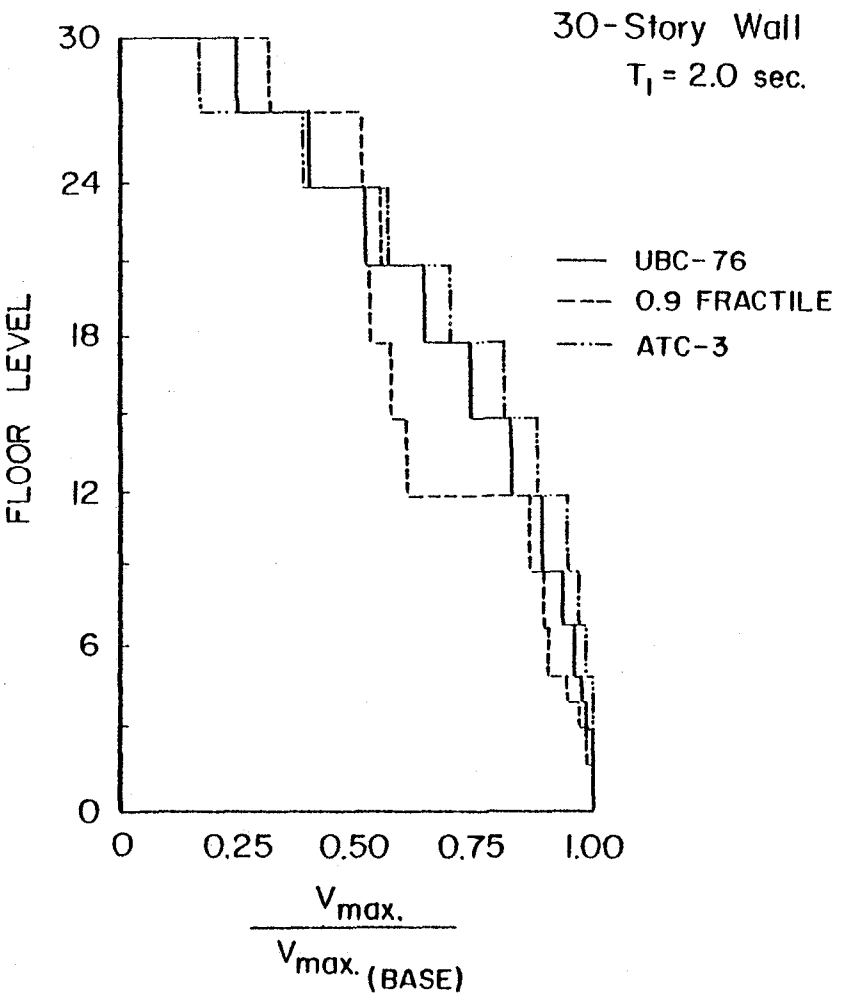

(c)

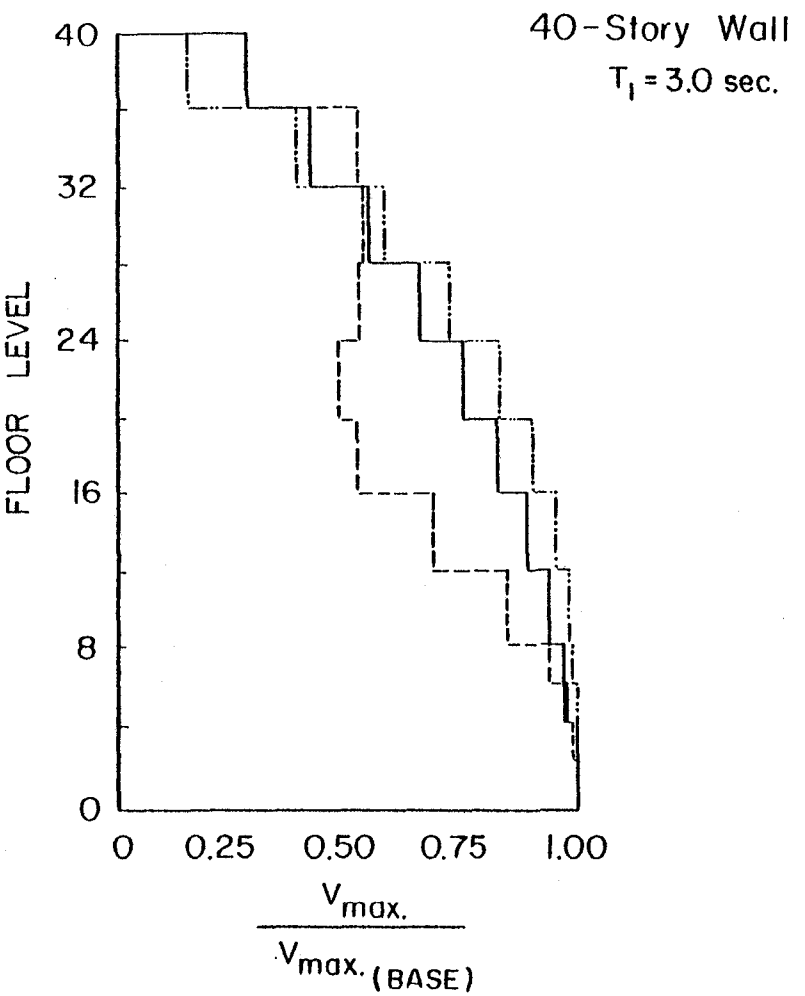

(d)

Fig. 75 (contd.) Normalized Story Shear Distributions Over Height for Different Wall Heights

period, low walls and diminishes with the longer-period, taller walls. For comparison, the distribution corresponding to the ATC-3[1] equivalent lateral force procedure is also shown in Fig. 75. The observations made relative to the UBC-76 distribution when compared to the 0.9 fractile shears also apply to the ATC-3 distribution.

To obtain design story shears that are in close agreement with the distribution indicated by the 0.9 F.D. shears from dynamic inelastic analysis, the following modification to the story shears resulting from lateral forces distributed according to UBC-76 is proposed:

(1) The story shears in the top 25% of the wall should be increased by a factor

$$\beta_1 = 2 - T/3, \qquad \text{where } 1.0 \leq \beta_1 \leq 1.50$$

(2) Use of β_1 should not result in a story shear greater than that calculated from the UBC-76 lateral force distribution for any portion in the lower 75% of the wall.

The factor β_1 was determined using regression analysis. The proposed correction represents a simple method of modifying the story shears from the familiar UBC lateral force distribution to obtain results closely conforming to that indicated by dynamic inelastic analysis.

The above proposed correction is to be applied directly to story shears resulting from the lateral forces distributed according to UBC-76. Thus, no change need be made in the procedure developed earlier for determining design forces for the hinging region near the base of the wall. The correction proposed above need be applied only to the story shears in the top 25% of the wall to remedy the unconservativeness of the shears associated with the UBC-76 lateral force distribution.

Figure 76 shows a comparison of normalized story shears for the same cases considered in Fig. 75, with the above-proposed correction included in the UBC shears. In most practical cases, the design of the upper 25% of a wall is governed by code wall-slenderness requirements so that the application of the proposed story shear correction may not alter wall dimensions.

Distribution of Normalized Bending Moments

Normalized bending moments for the four cases examined earlier, corresponding to the 0.9 fractile of the dynamic analysis results and the UBC-76 lateral force distribution are shown in Fig. 77. Also shown for comparison are normalized moments corresponding to the ATC-3 equivalent lateral forces. It will be noted that insofar as distribution over the height is concerned, UBC-76 and ATC-3 are very close to each other.

Figure 77 shows that the UBC-76 (as well as the ATC-3) normalized moment requirements are less than the 0.9 fractile moments for all four cases considered. The difference between UBC-76 and 0.9 fractile normalized moments is particularly significant near midheight. At about two-thirds of the height of the walls, the 0.9 fractile moments exceed the corresponding UBC moments by as much as 100 percent for the longer period walls.

To bring the normalized moments calculated from the UBC-76 lateral force distribution into closer agreement with the 0.9 fractile moments, it is proposed that the former be multiplied by a factor, β_2, given by

$$\beta_2 = k \left(\frac{x}{H}\right) \left[1 - \left(\frac{x}{H}\right)\right] ,$$

where

H = total height of wall
x = distance of level "x" from base
k = a constant, equal to the initial fundamental period, T_1, but not greater than 1.2.

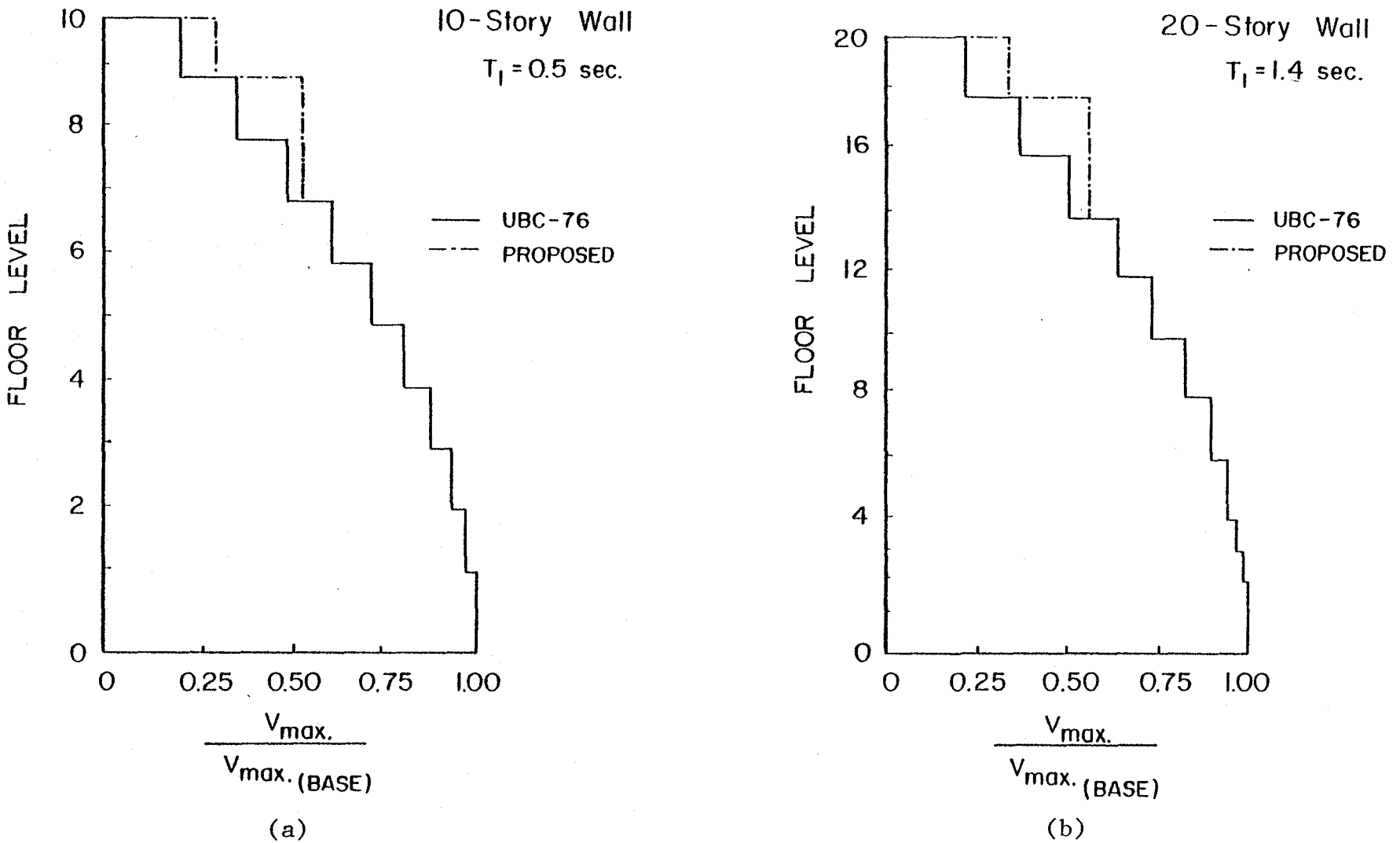

Fig. 76 Proposed Modification to UBC Story Shear Distribution

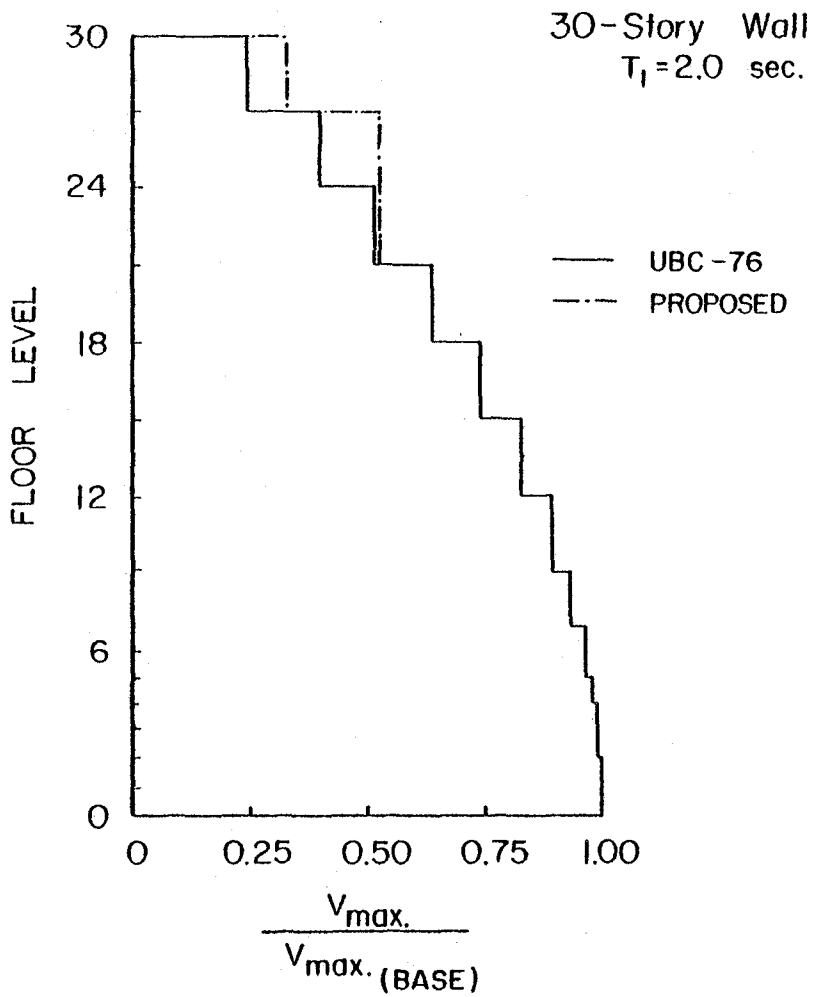

(c)

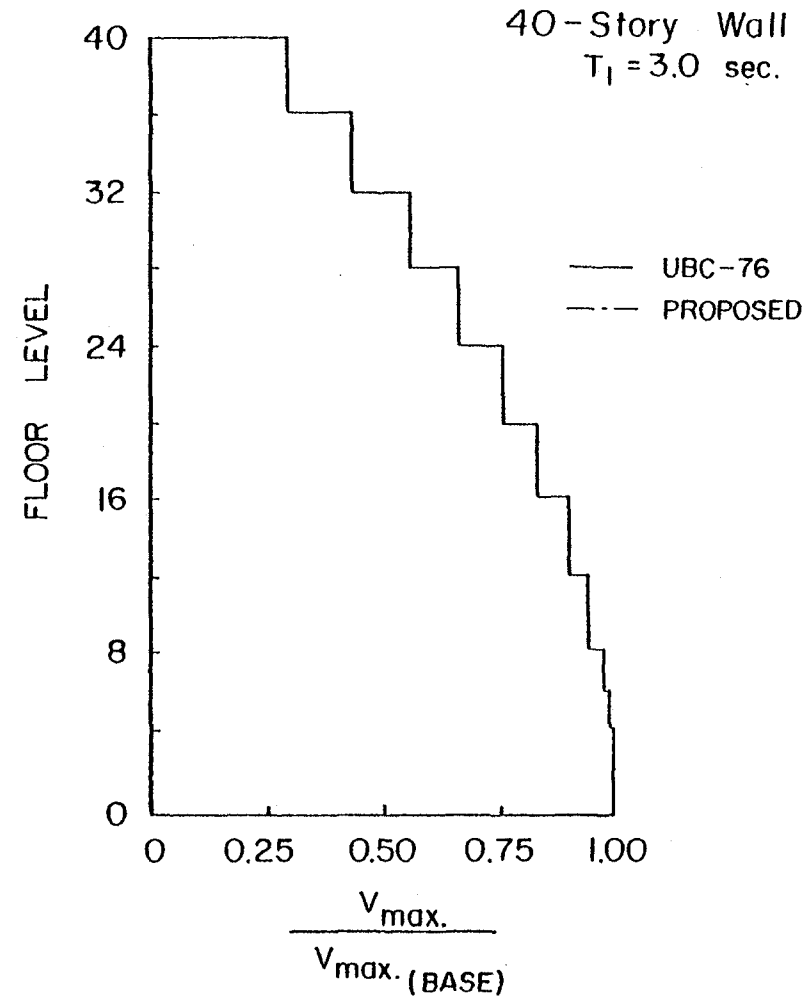

(d)

Fig. 76 (contd.) Proposed Modifications to UBC Story Shear Distribution

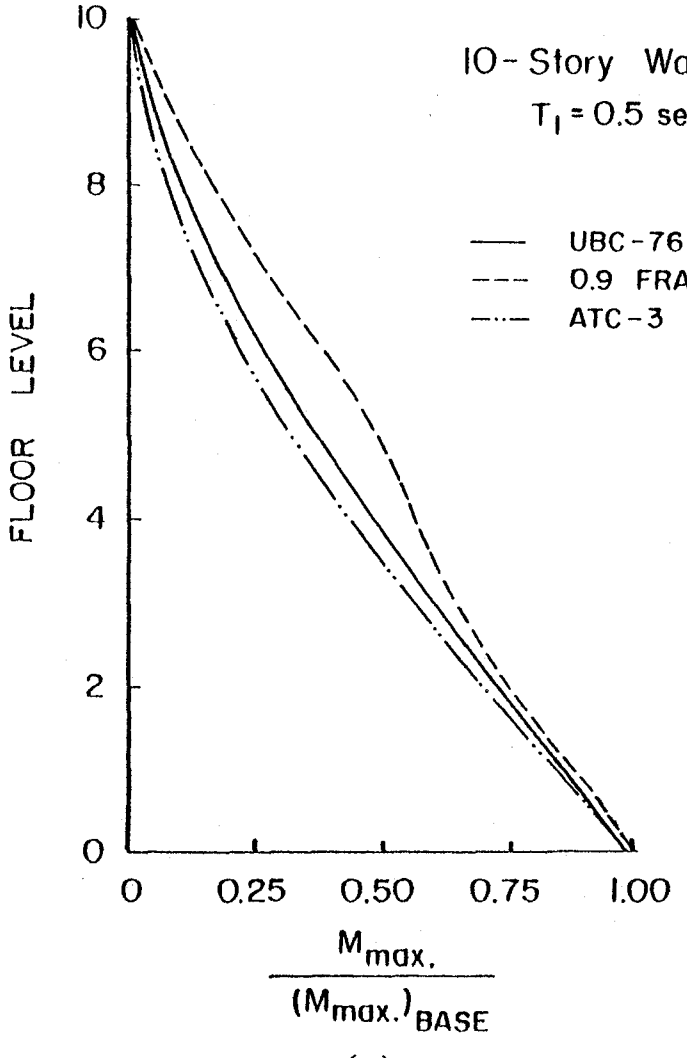

(a)

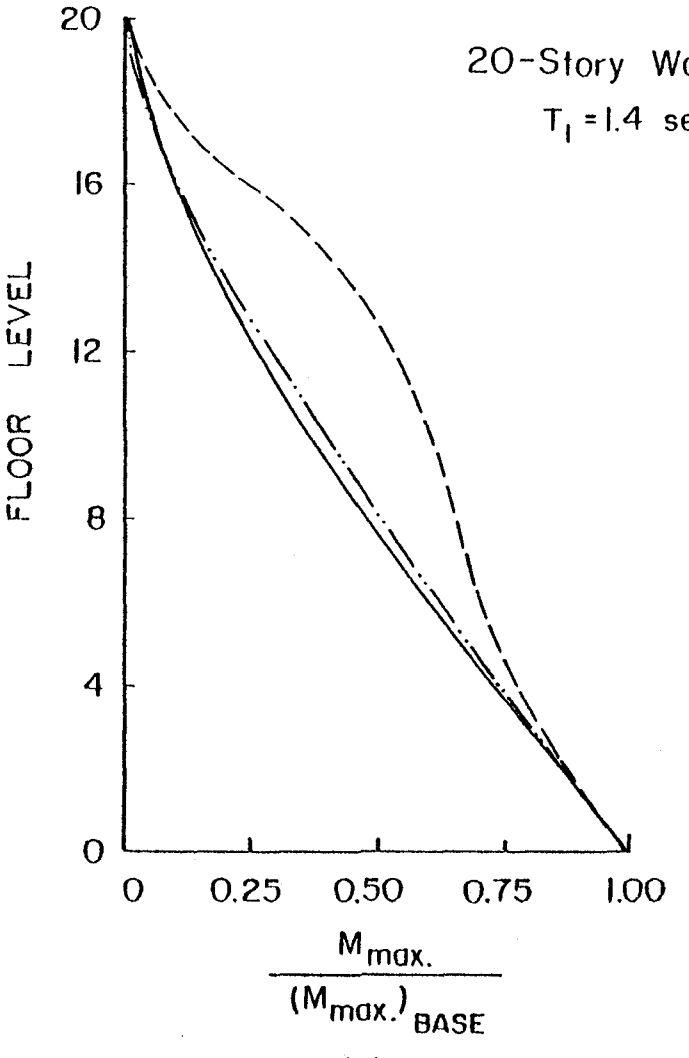

(b)

Fig. 77 Normalized Maximum Moment Distributions Over Height for Different Wall Heights

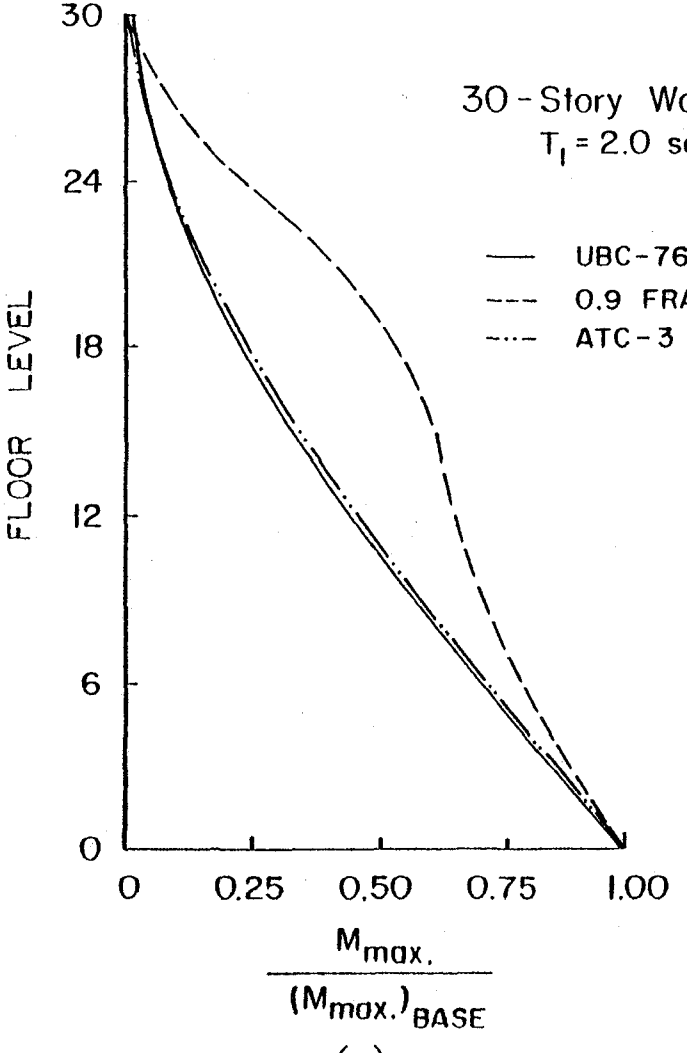

(c)

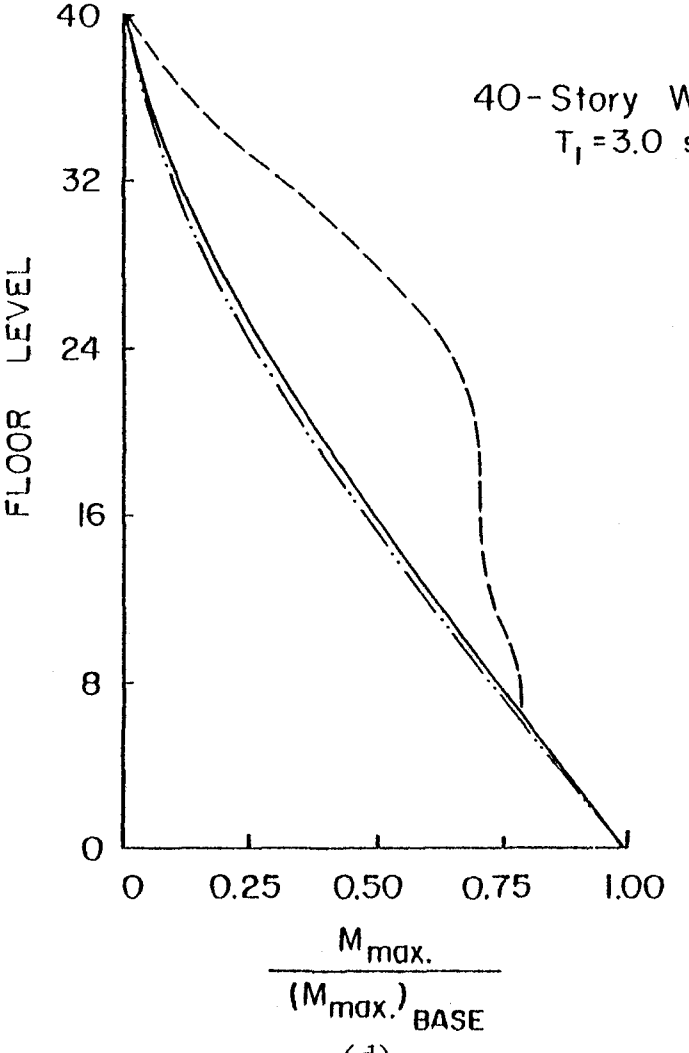

(d)

Fig. 77 (contd.) Normalized Maximum Moment Distributions Over Height for Different Wall Heights

The expression for β_2 was also determined using regression analysis. Normalized UBC moments for the four cases considered, with the correction factor β_2 applied, are shown plotted in Fig. 78. Also shown for comparison are the 0.9 fractile moments from dynamic analysis.

It should be pointed out that the proposed modifications to the design forces for the upper portions of walls are based on results for isolated walls with uniformly distributed mass and stiffness over their height.

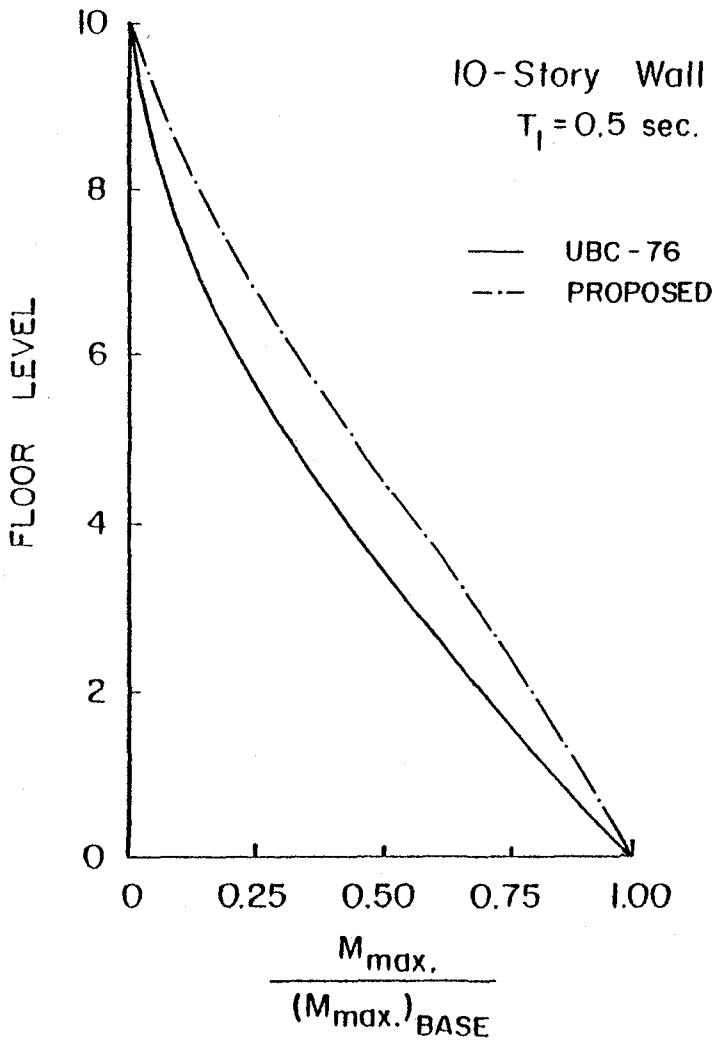

(a)

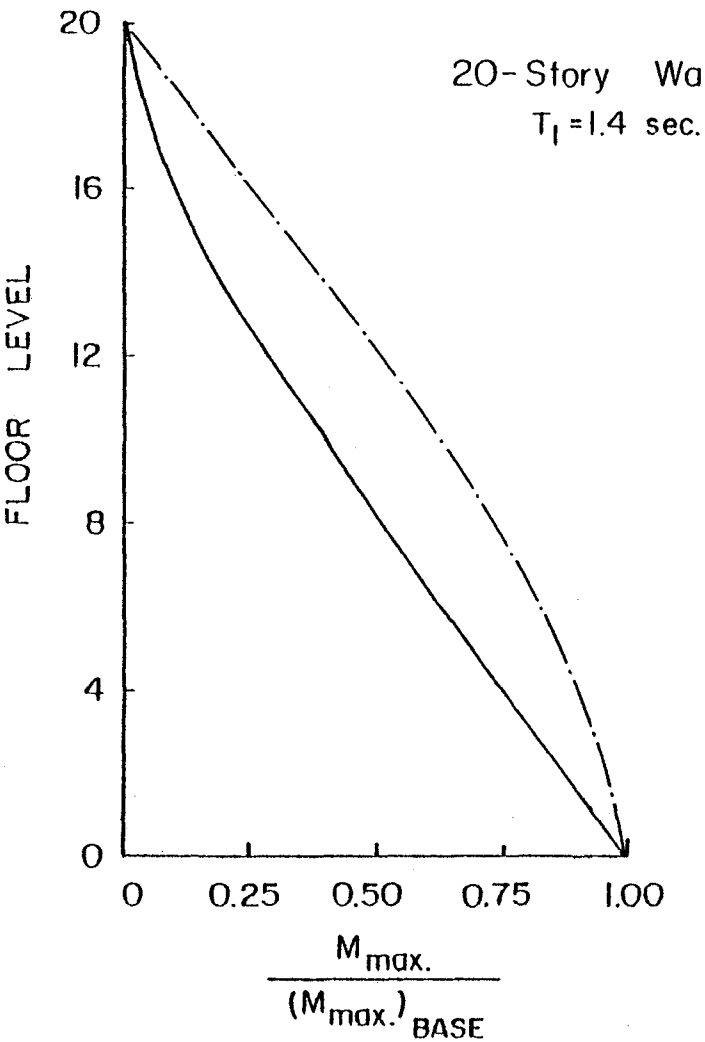

(b)

Fig. 78 Proposed Modification to UBC Story Shear Distribution

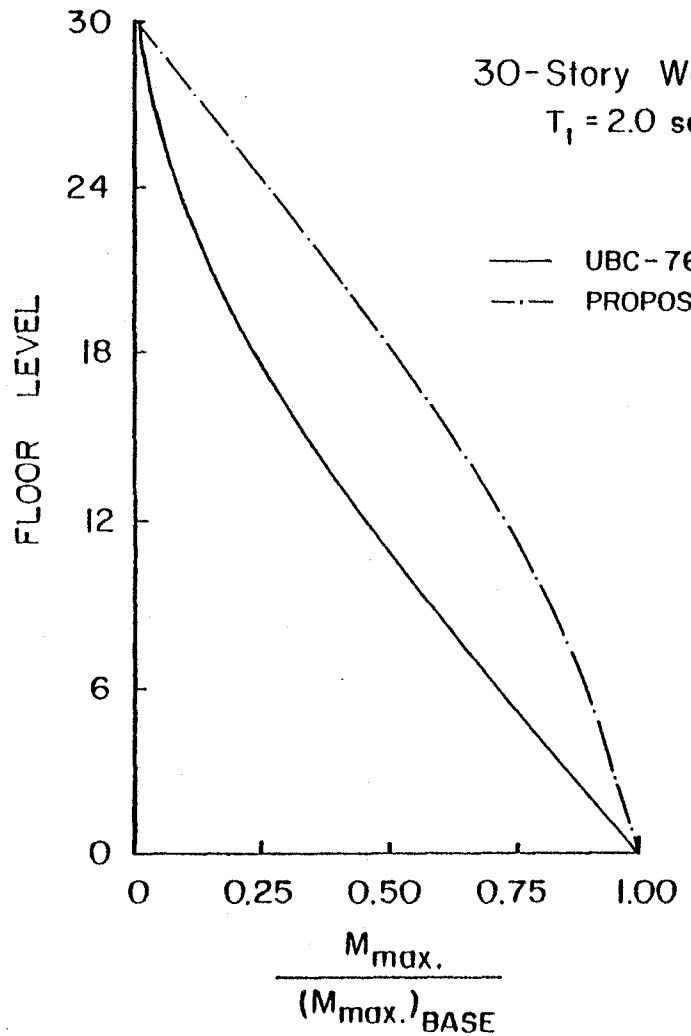

(c)

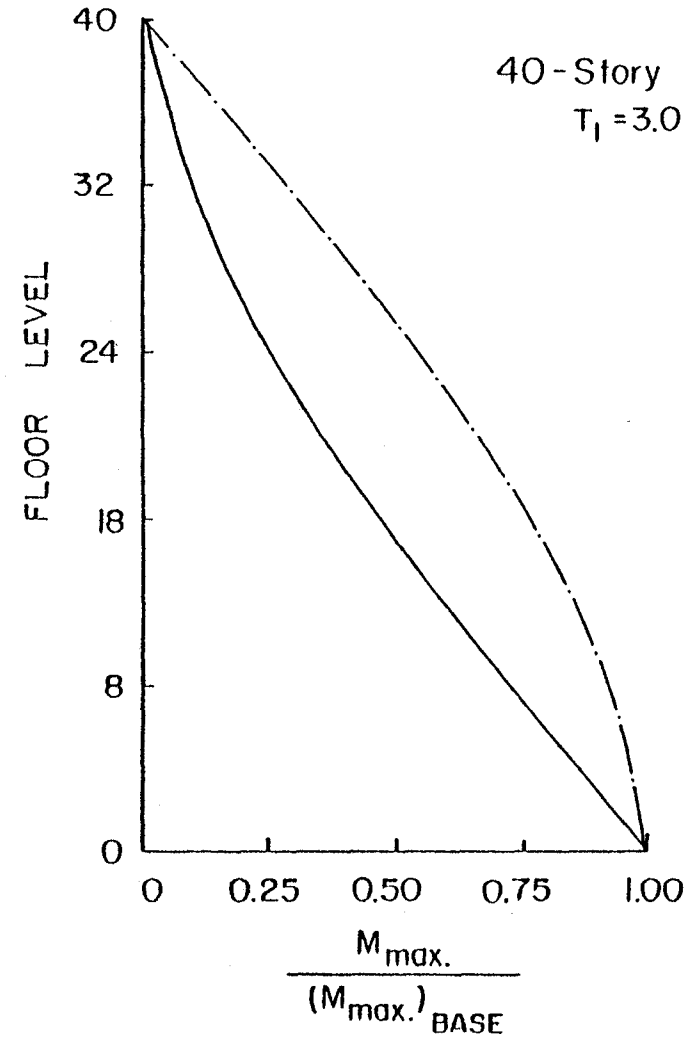

(d)

Fig. 78 (contd.) Proposed Modification to UBC Story Shear Distribution

PROPOSED DESIGN PROCEDURE - SUMMARY

The proposed design procedure follows essentially the same basic steps presently used in designing for earthquake resistance. Development of a design procedure has been made easier by the existence, both in current codes and in recently published literature, of a strong and logical basis for the design of structures for earthquake resistance.

The availability of analytical and experimental data has allowed the treatment of such major design parameters as ductility, yield level, and earthquake intensity in a more explicit manner than was possible before.

The basic steps in the design procedure are summarized below for the particular case of isolated structural wall buildings. A similar general procedure can be developed for wall systems, with appropriate modifications to cover the additional considerations involved in the more complex systems.

(1) Preliminary Design. A logical first step is a design satisfying gravity and wind loading requirements. From the preliminary design, an effective initial stiffness and the corresponding initial fundamental period, T_1, can be determined.

(2) Stiffness Design for Damage Control. As far as stiffness and the associated displacements due to ground motion are concerned, the major design considerations are (a) stability of the structure, and (b) damage control. Generally, the considerations related to damage control govern.

Figures 53 and 54, used in conjunction with Figs. 63 and 64, can be used as guides in selecting the appropriate fundamental period, and hence stiffness, once the tolerable maximum displacements have been determined. For convenient reference, the above four figures have been reproduced as Figs. B through E in the following pages.

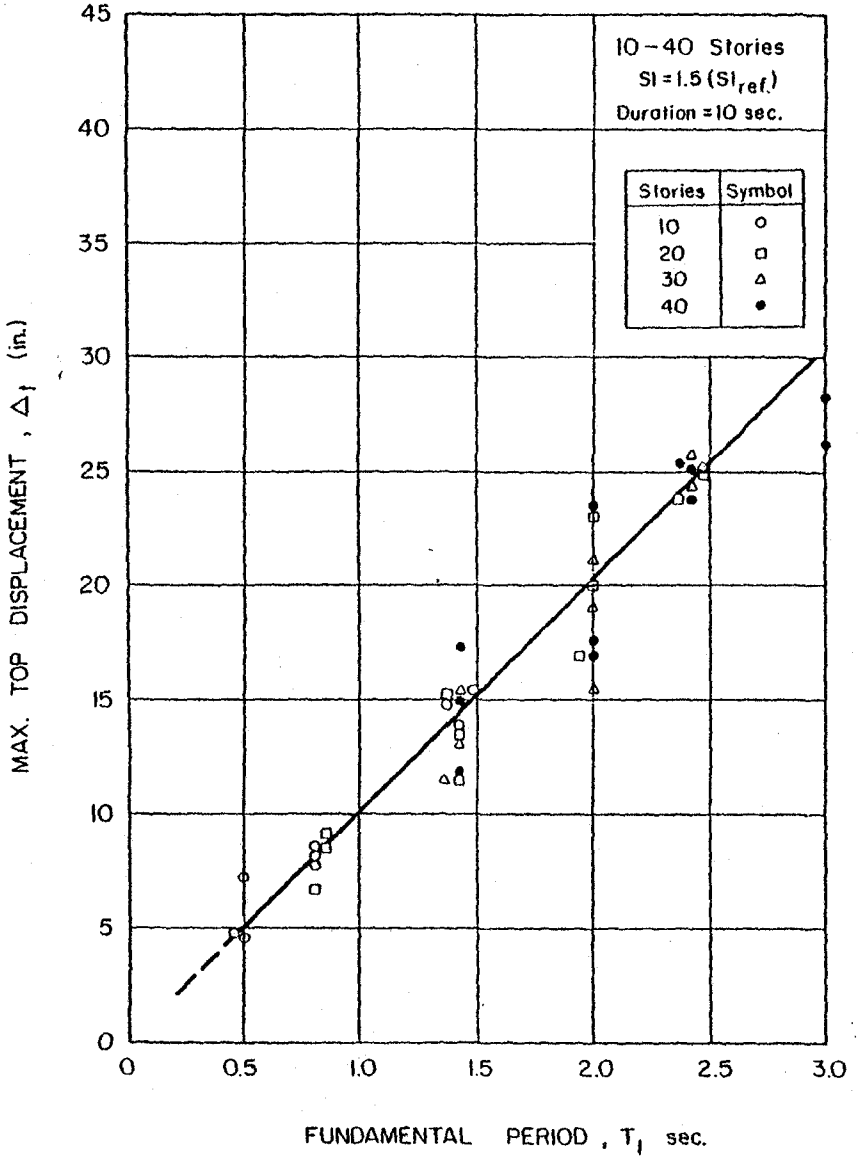

(a)

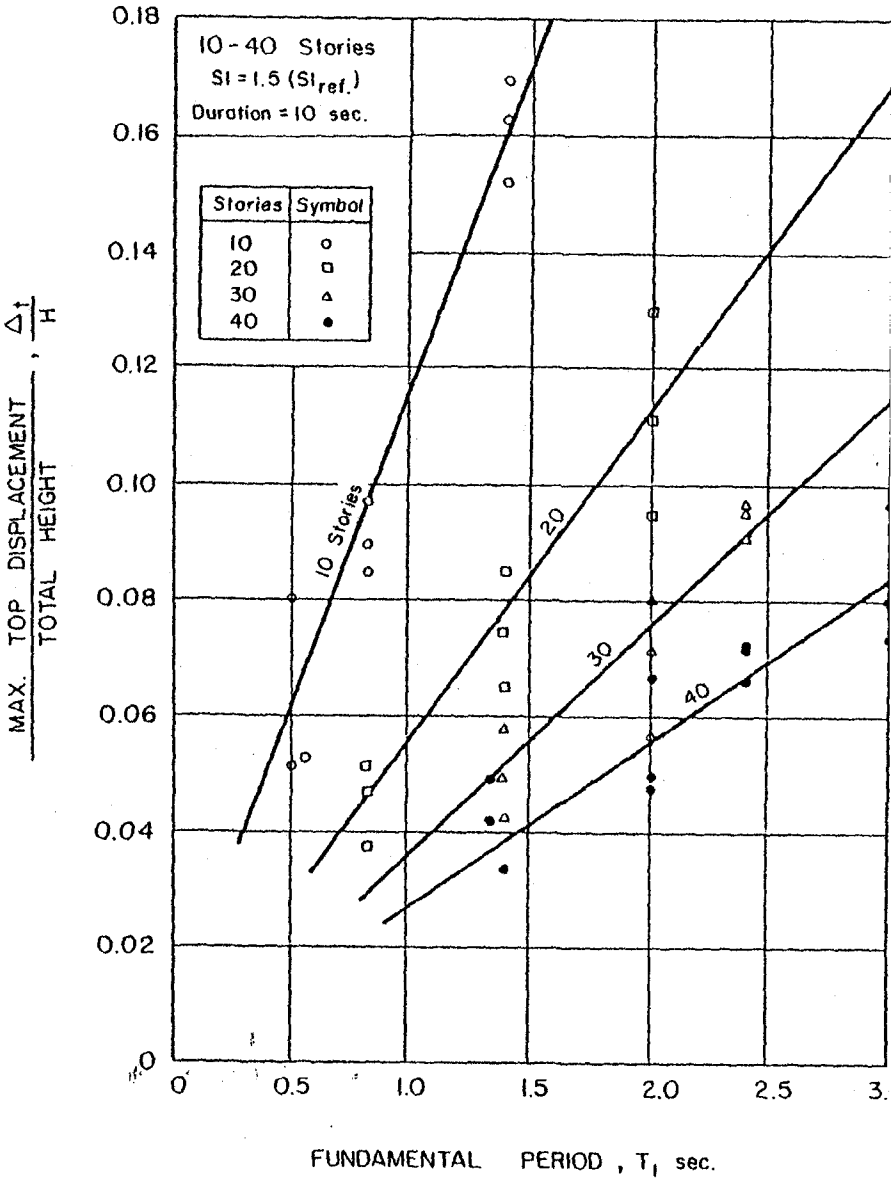

(b)

Fig. B Maximum Top Displacement as a Function of Fundamental Period
(a) Absolute Value (b) As a Ratio Δ_t/H. (Same as Figs. 53a and 53b)

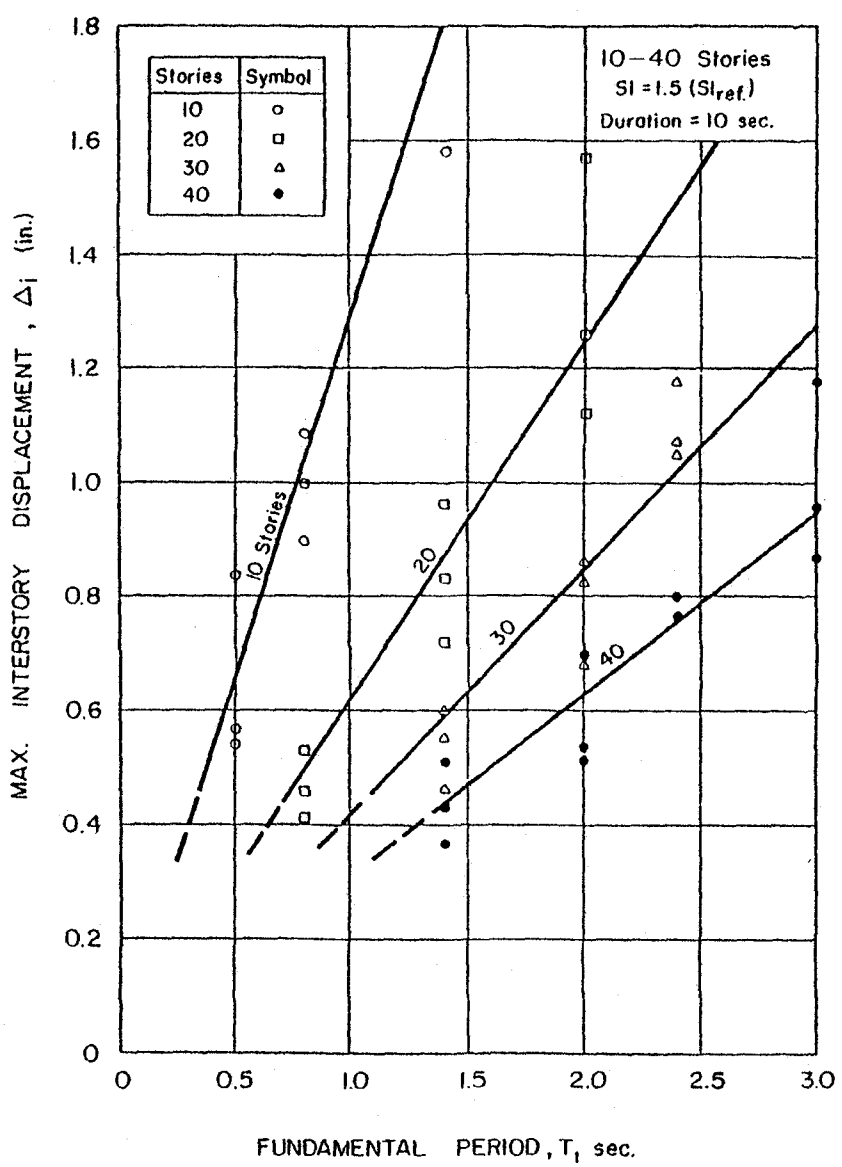

(a)

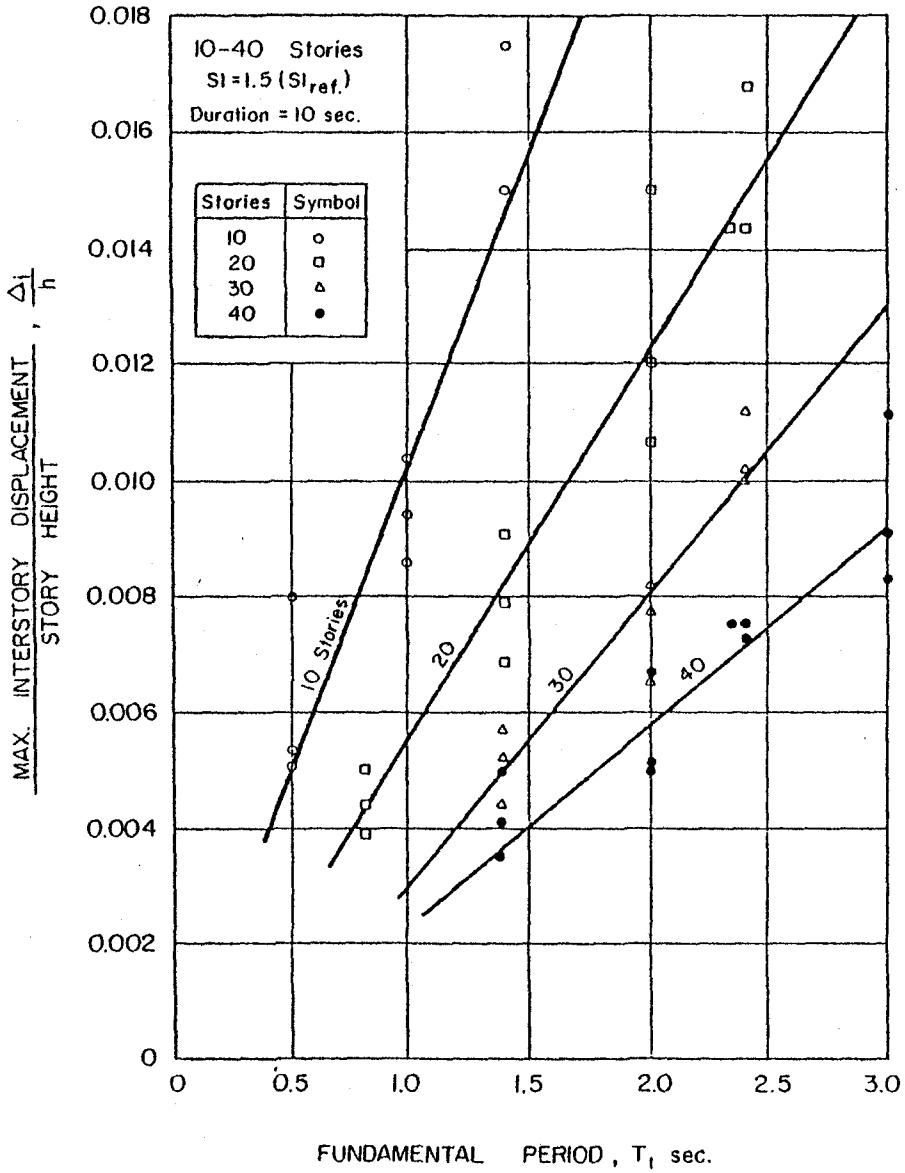

(b)

Fig. C Maximum Interstory Displacement as a Function of Period and Wall Height. (a) Absolute Value (b) As a Ratio Δ_t/h. (Same as Figs. 54a and 54b)

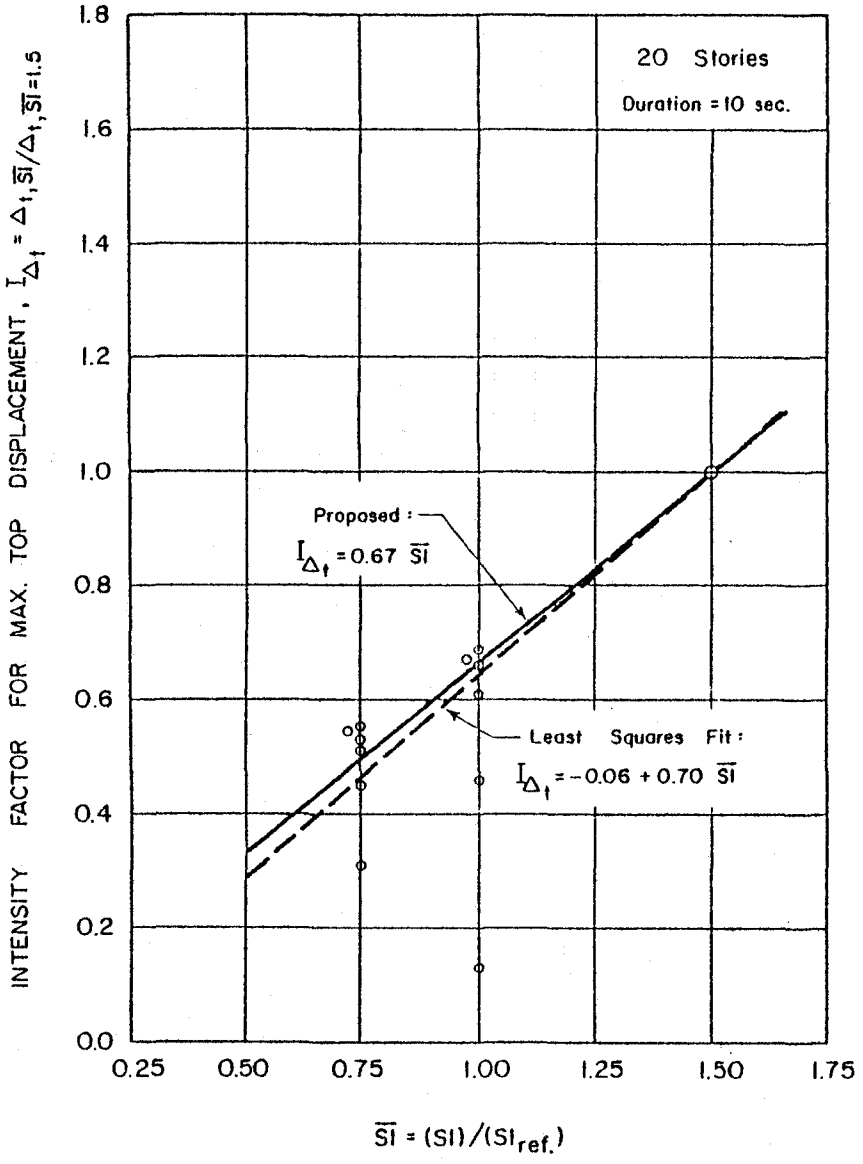

Fig. D Intensity Factor for Maximum Top Displacement, Δ_t (same as Fig. 63)

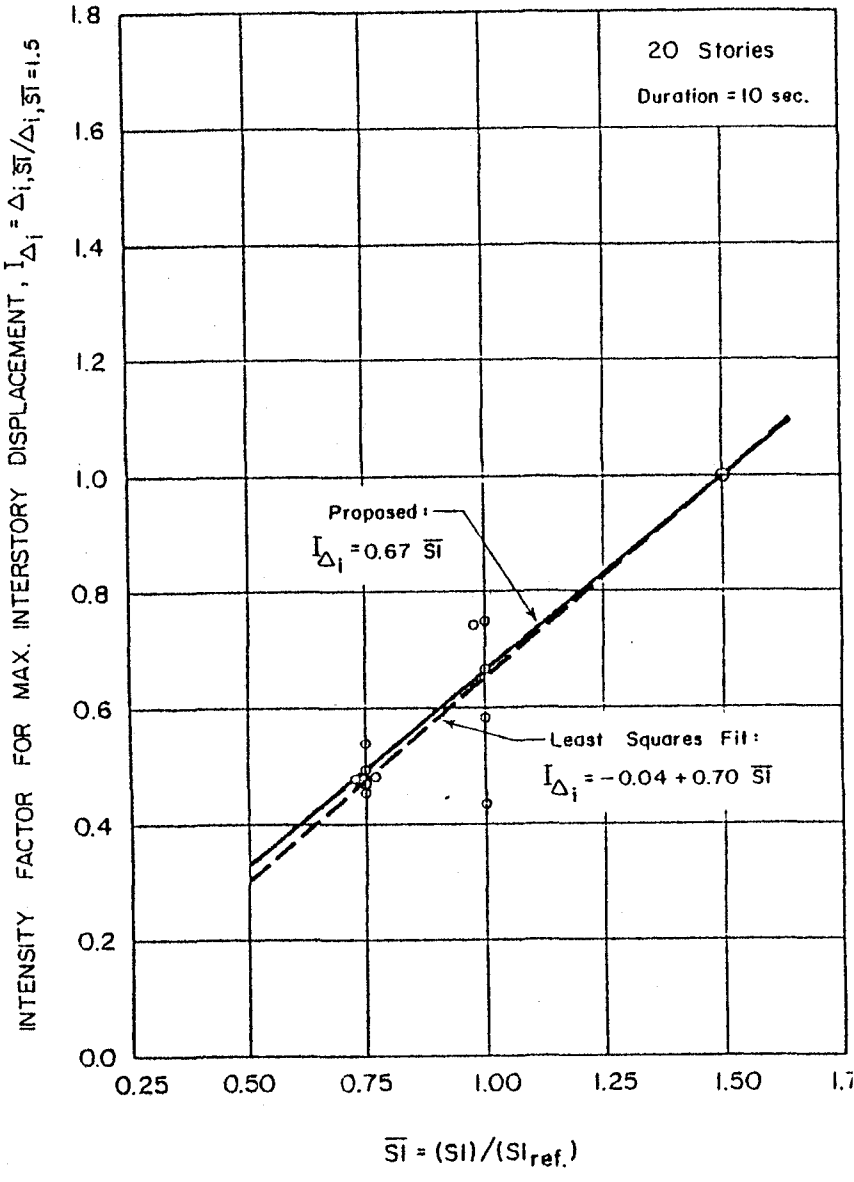

Fig. E Intensity Factor for Maximum Interstory Displacement, Δ_i (same as Fig. 64)

(3) Design for Strength and Deformation Capacity - Base of Wall. This step in the design may be conveniently divided into the following sub-steps:

(a) Determination of Design Forces - Assume an available rotational ductility, μ_r^a, at the base of the wall. A trial value may be obtained from a chart similar to Fig. F. This chart based on experimental data from Ref. 19 shows available rotational ductility as a function of nominal shear stress. A trial value of rotational ductility can be obtained by entering the chart with an estimate of the maximum nominal design shear stress.

(b) Calculate the minimum required flexural yield level at the base of the wall, M_y^{min}, by determining α_f from Fig. 51 (reproduced as Fig. G) and distributing the resulting total horizontal force, $V_T = \alpha_f W$, in accordance with UBC-76. Values from Fig. 51 may be adjusted for design earthquake intensities other than $\overline{SI} = 1.5$ by using Fig. 61 (reproduced as Fig. I).

From M_y^{min}, determine the required flexural reinforcement at the base.

(c) Determine the shear design factor $\bar{\alpha}_v$ from Fig. 52 (reproduced as Fig. H). Values of $\bar{\alpha}_v$ from Fig. 52 may be adjusted for design earthquake intensities other than $\overline{SI} = 1.5$ by using Fig. 62 (reproduced as Fig. J). Calculate the effective static design shear for proportioning the shear reinforcement at the base,

$$V_{TS} = r_v \bar{\alpha}_v \alpha_f W = r_v \bar{\alpha}_v V_T$$

where r_v is an appropriate reduction factor

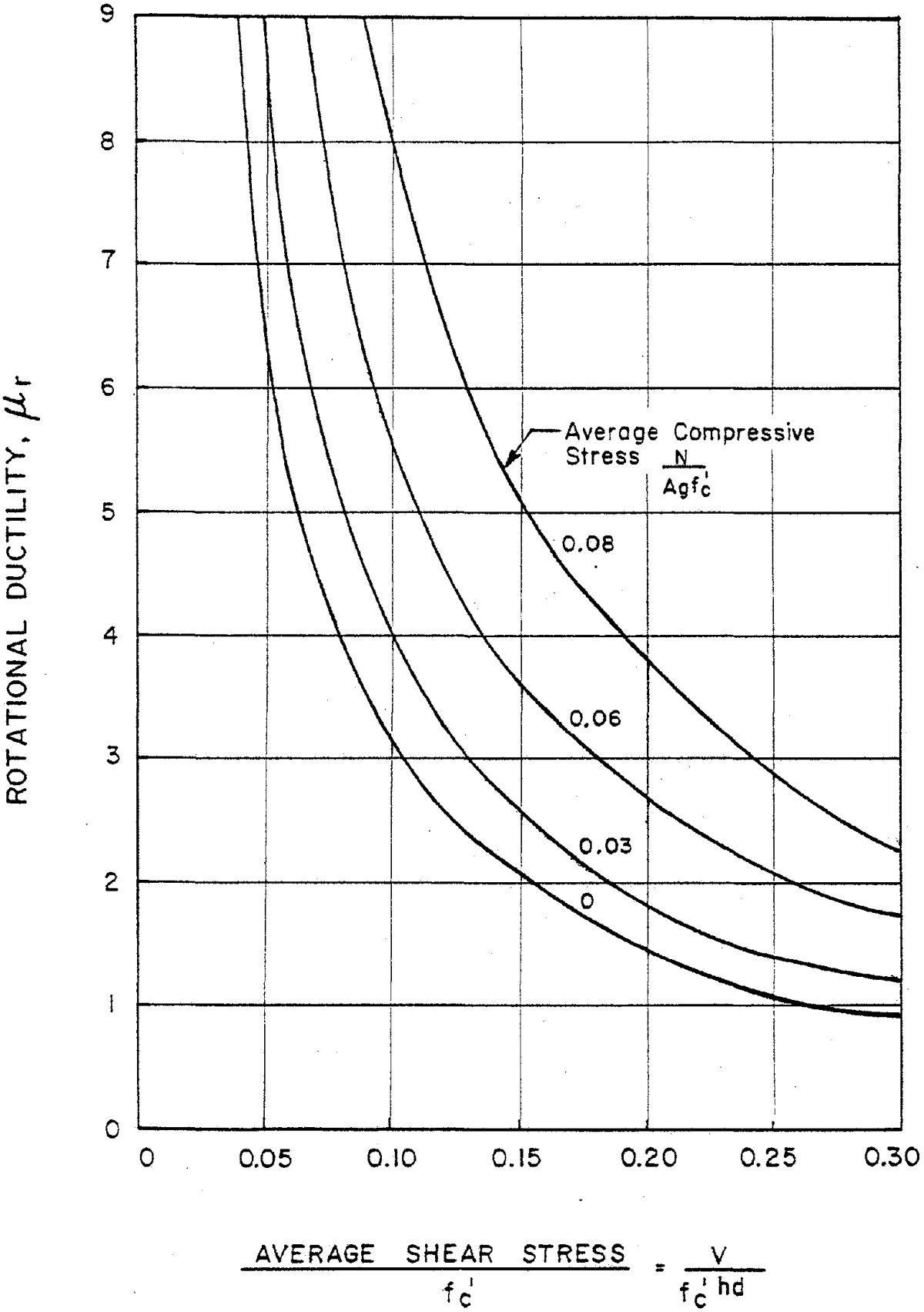

Fig. F Variation of Available Rotational Ductility, μ_r With Maximum Average Shear Stress (from Ref. 19)

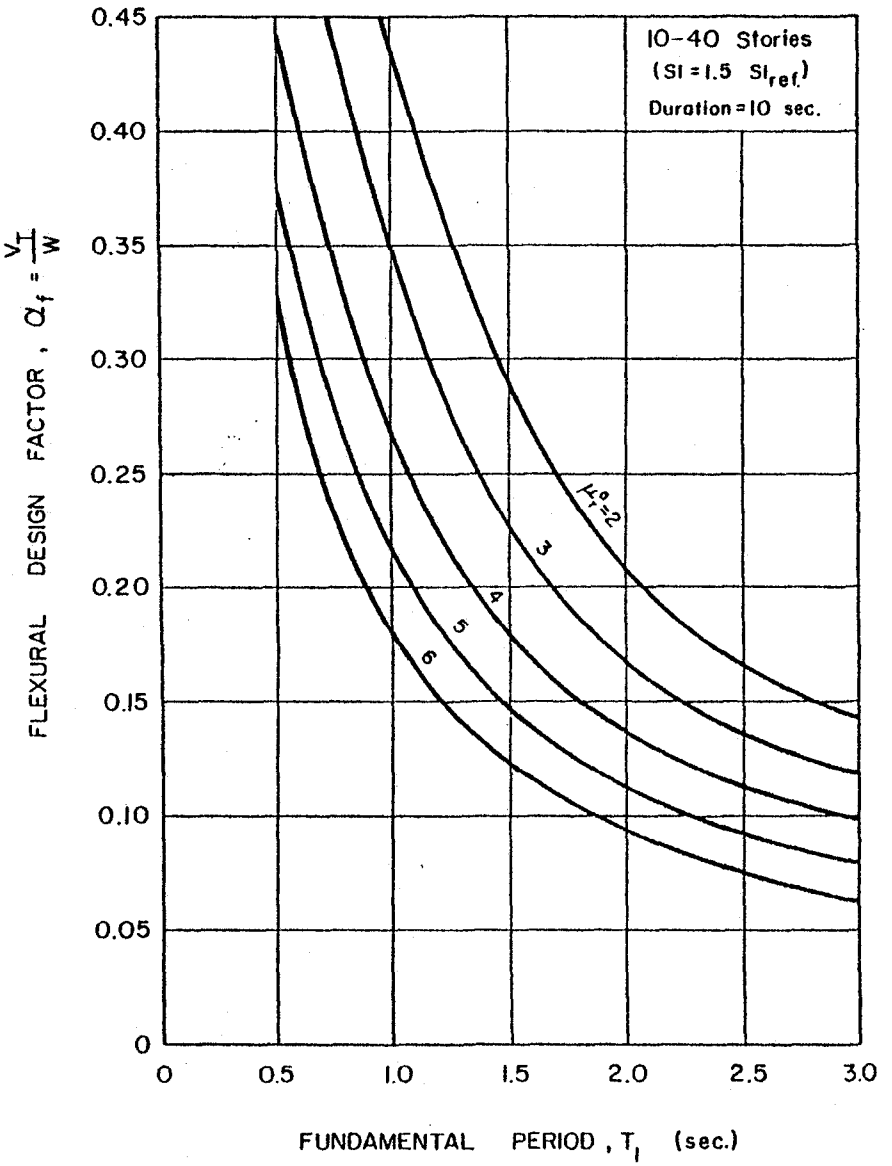

Fig. G Flexural Design Factor
(same as Fig. 51)

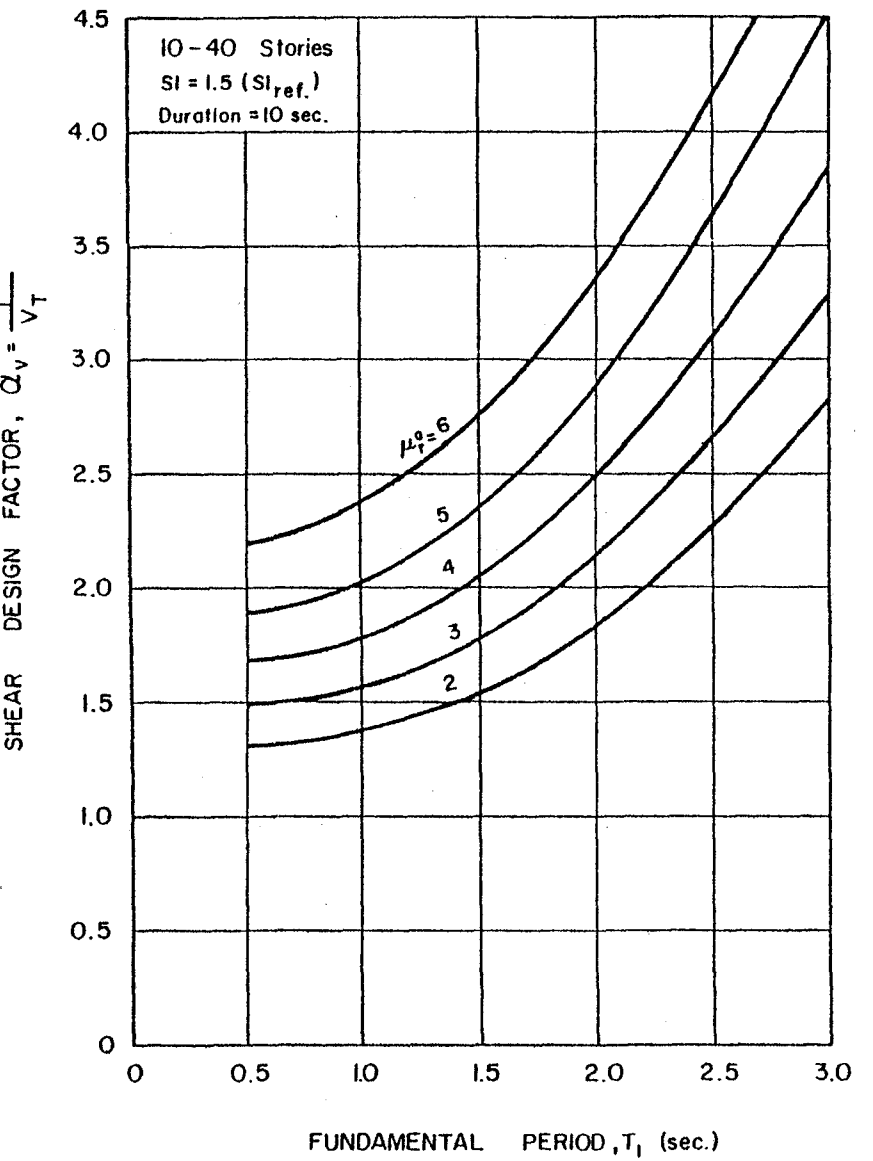

Fig. H Shear Design Factor
(same as Fig. 52)

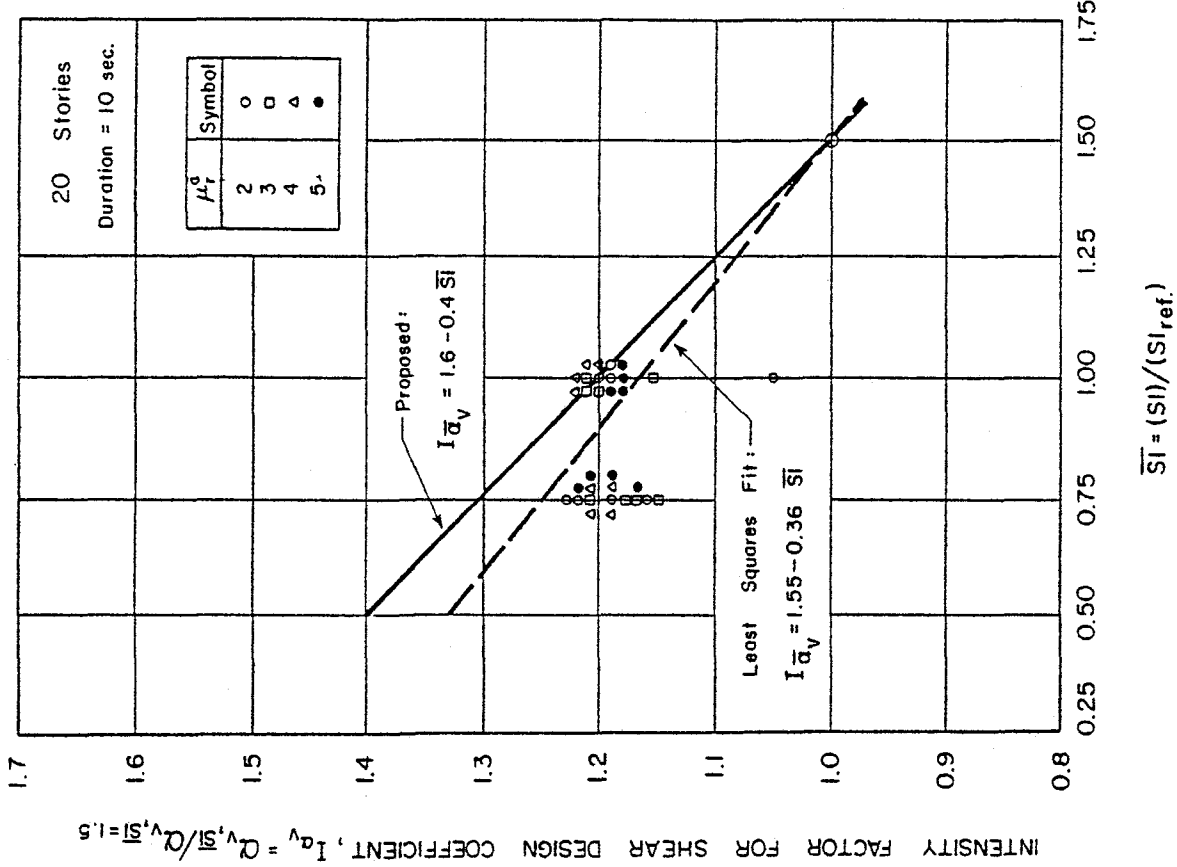

Fig. J Intensity Factor for $\overline{\alpha}_v$
(same as Fig. 62)

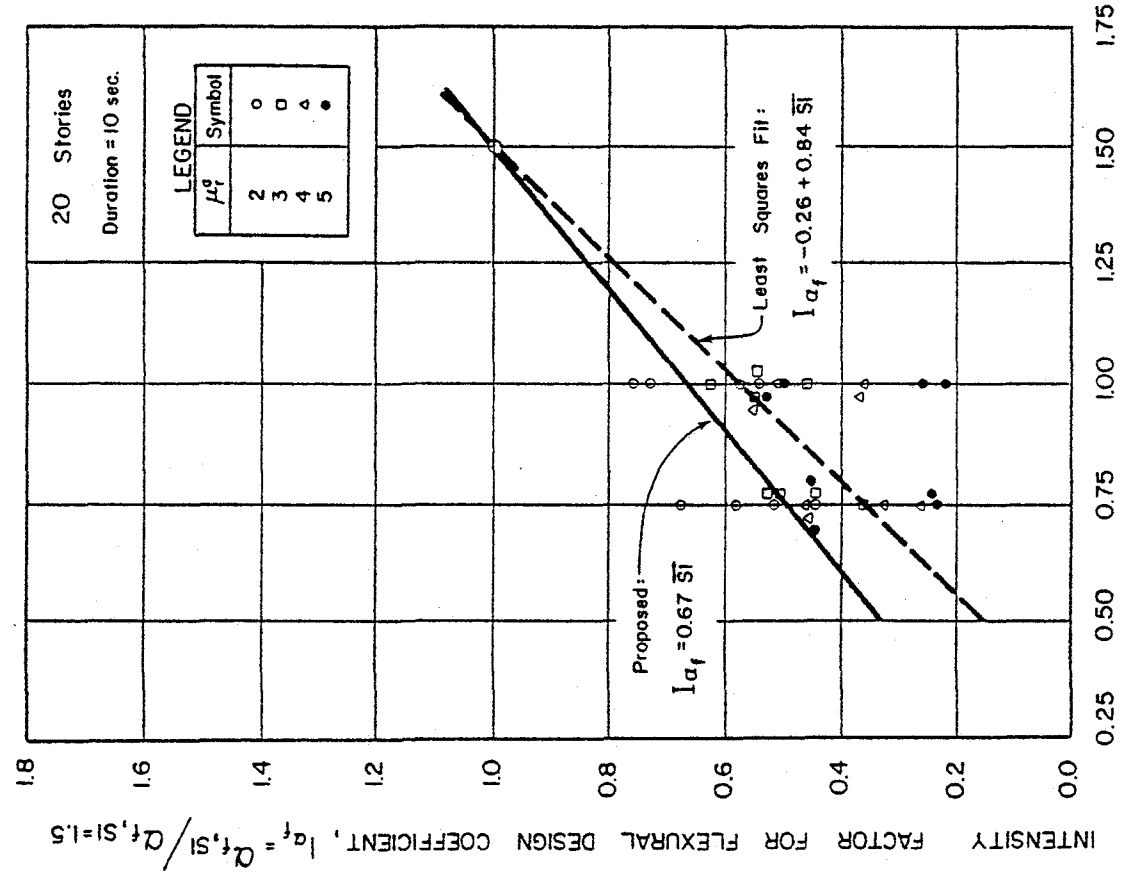

Fig. I Intensity Factor for α_f
(same as Fig. 61)

to account for the overconservatism inherent in the critical dynamic shears as determined in this study when compared to the shear capacity obtained from the experimental program.

(d) Using a chart similar to Fig. F, check if the available ductility, μ_r^a, assumed in Step (a) can be developed under the stress determined in Step (c).

If the assumed ductility can be developed, determine the required shear reinforcement using current codes or design and detailing recommendations developed on the basis of the results of experimental investigation.

If the assumed ductility cannot be developed under the calculated design stress, adjust the assumed ductility value, μ_r^a, or modify the section dimensions accordingly and repeat Steps (a) through (d) until reasonable agreement is obtained.

The above comparison between assumed and developable values can alternatively be carried out in terms of shear stress instead of ductility. Ductility can then be assumed fixed.

(4) Design of Upper Portions of Wall. Determine flexural and shear reinforcement required in upper portions of walls on the basis of the distribution of $V_T = (\alpha_f W)$ and $V_{TS} = (r_v \bar{\alpha}_v V_T)$ as specified in UBC-76, with corrections as follows:

(a) Bending Moments. The design bending moments corresponding to the distribution of V_T over the height of the wall according to UBC-76 should be multiplied by a factor β_2 given by

$$\beta_2 = k \left(\frac{x}{H}\right) \left[1 - \left(\frac{x}{H}\right)\right],$$

where

H = total height of wall

x = distance from base to level "x"

k = a constant, equal to fundamental period T_1, but not greater than 1.2.

(b) Story Shears. The story shears resulting from the application of the total design shear, $V_{TS} = r_v \bar{\alpha}_v V_T$, distributed according to UBC-76, should be modified in the top 25% of the wall by a factor β_1 given by

$$\beta_1 = 2 - T_1/3, \quad \text{where } 1.0 \leq \beta_1 \leq 1.50,$$

provided that the use of the factor β_1 shall not result in a story shear greater than the unmodified story shear calculated for any portion of the lower 75% of the wall.

DESIGN EXAMPLE

Application of the design charts will be illustrated for the particular case of a 24-story structural wall building as shown in Fig. K, with the following properties and loading:

No. of stories	= 24
Building height,	= 213.25 ft.
Tributary floor area/wall	= (24)(60) = 1440 sq. ft.
Floor live load	= 40 psf
Roof live load	= 20 psf
Partition load	= 20 psf
Roofing	= 5 psf
Floor/Roof slab thickness	= 8 in.

A ground motion characterized by a spectrum intensity, SI, equal to 1.2 ($SI_{ref.}$), as defined in this report, will be assumed. This intensity is considered to be approximately equivalent to UBC specified forces (Zone 4).

Material Properties:

Concrete unit weight,	w = 150 pcf
Concrete cylinder strength,	f'_c = 4000 psi
Steel yield strength,	f_y = 60 ksi
Concrete modulus of elasticity,	$E_c = w^{1.5} 33 \sqrt{f_c}$ = 3800 ksi

Assume the shear strength-available ductility curve shown in Fig. F*.

---

* The use of Fig. F for the particular case considered here is only a rough estimate since Fig. F is based on data for "barbell" sections, failing by 'web crushing'. Results of the few tests of rectangular section walls conducted at PCA[9,10,19] suggest that, for the same amount of reinforcement and loading conditions, barbell sections tend to exhibit relatively greater rotational ductility than rectangular sections.

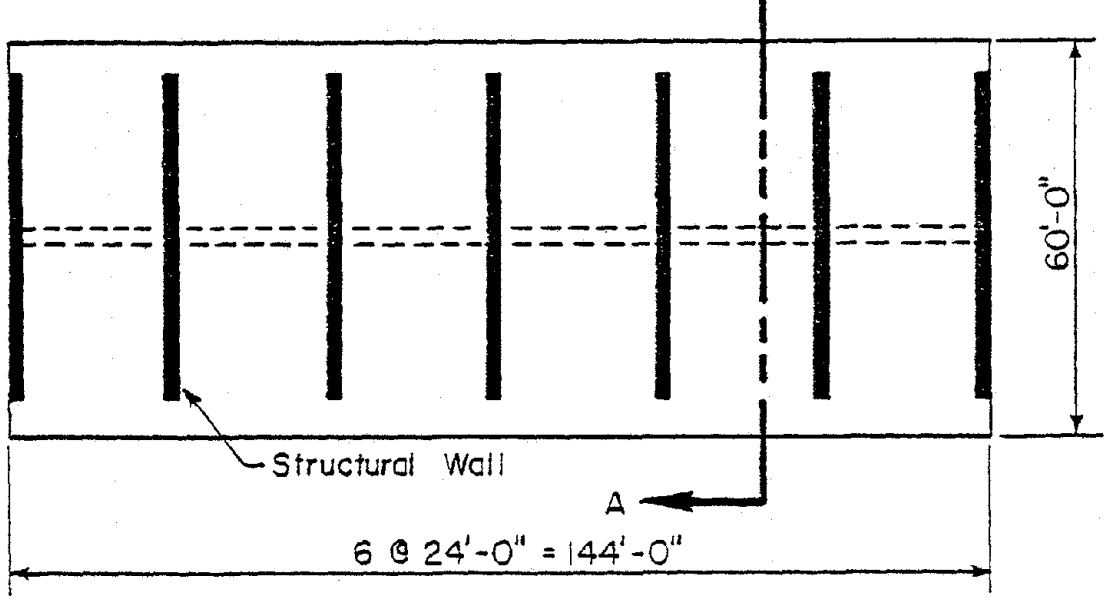

PLAN

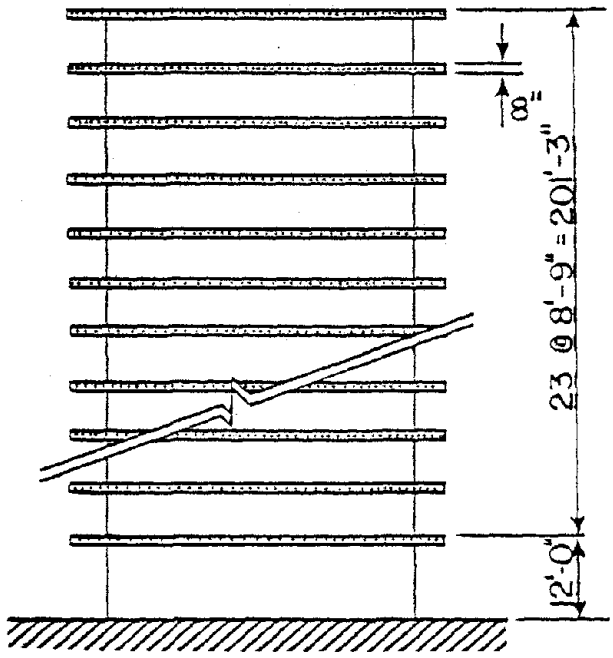

SECTION A-A

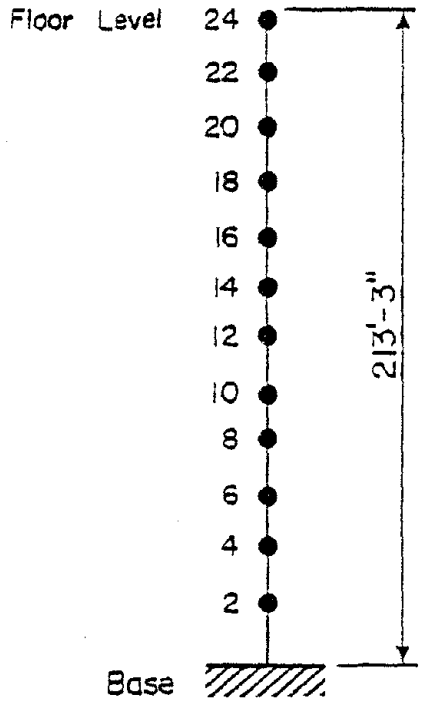

12-MASS MODEL

Fig. K Plan and Elevation of 24-Story Structural Wall Building of Design Example

SOLUTION

Calculations given below cover only the determination of basic wall properties as influenced by drift, ductility and shear stress. Determination of required reinforcement can be carried out using the design provisions in either UBC-76[16] or ACI 318-77[2].

From the given data and assuming a wall of rectangular section, the following preliminary values are obtained:

Wall width, d	= 34 ft.
Wall thickness, b_w	= 10 in.
Weight/floor	= 230 kips
Weight/wall (including tributary loads for mass computations)	= 5500 kips
Wall moment of inertia (gross), I	= 5.66×10^7 in.^{4}
EI	= 2.15×10^{11} kip-in^2
Fundamental period, T_1 (from Fig. L*)	= 2.0 sec.
Drift under wind loading, δ_t/H (UBC-76 20 psf basic pressure zone)	= 1/1670

(A) Flexural Design of Base of Wall

Using Fig. F as a guide, assume an available rotational ductility ratio $\mu_r^a = 3$, corresponding to a nominal shear stress (with $N/A_g = 0$)

---

* Figure L, which shows the variation of the fundamental period, T_1, and the ratio, H/δ_t (where H is the total height of the wall and δ_t is the displacement at the top due to wind) with the stiffness parameter, EI, was prepared for the particular 24-story wall structure considered here. The mass of the structure was assumed to remain essentially unchanged with changing width of the wall. The wind loading corresponds to the UBC-75 20-psf wind pressure zone. A 12-mass lumped parameter model, as shown in Fig. K, was used for the period determination.

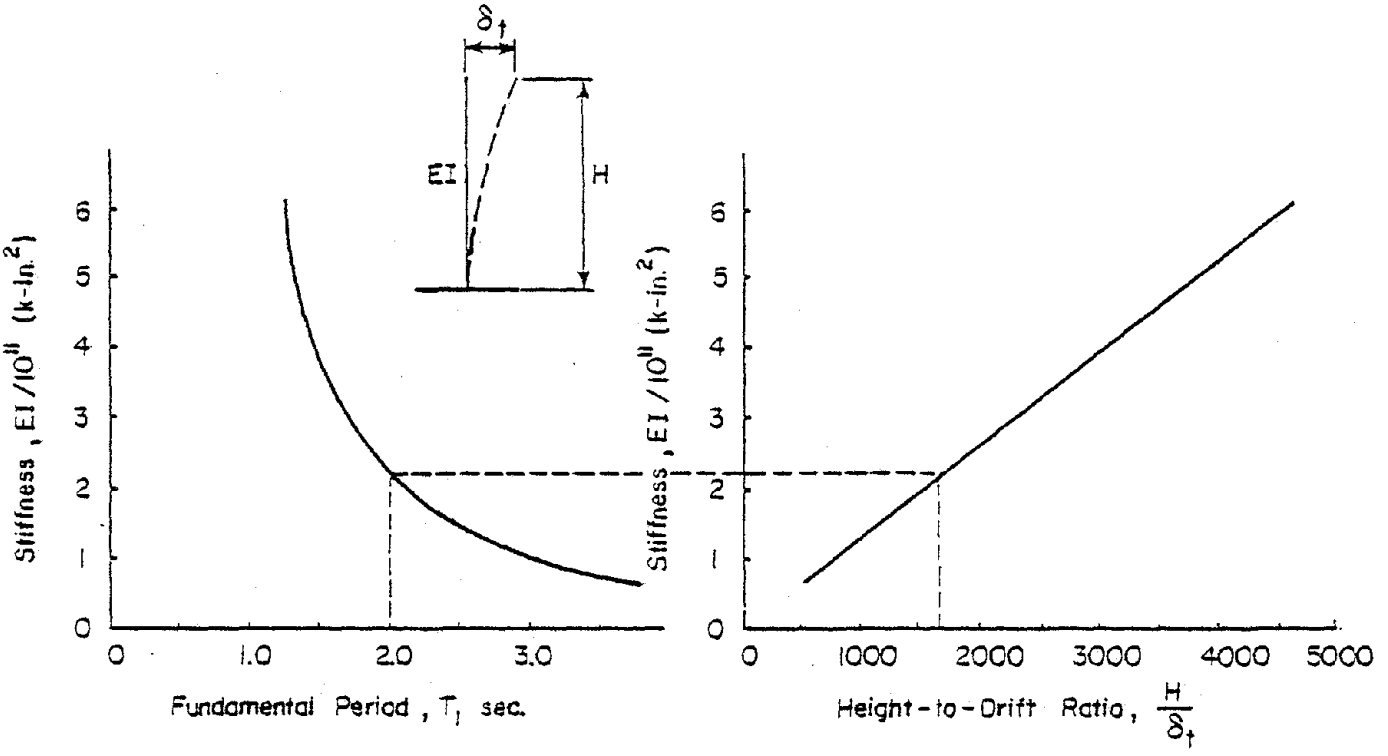

Fig. L Stiffness-Period-Wind Drift Relationship for Example Structure

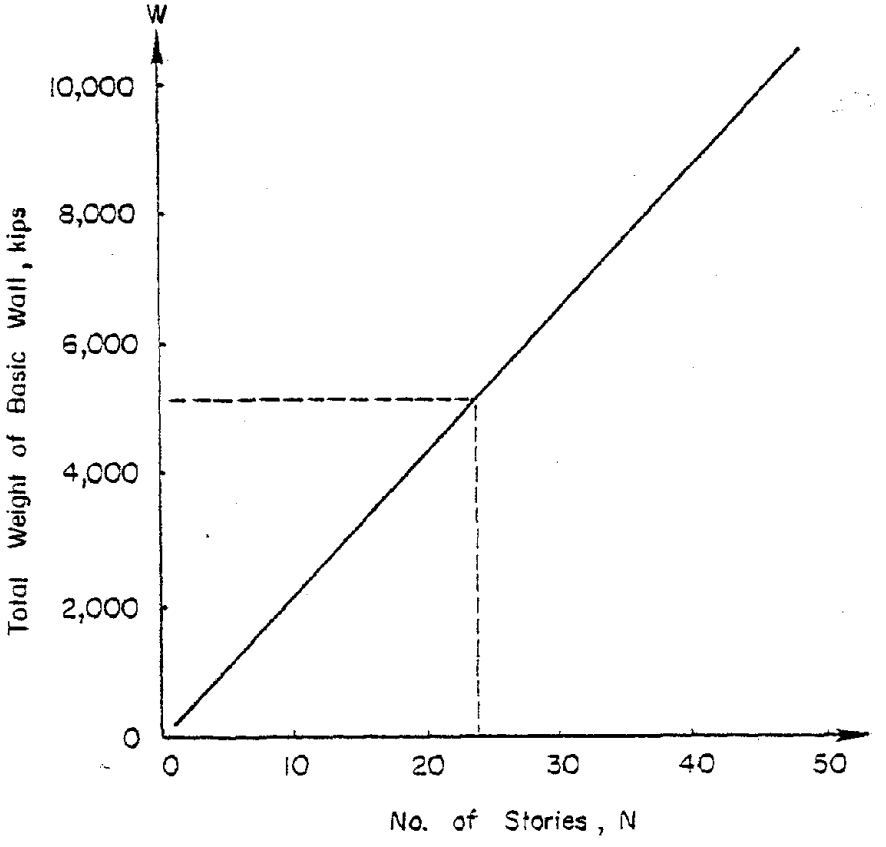

Fig. M Variation of Total Weight of "Basic Wall" with Number of Stories, N

$$v_\mu = \frac{V}{hd} = 0.105 f'_c = 0.105(4000) = 420 \text{ psi.}$$

From Fig. 51 (reproduced as Fig. G) for $T_1 = 2.0$ sec. and $\mu_r^a = 3.0$, we obtain $\alpha_f = 0.165$.

Adjust α_f for variation of mass of example structure from mass of corresponding 'basic structure':

Figure M gives the variation of the total weight of the 'basic structures' with the number of stories. This figure can be used to estimate the weight corresponding to any 'basic structure' between 10 and 40 stories high. For a 24-story basic structure, Fig. M gives a weight of 5250 kips. Hence,

$$\frac{W_{str.}}{W_{basic\ str.}} = \frac{5500}{5250} = 1.05 \text{ (correction factor for mass)}$$

Adjust α_f for particular earthquake intensity:

For an assumed earthquake intensity $SI = 1.2\ (SI_{ref.})$, Fig. 61 (reproduced as Fig. I) gives an intensity factor of 0.8 (correction factor for intensity).

Incorporating the above two correction factors into α_f yields:

$$\alpha_f \text{ (adjusted for mass and intensity)} = (0.165)(1.05)(0.8) = \underline{0.139}$$

Total lateral force for flexural design of base

$$V_T = \alpha_f W = (0.139)(5500) = 765 \text{ kips.}$$

For a distribution of V_T along the height of the wall according to UBC-76, it can shown that the moment at the base, M_b is given by

$$M_b = (0.67 + 0.023\ T_1)HV_T,$$

where H is the total height of the wall. For the structure considered,

$$M_b = M_y^{min} \text{ (at base)} = (0.67 + (0.023)(2.0))\ (213.25)(765)$$
$$= 116{,}800 \text{ ft-kips}$$

This minimum flexural yield level has to be provided at the base of the wall if the assumed available ductility μ_r^a is not to be exceeded under the design earthquake intensity.

Flexural Design of Upper Portions of Wall

For flexural design of portions of the wall above the base, moments obtained from a distribution of V_T over the height of the wall according to UBC-76 should be modified by a factor β_2 given by

$$\beta_2 = 1.2 \left(\frac{x}{213}\right) \left[1 - \left(\frac{x}{213}\right)\right],$$

where x is the distance, in feet, from the base of the wall to the point considered.

(B) Shear Design of Base of Wall

Dynamic base shears are obtained from Figs. 51 and 52 (Figs. G and H). From Fig. 52 (Fig. H):

For $T_1 = 2.0$ secs, $\mu_r^a = 3$, $\overline{SI} = 1.5$

$\bar{\alpha}_v = 2.15$

Adjust $\bar{\alpha}_v$ for intensity ($\overline{SI} = 1.2$) using Fig. 62 (Fig. J)

$I\bar{\alpha}_v = 1.6 - 0.4\ \overline{SI} = 1.6 - (0.4)\ (1.2) = 1.12$

$\bar{\alpha}_v = (1.12)\ (2.15) = 2.41$

Unadjusted base shear is obtained from

$V_{TS} = \bar{\alpha}_v\ V_T = (2.41)\ (765) = 1844$ kips

As pointed out under the heading "Reduction in Critical Dynamic Base Shears for Design Use" a reduction factor, r_v, is applied to critical dynamic base shears obtained from the inelastic dynamic analyses. An indication of the probable range of values for r_v can be obtained by comparing V_{TS}

with the design shear obtained for flexure and also with design shears obtained from current UBC requirements.

(a) Based on total shear used for flexural design, V_T = 765,

$$r_v = \frac{765}{1844} = 0.41$$

(b) Unfactored shear obtained from UBC requirements is 516 kips as shown in Item (D).

Based on UBC shear with load factor of 1.4,

$$r_v = \frac{(1.4)(516)}{(1844)} = 0.39$$

Based on UBC shear with load factor of 2.0

$$r_v = \frac{(2.0)(516)}{(1844)} = 0.56$$

These simple comparisons suggest that a reduction factor, r_v, in the range of 0.40 to 0.60 may be appropriate for design use.

Nominal shear stress at base (using r_v = 0.40),

$$V = \frac{V_{TS}}{\varphi b_w d}$$

$$= \frac{(0.40)\ (1{,}843{,}000}{(0.85)\ (10)\ (34)\ (12)}$$

$$= 222 \text{ psi}$$

$$< 420 \text{ psi} \qquad \text{OK}$$

Shear Design of Upper Portions of Walls

For shear design of upper portions of the wall, the story shears in the top 25% of the wall height corresponding to the distribution of the total base shear, V_{TS}, are adjusted by the factor

$$\beta_1 = 2 - T_1/3 \qquad 1.0 < \beta_1 < 1.5$$

$$= 2 - 2/3 = 1.33.$$

However, in no case should the shear obtained by applying β_1 be greater than that calculated for the lower 75% of the wall.

(C) Calculation of Drift

The horizontal displacement at the top of the wall under the total lateral load V_T, distributed according to UBC-76 as shown in Fig. 41 can be shown to be given approximately by

$$\delta_t(\text{UBC dist. of } V_T) = \frac{11}{60}(V_T - F_t)\frac{H^3}{EI} + \frac{F_t H^3}{3EI} = 12 \text{ in.}$$

The above value of top displacement, obtained from the static application of V_T, can be compared with the maximum displacement from dynamic analysis. Thus, from Fig. 53a (Fig. B) and Fig. 63 (Fig. D),

$$\Delta_{t(max)} = (0.8)(20) = 16 \text{ in.}$$
$$\text{or } \frac{\Delta_t}{H} = \frac{16}{(213.25)(12)} = \frac{1}{160} = 0.0063$$

The corresponding maximum dynamic interstory displacement - from Fig. 54a (Fig. C) - interpolating linearly between curves for 20- and 30- stories) and Fig. 64 (Fig. E) - is given by

$$i_{(max)} = (0.8)(1.1) = 0.9 \text{ in.}$$
$$\text{or } \frac{i}{h} = \frac{0.9}{(8.75)(12)} = .0086$$

The above estimated value of the interstory displacement should be compared with the tolerable distortion in the most critical nonstructural element to determine if the stiffness provided by the wall is adequate.

(D) Comparison with UBC-76

In UBC-76, the design base shear, V, is given by

$$V=ZIKCSW.$$

It will be assumed that a spectrum intensity of 1.2 ($SI_{ref.}$) corresponds to UBC Zone 4, for which Z = 1.0. For the case considered,

$$I = 1.0$$
$$S = 1.5$$
$$K = 1.33$$

and $$C = \frac{1}{15\sqrt{T_1}} = 0.047$$

Thus,

$$V = (1.0)(1.0)(1.33)(0.047)(1.5)(5500) = 516 \text{ kips}$$

For flexural design, the applicable load factor is 1.4,

$$V_{design}(\text{flexure}) = 1.4(516) = 722 \text{ kips}$$

The corresponding required ultimate moment at the base (assumed equal to M_y in UBC) is

$$M_y(\text{base}) = (0.67 + 0.023T_1)H\, V_{design}$$
$$= 0.67 + (0.023)(2.0)\ (213.25)(722)$$
$$= 109{,}935 \text{ ft-kips.}$$

For shear design of walls UBC-76 requires a load factor of 2.0. Thus,

$$V_{design}(\text{shear}) = 2.0(516) = 1032 \text{ kips.}$$

It is important to observe that the UBC design forces imply a certain minimum available ductility, with the specified forces remaining unchanged for any given material or type of construction. In contrast, the procedure in this investigation determines the design forces as a function of both fundamental period and available ductility. An increase in the available ductility would lead to a corresponding reduction in design forces.

SUMMARY

This report presents a procedure for determining design force levels for earthquake-resistant reinforced concrete structural walls. The procedure is the result of an extensive analytical investigation that considers the following problems:

(a) characterization of earthquake ground motions for the purpose of selecting critical input motions.

(b) identification of the most significant structural and ground motion parameters.

(c) formulation of a simple design procedure for correlating earthquake demands with structural capacities.

Previous reports on this investigation presented results of studies addressing to the first two aspects of the investigation. This report considers Item (c).

The main purpose of the extensive parametric study reported previously was to identify the most significant variables affecting dynamic response. These parameters were then incorporated in the proposed design procedure.

Some 400 dynamic inelastic analyses were undertaken to develop data for this investigation. The bulk of the data pertains to 20-story walls subjected to ground motions of intensity SI = 1.5 ($SI_{ref.}$). The reference intensity, SI , used in this study corresponds to that of the N-S component of the 1940 El Centro record. The principal structural variables, as indentified in the parametric study reported in Ref. 7, are fundamental period and flexural yield level. Six different input motions were used to obtain critical or near-maximum response for each combination of the principal variables.

The basic procedure is illustrated for the case of 20-story walls subjected to input motions of intensity SI = 1.5 ($SI_{ref.}$). This illustration establishes the logical sequence of data reduction leading to the practical results sought.

To extend application of the results to walls of different heights and other ground motion intensities, two additional series of analyses were made to establish a basis for adjusting the results for the basic 20-story, SI = 1.5 ($SI_{ref.}$) case for these other conditions. Other variables characterizing the structure were held constant. The constant values assumed for these other parameters were those considered as averages for the normal range of variation of each parameter. The values assumed for these constant parameters are as follows:

(a) Yield stiffness ratio, $r_y = 0.05$

(b) Parameters characterizing hysteretic loop (see Fig. 4b):
Unloading parameter, $\alpha = 0.10$
Reloading parameter, $\beta = 0$

(c) Viscous damping coefficient (for first and second modes) = 0.05

(d) Uniform stiffness throughout height of wall
Strength (M_y) uniform throughout height except for adjustments to reflect effect of axial load due to dead weight

(e) Wall fully fixed at base

Another series of analyses was made to investigate the effect of varying the degree of base fixity. The results of this series are given in Appendix C.

The basic results are presented in Figs. 51 and 52. These figures, as well as other related figures developed as aids in the application of the procedure for determining design force levels for earthquake-resistant isolated walls have been reproduced as part of the Design Example.

As more test data on structural walls become available, it will be possible to establish relationships similar to that

shown in Fig. F for other types of failure mechanisms. It will be noted that Fig. F is based on data for walls that failed by web crushing. This type of failure is usually associated with flanged sections.

A major feature of the proposed method is the explicit relationship established between the principal structural parameters, i.e., fundamental period and yield level, and the force and deformation (ductility) requirements.

Another major aspect of the study is the comparison of ductility demand as indicated by analysis with deformation capacity of test specimens in terms of various quantities representing maximum amplitude of flexural deformation as well as cumulative deformation and energy. This comparison has led to the important observation that, at least for the cases considered, the satisfaction of the rotational ductility requirement generally ensures the satisfaction of the deformation requirements in terms of other measures of ductility. This observation and the explicit relationship established between the principal structural parameters and the corresponding force and deformation demands have allowed the correlation between analytical and experimental results in a simple and practical manner suitable for design.

Although several ground motion intensities were considered in the study, no specific effort was made to relate these intensities to the different seismic zones defined in seismic risk or regionalization maps found in some codes. This correlation is beyond the scope of this study.

ACKNOWLEDGEMENTS

The initial phase of this investigation was carried out in the Engineering Services Department of the Portland Cement Association, Skokie, Illinois. Mr. Mark Fintel, then Director of Engineering Services, now Director of Advanced Engineering Services, served as overall Project Director of the combined analytical and experimental program. Dr. T. Takayanagi generated a major part of the response data on effects of partial base fixity given in Appendix C. The valuable help provided by Jaidev Sharma and particularly Ralph Reichenbach, Jr. in performing the calculations for the least-squares-fit lines and in preparing most of the figures in this report is gratefully acknowledged.

This project was sponsored in major part by the National Science Foundation, ASRA Program, through Grant No. ENV77-15333. Any opinions, findings and conclusions expressed in this report are those of the authors and do not necessarily reflect the views of the National Science Foundation.

REFERENCES

1. Applied Technology Council, Tentative Provisions for the Development of Seismic Regulations for Buildings," (ATC3-06; also, NBS Special Publication 5100, or NSF Publication 78-8), U.S. Government Printing Office, Washington, D.C. 20402, 505 pp., June 1978.

2. Appendix A, Building Code Requirements for Reinforced Concrete (ACI 318-77), American Concrete Institute, P.O. Box 19150, Redford Station, Detroit, Michigan 48219.

3. The Behavior of Reinforced Concrete Buildings Subjected to the Chilean Earthquakes of May 1960," Advance Engineering Bulletin No. 6, Portland Cement Association, Skokie, Illinois, 1963.

4. Fintel, M., "Quake lesson from Managua: Revise Concrete Building Design?" Civil Engineering, ASCE, August 1973, pp. 60-63.

5. Anonymous, "Managua, If Rebuilt on Same Site, Could Survive Temblor," Engineering News Record, December 6, 1973, p. 16.

6. Derecho, A.T., Fugelso, L.E. and Fintel, M., "Structural Walls in Earthquake-Resistant Buildings - Analytical Investigation, Dynamic Analysis of Isolated Structural Walls - INPUT MOTIONS," Final Report to the National Science Foundation, RANN, under Grant No. ENV74-14766, Portland Cement Association, December 1977.

7. Derecho, A.T., Ghosh, S.K., Iqbal, M., Freskakis, G.N. and Fintel, M., "Structural Walls in Earthquake-Resistant Buildings - Analytical Investigation, Dynamic Analysis of Isolated Structural Walls - PARAMETRIC STUDIES," Final Report to the National Science Foundation, RANN, under Grant No. ENV74-14766, Portland Cement Association, March 1978.

8. Derecho, A.T., Ghosh, S.K., Iqbal, M., and Fintel, M., "Structural Walls in Earthquake-Resistant Buildings - Analytical Investigation, Dynamic Analysis of Isolated Structural Walls - (Part C: Development of Design Procedure - Design Force Levels)," Interim Report to the National Science Foundation, RANN, under Grant No. GI-43880, Portland Cement Association, November 1976.

9. Oesterle, R.G., Fiorato, A.E., Johal, L.S., Carpenter, J.E., Russell, H.G. and Corley, W.G., "Earthquake-Resistant Structural Walls - Tests of Isolated Walls," Report to the National Science Foundation, Portland Cement Association, November 1976, 44 pp. (Appendix A, 38 pp.; Appendix B, 233 pp.).

10. Oesterle, R.G., Aristizabal-Ochoa, D., Fiorato, A.E., Russell, H.G. and Corley, W.G., "Earthquake-Resistant Structural Walls - Tests of Isolated Walls - Phase II," Report to the National Science Foundation, Portland Cement Association, March 1978.

11. Derecho, A.T., Iqbal, M., Ghosh, S.K., Fintel, M. and Corley, W.G., "Structural Walls in Earthquake-Resistant Buildings - Analytical Investigation, Dynamic Analysis of Isolated Structural Walls - REPRESENTATIVE LOADING HISTORY," Final Report to the National Science Foundation, RANN, under Grant No. ENV74-14766, Portland Cement Association, August 1978.

12. Kanaan, A.E. and Powell, G.H., "General Purpose Computer Program for Dynamic Analysis of Plane Inelastic Structures," (DRAIN-2D), Report No. EERC 73-6, Earthquake Engineering Research Center, University of California, Berkeley, April 1973.

13. Ghosh, S.K. and Derecho, A.T., "Supplementary Output Package for DRAIN-2D, General Purpose Computer Program for Dynamic Analysis of Plane Inelastic Structures," Supplement No. 1 to an Interim Report on the PCA Investigation "Structural Walls in Earthquake-Resistant Structures," NSF-RANN Grant No. GI-43880, Portland Cement Association, Skokie, Illinois, August 1975.

14. Takeda, T., Sozen, M.A. and Nielsen, N.N., "Reinforced Concrete Response to Simulated Earthquakes," Journal of the Structural Division, ASCE, Proceedings Vol. 96, No. ST12, December 1970.

15. Analysis of Strong Motion Earthquake Accelerograms, Vol. II, Corrected Accelerograms Parts A, B, C, Report EERL 72-79, California Institute of Technology, Earthquake Engineering Research Laboratory, 1972, 1973, 1974.

16. Uniform Building Code, 1976 Edition, International Conference of Building Officials, 5360 South Workman Mill Road, Whittier, California 90601.

17. Park, R. and Paulay, T., Reinforced Concrete Structures, John Wiley & Sons, New York, 1975.

18. Bertero, V.V., Popov, E.P. and Wang, T.Y., "Seismic Design Implications of Hysteretic Behavior of Reinforced Concrete Elements Under High Shear," Proceedings of the Review Meeting, U.S. - Japan Cooperative Research Program in Earthquake Engineering with Emphasis on the Safety of School Buildings, August 18-20, 1975, Honolulu, Hawaii, The Japan Earthquake Engineering Promotion Society, Tokyo, 1976.

19. Oesterle, R. G., Fiorato, A.E., Russell, H.G., and Corley, W.G., "Earthquake-Resistant Structural Walls - Tests of Isolated Walls, Phase III," Report to National Science Foundation Portland Cement Association, Construction Technology Laboratories, Skokie, July, 1981

APPENDIX A

DATA FROM DYNAMIC INELASTIC ANALYSIS

APPENDIX A

Tables A1-A13	Maximum Response Values 10-40 Story Walls, SI = 1.5(SI $_{ref.}$)
Table A14	Effect of Duration of Input Motion on Maximum Response Values 20-Story Walls, SI = 1.5($SI_{ref.}$)
Tables A15-A20	Effects of Intensity of Input Motion on Maximum Response Values 20-Story Walls, SI = 1.0($SI_{ref.}$)
Tables A21-A26	Effects of Intensity of Input Motion on Maximum Response Values 20-Story Walls, SI = 0.75($SI_{ref.}$)
Figures A1-A16	Response Value for Different Input Motions 10-40 Story Walls, SI = 1.5($SI_{ref.}$)
Figures A16-A20	Critical Response Values 10-40 Story Walls, SI = 1.5($SI_{ref.}$)
Figures A21-A23	Critical Response Values 20-Story Walls, SI = 1.0 and 0.75($SI_{ref.}$)

List of Tables

List of Tables (cont'd)

List of Tables (cont'd)

List of Figures

List of Figures (cont'd)

Table A1

RESPONSE VALUES CORRESPONDING TO DIFFERENT EARTHQUAKE INPUT MOTIONS
[SI = 15(SI$_{ref.}$), Duration = 10 sec.]

10-Story Isolated Structural Walls
M_y = 150,000 IN-K

EARTHQUAKE INPUT NUMBER	EARTHQUAKE INPUT	FUNDAMENTAL PERIOD, T_1 (SEC.) 0.5 M_y x 10^4 in-kips	0.5 θ_y^{ϕ} x 10^{-3} rad.	0.5 θ_y^{w} x 10^{-3} rad.	0.8 M_y x 10^4 in-kips	0.8 θ_y^{ϕ} x 10^{-3} rad.	0.8 θ_y^{w} x 10^{-3} rad.	1.4 M_y x 10^4 in-kips	1.4 θ_y^{ϕ} x 10^{-3} rad.	1.4 θ_y^{w} x 10^{-3} rad.
1	1971 Pacoima Dam, S16E	.150	.09	.17	.150	.23	.43	.150	.76	1.29
2	1971 Holiday Orion, E-W	.150	.12	.19	.150	.22	.39	.150	.66	1.19
3	1952 Taft, S69E	.150	.10	.18	.150	.23	.44	.150	.66	1.22
4	1940 El Centro, E-W	.150	.09	.17	.150	.24	.44	.150	.69	1.32
5	Artificial Acc. (S1)	.150	.13	.21	.150	.24	.43	.150		
6	1940 El Centro, N-S	.150	.09	.17	.150	.23	.42	.150	.70	1.25
	AVERAGE		.103	.182		.23	.43		.68	1.22

$^{\phi}$ at midheight of 1st story
^{w} at 1st floor level

DUCTILITY DEMAND BASED ON NODAL ROTATIONS AT MID-HEIGHT OF 1st STORY

E.Q. INPUT NO.	FUNDAMENTAL PERIOD, T_1, (SEC) 0.5	0.8	1.4
	ROTATIONAL DUCTILITY, $\mu_{r\phi}$		
1	17.75*	12.93*	6.89
2	14.27	8.54	6.58
3	14.35	9.3	6.01
4	10.01	10.58	7.62*
5	11.17	8.58	6.62
6	12.70	9.76	4.79
	CYCLIC ROT. INCTILITY $\mu_{rc\phi}$		
1	28.45*	20.13*	9.38
2	19.60	13.54	9.72*
3	18.40	11.90	7.47
4	17.25	14.74	8.76
5	16.50	12.70	7.66
6	19.58	11.10	6.55
	CUMULATIVE DUCTILITY, $\sum\mu_{rc\phi}$		
1	142.77	219.23*	55.60
2	143.61	99.36	55.06
3	136.16	98.10	54.71
4	136.37	105.71	55.86
5	195.92*	129.46	75.44*
6	168.17	92.35	40.82
	CUMULATIVE ROT. ENERGY, $\sum A_{r\phi}$		
1	173.72	101.36	43.78
2	200.16	110.20	65.40
3	179.66	101.66	55.48
4	158.30	116.22*	54.38
5	207.90	116.20	66.08*
6	213.32*	96.18	37.64

DUCTILITY DEMAND BASED ON NODAL ROTATIONS AT 1st FLOOR LEVEL

E.Q. INPUT NO.	FUNDAMENTAL PERIOD, T_1, (SEC) 0.5	0.8	1.4
	ROTATIONAL DUCTILITY, μ_{rw}		
1	18.41*	11.76*	5.99
2	14.30	7.74	5.81
3	14.50	8.36	5.40
4	10.03	10.09	7.37*
5	11.37	7.20	5.86
6	12.83	9.23	4.32
	CYCLIC ROT. DUCTILITY μ_{rcw}		
1	28.74*	18.93*	8.24*
2	20.92	12.19	7.74
3	18.94	10.81	6.30
4	17.16	12.99	7.59
5	15.77	10.58	5.86
6	19.13	10.26	5.04
	CUMULATIVE DUCTILITY, $\sum\mu_{rcw}$		
1	138.11	86.24	45.69
2	143.00	85.90	47.09
3	135.42	86.39	45.10
4	136.31	91.41	47.63
5	183.85*	103.19*	59.23*
6	116.95	83.11	34.32
	CUMULATIVE ROT. ENERGY, $\sum A_{rw}$		
1	172.80	93.80	36.72
2	197.56	95.36	53.18*
3	181.20	91.40	44.0
4	157.64	101.00*	45.32
5	201.24*	95.16	51.32
6	191.58	86.48	29.76

*Critical (maximum) value for particular T_1
E - no yielding, i.e., linearly elastic response

MAXIMUM RESPONSE VALUES

E.Q. INPUT NO.	FUNDAMENTAL PERIOD, T_1, (SEC) 0.5	0.8	1.4
	MAX. TOP DISPL. (IN)		
1	7.3*	8.8*	10.8
2	5.1	5.8	10.9
3	5.9	6.9	9.4
4	3.3	7.7	13.9*
5	4.4	5.5	10.3
6	4.3	7.2	9.3
	MAX. INTERSTORY DISPL. (IN)		
1	0.84*	1.0*	1.32
2	0.58	0.66	1.29
3	0.70	0.82	1.11
4	0.37	0.86	1.58*
5	0.52	0.67	1.24
6	0.49	0.82	1.12
	MAX. BASE SHEAR (KIPS)		
1	565	524	413
2	506	521	577
3	558	523	475
4	445	513	399
5	669*	528*	626*
6	523	444	527
	MAX. BASE MOMENT (IN-KIPS)		
1	305,000*	242,000*	195,000
2	273,000	208,000	193,000
3	277,000	214,000	189,000
4	234,000	224,000	200,600*
5	246,000	209,000	193,000
6	258,000	217,000	178,000
	NOTATIONAL DUCTILITY, $\mu_{r\phi}$ **		
1	21.6*	13.2*	7.0
2	17.4	8.7	6.7
3	17.9	9.5	6.2
4	12.2	10.9	7.6*
5	14.8	8.9	6.7
6	15.4	9.9	4.7

** $\mu_{r\phi}$ Based on Eq. (1)

Table A2

RESPONSE VALUES CORRESPONDING TO DIFFERENT EARTHQUAKE INPUT MOTIONS
[SI = 15(SI$_{rel}$), Duration = 10 sec.]

10-Story Isolated Structural Walls
M_y = 500,000 IN-K

EARTHQUAKE INPUT NUMBER	EARTHQUAKE INPUT	FUNDAMENTAL PERIOD, T_1 (SEC.) 0.5 M_y $\times 10^6$ in-kips	0.5 θ_y' $\times 10^{-3}$ rad.	0.5 θ_y^* $\times 10^{-3}$ rad.	0.8 M_y $\times 10^6$ in-kips	0.8 θ_y' $\times 10^{-3}$ rad.	0.8 θ_y^* $\times 10^{-3}$ rad.	1.4 M_y $\times 10^6$ in-kips	1.4 θ_y' $\times 10^{-3}$ rad.	1.4 θ_y^* $\times 10^{-3}$ rad.
1	1971 Pacoima Dam, S16E	.525	.34	.60	.525	.82	1.61	.525	2.45	4.65
2	1971 Holiday Orion, E-W	.525	.33	.64	.525	.78	1.58	.525	E	E
3	1952 Taft, S69E	.525	.36	.62	.525	.80	1.52	.525	2.39	4.46
4	1940 El Centro, E-W	.525	.33	.60	.525	.80	1.53	.525	E	E
5	Artificial Acc. (SI)	.525	.31	.58	.525	.80	1.51	.525	2.34	4.27
6	1940 El Centro, N-S	.525	.33	.61	.525	.79	1.52	.525		
	AVERAGE		.33	.61		.80	1.55		2.39	4.46

θ_y' at midheight of 1st story
θ_y^* at 1st floor level

DUCTILITY DEMAND BASED ON NODAL ROTATIONS AT MID-HEIGHT OF 1st STORY

E.Q. INPUT NO.	FUNDAMENTAL PERIOD, T_1, (SEC) 0.5	0.8	1.4
	ROTATIONAL DUCTILITY, μ_{r1}		
1	2.37	2.69	2.06*
2	4.66	2.21	E
3	3.47	3.90*	E
4	4.6	1.90	E
5	3.48	2.05	1.28
6	4.75*	3.17	E
	CYCLIC ROT. DUCTILITY μ_{rc1}		
1	3.61	2.69	2.16*
2	4.79	2.21	E
3	4.03	4.80*	E
4	6.7	1.90	E
5	5.15	2.28	1.31
6	7.74*	4.36	E
	CUMULATIVE DUCTILITY, $\Sigma\mu_{rc1}$		
1	38.42	26.98	15.97
2	57.47	20.83	E
3	59.25	32.00	E
4	53.0	21.60	E
5	78.00*	34.28	17.28*
6	59.58	37.72*	E
	CUMULATIVE ROT. ENERGY, ΣA_{r1}		
1	25.58	14.28	8.44*
2	48.04	11.10	E
3	53.56	22.20	E
4	38.18	9.80	E
5	58.60*	19.18	6.72
6	45.60	25.14*	E

*Critical (maximum) value for particular T_1
E - no yielding, i.e., linearly elastic response

DUCTILITY DEMAND BASED ON NODAL ROTATIONS AT 1st FLOOR LEVEL

E.Q. INPUT NO.	FUNDAMENTAL PERIOD, T_1, (SEC) 0.5	0.8	1.4
	ROTATIONAL DUCTILITY, μ_{r2}		
1	1.90	1.88	1.59*
2	4.25	1.69	E
3	2.99	3.14*	E
4	3.92	1.49	E
5	2.92	1.54	1.12
6	4.50*	2.35	E
	CYCLIC ROT. DUCTILITY μ_{rc2}		
1	2.6	1.88	1.66*
2	4.25	1.69	E
3	3.30	3.63*	E
4	5.49	1.49	E
5	3.92	1.61	1.15
6	6.93*	2.94	E
	CUMULATIVE DUCTILITY, $\Sigma\mu_{rc2}$		
1	30.9	20.59	22.05*
2	50.27	18.05	E
3	48.93	24.89	E
4	44.59	19.01	E
5	61.75*	30.44*	14.98
6	53.82	27.44	E
	CUMULATIVE ROT. ENERGY, ΣA_{r2}		
1	17.98	9.38	5.54*
2	39.68	8.46	E
3	41.40	15.10*	E
4	29.90	7.52	E
5	43.24*	13.68	5.30
6	40.12	15.68	E

MAXIMUM RESPONSE VALUES

E.Q. INPUT NO.	FUNDAMENTAL PERIOD, T_1, (SEC) 0.5	0.8	1.4
	MAX. TOP DISPL. (IN)		
1	2.4	5.6	14.8*
2	4.4	5.3	12.6(E)
3	3.1	7.7*	11.0(E)
4	3.8	4.8	11.0(E)
5	3.0	5.1	11.4
6	4.7*	6.0	7.6(E)
	MAX. INTERSTORY DISPL. (IN)		
1	0.30	0.70	1.84*
2	0.50	0.67	1.89(E)
3	0.36	0.90*	1.53(E)
4	0.43	0.61	1.52(E)
5	0.35	0.66	1.70
6	0.54*	0.79	1.02(E)
	MAX. BASE SHEAR (KIPS)		
1	966	974	815
2	953	797	827(E)
3	978	983	1,022(E)
4	987	787	806(E)
5	1,234*	1,109	1,203*
6	1,140	1,116*	571(E)
	MAX. BASE MOMENT (IN-KIPS)		
1	558,000	572,000	553,000*
2	634,000	559,000	518,000(E)
3	600,000	602,000*	525,000(E)
4	631,000	549,000	465,000(E)
5	600,000	554,000	534,000
6	636,000*	585,000	330,000(E)
	ROTATIONAL DUCTILITY, μ_{r0} **		
1	2.6	2.8	2.1*
2	5.2	2.3	1.0(E)
3	3.9	3.9*	1.0(E)
4	5.0	1.9	0.9(E)
5	3.9	2.1	1.3
6	5.2*	3.3	0.6(E)

** μ_{r0} Based on Eq. (1)

Table A3

RESPONSE VALUES CORRESPONDING TO DIFFERENT EARTHQUAKE INPUT MOTIONS
[SI = 15(SI$_{ref.}$), Duration = 10 sec.]

10-Story Isolated Structural Walls
M_y = 1,000,000 IN-K

EARTHQUAKE INPUT NUMBER	EARTHQUAKE INPUT	FUNDAMENTAL PERIOD, T_1 (SEC.)				
		0.5			0.8	1.4
		M_y x 10^6 in-kips	$\theta_y^{\#}$ x 10^{-3} rad.	θ_y^{*} x 10^{-3} rad.		
1	1971 Pacoima Dam, S16E	1.05	.61	1.17		
2	1971 Holiday Orion, E-W	1.05	E	E		
3	1952 Taft, S69E	1.05	.64	1.21		
4	1940 El Centro, E-W	1.05	.60	1.14		
5	(Artificial Acc. (SI)	1.05	.70	1.24		
6	1940 El Centro, N-S	1.05	.61	1.16		
	AVERAGE		.63	1.18		

$^{\#}$at midheight of 1st story
*at 1st floor level

MAXIMUM RESPONSE VALUES

E.Q. INPUT NO.	FUNDAMENTAL PERIOD, T_1, (SEC)		
	0.5	0.8	1.4
	MAX. TOP DISPL. (IN)		
1	3.5	5.3(E)	15.4*(E)
2	2.9(E)	5.3(E)	12.6(E)
3	4.0	8.2*(E)	11.0(E)
4	4.4	4.8(E)	11.0(E)
5	3.6	6.1(E)	11.8(E)
6	4.8*	7.7(E)	7.6(E)
	MAX. INTERSTORY DISPL. (IN)		
1	0.45	0.70(E)	2.07*(E)
2	0.37(E)	0.71(E)	1.68(E)
3	0.49	1.09*(E)	1.58(E)
4	0.54	0.65(E)	1.52(E)
5	0.47	0.84(E)	1.78(E)
6	0.57*	1.03(E)	1.02(E)
	MAX. BASE SHEAR (KIPS)		
1	1,666	1,092(E)	1,061(E)
2	1,196(E)	1,026(E)	827(E)
3	1,535	1,372(E)	1,027(E)
4	1,844	855(E)	805(E)
5	1,812	1,473*(E)	1,359*(E)
6	1,969*	1,473*(E)	571(E)
	MAX. BASE MOMENT (IN-KIPS)		
1	1,080,000	704,000(E)	720,000*(E)
2	960,000(E)	720,000(E)	518,000(E)
3	1,105,000	1,051,000*(E)	531,000(E)
4	1,155,000	641,000(E)	466,000(E)
5	1,094,000	893,000(E)	596,000(E)
6	1,172,000*	997,000(E)	330,000(E)
	ROTATIONAL DUCTILITY, μ_{ro} **		
1	1.57	0.7(E)	0.7*(E)
2	0.9(E)	0.7(E)	0.5(E)
3	2.0	1.0*(E)	0.5(E)
4	3.0	0.6(E)	0.6(E)
5	1.8	0.8(E)	0.6(E)
6	3.3*	0.9(E)	0.3(E)

** μ_{ro} Based on Eq. (1)

DUCTILITY DEMAND BASED ON NODAL ROTATIONS AT MID-HEIGHT OF 1st STORY

E.Q. INPUT NO.	FUNDAMENTAL PERIOD, T_1, (SEC)		
	0.5	0.8	1.4
	ROTATIONAL DUCTILITY, μ_{r1}		
1	1.46	E	E
2	0.87(E)	E	E
3	1.94	E	E
4	2.85	E	E
5	1.70	E	E
6	3.10*	E	E
	CYCLIC ROT. DUCTILITY μ_{rc1}		
1	1.46	E	E
2	E	E	E
3	1.94	E	E
4	2.85	E	E
5	2.03	E	E
6	3.20*	E	E
	CUMULATIVE DUCTILITY, $\Sigma\mu_{rc1}$		
1	24.64	E	E
2	E	E	E
3	28.36	E	E
4	28.31	E	E
5	32.87*	E	E
6	26.87	E	E
	CUMULATIVE ROT. ENERGY, ΣA_{r1}		
1	12.62	E	E
2	E	E	E
3	15.50	E	E
4	14.26	E	E
5	17.02*	E	E
6	14.56	E	E

DUCTILITY DEMAND BASED ON NODAL ROTATIONS AT 1st FLOOR LEVEL

E.Q. INPUT NO.	FUNDAMENTAL PERIOD, T_1, (SEC)		
	0.5	0.8	1.4
	ROTATIONAL DUCTILITY, μ_{r2}		
1	1.29	E	E
2	0.84(E)	E	E
3	1.56	E	E
4	2.04	E	E
5	1.36	E	E
6	2.25*	E	E
	CYCLIC ROT. DUCTILITY μ_{rc2}		
1	1.29	E	E
2	E	E	E
3	1.56	E	E
4	2.04	E	E
5	1.55	E	E
6	2.25*	E	E
	CUMULATIVE DUCTILITY, $\Sigma\mu_{rc2}$		
1	23.96	E	E
2	E	E	E
3	26.57	E	E
4	23.47	E	E
5	28.00*	E	E
6	21.85	E	E
	CUMULATIVE ROT. ENERGY, ΣA_{r2}		
1	11.88	E	E
2	E	E	E
3	13.80*	E	E
4	10.28	E	E
5	13.62	E	E
6	10.20	E	E

*Critical (maximum) value for particular T_1
E - no yielding, i.e., linearly elastic response

Table A4

RESPONSE VALUES CORRESPONDING TO DIFFERENT EARTHQUAKE INPUT MOTIONS
[SI = 15(SI$_{ref}$), Duration = 10 sec.]

20-Story Isolated Structural Walls
M_y = 750,000 IN-K

EARTHQUAKE INPUT NUMBER	EARTHQUAKE INPUT	FUNDAMENTAL PERIOD, T_1 (SEC.) 0.8			1.4			2.0			2.4		
		M_y x 10^6 in-kips	θ_y* x 10^{-3} rad.	θ_y@ x 10^{-3} rad.	M_y x 10^6 in-kips	θ_y* x 10^{-3} rad.	θ_y@ x 10^{-3} rad.	M_y x 10^6 in-kips	θ_y* x 10^{-3} rad.	θ_y@ x 10^{-3} rad.	M_y x 10^6 in-kips	θ_y* x 10^{-3} rad.	θ_y@ x 10^{-3} rad.
1	1971 Pacoima Dam, S16E	.7875	.20	.32	.7875	.53	.85	.7875	1.11	1.82	.7858	1.60	2.65
2	1971 Holiday Orion, E-W	.7875	.18	.30	.7875	.53	.88	.7875	1.07	1.70	.7875	1.57	2.60
3	1952 Taft, S69E	.7875	.20	.31	.7875	.59	.94	.7875	1.06	1.71	.7875	1.60	2.49
4	1940 El Centro, E-W	.7875	.17	.29	.7875	.50	.80	.7875	1.06	1.68	.7875	1.50	2.38
5	SI (Artificial Acc.)	.7875	.17	.28	.7875	.59	.92	.7875	1.12	1.77	.7875	1.59	2.53
6	1940 El Centro, N-S	.7875	.18	.29	.7875	.60	.98	.7875	1.08	1.76	.7875	1.57	2.57
	AVERAGE		.18	.30		.55	.90		1.08	1.74		1.57	2.54

*at 1st floor level
@at 2nd floor level

DUCTILITY DEMAND BASED ON NODAL ROTATIONS AT 1st FLOOR LEVEL

E.Q. INPUT NO.	FUNDAMENTAL PERIOD, T_1, (SEC) 0.8	1.4	2.0	2.4
	ROTATIONAL DUCTILITY, μ_{r1}			
1	9.22*	4.70	2.78	1.55
2	7.05	4.80*	3.28*	1.40
3	5.84	4.28	2.59	1.34
4	5.89	4.55	2.85	3.94*
5	5.15	4.28	2.73	1.97
6	7.11	2.78	2.40	2.43
	CYCLIC ROT. DUCTILITY μ_{rc1}			
1	15.44*	7.58*	2.57	1.34
2	10.90	7.58*	4.82*	1.30
3	7.28	5.28	2.88	1.24
4	8.89	6.28	2.85	4.03*
5	6.91	5.02	3.38	2.63
6	9.00	3.55	2.44	2.90
	CUMULATIVE DUCTILITY, $\Sigma\mu_{rc1}$			
1	75.06	42.05	16.93	13.60
2	64.11	43.87	30.49*	14.60
3	71.12	48.50	27.07	18.85
4	69.50	37.77	21.00	20.83*
5	99.08*	53.29*	26.88	19.46
6	71.22	25.09	16.56	15.48
	CUMULATIVE ROT. ENERGY, ΣA_{r1}			
1	71.76	35.50	7.52	7.00
2	65.68	39.58	23.06*	6.80
3	76.68	45.32*	14.44	8.66
4	63.32	34.38	16.90	12.10*
5	76.98*	35.14	17.48	12.10
6	68.72	18.92	9.28	9.26

*Critical (maximum) value for particular T_1
E - no yielding, i.e., linearly elastic response

DUCTILITY DEMAND BASED ON NODAL ROTATIONS AT 2nd FLOOR LEVEL

E.Q. INPUT NO.	FUNDAMENTAL PERIOD, T_1, (SEC) 0.8	1.4	2.0	2.4
	ROTATIONAL DUCTILITY, μ_{r2}			
1	8.43*	4.04*	2.16	1.34
2	6.31	3.72	2.39*	1.22
3	5.38	3.60	1.94	1.19
4	4.93	3.74	2.38	2.91*
5	4.62	3.40	2.07	1.67
6	6.53	2.31	2.07	1.99
	CYCLIC ROT. DUCTILITY μ_{rc2}			
1	13.50*	6.02*	2.37	1.13
2	9.60	5.59	3.40*	1.22
3	6.89	4.13	2.13	1.10
4	7.10	4.63	3.04	3.01*
5	5.54	4.05	2.35	1.95
6	7.80	2.86	2.06	2.33
	CUMULATIVE DUCTILITY, $\Sigma\mu_{rc2}$			
1	63.63	33.18	14.83	15.86
2	54.22	35.48	27.75*	13.57
3	65.52	38.58	21.92	17.03*
4	57.67	30.26	17.29	16.12
5	79.60*	40.85*	21.62	15.90
6	62.70	21.45	14.79	13.14
	CUMULATIVE ROT. ENERGY, ΣA_{r2}			
1	61.54	27.18	6.18	10.10
2	54.72	29.60	17.12*	6.18
3	65.40*	32.64*	11.06	7.29
4	50.78	26.04	12.54	10.52*
5	60.50	26.20	12.84	9.02
6	59.32	14.74	7.76	6.94

MAXIMUM RESPONSE VALUES

E.Q. INPUT NO.	FUNDAMENTAL PERIOD, T_1, (SEC) 0.8	1.4	2.0	2.4
	MAX. TOP DISPL. (IN)			
1	9.2*	11.5*	16.1	15.4
2	6.3	10.7	15.7	15.2
3	6.4	10.5	11.3	14.9
4	4.7	10.9	17.0*	23.7*
5	4.7	9.3	13.2	19.0
6	7.0	7.9	15.3	22.6
	MAX. INTERSTORY DISPL. (IN)			
1	0.53*	0.72*	1.04	1.13
2	0.36	0.67	1.07	1.17
3	0.37	0.64	0.90	1.16
4	0.28	0.65	1.12*	1.51*
5	0.28	0.60	0.52	1.32
6	-	0.49	-	-
	MAX. BASE SHEAR (KIPS)			
1	1,315	1,064	1,472*	1,434
2	1,156	1,367	1,227	1,078
3	1,152	1,133	1,444	1,479*
4	1,185	950	1,070	1,179
5	1,700*	1,463*	1,442	1,263
6	1,018	1,247	1,190	1,136
	MAX. BASE MOMENT (IN-KIPS)			
1	1,133,000*	945,000	839,000	815,000
2	1,045,000	948,000*	881,000*	802,000
3	1,017,000	925,000	854,000	801,000
4	996,000	941,000	862,000	903,000*
5	957,000	924,000	858,000	828,000
6	1,045,000	863,000	845,000	844,000
	ROTATIONAL DUCTILITY, μ_{r0} **			
1	9.77*	5.00	2.01	1.70
2	7.54	5.08*	3.37*	1.37
3	6.83	4.49	2.69	1.34
4	6.30	4.90	2.90	3.92*
5	5.30	4.47	2.79	2.03
6	7.54	2.52	2.46	2.43

** μ_{r0} Based on Eq. (1)

Table A5

RESPONSE VALUES CORRESPONDING TO DIFFERENT EARTHQUAKE INPUT MOTIONS
[SI = 15(SI$_{ref.}$), Duration = 10 sec.]

20-Story Isolated Structural Walls
M_y = 1,000,000 IN-K

EARTHQUAKE INPUT NUMBER	EARTHQUAKE INPUT	FUNDAMENTAL PERIOD, T_1 (SEC.) 0.8 M_y x 10^6 in-kips	0.8 θ_y' x 10^{-3} rad.	0.8 θ_y^* x 10^{-3} rad.	1.4 M_y x 10^6 in-kips	1.4 θ_y' x 10^{-3} rad.	1.4 θ_y^* x 10^{-3} rad.	2.0 M_y x 10^6 in-kips	2.0 θ_y' x 10^{-3} rad.	2.0 θ_y^* x 10^{-3} rad.	2.4 M_y x 10^6 in-kips	2.4 θ_y' x 10^{-3} rad.	2.4 θ_y^* x 10^{-3} rad.
1	1971 Pacoima Dam, S16E	1.05	.23	.38	1.05	.71	1.18	1.05	1.46	2.44	1.05	E	E
2	1971 Holiday Orion, E-W	1.05	.23	.38	1.05	.71	1.16	1.05	1.53	2.48	1.05	E	E
3	1952 Taft, S69E	1.05	.26	.40	1.05	.71	1.17	1.05	1.45	2.37	1.05	E	E
4	1940 El Centro, E-W	1.05	.23	.40	1.05	.71	1.18	1.05	1.53	2.48	1.05	2.15	3.55
5	Artificial Acc. (SI)	1.05	.26	.40	1.05	.71	1.14	1.05	1.45	2.38	1.05	2.02	3.23
6	1940 El Centro, N-S	1.05	.22	.36	1.05	.70	1.17	1.05	1.43	2.36	1.05	2.06	3.37
	AVERAGE		.24	.39		.71	1.17		1.48	2.42		2.08	3.38

θ_y' at 1st floor level
θ_y^* at 2nd floor level

DUCTILITY DEMAND BASED ON NODAL ROTATIONS AT 1st FLOOR LEVEL

E.Q. INPUT NO.	FUNDAMENTAL PERIOD, T_1, (SEC) 0.8	1.4	2.0	2.4
	ROTATIONAL DUCTILITY, μ_{r1}			
1	6.81*	4.50*	1.36	E
2	5.58	3.41	2.69*	E
3	4.26	3.24	1.90	E
4	3.84	-	2.41	2.08*
5	3.79	3.14	1.76	1.24
6	7.87	1.56	1.57	1.50
	CYCLIC ROT. DUCTILITY μ_{rc1}			
1	10.23*	5.90*	1.36	E
2	7.63	5.21	3.71*	E
3	5.93	4.41	1.89	E
4	5.09	-	2.61	2.08*
5	5.25	3.63	1.78	1.40
6	7.87	1.56	1.57	1.54
	CUMULATIVE DUCTILITY, $\Sigma\mu_{rc1}$			
1	53.27	33.80	11.85	E
2	49.46	34.03	23.81*	E
3	47.74	26.01	17.78	E
4	49.34	-	14.49	14.85*
5	61.25	37.94*	18.07	14.20
6	62.82*	19.82	14.45	12.53
	CUMULATIVE ROT. ENERGY, ΣA_{r1}			
1	49.68	26.20	5.06	E
2	48.40	27.04*	17.04*	E
3	42.42	19.78	10.64	E
4	39.56	-	9.80	10.26*
5	46.02	21.76	7.54	6.02
6	59.66*	12.72	8.64	3.46

*Critical (maximum) value for particular T_1
E - no yielding, i.e., linearly elastic response

DUCTILITY DEMAND BASED ON NODAL ROTATIONS AT 2nd FLOOR LEVEL

E.Q. INPUT NO.	FUNDAMENTAL PERIOD, T_1, (SEC) 0.8	1.4	2.0	2.4
	ROTATIONAL DUCTILITY, μ_{r2}			
1	6.27*	3.54*	1.24	E
2	5.00	2.56	2.06*	E
3	4.12	2.36	1.50	E
4	3.09	-	2.00	1.73*
5	3.38	2.44	1.45	1.17
6	5.08	1.34	1.36	1.33
	CYCLIC ROT. DUCTILITY μ_{rc2}			
1	8.93*	4.44*	1.26	E
2	6.36	3.76	2.54*	E
3	5.15	3.09	1.49	E
4	3.81	-	2.18	1.73*
5	4.51	2.77	1.50	1.28
6	6.41	1.38	1.36	1.40
	CUMULATIVE DUCTILITY, $\Sigma\mu_{rc2}$			
1	45.98	25.76	10.88	E
2	42.10	27.09	19.84*	E
3	43.57	20.04	14.27	E
4	39.76	-	12.74	12.14
5	53.31	28.88*	15.60	14.23*
6	53.85*	18.41	13.36	11.46
	CUMULATIVE ROT. ENERGY, ΣA_{r2}			
1	42.40	18.78	4.42	E
2	39.20	19.72*	13.14*,	E
3	37.64	12.94	6.80	E
4	29.88	-	7.56	7.64
5	40.38	15.34	6.18	8.56*
6	48.70*	11.34	7.66	3.00

MAXIMUM RESPONSE VALUES

E.Q. INPUT NO.	FUNDAMENTAL PERIOD, T_1, (SEC) 0.8	1.4	2.0	2.4
	MAX. TOP DISPL. (IN)			
1	8.4*	13.4*	17.2	15.4 (E)
2	6.3	10.4	18.6	15.2 (E)
3	6.2	9.5	13.9	14.9 (E)
4	4.0	9.2	20.0*	22.4
5	4.5	10.0	13.4	14.2
6	6.6	7.9	15.9	24.9*
	MAX. INTERSTORY DISPL. (IN)			
1	0.46*	0.83*	1.18	1.13 (E)
2	0.36	0.68	1.26*	1.22 (E)
3	0.37	0.63	1.10	1.21 (E)
4	0.24	0.58	1.25	1.51*
5	0.28	0.77	0.97	-
6	0.38	-	-	-
	MAX. BASE SHEAR (KIPS)			
1	1,530	1,210	1,470	1,680*(E)
2	1,330	1,550*	1,550	1,180 (E)
3	1,270	1,419	1,620*	1,437 (E)
4	1,330	1,190	1,120	1,240
5	1,730*	1,510	1,470	1,488
6	1,227	1,367	1,799	1,235
	MAX. BASE MOMENT (IN-KIPS)			
1	1,375,000*	1,243,000*	1,070,000	1,018,000(E)
2	1,306,000	1,182,000	1,147,000*	907,000(E)
3	1,237,000	1,116,000	1,103,000	916,000(E)
4	1,214,000	1,149,000	1,126,000	1,107,000*
5	1,208,000	1,165,000	1,093,000	1,061,000
6	1,318,000	1,080,000	1,081,000	1,076,000
	ROTATIONAL DUCTILITY, μ_{ro}			
1	7.2*	4.7*	1.4	0.95(E)
2	5.9	3.5	2.9*	0.9 (E)
3	4.6	2.3	2.0	1.0 (E)
4	4.1	2.9	2.5	2.1*
5	4.0	2.2	1.8	1.2
6	6.1	1.6	1.6	1.5

** μ_{ro} Based on Eq. (1)

Table A6

RESPONSE VALUES CORRESPONDING TO DIFFERENT EARTHQUAKE INPUT MOTIONS

[SI = 15(SI$_{ref.}$), Duration = 10 sec.]

20-Story Isolated Structural Walls

M_y = 1,500,000 IN-K

EARTHQUAKE INPUT NUMBER	EARTHQUAKE INPUT	FUNDAMENTAL PERIOD, T_1 (SEC.)											
		0.8			1.4			2.0			2.4		
		M_y x 10^6 in-kips	θ_y^* x 10^{-3} rad.	θ_y^{**} x 10^{-3} rad.	M_y x 10^6 in-kips	θ_y^* x 10^{-3} rad.	θ_y^{**} x 10^{-3} rad.	M_y x 10^6 in-kips	θ_y^* x 10^{-3} rad.	θ_y^{**} x 10^{-3} rad.	M_y x 10^6 in-kips	θ_y^* x 10^{-3} rad.	θ_y^{**} x 10^{-3} rad.
1	1971 Pacoima Dam, S16E	1.575	.34	.56	1.575	1.04	1.71	1.575	E	E	1.575	E	E
2	1971 Holliday Orion, E-W	1.575	.38	.61	1.575	1.06	1.75	1.575	2.24	3.67	1.575	E	E
3	1952 Taft, S69E	1.575	.34	.55	1.575	1.07	1.77	1.575	E	E	1.575	E	E
4	1940 El Centro, E-W	1.575	.35	.60	1.575	1.07	1.78	1.575	2.23	3.70	1.575	E	E
5	(Artificial Acc.), SI	1.575	.34	.57	1.575	1.04	1.67	1.575	E	E	1.575	E	E
6	1940 El Centro, N-S	1.575	.35	.58	1.575	E	E	1.575	E	E	1.575	E	E
	AVERAGE		.35	.58		1.06	1.74		2.23	3.68			

*at 1st floor level
**at 2nd floor level

MAXIMUM RESPONSE VALUES

E.Q. INPUT NO.	FUNDAMENTAL PERIOD, T_1, (SEC)			
	0.8	1.4	2.0	2.4
	MAX. TOP DISPL. (IN)			
1	6.7*	15.2*	17.2(E)	15.4(E)
2	4.6	13.4	20.1	15.2(E)
3	5.8	11.4	16.0(E)	14.9(E)
4	4.5	11.0	23.1*	24.5(E)
5	5.4	11.8	13.7(E)	20.7(E)
6	5.7	8.0(E)	16.0(E)	24.9*(E)
	MAX. INTERSTORY DISPL. (IN)			
1	0.41*	0.96*	1.21(E)	1.13(E)
2	0.30	0.87	1.57*	1.22(E)
3	0.37	0.80	1.17(E)	1.21(E)
4	0.29	0.75	1.57	1.76*(E)
5	0.39	0.84	1.04(E)	1.57(E)
6	-	0.49	-	-
	MAX. BASE SHEAR (KIPS)			
1	1,830	1,690	1,490(E)	1,680*(E)
2	1,550	1,660	2,120*	1,180(E)
3	2,000	1,681	1,800(E)	1,437(E)
4	1,610	1,300	1,150	1,300(E)
5	2,030*	1,900*	1,660(E)	1,580(E)
6	1,710	1,423(E)	1,200(E)	1,235(E)
	MAX. BASE MOMENT (IN-KIPS)			
1	1,828,000*	1,774,000*	1,144,000(E)	1,018,000(E)
2	1,714,000	1,655,000	1,647,000*	907,000(E)
3	1,824,000	1,614,000	1,407,000(E)	916,000(E)
4	1,701,000	1,583,000	1,609,000	1,519,000*(E)
5	1,739,000	1,647,000	1,387,000(E)	1,218,000(E)
6	1,799,000	1,191,000(E)	1,226,000(E)	1,076,000(E)
	ROTATIONAL DUCTILITY, μ_{ro} **			
1	4.2*	3.6*	0.7(E)	0.6(E)
2	2.8	2.0	1.9*	0.6(E)
3	4.2	1.5	0.9(E)	0.6(E)
4	2.6	1.1	1.4	1.0*(E)
5	3.1	1.9	0.9(E)	0.8(E)
6	3.9	0.8(E)	0.8(E)	0.7(E)

** μ_{ro} Based on Eq. (1)

DUCTILITY DEMAND BASED ON NODAL ROTATIONS AT 1st FLOOR LEVEL

E.Q. INPUT NO.	FUNDAMENTAL PERIOD, T_1, (SEC)			
	0.8	1.4	2.0	2.4
	ROTATIONAL DUCTILITY, μ_{r1}			
1	4.03*	3.42*	E	E
2	2.6	1.99	1.80*	E
3	3.6	1.47	E	E
4	2.6	1.10	1.38	E
5	3.0	1.88	E	E
6	3.7	E	E	E
	CYCLIC ROT. DUCTILITY μ_{rc1}			
1	4.66	3.42*	E	E
2	3.29	2.00	1.8*	E
3	4.94	1.46	E	E
4	3.46	-	1.38	E
5	3.29	1.89	E	E
6	5.55*	E	E	E
	CUMULATIVE DUCTILITY, $\Sigma\mu_{rc1}$			
1	34.54	22.15	E	E
2	26.89	18.64	16.2*	E
3	35.86	16.34	E	E
4	31.12	-	12.72	E
5	43.60	23.97*	E	E
6	45.59*	E	E	E
	CUMULATIVE ROT. ENERGY, ΣA_{r1}			
1	21.80	15.62*	E	E
2	17.88	10.50	10.00*	E
3	25.90	11.36	E	E
4	22.28	-	9.00	E
5	29.40	12.08	E	E
6	38.16*	E	E	E

DUCTILITY DEMAND BASED ON NODAL ROTATIONS AT 2nd FLOOR LEVEL

E.Q. INPUT NO.	FUNDAMENTAL PERIOD, T_1, (SEC)			
	0.8	1.4	2.0	2.4
	ROTATIONAL DUCTILITY, μ_{r2}			
1	3.41*	2.53*	E	E
2	1.97	1.61	1.44*	E
3	2.93	1.31	E	E
4	1.90	1.08	1.24	E
5	2.38	1.53	E	E
6	2.95	E	E	E
	CYCLIC ROT. DUCTILITY μ_{rc2}			
1	3.81	2.61*	E	E
2	2.47	1.65	1.41*	E
3	4.02	1.30	E	E
4	2.57	-	1.23	E
5	2.52	1.53	E	E
6	4.09*	E	E	E
	CUMULATIVE DUCTILITY, $\Sigma\mu_{rc2}$			
1	28.65	18.60	E	E
2	23.10	16.37	14.25*	E
3	31.12	15.53	E	E
4	25.46	-	12.30	E
5	35.90	19.95*	E	E
6	35.91*	E	E	E
	CUMULATIVE ROT. ENERGY, ΣA_{r2}			
1	16.74	11.22*	E	E
2	13.52	8.60	8.38	E
3	21.22	10.48	E	E
4	16.36	-	8.50*	E
5	22.60	9.28	E	E
6	27.54*	E	E	E

*Critical (maximum) value for particular T_1
E - no yielding, i.e., linearly elastic response

Table A7

RESPONSE VALUES CORRESPONDING TO DIFFERENT EARTHQUAKE INPUT MOTIONS
[SI = 1.5(SI)$_{ref.}$), Duration = 10 sec.]

30-Story Isolated Structural Walls
M_y = 1,000,000 IN-K

EARTHQUAKE INPUT NUMBER	EARTHQUAKE INPUT	FUNDAMENTAL PERIOD, T_1 (SEC.) 1.4 M_y x 10^6 in-kips	1.4 θ_y^a x 10^{-3} rad.	1.4 θ_y^b x 10^{-3} rad.	2.0 M_y x 10^6 in-kips	2.0 θ_y^a x 10^{-3} rad.	2.0 θ_y^b x 10^{-3} rad.	2.4 M_y x 10^6 in-kips	2.4 θ_y^a x 10^{-3} rad.	2.4 θ_y^b x 10^{-3} rad.
1	1971 Pacoima Dam, S16E	1.050	.19	.29	1.050	.32	.54	1.050	.42	.69
2	1971 Holiday Orion, E-W	1.050	.16	.25	1.050	.30	.55	1.050	.47	.75
3	1952 Taft, S69E	1.050	.15	.25	1.050	.34	.56	1.050	.44	.74
4	1940 El Centro, E-W	1.050	.15	.25	1.050	.33	.54	1.050	.44	.73
5	(Artificial Acc. (S1)	1.050	.16	.24	1.050	.34	.55	1.050	.45	.73
6	1940 El Centro, N-S	1.050	.16	.27	1.050	.32	.51	1.050	.45	.78
	AVERAGE		.16	.26		.33	.54		.45	.78

^{a}at 1st floor level
^{b}at 2nd floor level

DUCTILITY DEMAND BASED ON NODAL ROTATIONS AT 1st FLOOR LEVEL

E.Q. INPUT NO.	FUNDAMENTAL PERIOD, T_1, (SEC) 1.4	2.0	2.4
	ROTATIONAL DUCTILITY, μ_{r1}		
1	8.00	4.21	3.91
2	6.49	5.52	5.58
3	5.92	3.96	3.04
4	8.95*	6.67*	6.96*
5	7.50	5.41	4.70
6	5.83	3.61	4.61
	CYCLIC ROT. DUCTILITY μ_{rc1}		
1	9.50	4.06	3.26
2	10.81	7.43	6.88
3	7.61	4.93	3.04
4	11.72*	9.00*	10.19*
5	9.38	7.10	7.10
6	7.31	5.87	6.66
	CUMULATIVE DUCTILITY, $\Sigma\mu_{rc1}$		
1	61.13	31.61	29.20
2	75.29	50.95	30.50
3	65.42	40.04	34.50
4	84.75	40.61	46.35*
5	88.5*	58.41*	41.50
6	48.97	35.33	34.79
	CUMULATIVE ROT. ENERGY, ΣA_{r1}		
1	49.78	21.84	22.76
2	72.58	49.44	26.12
3	59.98	31.42	27.36
4	83.10	35.18	42.14*
5	75.16*	50.30*	33.60
6	42.80	31.40	32.88

DUCTILITY DEMAND BASED ON NODAL ROTATIONS AT 2nd FLOOR LEVEL

E.Q. INPUT NO.	FUNDAMENTAL PERIOD, T_1, (SEC) 1.4	2.0	2.4
	ROTATIONAL DUCTILITY, μ_{r2}		
1	7.36	3.59	2.98
2	5.80	4.23	4.97
3	5.57	3.61	2.40
4	8.48*	6.11*	6.14*
5	6.78	4.06	3.66
6	5.31	2.63	3.30
	CYCLIC ROT. DUCTILITY μ_{rc2}		
1	8.74	3.62	2.51
2	9.38	5.64	5.62
3	6.25	3.92	2.40
4	10.55*	7.74*	8.32*
5	7.62	5.62	6.45
6	6.37	3.95	4.74
	CUMULATIVE DUCTILITY, $\Sigma\mu_{rc2}$		
1	54.40	27.30	24.09
2	65.23	42.02	24.84
3	56.26	34.66	29.90
4	56.57	34.28	37.42*
5	75.80*	46.80*	31.68
6	41.95	25.00	27.09
	CUMULATIVE ROT. ENERGY, ΣA_{r2}		
1	45.32	18.60	17.10
2	62.20*	38.54	15.84
3	50.68	24.64	20.56
4	55.14	29.10	32.68*
5	64.90	39.06*	22.36
6	34.02	20.90	23.60

*Critical (maximum) value for particular T_1
E - no yielding, i.e., linearly elastic response

MAXIMUM RESPONSE VALUES

E.Q. INPUT NO.	FUNDAMENTAL PERIOD, T_1, (SEC) 1.4	2.0	2.4
	MAX. TOP DISPL. (IN)		
1	11.8	13.4	15.4
2	10.9	11.1	10.2
3	9.4	12.5	11.7
4	15.4*	21.2*	25.8*
5	11.7	15.2	10.5
6	10.5	13.4	13.5
	MAX. INTERSTORY DISPL. (IN)		
1	0.48	0.58	0.43
2	0.44	0.57	0.84
3	0.38	0.56	0.62
4	0.60*	0.86*	1.07*
5	0.49	0.67	0.87
6	0.43	0.58	0.69
	MAX. BASE SHEAR (KIPS)		
1	1339	1626	1402
2	1738*	2038*	1319
3	1338	1457	1922*
4	1194	1503	1567
5	1937	1690	1378
6	1657	1592	1525
	MAX. BASE MOMENT (IN-KIPS)		
1	1,450,000	1,240,000	1,210,000
2	1,374,000	1,306,000	1,301,000
3	1,337,000	1,219,000	1,164,000
4	1,510,000*	1,380,000*	1,370,000*
5	1,426,000	1,310,000	1,291,000
6	1,332,000	1,204,000	1,248,000
	ROTATIONAL DUCTILITY, μ_{ro} **		
1	8.6	4.6	4.1
2	7.2	5.9	5.8
3	6.5	4.2	3.2
4	9.8*	7.3*	7.1*
5	8.2	6.0	4.8
6	6.4	3.9	4.8

** μ_{ro} Based on Eq. (1)

Table A8

RESPONSE VALUES CORRESPONDING TO DIFFERENT EARTHQUAKE INPUT MOTIONS
[SI = 15(SI$_{ref.}$), Duration = 10 sec.]

30-Story Isolated Structural Walls
M_y = 1,500,000 IN-K

EARTHQUAKE INPUT NUMBER	EARTHQUAKE INPUT	FUNDAMENTAL PERIOD, T_1 (SEC.)								
		0.6			0.8			1.4		
		M_y x 10^6 in-kips	$\theta_y^{\#}$ x 10^{-3} rad.	$\theta_y^{@}$ x 10^{-3} rad.	M_y x 10^6 in-kips	$\theta_y^{\#}$ x 10^{-3} rad.	$\theta_y^{@}$ x 10^{-3} rad.	M_y x 10^6 in-kips	$\theta_y^{\#}$ x 10^{-3} rad.	$\theta_y^{@}$ x 10^{-3} rad.
1	1971 Pacoima Dam, S16E	1.575	.22	.35	1.575	.46	.77	1.575	.70	1.18
2	1971 Holiday Orion, E-W	1.575	.24	.39	1.575	.48	.80	1.575	.70	1.15
3	1952 Taft, S69E	1.575	.22	.37	1.575	.45	.78	1.575	.66	1.07
4	1940 El Centro, E-W	1.575	.23	.37	1.575	.46	.75	1.575	.64	1.05
5	Artificial Acc. (SI)	1.575	.22	.37	1.575	.46	.76	1.575	.70	1.14
6	1940 El Centro, N-S	1.575	.23	.39	1.575	.48	.79	1.575	.66	1.11
	AVERAGE		.23	.37		.47	.78		.68	1.12

#at 1st floor level
@at 2nd floor level

DUCTILITY DEMAND BASED ON NODAL ROTATIONS AT 1st FLOOR LEVEL

E.Q. INPUT NO.	FUNDAMENTAL PERIOD, T_1, (SEC)		
	1.4	2.0	2.4
	ROTATIONAL DUCTILITY, μ_{r1}		
1	5.57	2.47	2.37
2	5.61	4.28*	1.77
3	5.42	3.48	1.85
4	5.65*	4.02	4.73*
5	5.23	3.82	2.91
6	3.28	2.96	2.90
	CYCLIC ROT. DUCTILITY μ_{rc1}		
1	9.31*	3.15	2.06
2	9.22	6.32*	1.67
3	6.38	4.23	2.37
4	7.91	4.31	5.49*
5	6.98	4.61	3.67
6	5.09	3.16	4.06
	CUMULATIVE DUCTILITY, $\Sigma\mu_{rc1}$		
1	52.70	20.72	18.13
2	55.57	40.29*	16.55
3	47.91	30.08	23.90
4	47.80	27.34	27.12*
5	70.20*	38.12	24.82
6	32.88	20.20	20.88
	CUMULATIVE ROT. ENERGY, ΣA_{r1}		
1	41.66	10.88	11.74
2	52.44*	33.86*	8.38
3	43.86	21.60	15.66
4	43.10	23.12	20.54*
5	49.50	25.88	16.74
6	25.54	12.64	16.14

DUCTILITY DEMAND BASED ON NODAL ROTATIONS AT 2nd FLOOR LEVEL

E.Q. INPUT NO.	FUNDAMENTAL PERIOD, T_1, (SEC)		
	1.4	2.0	2.4
	ROTATIONAL DUCTILITY, μ_{r2}		
1	5.04	2.23	1.68
2	4.86	3.40*	1.49
3	5.02	2.30	1.56
4	5.08*	3.26	3.96*
5	4.66	2.91	2.66
6	2.96	2.53	2.49
	CYCLIC ROT. DUCTILITY μ_{rc2}		
1	8.27*	2.68	1.58
2	7.92	4.64*	1.40
3	5.77	2.78	1.77
4	6.70	3.36	4.23*
5	5.77	3.40	2.63
6	4.10	2.63	3.16
	CUMULATIVE DUCTILITY, $\Sigma\mu_{rc2}$		
1	46.46	17.46	16.54
2	49.05	33.06*	15.16
3	40.73	23.04	20.28
4	41.80	21.89	22.63*
5	59.05*	29.78	19.46
6	28.27	17.57	17.29
	CUMULATIVE ROT. ENERGY, ΣA_{r2}		
1	36.10	8.40	9.32
2	44.58*	25.34*	6.92
3	35.82	14.72	12.48
4	36.62	24.20	16.20*
5	41.00	18.22	11.34
6	20.02	10.20	12.08

MAXIMUM RESPONSE VALUES

E.Q. INPUT NO.	FUNDAMENTAL PERIOD, T_1, (SEC)		
	1.4	2.0	2.4
	MAX. TOP DISPL. (IN)		
1	11.4	15.1	15.5
2	10.9	14.8	14.8
3	10.8	12.3	16.6
4	11.5*	15.5*	24.3*
5	9.4	13.2	20.2
6	7.5	15.2	20.7
	MAX. INTERSTORY DISPL. (IN)		
1	0.48	0.66	0.76
2	0.45	0.68*	0.73
3	0.45	0.57	0.79
4	0.46*	0.68*	1.05*
5	0.40	0.62	0.92
6	0.32	0.65	0.58
	MAX. BASE SHEAR (KIPS)		
1	1588	2031	2042
2	1977	1815	1601
3	1658	2078	2179*
4	1334	1513	1689
5	2158*	2302*	1767
6	1802	1748	1729
	MAX. BASE MOMENT (IN-KIPS)		
1	1,950,000	1,690,000	1,700,000
2	1,965,000	1,864,000*	1,639,000
3	1,953,000	1,778,000	1,649,000
4	1,970,000*	1,820,000	1,830,000*
5	1,931,000	1,810,000	1,734,000
6	1,763,000	1,732,000	1,735,000
	ROTATIONAL DUCTILITY, μ_{ro} **		
1	5.8	2.5	2.6
2	6.0	4.7*	1.8
3	5.8	3.6	1.9
4	6.0*	4.1	4.9*
5	5.5	4.0	3.0
6	3.5	3.0	3.0

*Critical (maximum) value for particular T_1
E - no yielding, i.e., linearly elastic response

** μ_{ro} Based on Eq. (1)

Table A9

RESPONSE VALUES CORRESPONDING TO DIFFERENT EARTHQUAKE INPUT MOTIONS

[SI = 15(SI$_{ref.}$), Duration = 10 sec.]

30-Story Isolated Structural Walls

M_y = 2,000,000 IN-K

EARTHQUAKE INPUT NUMBER	EARTHQUAKE INPUT	FUNDAMENTAL PERIOD, T_1 (SEC.)								
		1.4			2.0			2.4		
		M_y x 10^6 in-kips	θ_y^a x 10^{-3} rad.	θ_y^e x 10^{-3} rad.	M_y x 10^6 in-kips	θ_y^a x 10^{-3} rad.	θ_y^e x 10^{-3} rad.	M_y x 10^6 in-kips	θ_y^a x 10^{-3} rad.	θ_y^e x 10^{-3} rad.
1	1971 Pacoima Dam, S16E	2.11	.29	.54	2.11	.64	1.09	2.11	.86	1.40
2	1971 Holiday Orion, E-W	2.11	.30	.60	2.11	.62	1.02	2.11	E	E
3	1952 Taft, S69E	2.11	.30	.51	2.11	.68	1.06	2.11	E	E
4	1940 El Centro, E-W	2.11	.30	.52	2.11	.64	1.07	2.11	.91	1.56
5	Artificial Acc. (SI)	2.11	.29	.49	2.11	.62	1.04	2.11	.88	1.46
6	1940 El Centro, N-S	2.11	.32	.53	2.11	.63	1.05	2.11	.89	1.47
	AVERAGE		.30	.52		.64	1.06		.88	1.46

^{a}at 1st floor level
^{e}at 2nd floor level

DUCTILITY DEMAND BASED ON NODAL ROTATIONS AT 1st FLOOR LEVEL

E.Q. INPUT NO.	FUNDAMENTAL PERIOD, T_1, (SEC)		
	1.4	2.0	2.4
	ROTATIONAL DUCTILITY, μ_{r1}		
1	5.34	1.81	1.27
2	4.70*	3.85*	E
3	3.84	2.30	E
4	3.90	2.60	3.26*
5	4.13	2.48	1.67
6	2.31	1.73	2.24
	CYCLIC ROT. DUCTILITY μ_{rc1}		
1	7.66*	1.81	1.18
2	7.20	5.36*	E
3	5.65	2.30	E
4	5.80	3.10	3.26*
5	4.87	2.50	2.01
6	2.42	1.97	2.36
	CUMULATIVE DUCTILITY, $\Sigma\mu_{rc1}$		
1	43.17	13.41	16.27
2	42.70	30.93*	E
3	34.80	20.35	E
4	34.50	18.80	20.71*
5	50.83*	23.22	18.85
6	24.75	15.34	16.28
	CUMULATIVE ROT. ENERGY, ΣA_{r1}		
1	32.76	5.82	9.56
2	36.52*	24.20*	E
3	30.10	14.42	E
4	27.64	14.60	14.54*
5	32.24	11.74	10.98
6	19.32	9.00	11.32

DUCTILITY DEMAND BASED ON NODAL ROTATIONS AT 2nd FLOOR LEVEL

E.Q. INPUT NO.	FUNDAMENTAL PERIOD, T_1, (SEC)		
	1.4	2.0	2.4
	ROTATIONAL DUCTILITY, μ_{r2}		
1	4.48*	1.52	1.15
2	3.44	2.76*	E
3	2.86	1.80	E
4	3.04	2.22	2.42*
5	3.21	1.91	1.43
6	1.80	1.47	1.82
	CYCLIC ROT. DUCTILITY μ_{rc2}		
1	6.05*	1.53	1.06
2	5.35	3.71*	E
3	4.13	1.80	E
4	4.12	2.53	2.42*
5	3.79	1.94	1.63
6	1.91	1.60	1.94
	CUMULATIVE DUCTILITY, $\Sigma\mu_{rc2}$		
1	33.94	11.84	15.36
2	34.65	25.37*	E
3	26.87	17.64	E
4	26.56	15.76	16.49
5	38.71*	19.74	16.51*
6	21.73	13.92	14.36
	CUMULATIVE ROT. ENERGY, ΣA_{r2}		
1	23.10	4.62	8.84
2	28.74*	17.84*	E
3	20.98	11.96	E
4	19.78	10.70	10.30*
5	23.26	9.14	8.72
6	16.12	7.54	9.44

*Critical (maximum) value for particular T_1
E - no yielding, i.e., linearly elastic response

MAXIMUM RESPONSE VALUES

E.Q. INPUT NO.	FUNDAMENTAL PERIOD, T_1, (SEC)		
	1.4	2.0	2.4
	MAX. TOP DISPL. (IN)		
1	13.1*	16.7	15.5
2	10.9	17.9	15.3(E)
3	9.5	13.2	16.7(E)
4	9.6	19.1*	22.6
5	9.5	13.5	18.8
6	8.0	14.9	25.2*
	MAX. INTERSTORY DISPL. (IN)		
1	0.55*	0.77	0.76
2	0.45	0.82*	0.82(E)
3	0.43	0.69	0.85(E)
4	0.41	0.82*	1.01
5	0.44	0.66	0.94
6	0.34	0.68	1.18*
	MAX. BASE SHEAR (KIPS)		
1	1681	2118	2380*
2	2298	2261	1744(E)
3	2013	2271*	2136(E)
4	1697	1680	1808
5	2340*	2192	2190
6	2108	1748	1945
	MAX. BASE MOMENT (IN-KIPS)		
1	2,450,000	2,200,000	2,140,000
2	2,513,000*	2,432,000*	1,984,000(E)
3	2,415,000	2,266,000	2,048,000(E)
4	2,420,000	2,290,000	2,350,000*
5	2,445,000	2,279,000	2,180,000
6	2,252,000	2,194,000	2,247,000
	ROTATIONAL DUCTILITY, μ_{ro} **		
1	4.3	2.0	1.4
2	4.9*	4.2*	0.9(E)
3	4.0	2.6	1.0(E)
4	4.1	2.8	3.4*
5	4.3	2.7	1.8
6	2.4	1.9	2.4

** μ_{ro} Based on Eq. (1)

Table A10

RESPONSE VALUES CORRESPONDING TO DIFFERENT EARTHQUAKE INPUT MOTIONS
[SI = 15(SI$_{ref.}$), Duration = 10 sec]

40-Story Isolated Structural Walls
M_y = 1,500,000 IN-K

EARTHQUAKE INPUT NUMBER	EARTHQUAKE INPUT	FUNDAMENTAL PERIOD, T_1 (SEC.) 1.4 M_y x 10^6 in-kips	1.4 θ_y' x 10^{-3} rad.	1.4 θ_y'' x 10^{-3} rad.	2.0 M_y x 10^6 in-kips	2.0 θ_y' x 10^{-3} rad.	2.0 θ_y'' x 10^{-3} rad.	2.4 M_y x 10^6 in-kips	2.4 θ_y' x 10^{-3} rad.	2.4 θ_y'' x 10^{-3} rad.	3.0 M_y x 10^6 in-kips	3.0 θ_y' x 10^{-3} rad.	3.0 θ_y'' x 10^{-3} rad.
1	1971 Pacoima Dam, S16E	1.575	.12	.20	1.575	.25	.41	1.575	.40	.68	1.575	.58	.99
2	1971 Holliday Orion, E-W	1.575	.10	.16	1.575	.24	.38	1.575	.38	.64	1.575	.58	1.02
3	1952 Taft, S69E	1.575	.12	.21	1.575	.38	.67	1.575	.38	.67	1.575	.57	.97
4	1940 El Centro, E-W	1.575	.12	.21	1.575	.27	.44	1.575	.35	.60	1.575	.60	.99
5	Artificial Acc. (SE)	1.575	.12	.18	1.575	.25	.44	1.575	.35	.60	1.575	.57	.97
6	1940 El Centro, N-S	1.575	.12	.22	1.575	.25	.42	1.575	.36	.61	1.575	.56	.95
	AVERAGE		.12	.19		.25	.41		.37	.63		.58	.98

θ_y' at 2nd floor level
θ_y'' at 4th floor level

DUCTILITY DEMAND BASED ON NODAL ROTATIONS AT 2nd FLOOR LEVEL

E.Q. INPUT NO.	FUNDAMENTAL PERIOD, T_1, (SEC) 1.4	2.0	2.4	3.0
	ROTATIONAL DUCTILITY, $\mu_{r\theta}$			
1	9.00	5.10	4.10	2.10
2	7.50	5.38	3.19	1.80
3	6.72	5.37	3.10	3.14
4	11.88*	7.95*	6.18*	5.49*
5	9.00	5.70	5.06	5.29
6	6.05	4.70	5.14	4.88
	CYCLIC ROT. DUCTILITY $\mu_{rc\theta}$			
1	9.20	4.80	2.81	1.50
2	11.20	7.87	3.71	1.80
3	7.73	5.37	2.90	2.38
4	16.00*	11.31*	10.36*	8.28*
5	10.75	6.20	7.27	6.57
6	8.95	6.70	6.89	4.88
	CUMULATIVE DUCTILITY, $\Sigma\mu_{rc\theta}$			
1	63.40	36.90	28.30	15.00
2	76.80	52.03	31.52	17.30
3	69.18	44.35	32.00	21.19
4	67.25	45.47	41.71	27.81
5	95.42*	57.70*	43.79*	30.48*
6	59.53	38.80	30.94	24.16
	CUMULATIVE ROT. ENERGY, $\Sigma A_{r\theta}$			
1	54.18	26.86	20.96	7.80
2	87.58*	50.82*	24.52	9.80
3	67.16	35.72	25.08	15.06
4	75.18	44.30	39.52*	27.72*
5	85.42	50.26	36.36	24.56
6	58.06	36.24	28.02	19.84

DUCTILITY DEMAND BASED ON NODAL ROTATIONS AT 4th FLOOR LEVEL

E.Q. INPUT NO.	FUNDAMENTAL PERIOD, T_1, (SEC) 1.4	2.0	2.4	3.0
	ROTATIONAL DUCTILITY, μ_{r2}			
1	9.14	4.59	3.30	1.72
2	7.77	4.19	2.35	1.56
3	7.04	5.02	2.73	2.50
4	12.41*	7.70*	5.70*	3.76
5	8.89	4.82	3.85	4.16*
6	5.68	3.77	3.78	3.39
	CYCLIC ROT. DUCTILITY μ_{rc2}			
1	9.35	4.59	2.64	1.41
2	10.55	5.95	3.26	1.56
3	7.04	5.02	2.63	1.82
4	15.71*	10.23*	8.27*	6.11*
5	9.37	6.10	5.17	4.95
6	8.16	5.10	4.95	3.39
	CUMULATIVE DUCTILITY, $\Sigma\mu_{rc2}$			
1	60.27	32.23	23.76	13.74
2	71.26	42.13	24.68	15.50
3	63.42	39.80	26.67	17.76
4	65.08	39.82	32.76*	20.77
5	85.89*	46.01*	32.62	23.96*
6	49.40	29.89	24.25	18.34
	CUMULATIVE ROT. ENERGY, ΣA_{r2}			
1	52.36	23.48	16.72	6.86
2	76.82	38.54	17.14	8.32
3	63.22	32.00	19.98	11.84
4	73.96	39.58	30.52*	19.30*
5	79.38*	40.18*	25.40	18.22
6	39.68	26.66	20.18	13.82

*Critical (maximum) value for particular T_1
E - no yielding, i.e., linearly elastic response

MAXIMUM RESPONSE VALUES

E.Q. INPUT NO.	FUNDAMENTAL PERIOD, T_1, (SEC) 1.4	2.0	2.4	3.0
	MAX. TOP DISPL. (IN)			
1	12.6	14.0	15.7	17.8
2	11.2	10.5	12.3	14.1
3	9.8	13.2	13.7	18.0
4	17.3*	23.5*	25.1*	26.2*
5	13.9	16.5	20.0	22.2
6	10.1	11.6	15.9	20.1
	MAX. INTERSTORY DISPL. (IN)			
1	0.38	0.44	0.59	0.66
2	0.34	0.40	0.42	0.47
3	0.38	0.44	0.48	0.69
4	0.51*	0.70*	0.77*	0.87*
5	0.43	0.54	0.59	0.76
6	0.30	0.41	0.58	0.75
	MAX. BASE SHEAR (KIPS)			
1	1,702	2,015*	1,756	1,607
2	2,252	1,985	1,558	1,609
3	1,692	1,961	2,205*	1,524
4	1,409	1,905	1,936	1,893
5	2,326*	1,981	1,659	1,661
6	1,896	1,774	2,044	2,268*
	MAX. BASE MOMENT (IN-KIPS)			
1	2,240,000	1,950,000	1,830,000	1,670,000
2	2,116,000	1,978,000	1,754,000	1,639,000
3	2,046,000	1,968,000	1,756,000	1,743,000
4	2,478,000*	2,194,000*	1,989,000*	1,942,000*
5	2,240,000	2,000,000	1,900,000	1,920,000
6	1,984,000	1,918,000	1,916,000	1,888,000
	ROTATIONAL DUCTILITY, $\mu_{r\theta}$ **			
1	9.4	5.8	4.2	2.2
2	7.9	6.1	3.3	1.8
3	7.0	6.0	3.3	3.1
4	12.5*	8.9*	6.3*	5.7*
5	9.4	6.4	5.1	5.4
6	6.2	5.4	5.3	5.0

** $\mu_{r\theta}$ Based on Eq. (1)

Table AII

RESPONSE VALUES CORRESPONDING TO DIFFERENT EARTHQUAKE INPUT MOTIONS
[SI = 1.5(SI$_{ref.}$), Duration = 10 sec.]

40-Story Isolated Structural Walls
M_y = 2,000,000 IN-K

EARTHQUAKE INPUT NUMBER	EARTHQUAKE INPUT	FUNDAMENTAL PERIOD, T_1 (SEC.) 1.4			2.0			2.4			3.0		
		M_y x 10^6 in-kips	θ_y^a x 10^{-3} rad.	θ_y^e x 10^{-3} rad.	M_y x 10^6 in-kips	θ_y^a x 10^{-3} rad.	θ_y^e x 10^{-3} rad.	M_y x 10^6 in-kips	θ_y^a x 10^{-3} rad.	θ_y^e x 10^{-3} rad.	M_y x 10^6 in-kips	θ_y^a x 10^{-3} rad.	θ_y^e x 10^{-3} rad.
1	1971 Pacoima Dam, S16E	2.11	.16	.27	2.11	.30	.53	2.11	.48	.82	2.11	.80	1.30
2	1978 Holiday Orion, E-W	2.11	.17	.28	2.11	.29	.47	2.11	.47	.81	2.11	E	E
3	1952 Taft, S69E	2.11	.17	.29	2.11	.33	.57	2.11	.50	.89	2.11	.76	1.30
4	1940 El Centro, E-W	2.11	.16	.26	2.11	.31	.51	2.11	.50	.86	2.11	.75	1.29
5	Artificial Acc. (S1)	2.11	.18	.31	2.11	.32	.56	2.11	.48	.81	2.11	.75	1.29
6	1940 El Centro, N-S	2.11	.16	.27	2.11	.30	.51	2.11	.52	.92	2.11	.75	1.20
	AVERAGE		.17	.28		.31	.53		.49	.85		.76	1.28

θ_y^a at 2nd floor level
θ_y^e at 4th floor level

DUCTILITY DEMAND BASED ON NODAL ROTATIONS AT 2nd FLOOR LEVEL

E.Q. INPUT NO.	FUNDAMENTAL PERIOD, T_1, (SEC) 1.4	2.0	2.4	3.0
	ROTATIONAL DUCTILITY, μ_{r2}			
1	6.58	3.52	3.14	1.84
2	5.93	5.19	2.36	E
3	5.40	3.76	3.06	2.66
4	7.21*	5.60*	5.51*	3.73
5	6.04	4.29	3.43	4.28*
6	4.93	3.40	3.58	3.86
	CYCLIC ROT. DUCTILITY μ_{rc2}			
1	8.74*	4.40	2.84	1.84
2	8.34*	7.84*	3.01	E
3	6.90	4.70	2.86	2.50
4	8.69	6.80	7.34*	6.10*
5	7.21	7.04	5.19	4.28
6	6.05	4.22	4.82	3.76
	CUMULATIVE DUCTILITY, $\Sigma\mu_{r2}$			
1	51.42	29.15	23.32	15.18
2	61.15	52.63*	24.50	E
3	52.60	40.61	28.66	15.60
4	54.06	37.70	33.35*	22.81
5	75.42*	52.14	32.54	23.21*
6	44.58	26.68	27.66	17.92
	CUMULATIVE ROT. ENERGY, ΣA_{r2}			
1	41.42	19.36	16.26	10.68
2	60.90*	48.12*	16.36	E
3	48.60	32.76	21.01	9.40
4	48.82	33.00	28.64*	20.30*
5	58.86	42.64	24.90	16.70
6	43.06	22.26	23.96	12.88

DUCTILITY DEMAND BASED ON NODAL ROTATIONS AT 4th FLOOR LEVEL

E.Q. INPUT NO.	FUNDAMENTAL PERIOD, T_1, (SEC) 1.4	2.0	2.4	3.0
	ROTATIONAL DUCTILITY, μ_{r2}			
1	6.14	3.13	2.30	1.47
2	5.72	3.48	1.79	E
3	5.08	3.36	2.31	2.04
4	7.07*	4.90*	4.75*	2.89
5	5.55	3.05	2.66	3.03*
6	4.65	3.39	2.61	2.82
	CYCLIC ROT. DUCTILITY μ_{rc2}			
1	8.16*	3.78	1.92	1.47
2	8.01	5.45	2.26	E
3	6.17	3.74	2.10	1.94
4	8.00	5.60*	5.76*	4.28*
5	6.33	4.91	3.61	3.03
6	5.10	3.82	3.31	2.73
	CUMULATIVE DUCTILITY, $\Sigma\mu_{rc2}$			
1	45.89	24.41	18.62	14.17
2	53.20	40.33*	19.99	E
3	45.25	33.12	23.42	13.26
4	50.03	30.70	26.16*	16.69
5	63.60*	39.35	23.66	16.97*
6	34.80	23.11	20.86	14.29
	CUMULATIVE ROT. ENERGY, ΣA_{r2}			
1	37.64	15.76	11.72	9.62
2	52.64*	34.78*	12.10	E
3	40.26	26.04	16.18	7.14
4	45.94	25.80	21.42*	14.04*
5	51.30	30.36	16.72	9.90
6	29.26	18.44	16.34	8.84

*Critical (maximum) value for particular T_1
E - no yielding, i.e., linearly elastic response

MAXIMUM RESPONSE VALUES

E.Q. INPUT NO.	FUNDAMENTAL PERIOD, T_1, (SEC) 1.4	2.0	2.4	3.0
	MAX. TOP DISPL. (IN)			
1	11.2	12.9	15.4	17.9
2	11.8	12.6	13.2	14.2(E)
3	9.4	12.2	14.5	17.8
4	14.9*	17.6*	25.4*	28.2*
5	10.6	12.8	18.8	23.2
6	10.3	14.6	14.8	21.6
	MAX. INTERSTORY DISPL. (IN)			
1	0.35	0.42	0.54	0.69
2	0.33	0.43	0.47	0.53(E)
3	0.29	0.41	0.53	0.72
4	0.43*	0.52*	0.80*	0.96*
5	0.32	0.44	0.64	0.83
6	0.31	0.46	0.56	0.79
	MAX. BASE SHEAR (KIPS)			
1	1,848	2,657	2,159	1,751
2	2,343	2,326	1,763	1,562(E)
3	1,922	2,336	2,688*	1,897
4	1,641	2,038	2,097	2,367
5	2,682*	2,771*	1,683	2,112
6	2,280	2,403	2,165	2,637*
	MAX. BASE MOMENT (IN-KIPS)			
1	2,770,000	2,380,000	2,340,000	2,200,000
2	2,686,000	2,575,000	2,249,000	1,992,000(E)
3	2,640,000	2,418,000	2,331,000	2,277,000
4	2,860,000*	2,616,000*	2,589,000*	2,388,000
5	2,711,000	2,480,000	2,374,000	2,451,000*
6	2,576,000	2,381,000	2,387,000	2,413,000
	ROTATIONAL DUCTILITY, μ_{ro} **			
1	7.3	3.6	3.2	1.8
2	6.5	5.4	2.4	0.9(E)
3	6.0	3.9	3.1	2.6
4	8.2*	5.8*	5.7*	3.7
5	6.7	4.5	3.5	4.3*
6	5.4	3.6	3.6	4.0

** μ_{ro} Based on Eq. (1)

Table A12

RESPONSE VALUES CORRESPONDING TO DIFFERENT EARTHQUAKE INPUT MOTIONS

[SI = 15(SI$_{ref.}$), Duration = 10 sec.]

40-Story Isolated Structural Walls

M_y = 3,000,000 IN-K

EARTHQUAKE INPUT NUMBER	EARTHQUAKE INPUT	FUNDAMENTAL PERIOD, T_1 (SEC.) 1.4			2.0			2.4			3.0		
		M_y x 10^6 in-kips	θ_y' x 10^{-3} rad.	θ_y^* x 10^{-3} rad.	M_y x 10^6 in-kips	θ_y' x 10^{-3} rad.	θ_y^* x 10^{-3} rad.	M_y x 10^6 in-kips	θ_y' x 10^{-3} rad.	θ_y^* x 10^{-3} rad.	M_y x 10^6 in-kips	θ_y' x 10^{-3} rad.	θ_y^* x 10^{-3} rad.
1	1971 Pacoima Dam, S16E	3.15	.23	.40	3.15	.45	.79	3.15	.73	1.28	3.15	E	E
2	1971 Holliday Orion, E-W	3.15	.23	.42	3.15	.48	.80	3.15	.75	1.30	3.15	E	E
3	1952 Taft, S69E	3.15	.23	.40	3.15	.47	.82	3.15	.74	1.29	3.15	1.10	1.85
4	1940 El Centro, E-W	3.15	.24	.42	3.15	.47	.81	3.15	.72	1.21	3.15	1.10	1.87
5	Artificial Acc. (SI)	3.15	.23	.40	3.15	.44	.75	3.15	.71	1.22	3.15	1.16	2.01
6	1940 El Centro, N-S	3.15	.24	.43	3.15	.45	.80	3.15	.75	1.20	3.15	1.18	2.04
	AVERAGE		.23	.41		.46	.80		.73	1.27		1.14	1.94

θ_y' at 2nd floor level
θ_y^* at 4th floor level

DUCTILITY DEMAND BASED ON NODAL ROTATIONS AT 2nd FLOOR LEVEL

E.Q. INPUT NO.	FUNDAMENTAL PERIOD, T_1, (SEC) 1.4	2.0	2.4	3.0
	ROTATIONAL DUCTILITY, μ_{r1}			
1	5.20*	2.65	1.39	E
2	8.30	3.54*	1.25	E
3	4.44	2.91	1.49	1.02
4	4.99	3.33	3.74*	2.38*
5	4.60	2.88	1.89	1.84
6	3.02	2.06	2.52	1.70
	CYCLIC ROT. DUCTILITY μ_{rc1}			
1	8.30*	3.14	1.18	E
2	7.84	5.62*	1.15	E
3	5.77	3.33	1.49	1.02
4	6.86	4.02	3.84*	2.81*
5	5.40	3.34	2.60	1.84
6	3.85	2.84	2.84	1.70
	CUMULATIVE DUCTILITY, $\Sigma\mu_{rc1}$			
1	45.00	18.82	16.91	E
2	46.80	33.49*	14.02	E
3	39.52	25.69	18.61	8.22
4	39.21	22.83	21.41*	13.28*
5	54.80*	27.37	20.65	13.16
6	26.10	21.76	16.59	13.04
	CUMULATIVE ROT. ENERGY, ΣA_{r1}			
1	34.20	10.98	10.58	E
2	46.74*	27.10*	6.88	E
3	34.32	16.18	11.28	2.26
4	36.72	19.60	16.16	9.60*
5	36.20	14.62	16.42*	7.54
6	17.10	16.66	12.30	7.42

DUCTILITY DEMAND BASED ON NODAL ROTATIONS AT 4th FLOOR LEVEL

E.Q. INPUT NO.	FUNDAMENTAL PERIOD, T_1, (SEC) 1.4	2.0	2.4	3.0
	ROTATIONAL DUCTILITY, μ_{r2}			
1	4.51*	2.48	1.13	E
2	3.60	2.93*	1.16	E
3	3.76	2.08	1.25	1.04
4	4.18	2.87	2.83*	1.87*
5	3.72	2.27	1.55	1.56
6	2.52	1.68	2.03	1.40
	CYCLIC ROT. DUCTILITY μ_{rc2}			
1	6.66*	2.77	1.03	E
2	5.70	4.04*	1.07	E
3	4.45	2.29	1.25	1.04
4	5.00	3.27	2.93*	2.18*
5	4.41	2.59	1.89	1.56
6	3.05	2.08	2.25	1.51
	CUMULATIVE DUCTILITY, $\Sigma\mu_{rc2}$			
1	35.77	16.04	15.97	E
2	37.32	26.87*	13.00	E
3	30.95	19.14	16.32	7.88
4	31.11	15.44	17.17*	10.71
5	41.94*	21.71	16.87	11.44
6	22.05	18.41	13.91	11.77
	CUMULATIVE ROT. ENERGY, ΣA_{r2}			
1	26.66	8.92	10.60	E
2	33.26*	20.20*	6.40	E
3	24.98	10.40	9.80	2.16
4	27.82	14.50	12.12	6.66*
5	27.44	10.46	12.54*	6.04
6	13.02	12.88	9.42	6.26

*Critical (maximum) value for particular T_1
E - no yielding, i.e., linearly elastic response

MAXIMUM RESPONSE VALUES

E.Q. INPUT NO.	FUNDAMENTAL PERIOD, T_1, (SEC) 1.4	2.0	2.4	3.0
	MAX. TOP DISPL. (IN)			
1	11.9*	16.4	15.6	17.9(E)
2	10.2	17.0*	15.4	14.2(E)
3	9.9	12.0	16.8	20.1
4	10.9	16.7	23.7*	34.3*
5	9.4	12.1	18.6	23.4
6	7.9	12.0	23.7*	22.4
	MAX. INTERSTORY DISPL. (IN)			
1	0.37*	0.52	0.57	0.69(E)
2	0.32	0.54*	0.59	0.53(E)
3	0.31	0.45	0.64	0.78
4	0.33	0.51	0.76	1.18*
5	0.33	0.46	0.66	0.84
6	0.25	0.39	0.80*	0.85
	MAX. BASE SHEAR (KIPS)			
1	2,135	2,796	2,926	2,088(E)
2	2,945*	2,884	2,168	1,562(E)
3	2,336	2,898*	3,077*	2,371
4	1,942	2,081	2,363	2,625
5	2,840	2,606	2,561	2,600
6	2,508	2,552	2,311	3,058*
	MAX. BASE MOMENT (IN-KIPS)			
1	3,816,000*	3,423,000	3,232,000	2,780,000(E)
2	3,804,000	3,584,000*	3,189,000	1,992,000(E)
3	3,683,000	3,478,000	3,228,000	3,155,000
4	3,804,000	3,523,000	3,595,000*	3,356,000*
5	3,720,000	3,466,000	3,294,000	3,294,000
6	3,467,000	3,332,000	3,399,000	3,264,000
	ROTATIONAL DUCTILITY, μ_{ro} **			
1	4.2*	2.7	1.5	0.9(E)
2	5.2	3.8*	1.2	0.6(E)
3	4.4	3.1	1.5	1.0
4	5.2	3.4	3.8*	2.3*
5	4.6	3.0	1.9	1.9
6	3.0	2.2	2.6	1.7

** μ_{ro} Based on Eq. (1)

EARTHQUAKE INPUT MOTIONS
[SI = 1.5($SI_{ref.}$), Duration = 10 sec.]
M_y = Very Large (Elastic)

10-Story Isolated Structural Wall

E.Q. Input No.	Fundamental Period, T_1 (sec.)		
	0.5	0.8	1.4
	MAX. TOP DISPLACEMENT (IN.)		
1	3.5	5.3	15.4*
2	2.9	5.3	12.6
3	4.0	8.2*	11.0
4	4.4	4.8	11.0
5	4.3	6.1	11.8
6	4.6*	7.7	7.6
	MAX. INTERSTORY DISPLACEMENT (IN.)		
1	0.45	0.70	2.70*
2	0.37	0.71	1.68
3	0.51	1.09*	1.38
4	0.56	0.65	1.52
5	0.56	0.84	1.78
6	0.59*	1.03	1.02
	MAX. BASE SHEAR (KIPS)		
1	1,766	1,092	1,061
2	1,196	1,026	827
3	1,644	1,372	1,027
4	1,843	855	805
5	2,346*	1,473*	1,359*
6	2,206	1,473	571
	MAX. BASE MOMENT (IN-KIPS)		
1	1,210,000	704,000	720,000*
2	960,000	720,000	518,000
3	1,301,000	1,051,000*	531,000
4	1,447,000	641,000	466,000
5	1,460,000	893,000	569,000
6	1,537,000*	997,000	330,000

20-Story Isolated Structural Wall

E.Q. Input No.	Fundamental Period, T_1 (sec.)			
	0.8	2.4	2.0	2.4
	MAX. TOP DISPLACEMENT (IN.)			
1	5.6	15.7*	17.2	15.4
2	5.5	13.4	21.6	15.2
3	8.8*	11.5	16.0	14.9
4	5.2	11.0	23.3*	24.5
5	6.0	12.5	13.7	20.7
6	7.9	8.0	16.0	24.9*
	MAX. INTERSTORY DISPLACEMENT (IN.)			
1	0.38	1.03*	1.21	1.13
2	0.37	0.92	1.82*	1.22
3	0.61*	0.82	1.17	1.21
4	0.35	0.76	1.57	1.76*
5	0.41	0.91	1.04	1.57
6	0.54	0.54	1.06	-
	MAX. BASE SHEAR (KIPS)			
1	2,380	2,090	1,490	1,580*
2	1,900	1,750	2,400*	1,180
3	2,734	1,857	1,800	1,437
4	1,700	1,420	1,240	1,300
5	2,910*	2,400*	1,660	1,560
6	2,780	1,423	1,200	1,234
	MAX. BASE MOMENT (IN-KIPS)			
1	2,764,000	2,582,000*	1,144,000	1,018,000
2	2,490,000	1,905,000	2,091,000*	907,000
3	4,025,000*	1,799,000	1,407,000	916,000
4	2,419,000	1,667,000	1,782,000	1,519,000*
5	3,023,000	2,192,000	1,387,000	1,218,000
6	3,635,000	1,191,000	1,225,000	1,028,000

30-Story Isolated Structural Wall

E.Q. Input No.	Fundamental Period, T_1 (sec.)		
	1.4	2.0	2.4
	MAX. TOP DISPLACEMENT (IN.)		
1	15.9*	16.9	15.5
2	13.6	22.0*	15.3
3	11.7	15.1	16.7
4	8.5	17.2	18.4
5	12.5	13.8	21.0
6	8.1	15.5	25.3*
	MAX. INTERSTORY DISPLACEMENT (IN.)		
1	0.71*	0.80	0.76
2	0.62	1.12*	0.82
3	0.56	0.76	0.85
4	0.55	1.10	1.20
5	.62	0.71	1.06
6	0.37	0.70	1.24*
	MAX. BASE SHEAR (KIPS)		
1	3,006	2,122	2,593*
2	2,662	3,689*	1,744
3	2,887	2,491	2,136
4	2,014	1,868	1,955
5	3,647*	2,478	2,302
6	2,108	1,747	1,945
	MAX. BASE MOMENT (IN-KIPS)		
1	5,540,000*	2,410,000	2,320,000
2	4,211,000	4,642,000*	1,984,000
3	4,041,000	2,978,000	2,046,000
4	3,790,000	3,920,000	3,350,000*
5	4,889,000	3,030,000	3,710,000
6	2,599,000	2,568,000	2,743,000

40-Story Isolated Structural Wall

E.Q. Input No.	Fundamental Period, T_1 (sec.)			
	1.8	2.0	2.4	3.0
	MAX. TOP DISPLACEMENT (IN.)			
1	15.8*	17.7	15.5	17.9
2	12.9	22.5*	15.4	14.2
3	11.2	17.6	24.8*	37.0*
4	11.3	17.5	24.3	37.0
5	12.0	13.4	21.0	30.2
6	8.0	11.9	25.3	22.9
	MAX. INTERSTORY DISPLACEMENT (IN.)			
1	0.50*	0.62	.57	.69
2	0.44	.86*	.62	.53
3	.39	.54	.66	0.78
4	0.39	.59	.90	1.35*
5	0.44	.51	.80	1.12
6	0.27	.47	.92*	0.92
	MAX. BASE SHEAR (KIPS)			
1	4,120	3,421	3,244*	2,088
2	3,270	5,058*	2,304	1,562
3	3,464	4,109	3,020	2,271
4	2,702	2,720	2,545	2,843
5	4,333*	3,544	3,149	2,979
6	2,738	2,552	2,408	3,058*
	MAX. BASE MOMENT (IN-KIPS)			
1	10,360,000*	5,460,000	3,860,000	2,780,000
2	7,511,000	9,308,000*	3,514,000	1,992,000
3	7,225,000	6,804,000	3,649,000	3,252,000
4	6,430,000	6,166,000	5,847,000*	4,730,000*
5	8,210,000	5,950,000	4,630,000	4,120,000
6	4,716,000	4,671,000	4,681,000	4,061,000

*Critical (maximum) value for particular T_1

Table A14

Effect of Duration of Input Motion on Maximum Response Values and Cumulative Measures of Deformation

20-Story Isolated Structural Walls - SI = 1.5 ($SI_{ref.}$)

Earthquake Input	Fundamental Period, T_1 sec.	Yield Level, M_y (in-kips)	Maximum or Cumulative Values Corresponding to: 10-sec. Duration (R_{10})	20-sec. Duration (R_{20})	Ratio $\frac{R_{20}}{R_{10}}$
Top Displacement (in.)					
El Centro, E-W	0.8	500,000	8.3	-	-
Holiday Orion, E-W	1.4	500,000	11.0	12.0	1.09
El Centro, E-W	2.0	500,000	20.5	29.3	1.43
El Centro, E-W	2.4	500,000	25.1	29.4	1.17
Pacoima Dam, S16E	0.8	1,000,000	8.8	11.1	1.26
Pacoima Dam, S16E	1.4	1,000,000	13.6	16.0	1.18
Holiday Orion, E-W	2.0	1,000,000	18.6	18.6	1.00
El Centro, E-W	2.4	1,000,000	22.4	26.2	1.17
El Centro, N-S	0.8	1,500,000	5.7	6.7	1.17
Pacoima Dam, S16E	1.4	1,500,000	15.3	18.7	1.22
Holiday Orion, E-W	2.0	1,500,000	20.1	20.7	1.03
El Centro, E-W	2.4	1,500,000	24.5	25.4	1.04
Interstory Displacement (in.)					
El Centro, E-W	0.8	500,000	0.47	-	-
Holiday Orion, E-W	1.4	500,000	0.66	0.79	1.20
El Centro, E-W	2.0	500,000	1.23	1.73	1.41
El Centro, E-W	2.4	500,000	1.56	1.77	1.13
Pacoima Dam, S16E	0.8	1,000,000	0.48	0.63	1.31
Pacoima Dam, S16E	1.4	1,000,000	0.82	0.97	1.18
Holiday Orion, E-W	2.0	1,000,000	1.27	1.27	1.00
El Centro, E-W	2.4	1,000,000	1.50	1.72	1.15
El Centro, N-S	0.8	1,500,000	0.34	0.39	1.17
Pacoima Dam, S16E	1.4	1,500,000	0.96	1.14	1.19
Holiday Orion, E-W	2.0	1,500,000	1.57	1.57	1.00
El Centro, E-W	2.4	1,500,000	1.75	1.85	1.05
Horizontal Shear at Base (kips)					
El Centro, E-W	0.8	500,000	1,240	-	-
Holiday Orion, E-W	1.4	500,000	1,148	1,148	1.00
El Centro, E-W	2.0	500,000	1,044	1,044	1.00
El Centro, E-W	2.4	500,000	1,052	1,227	1.17
Pacoima Dam, S16E	0.8	1,000,000	1,515	1,521	1.00
Pacoima Dam, S16E	1.4	1,000,000	1,146	1,183	1.03
Holiday Orion, E-W	2.0	1,000,000	1,547	1,547	1.00
El Centro, E-W	2.4	1,000,000	1,232	1,542	1.25
El Centro, N-S	0.8	1,500,000	-	1,794	-
Pacoima Dam, S16E	1.4	1,500,000	1,613	1,163	1.00
Holiday Orion, E-W	2.0	1,500,000	2,114	2,114	1.00
El Centro, E-W	2.4	1,500,000	1,297	1,468	1.13

Table A14 (contd)

Effect of Duration of Input Motion on Maximum Response Values and Cumulative Measures of Deformation

20-Story Isolated Structural Walls - SI = 1.5 ($SI_{ref.}$)

Earthquake Input	Fundamental Period, T_1 sec.	Yield Level, M_y (in-kips)	Maximum or Cumulative Values Corresponding to: 10-sec. Duration (R_{10})	20-sec. Duration (R_{20})	Ratio $\frac{R_{20}}{R_{10}}$
Bending Moment at Base (in.kips)					
El Centro, E-W	0.8	500,000	813,000	-	-
Holiday Orion, E-W	1.4	500,000	658,000	704,000	1.07
El Centro, E-W	2.0	500,000	661,000	725,000	1.10
El Centro, E-W	2.4	500,000	648,000	648,000	1.00
Pacoima Dam, S16E	0.8	1,000,000	1,375,000	1,486,000	1.08
Pacoima Dam, S16E	1.4	1,000,000	1,231,000	1,240,000	1.01
Holiday Orion, E-W	2.0	1,000,000	1,147,000	1,147,000	1.00
El Centro, E-W	2.4	1,000,000	1,106,000	1,143,000	1.03
El Centro, N-S	0.8	1,500,000	1,780,000	1,850,000	1.04
Pacoima Dam, S16E	1.4	1,500,000	1,772,000	1,797,000	1.01
Holiday Orion, E-W	2.0	1,500,000	1,547,000	1,561,000	1.01
El Centro, E-W	2.4	1,500,000	1,519,000	1,522,000	1.00
Rotational Ductility Ratio at Base, μ_r (Based on Equation 1)					
El Centro, E-W	0.8	500,000	13.60	-	-
Holiday Orion, E-W	1.4	500,000	6.07	7.82	1.29
El Centro, E-W	2.0	500,000	6.18	8.62	1.39
El Centro, E-W	2.4	500,000	5.69	5.69	1.00
Pacoima Dam, S16E	0.8	1,000,000	7.25	9.30	1.28
Pacoima Dam, S16E	1.4	1,000,000	4.56	4.62	1.01
Holiday Orion, E-W	2.0	1,000,000	2.85	2.85	1.00
El Centro, E-W	2.4	1,000,000	2.07	2.77	1.34
El Centro, N-S	0.8	1,500,000	3.60	4.49	1.25
Pacoima Dam, S16E	1.4	1,500,000	3.50	3.82	1.09
Holiday Orion, E-W	2.0	1,500,000	1.90	2.09	1.10
El Centro, E-W	2.4	1,500,000	0.96	0.97	1.01
Rotational Ductility Ratio at Base, μ_r (Based on Nodal Rotation at 1st Floor Level)					
El Centro, E-W	0.8	500,000	9.6	-	-
Holiday Orion, E-W	1.4	500,000	6.7	8.4	1.27
El Centro, E-W	2.0	500,000	6.4	9.0	1.41
El Centro, E-W	2.4	500,000	5.1	5.1	1.00
Pacoima Dam, S16E	0.8	1,000,000	6.8	8.8	1.29
Pacoima Dam, S16E	1.4	1,000,000	4.5	4.6	1.02
Holiday Orion, E-W	2.0	1,000,000	2.7	2.7	1.00
El Centro, E-W	2.4	1,000,000	2.1	2.8	1.33
El Centro, N-S	0.8	1,500,000	3.7	4.5	1.22
Pacoima Dam, S16E	1.4	1,500,000	3.4	3.7	1.10
Holiday Orion, E-W	2.0	1,500,000	1.8	2.0	1.10
El Centro, E-W	2.4	1,500,000	elastic	elastic	-

Table A14 (contd)

Effect of Duration of Input Motion on Maximum Response Values and Cumulative Measures of Deformation

20-Story Isolated Structural Walls - SI = 1.5 ($SI_{ref.}$)

Earthquake Input	Fundamental Period, T_1 sec.	Yield Level, M_y (in-kips)	Maximum or Cumulative Values Corresponding to: 10-sec. Duration (R_{10})	20-sec. Duration (R_{20})	Ratio $\frac{R_{20}}{R_{10}}$
Rotational Ductility Ratio (at Base), μ_θ					
(Based on Nodal Rotation at 2nd Floor Level)					
El Centro, E-W	0.8	500,000	9.6	-	-
Holiday Orion, E-W	1.4	500,000	6.1	6.6	1.08
El Centro, E-W	2.0	500,000	5.4	7.8	1.43
El Centro, E-W	2.4	500,000	4.6	4.7	1.03
Pacoima Dam, S16E	0.8	1,000,000	6.3	8.1	1.30
Pacoima Dam, S16E	1.4	1,000,000	3.5	3.9	1.11
Holiday Orion, E-W	2.0	1,000,000	2.1	2.1	1.00
El Centro, E-W	2.4	1,000,000	1.7	2.1	1.25
El Centro, N-S	0.8	1,500,000	3.0	3.7	1.26
Pacoima Dam, S16E	1.4	1,500,000	2.5	3.2	1.24
Holiday Orion, E-W	2.0	1,500,000	1.4	1.6	1.09
El Centro, E-W	2.4	1,500,000	elastic	elastic	-
Cyclic Rotational Ductility Ratio (at Base), μ_θ					
(Based on Nodal Rotation at 2nd Floor Level)					
El Centro, E-W	0.8	500,000	12.6	-	-
Holiday Orion, E-W	1.4	500,000	8.9	9.4	1.05
El Centro, E-W	2.0	500,000	6.4	8.7	1.37
El Centro, E-W	2.4	500,000	5.7	6.1	1.07
Pacoima Dam, S16E	0.8	1,000,000	8.9	10.7	1.20
Pacoima Dam, S16E	1.4	1,000,000	4.4	4.6	1.04
Holiday Orion, E-W	2.0	1,000,000	2.5	2.5	1.00
El Centro, E-W	2.4	1,000,000	1.7	2.1	1.28
El Centro, N-S	0.8	1,500,000	4.1	4.5	1.09
Pacoima Dam, S16E	1.4	1,500,000	2.6	2.9	1.12
Holiday Orion, E-W	2.0	1,500,000	1.4	1.5	1.03
El Centro, E-W	2.4	1,500,000	elastic	elastic	-
Cumulative Cyclic Rotational Ductility Ratio (at Base), $\Sigma\mu_\theta$					
(Based on Nodal Rotation at 2nd Floor Level)					
El Centro, E-W	0.8	500,000	86.0	-	-
Holiday Orion, E-W	1.4	500,000	57.7	144.6	2.51
El Centro, E-W	2.0	500,000	30.2	69.1	2.29
El Centro, E-W	2.4	500,000	26.0	55.9	2.15
Pacoima Dam, S16E	0.8	1,000,000	46.0	95.3	2.07
Pacoima Dam, S16E	1.4	1,000,000	25.8	52.9	2.05
Holiday Orion, E-W	2.0	1,000,000	19.8	40.3	2.04
El Centro, E-W	2.4	1,000,000	12.1	27.6	2.28
El Centro, N-S	0.8	1,500,000	35.9	72.9	2.03
Pacoima Dam, S16E	1.4	1,500,000	17.6	36.3	2.06
Holiday Orion, E-W	2.0	1,500,000	14.3	27.1	1.90
El Centro, E-W	2.4	1,500,000	elastic	elastic	-

Table A14 (contd)

Effect of Duration of Input Motion on Maximum Response Values and Cumulative Measures of Deformation

20-Story Isolated Structural Walls - SI = 1.5 ($SI_{ref.}$)

Earthquake Input	Fundamental Period, T_1 sec.	Yield Level, M_y (in-kips)	Maximum or Cumulative Values Corresponding to: 10-sec. Duration (R_{10})	20-sec. Duration (R_{20})	Ratio $\frac{R_{20}}{R_{10}}$
Cyclic Rotational Ductility Ratio (at Base), μ_θ					
(Based on Nodal Rotation at 1st Floor Level)					
El Centro, E-W	0.8	500,000	13.6	-	-
Holiday Orion, E-W	1.4	500,000	11.0	11.3	1.03
El Centro, E-W	2.0	500,000	7.8	11.0	1.39
El Centro, E-W	2.4	500,000	6.9	7.4	1.08
Pacoima Dam, S16E	0.8	1,000,000	10.2	12.2	1.19
Pacoima Dam, S16E	1.4	1,000,000	5.9	5.9	1.00
Holiday Orion, E-W	2.0	1,000,000	3.7	3.7	1.00
El Centro, E-W	2.4	1,000,000	2.1	2.9	1.39
El Centro, N-S	0.8	1,500,000	5.6	6.0	1.06
Pacoima Dam, S16E	1.4	1,500,000	3.4	3.5	1.01
Holiday Orion, E-W	2.0	1,500,000	1.8	1.8	1.01
El Centro, E-W	2.4	1,500,000	elastic	elastic	-
Cumulative Cyclic Rotational Ductility Ratio (at Base), $\Sigma\mu_\theta$					
(Based on Nodal Rotation at 1st Floor Level)					
El Centro, E-W	0.8	500,000	92.6	-	-
Holiday Orion, E-W	1.4	500,000	70.5	178.3	2.53
El Centro, E-W	2.0	500,000	38.0	86.7	2.28
El Centro, E-W	2.4	500,000	31.3	68.0	2.17
Pacoima Dam, S16E	0.8	1,000,000	53.3	110.4	2.07
Pacoima Dam, S16E	1.4	1,000,000	33.8	67.7	2.00
Holiday Orion, E-W	2.0	1,000,000	23.8	50.8	2.13
El Centro, E-W	2.4	1,000,000	14.9	34.8	2.34
El Centro, N-S	0.8	1,500,000	45.6	92.0	2.02
Pacoima Dam, S16E	1.4	1,500,000	22.2	44.5	2.01
Holiday Orion, E-W	2.0	1,500,000	16.2	31.3	1.94
El Centro, E-W	2.4	1,500,000	elastic	elastic	-
Cumulative Rotational Energy (at Base), Σw					
(Based on Nodal Rotation at 1st Floor Level)					
El Centro, E-W	0.8	500,000	56.1	-	-
Holiday Orion, E-W	1.4	500,000	37.9	91.2	2.41
El Centro, E-W	2.0	500,000	17.6	38.6	2.19
El Centro, E-W	2.4	500,000	13.3	25.7	1.94
Pacoima Dam, S16E	0.8	1,000,000	49.7	96.0	1.94
Pacoima Dam, S16E	1.4	1,000,000	26.2	47.8	1.82
Holiday Orion, E-W	2.0	1,000,000	17.0	31.4	1.85
El Centro, E-W	2.4	1,000,000	10.3	23.4	2.26
El Centro, N-S	0.8	1,500,000	38.2	72.5	1.89
Pacoima Dam, S16E	1.4	1,500,000	15.6	28.2	1.82
Holiday Orion, E-W	2.0	1,500,000	10.0	16.4	1.64
El Centro, E-W	2.4	1,500,000	elastic	elastic	-

Table A14 (contd)

Effect of Duration of Input Motion on Maximum Response Values and Cumulative Measures of Deformation

20-Story Isolated Structural Walls - SI = 1.5 ($SI_{ref.}$)

Earthquake Input	Fundamental Period, T_1 sec.	Yield Level, M_y (in-kips)	Maximum or Cumulative Values Corresponding to: 10-sec. Duration (R_{10})	20-sec. Duration (R_{20})	Ratio $\frac{R_{20}}{R_{10}}$
Cumulative Rotational Energy (at Base), ΣAr (Based on Nodal Rotation at 2nd Floor Level)					
El Centro, E-W	0.8	500,000	103.6	-	-
Holiday Orion, E-W	1.4	500,000	60.6	72.3	2.39
El Centro, E-W	2.0	500,000	27.2	30.1	2.22
El Centro, E-W	2.4	500,000	21.2	20.4	1.92
Pacoima Dam, S1SE	0.8	1,000,000	42.4	82.4	1.94
Pacoima Dam, S16E	1.4	1,000,000	18.3	35.6	1.89
Holiday Orion, E-W	2.0	1,000,000	13.1	23.0	1.77
El Centro, E-W	2.4	1,000,000	7.6	17.0	2.20
El Centro, N-S	0.8	1,500,000	27.5	53.6	1.94
Pacoima Dam, S16E	1.4	1,500,000	11.2	21.5	1.93
Holiday Orion, E-W	2.0	1,500,000	8.4	13.2	1.58
El Centro, E-W	2.4	1,500,000	elastic	elastic	-

Table A15

RESPONSE VALUES CORRESPONDING TO DIFFERENT EARTHQUAKE INPUT MOTIONS
[SI = 1.0(SI$_{ref}$), Duration = 10 sec]

20-Story Isolated Structural Walls
M_y = 250,000 IN-K

EARTHQUAKE INPUT NUMBER	EARTHQUAKE INPUT	FUNDAMENTAL PERIOD, T_1 (sec.)											
		0.8			1.4			2.0			2.4		
								M_y x 10^6 in-kips	$\theta_y^{\#}$ x 10^{-3} rad.	$\theta_y^{@}$ x 10^{-3} rad.	M_y x 10^6 in-kips	$\theta_y^{\#}$ x 10^{-3} rad.	$\theta_y^{@}$ x 10^{-3} rad.
1	1971 Pacoima Dam , S16E	-	-	-	-	-	-	-	-	-	.263	.54	.90
2	1971 Holiday Orion, E-W	-	-	-	-	-	-	-	-	-	-	-	-
3	1952 Taft S69E	-	-	-	-	-	-	-	-	-	.263	.51	.82
4	1940 El Centro, E-W	-	-	-	-	-	-	.263	.35	.58	.263	.50	.80
5	Artificial Acc. (SI)	-	-	-	-	-	-	.263	.37	.64	-	-	-
6	1940 El Centro, N-S	-	-	-	-	-	-	-	-	-	-	-	-
	Average	-	-	-	-	-	-	.263	.36	.61	.263	.52	.84

at 1st floor level
@ at 2nd floor level

DUCTILITY DEMAND BASED ON NODAL ROTATIONS AT 1st FLOOR LEVEL

E.Q. INPUT NO.	FUNDAMENTAL PERIOD			
	0.8	1.4	2.0	2.4
	ROTATIONAL DUCTILITY μ_{r1}			
1	-	-	-	4.07
2	-	-	-	-
3	-	-	-	3.67
4	-	-	9.17*	6.54*
5	-	-	5.31	-
6	-	-	-	-

*Critical (maximum) value for particular T_1

DUCTILITY DEMAND BASED ON NODAL ROTATIONS AT 2nd FLOOR LEVEL

E.Q. INPUT NO.	FUNDAMENTAL PERIOD			
	0.8	1.4	2.0	2.4
	ROTATIONAL DUCTILITY μ_{r2}			
1	-	-	-	3.24
2	-	-	-	-
3	-	-	-	3.07
4	-	-	7.85*	5.95*
5	-	-	4.26	-
6	-	-	-	-

MAXIMUM RESPONSE VALUES

E.Q. Input No.	Fundamental Period T_1 (sec).			
	0.8	1.4	2.0	2.4
	Top Displacement (in.)			
1	-	-	-	10.4
2	-	-	-	-
3	-	-	-	9.0
4	-	-	15.6*	16.2*
5	-	-	11.3	-
6	-	-	-	-
	Interstory Displacement (in.)			
1	-	-	-	0.75
2	-	-	-	-
3	-	-	-	0.62
4	-	-	0.93*	0.96*
5	-	-	0.74	-
6	-	-	-	-
	Horizontal Shear at Base (k)			
1	-	-	-	596
2	-	-	-	-
3	-	-	-	757*
4	-	-	661*	672
5	-	-	640	-
6	-	-	-	-
	Bending Moment at Base (in-k)			
1	-	-	-	306,000
2	-	-	-	-
3	-	-	-	298,000
4	-	-	367,000*	332,000*
5	-	-	329,000	-
6	-	-	-	-
	Rotational Ductility μ_{r0} **			
1	-	-	-	4.27
2	-	-	-	-
3	-	-	-	3.66
4	-	-	8.91*	6.25*
5	-	-	6.02	-
6	-	-	-	-

** Based on Eq. (1)

Table A16

RESPONSE VALUES CORRESPONDING TO DIFFERENT EARTHQUAKE INPUT MOTIONS
[SI = 10(SI$_{ref.}$), Duration = 10 sec.]

20-Story Isolated Structural Walls
M_y = 500,000 IN-K

EARTHQUAKE INPUT NUMBER	EARTHQUAKE INPUT	FUNDAMENTAL PERIOD, T_1 (sec.)											
		0.8			1.4			2.0			2.4		
					M_y x 10^6 in-kips	$\theta_y^{\#}$ x 10^{-3} rad.	$\theta_y^{@}$ x 10^{-3} rad.	M_y x 10^6 in-kips	$\theta_y^{\#}$ x 10^{-3} rad.	$\theta_y^{@}$ x 10^{-3} rad.	M_y x 10^6 in-kips	$\theta_y^{\#}$ x 10^{-3} rad.	$\theta_y^{@}$ x 10^{-3} rad.
1	1971 Pacoima Dam , S16E	-	-	-	-	-	-	-	-	-	.525	1.05	1.76
2	1971 Holiday Orion, E-W	-	-	-	.525	.36	.60	.525	.64	1.04	-	-	-
3	1952 Taft S69E	-	-	-	-	-	-	.525	.72	1.19	-	-	-
4	1940 El Centro, E-W	-	-	-	.525	.30	.49	.525	.68	1.09	.525	0.99	1.54
5	Artificial Acc, (S1)	-	-	-	.525	.34	.56	-	-	-	-	-	-
6	1940 El Centro, N-S	-	-	-	-	-	-	-	-	-	-	-	-
	Average	-	-	-	.525	.33	.55	.525	.68	1.11	.525	1.01	1.65

$^{\#}$at 1st floor level
$^{@}$at 2nd floor level

DUCTILITY DEMAND BASED ON NODAL ROTATIONS AT 2nd FLOOR LEVEL

E.Q. INPUT NO.	FUNDAMENTAL PERIOD			
	0.8	1.4	2.0	2.4
	ROTATIONAL DUCTILITY μ_{r1}			
1	-	-	-	1.27
2	-	3.25	2.64*	-
3	-	-	2.02	-
4	-	4.55*	2.37	3.23*
5	-	3.45	-	-
6	-	-	-	-

*Critical (maximum) value for particular T_1

DUCTILITY DEMAND BASED ON NODAL ROTATIONS AT 1st FLOOR LEVEL

E.Q. INPUT NO.	FUNDAMENTAL PERIOD			
	0.8	1.4	2.0	2.4
	ROTATIONAL DUCTILITY μ_{r2}			
1	-	-	-	1.61
2	-	4.81	3.58*	-
3	-	-	2.74	-
4	-	5.60*	3.06	4.24*
5	-	4.62	-	-
6	-	-	-	-

MAXIMUM RESPONSE VALUES

E.Q. Input No.	Fundamental Period T_1 (sec).			
	0.8	1.4	2.0	2.4
	Top Displacement (in.)			
1	-	-	-	10.2
2	-	7.0	10.5	-
3	-	-	8.3	-
4	-	7.2*	11.3*	15.8*
5	-	6.2	-	-
6	-	-	-	-
	Interstory Displacement (in.)			
1	-	-	-	0.75
2	-	0.44	0.71	-
3	-	-	0.58	-
4	-	0.44*	0.74*	1.01*
5	-	0.39	-	-
6	-	-	-	-
	Horizontal Shear at Base (k)			
1	-	-	-	956*
2	-	924	782	-
3	-	-	903*	-
4	-	632	710	786
5	-	950*	-	-
6	-	-	-	-
	Bending Moment at Base (in-k)			
1	-	-	-	543,000
2	-	630,000*	583,000*	-
3	-	-	572,000	-
4	-	627,000	574,000	602,000*
5	-	618,000	-	-
6	-	-	-	-
	Rotational Ductility μ_{ro} **			
1	-	-	-	1.69
2	-	5.00*	3.21*	-
3	-	-	2.79	-
4	-	4.89	2.87	3.93*
5	-	4.54	-	-
6	-	-	-	-

** Based on Eq. (1)

Table A17

RESPONSE VALUES CORRESPONDING TO DIFFERENT EARTHQUAKE INPUT MOTIONS
[SI = 1.0(SI$_{ref.}$), Duration = 10 sec.]

20-Story Isolated Structural Walls
M_y = 750,000 IN-K

EARTHQUAKE INPUT NO.	EARTHQUAKE INPUT	FUNDAMENTAL PERIOD, T_1 (sec.)											
		0.8			1.4			2.0			2.4		
		M_y x 10^6 in-kips	$\theta_y^{\prime}$ x 10^{-3} rad.	$\theta_y^{@}$ x 10^{-3} rad.	M_y x 10^6 in-kips	$\theta_y^{\prime}$ x 10^{-3} rad.	$\theta_y^{@}$ x 10^{-3} rad.	M_y x 10^5 in-kips	$\theta_y^{\prime}$ x 10^{-3} rad.	$\theta_y^{@}$ x 10^{-3} rad.	M_y x 10^6 in-kips	$\theta_y^{\prime}$ x 10^{-3} rad.	$\theta_y^{@}$ x 10^{-3} rad.
1	1971 Pacoima Dam , S16E	.7875	.17	.29	.7875	.52	.87	-	-	-	.7875	E	E
2	1971 Holliday Orion, E-W	-	-	-	.7875	.58	.85	.7875	1.07	1.76	-	-	-
3	1952 Taft S69E	-	-	-	-	-	-	-	-	-	-	-	-
4	1940 El Centro, E-W	-	-	-	-	-	-	-	-	-	.7875	1.59	2.65
5	Artificial Acc. (SI)	.7875	.16	.26	.7875	.52	.84	-	-	-	-	-	-
6	1940 El Centro, N-S	-	-	-	-	-	-	-	-	-	-	-	-
	Average	.7875	.16	.28	.7875	.54	.85	.7875	1.07	1.76	.7875	1.59	2.65

$^{\prime}$at 1st floor level
$^{@}$at 2nd floor level

DUCTILITY DEMAND BASED ON NODAL ROTATIONS AT 1st FLOOR LEVEL

E.Q. INPUT NO.	FUNDAMENTAL PERIOD			
	0.8	1.4	2.0	2.4
	ROTATIONAL DUCTILITY μ_{r1}			
1	6.29*	4.33*	-	E
2	-	2.68	2.68*	-
3	-	-	-	-
4	-	-	-	1.52*
5	3.69	2.62	-	-
6	-	-	-	-

DUCTILITY DEMAND BASED ON NODAL ROTATIONS AT 2nd FLOOR LEVEL

E.Q. INPUT NO.	FUNDAMENTAL PERIOD			
	0.8	1.4	2.0	2.4
	ROTATIONAL DUCTILITY μ_{r2}			
1	5.52*	3.37*	-	E
2	-	2.32	2.02*	-
3	-	-	-	-
4	-	-	-	1.29*
5	2.88	2.10	-	-
6	-	-	-	-

*Critical (maximum) value for particular T_1
E - no yielding, i.e., linearly elastic response

MAXIMUM RESPONSE VALUES

E.Q. Input No.	Fundamental Period T_1 (sec).			
	0.8	1.4	2.0	2.4
	Top Displacement (in.)			
1	5.3*	9.3*	-	10.7(E)
2	-	7.0	12.4	-
3	-	-	-	-
4	-	-	14.6*	15.0*
5	2.9	6.7	-	-
6	-	-	-	-
	Interstory Displacement (in.)			
1	0.30*	0.58*	-	0.75(E)
2	-	0.47	0.88	-
3	-	-	-	-
4	-	-	0.9*	1.0*
5	0.18	0.48	-	-
6	-	-	-	-
	Horizontal Shear at Base (k)			
1	1,032	884	-	1,102*(E)
2	-	1,055*	1,193*	-
3	-	-	-	-
4	-	-	742	833
5	1,223*	1,022	-	-
6	-	-	-	-
	Bending Moment at Base (in-k)			
1	996,000*	919,000*	-	679,000(E)
2	-	865,000	854,000	-
3	-	-	-	-
4	-	-	860,000*	809,000*
5	885,000	851,000	-	-
6	-	-	-	-
	Rotational Ductility $\mu_{r\theta}$ **			
1	6.30*	4.34*	-	0.86(E)
2	-	2.97	2.69	-
3	-	-	-	-
4	-	-	2.84*	1.57*
5	3.48	2.61	-	-
6	-	-	-	-

** Based on Eq. (1)

Table A18

RESPONSE VALUES CORRESPONDING TO DIFFERENT EARTHQUAKE INPUT MOTIONS
[SI = 1.0(SI$_{ref.}$), Duration = 10 sec.]

20-Story Isolated Structural Walls
M_y = 1,000,000 IN-K

EARTHQUAKE INPUT NUMBER	EARTHQUAKE INPUT	FUNDAMENTAL PERIOD, T_1 (sec.)											
		0.8			1.4			2.0			2.4		
		M_y x 10^6 in-kips	$\theta_y^{\#}$ x 10^{-3} rad.	$\theta_y^{@}$ x 10^{-3} rad.	M_y x 10^6 in-kips	$\theta_y^{\#}$ x 10^{-3} rad.	$\theta_y^{@}$ x 10^{-3} rad.	M_y x 10^6 in-kips	$\theta_y^{\#}$ x 10^{-3} rad.	$\theta_y^{@}$ x 10^{-3} rad.	M_y x 10^6 in-kips	$\theta_y^{\#}$ x 10^{-3} rad.	$\theta_y^{@}$ x 10^{-3} rad.
1	1971 Pacoima Dam, S16E	-	-	-	1.05	.73	1.25	-	-	-	1.05	E	E
2	1971 Holiday Orion, E-W	-	-	-	-	-	-	1.05	1.43	2.35	-	-	-
3	1952 Taft S69E	1.05	.22	.36	-	-	-	-	-	-	-	-	-
4	1940 El Centro, E-W	1.05	.25	.41	-	-	-	-	-	-	1.05	E	E
5	Artificial Acc, (SI)	1.05	.23	.39	1.05	.61	1.08	-	-	-	-	-	-
6	1940 El Centro, N-S	-	-	-	-	-	-	-	-	-	-	-	-
	Average	1.05	.23	.39	1.05	.65	1.17	1.05	1.43	2.35	1.05	-	-

at 1st floor level
@ at 2nd floor level

DUCTILITY DEMAND BASED ON NODAL ROTATIONS AT 1st FLOOR LEVEL

E.Q. INPUT NO.	FUNDAMENTAL PERIOD			
	0.8	1.4	2.0	2.4
	ROTATIONAL DUCTILITY μ_{r1}			
1	-	3.36*	-	E
2	-	-	1.88*	-
3	4.27*	-	-	-
4	2.36	-	-	E
5	3.04	2.18	-	-
6	-	-	-	-

DUCTILITY DEMAND BASED ON NODAL ROTATIONS AT 2nd FLOOR LEVEL

E.Q. INPUT NO.	FUNDAMENTAL PERIOD			
	0.8	1.4	2.0	2.4
	ROTATIONAL DUCTILITY μ_{r2}			
1	-	2.42*	-	E
2	-	-	1.52*	-
3	3.17*	-	-	-
4	1.80	-	-	E
5	2.36	1.65	-	-
6	-	-	-	-

*Critical (maximum) value for particular T_1
E - no yielding, i.e., linearly elastic response

MAXIMUM RESPONSE VALUES

E.Q. Input No.	Fundamental Period T_1 (sec).			
	0.8	1.4	2.0	2.4
	Top Displacement (in.)			
1	-	10.1*	-	10.2(E)
2	-	-	13.4*	-
3	3.9*	-	-	-
4	3.0	-	-	16.3*(E)
5	3.6	7.9	-	-
6	-	-	-	-
	Interstory Displacement (in.)			
1	-	.64*	-	0.75(E)
2	-	-	1.05*	-
3	.25*	-	-	-
4	0.19	-	-	1.17*(E)
5	.23	.56	-	-
6	-	-	-	-
	Horizontal Shear at Base (k)			
1	-	1,124*	-	1,120*(E)
2	-	-	1,409*	-
3	1,336	-	-	-
4	1,069	-	-	865(E)
5	1,412*	1,271	-	-
6	-	-	-	-
	Bending Moment at Base (in-k)			
1	-	1,182,000*	-	679,000(E)
2	-	-	1,097,000*	-
3	1,217,000*	-	-	-
4	1,134,000	-	-	1,013,000*(E)
5	1,159,000	1,099,000	-	-
6	-	-	-	-
	Rotational Ductility μ_{ro} **			
1	-	3.51*	-	0.65(E)
2	-	-	1.90*	-
3	4.18*	-	-	-
4	1.60	-	-	0.96*(E)
5	3.08	1.93	-	-
6	-	-	-	-

** Based on Eq. (1)

Table A19

RESPONSE VALUES CORRESPONDING TO DIFFERENT EARTHQUAKE INPUT MOTIONS
[SI = 10(SI$_{ref}$), Duration = 10 sec.]

20-Story Isolated Structural Walls
M_y = 1,500,000 IN-K

EARTHQUAKE INPUT NUMBER	EARTHQUAKE INPUT	FUNDAMENTAL PERIOD, T_1 (sec.)											
		0.8			1.4			2.0			2.4		
		M_y x 10^6 in-kips	$\theta_y^{\#}$ x 10^{-3} rad.	$\theta_y^{@}$ x 10^{-3} rad.	M_y x 10^6 in-kips	$\theta_y^{\#}$ x 10^{-3} rad.	$\theta_y^{@}$ x 10^{-3} rad.	M_y x 10^6 in-kips	$\theta_y^{\#}$ x 10^{-3} rad.	$\theta_y^{@}$ x 10^{-3} rad.	M_y x 10^6 in-kips	$\theta_y^{\#}$ x 10^{-3} rad.	$\theta_y^{@}$ x 10^{-3} rad.
1	1971 Pacoima Dam, S16E	-	-	-	1.575	1.04	1.73	-	-	-	1.575	E	E
2	1971 Holiday Orion, E-W	-	-	-	-	-	-	1.575	E	E	-	-	-
3	1952 Taft S69E	1.575	.36	.61	-	-	-	-	-	-	-	-	-
4	1940 El Centro, E-W	-	-	-	-	-	-	-	-	-	1.575	E	E
5	Artificial Acc. (S1)	1.575	.35	.56	E	E	E	-	-	-	-	-	-
6	1940 El Centro, N-S	-	-	-	-	-	-	-	-	-	-	-	-
	Average	1.575	.36	.59	1.575	1.04	1.73	1.575	-	-	1.575	-	-

\# at 1st floor level
@ at 2nd floor level

DUCTILITY DEMAND BASED ON NODAL ROTATIONS AT 1st FLOOR LEVEL

E.Q. INPUT NO.	FUNDAMENTAL PERIOD			
	0.8	1.4	2.0	2.4
	ROTATIONAL DUCTILITY μ_{r1}			
1	-	1.15*	-	E
2	-	-	E	-
3	3.11*	-	-	-
4	-	-	-	E
5	1.29	E		
6	-	-	-	-

*Critical (maximum) value for particular T_1
E - no yielding, i.e., linearly elastic response

DUCTILITY DEMAND BASED ON NODAL ROTATIONS AT 2nd FLOOR LEVEL

E.Q. INPUT NO.	FUNDAMENTAL PERIOD			
	0.8	1.4	2.0	2.4
	ROTATIONAL DUCTILITY μ_{r2}			
1	-	1.09*	-	-
2	-	-	E	-
3	2.51*	-	-	-
4	-	-	-	E
5	1.20	E	-	-
6	-	-	-	-

MAXIMUM RESPONSE VALUES

E.Q. Input No.	Fundamental Period T_1 (sec).			
	0.8	1.4	2.0	2.4
	Top Displacement (in.)			
1	-	10.2*	-	10.2(F)
2	-	-	12.4*(E)	-
3	5.5*	-	-	-
4	-	-	-	16.3*(E)
5	3.5	8.3(E)	-	-
6	-	-	-	-
	Interstory Displacement (in.)			
1	-	0.68*	-	0.75(E)
2	-	-	1.08*(E)	-
3	0.33*	-	-	-
4	-	-	-	1.17*(E)
5	-	0.60(E)	-	-
6	-	-	-	-
	Horizontal Shear at Base (k)			
1	-	1,304	-	1,120*(E)
2	-	-	1,595*(E)	-
3	1,387	-	-	-
4	-	-	-	865(E)
5	1,669*	1,614*(E)	-	-
6	-	-	-	-
	Bending Moment at Base (in-k)			
1	-	1,587,000*	-	670,000(E)
2	-	-	1,394,000*(E)	-
3	1,755,000*	-	-	-
4	-	-	-	1,031,000*(E)
5	1,599,000	1,466,000(E)	-	-
6	-	-	-	-
	Rotational Ductility μ_{ro}**			
1	-	1.15*	-	0.43(E)
2	3.29*	-	0.89*(E)	-
3	-	-	-	-
4	-	-	-	0.64*(E)
5	1.30	0.93(E)	-	-
6	-	-	-	-

** Based on Eq. (1)

Table A 20

RESPONSE VALUES CORRESPONDING TO DIFFERENT EARTHQUAKE INPUT MOTIONS
[SI = 10(SI$_{ref.}$), Duration = 10 sec.]

20-Story Isolated Structural Walls
M_y = Very Large (Elastic)

E.Q. Input No.	Fundamental Period T_1 (sec).			
	0.8	1.4	2.0	2.4
	Top Displacement (in.)			
1	-	1.05*	-	10.2
2	-	-	12.4*	-
3	5.9*	-	-	-
4	-	-	-	16.3*
5	4.0	8.3	-	-
6	-	-	-	-
	Interstory Displacement (in.)			
1	-	0.69*	-	0.75
2	-	-	1.08*	-
3	0.39*	-	-	-
4	-	-	-	1.17*
5	-	0.60	-	-
6	-	-	-	-
	Horizontal Shear at Base (k)			
1	-	1,339	-	1,120*
2	-	-	1,595*	-
3	1,838	-	-	-
4	-	-	-	865
5	1,923*	1,614*	-	-
6	-	-	-	-
	Bending Moment at Base (in-k)			
1		1,699,000*	-	679,000
2	2,673,000*	-	1,394,000*	-
3	-	-	-	-
4	-	-	-	1,013,000*
5	2,082,000	1,466,000	-	-
6	-	-	-	-

*Critical (maximum) value for particular T_1

Table A 21

RESPONSE VALUES CORRESPONDING TO DIFFERENT
EARTHQUAKE INPUT MOTIONS
[SI = 0.75(SI$_{ref.}$), Duration = 10 sec.]

20-Story Isolated Structural Walls
M_y = 250,000 IN-K

EARTHQUAKE INPUT NUMBER	EARTHQUAKE INPUT	FUNDAMENTAL PERIOD, T_1 (SEC.) 0.8 M_y x 10^6 in-kips	0.8	0.8	1.4 M_y x 10^6 in-kips	1.4 $\theta_y^{\#}$ x 10^{-3} rad.	1.4 $\theta_y^{@}$ x 10^{-3} rad.	2.0 M_y x 10^6 in-kips	2.0 $\theta_y^{\#}$ x 10^{-3} rad.	2.0 $\theta_y^{@}$ x 10^{-3} rad.	2.4 M_y x 10^6 in-kips	2.4 $\theta_y^{\#}$ x 10^{-3} rad.	2.4 $\theta_y^{@}$ x 10^{-3} rad.
1	1971 Pacoima Dam, S16E	.263	-	-	.263	-	-	.263	-	-	.263	-	-
2	1971 Holiday Orion, E-W	.263	-	-	.263	-	-	.263	.32	.49	.263	-	-
3	1952 Taft, S69E	.263	-	-	.263	-	-	.263	-	-	.263	.54	.91
4	1940 El Centro, E-W	.263	-	-	.263	.17	.29	.263	-	-	.263	.51	.81
5	Artificial Acc. (SI)	.263	-	-	.263	-	-	.263	.40	.63	.263	-	-
6	1940 El Centro, N-S	.263	-	-	.263	-	-	.263	-	-	.263	-	-
	AVERAGE					.17	.29		.36	.56		.53	.86

$^{\#}\theta$ at 1st floor level
$^{@}\theta$ at 2nd floor level

DUCTILITY DEMAND BASED ON NODAL ROTATIONS AT 1st FLOOR LEVEL

E.Q. INPUT NO.	FUNDAMENTAL PERIOD, T_1, (SEC) 0.8	1.4	2.0	2.4
	ROTATIONAL DUCTILITY, μ_{r1}			
1	--	--	--	--
2	--	--	4.97	--
3	--	--	--	2.91
4	--	8.29*	6.40*	5.84*
5	--	6.76	4.10	--
6	--	--	--	--

*Critical (maximum) value for particular T_1

DUCTILITY DEMAND BASED ON NODAL ROTATIONS AT 2nd FLOOR LEVEL

E.Q. INPUT NO.	FUNDAMENTAL PERIOD, T_1, (SEC) 0.8	1.4	2.0	2.4
	ROTATIONAL DUCTILITY, μ_{r2}			
1	--	--	--	--
2	--	--	3.71	--
3	--	--	--	2.20
4	--	7.03*	5.35*	4.99*
5	--	6.27	2.90	--
6	--	--	--	--

MAXIMUM RESPONSE VALUES

E.Q. Input No.	Fundamental Period, T_1 (sec.) 0.8	1.4	2.0	2.4
	Top Displacement (in.)			
1	-	-	-	-
2	-	-	5.7	-
3	-	-	-	7.3
4	-	7.5*	10.2*	12.6*
5	-	5.3	6.9	-
6	-	-	-	-
	Interstory Displacement (in.)			
1	-	-	-	-
2	-	-	0.40	-
3	-	-	-	0.50
4	-	0.43*	0.61*	0.78*
5	-	0.32	0.46	-
6	-	-	-	-
	Horizontal Shear at Base (k)			
1	-	-	-	-
2	-	-	536	-
3	-	-	-	659*
4	-	413	522	526
5	-	684*	630*	-
6	-	-	-	-
	Bending Moment at Base (in-k)			
1	-	-	-	-
2	-	-	308,000	-
3	-	-	-	290,000
4	-	356,000*	331,000*	325,000*
5	-	337,000	311,000	-
6	-	-	-	-
	Rotational Ductility μ_{ro} **			
1	-	-	-	-
2	-	-	4.42	-
3	-	-	-	3.05
4	-	8.07*	6.10*	5.71*
5	-	-	4.65	-
6	-	-	-	-

** Based on Eq. (1)

Table A22

RESPONSE VALUES CORRESPONDING TO DIFFERENT
EARTHQUAKE INPUT MOTIONS
[SI = 0.75(SI$_{ref.}$), Duration = 10 sec.]

20-Story Isolated Structural Walls
M_y = 500,000 IN-K

EARTHQUAKE INPUT NUMBER	EARTHQUAKE INPUT	FUNDAMENTAL PERIOD, T_1 (SEC.) 0.8 M_y x 10^6 in-kips	0.8 θ_y' x 10^{-3} rad.	0.8 θ_y^* x 10^{-3} rad.	1.4 M_y x 10^6 in-kips	1.4 θ_y' x 10^{-3} rad.	1.4 θ_y^* x 10^{-3} rad.	2.0 M_y x 10^6 in-kips	2.0 θ_y' x 10^{-3} rad.	2.0 θ_y^* x 10^{-3} rad.	2.4 M_y x 10^6 in-kips	2.4 θ_y' x 10^{-3} rad.	2.4 θ_y^* x 10^{-3} rad.
1	1971 Pacoima Dam, S16E	.525	.10	.19	.525	.35	.59	.525	-	-	.525	E	E
2	1971 Holiday Orion, E-W	.525	-	-	.525	.36	.58	.525	.71	1.13	.525	-	-
3	1952 Taft, S69E	.525	-	-	.525	-	-	.525	.72	1.19	.525	E	E
4	1940 El Centro, E-W	.525	-	-	.525	.42	.62	.525	-	-	.263	1.03	1.77
5	Artificial Acc. (SI)	.525	.11	.18	.525	.34	.56	.525	-	-	.525	-	-
6	1940 El Centro, N-S	.525	.11	.19	.525	-	-	.525	-	-	.525	-	-
	AVERAGE		.11	.19		.37	.59		.72	1.16		1.03	1.77

θ_y' at 1st floor level
θ_y^* at 2nd floor level

DUCTILITY DEMAND BASED ON NODAL ROTATIONS AT 1st FLOOR LEVEL

E.Q. INPUT NO.	FUNDAMENTAL PERIOD, T_1, (SEC) 0.8	1.4	2.0	2.4
	ROTATIONAL DUCTILITY, μ_{r1}			
1	8.10*	4.66*	--	E
2	--	3.36	2.86*	--
3	--	--	1.96	E
4	--	1.95	--	2.10*
5	4.18	3.26	--	--
6	6.27	--	--	--

*Critical (maximum) value for particular T_1
E - no yielding, i.e., linearly elastic response

DUCTILITY DEMAND BASED ON NODAL ROTATIONS AT 2nd FLOOR LEVEL

E.Q. INPUT NO.	FUNDAMENTAL PERIOD, T_1, (SEC) 0.8	1.4	2.0	2.4
	ROTATIONAL DUCTILITY, μ_{r2}			
1	6.42*	3.58	--	E
2	--	4.17*	2.19*	--
3	--	--	1.54	E
4	--	1.69	--	1.61*
5	3.67	2.54	--	--
6	5.21	--	--	--

MAXIMUM RESPONSE VALUES

E.Q. Input No.	Fundamental Period, T_1 (sec.) 0.8	1.4	2.0	2.4
	Top Displacement (in.)			
1	4.2*	6.7*	-	7.7 (E)
2	-	5.2	9.3*	-
3	-	-	7.0	7.5 (E)
4	-	4.6	-	11.2*
5	2.3	5.0	-	-
6	3.3	-	-	-
	Interstory Displacement (in.)			
1	0.24*	0.41*	-	0.56 (E)
2	-	0.34	0.63*	-
3	-	-	0.55	0.60 (E)
4	-	0.29	-	0.76*
5	0.14	0.33	-	-
6	0.19	-	-	-
	Horizontal Shear at Base (k)			
1	760	603	-	840* (E)
2	-	775*	774	-
3	-	-	811*	718 (E)
4	-	591	-	616
5	850*	754	-	-
6	613	-	-	-
	Bending Moment at Base (in-k)			
1	688,000*	621,000*	-	509,000 (E)
2	-	591,000	573,000*	-
3	-	-	551,000	458,000 (E)
4	-	574,000	-	553,000*
5	605,000	582,000	-	-
6	659,000	-	-	-
	Rotational Ductility μ_{ro} **			
1	7.21*	4.66*	-	0.97 (E)
2	-	3.5	2.83*	-
3	-	-	2.00	0.87 (E)
4	-	2.87	-	2.10*
5	4.05	3.17	-	-
6	6.10	-	-	-

** Based on Eq. (1)

Table A23

RESPONSE VALUES CORRESPONDING TO DIFFERENT EARTHQUAKE INPUT MOTIONS

[SI = 0.75(SI$_{ref}$), Duration = 10 sec.]

20-Story Isolated Structural Walls

M_y = 750,000 IN-K

EARTHQUAKE INPUT NUMBER	EARTHQUAKE INPUT	FUNDAMENTAL PERIOD, T_1 (SEC.) 0.8: M_y x 10^6 in-kips	0.8: $\theta_y^\ast$ x 10^{-3} rad.	0.8: $\theta_y^\#$ x 10^{-3} rad.	1.4: M_y x 10^6 in-kips	1.4: $\theta_y^\ast$ x 10^{-3} rad.	1.4: $\theta_y^\#$ x 10^{-3} rad.	2.0: M_y x 10^6 in-kips	2.0: $\theta_y^\ast$ x 10^{-3} rad.	2.0: $\theta_y^\#$ x 10^{-3} rad.	2.4: M_y x 10^6 in-kips	2.4: $\theta_y^\ast$ x 10^{-3} rad.	2.4: $\theta_y^\#$ x 10^{-3} rad.
1	1971 Pacoima Dam, S16E	.7875	.17	.28	.7875	.52	.85	.7875	-	-	.7875	E	E
2	1971 Holiday Orion, E-W	.7875	-	-	.7875	.52	.88	.7875	1.02	1.81	.7875	-	-
3	1952 Taft, S69E	.7875	.17	.27	.7875	-	-	.7875	-	-	.7875	E	E
4	1940 El Centro, E-W	.7875	-	-	.7875	-		.7875	1.10	1.82	.7875	E	E
5	Artificial Acc. (S1)	.7875	.17	.30	.7875	.51	.81	.7875	-	-	.7875	-	-
6	1940 El Centro, N-S	.7875	-	-	.7875	-		.7875	-	-	.7875	-	-
	AVERAGE		.17	.28		.52	.85		1.06	1.82			

*at 1st floor level
#at 2nd floor level

DUCTILITY DEMAND BASED ON NODAL ROTATIONS AT 1st FLOOR LEVEL

E.Q. INPUT NO.	FUNDAMENTAL PERIOD, T_1, (SEC) 0.8	1.4	2.0	2.4
	ROTATIONAL DUCTILITY, μ_{r1}			
1	4.12*	3.48*	--	E
2	--	2.62	1.95*	--
3	3.76	--	--	E
4	--	--	1.39	E
5	3.06	1.94	--	--
6	--	--	--	--

DUCTILITY DEMAND BASED ON NODAL ROTATIONS AT 2nd FLOOR LEVEL

E.Q. INPUT NO.	FUNDAMENTAL PERIOD, T_1, (SEC) 0.8	1.4	2.0	2.4
	ROTATIONAL DUCTILITY, μ_{r2}			
1	3.54*	2.62*	--	E
2	--	1.63	1.46*	--
3	3.15	--	--	E
4	--	--	1.25	E
5	2.30	1.64	--	--
6	--	--	--	--

*Critical (maximum) value for particular T_1
E - no yielding, i.e., linearly elastic response

MAXIMUM RESPONSE VALUES

E.Q. Input No.	Fundamental Period, T_1 (sec.) 0.8	1.4	2.0	2.4
	Top Displacement (in.)			
1	3.4*	7.7*	-	7.7 (E)
2	-	6.7	10.1	-
3	3.0	-	-	7.5 (E)
4	-	-	11.5*	12.3*(E)
5	2.7	5.9	-	-
6	-	-	-	-
	Interstory Displacement (in.)			
1	0.20*	0.48*	-	0.56 (E)
2	-	0.43	0.78*	-
3	0.18	-	-	0.60*(E)
4	-	-	0.76	-
5	0.17	0.42	-	-
6	-	-	-	-
	Horizontal Shear at Base (k)			
1	898	806	-	840* (E)
2	-	813	1,057*	-
3	867			718 (E)
4	-	-	575	649 (E)
5	1,059*	946*	-	-
6	-	-	-	-
	Bending Moment at Base (in-k)			
1	911,000*	886,000*	-	509,000 (E)
2	-	827,000	824,000*	-
3	896,000	-	-	458,000 (E)
4	-	-	804,000	760,000*(E)
5	869,000	823,000	-	-
6	-	-	-	-
	Rotational Ductility μ_{ro}**			
1	4.14*	3.50*	-	0.65 (E)
2	-	2.0	1.90*	-
3	3.8	-	-	0.58 (E)
4	-	-	1.32	0.97*(E)
5	3.1	1.90	-	-
6	-	-	-	-

** Based on Eq. (1)

Table A24

RESPONSE VALUES CORRESPONDING TO DIFFERENT EARTHQUAKE INPUT MOTIONS
[SI = 0.75(SI$_{rel}$), Duration = 10 sec]

20-Story Isolated Structural Walls
M_y = 1,000,000 IN-K

EARTHQUAKE INPUT NUMBER	EARTHQUAKE INPUT	FUNDAMENTAL PERIOD, T_1 (SEC.) 0.8: M_y x 10^6 in-kips	0.8: $\theta_y^{\#}$ x 10^{-3} rad.	0.8: $\theta_y^{@}$ x 10^{-3} rad.	1.4: M_y x 10^6 in-kips	1.4: $\theta_y^{\#}$ x 10^{-3} rad.	1.4: $\theta_y^{@}$ x 10^{-3} rad.	2.0: M_y x 10^6 in-kips	2.0: $\theta_y^{\#}$ x 10^{-3} rad.	2.0: $\theta_y^{@}$ x 10^{-3} rad.	2.4: M_y x 10^6 in-kips	2.4: $\theta_y^{\#}$ x 10^{-3} rad.	2.4: $\theta_y^{@}$ x 10^{-3} rad.
1	1971 Pacoima Dam, S16E	1.05	.23	.38	1.05	.70	1.18	1.05	-	-	1.05	E	E
2	1971 Holiday Orion, E-W	1.05	-	-	1.05	-	-	1.05	E	E	1.05	-	-
3	1952 Taft, S69E	1.05	.16	.76	1.05	E	E	1.05	-	-	1.05	E	E
4	1940 El Centro, E-W	1.05	-	-	1.05	-	-	1.05	E	E	1.05	E	E
5	Artificial Acc. (SI)	1.05	.23	.37	1.05	.69	1.11	1.05	-	-	1.05	-	-
6	1940 El Centro, N-S	1.05	.23	.37	1.05	-	-	1.05	-	-	1.05	-	-
	AVERAGE		.21	.35		.70	1.15						

\# at 1st floor level
@ at 2nd floor level

MAXIMUM RESPONSE VALUES

E.Q. Input No.	Fundamental Period, T_1 (sec.) 0.8	1.4	2.0	2.4
	Top Displacement (in.)			
1	2.9	7.6*	-	7.7 (E)
2	-	-	10.8 (E)	-
3	4.1*	5.8 (E)	-	7.5 (E)
4	-	-	11.6* (E)	12.3* (E)
5	2.5	6.2	-	-
6	3.1	-	-	-
	Interstory Displacement (in.)			
1	0.18	0.48*	-	0.56 (E)
2	-	-	0.81*(E)	-
3	0.24*	0.41 (E)	-	0.60*(E)
4	-	-	0.78 (E)	-
5	0.17	0.45	-	-
6	-	-	-	-
	Horizontal Shear at Base (k)			
1	964	929	-	840* (E)
2	-	-	1,196*(E)	-
3	1,051	940 (E)	-	718 (E)
4	-	-	617 (E)	649 (E)
5	1,200*	1,157*	-	-
6	1,195	-	-	-
	Bending Moment at Base (in-k)			
1	1,123,000	1,084,000*	-	509,000 (E)
2	-	-	1,045,000* (E)	-
3	1,195,000*	933,000 (E)	-	458,000 (E)
4	-	-	891,000 (E)	760,000* (E)
5	1,087,000	1,054,000	-	-
6	1,157,000	-	-	-
	Rotational Ductility μ_{ro} **			
1	2.40	1.65*	-	0.48(E)
2	-	-	0.99*(E)	-
3	3.80*	0.89 (E)	-	0.44(E)
4	-	-	0.80 (E)	0.72*(E)
5	1.70	1.08	-	-
6	3.04	-	-	-

** Based on Eq. (1)

DUCTILITY DEMAND BASED ON NODAL ROTATIONS AT 1st FLOOR LEVEL

E.Q. INPUT NO.	FUNDAMENTAL PERIOD, T_1 (SEC) 0.8	1.4	2.0	2.4
	ROTATIONAL DUCTILITY, μ_{r1}			
1	1.79	1.31*	--	E
2	--	--	E	--
3	4.54*	E	--	E
4	--	--	E	E
5	1.43	1.05	--	--
6	2.11	--	--	--

DUCTILITY DEMAND BASED ON NODAL ROTATIONS AT 2nd FLOOR LEVEL

E.Q. INPUT NO.	FUNDAMENTAL PERIOD, T_1, (SEC) 0.8	1.4	2.0	2.4
	ROTATIONAL DUCTILITY, μ_{r2}			
1	2.30	1.56*	--	E
2	--	--	E	--
3	5.31*	E	--	E
4	--	--	E	E
5	1.65	1.07	--	--
6	2.39	--	--	--

*Critical (maximum) value for particular T_1
E - no yielding, i.e., linearly elastic response

Table A 25

RESPONSE VALUES CORRESPONDING TO DIFFERENT
EARTHQUAKE INPUT MOTIONS
[SI = 0.75(SI$_{ref.}$), Duration = 10 sec.]

20 - Story Isolated Structural Walls
M_y = 1,500,000 IN-K

EARTHQUAKE INPUT NUMBER	EARTHQUAKE INPUT	FUNDAMENTAL PERIOD, T_1 (SEC.)											
		0.8			1.4			2.0			2.4		
		M_y x 10^6 in-kips	θ_y [a] x 10^{-3} rad.	θ_y [b] x 10^{-3} rad.	M_y x 10^6 in-kips	θ_y [a] x 10^{-3} rad.	θ_y [b] x 10^{-3} rad.	M_y x 10^6 in-kips	θ_y [a] x 10^{-3} rad.	θ_y [b] x 10^{-3} rad.	M_y x 10^6 in-kips	θ_y [a] x 10^{-3} rad.	θ_y [b] x 10^{-3} rad.
1	1971 Pacoima Dam, S16E	1.575	-	-	1.575	E	E	1.575	-	-	1.575	E	E
2	1971 Holiday Orion, E-W	1.575	-	-	1.575	-	-	1.575	E	E	1.575	-	-
3	1952 Taft, S69E	1.575	.34	.56	1.575	E	E	1.575	-	-	1.575	E	E
4	1940 El Centro, E-W	1.575	-	-	1.575	-	-	1.575	E	E	1.575	E	E
5	Artificial Acc. (S1)	1.575	E	E	1.575	E	E	1.575	-	-	1.575	-	-
6	1940 El Centro, N-S	1.575	.34	.55	1.575	-	-	1.575	-	-	1.575	-	-
	AVERAGE		.34	.56									

[a] at 1st floor level
[b] at 2nd floor level

DUCTILITY DEMAND BASED ON NODAL ROTATIONS AT 1st FLOOR LEVEL

E.Q. INPUT NO.	FUNDAMENTAL PERIOD, T_1, (SEC)			
	0.8	1.4	2.0	2.4
	ROTATIONAL DUCTILITY, μ_{r1}			
1	--	E	--	E
2	--	--	E	--
3	1.82*	E	--	E
4	--	--	E	E
5	E	E	--	--
6	1.49	--	--	--

DUCTILITY DEMAND BASED ON NODAL ROTATIONS AT 2nd FLOOR LEVEL

E.Q. INPUT NO.	FUNDAMENTAL PERIOD, T_1, (SEC)			
	0.8	1.4	2.0	2.4
	ROTATIONAL DUCTILITY, μ_{r2}			
1	--	E	--	E
2	--	--	E	--
3	2.29*	E	--	E
4	--	--	E	E
5	E	E	--	--
6	1.94	--	--	--

*Critical (maximum) value for particular T_1
E - no yielding, i.e., linearly elastic response

MAXIMUM RESPONSE VALUES

E.Q. Input No.	Fundamental Period, T_1 (sec.)			
	0.8	1.4	2.0	2.4
	Top Displacement (in.)			
1	-	7.9*(E)	-	7.7 (E)
2	-	-	10.8 (E)	-
3	4.4*	5.8 (E)	-	7.5 (E)
4	-	-	11.6*(E)	12.3*(E)
5	3.0 (E)	6.23 (E)	-	-
6	3.9	-	-	-
	Interstory Displacement (in.)			
1	-	0.51*(E)	-	0.56 (E)
2	-	-	0.81*(E)	-
3	0.27*	0.41 (E)	-	0.60*(E)
4	-	-	0.78 (E)	-
5	0.21 (E)	0.45 (E)	-	-
6	-0.25	-	-	-
	Horizontal Shear at Base (k)			
1	-	1,041 (E)	-	840* (E)
2	-	-	1,196*(E)	-
3	1,304	940 (E)	-	718 (E)
4	-	-	617 (E)	649 (E)
5	1,442*(E)	1,210*(E)	-	-
6	1,357	-	-	-
	Bending Moment at Base (in-k)			
1	-	1,291,000* (E)	-	509,000 (E)
2	-	-	1,045,000* (E)	-
3	1,678,000*	933,000 (E)	-	458,000 (E)
4	-	-	891,000 (E)	760,000*,E)
5	1,561,000 (E)	1,099,000 (E)	-	-
6	1,628,000	-	-	-
	Rotational Ductility μ_{ro} **			
1	-	0.82*(E)	-	0.32(E)
2	-	-	0.66*(E)	-
3	3.01*	0.59 (E)	-	0.29(E)
4	-	-	0.57(E)	0.48*(E)
5	0.99(E)	0.70 (E)	-	-
6	1.67	-	-	-

** Based on Eq. (1)

Table A26

RESPONSE VALUES CORRESPONDING TO DIFFERENT EARTHQUAKE INPUT MOTIONS
[SI=0.75(SI$_{ref.}$), Duration = 10 sec.]

20-Story Isolated Structural Walls

M_y = Very Large (Elastic)

E.Q. Input No.	Fundamental Period, T_1 (sec.)			
	0.8	1.4	2.0	2.4
	Top Displacement (in.)			
1	-	-	-	7.7
2	-	-	10.8	-
3	4.4*	5.8	-	7.5
4	-	-	11.6*	12.3*
5	3.02	6.23*	-	-
6	-	-	-	-
	Interstory Displacement (in).			
1	-	-	-	0.56
2	-	-	0.81 *	-
3	0.29*	0.41	-	0.60*
4	-	-	0.78	-
5	0.21	0.45	-	-
6	-	-	-	-
	Horizontal Shear at Base (k)			
1	-	1,041	-	840*
2	-	-	1,196*	-
3	1,379	940	-	718
4	-	-	617	649
5	1,442*	1,210*	-	-
6	-	-	-	-
	Bending Moment at Base (in-k)			
1	-	1,291,000*	-	509,000
2	-	-	1,045,000*	-
3	2,005,000*	933,000	-	458,000
4	-	-	891,000	760,000*
5	1,561,000	1,099,000	-	-
6	-	-	-	-

*Critical (maximum) value for particular T_1

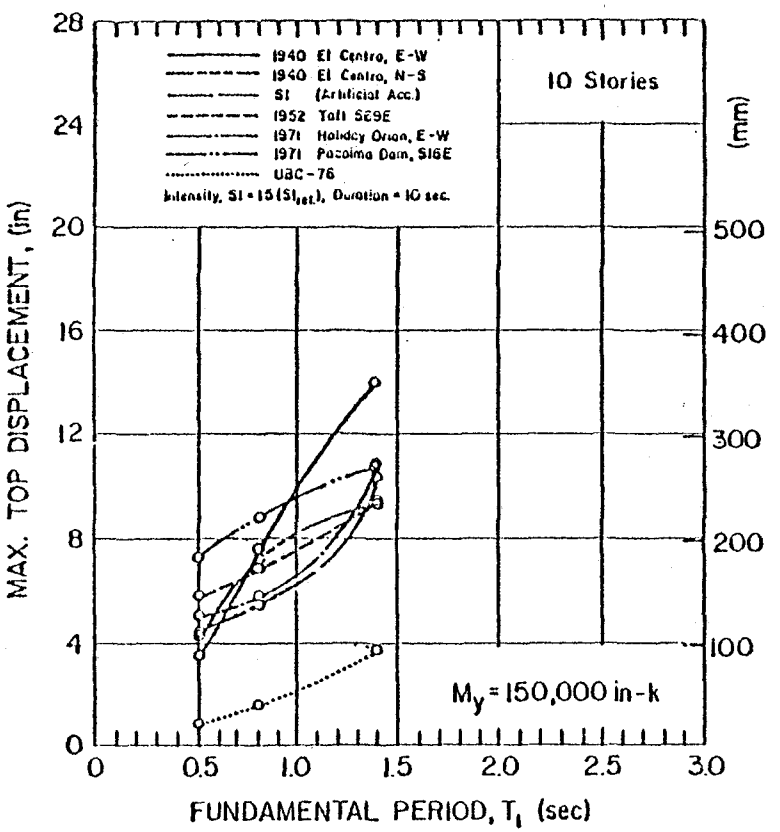

(a)

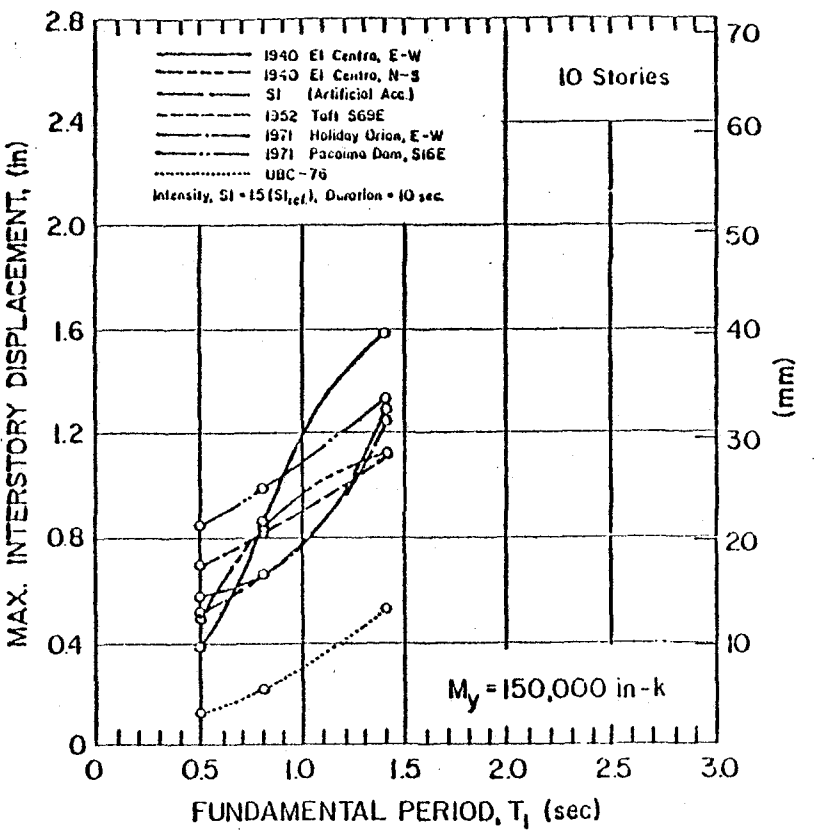

(b)

Fig. A1 Maximum Response Values for Different Input Motions
10-Story Isolated Structural Walls - M_y = 150,000 in.-k

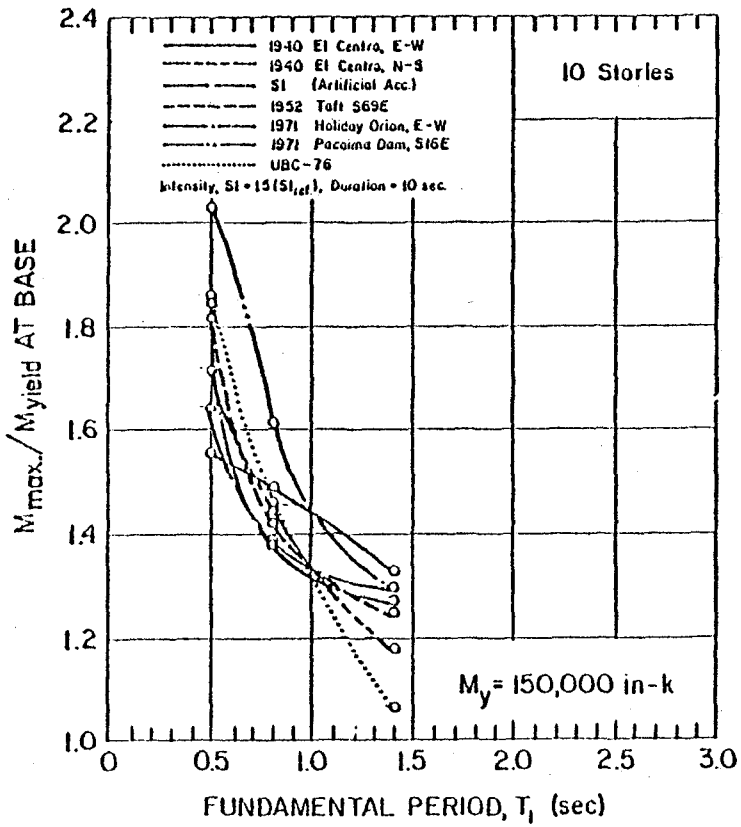

(c)

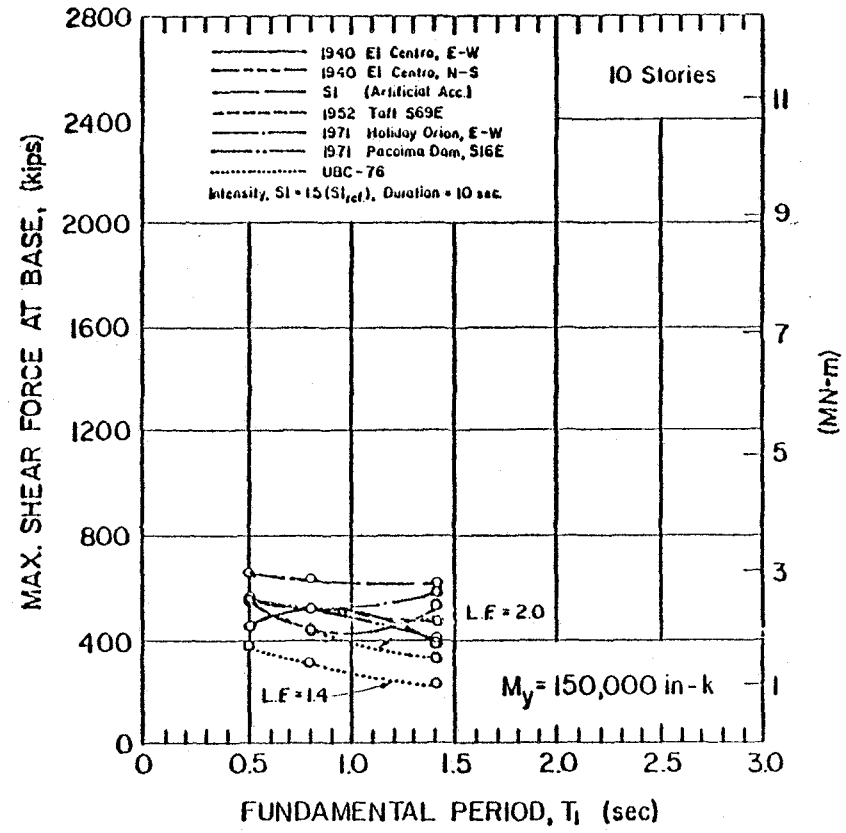

(d)

Fig. A1 (cont'd.) Maximum Response Values for Different Input Motions
10-Story Isolated Structural Walls - M_y = 150,000 in.-k

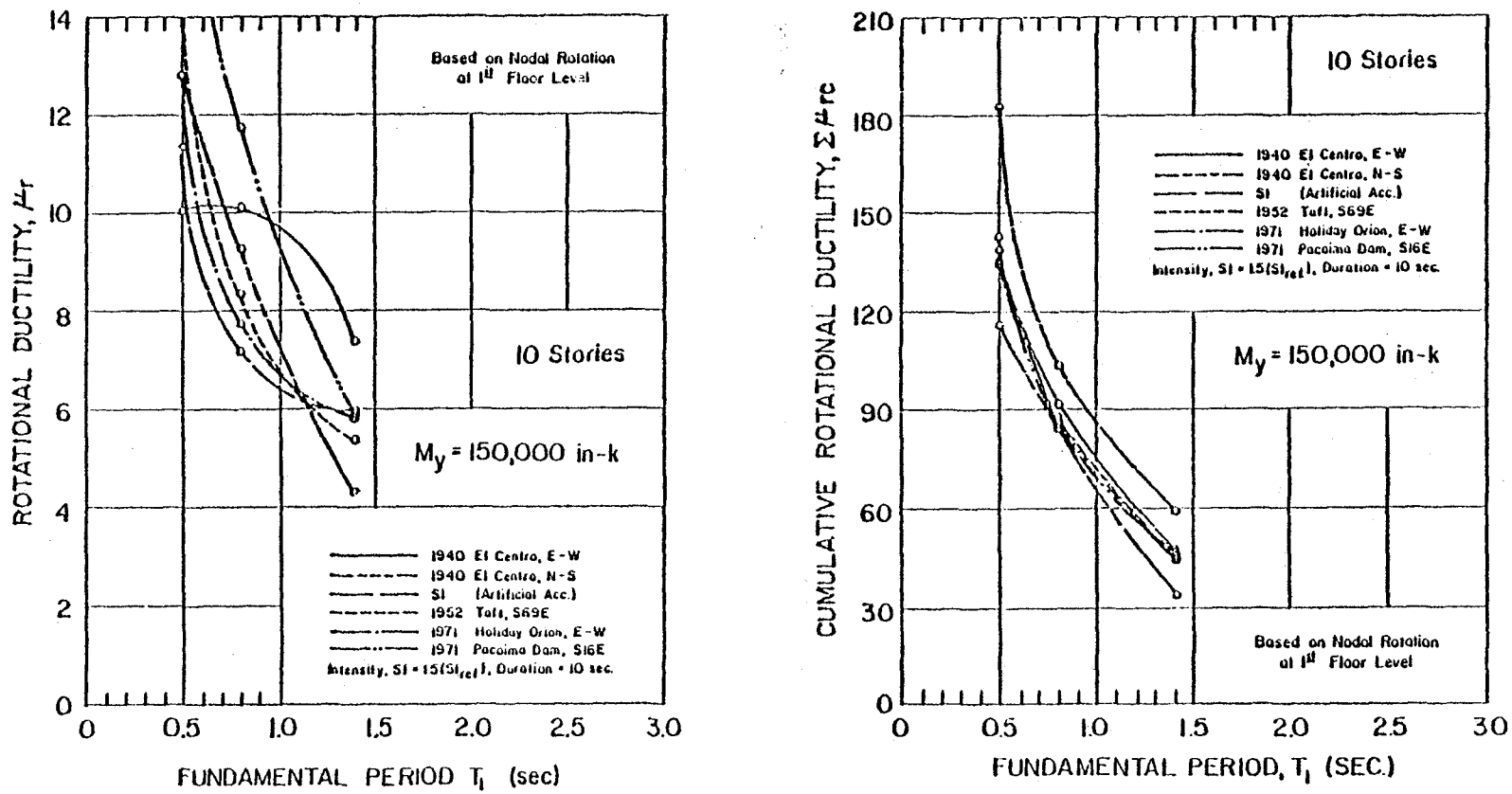

Fig. A1 (cont'd.) Maximum Response Values for Different Input Motions
10-Story Isolated Structural Walls - M_y = 150,000 in.-k

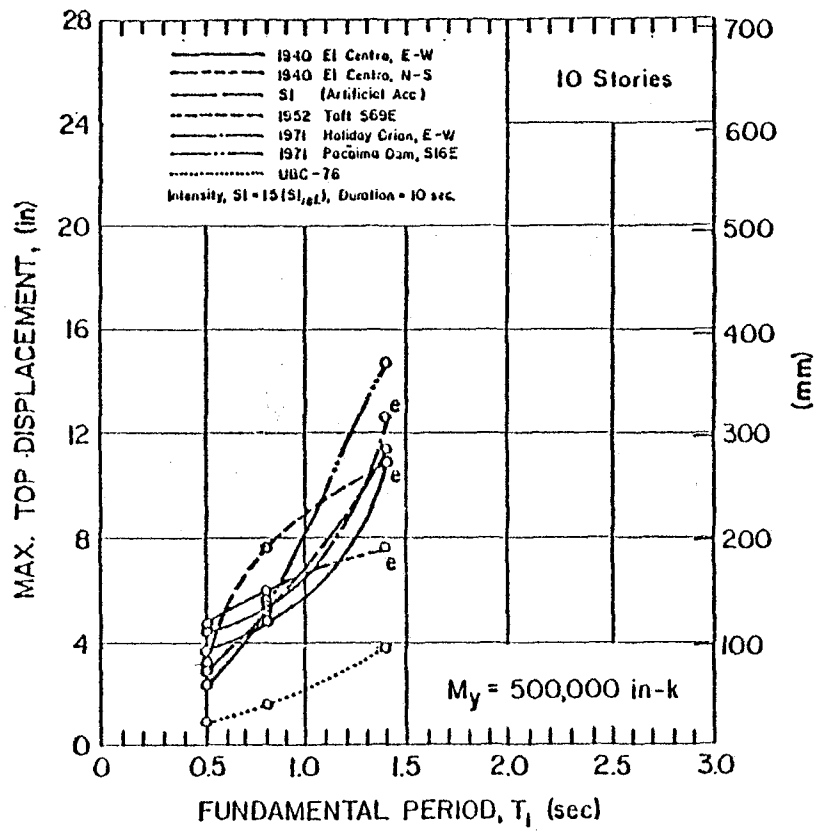

(a)

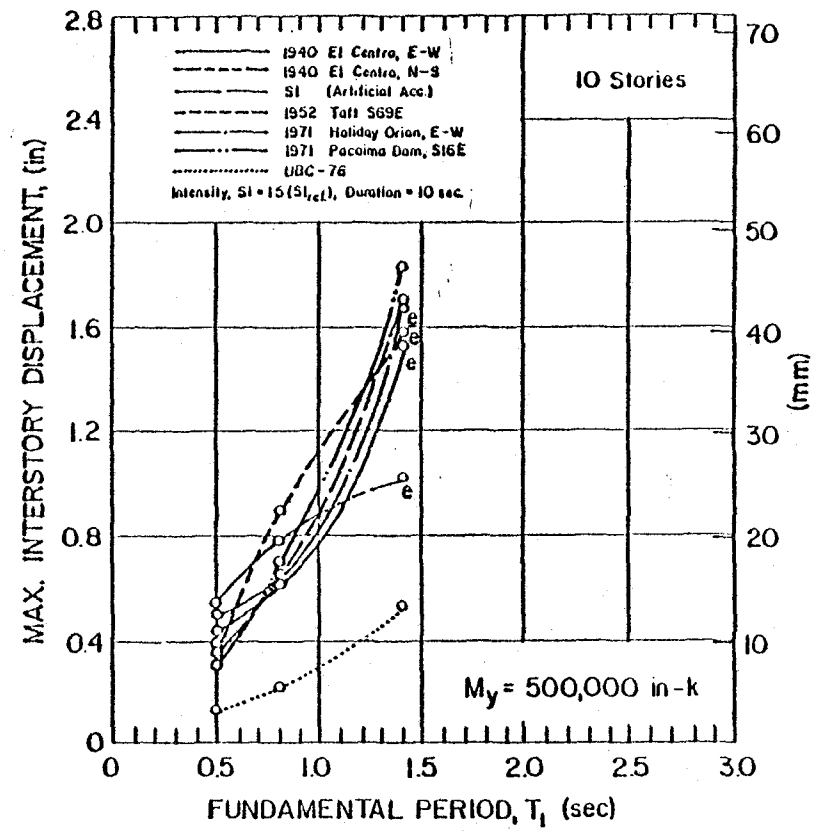

(b)

Fig. A2 Maximum Response Values for Different Input Motions
10-Story Isolated Structural Walls - M_y = 500,000 in.-k

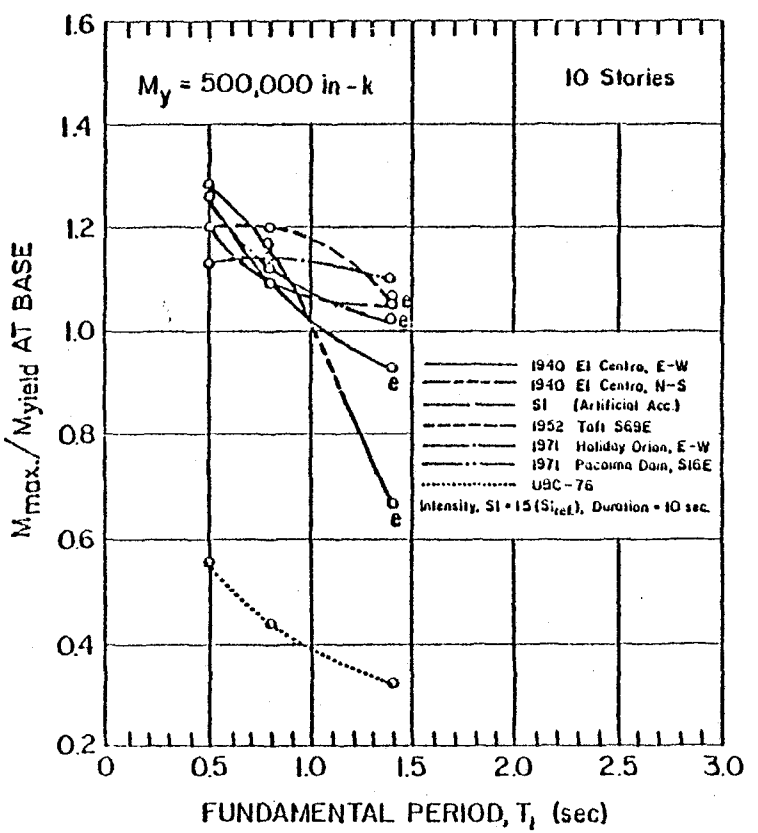

(c)

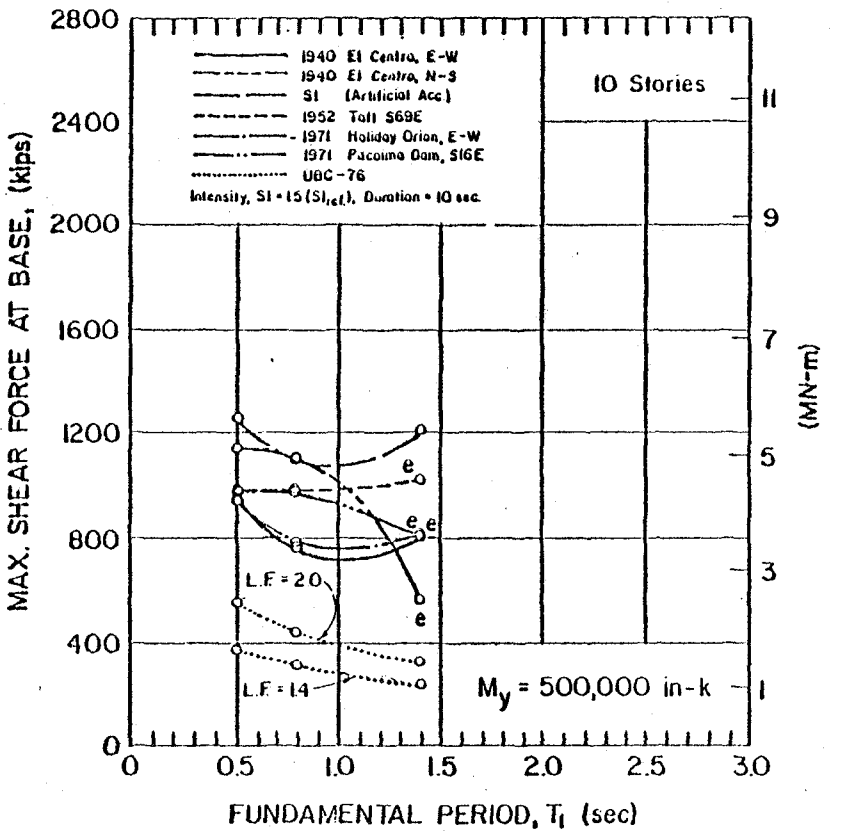

(d)

Fig. A2 (cont'd.) Maximum Response Values for Different Input Motions
10-Story Isolated Structural Walls - M_y = 500,000 in.-k

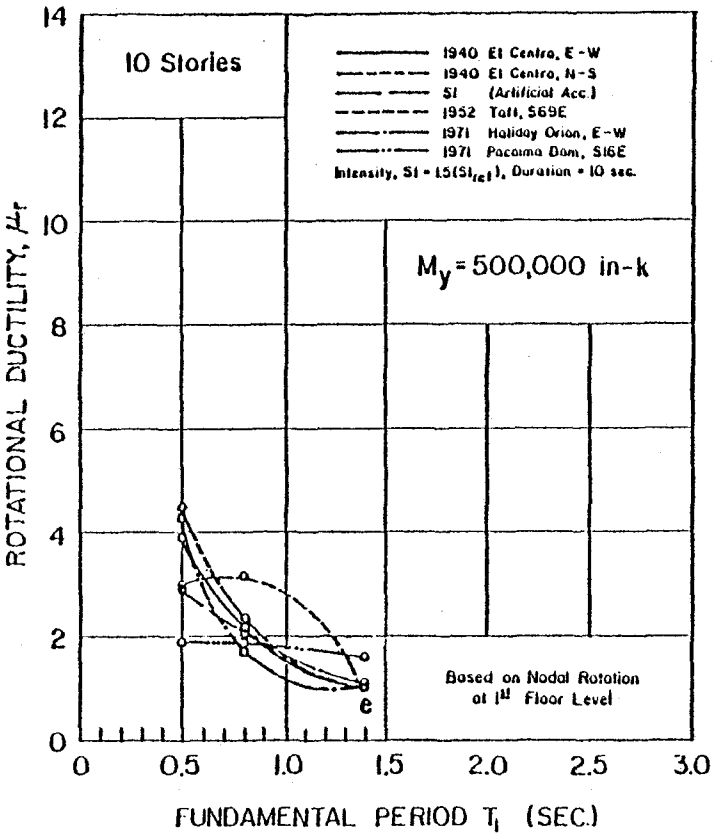

(e)

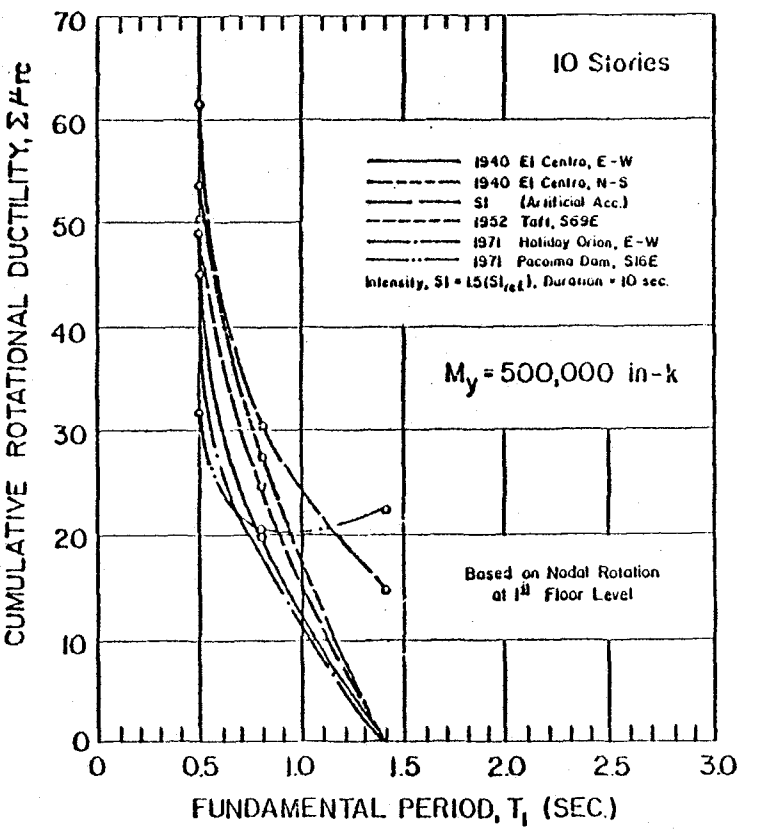

(f)

Fig. A2 (cont'd.) Maximum Response Values for Different Input Motions
10-Story Isolated Structural Walls - M_y = 500,000 in.-k

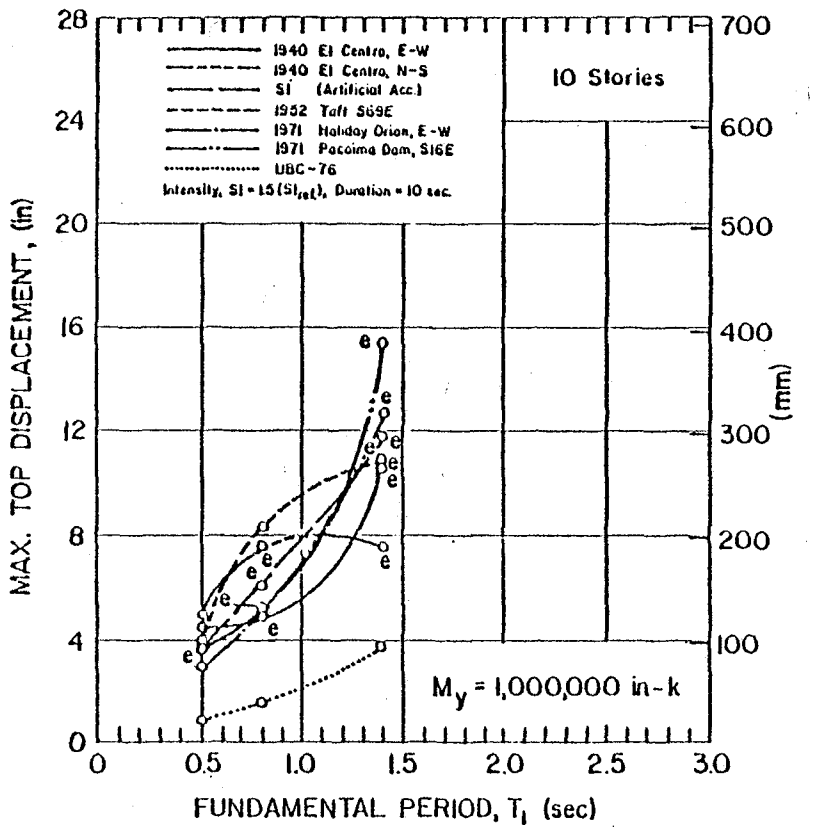

(a)

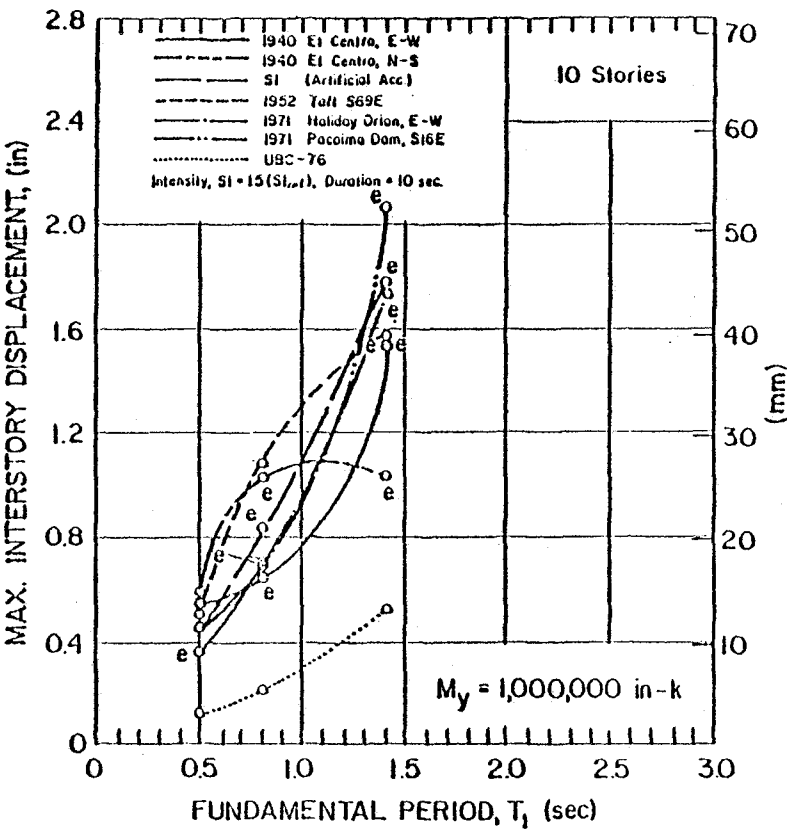

(b)

Fig. A3 Maximum Response Values for Different Input Motions
10-Story Isolated Structural Walls - M_y = 1,000,000 in.-k

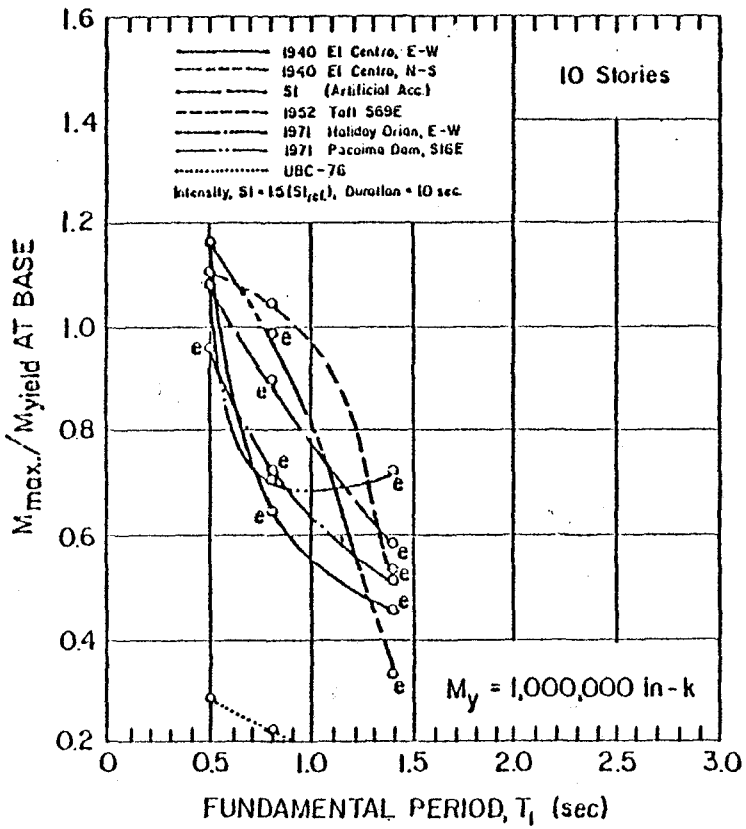

(c)

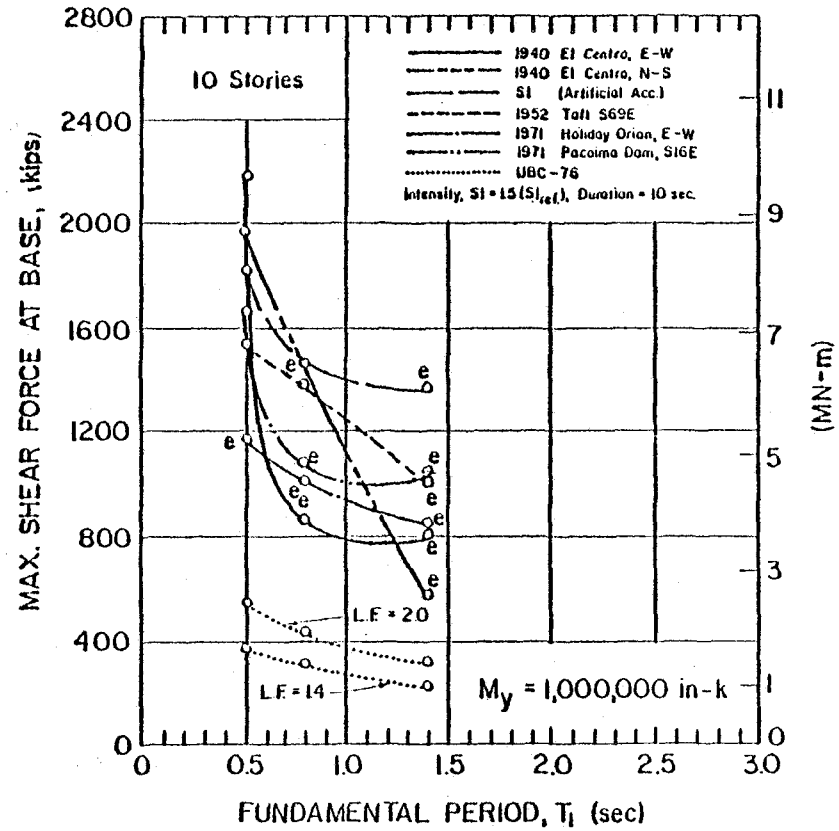

(d)

Fig. A3 (cont'd.) Maximum Response Values for Different Input Motions
10-Story Isolated Structural Walls - M_y = 1,000,000 in.-k

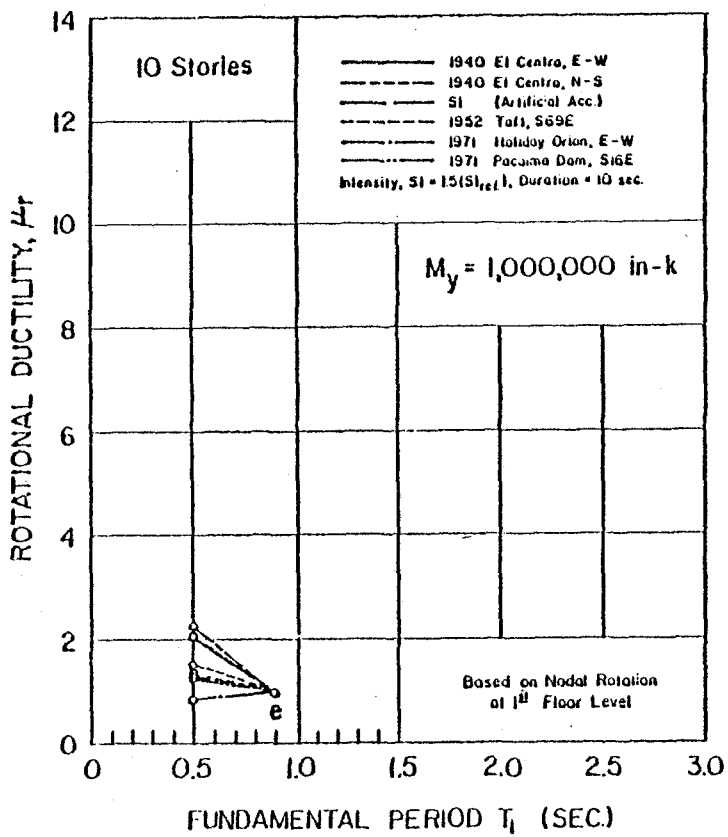

(e)

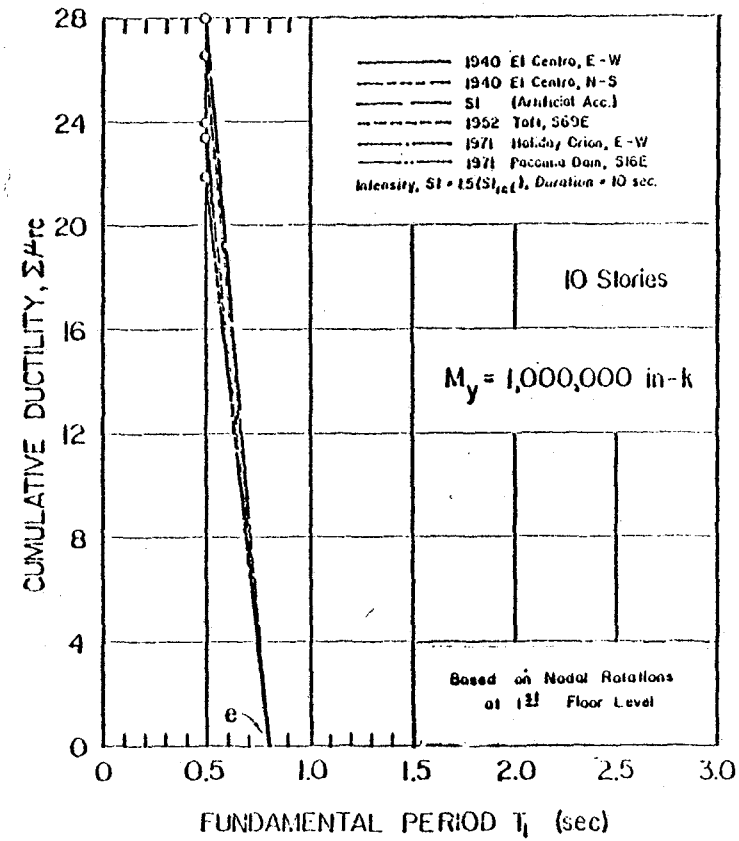

(f)

Fig. A3 (cont'd.) Maximum Response Values for Different Input Motions
10-Story Isolated Structural Walls - M_y = 1,000,000 in.-k

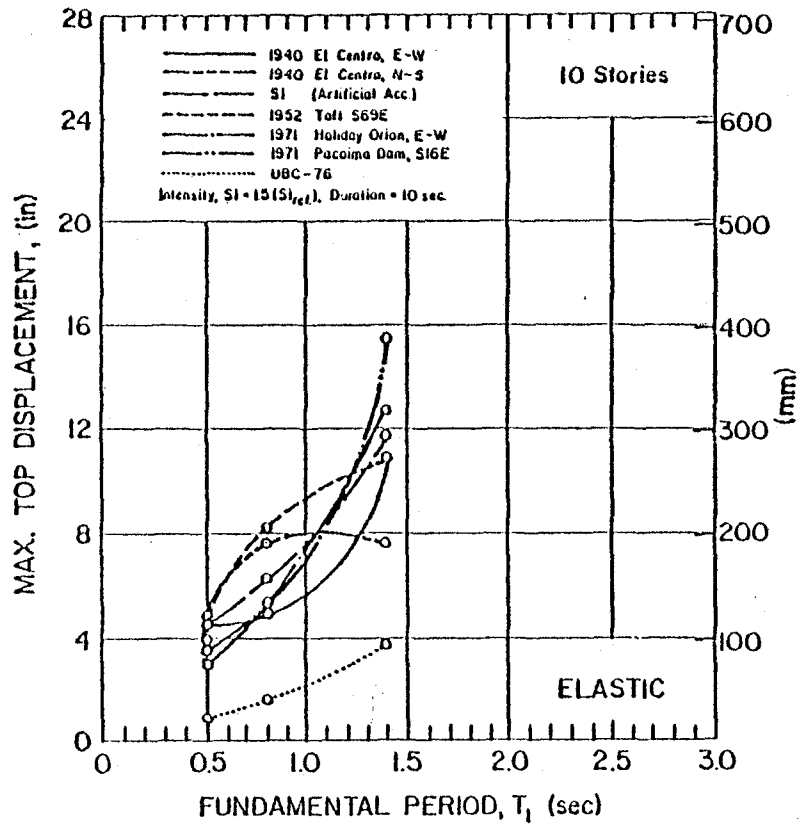

(a)

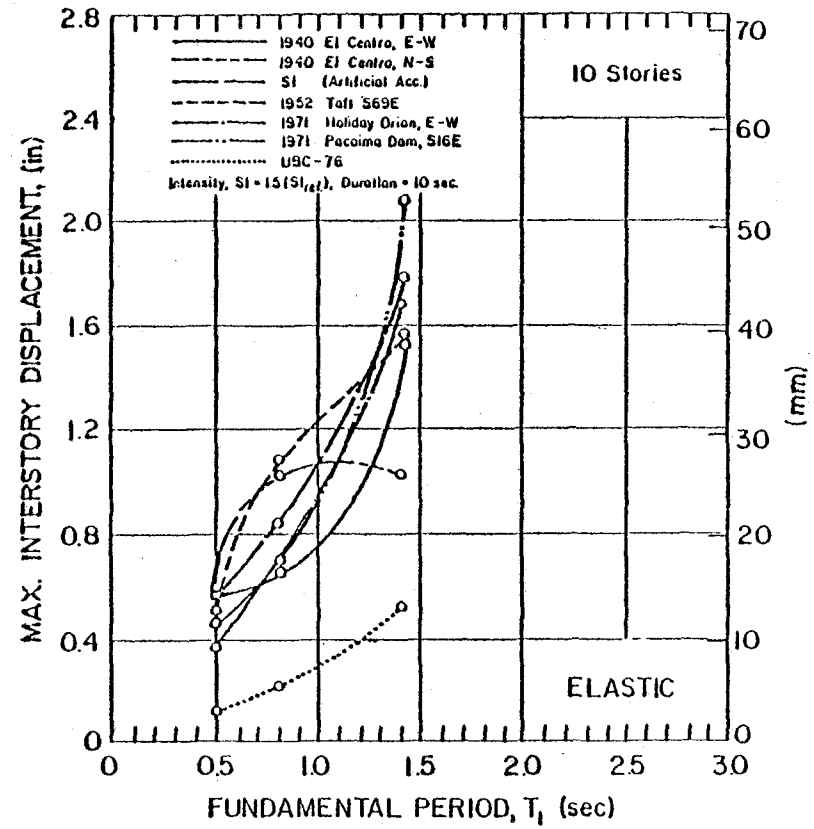

(b)

Fig. A4 Maximum Response Values for Different Input Motions
10-Story Isolated Structural Walls - Elastic Case

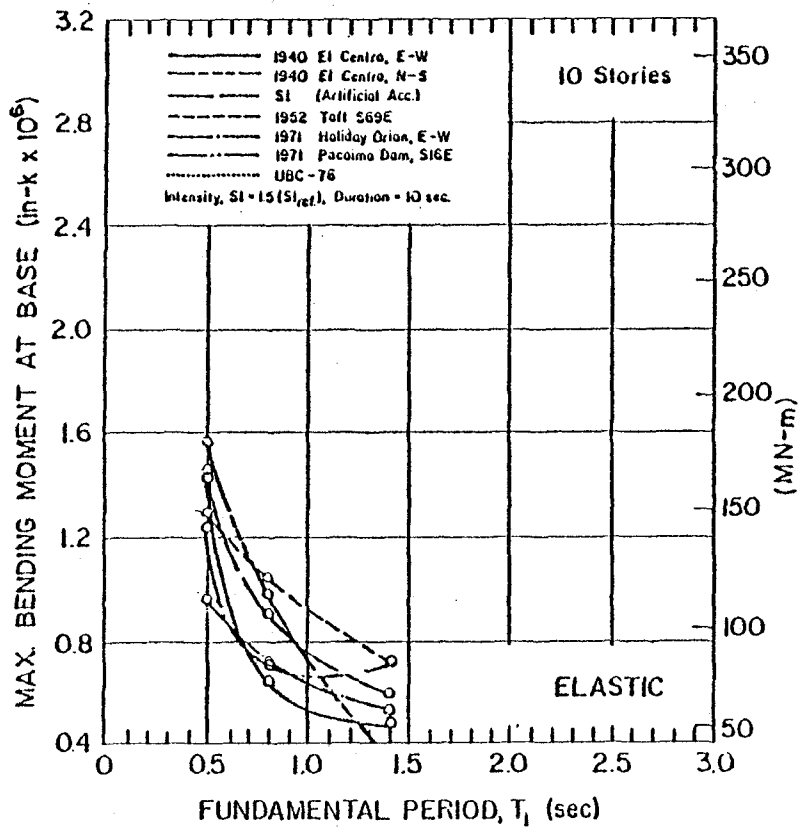

(c)

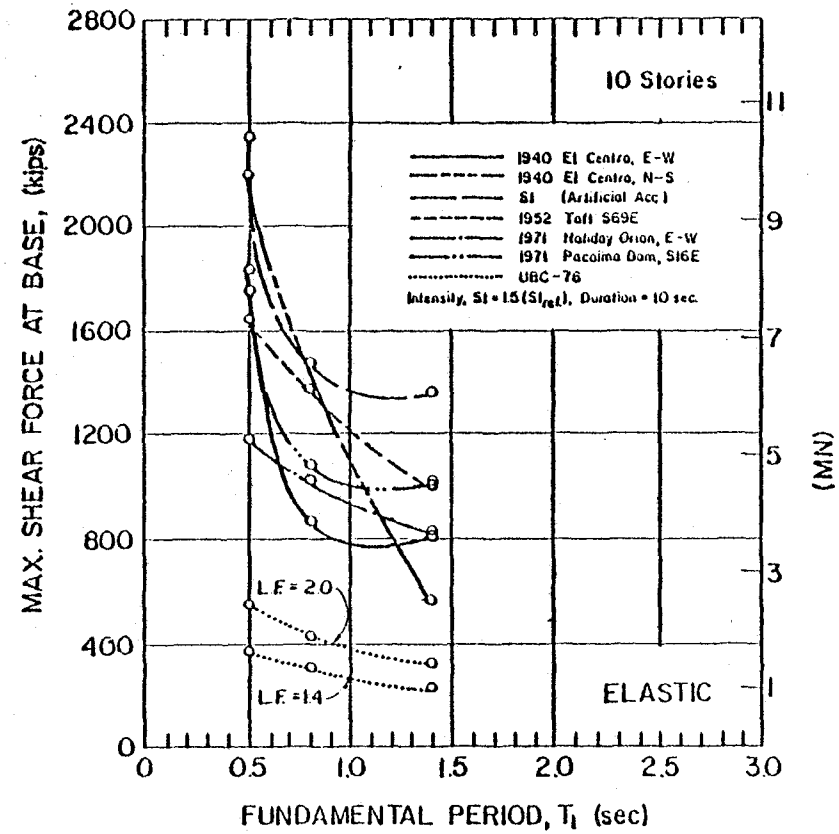

(d)

Fig. A4 (cont'd) Maximum Response Values for Different Input Motions
10-Story Isolated Structural Walls - Elastic Case

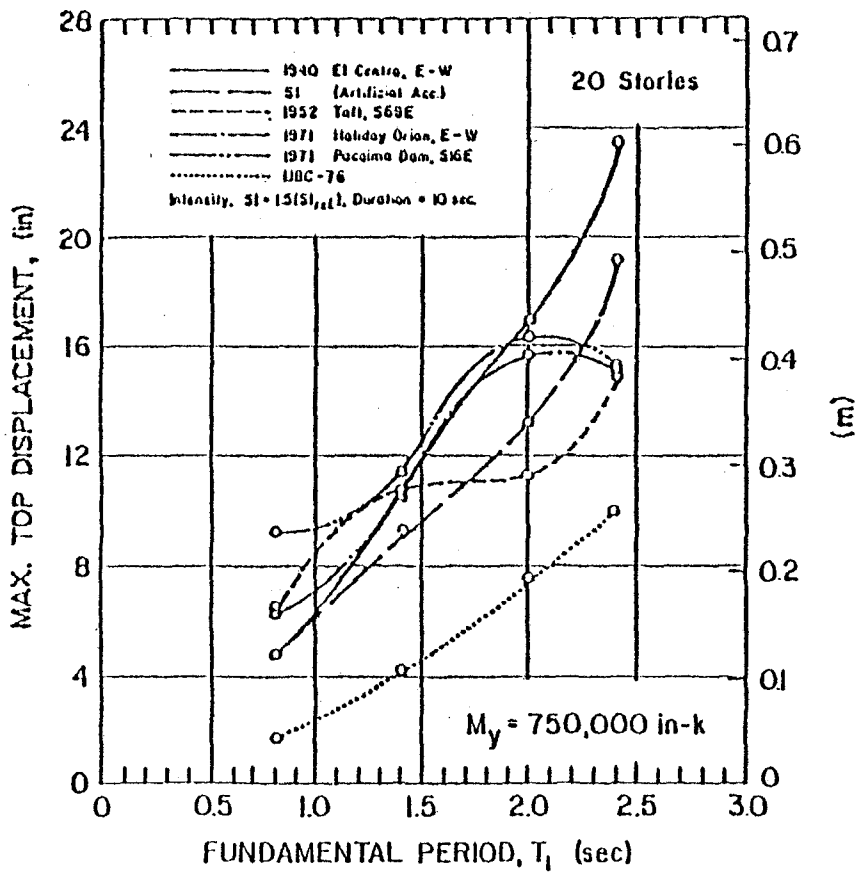

(a)

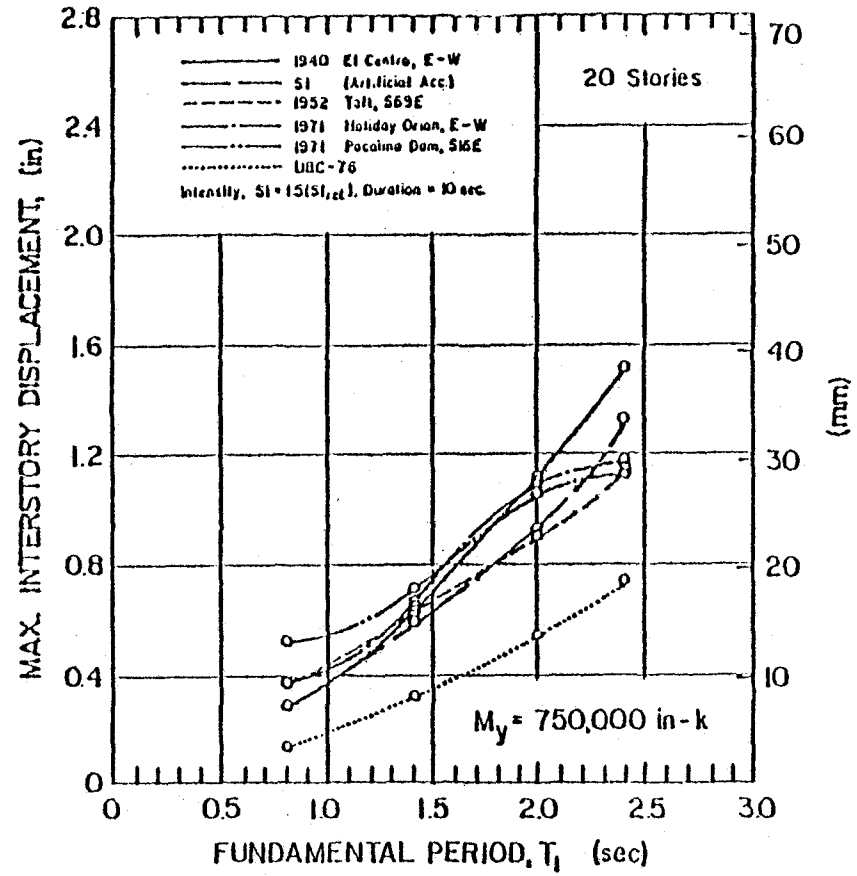

(b)

Fig. A5 Maximum Response Values for Different Input Motions
20-Story Isolated Structural Walls - M_y = 750,000 in.-k

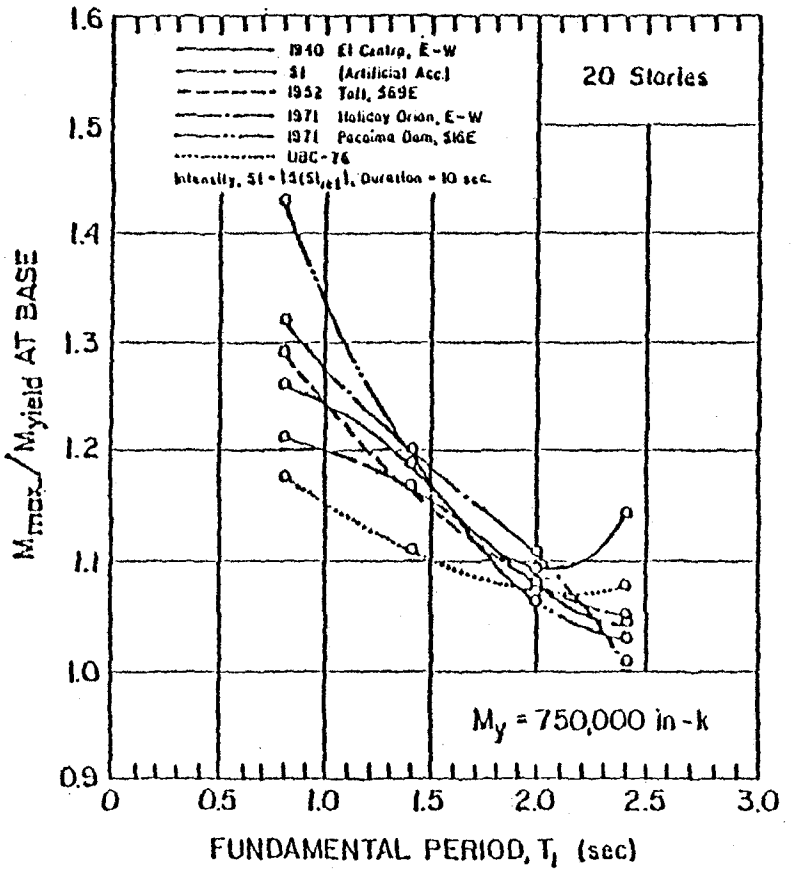

(c)

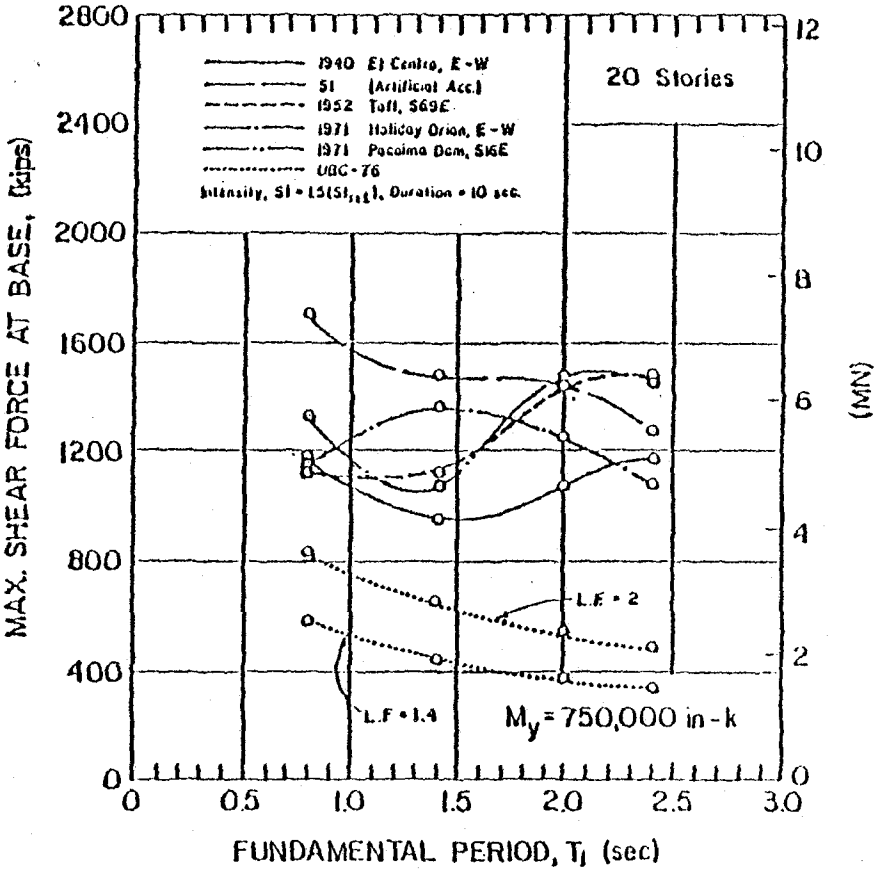

(d)

Fig. A5 (cont'd.) Maximum Response Values for Different Input Motions
20-Story Isolated Structural Walls - M_y = 750,000 in.-k

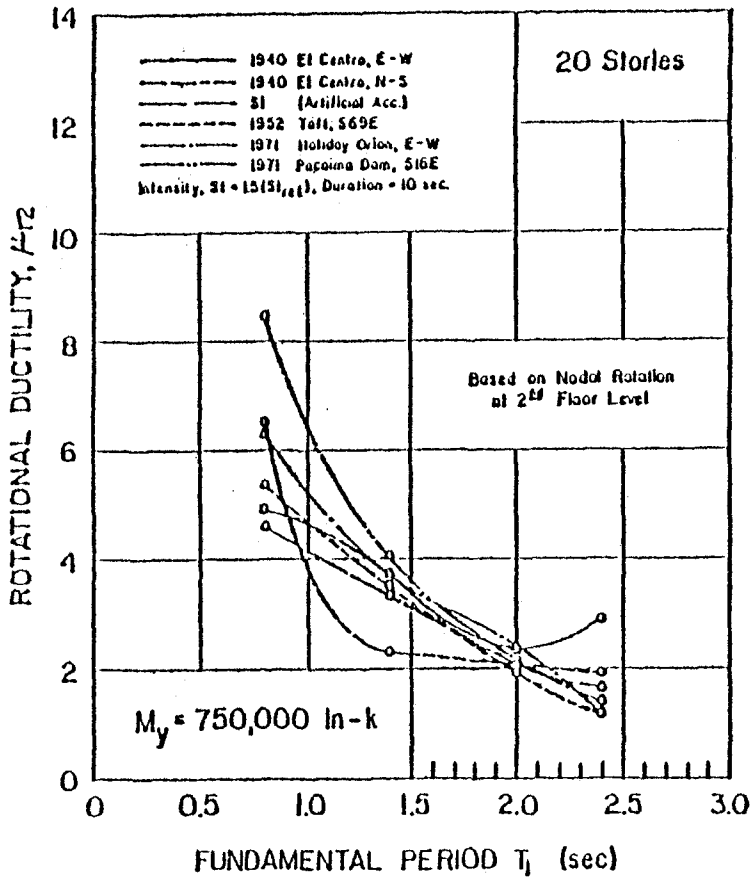

(e)

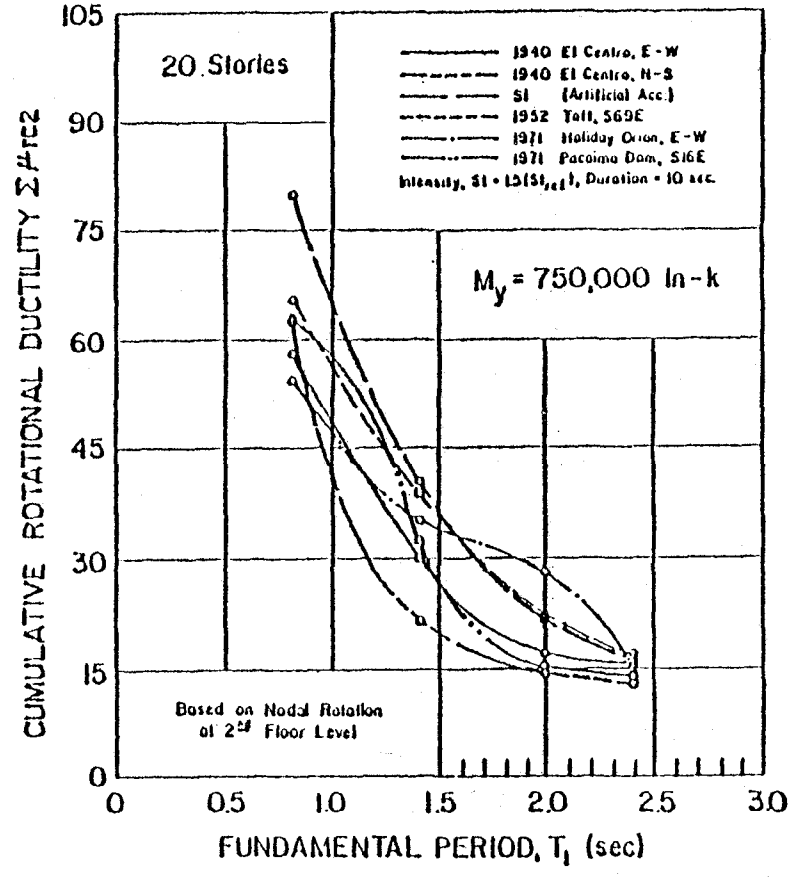

(f)

Fig. A5 (cont'd.) Maximum Response Values for Different Input Motions 20-Story Isolated Structural Walls - M_y = 750,000 in.-k

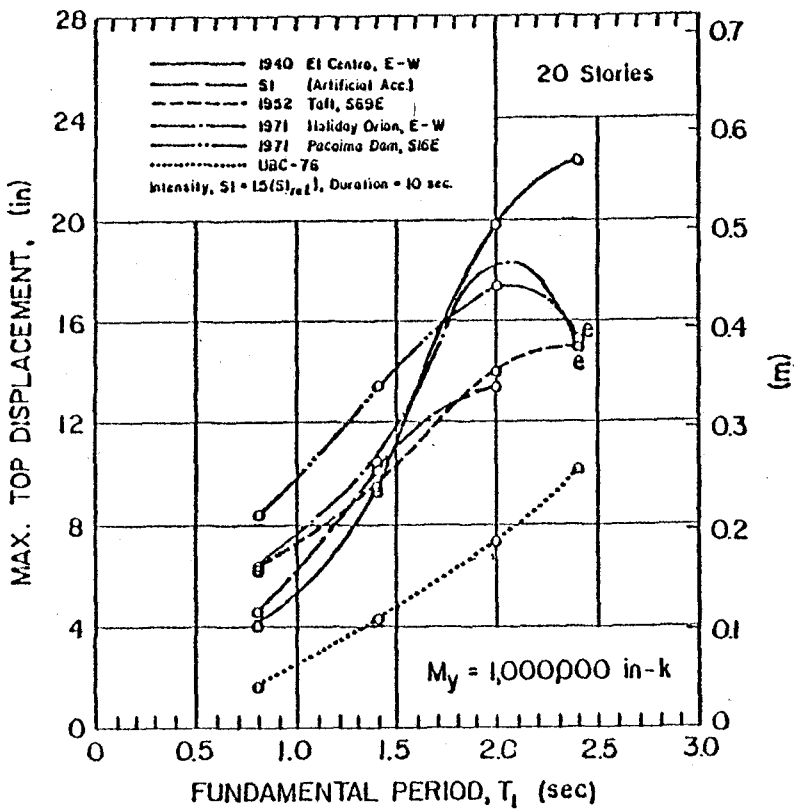

(a)

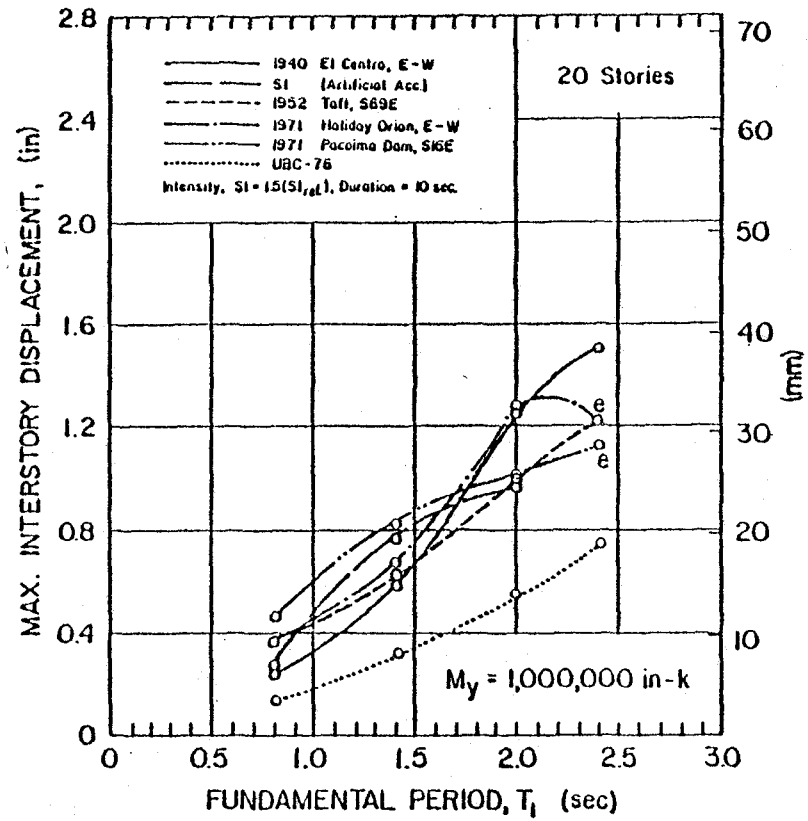

(b)

Fig. A6 Maximum Response Values for Different Input Motions
20-Story Isolated Structural Walls - M_y = 1,000,000 in.-k

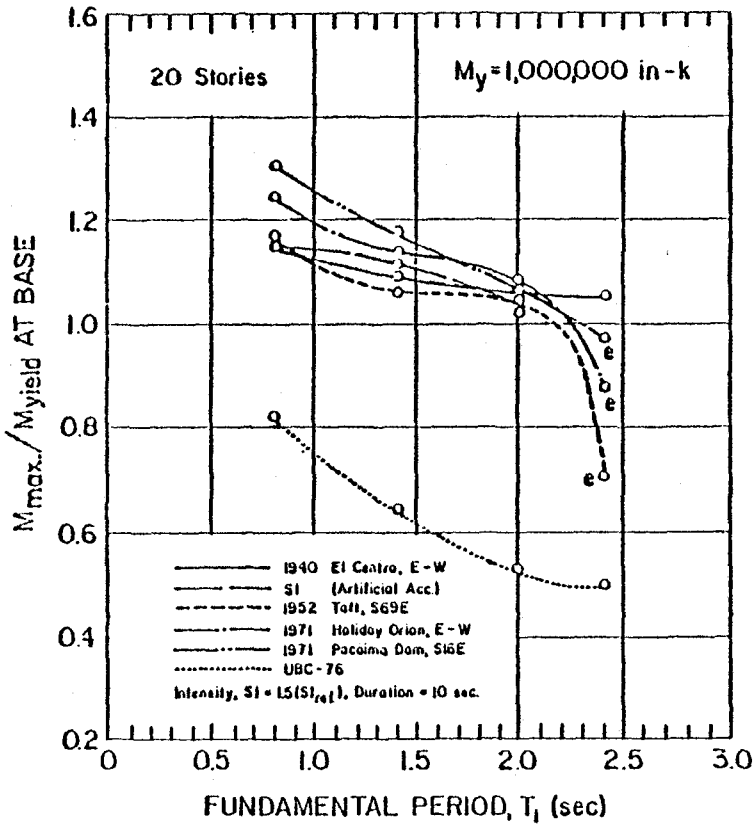

(c)

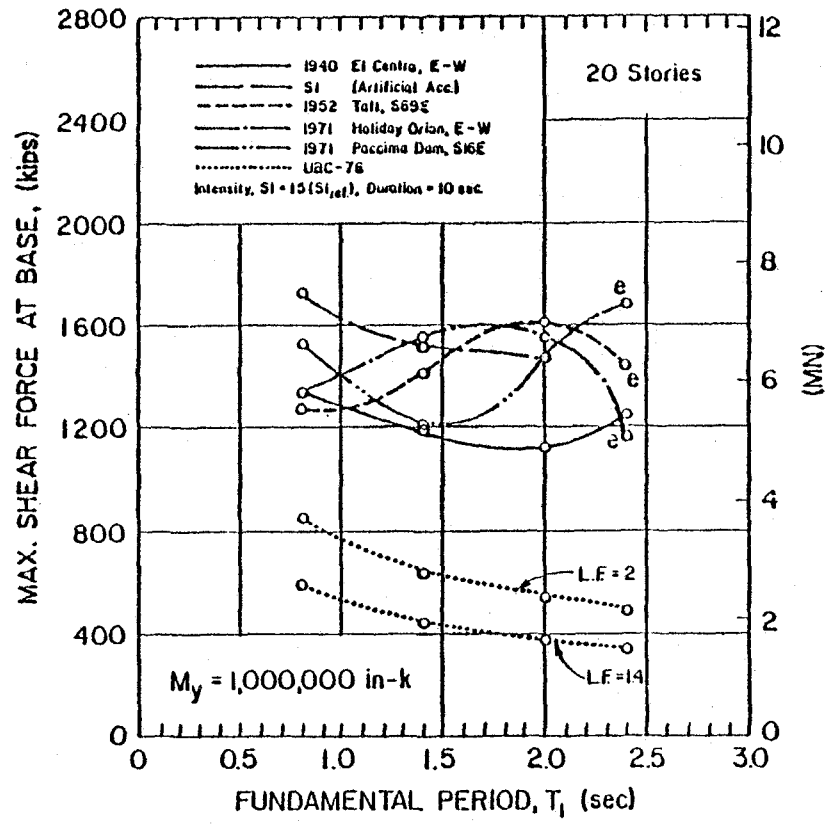

(d)

Fig. A6 (cont'd) Maximum Response Values for Different Input Motions 20-Story Isolated Structural Walls- M_y = 1,000,000 in.-k

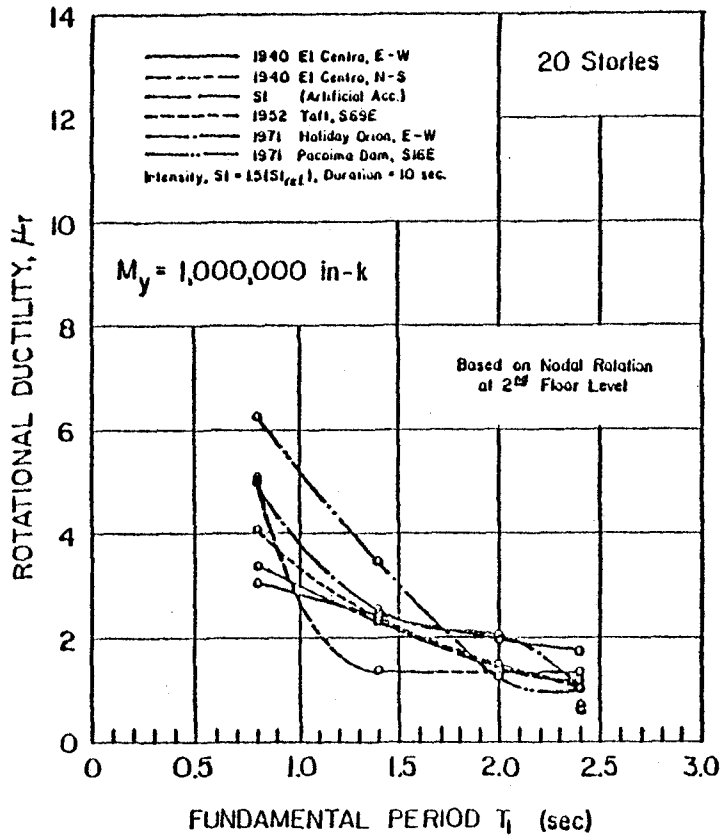

(e)

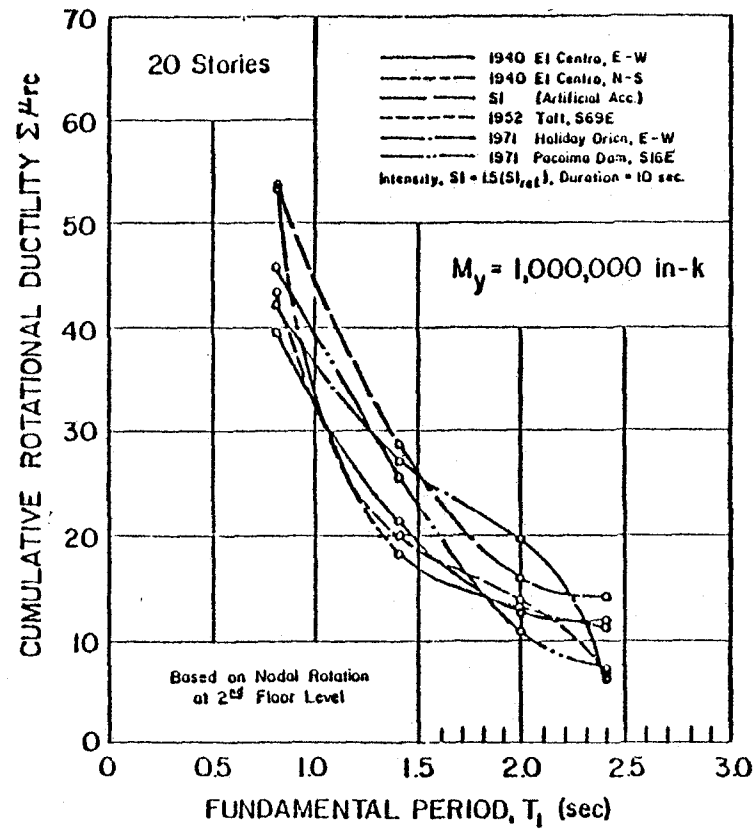

(f)

Fig. A6 (cont'd.) Maximum Response Values for Different Input Motions
20-Story Isolated Structural Walls - M_y = 1,000,000 in.-k

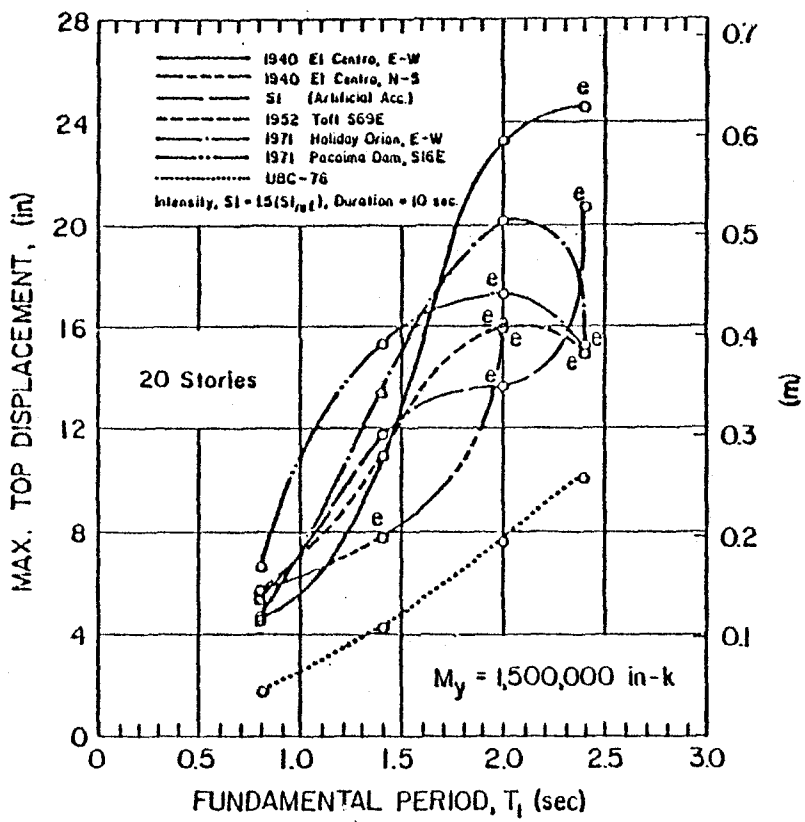

(a)

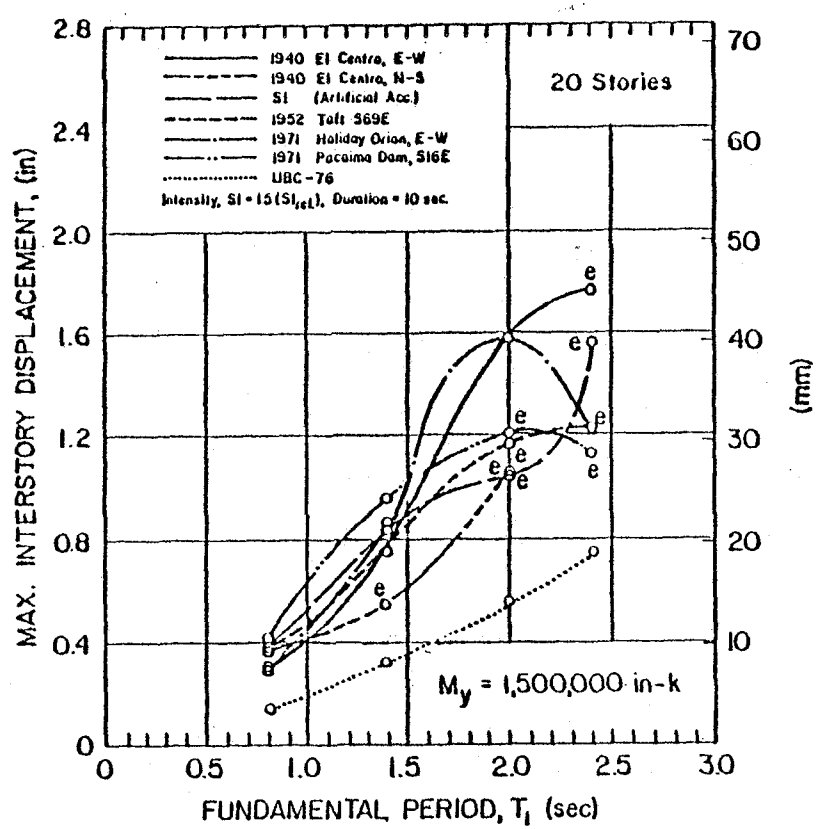

(b)

Fig. A7 Maximum Response Values for Different Input Motions
20-Story Isolated Structural Walls - M_y = 1,500,000 in.-k

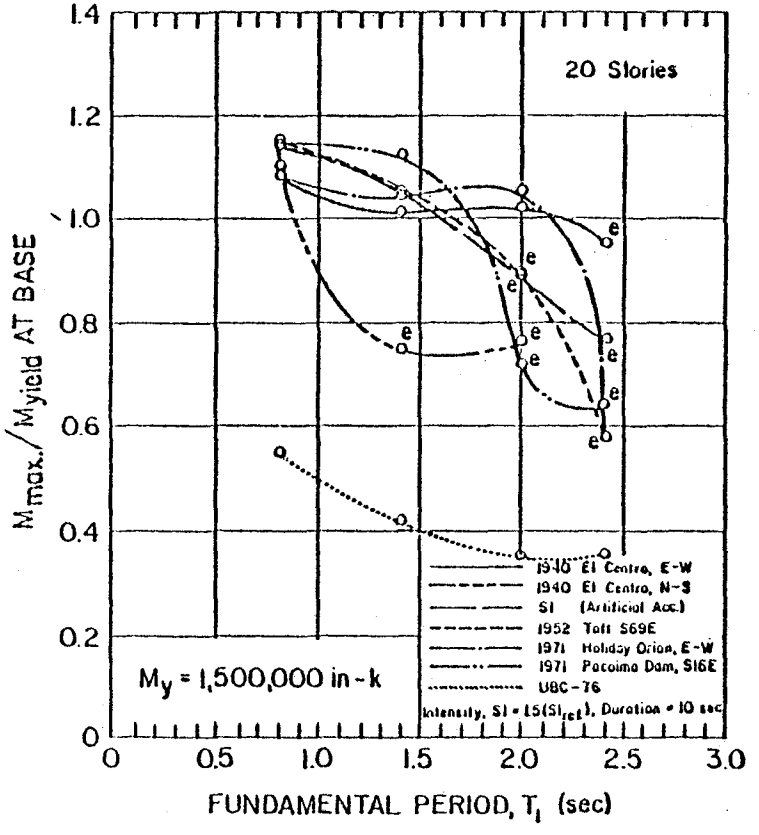

(c)

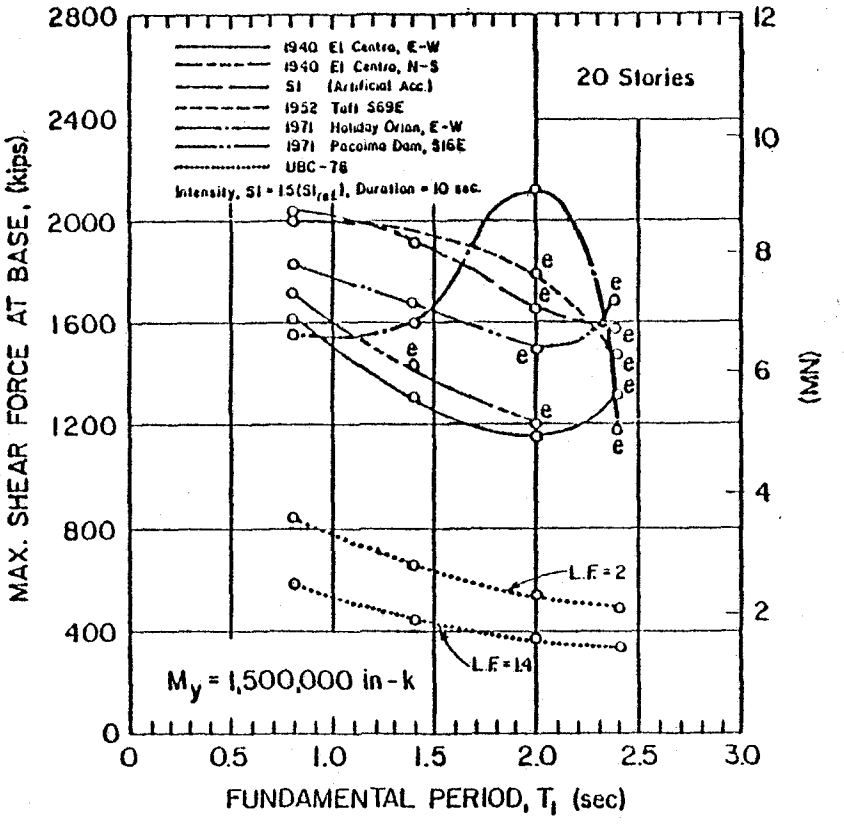

(d)

Fig. A7 (cont'd.) Maximum Response Values for Different Input Motions
20-Story Isolated Structural Walls - M_y = 1,500,000 in.-k

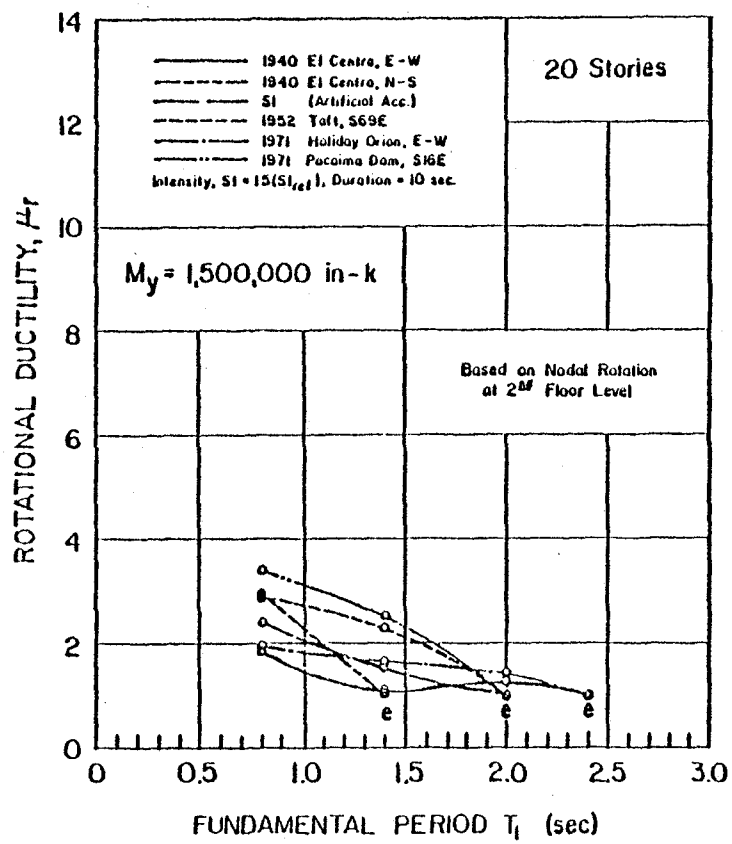

(e)

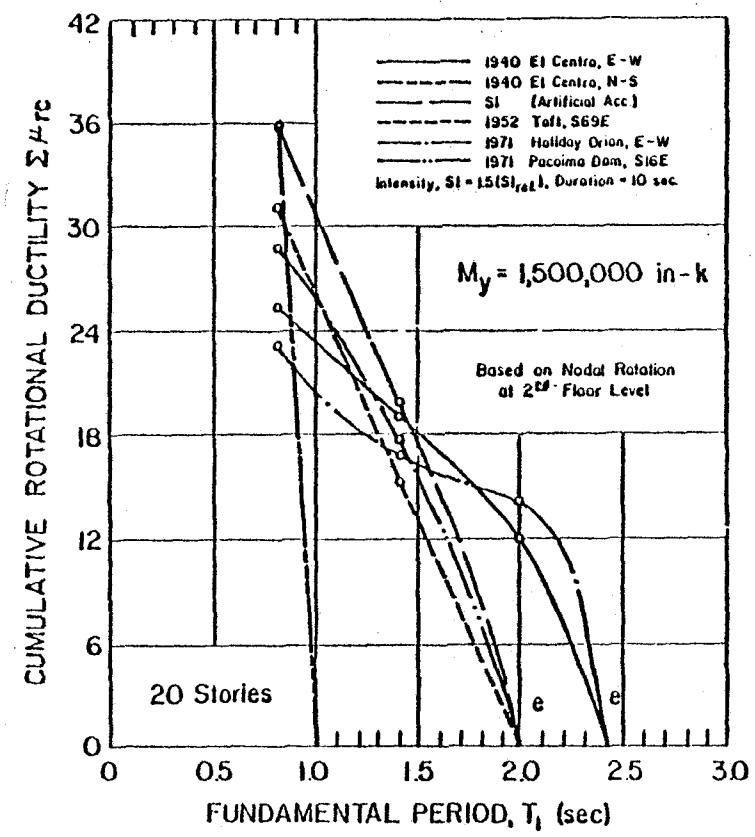

(f)

Fig. A7 (cont'd.) Maximum Response Values for Different Input Motions
20-Story Isolated Structural Walls - M_y = 1,500,000 in.-k

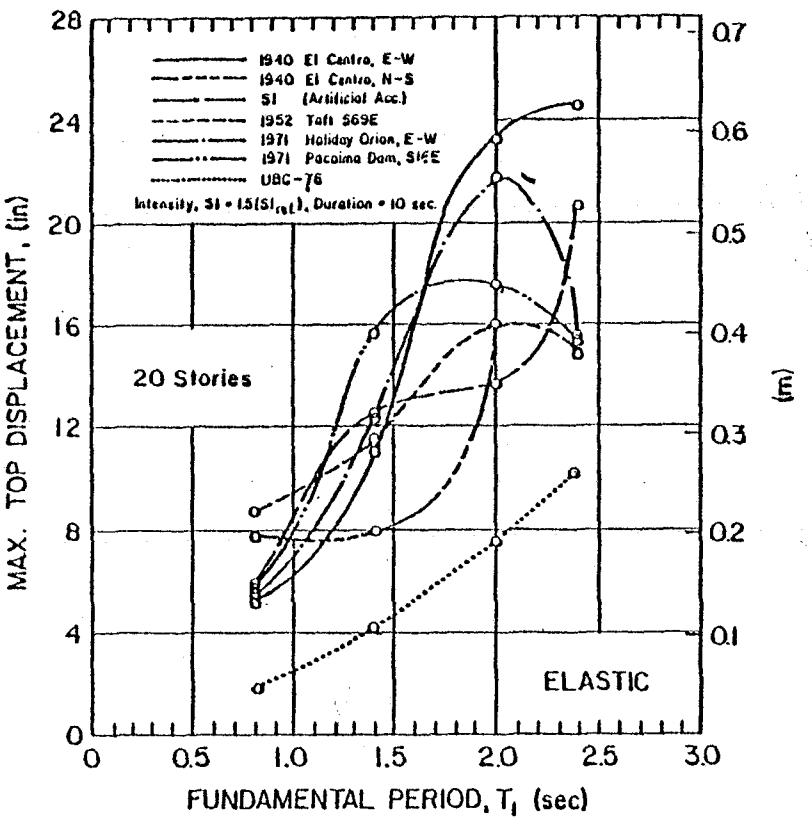

(a)

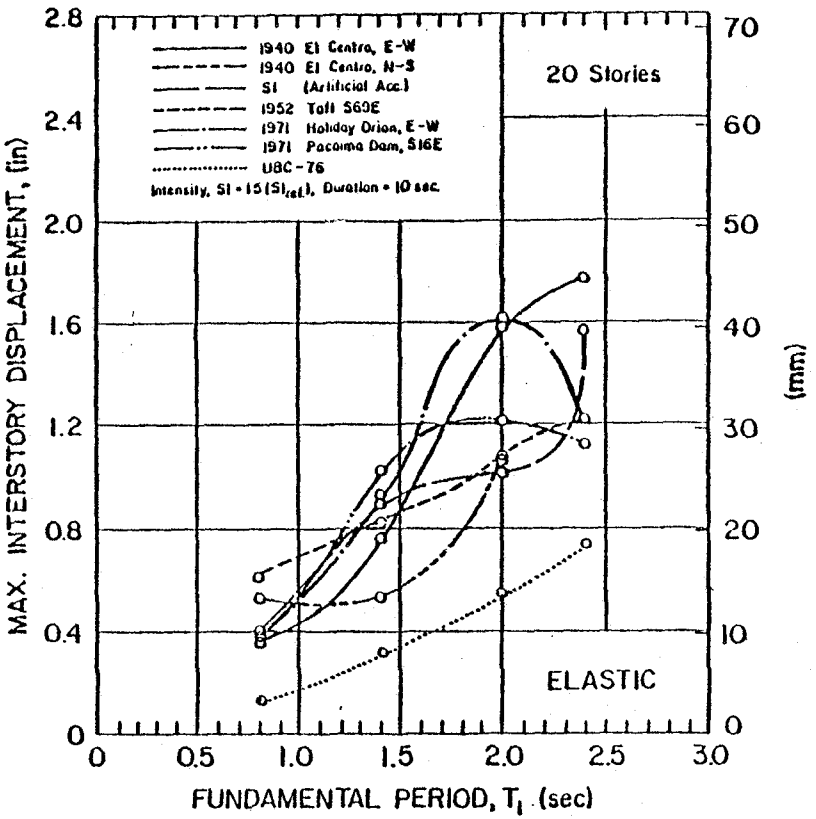

(b)

Fig. A8 Maximum Response Values for Different Input Motions
20-Story Isolated Structural Walls - Elastic Case

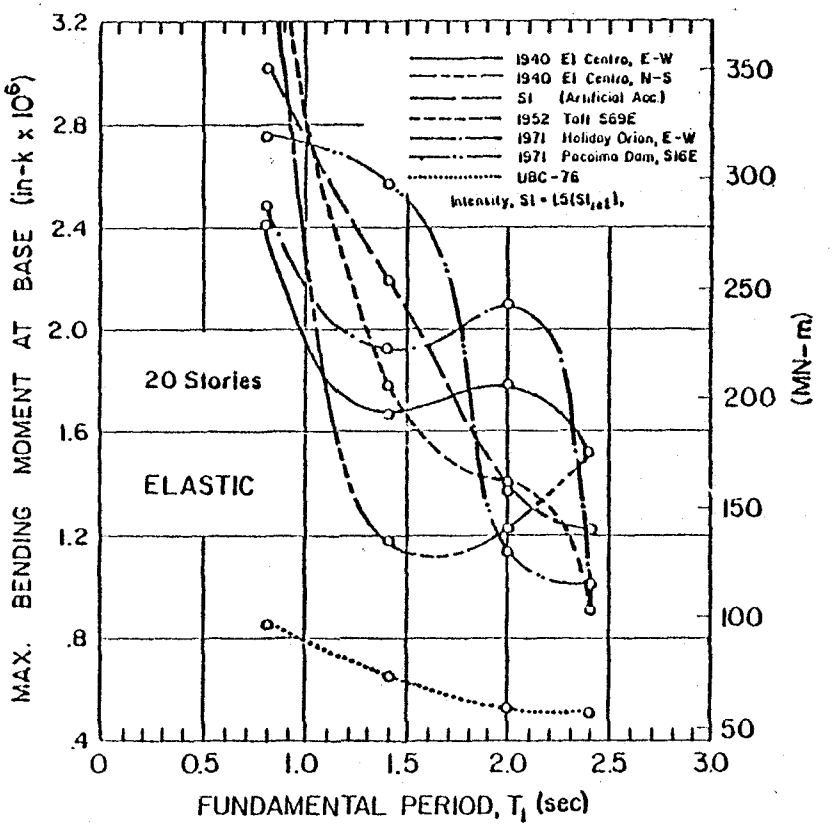

(c)

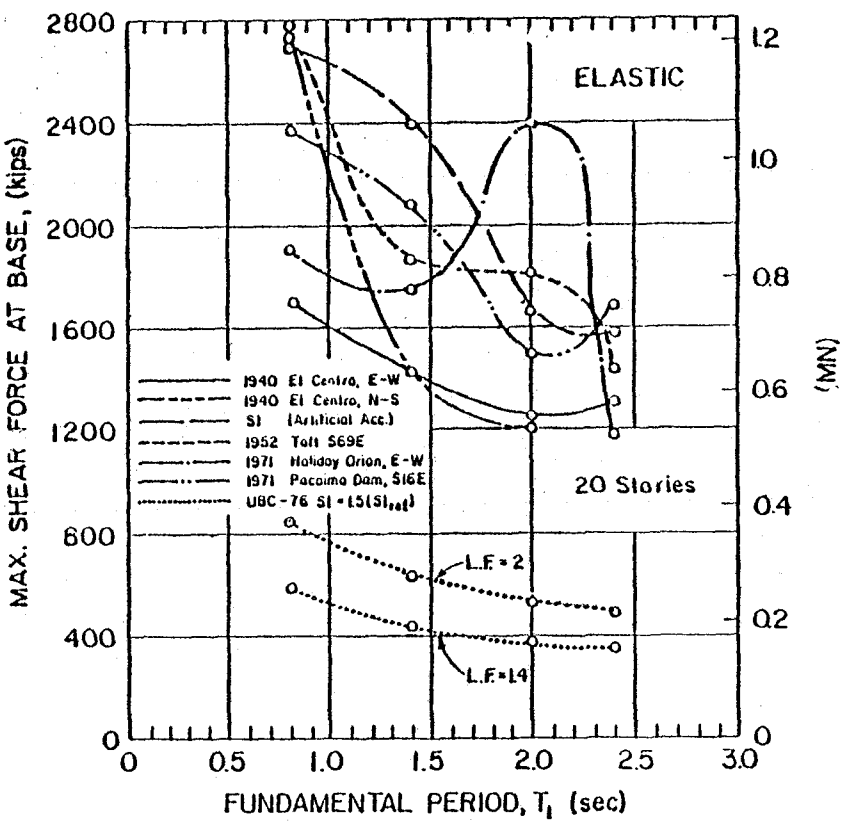

(d)

Fig. A8 (cont'd.) Maximum Response Values for Different Input Motions 20-Story Isolated Structural Walls - Elastic Case

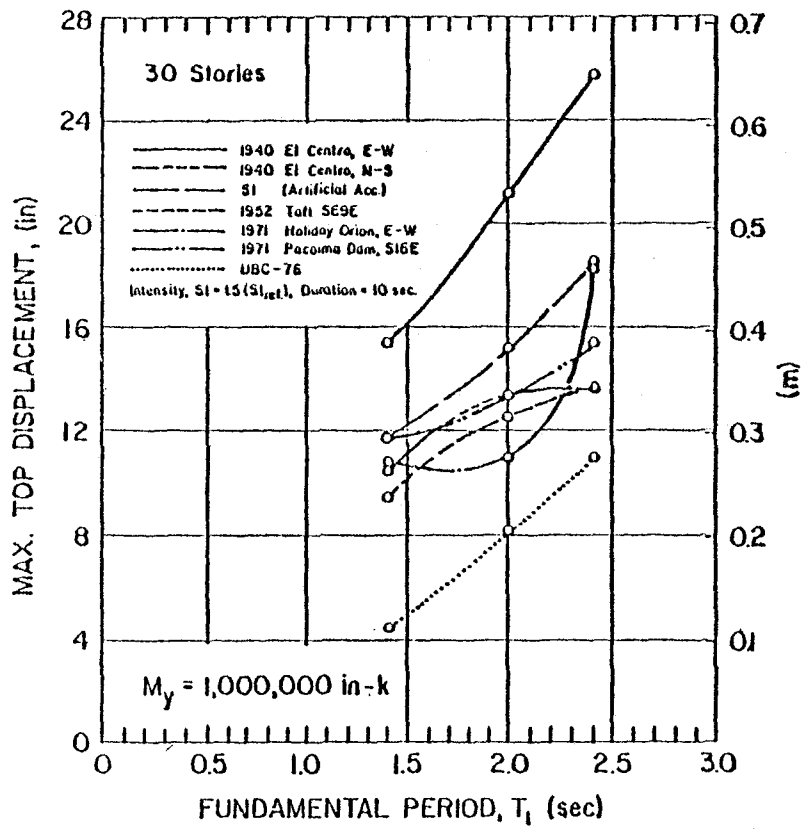

(a)

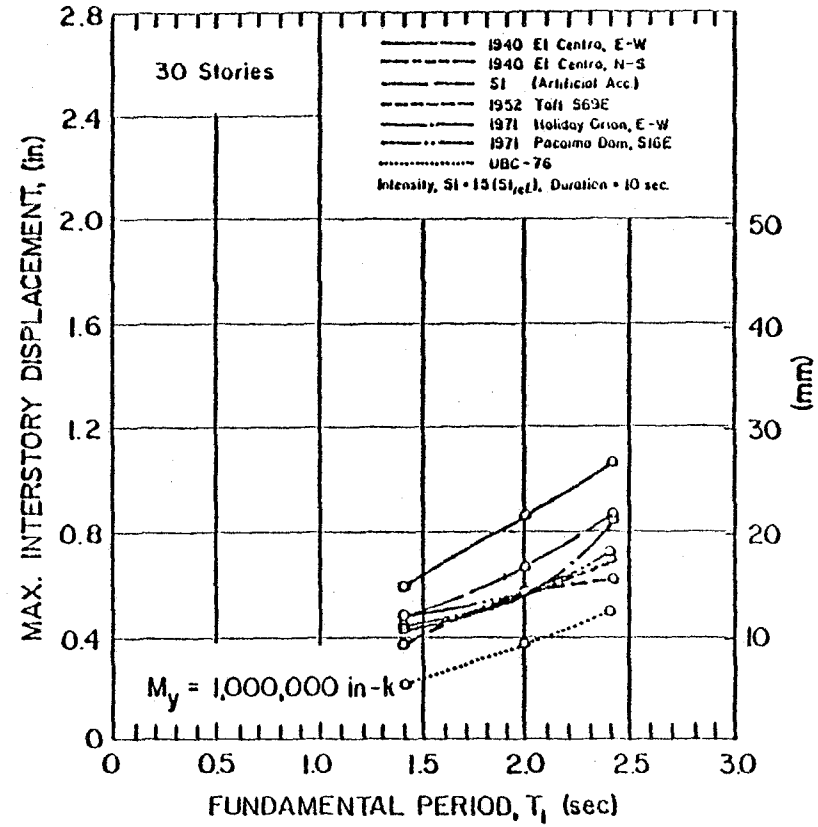

(b)

Fig. A9 Maximum Response Values for Different Input Motions
30-Story Isolated Structural Walls - M_y = 1,000,000 in.-k

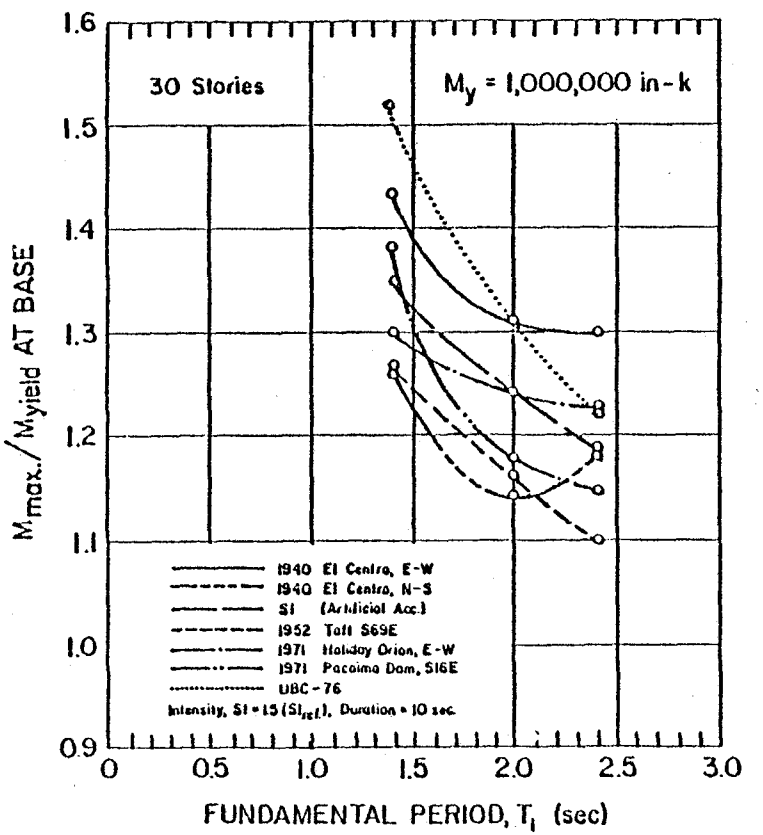

(c)

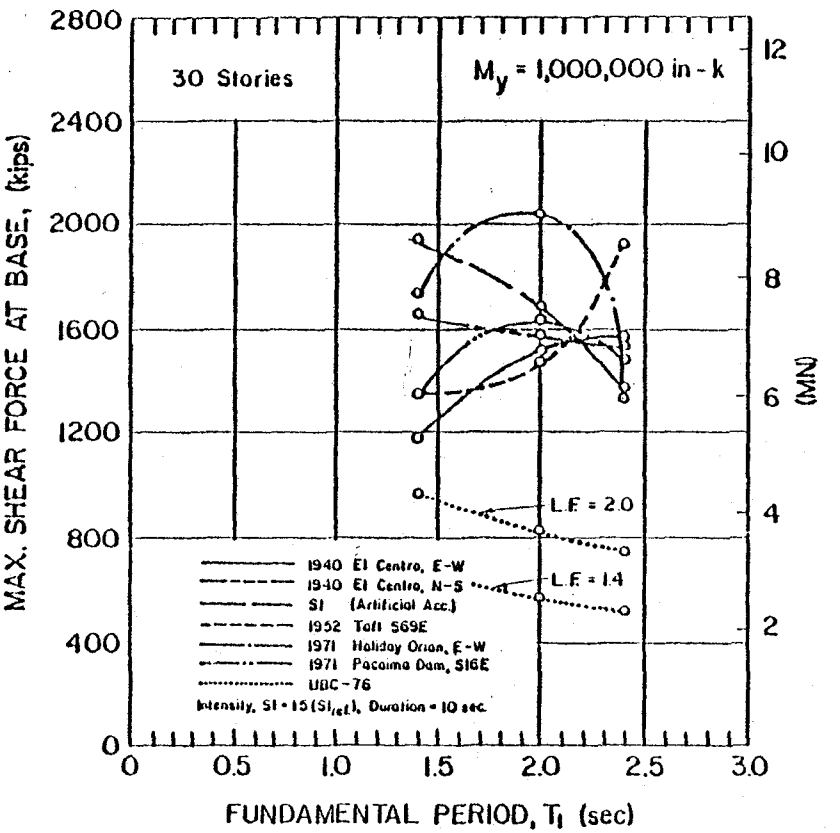

(d)

Fig. A9 (cont'd.) Maximum Response Values for Different Input Motions
30-Story Isolated Structural Walls - M_y = 1,000,000 in.-k

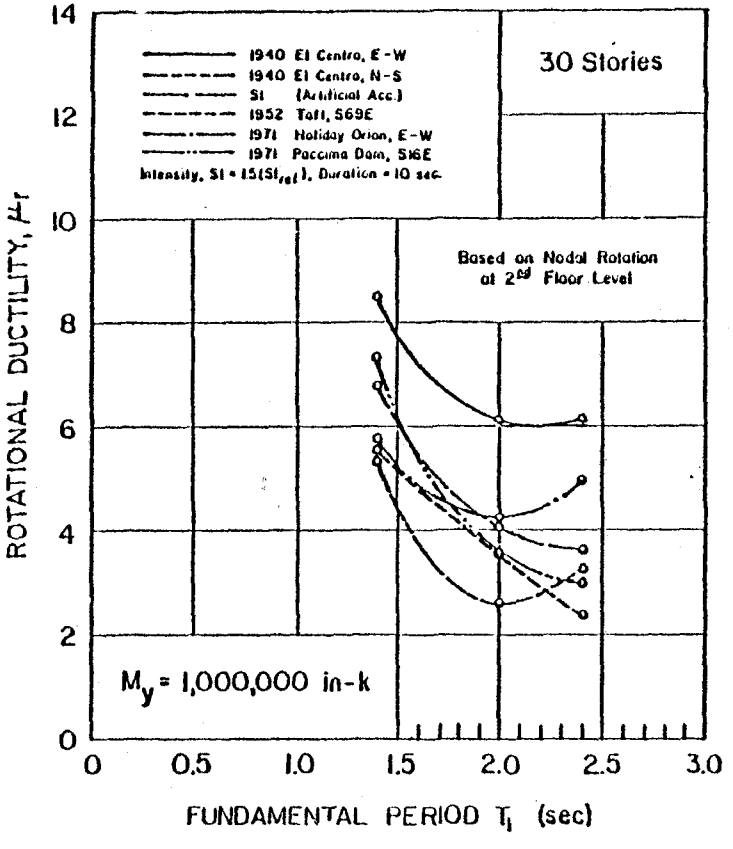

(e)

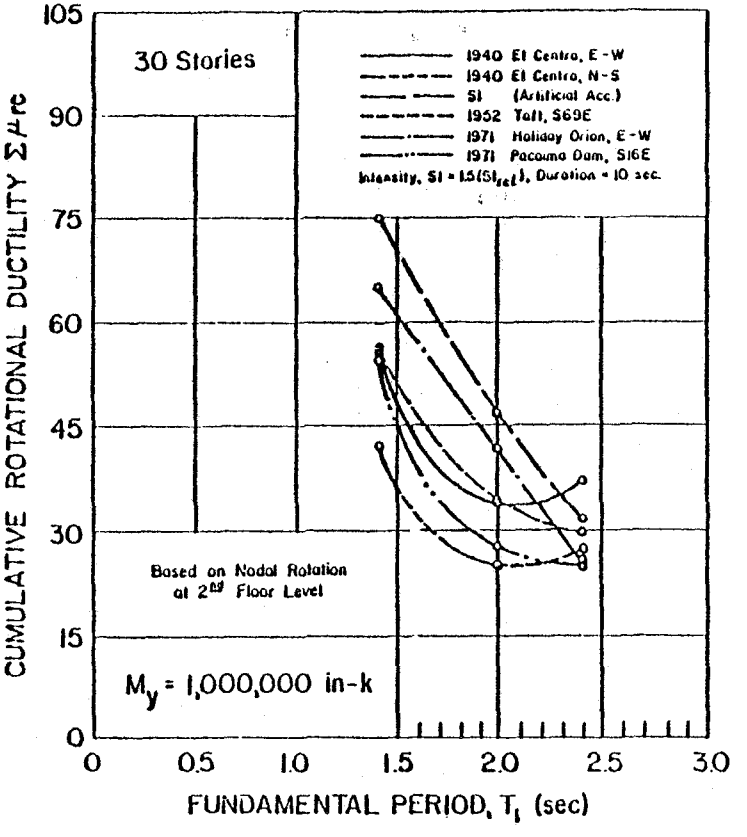

(f)

Fig. A9 (cont'd.) Maximum Response Values for Different Input Motions
30-Story Isolated Structural Walls - M_y = 1,000,000 in.-k

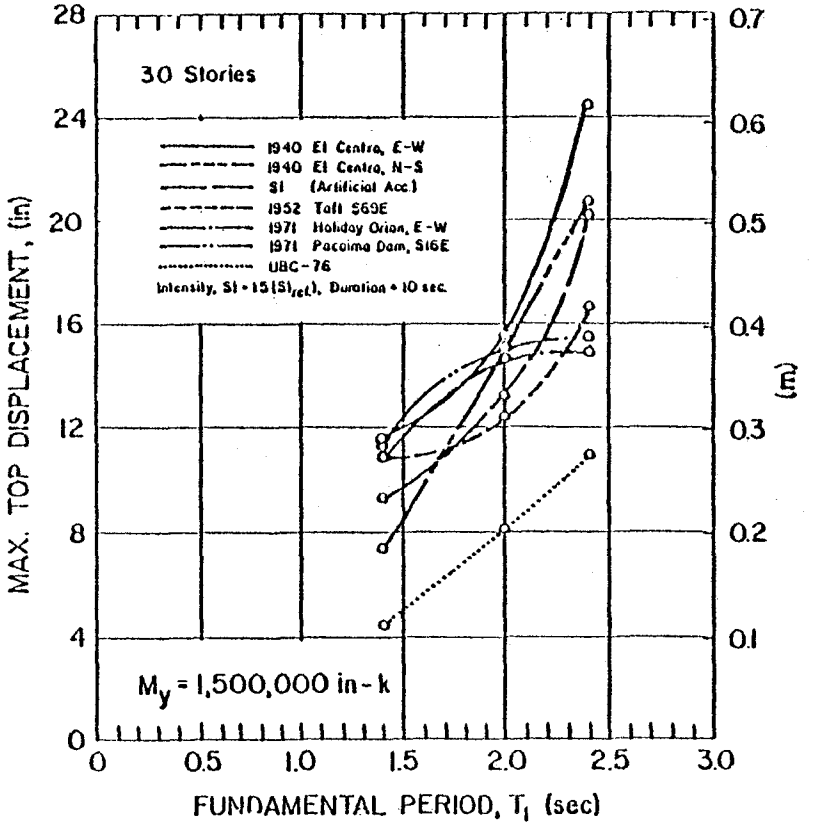

(a)

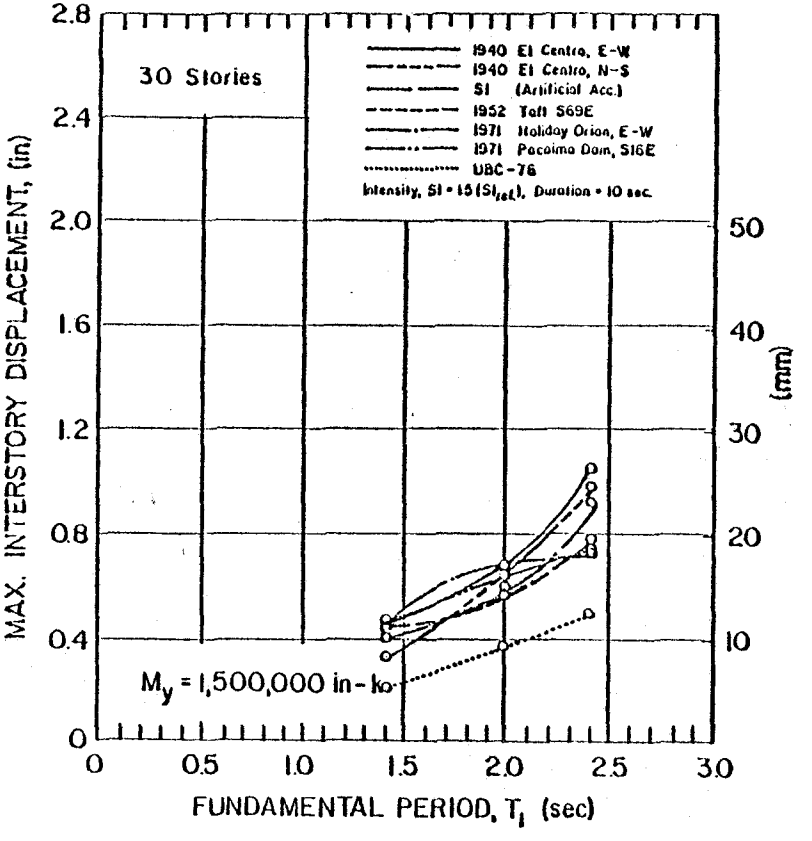

(b)

Fig. A10 Maximum Response Values for Different Input Motions
30-Story Isolated Structural Walls - M_y = 1,500,000 in.-k

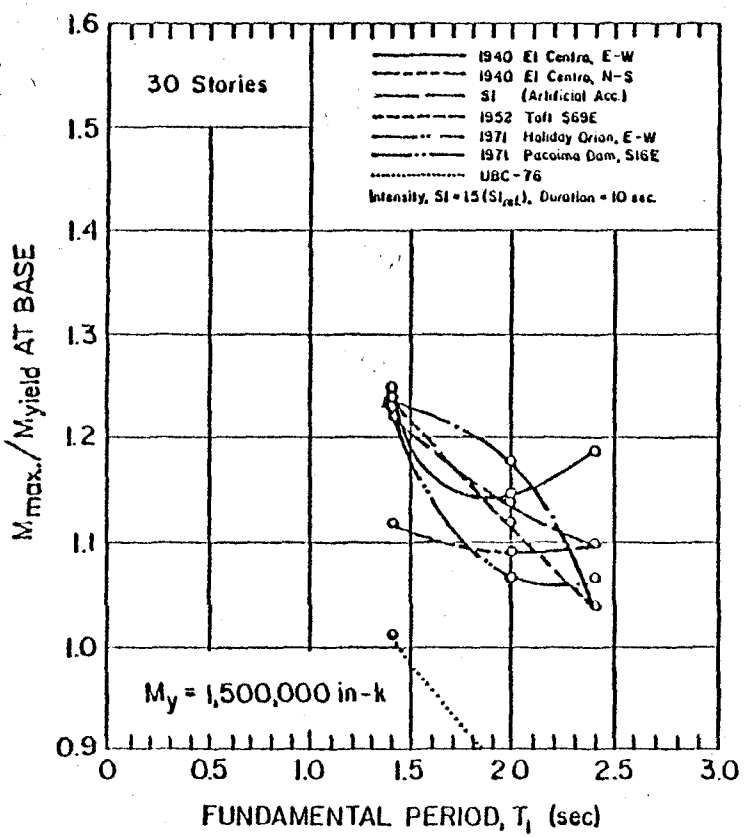

(c)

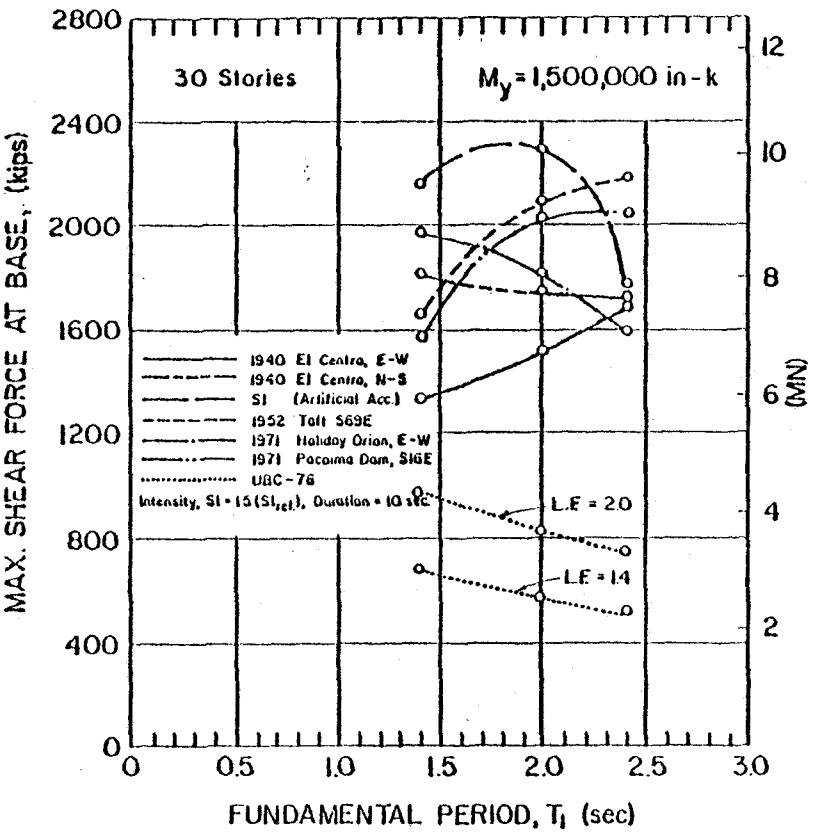

(d)

Fig. A10 (cont'd.) Maximum Response Values for Different Input Motions
30-Story Isolated Structural Walls - M_y = 1,500,000 in.-k

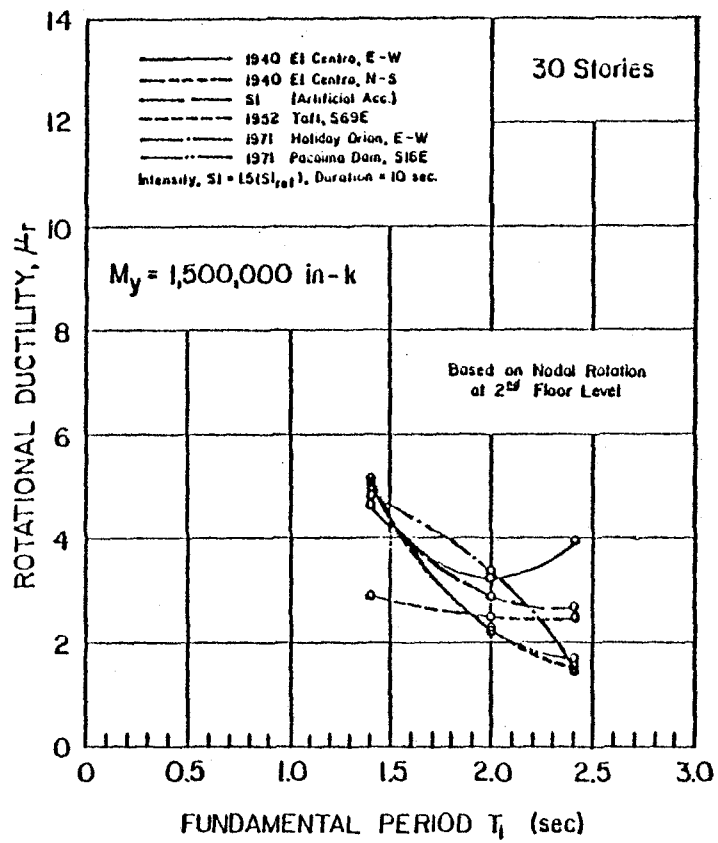

(e)

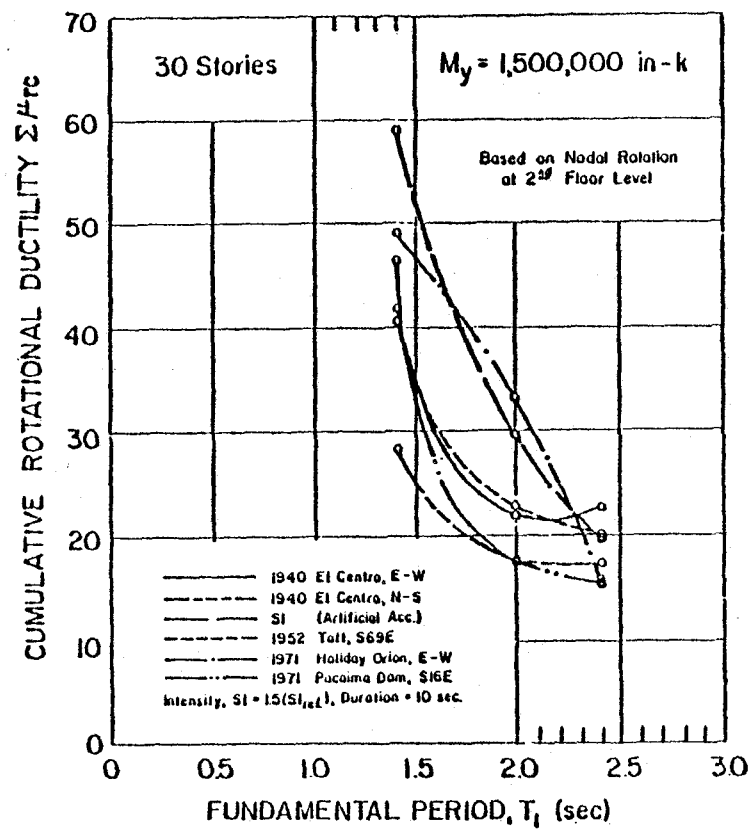

(f)

Fig. A10 (cont'd.) Maximum Response Values for Different Input Motions
30-Story Isolated Structural Walls - M_y = 1,500,000 in.-k

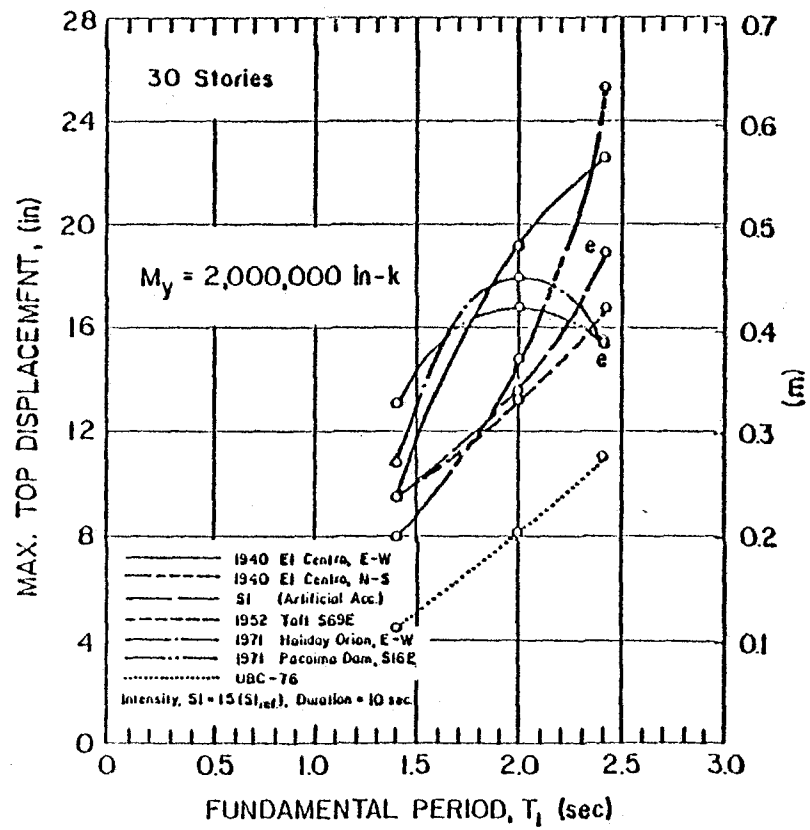

(a)

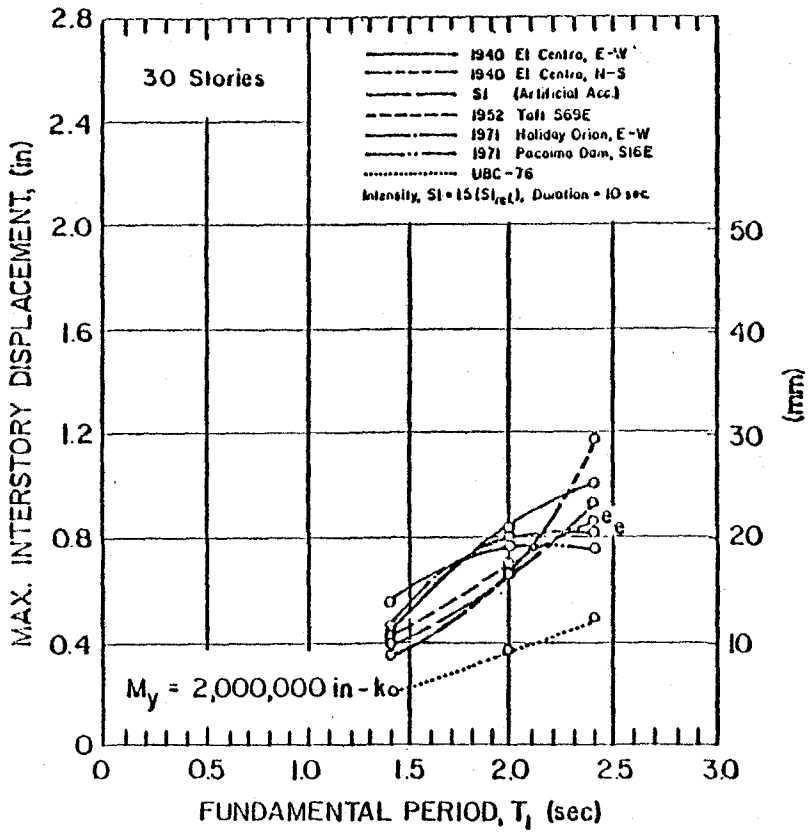

(b)

Fig. A11 Maximum Response Values for Different Input Motions
30-Story Isolated Structural Walls - M_y = 2,000,000 in.-k

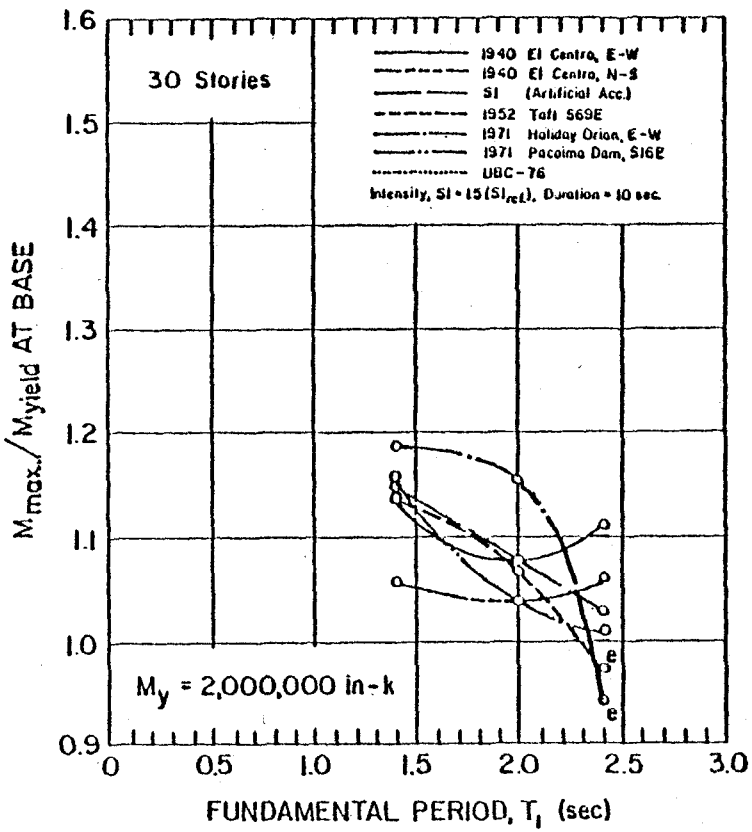

(c)

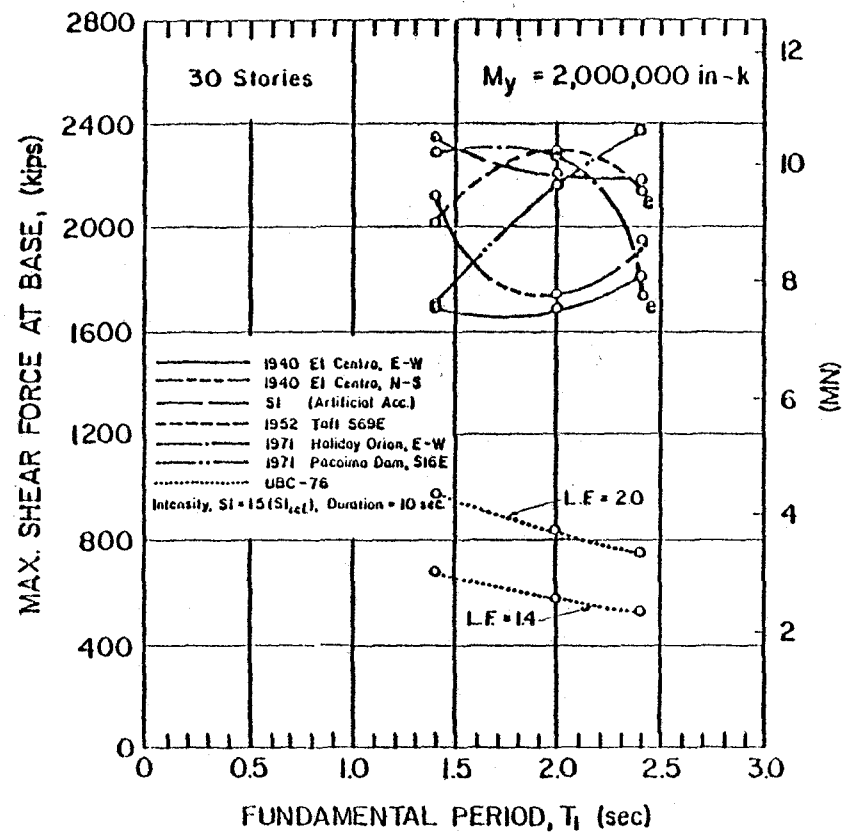

(d)

Fig. A11 (cont'd.) Maximum Response Values for Different Input Motions
30-Story Isolated Structural Walls - M_y = 2,000,000 in.-k

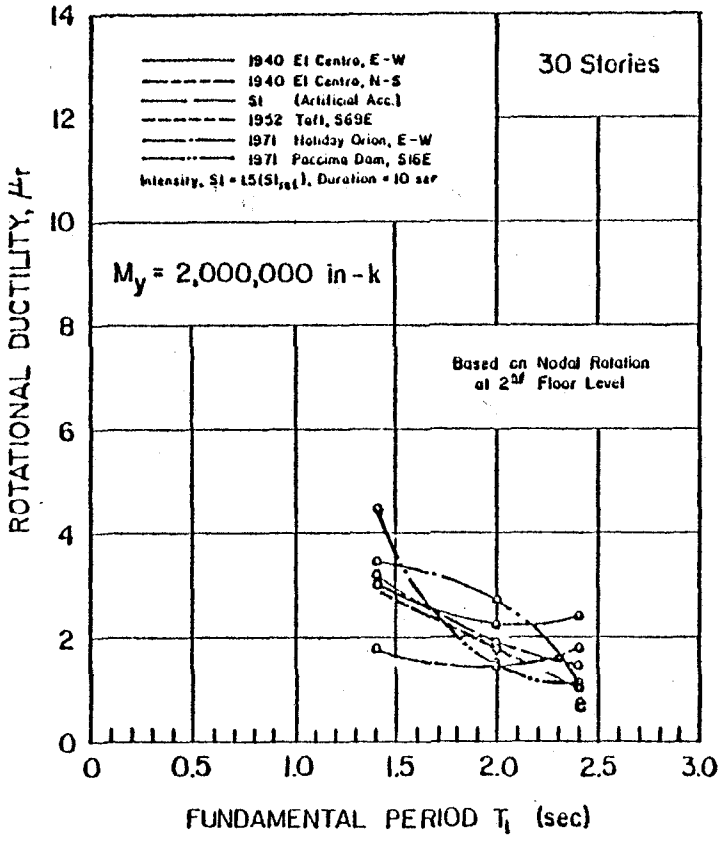

(e)

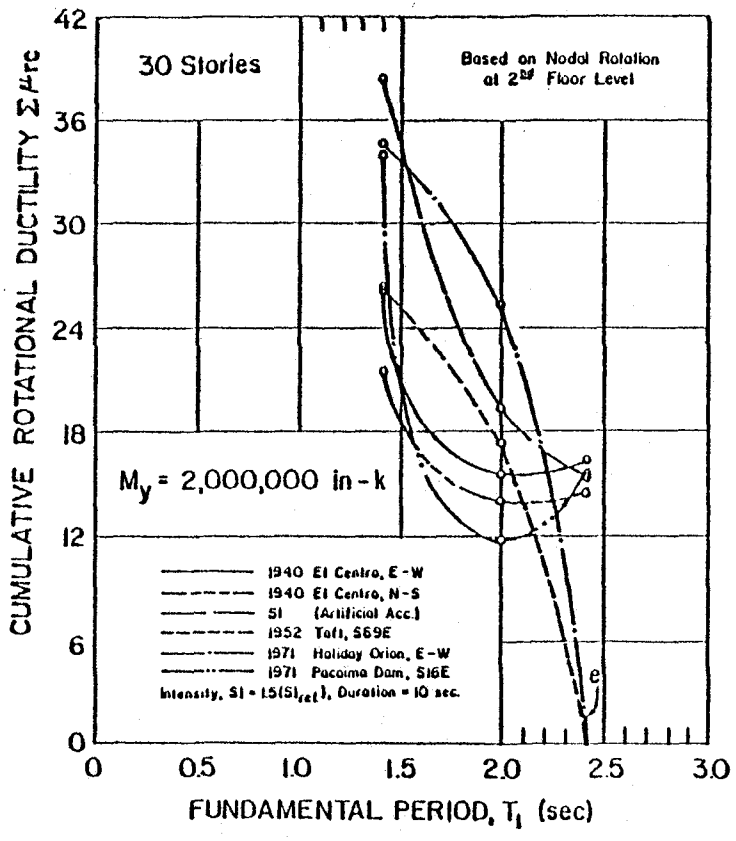

(f)

Fig. A11 (cont'd.) Maximum Response Values for Different Input Motions 30-Story Isolated Structural Walls - M_y = 2,000,000 in.-k

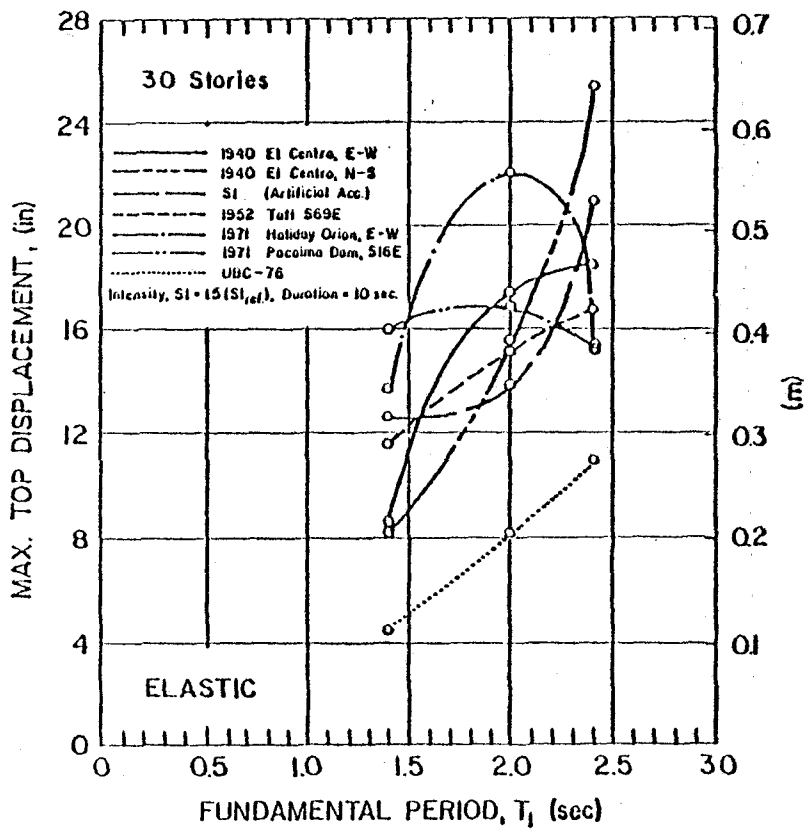

(a)

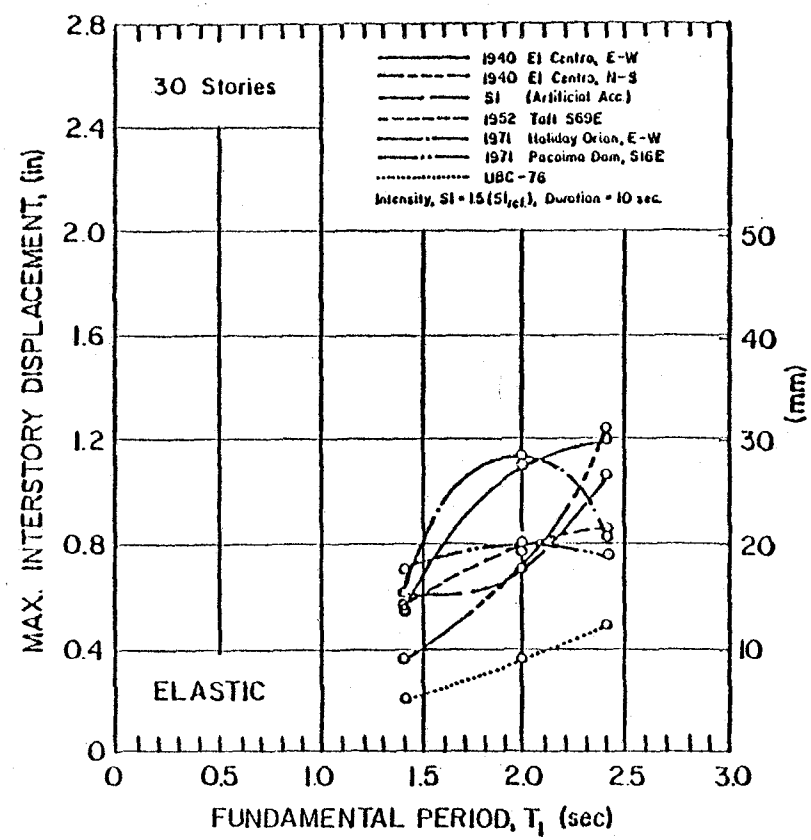

(b)

Fig. A12 Maximum Response Values for Different Input Motions
30-Story Isolated Structural Walls - Elastic Case

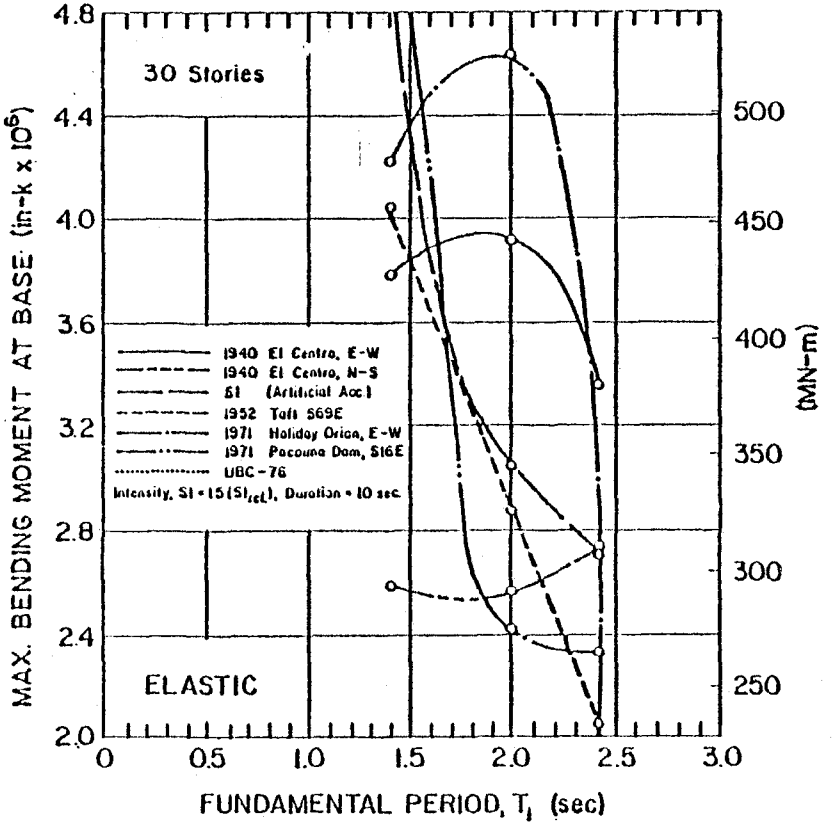

(c)

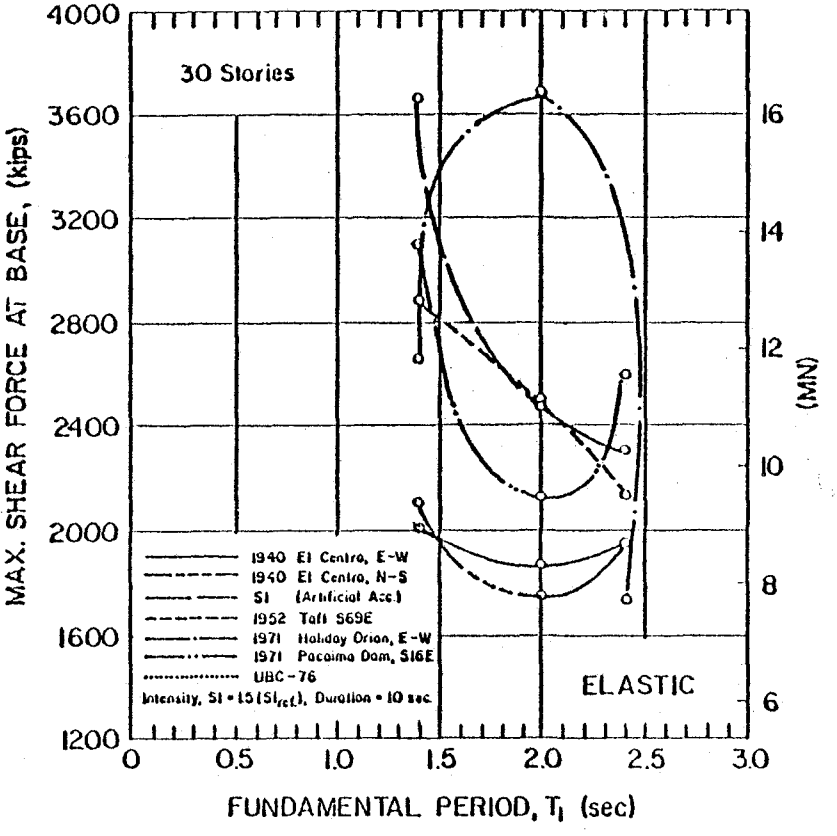

(d)

Fig. A12 (cont'd.) Maximum Response Values for Different Input Motions
30-Story Isolated Structural Walls - Elastic Case

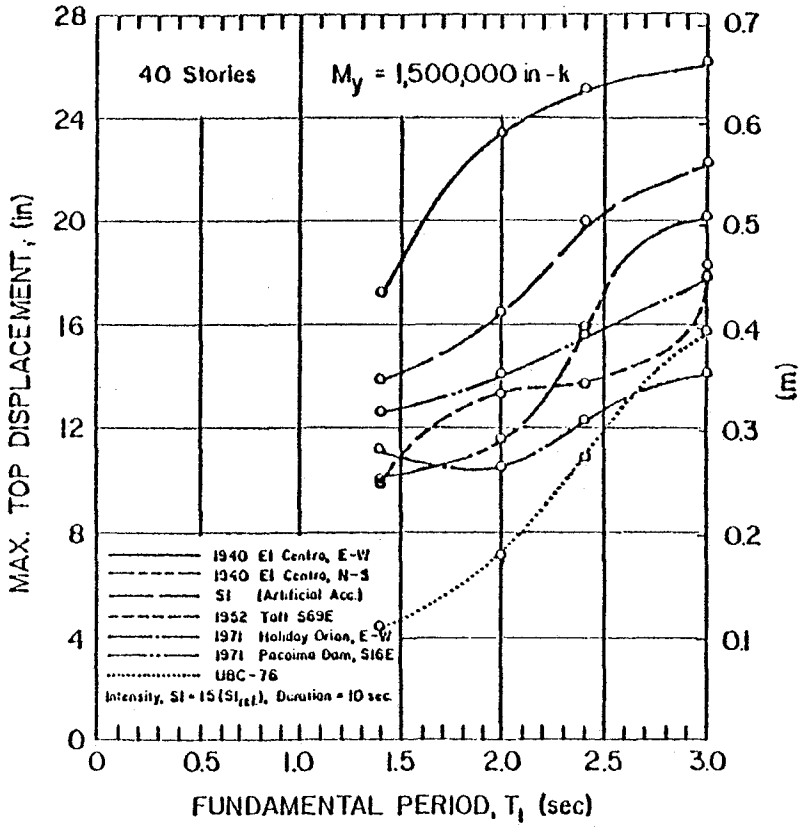

(a)

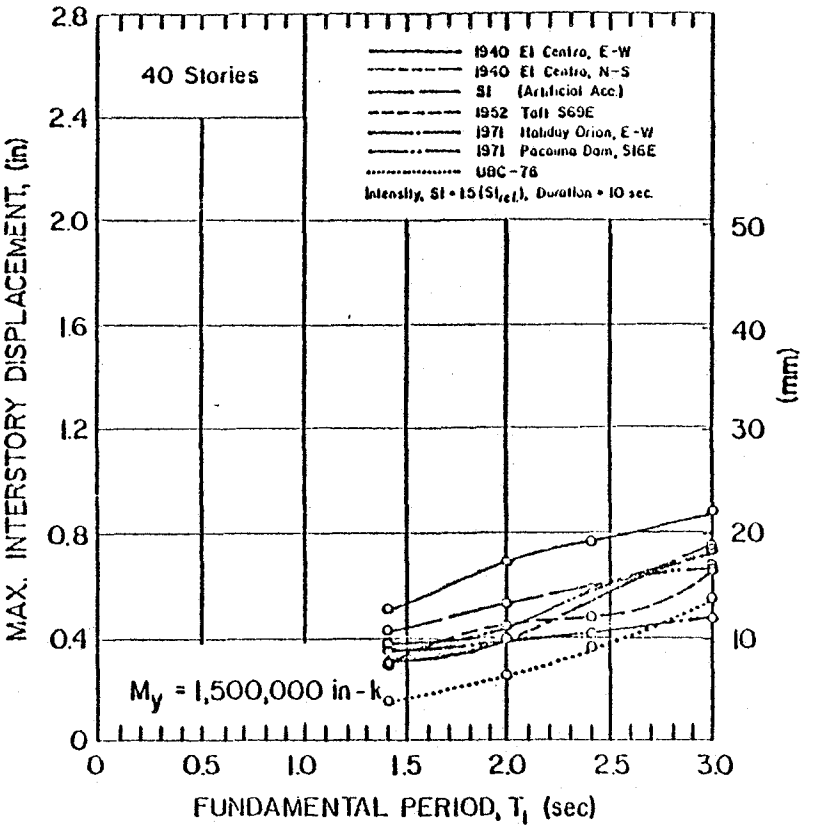

(b)

Fig. A13 Maximum Response Values for Different Input Motions
40-Story Isolated Structural Walls - M_y = 1,500,000 in.-k

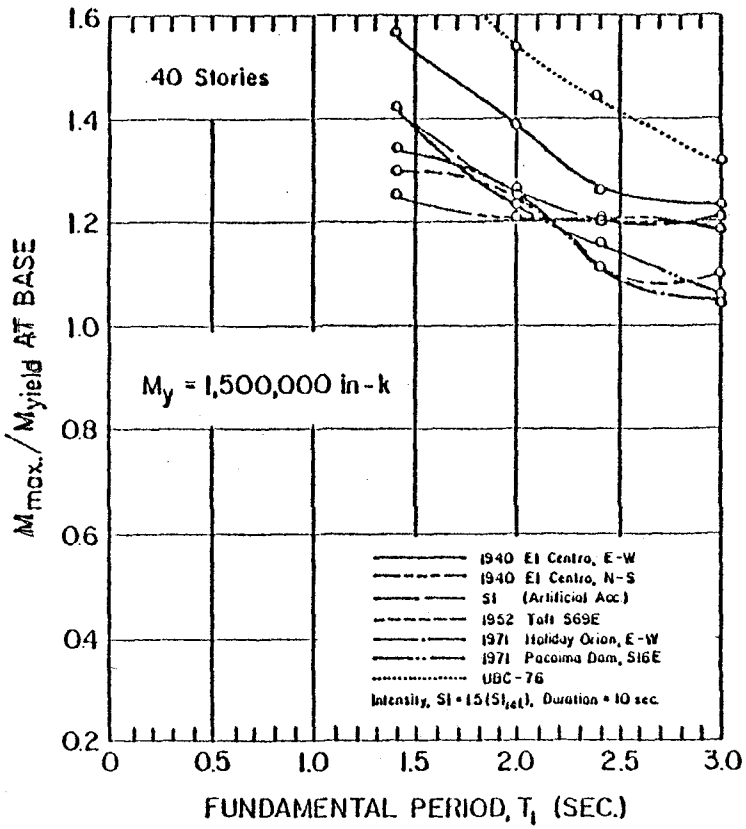

(c)

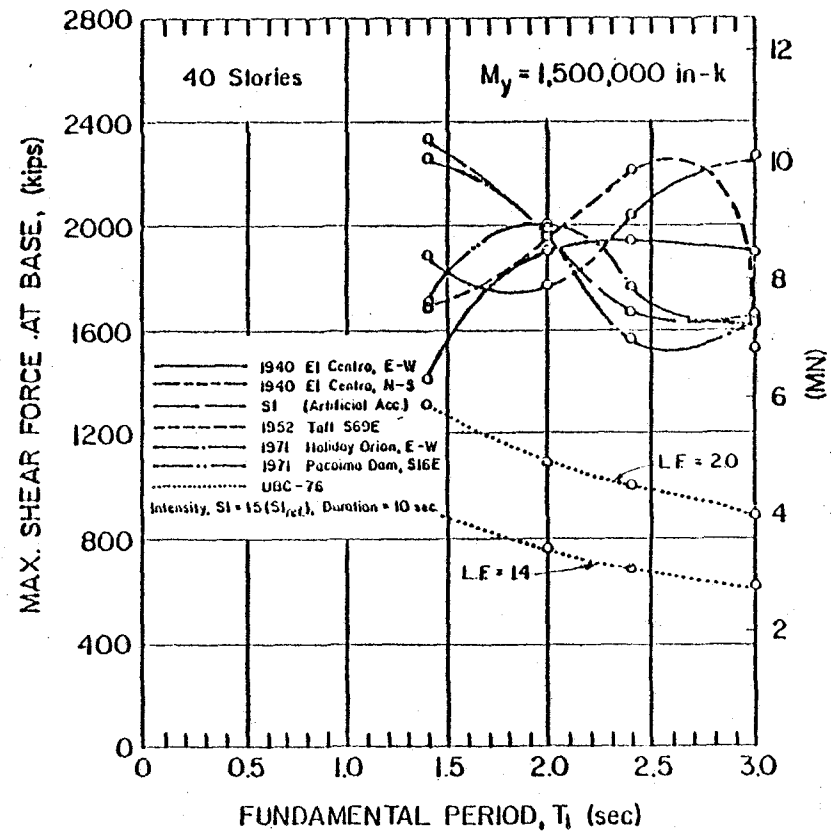

(d)

Fig. A13 (cont'd.) Maximum Response Values for Different Input Motions
40-Story Isolated Structural Walls - M_y = 1,500,000 in.-k

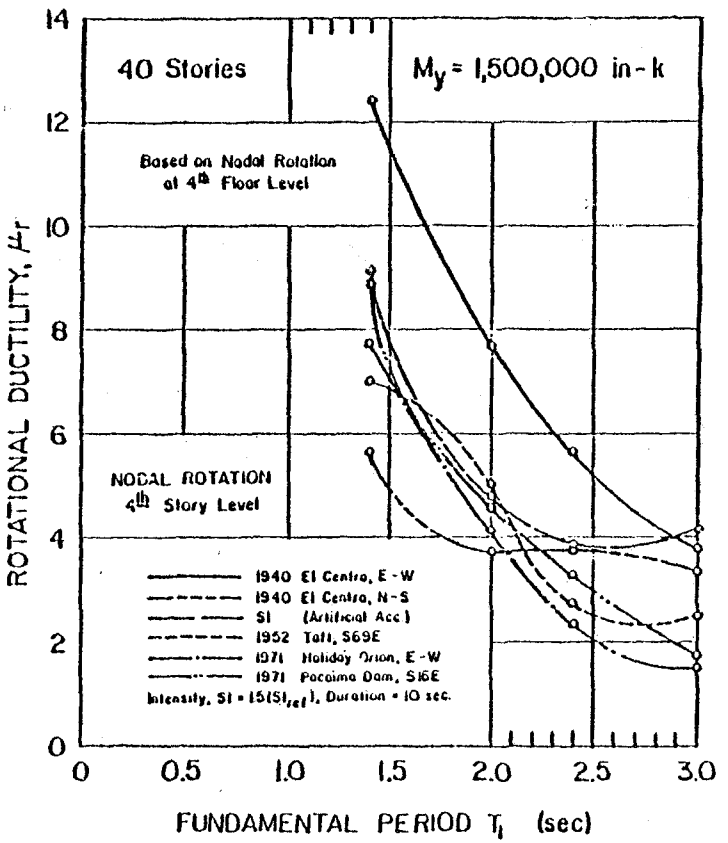

(e)

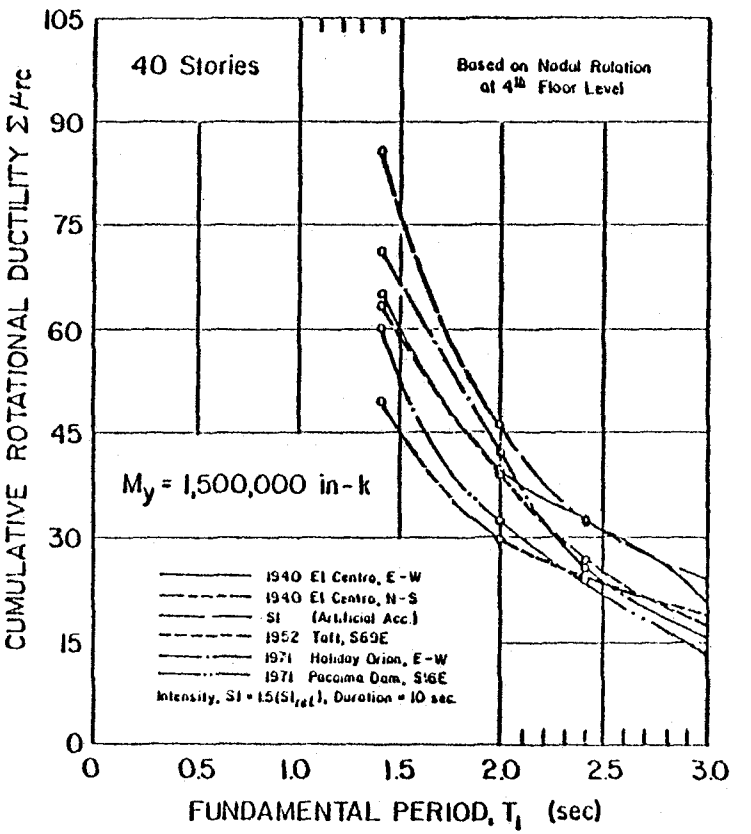

(f)

Fig. A13 (cont'd.) Maximum Response Values for Different Input Motions
40-Story Isolated Structural Walls - M_y = 1,500,000 in.-k

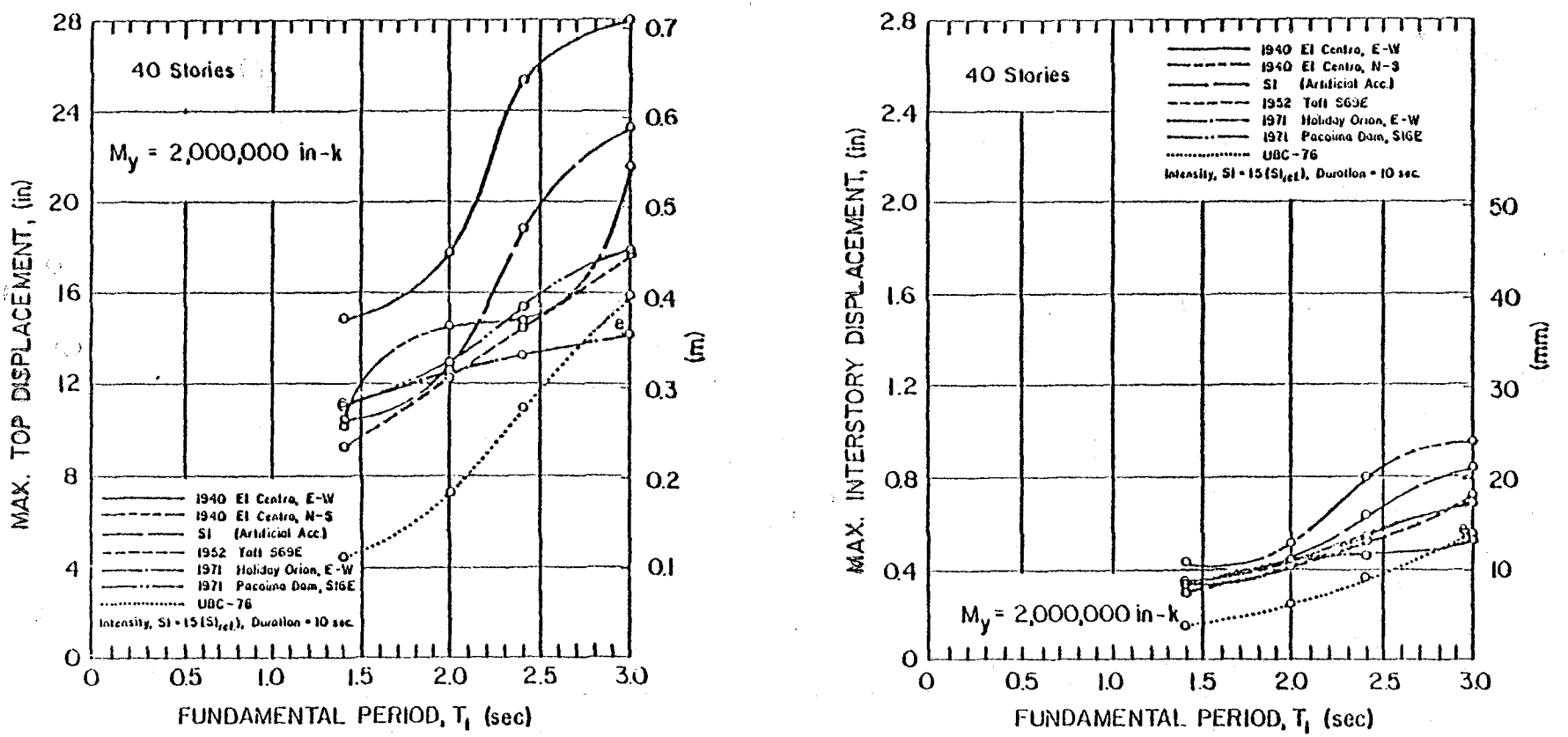

(a) (b)

Fig. A14 Maximum Response Values for Different Input Motions
40-Story Isolated Structural Walls - M_y = 2,000,000 in.-k

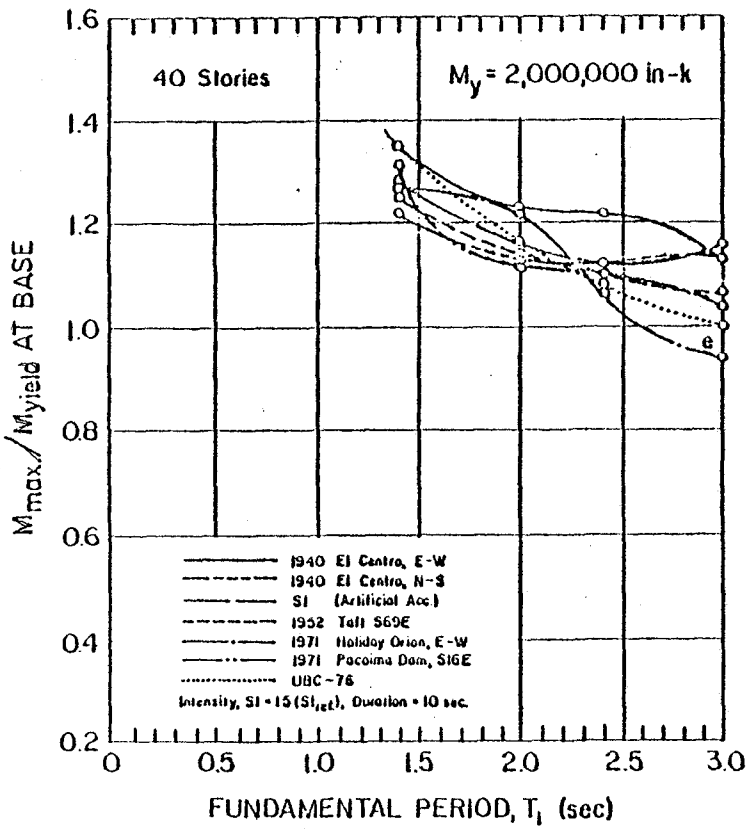

(c)

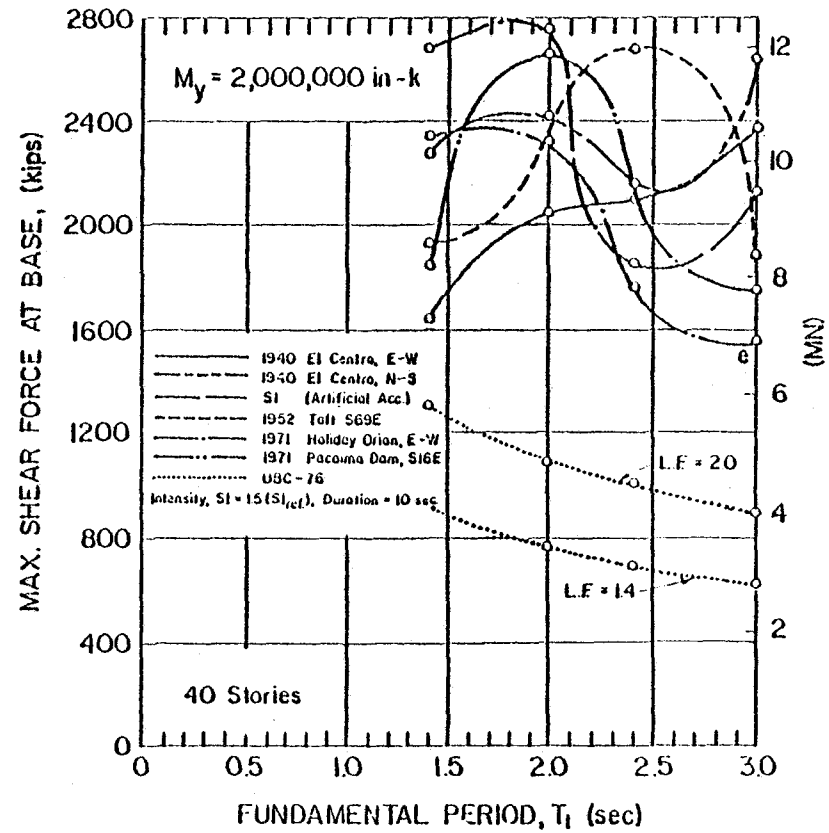

(d)

Fig. A14 (cont'd.) Maximum Response Values for Different Input Motions
40-Story Isolated Structural Walls - M_y = 2,000,000 in.-k

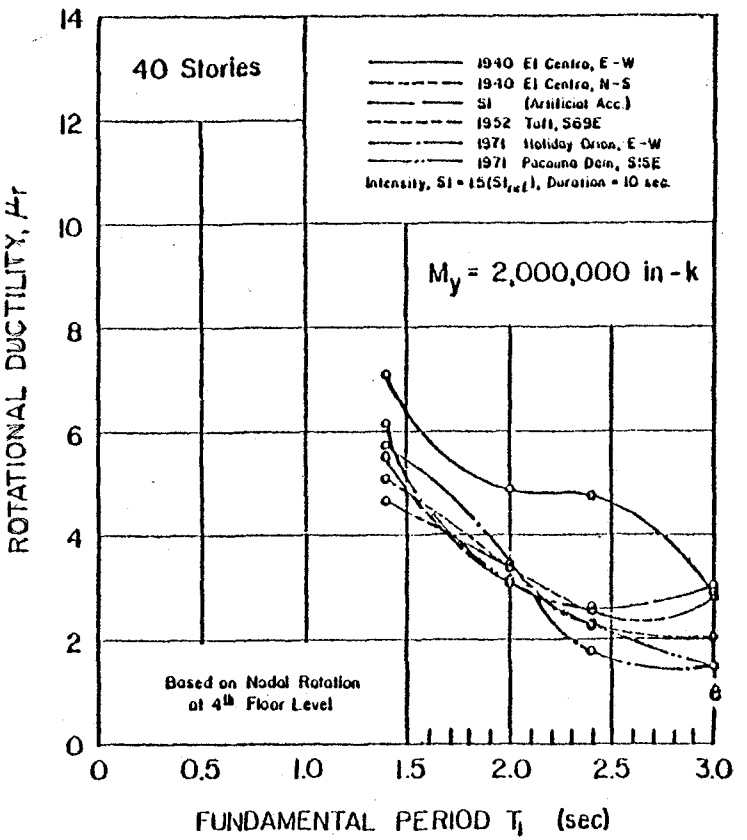

(e)

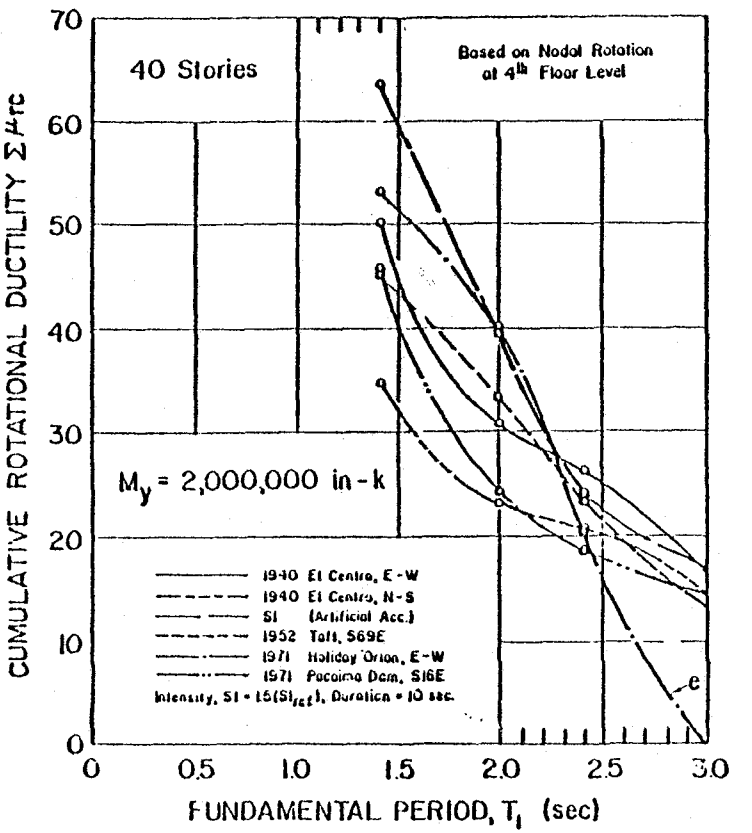

(f)

Fig. A14 (cont'd.) Maximum Response Values for Different Input Motions
40-Story Isolated Structural Walls - M_y = 2,000,000 in.-k

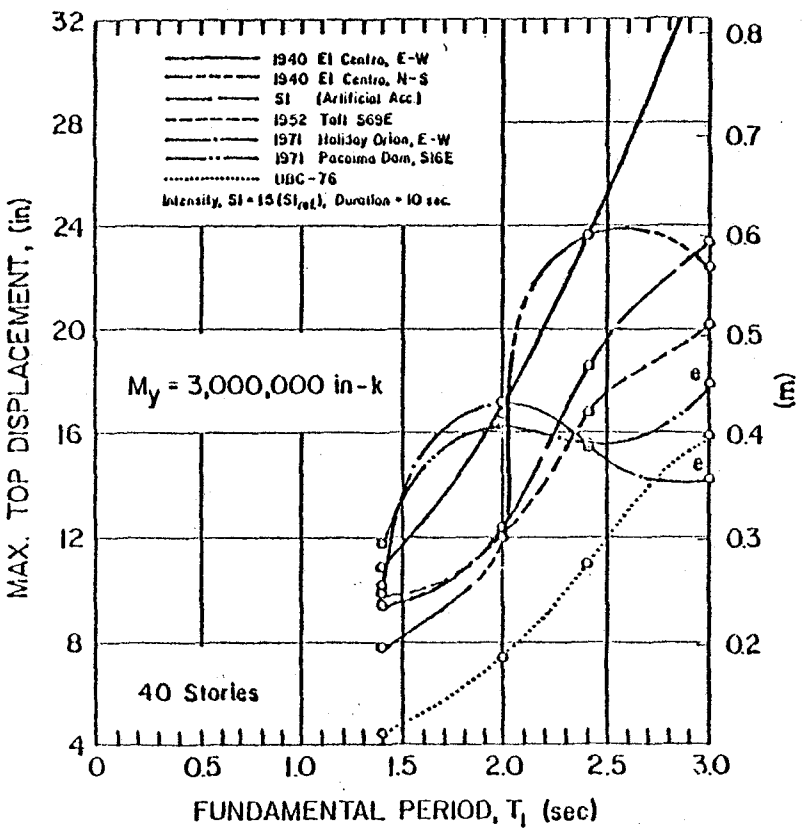

(a)

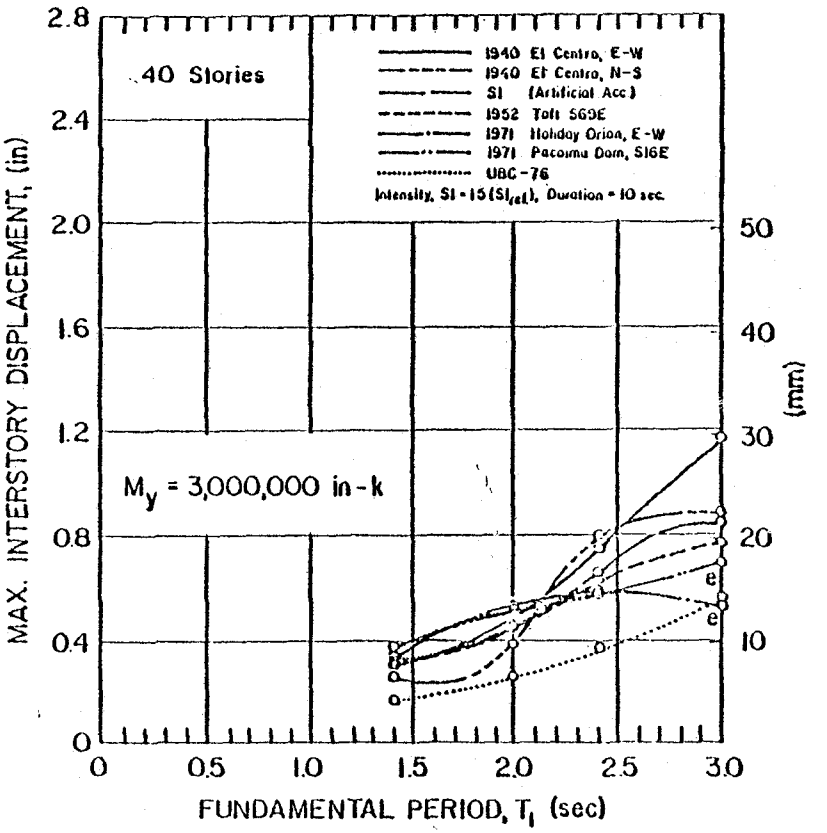

(b)

Fig. A15 Maximum Response Values for Different Input Motions
40-Story Isolated Structural Walls - M_y = 3,000,000 in.-k

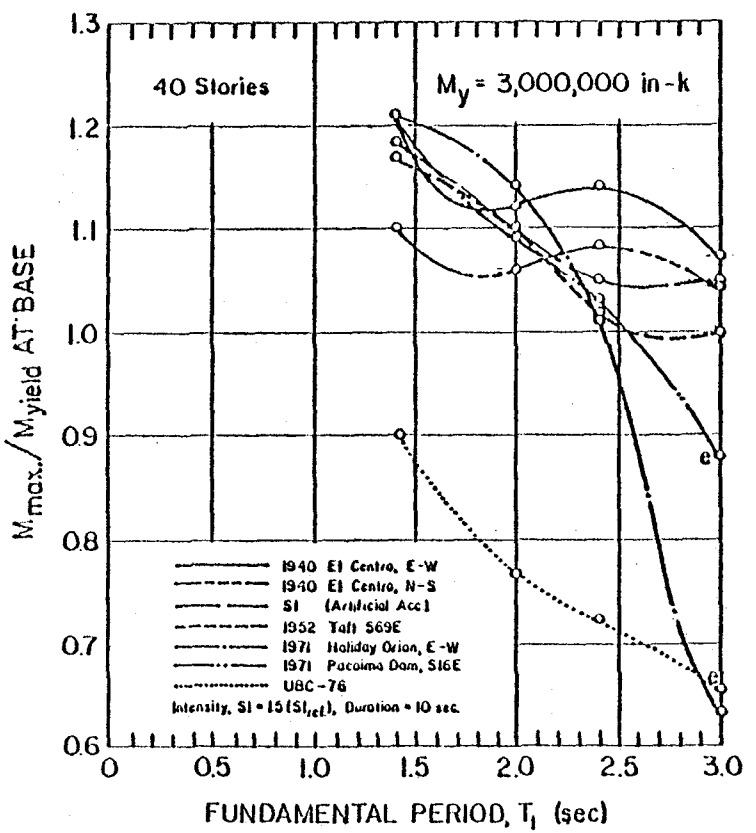

(c)

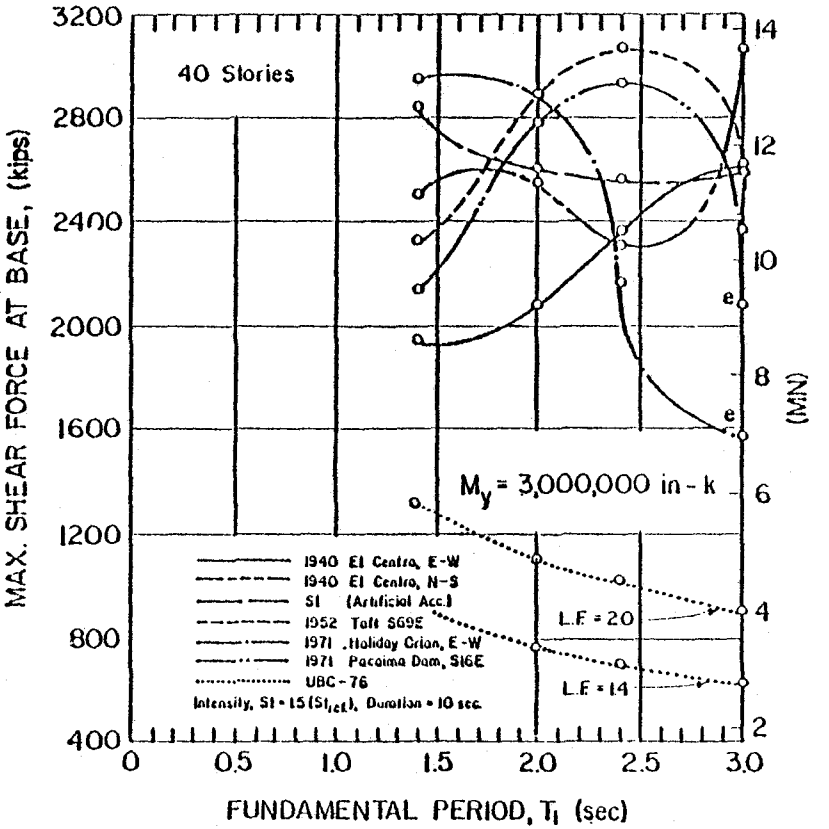

(d)

Fig. A15 (cont'd.) Maximum Response Values for Different Input Motions
40-Story Isolated Structural Walls - M_y = 3,000,000 in.-k

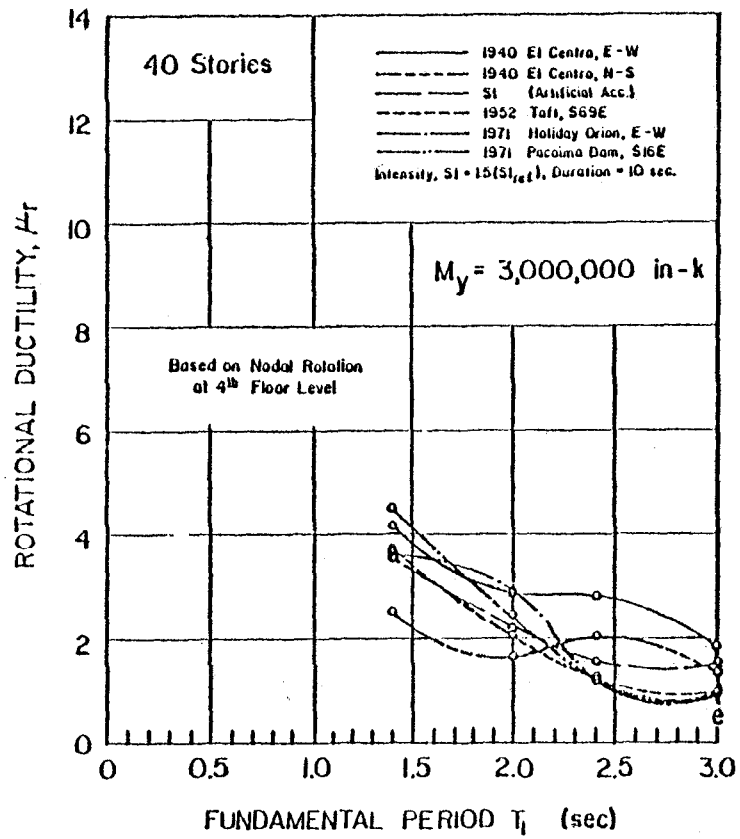

(e)

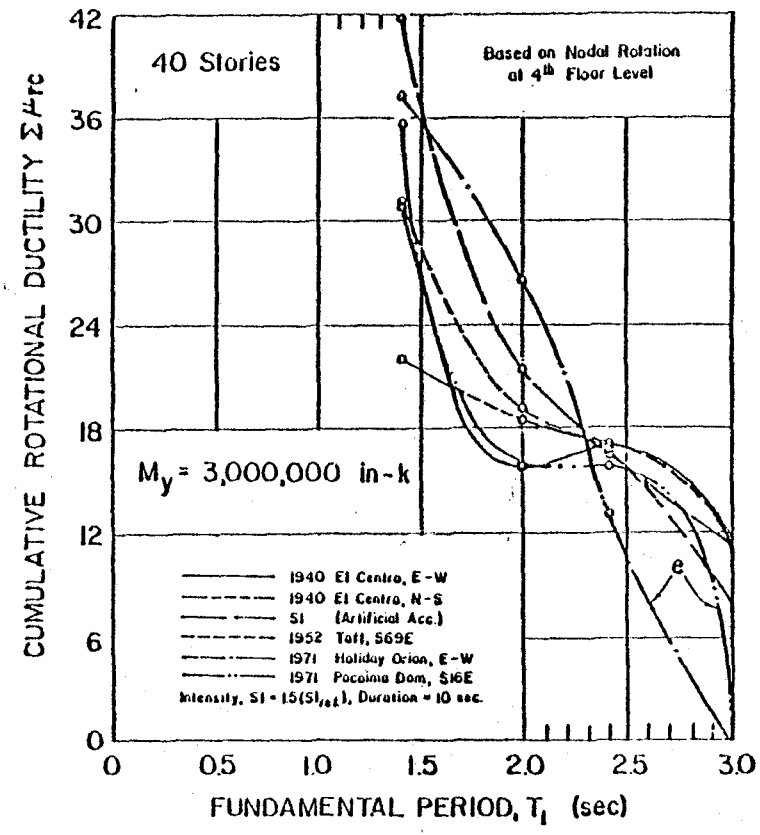

(f)

Fig. A15 (cont'd.) Maximum Response Values for Different Input Motions
40-Story Isolated Structural Walls - M_y = 3,000,000 in.-k

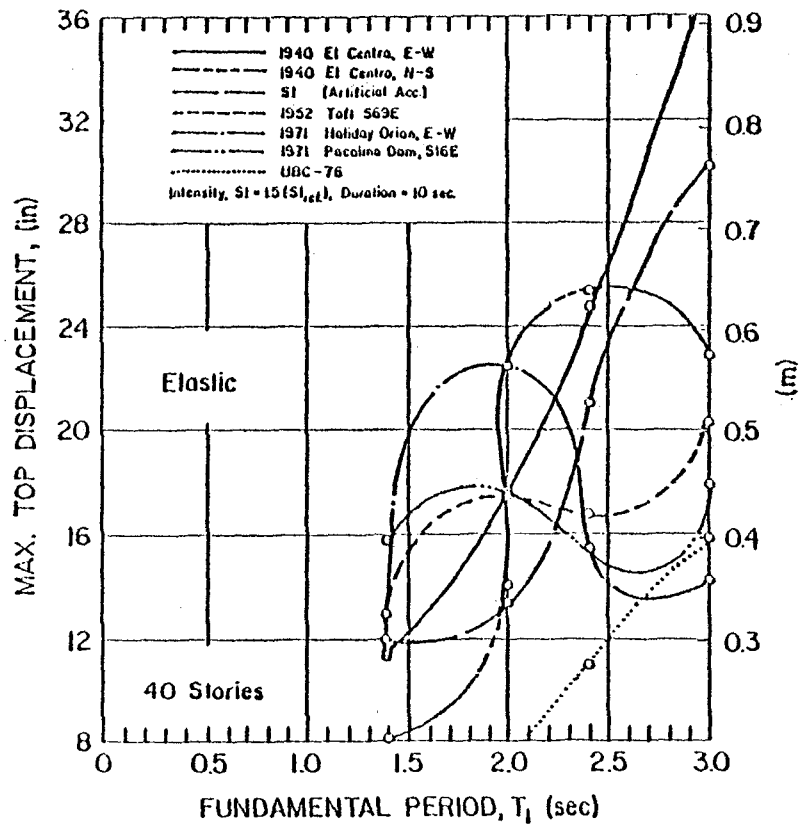

(a)

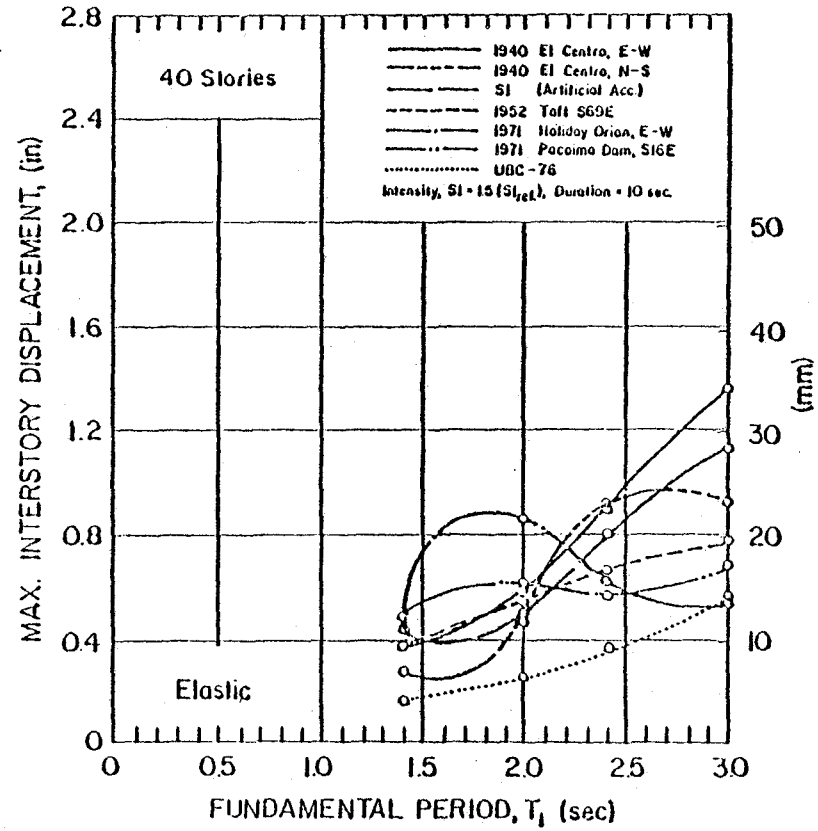

(b)

Fig. A16 Maximum Response Values for Different Input Motions
40-Story Isolated Structural Walls - Elastic Case

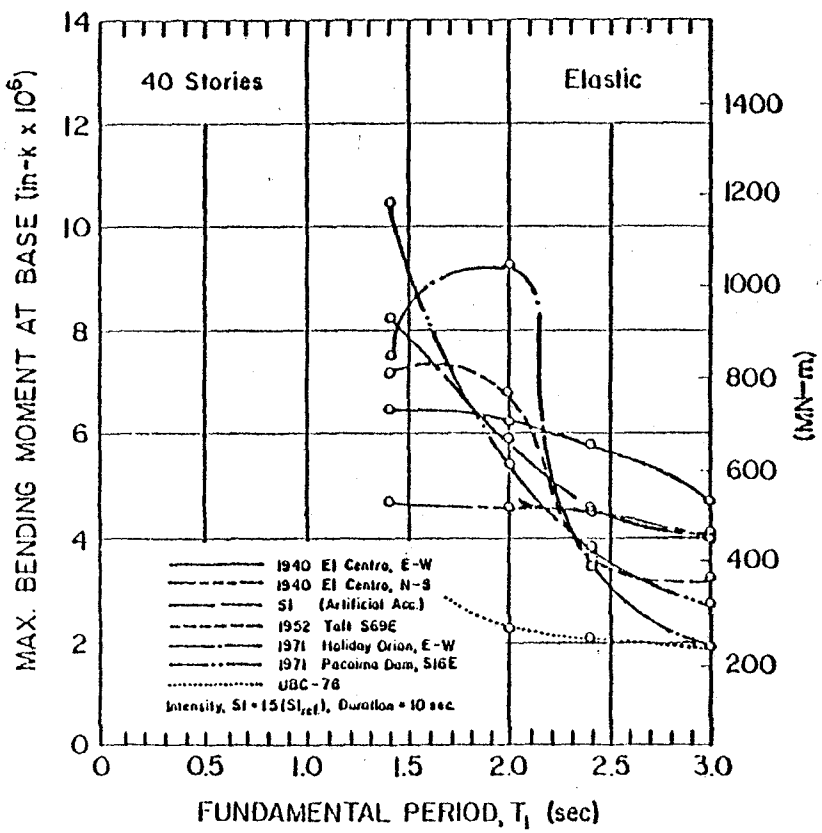

(c)

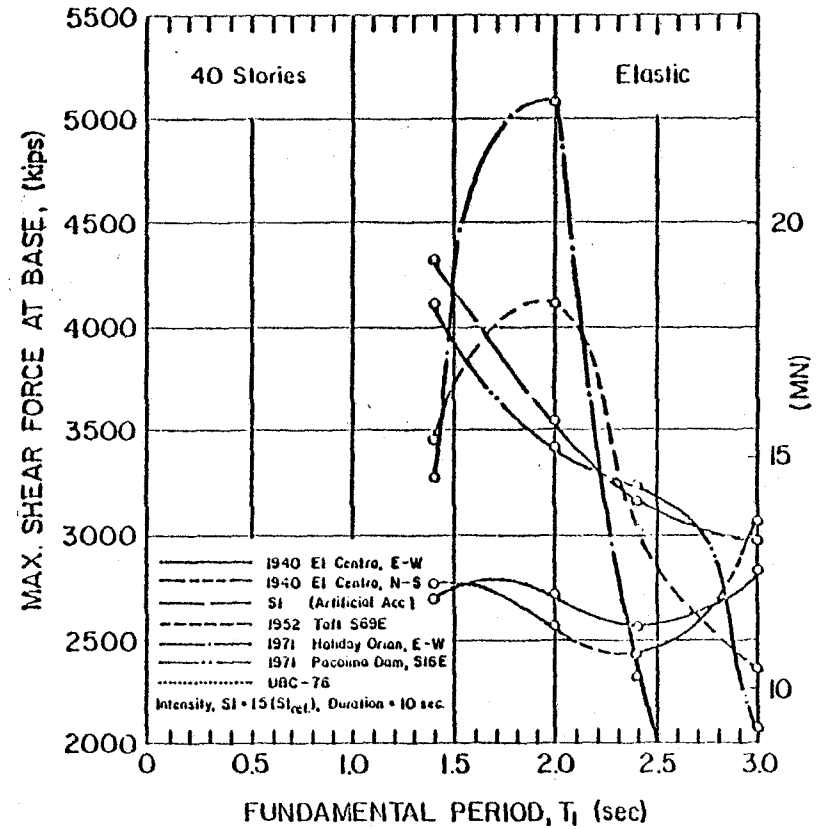

(d)

Fig. A16 (cont'd.) Maximum Response Values for Different Input Motions
40-Story Isolated Structural Walls - Elastic Case

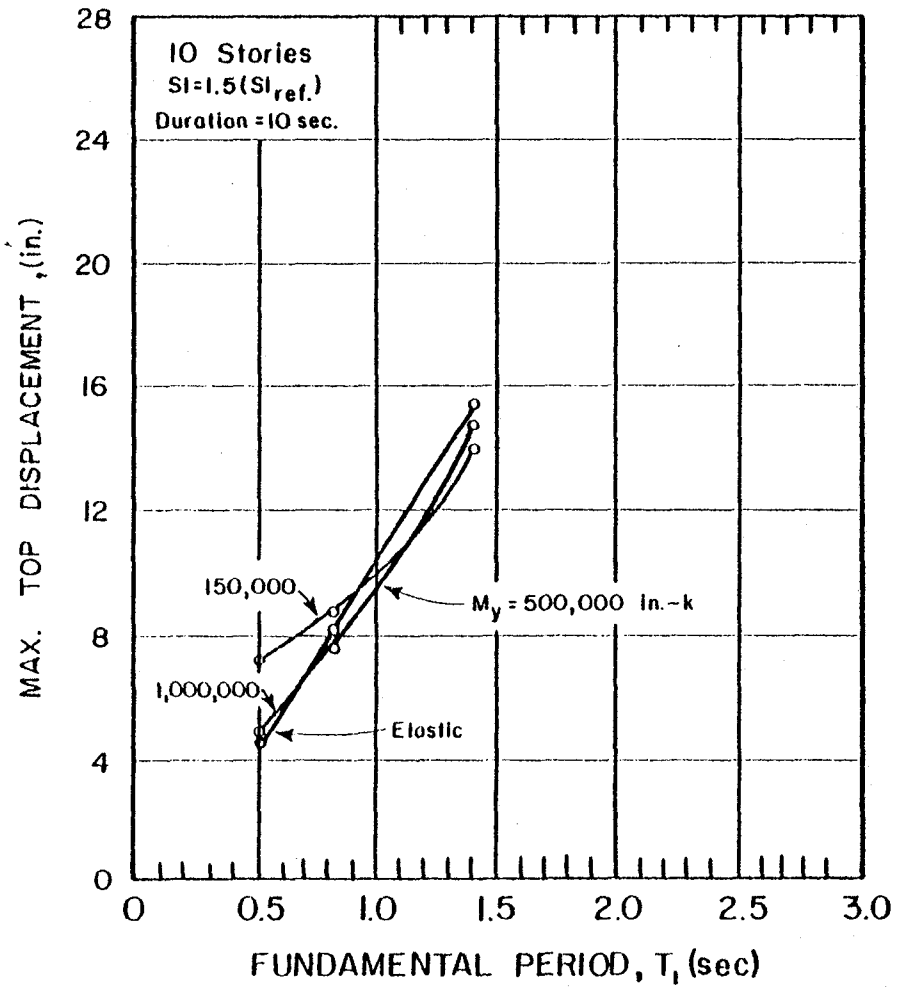

(a)

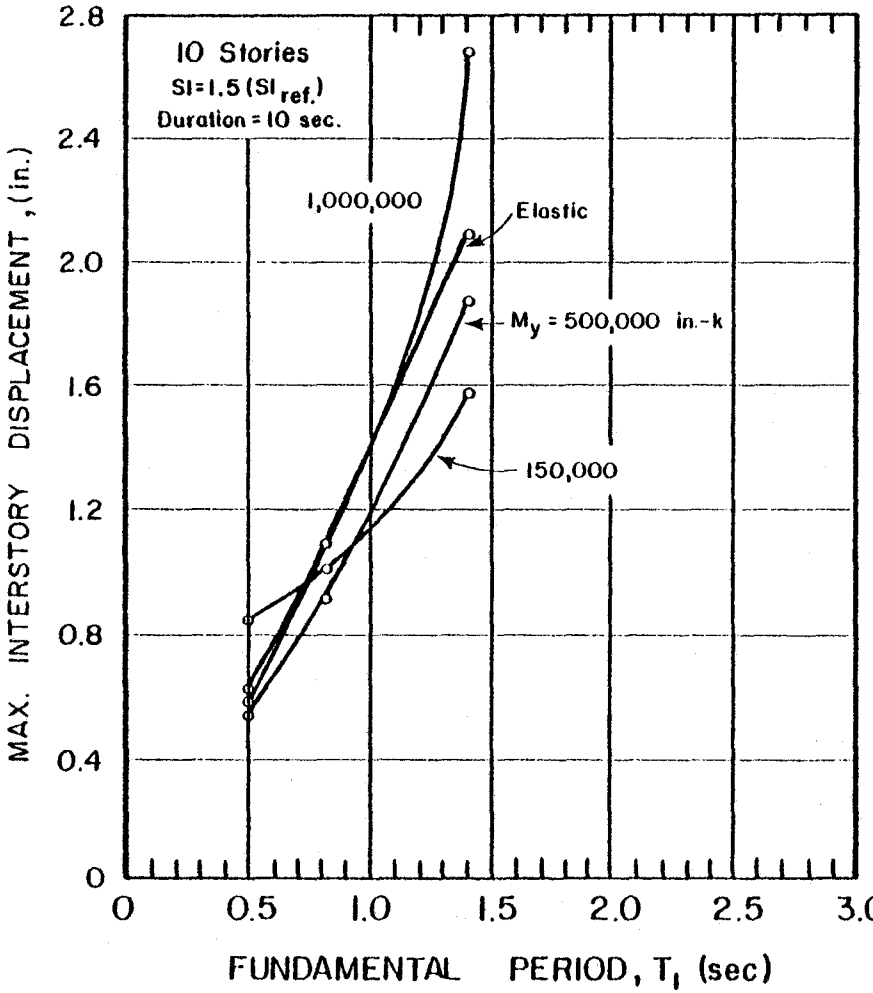

(b)

Fig. A17 Critical Response Values as Functions of Fundamental Period, T_1, and Yield Level, M_y, 10-Story Isolated Structural Walls

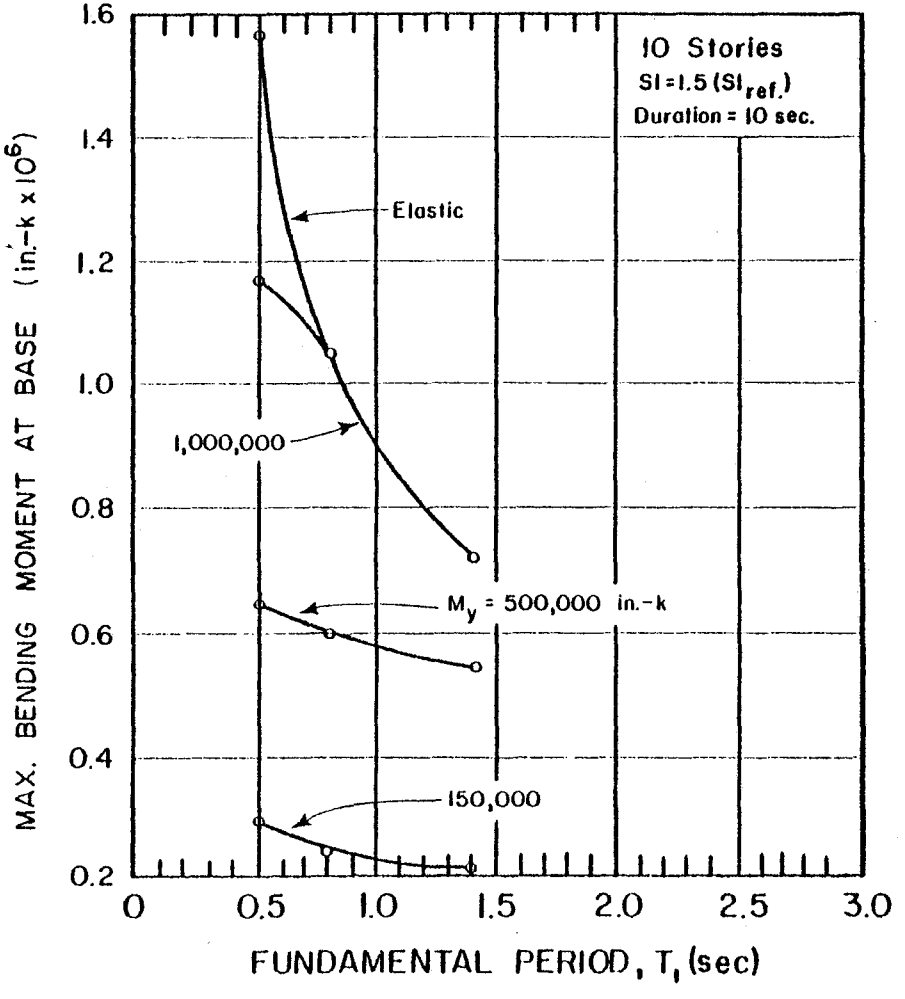

(c)

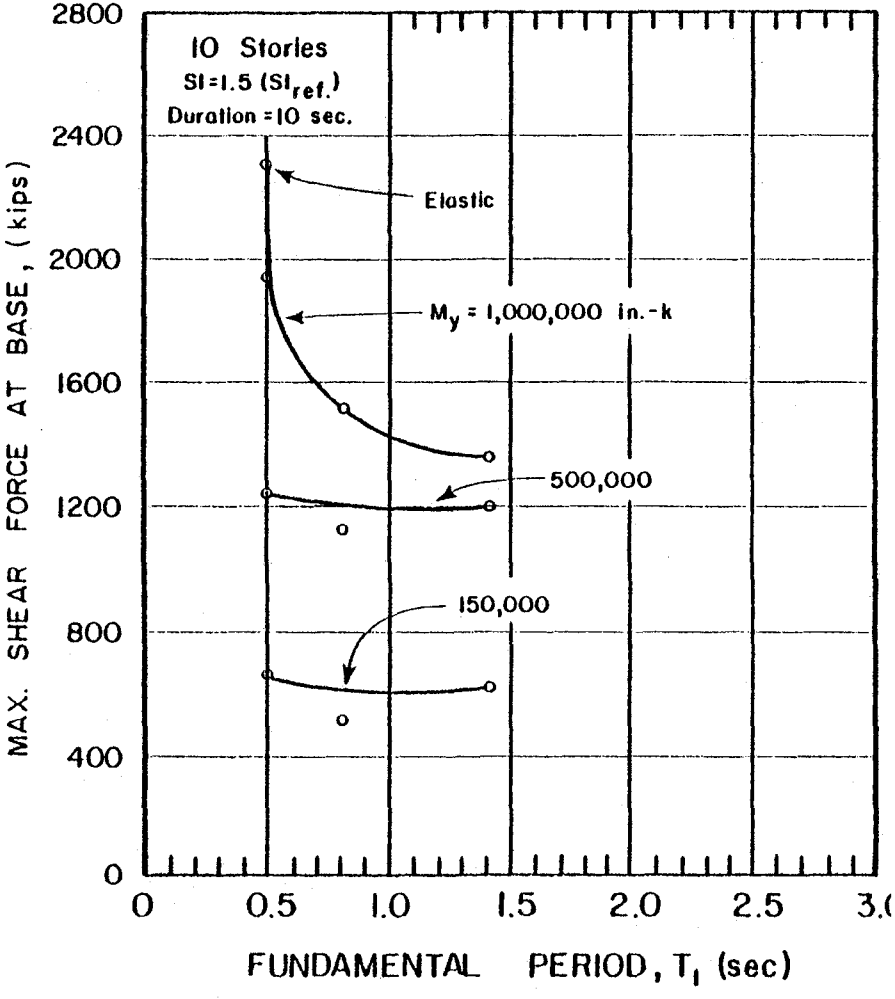

(d)

Fig. A17 (contd.) Critical Response Values as Functions of Fundamental Period, T_1, and Yield Level, M_y, 10-Story Isolated Structural Walls

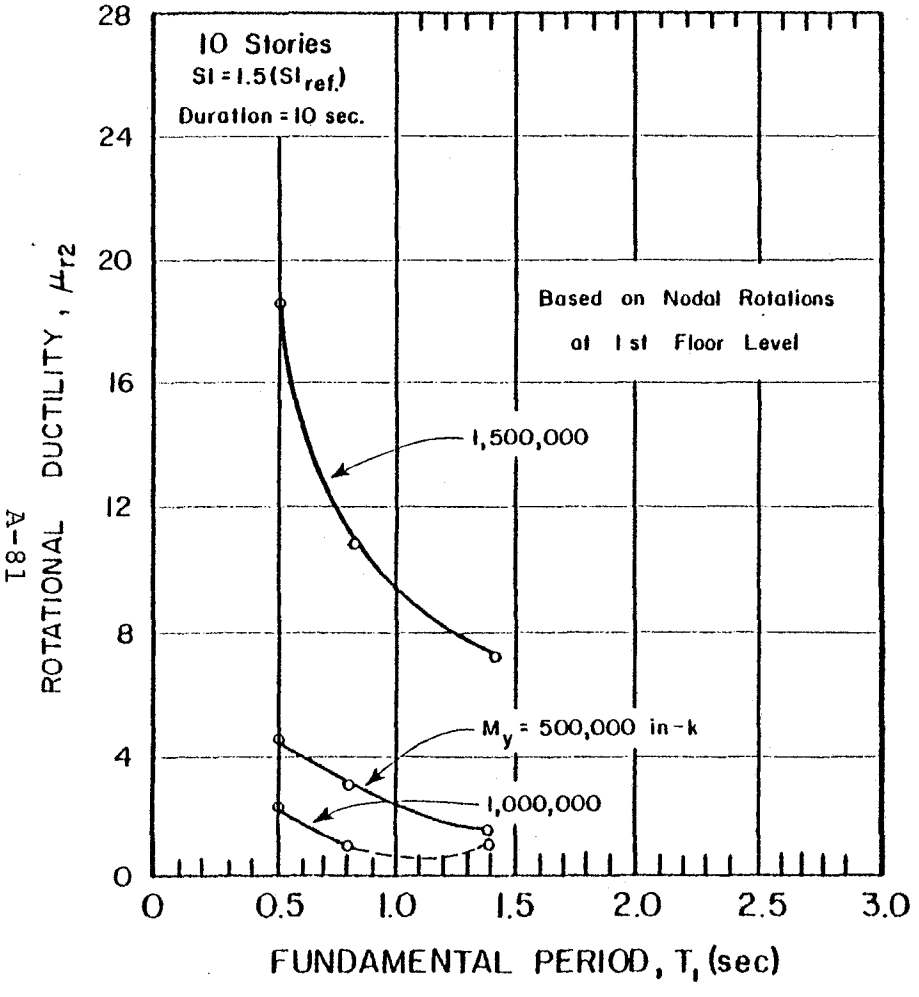

(e)

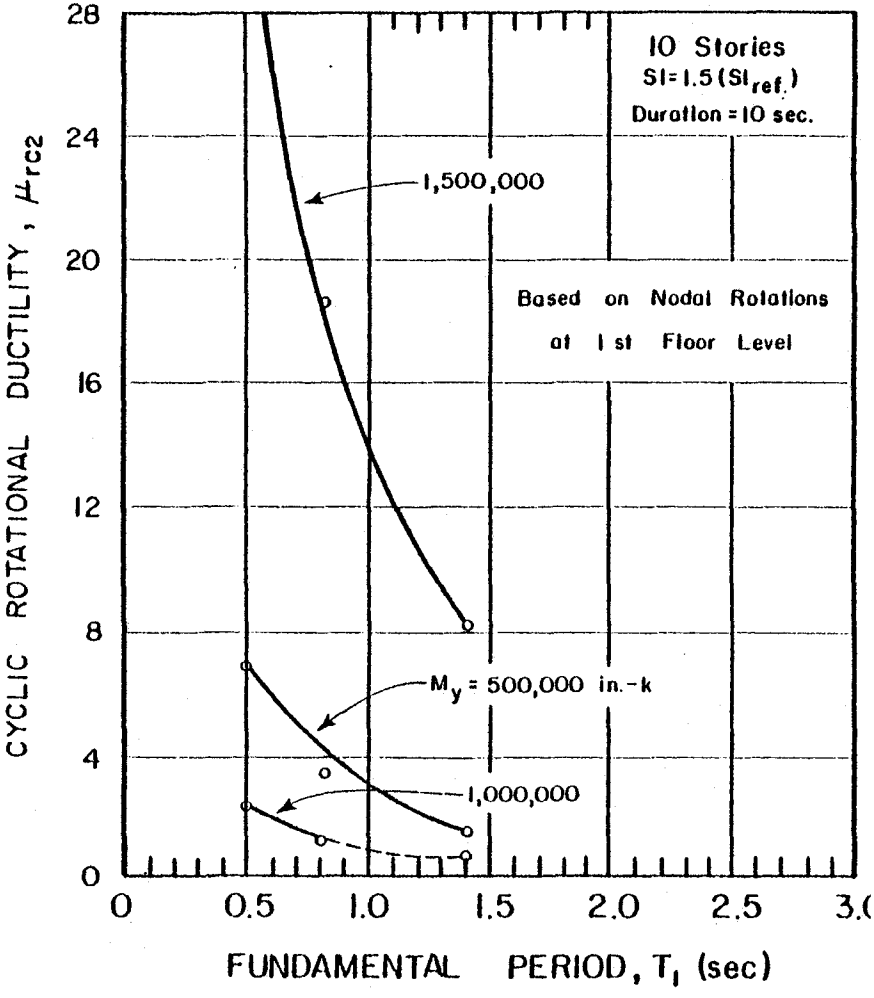

(f)

Fig. A17 (contd.) Critical Response Values as Functions of Fundamental Period, T_1, and Yield Level, M_y, 10-Story Isolated Structural Walls

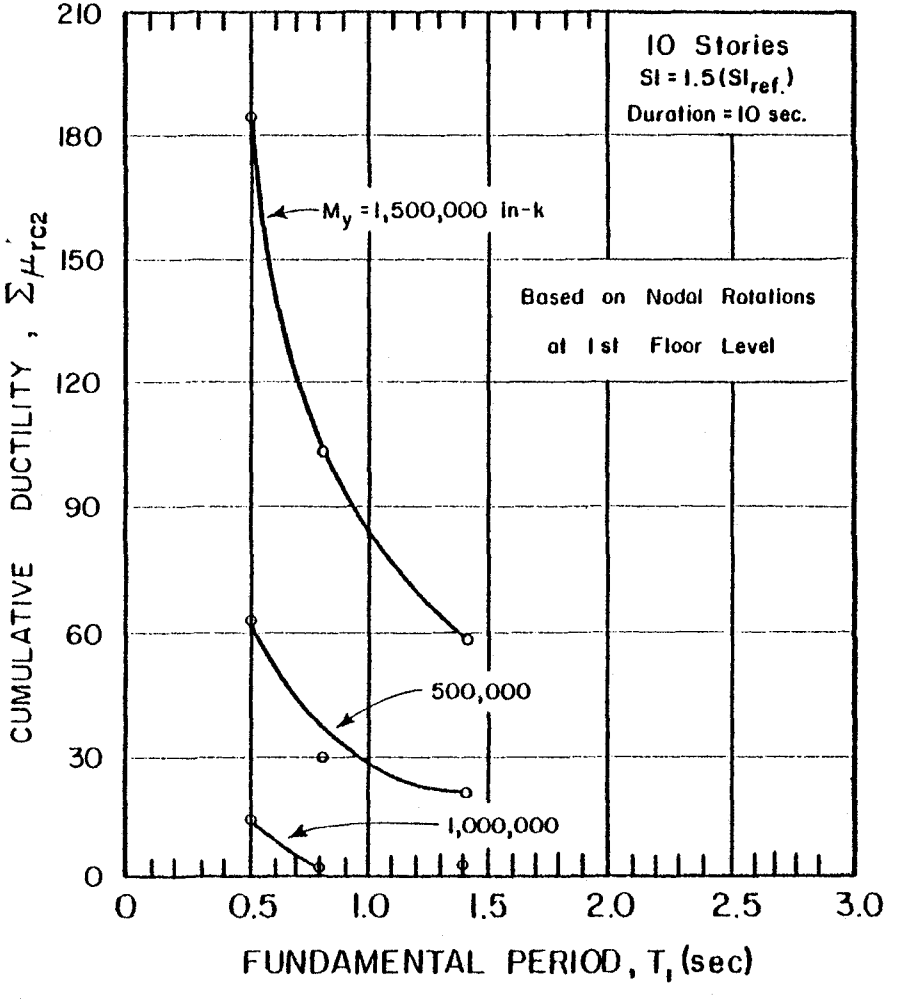

(g)

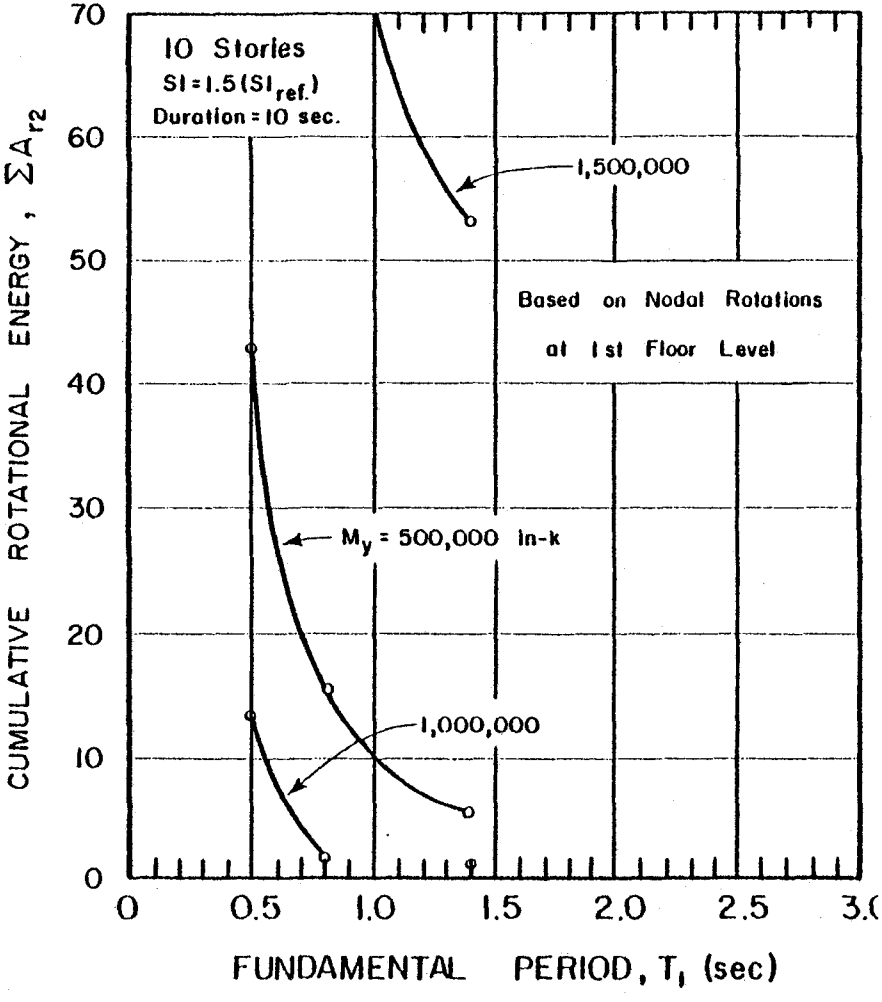

(h)

Fig. A17 (contd.) Critical Response Values as Functions of Fundamental Period, T_1, and Yield Level, M_y, 10-Story Isolated Structural Walls

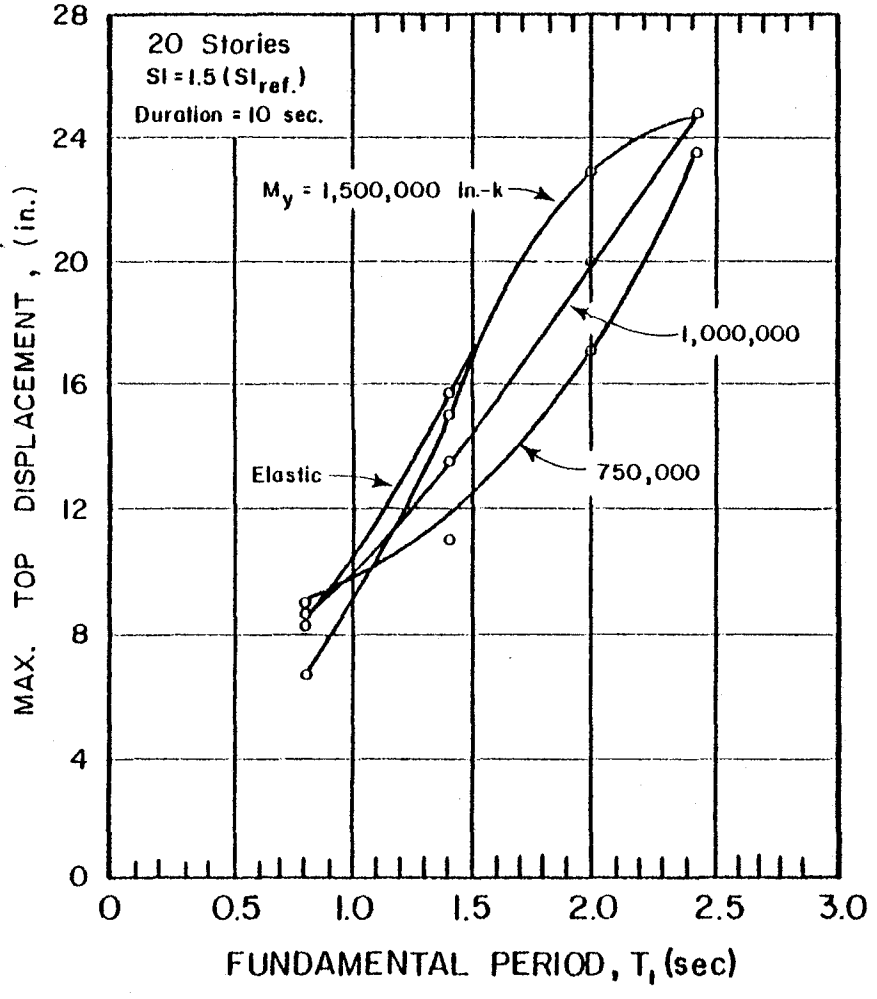

(a)

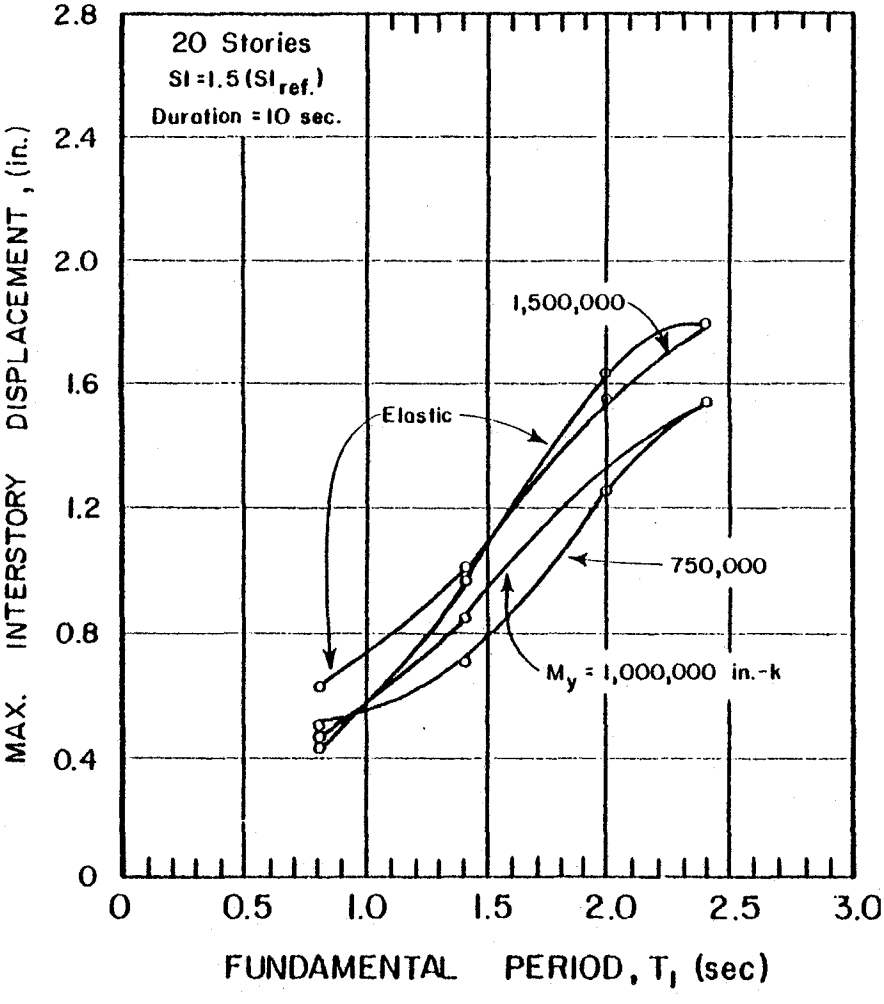

(b)

Fig. A18 Critical Response Values as Functions of Fundamental Period, T_1, and Yield Level, M_y, 20-Story Isolated Structural Walls

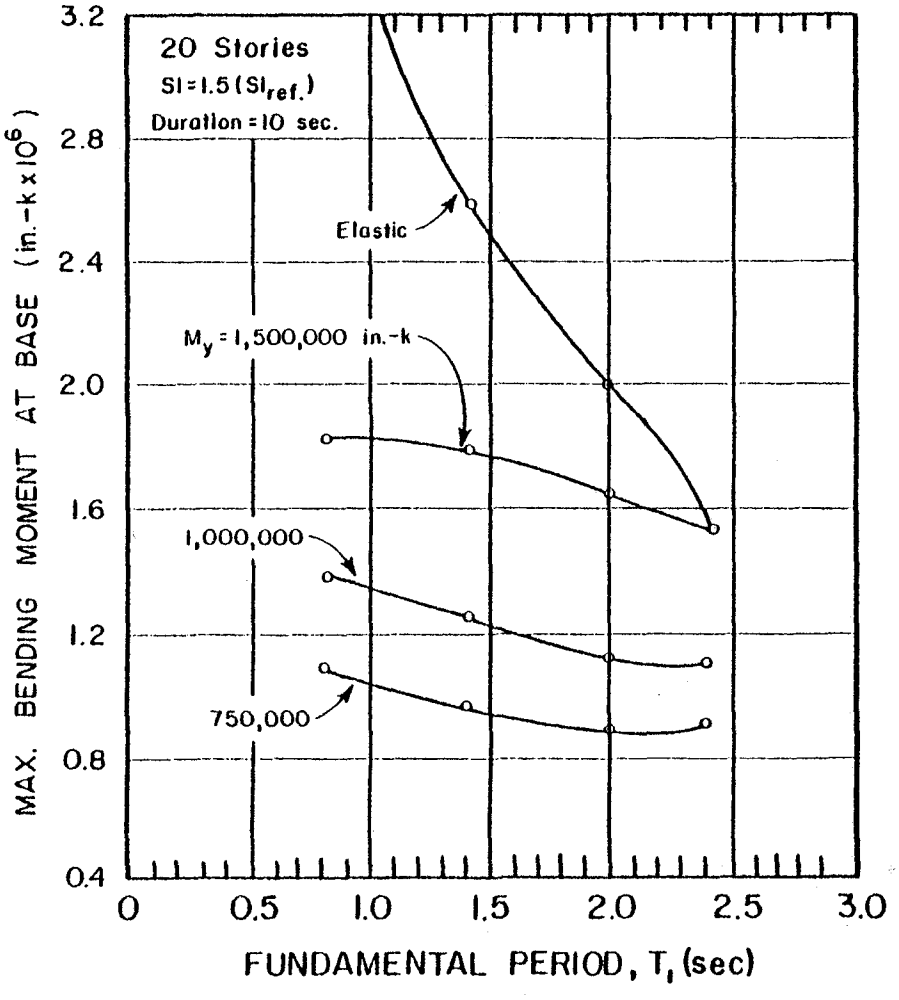

(c)

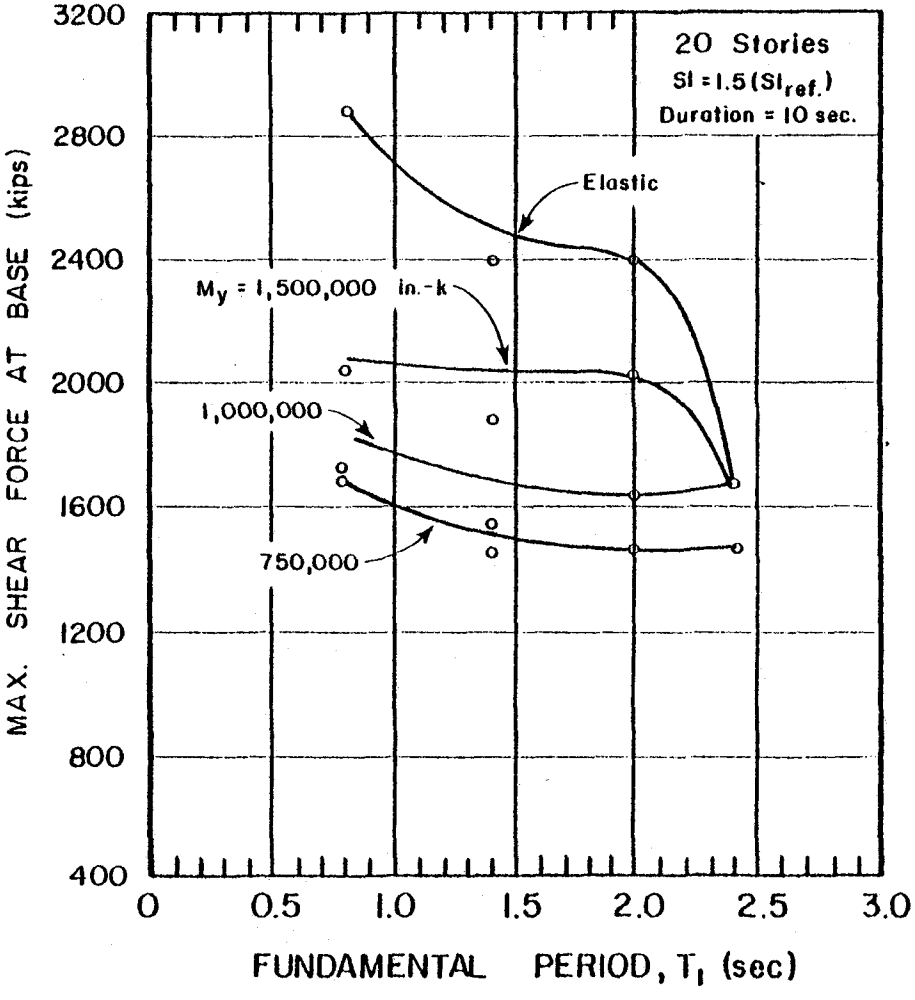

(d)

Fig. A18 (contd.) Critical Response Values as Functions of Fundamental Period, T_1, and Yield Level, M_y, 20-Story Isolated Structural Walls

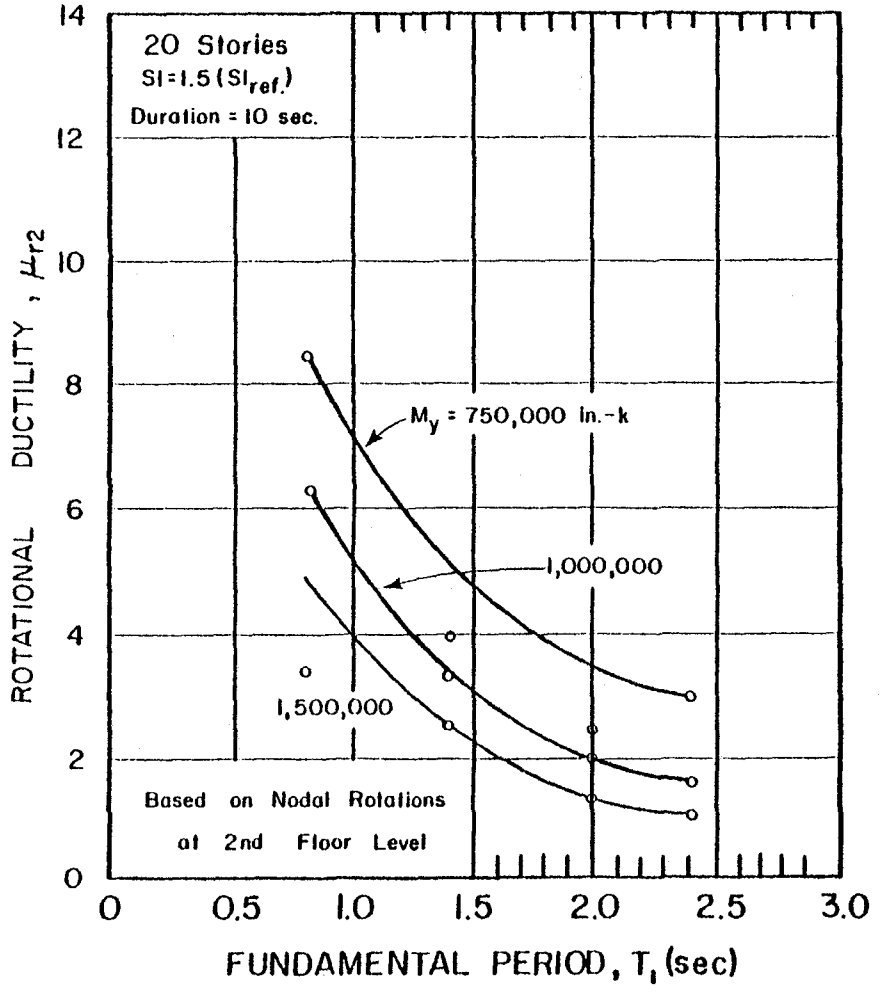

(e)

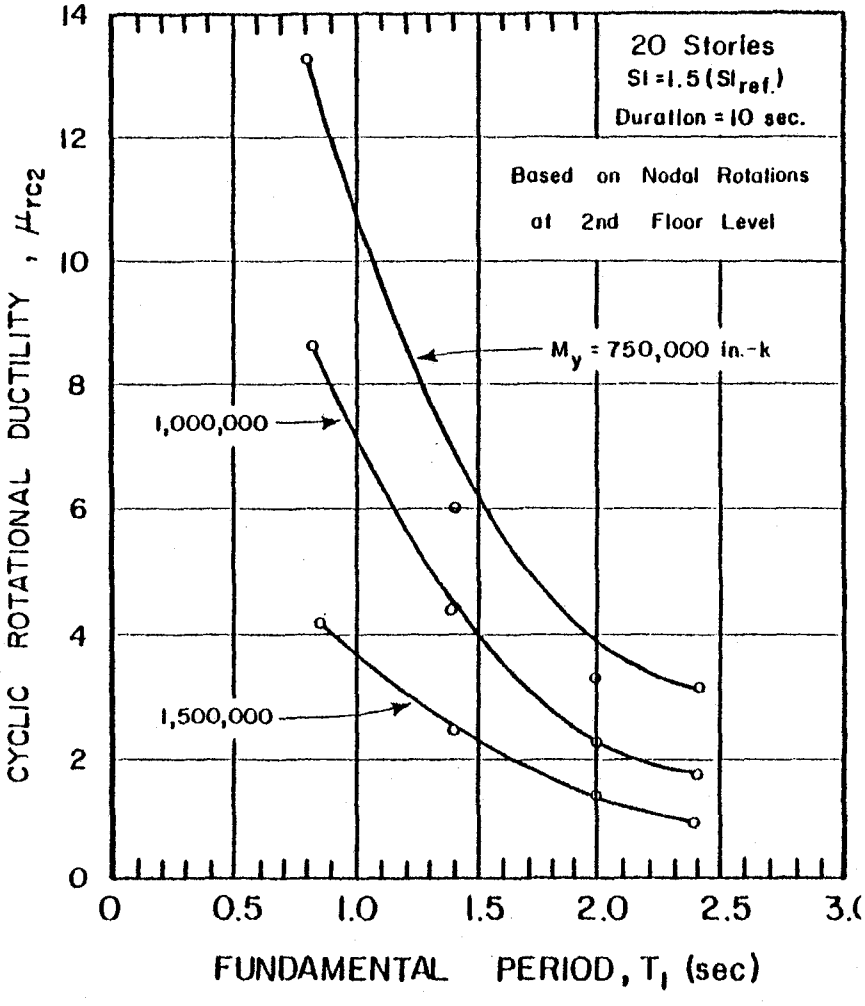

(f)

Fig. A18 (contd.) Critical Response Values as Functions of Fundamental Period, T_1, and Yield Level, M_y, 20-Story Isolated Structural Walls

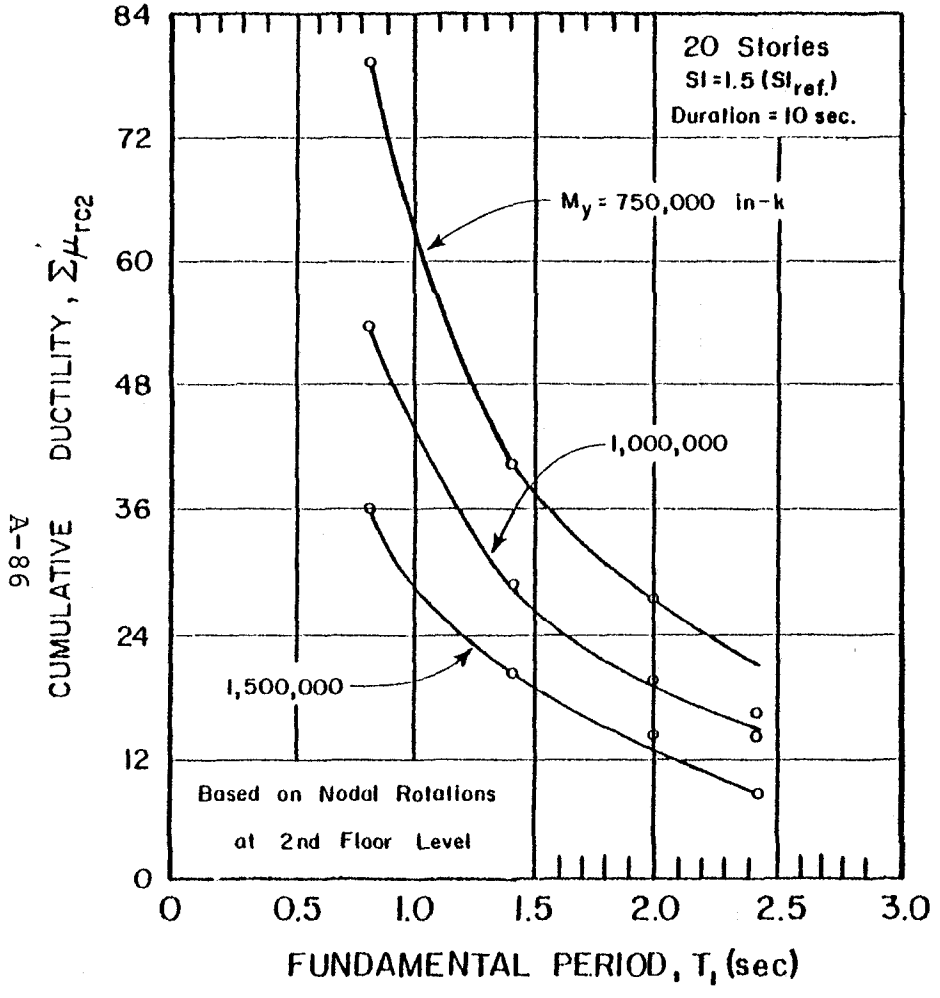

(g)

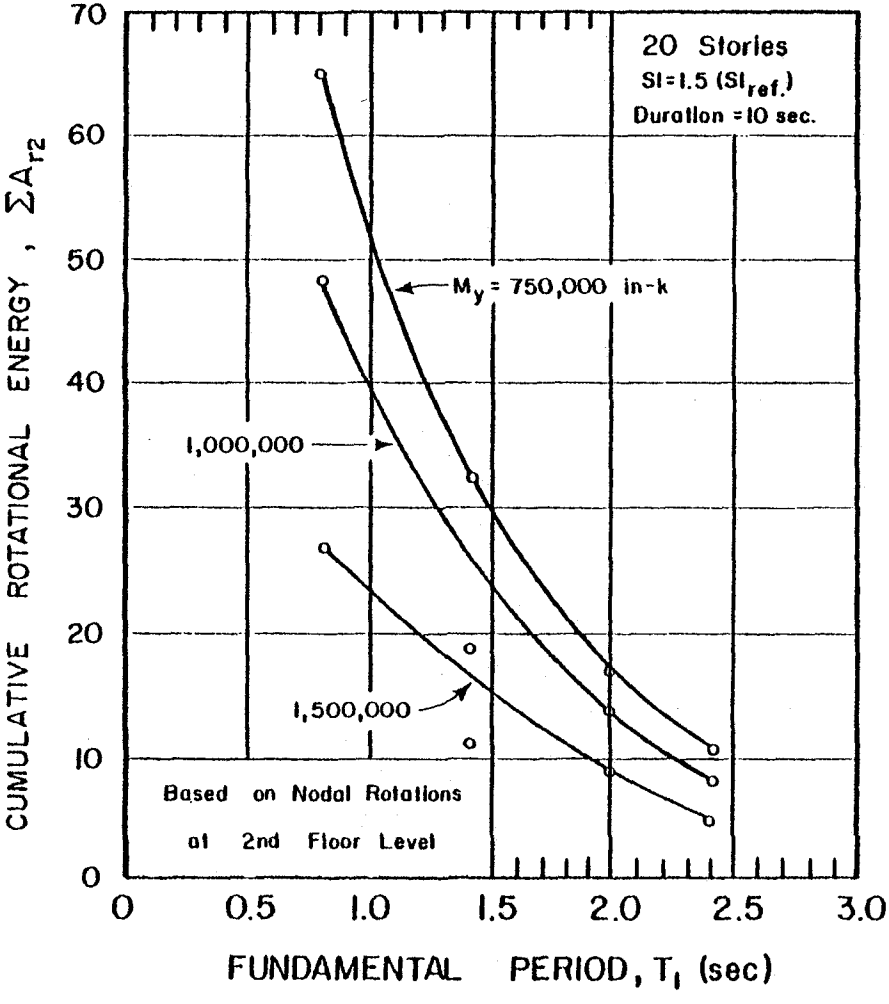

(h)

Fig. A18 (contd.) Critical Response Values as Functions of Fundamental Period, T_1, and Yield Level, M_y, 20-Story Isolated Structural Walls

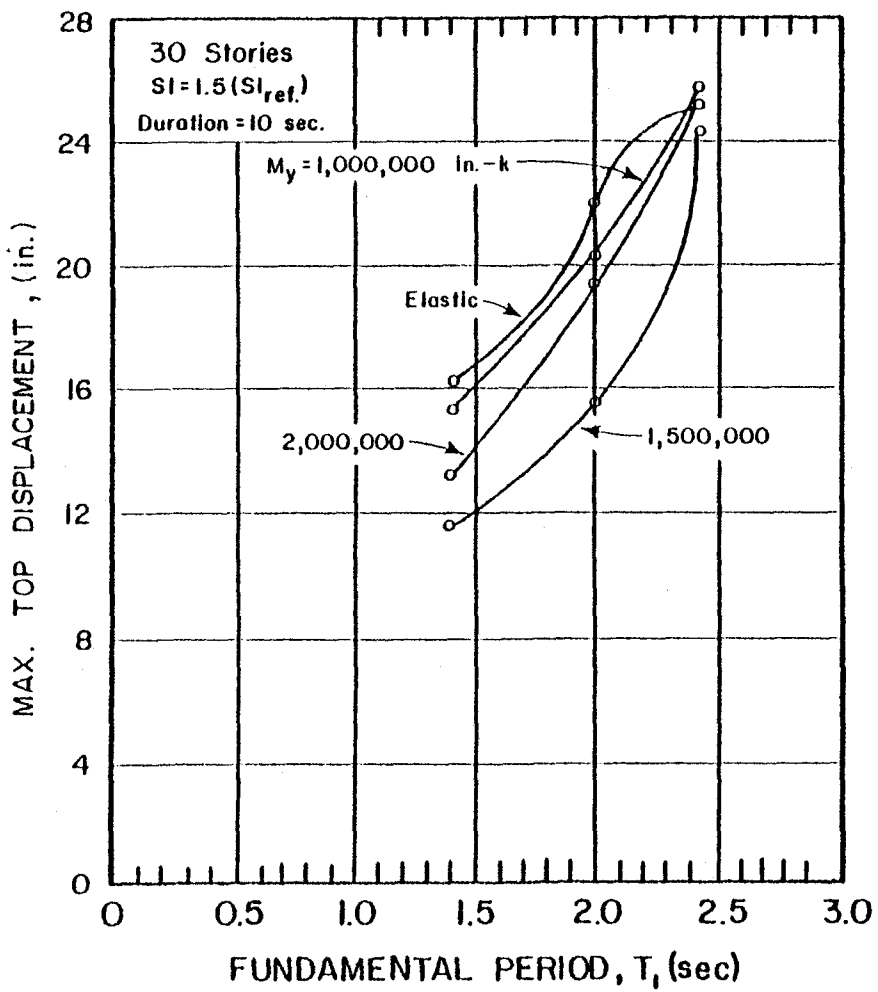

(a)

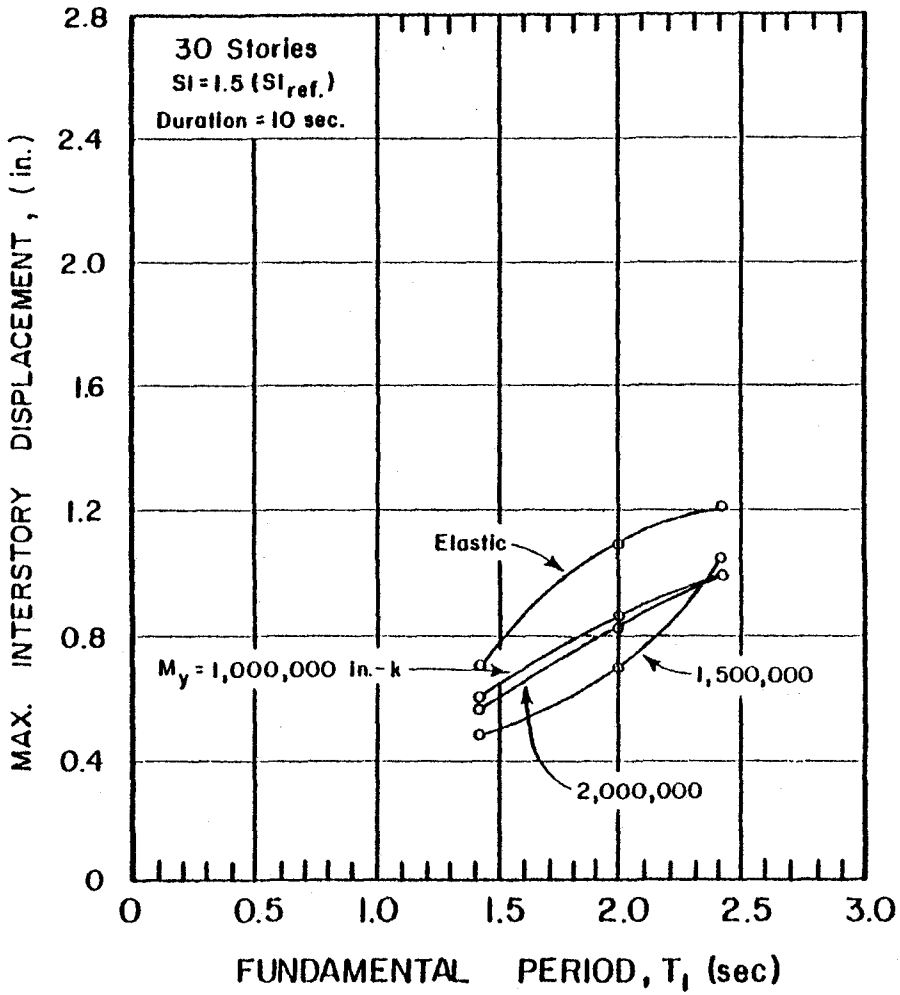

(b)

Fig. A19 Critical Response Values as Functions of Fundamental Period, T_1, and Yield Level, M_y, 30-Story Isolated Structural Walls

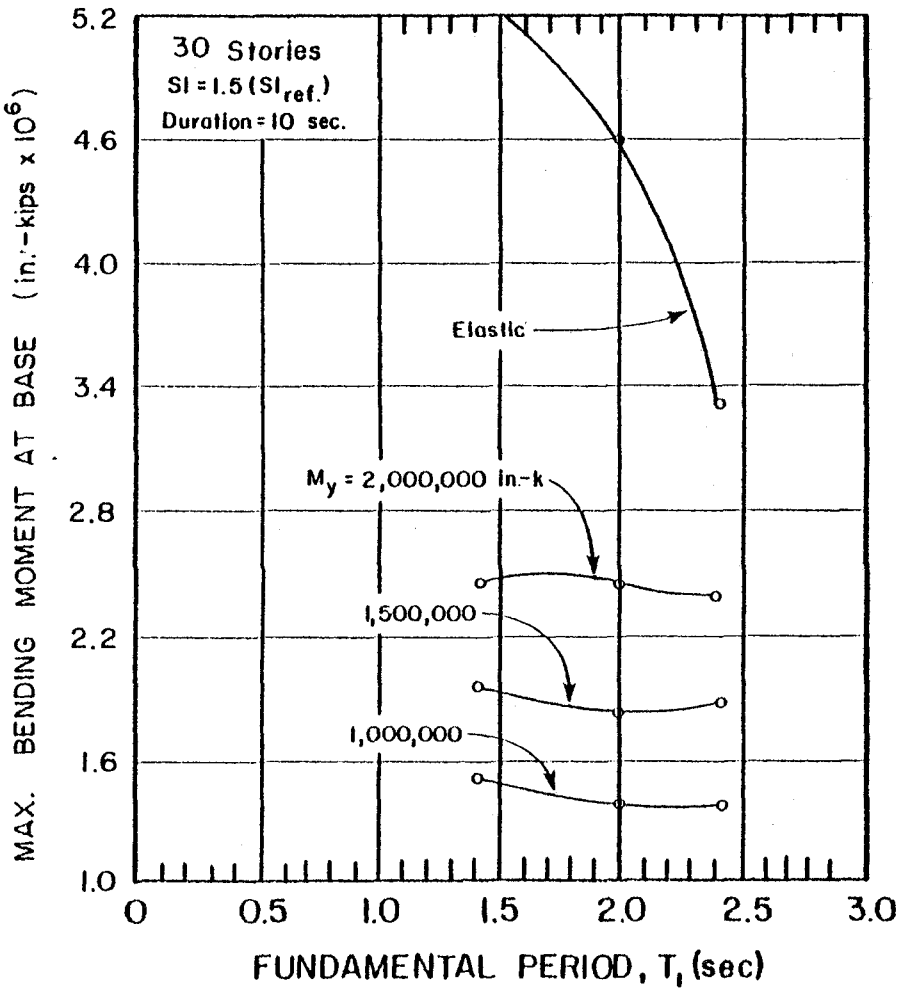

(c)

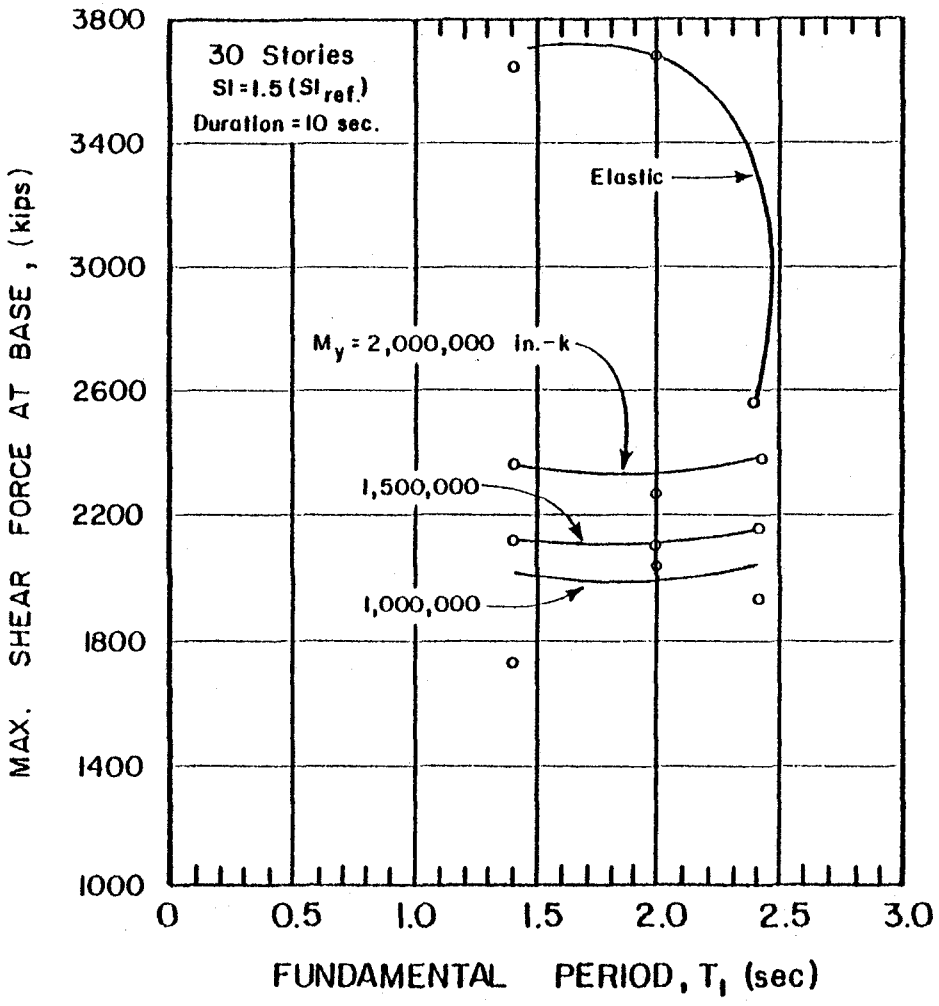

(d)

Fig. A19 (contd.) Critical Response Values as Functions of Fundamental Period, T_1, and Yield Level, M_y, 30-Story Isolated Structural Walls

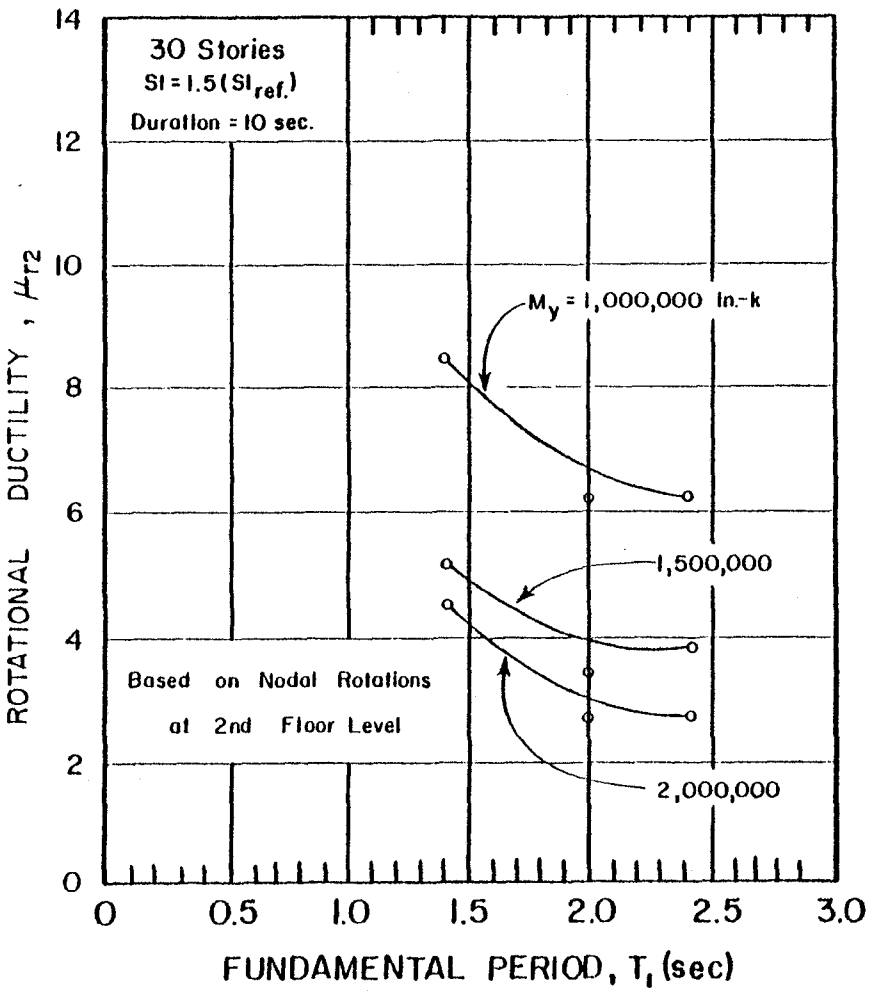

(e)

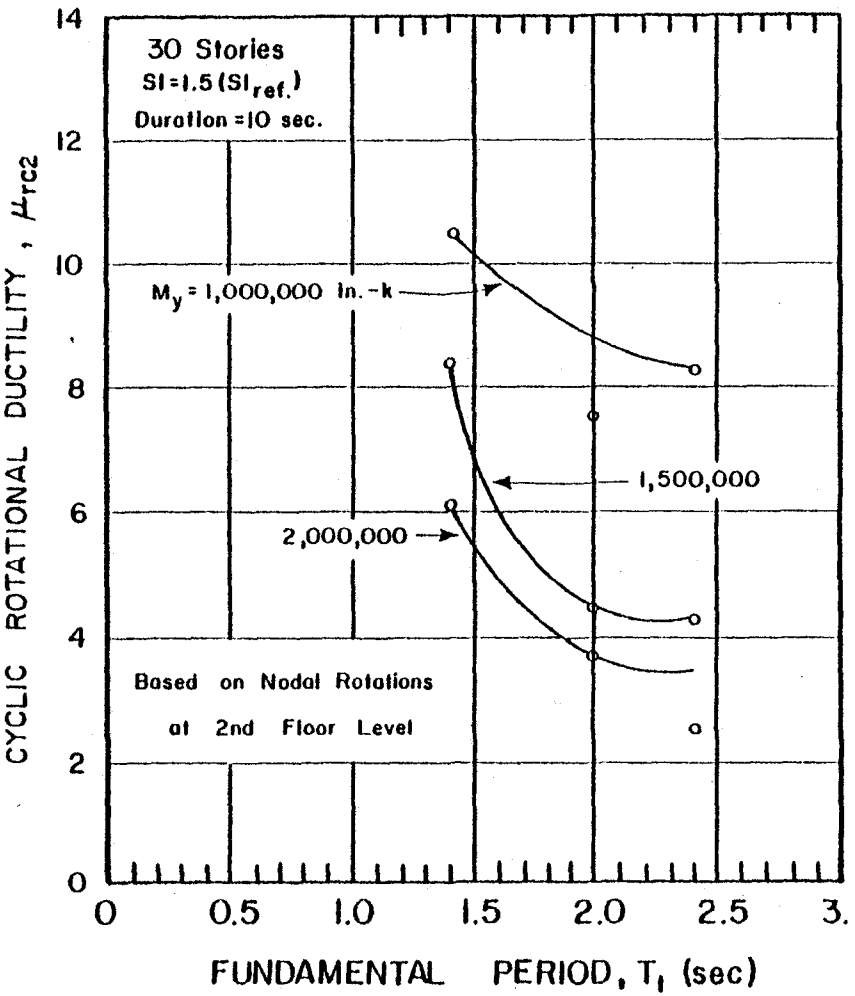

(f)

Fig. A19 (contd.) Critical Response Values as Functions of Fundamental Period, T_1, and Yield Level, M_y, 30-Story Isolated Structural Walls

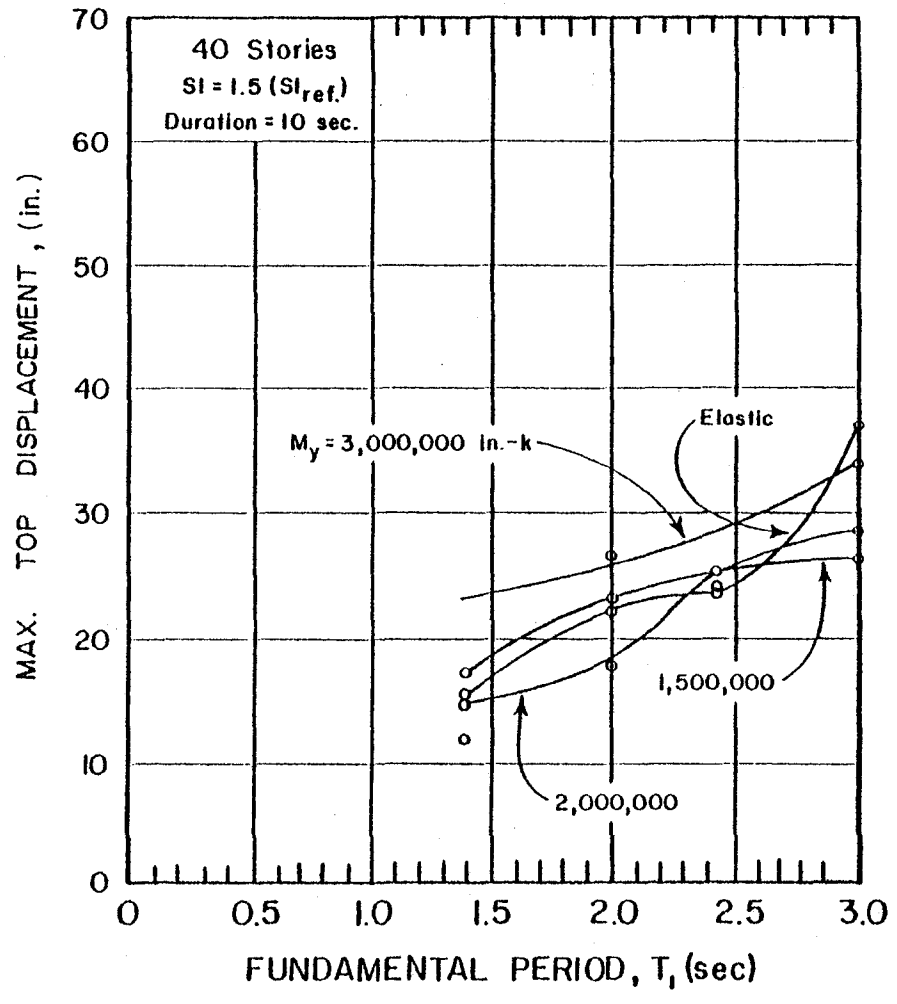

(a)

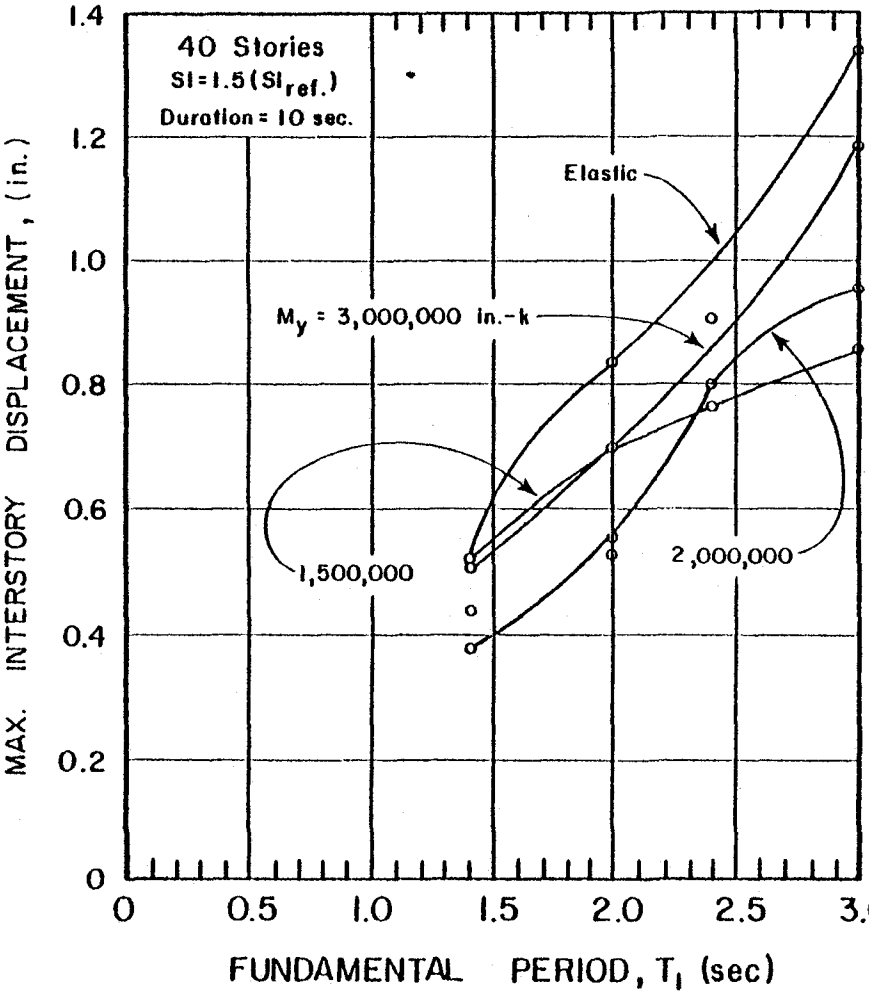

(b)

Fig. A20 Critical Response Values as Functions of Fundamental Period, T_1 and Yield Level, M_y, 40-Story Isolated Structural Walls

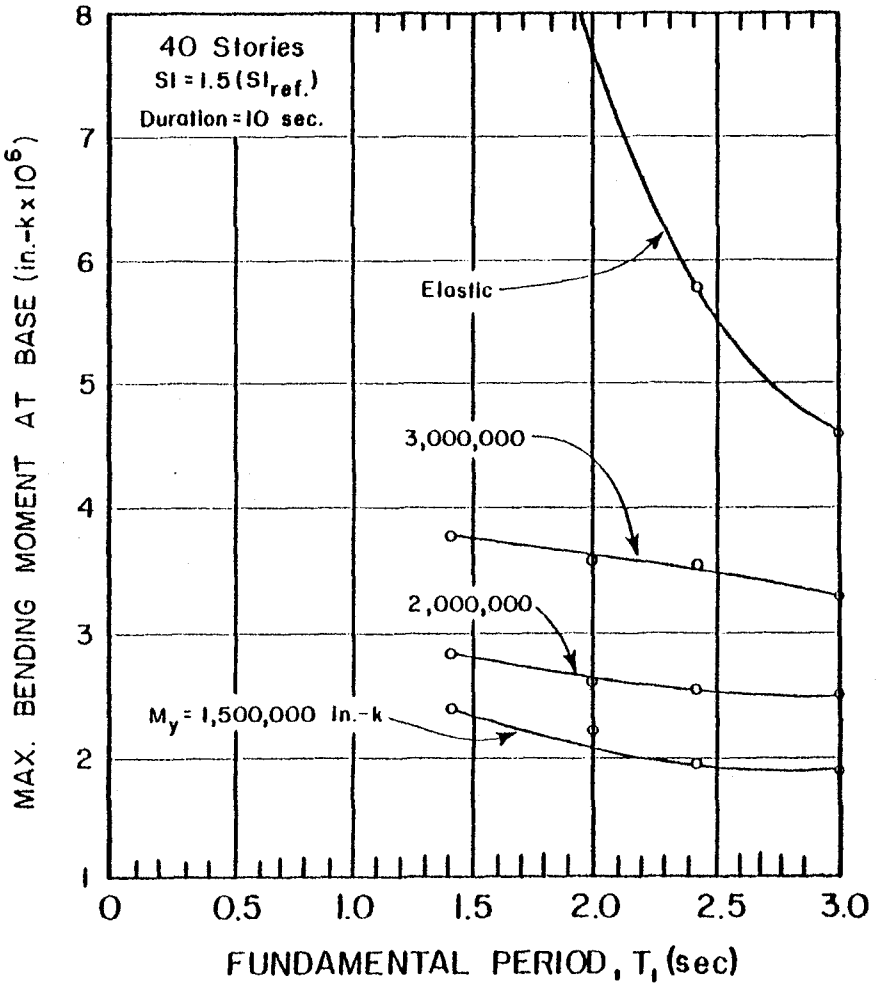

(c)

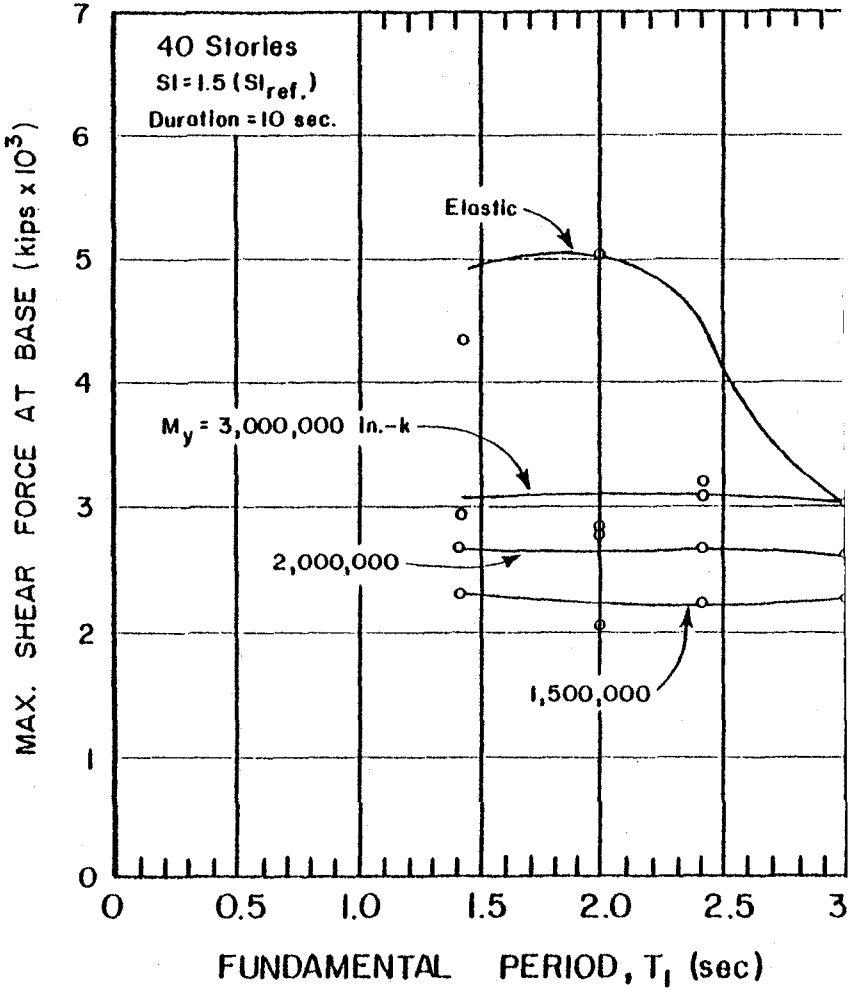

(d)

Fig. A20 (contd.) Critical Response Values as Functions of Fundamental Period, T_1, and Yield Level, M_y, 40-Story Structural Walls

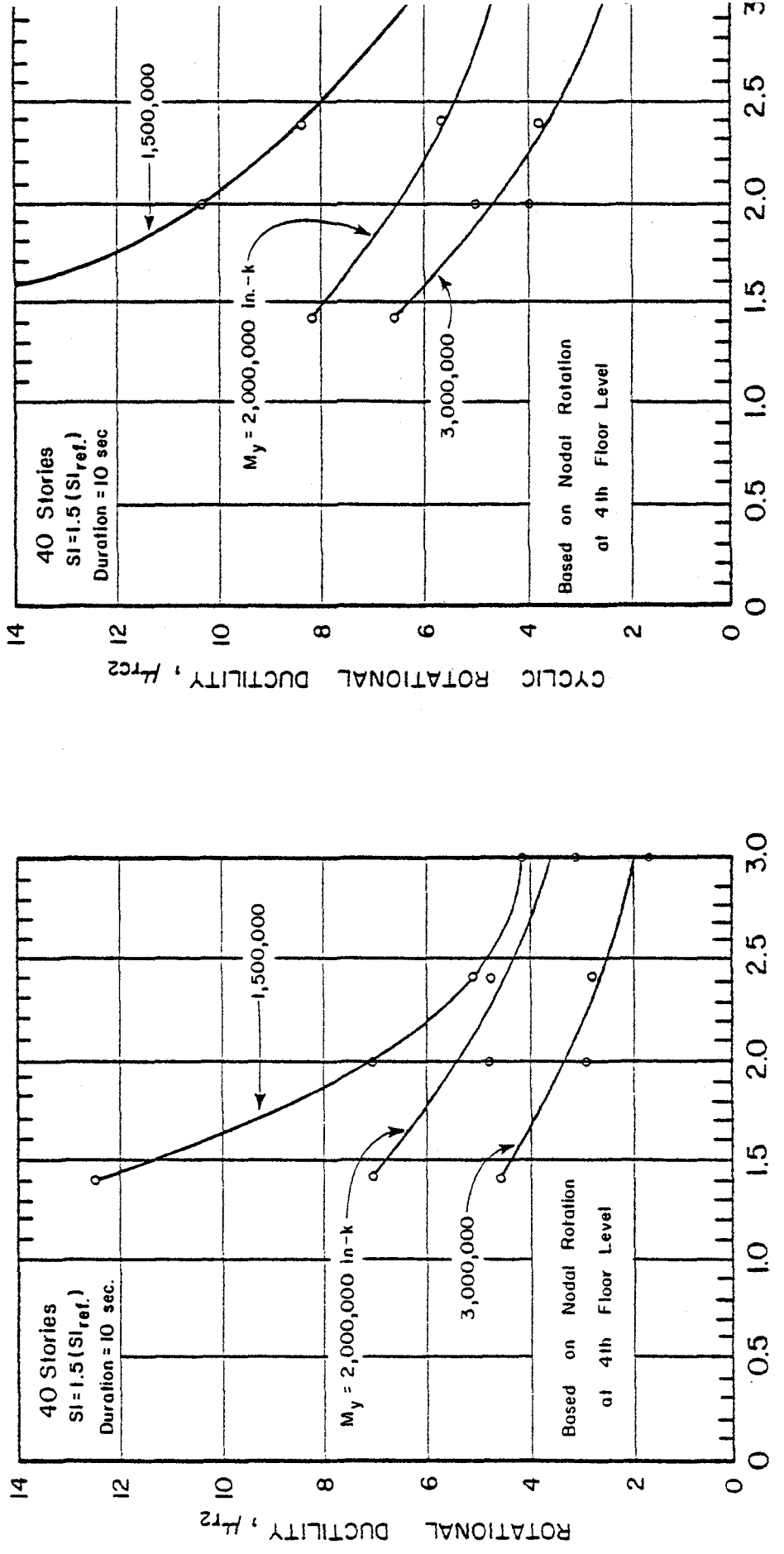

(e)

(f)

Fig. A20(contd.) Critical Response Values as Functions of Fundamental Period, T_1, and Yield Level, M_y, 40-Story Structural Walls

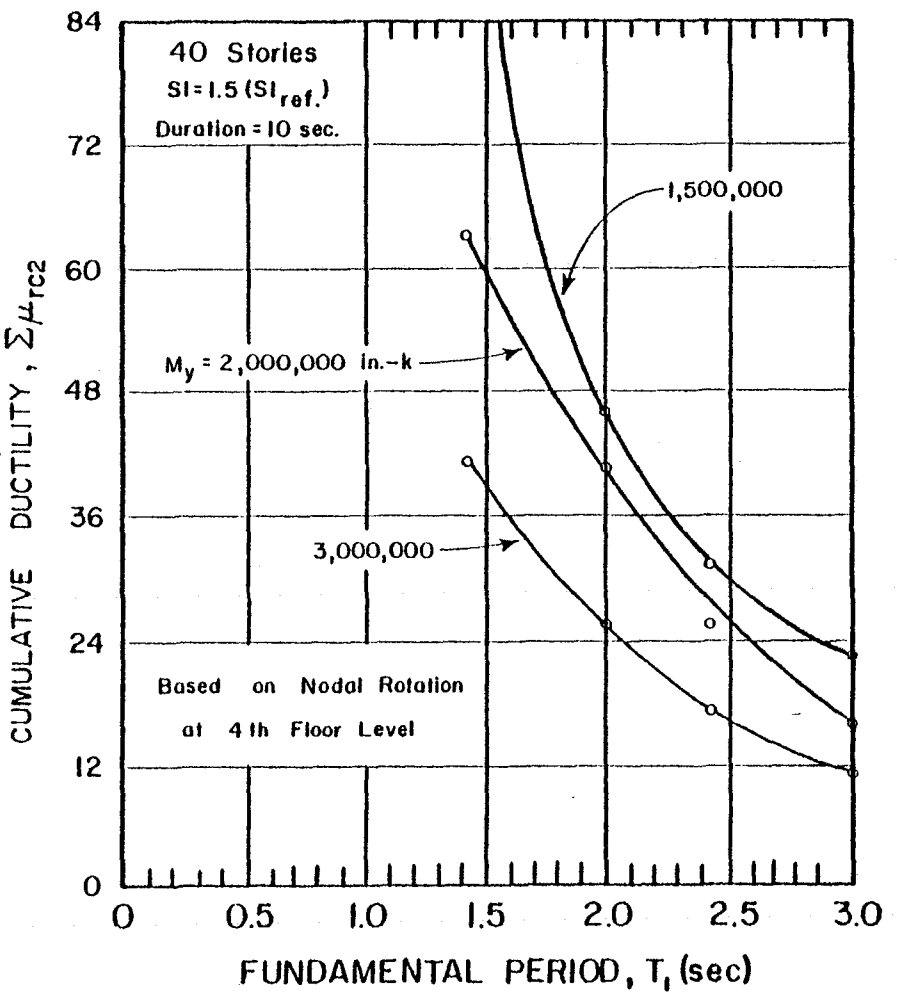

(g)

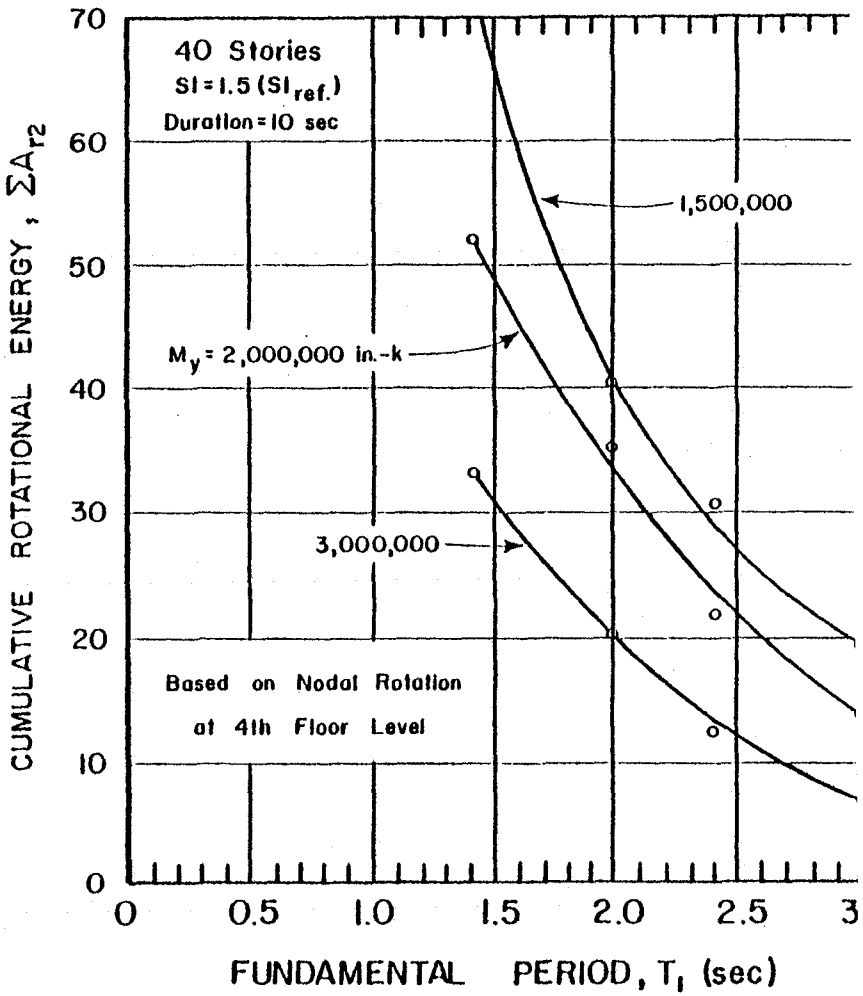

(h)

Fig. A20 (contd.) Critical Response Values as Functions of Fundamental Period, T_1, and Yield Level, M_y, 40-Story Structural Walls

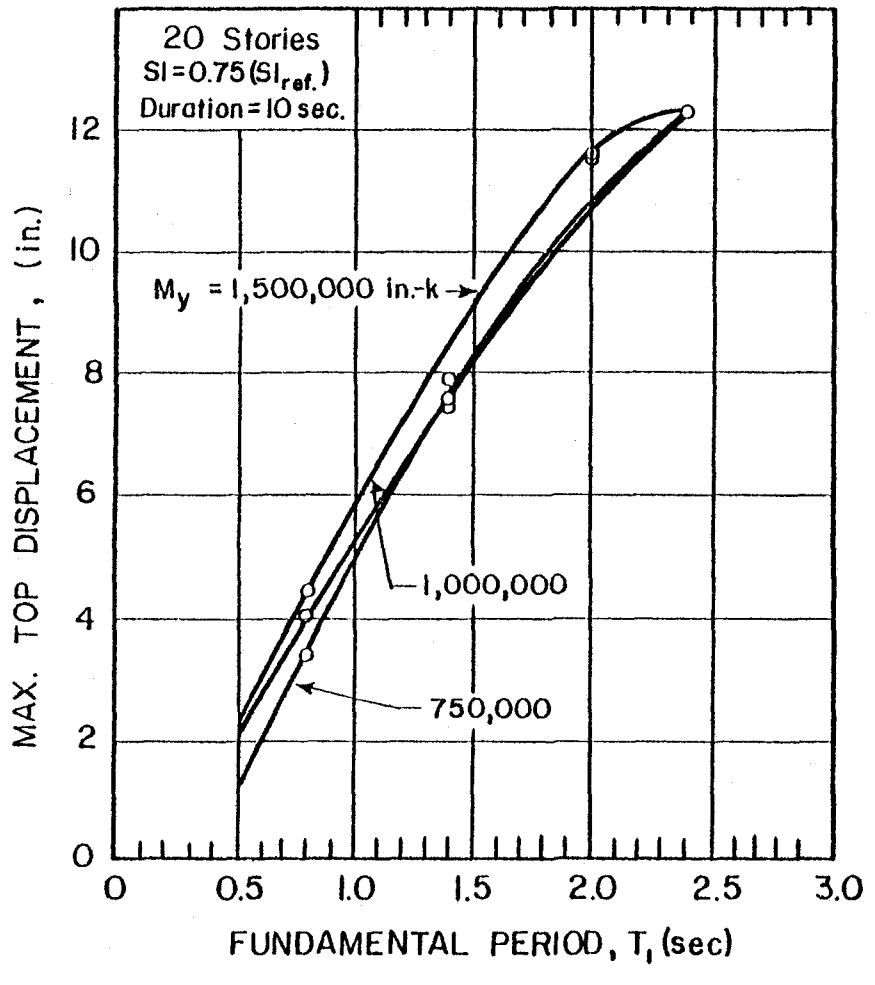

(a)

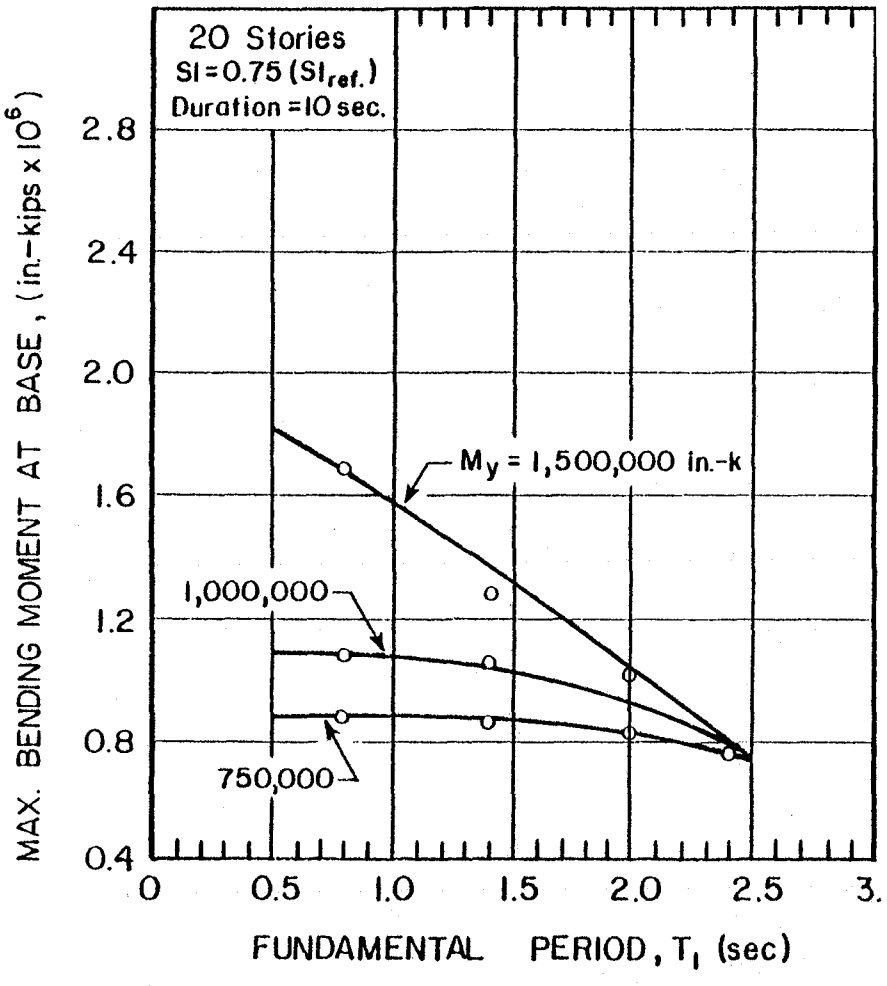

(b)

Fig. A21 Critical Response Values as Functions of Fundamental Period, T_1 and Yield Level, M_y, 20-Story Structural Walls - SI = 0.75($SI_{ref.}$)

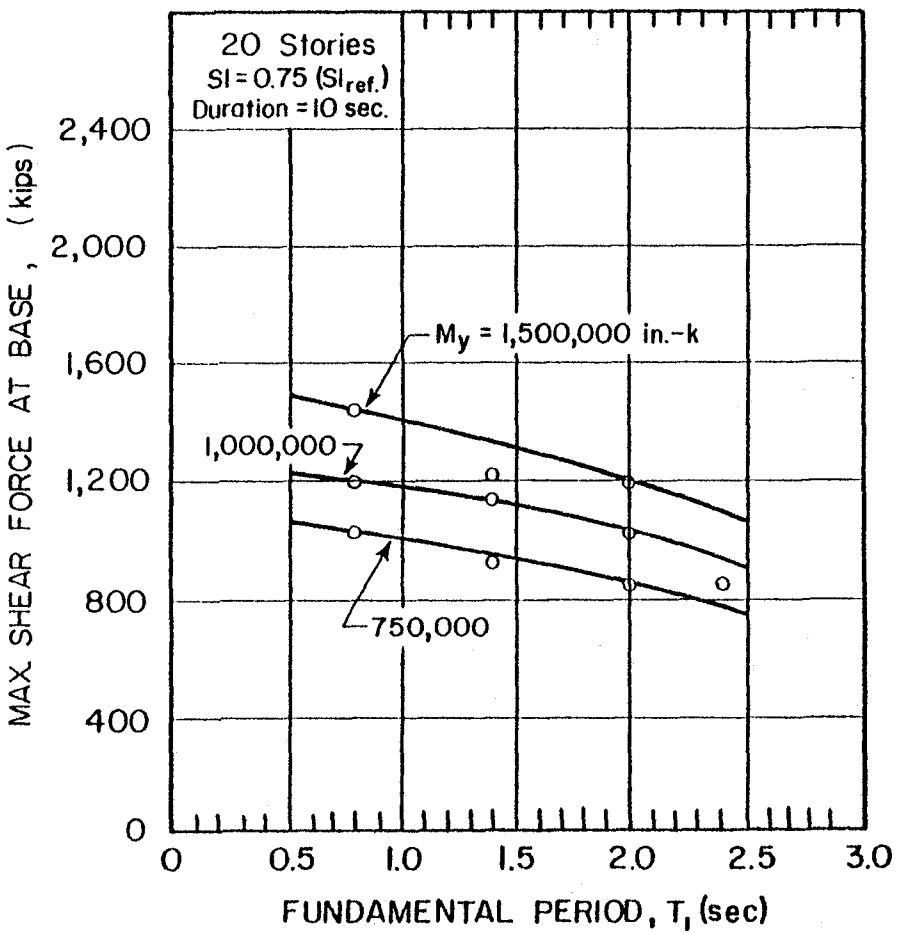

(c)

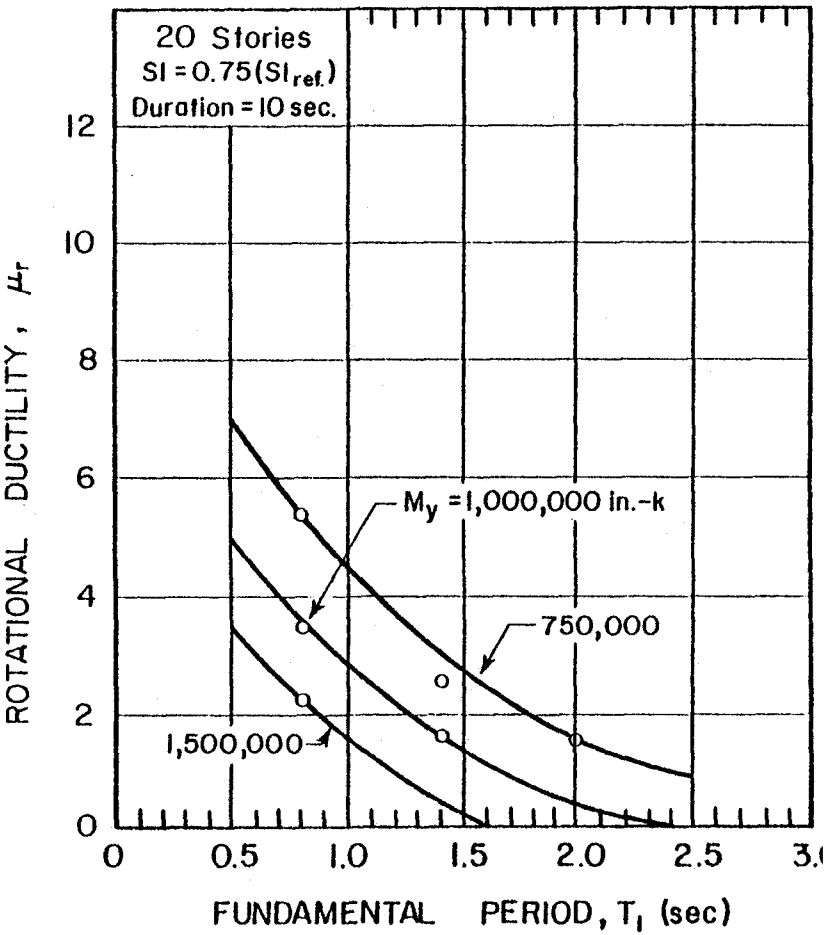

(d)

Fig. A21(contd.) Critical Response Values as Functions of Fundamental Period, T_1, and Yield Level, M_y, 20-Story Structural Walls - $SI = 0.75(SI_{ref.})$

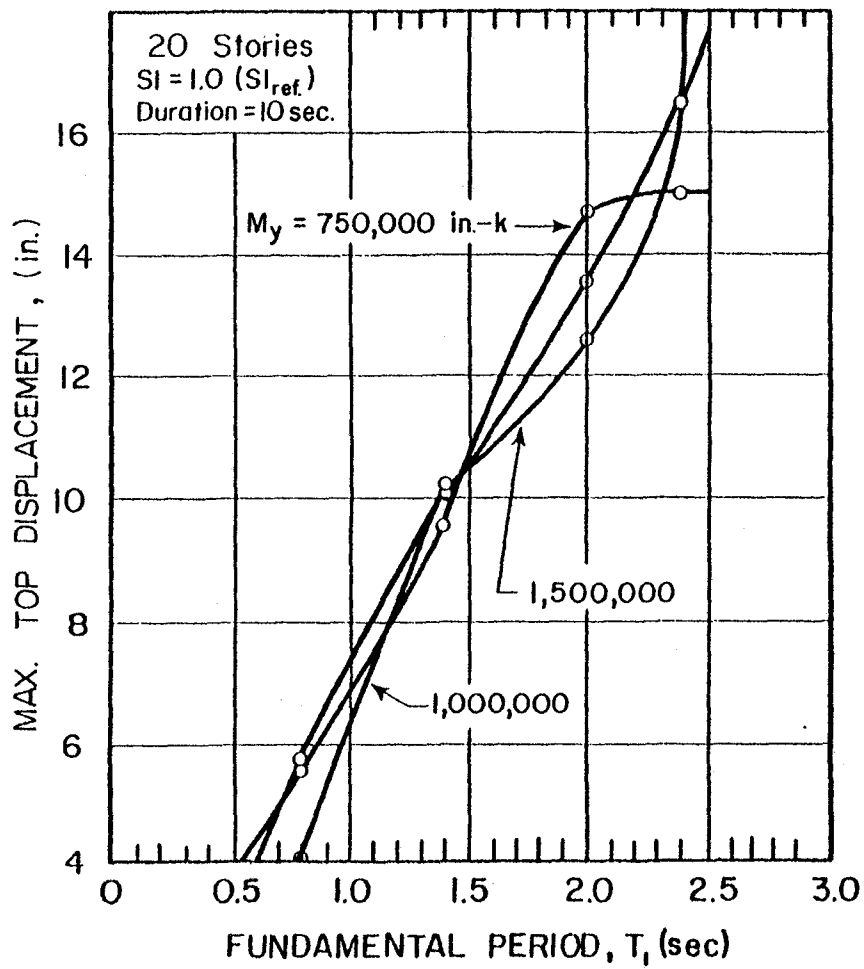

(a)

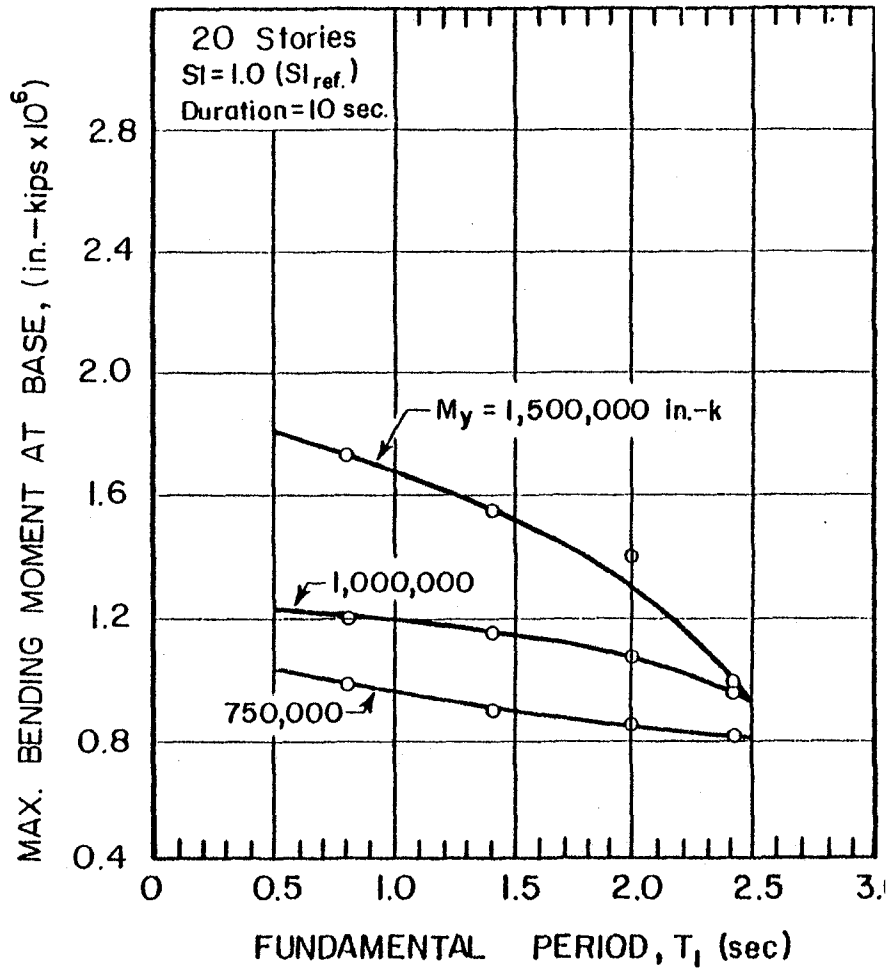

(b)

Fig. A22 Critical Response Values as Functions of Fundamental Period, T_1, and Yield Level, M_y, 20-Story Structural Walls - SI = $1.0(SI_{ref.})$

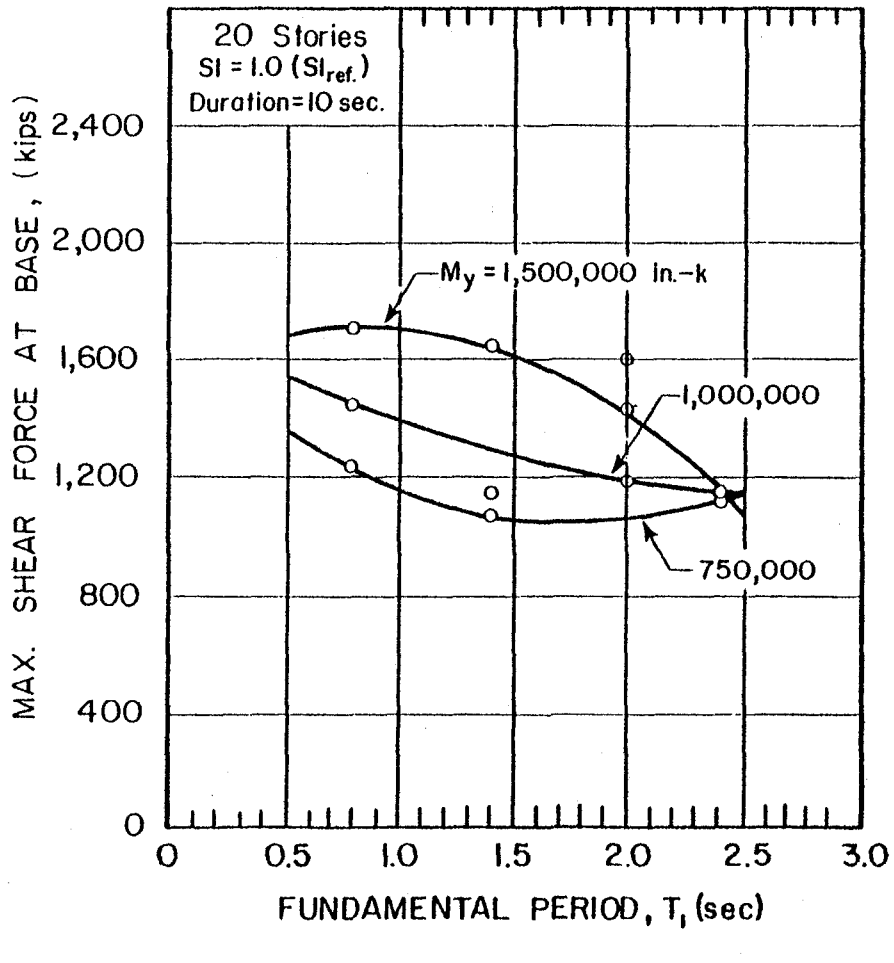

(c)

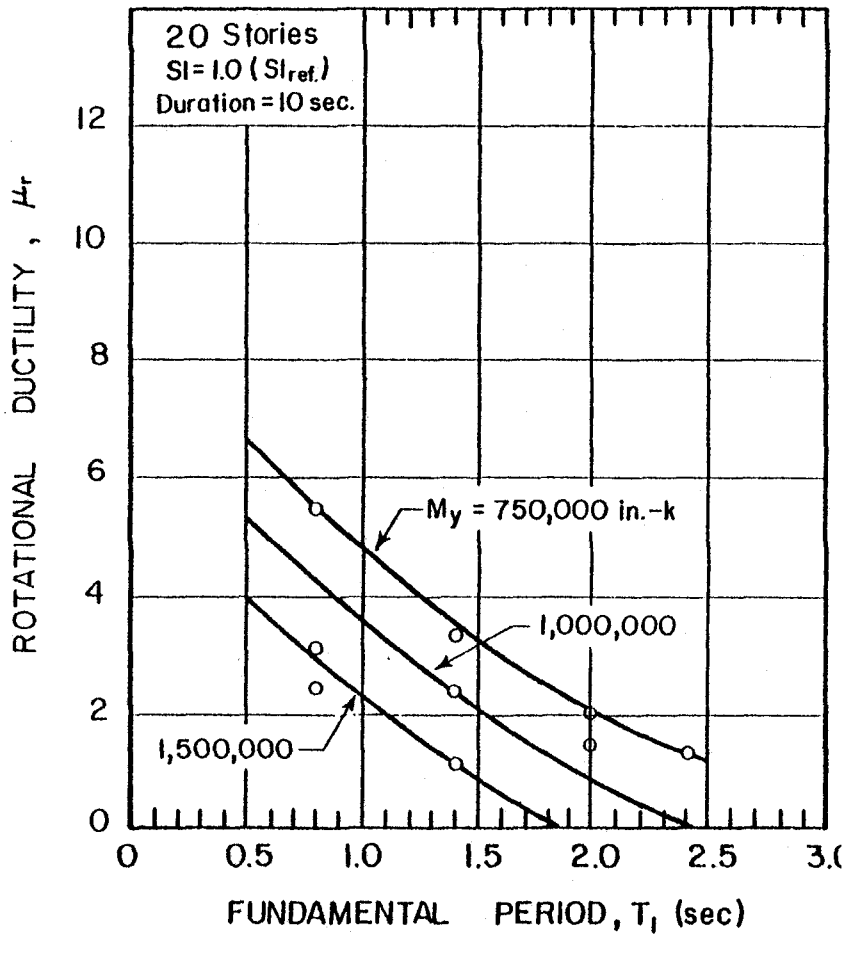

(d)

Fig. A22 (contd.) Critical Response Values as Functions of Fundamental Period, T_1, and Yield Level, M_y, 20-Story Isolated Structural Walls, SI = 1.0($SI_{ref.}$)

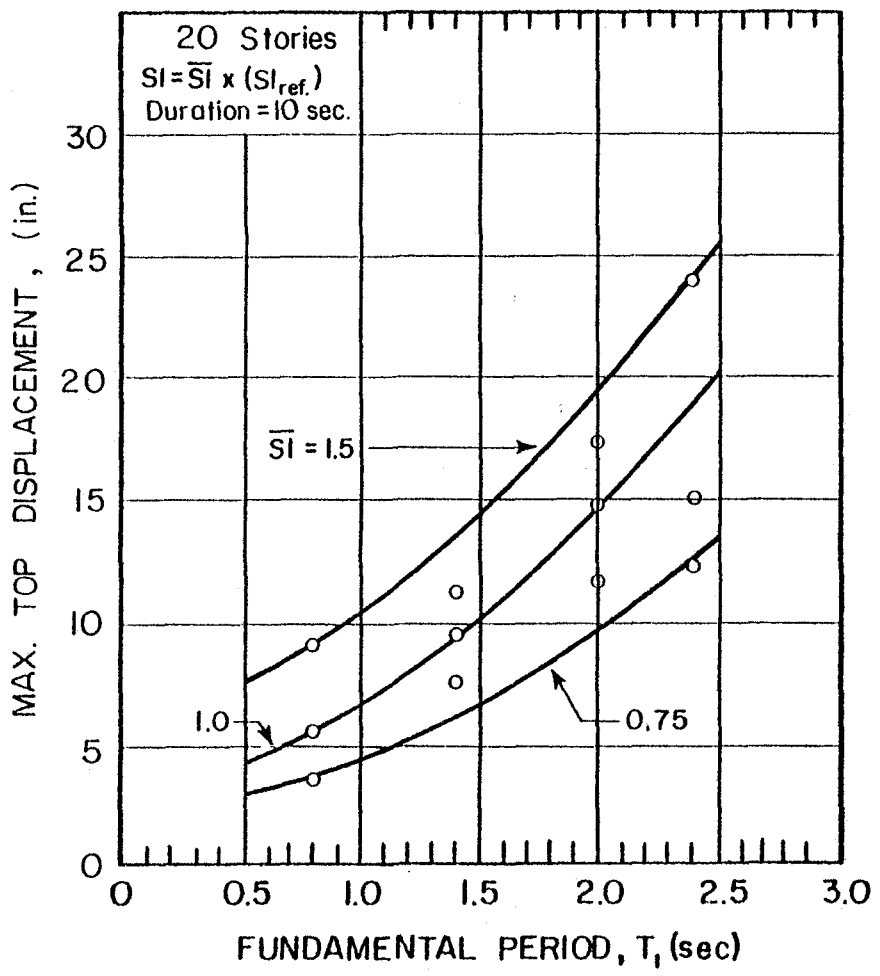

(a)

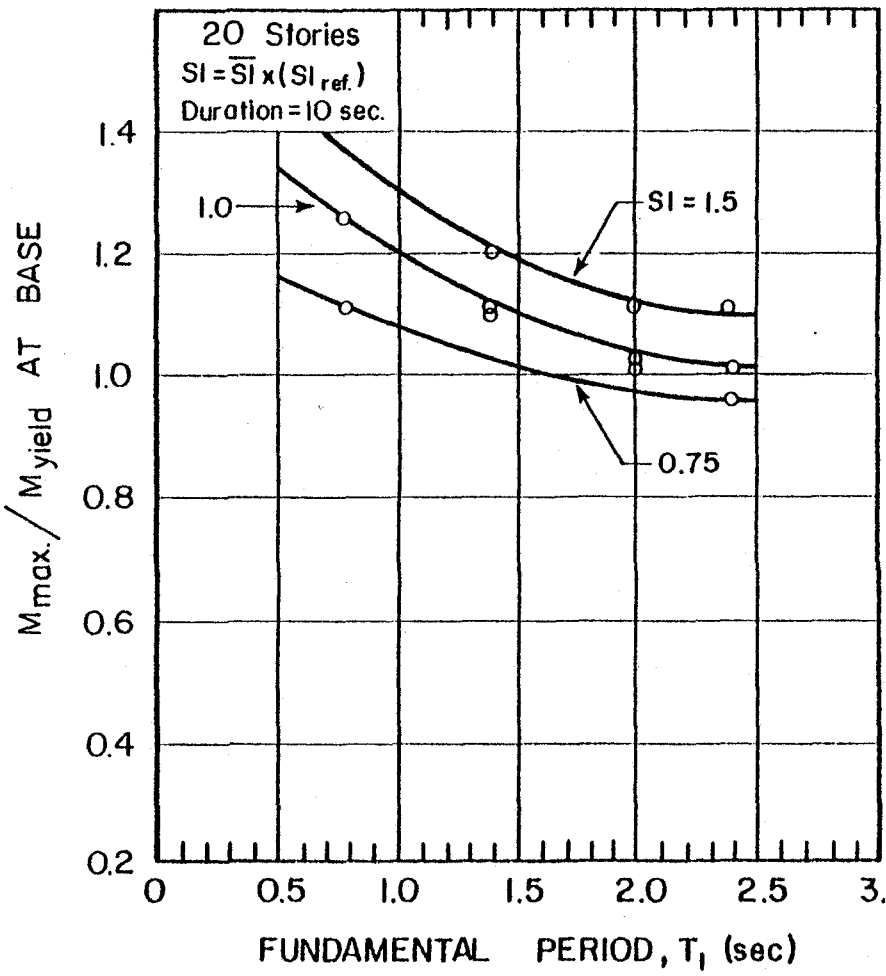

(b)

Fig. A23 Critical Response Values as Functions of Fundamental Period, T_1, and Earthquake Intensity, SI, 20-Story Isolated Structural Walls

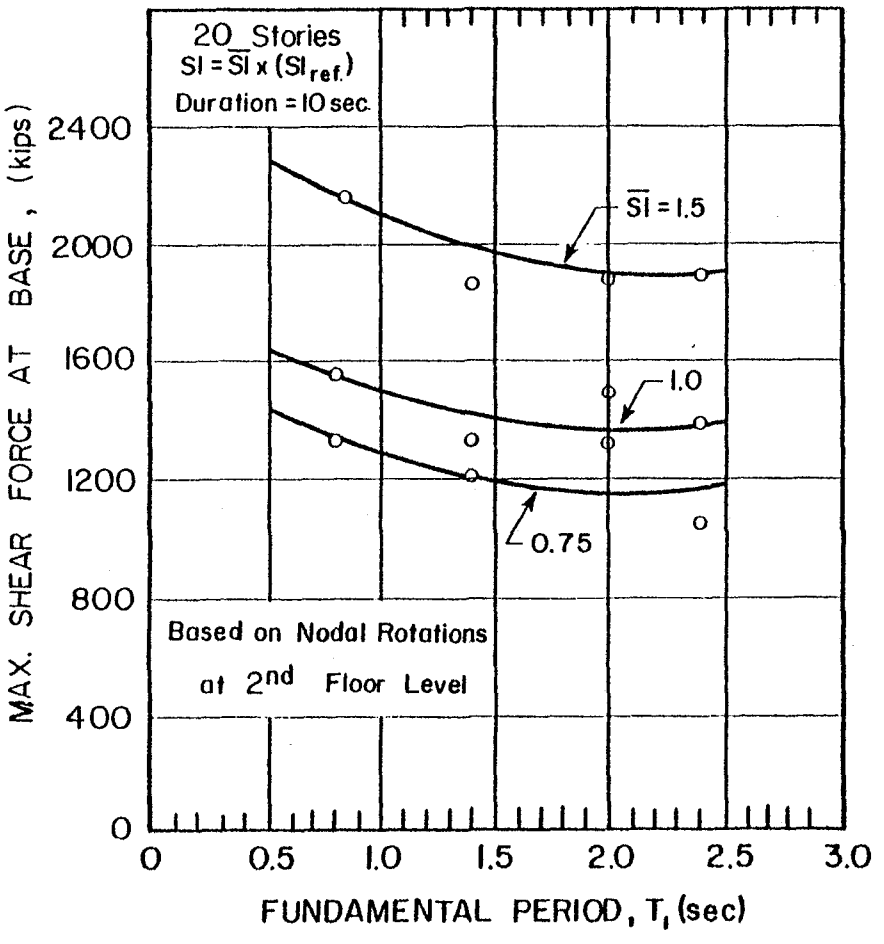

(c)

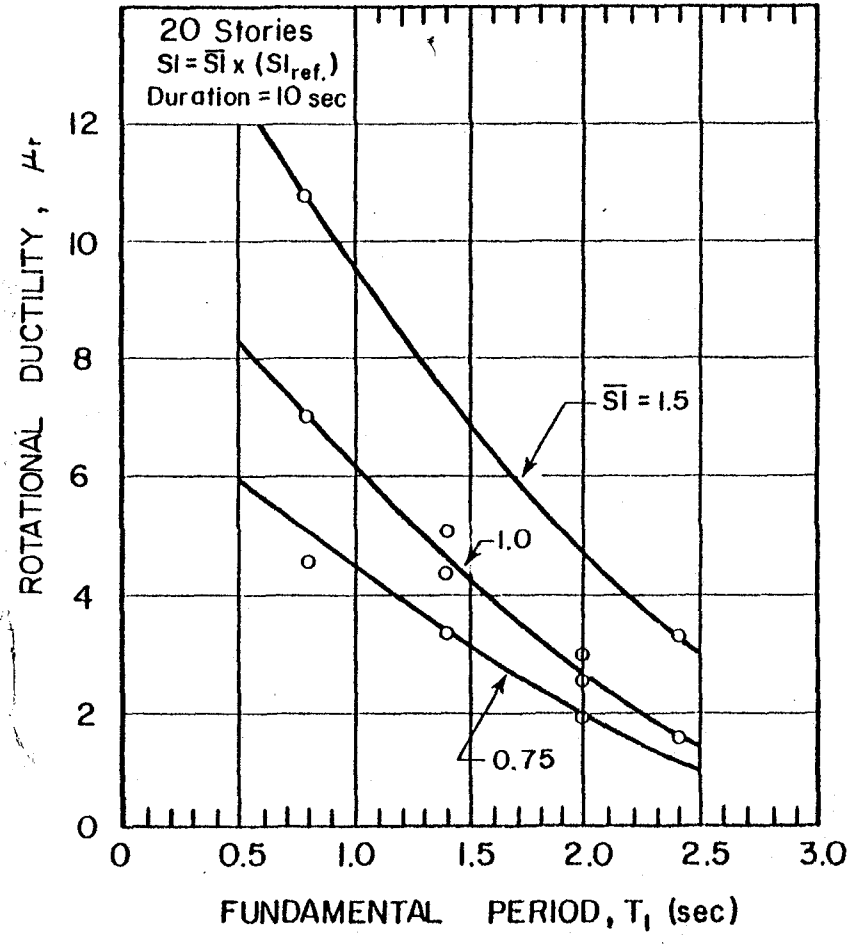

(d)

Fig. A23(contd.) Critical Response Values as Functions of Fundamental Period, T_1, and Earthquake Intensity, SI, 20-Story Isolated Structural Walls

APPENDIX B

EXPERIMENTAL DATA

APPENDIX B

Tables B1-B13 Ductilities by Various Definitions for Test Specimens

Figures B1-B15 Moment vs. Rotation Curves for Test Specimens

List of Tables

List of Tables (cont'd)

List of Figures

List of Figures (cont'd)

Table B1

Ductilities by Various Definitions - For the Hinging Region in Specimen R1
Based on Rotation of a Section 74.0 in. Above Base of Test Specimen

Observed Yield Moment (k-in.)	Rotation at Full Yield (Rad.)	Load Stage			Cycle No.	Rotational Ductility, μ_r	Cyclic Rotational Ductility, μ_{rc}	Cumulative Ductility, $\Sigma\mu_{rc}$	Cumulative Rotational Energy, ΣA_r @
		+Load (% Max)	-Load (% Max)	Avg. Load (% Max)					
3,600	0.0030	81.8	72.8	77.3	10	1.00	1.1	2.2	1.94
		80.3	72.6	76.5	11	1.04	1.3	4.6	2.48
		70.6	74.9	72.7	12	1.13	1.2	7.1	3.00
		92.5	84.8	88.7	13	2.09	2.7	12.0	6.70
		83.6	79.8	81.7	14	2.05	2.9	17.5	9.56
		81.4	77.9	79.7	15	2.04	2.8	22.9	12.16
		99.4	91.0	95.2	16	4.04	6.3	33.9	23.00
		90.1	85.3	87.7	17	4.02	6.3	46.3	32.24
		86.1	84.8	85.5	18	4.08	6.1	58.4	41.70
		100.0	94.1	97.1	19	6.13	9.8	75.8	59.04*
		90.5	89.0	89.7	20	6.08	9.7	95.0	75.10
		88.5	85.3	86.9	21	6.10	9.5	113.7	90.64
		98.3	93.3	95.8	25	7.93	12.9	134.9	116.30**
		90.8	64.8	77.8	26	7.85	12.7	160.1	135.32
		89.1	62.3	75.7	27	14.35	18.4	191.0	155.66
		64.7	66.9	65.8	28	18.17	25.3	236.6	189.72
		56.7	26.5	41.6	29	19.22	26.2	286.4	210.38
		51.6	17.9	34.7	30	19.39	27.0	339.8	227.36

@ The cumulative rotational energy has been normalized in terms of observed yield moment and the rotation at full yield.

* Maximum load stage.

** Last stable cycle.

Table B2

Ductilities by Various Definitions - For the Hinging Region in Specimen R2
Based on Rotation of a Section 74.0 in. Above Base of Test Specimen

Observed Yield Moment (k-in.)	Rotation at Full Yield (Rad.)	Load Stage			Cycle No.	Rotational Ductility, μ_r	Cyclic Rotational Ductility, μ_{rc}	Cumulative Ductility, $\Sigma\mu_{rc}$	Cumulative Rotational Energy, ΣA_r @
		+Load (% Max)	-Load (% Max)	Avg. Load (% Max)					
6,000	0.0046	86.4	83.6	85.0	19	1.08	1.3	2.4	3.10
		82.0	80.5	81.3	20	1.06	1.3	5.0	4.12
		80.3	79.2	79.7	21	1.05	1.3	7.5	5.02
		92.9	91.0	91.9	22	2.31	3.5	13.4	12.04
		87.8	87.4	87.6	23	2.26	3.3	20.0	17.18
		86.0	85.5	85.8	24	2.22	3.2	26.3	21.90
		94.5	96.5	95.5	25	3.38	5.3	35.8	34.24
		91.1	92.7	91.9	26	3.28	5.0	45.8	43.70
		89.7	91.2	90.4	27	3.19	4.9	55.5	52.58
		96.0	98.7	97.4	31	4.33	6.8	66.8	70.16
		92.0	87.5	89.7	32	4.14	6.2	79.1	82.30
		84.0	92.6	88.3	33	3.62	5.6	89.8	92.30
		94.8	100.0	97.4	34	4.62	7.7	104.4	112.02*
		89.5	92.4	91.0	35	4.39	7.5	118.7	125.96**
		78.3	78.9	78.6	36	4.44	6.8	131.9	137.33
		63.0	59.3	61.1	37	4.35	9.1	149.1	151.10
		43.9	36.1	40.0	38	5.28	10.0	169.2	161.34
		19.0	21.6	20.3	39	6.88	11.3	191.6	165.74

@ The cumulative rotational energy has been normalized in terms of observed yield moment and the rotation at full yield.

* Maximum load stage.

** Last stable cycle.

Table B 3

Ductilities by Various Definitions - For the Hinging Region in Specimen B1
Based on Rotation of a Section 74.0 in. Above Base of Test Specimen

Observed Yield Moment (k-in.)	Rotation at Full Yield (Rad.)	Load Stage			Cycle No.	Rotational Ductility, μ_r	Cyclic Rotational Ductility, μ_{rc}	Cumulative Ductility, $\Sigma\mu_{rc}$	Cumulative Rotational Energy, $\Sigma A_r^{@}$
		+Load (% Max)	-Load (% Max)	Avg. Load (% Max)					
8,100	0.0042	89.8	89.1	89.5	13	1.34	1.8	3.1	4.42
		81.7	84.8	83.3	14	1.32	1.6	6.4	5.90
		80.1	83.2	81.6	15	1.33	1.6	9.6	7.22
		98.0	93.2	95.6	19	2.74	4.3	16.7	16.54
		91.7	89.4	90.5	20	2.74	4.0	24.8	22.60
		88.9	87.0	88.0	21	2.59	3.9	32.6	28.32
		99.8	97.7	98.7	22	4.15	6.9	44.8	42.86
		93.9	93.7	93.8	23	4.09	6.7	58.0	55.18
		90.8	90.9	90.8	24	3.98	6.8	71.0	66.22
		99.2	100.0	99.6	28	5.53	8.9	85.4	86.54*
		94.3	94.1	94.2	29	5.03	8.8	102.4	102.46
		92.4	90.5	91.4	30	5.28	8.7	119.4	117.90
		91.2	98.4	94.8	31	6.40	10.7	139.4	138.90
		85.4	89.2	87.3	32	6.26	10.1	159.6	156.86 **
		80.9	69.8	75.4	33	5.74	9.9	179.0	172.16

Table B 4

Ductilities by Various Definitions - For the Hinging Region in Specimen B2
Based on Rotation of a Section 74.0 in. Above Base of Test Specimen

Observed Yield Moment (k-in.)	Rotation at Full Yield (Rad.)	Load Stage			Cycle No.	Rotational Ductility, μ_r	Cyclic Rotational Ductility, μ_{rc}	Cumulative Ductility, $\Sigma\mu_{rc}$	Cumulative Rotational Energy, $\Sigma A_r^{@}$
		+Load (% Max)	-Load (% Max)	Avg. Load (% Max)					
21,500	0.0052	93.9	91.4	92.6	19	1.76	2.7	4.5	7.08
		88.3	88.4	88.3	20	1.73	2.5	9.4	10.40
		86.7	86.8	86.7	21	1.69	2.4	14.2	13.46
		95.8	96.2	96.0	22	2.59	4.0	21.4	21.76
		93.3	94.0	93.7	23	2.47	3.8	28.9	27.58
		92.1	92.6	92.4	24	2.40	3.5	35.9	33.00
		99.1	100.0	99.6	25	3.11	5.0	45.0	43.80*
		95.9	97.5	96.7	26	2.95	4.6	54.1	51.66
		92.9	95.0	93.9	27	2.86	4.3	62.6	58.68**
		94.4	92.2	93.3	28	2.93	5.2	72.7	69.64
		34.9	25.8	30.4	29	--	3.9	79.7	--
		16.7	16.0	16.4	30	--	4.0	86.8	--

@ The cumulative rotational energy has been normalized in terms of observed yield moment and the rotation at full yield.

* Maximum load stage.

** Last stable cycle.

Table B 5

Ductilities by Various Definitions - For the Hinging Region in Specimen B3 Based on Rotation of a Section 74.0 in. Above Base of Test Specimen

Observed Yield Moment (k-in.)	Rotation at Full Yield (Rad.)	Load Stage			Cycle No.	Rotational Ductility, μ_r	Cyclic Rotational Ductility, μ_{rc}	Cumulative Ductility, $\Sigma\mu_{rc}$	Cumulative Rotational Energy, $\Sigma A_r^{@}$
		+Load (% Max)	-Load (% Max)	Avg. Load (% Max)					
8,100	0.0040	88.3	84.0	86.1	13	1.29	1.7	2.9	3.58
		82.3	80.6	81.4	14	1.28	1.6	5.0	4.84
		80.6	79.1	79.8	15	1.29	1.5	9.0	5.98
		94.8	88.5	91.6	19	2.69	4.1	15.6	14.18
		87.8	85.5	86.6	20	2.69	4.0	23.4	21.10
		85.5	83.5	84.5	21	2.66	3.8	31.0	25.36
		95.6	93.1	94.4	22	4.13	6.3	42.3	38.86
		90.7	90.0	90.3	23	4.02	6.2	54.3	49.30
		89.4	88.5	89.0	24	3.97	5.9	66.1	59.22
		97.6	94.8	96.2	28	5.09	8.2	79.9	78.70
		93.9	92.4	93.1	29	4.94	8.0	95.7	93.52
		92.4	90.8	91.5	30	4.78	7.7	110.8	107.74
		98.9	96.4	97.6	31	5.97	9.9	129.5	131.38
		96.4	93.8	95.1	32	5.82	9.6	148.4	149.38
		94.8	91.6	93.2	33	5.87	9.0	166.1	167.04
		100.0	96.6	98.3	34	6.53	10.3	186.9	193.32**
		97.4	93.3	95.3	35	6.21	10.5	207.6	213.62
		95.3	91.4	93.4	36	6.00	9.8	227.1	232.36
		99.1	95.1	97.1	37	6.38	11.3	248.7	257.72
		95.9	91.7	93.8	38	6.27	10.8	270.0	278.76
		87.6	84.4	86.0	39	6.02	10.2	290.2	296.84**
		81.8	78.4	80.1	40	7.07	11.9	313.0	316.54
		63.3	60.3	61.8	41	6.80	11.9	336.7	311.66
		55.5	49.3	52.4	42	6.77	11.8	359.3	344.08

Table B 6

Ductilities by Various Definitions - For the Hinging Region in Specimen B5 Based on Rotation of a Section 74.0 in. Above Base of Test Specimen

Observed Yield Moment (k-in.)	Rotation at Full Yield (Rad.)	Load Stage			Cycle No.	Rotational Ductility, μ_r	Cyclic Rotational Ductility, μ_{rc}	Cumulative Ductility, $\Sigma\mu_{rc}$	Cumulative Rotational Energy, $\Sigma A_r^{@}$
		+Load (% Max)	-Load (% Max)	Avg. Load (% Max)					
20,000	0.0064	86.9	87.4	87.1	19	1.44	2.1	3.4	5.20
		82.1	83.8	83.0	20	1.38	1.9	7.2	7.82
		81.2	82.6	81.9	21	1.36	1.8	10.9	10.26
		89.6	91.9	90.7	22	2.13	3.2	16.6	17.52
		87.6	89.7	88.7	23	2.06	3.0	22.5	22.80
		86.8	88.9	87.8	24	2.00	2.9	28.1	27.64
		93.3	96.5	94.9	25	2.64	4.1	35.5	37.82
		91.5	94.2	92.8	26	2.51	3.8	43.1	45.20
		90.1	92.9	91.5	27	2.43	3.6	50.3	51.92
		96.7	100.0	98.3	28	3.05	4.7	59.1	63.98***
		93.0	80.5	86.8	29	2.54	4.4	67.4	71.86
		65.5	58.5	62.0	30	2.12	3.2	73.6	75.52

@ The cumulative rotational energy has been normalized in terms of observed yield moment and the rotation at full yield.

* Maximum load stage.

** Last stable cycle.

Table B 7

Ductilities by Various Definitions - For the Hinging Region in Specimen F1
Based on Rotation of a Section 74.0 in. Above Base of Test Specimen

Observed Yield Moment (k-in.)	Rotation at Full Yield (Rad.)	Load Stage			Cycle No.	Rotational Ductility, μ_r	Cyclic Rotational Ductility, μ_{rc}	Cumulative Ductility, $\Sigma\mu_{rc}$	Cumulative Rotational Energy, ΣA_r @
		+Load (% Max)	-Load (% Max)	Avg. Load (% Max)					
27,000	0.0034	80.1	80.5	80.3	13	1.08	1.1	2.1	1.18
		78.5	80.8	79.7	14	1.13	1.2	4.4	1.36
		79.1	80.0	79.6	15	1.10	1.1	6.6	1.54
		91.0	90.6	90.8	19	2.73	3.7	12.7	7.34
		89.4	87.6	88.5	20	2.66	3.4	19.4	11.14
		87.7	86.0	86.9	21	2.51	3.2	25.8	14.50**
		100.0	94.1	97.1	22	4.32	6.8	38.4	31.18*
		22.0	18.9	20.4	23	--	9.3	50.9	--
		11.1	12.4	11.7	24	--	9.4	68.7	--
		13.2	9.0	11.1	25	--	18.5	102.3	--

@ The cumulative rotational energy has been normalized in terms of observed yield moment and the rotation at full yield.

* Maximum load stage.

** Last stable cycle.

Table B 8

Ductilities by Various Definitions - For the Hinging Region in Specimen B6
Based on Rotation of a Section 74.0 in. Above Base of Test Specimen

Observed Yield Moment (k-in.)	Rotation at Full Yield (rad.)	Load Stage			Cycle No.	Rotational Ductility, μ_r	Cyclic Rotational Ductility, μ_{rc}	Cumulative Ductility, $\Sigma\mu_{rc}$	Cumulative Rotational Energy, ΣA_r @
		+Load (% max)	-Load (% max)	Avg. Load (% max)					
31,300	0.0049	97.5	95.7	96.6	22	1.70	2.3	4.0	4.70
		91.9	93.3	92.6	23	1.70	2.3	8.6	8.69
		91.4	91.8	91.6	24	1.69	2.2	13.0	8.64**
		97.9	100.0	99.0	25	2.78	4.1	20.3	14.50*/**
		49.5	37.6	43.5	26/		3.4	26.7	

@ The cumulative rotational energy has been normalized in terms of observed yield moment and the rotation at full yield.

* Maximum load stage.

** Last stable cycle.

/ Web crushing occurs in this cycle.

Table B 9

Ductilities by Various Definitions - For the Hinging Region in Specimen B7
Based on Rotation of a Section 74.0 in. Above Base of Test Specimen

Observed Yield Moment (k-in.)	Rotation at Full Yield (rad.)	Load Stage			Cycle No.	Rotational Ductility, μ_r	Cyclic Rotational Ductility, μ_{rc}	Cumulative Ductility, $\Sigma\mu_{rc}$	Cumulative Rotational Energy, $\Sigma\Delta_r^{@}$
		+Load (% max)	-Load (% max)	Avg. Load (% max)					
33,750	0.0047	91.4	90.5	90.9	19	1.89	2.5	4.2	6.40
		87.6	88.8	88.2	20	1.89	2.4	9.0	9.72
		86.6	87.8	87.2	21	1.87	2.4	13.9	12.57
		93.4	95.0	94.2	22	3.03	4.3	21.6	20.53
		90.2	92.8	91.5	23	2.96	4.2	29.8	27.91
		89.1	91.8	90.4	24	2.94	4.1	38.1	34.81
		95.2	97.5	96.3	25	4.05	6.2	49.2	47.10
		91.9	95.6	93.7	26	3.98	6.0	61.2	59.73
		91.5	94.5	93.0	27	3.96	5.9	72.9	72.00
		97.2	100.0	98.6	28	5.18	8.1	87.8	93.98*
		93.7	97.5	95.6	29	5.08	7.7	103.3	119.16
		92.6	96.4	94.5	30	5.06	7.6	118.4	142.87**
		67.9	56.2	62.0	31	5.08	7.4	132.9	158.37

@ The cumulative rotational energy has been normalized in terms of observed yield moment and the rotation at full yield.

* Maximum load stage.

** Last stable cycle.

Table B 10

Ductilities by Various Definitions - For the Hinging Region in Specimen B8
Based on Rotation of a Section 74.0 in. Above Base of Test Specimen

Observed Yield Moment (k-in.)	Rotation at Full Yield (rad.)	Load Stage			Cycle No.	Rotational Ductility, μ_r	Cyclic Rotational Ductility, μ_{rc}	Cumulative Ductility, $\Sigma\mu_{rc}$	Cumulative Rotational Energy, $\Sigma\Delta_r^{@}$
		+Load (% max)	-Load (% max)	Avg. Load (% max)					
34,000	0.0049	90.5	90.2	90.3	19	1.93	2.5	4.3	6.73
		86.8	87.7	87.2	20	1.91	2.5	9.3	10.19
		85.6	86.6	86.1	21	1.93	2.5	14.3	13.41
		93.7	95.0	94.3	22	3.04	4.4	22.1	22.05
		90.7	92.5	91.6	23	2.99	4.3	30.7	30.00
		89.8	91.6	90.7	24	3.02	4.4	39.4	37.68
		96.6	98.2	97.4	25	4.11	6.2	50.9	50.89
		94.5	96.0	95.3	26	4.08	6.2	63.3	63.85
		93.7	94.7	94.2	27	4.06	6.1	75.5	76.79
		98.5	100.0	99.3	28	5.23	8.3	90.9	95.67*
		97.0	97.8	97.4	29	5.21	8.3	107.0	115.08
		95.7	96.5	96.1	30	5.19	8.3	123.2	133.21**
		99.3	40.7	70.0	31/	5.43	9.5	141.6	

@ The cumulative rotational energy has been normalized in terms of observed yield moment and the rotation at full yield.

* Maximum load stage.

** Last stable cycle.

/ Web crushing occurs in this cycle.

Table B 11

Ductilities by Various Definitions - For the Hinging Region in Specimen B9
Based on Rotation of a Section 74.0 in. Above Base of Test Specimen

Observed Yield Moment (k-in.)	Rotation at Full Yield (Rad.)	Load Stage			Cycle No.	Rotational Ductility, μ_r	Cyclic Rotational Ductility, μ_{rc}	Cumulative Cyclic Ductility, $\Sigma\mu_{rc}$	Cumulative Rotational Energy, ΣA_r^9
		Load (% Max)	Load (% Max)	Average Load (% Max)					
33,600	0.0048	100.0	99.7	99.8	2	4.96	8.2	13.2	19.85*
		59.3	33.1	46.2	3	1.10	4.0	18.5	22.73
		91.7	76.4	84.0	4	3.96	5.7	28.8	33.35

Table B 12

Ductilities by Various Definitions - For the Hinging Region in Specimen B10
Based on Rotation of a Section 74.0 in. Above Base of Test Specimen

Observed Yield Moment (k-in.)	Rotation at Full Yield (rad.)	Load Stage			Cycle No.	Rotational Ductility, μ_r	Cyclic Rotational Ductility, μ_{rc}	Cumulative Ductility, $\Sigma\mu_{rc}$	Cumulative Rotational Energy, $\Sigma A_r^{\#}$
		+Load (% max)	-Load (% max)	Avg. Load (% max)					
25,100	0.0048	100.0	93.3	96.6	2	5.0	8.3	13.4	19.77*
		58.8	45.9	52.3	3	1.1	4.2	19.0	22.00
		91.6	87.0	89.3	4	4.1	6.5	30.0	32.83
		52.3	46.7	49.5	5	1.2	3.2	34.6	34.42
		91.2	86.1	88.7	6	4.1	6.6	45.8	45.21
		54.1	46.8	50.5	7	1.2	3.5	50.7	46.86
		94.5	88.4	91.5	8	5.1	8.3	64.6	61.60
		50.4	42.6	46.5	9	1.2	4.4	70.4	63.53
		84.0	82.1	83.3	10	4.2	4.7	81.7	73.48
		46.3	41.3	43.8	11	1.3	3.6	86.7	74.98**
		76.4	84.0	80.2	12	5.1	7.7	100.1	87.64
		40.6	37.1	38.8	13	1.3	4.5	106.0	89.30
		66.4	69.5	67.9	14	5.9	7.9	118.6	101.12

The cumulative rotational energy has been normalized in terms of observed yield moment and the rotation at full yield.

* Maximum load stage.

Table B 13

Ductilities by Various Definitions - For the Hinging Region in Specimen F2
Based on Rotation of a Section 74.0 in. Above Base of Test Specimen

Observed Yield Moment (k-in.)	Rotation at Full Yield (rad.)	Load Stage			Cycle No.	Rotational Ductility, μ_r	Cyclic Rotational Ductility, μ_{rc}	Cumulative Ductility, $\Sigma\mu_{rc}$	Cumulative Rotational Energy, $\Sigma A_r^{@}$
		+Load (% max)	-Load (% max)	Avg. Load (% max)					
32,450	0.0037	92.3	91.6	91.9	19	2.26	3.1	5.3	7.91
		91.7	91.9	91.8	20	2.22	3.0	11.2	11.85
		90.5	90.9	90.7	21	2.21	3.0	17.2	15.57
		95.5	94.9	95.2	22	3.60	5.3	26.5	24.66
		95.2	96.3	95.7	23	3.57	5.2	36.8	33.48
		94.3	94.7	94.5	24	3.55	5.3	47.3	41.91
		100.0	96.5	96.9	25	4.86	7.6	61.1	55.88*
		97.2	97.0	97.1	26	4.80	7.4	75.8	69.79
		95.7	96.0	95.8	27	4.75	7.3	90.2	83.25**
		96.0	20.4	58.2	28	5.38	8.6	107.3	103.71
		0.0	0.0	0.0	29		0.0		

@ The cumulative rotational energy has been normalized in terms of observed yield moment and the rotation at full yield.

* Maximum load stage.

** Last stable cycle.

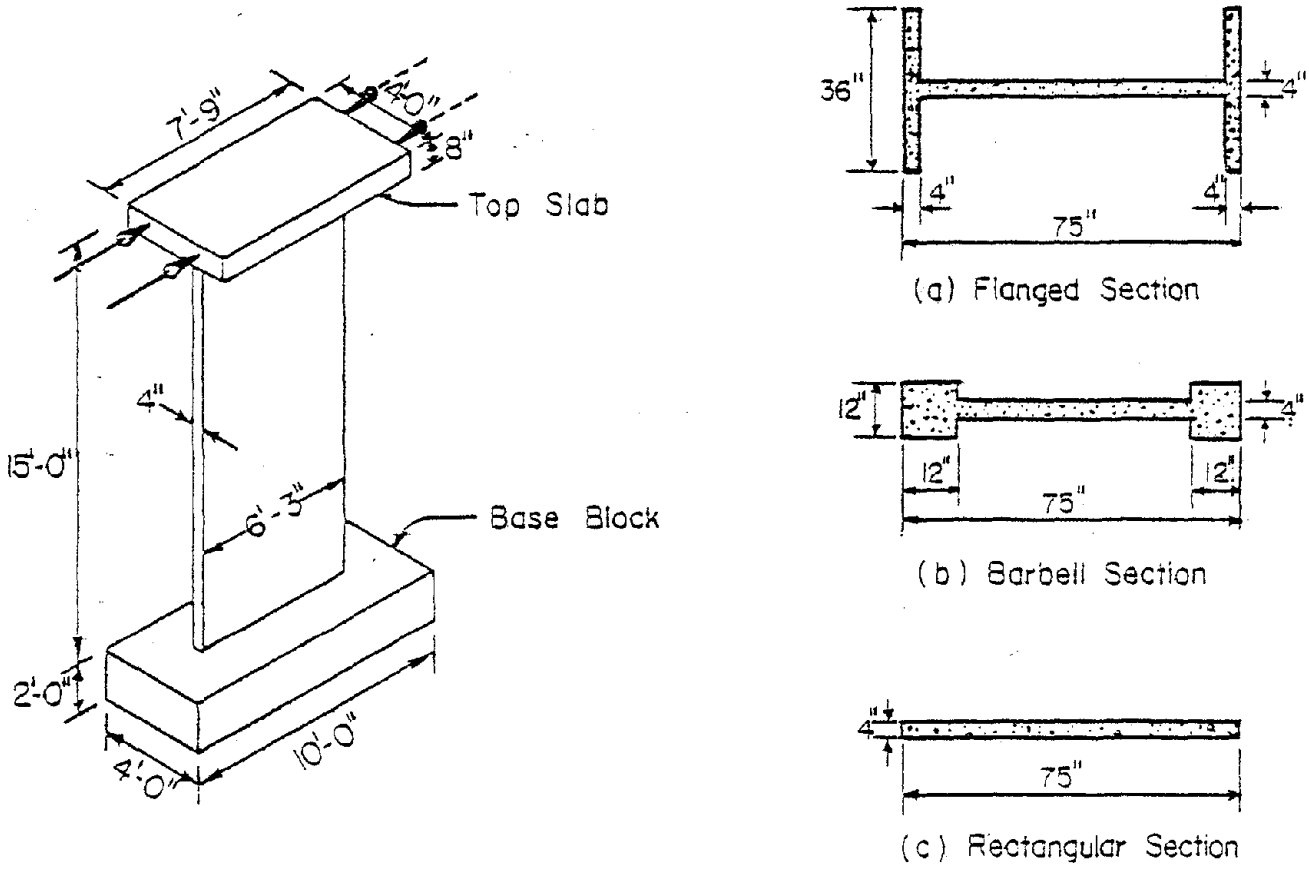

Fig. B1 Specimens and Loading in the Experimental Investigation on Isolated Structural Walls

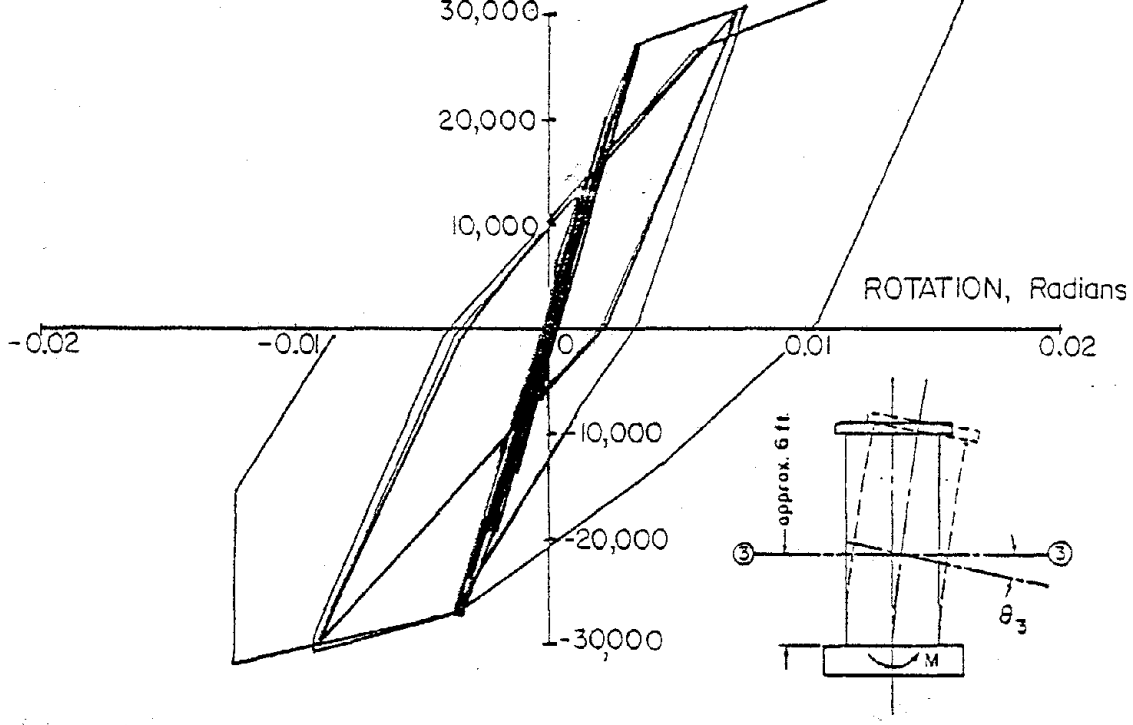

Fig. B2 Moment at Base Against Rotation Over Approximately 6 Ft. Length from Base - Specimen F1

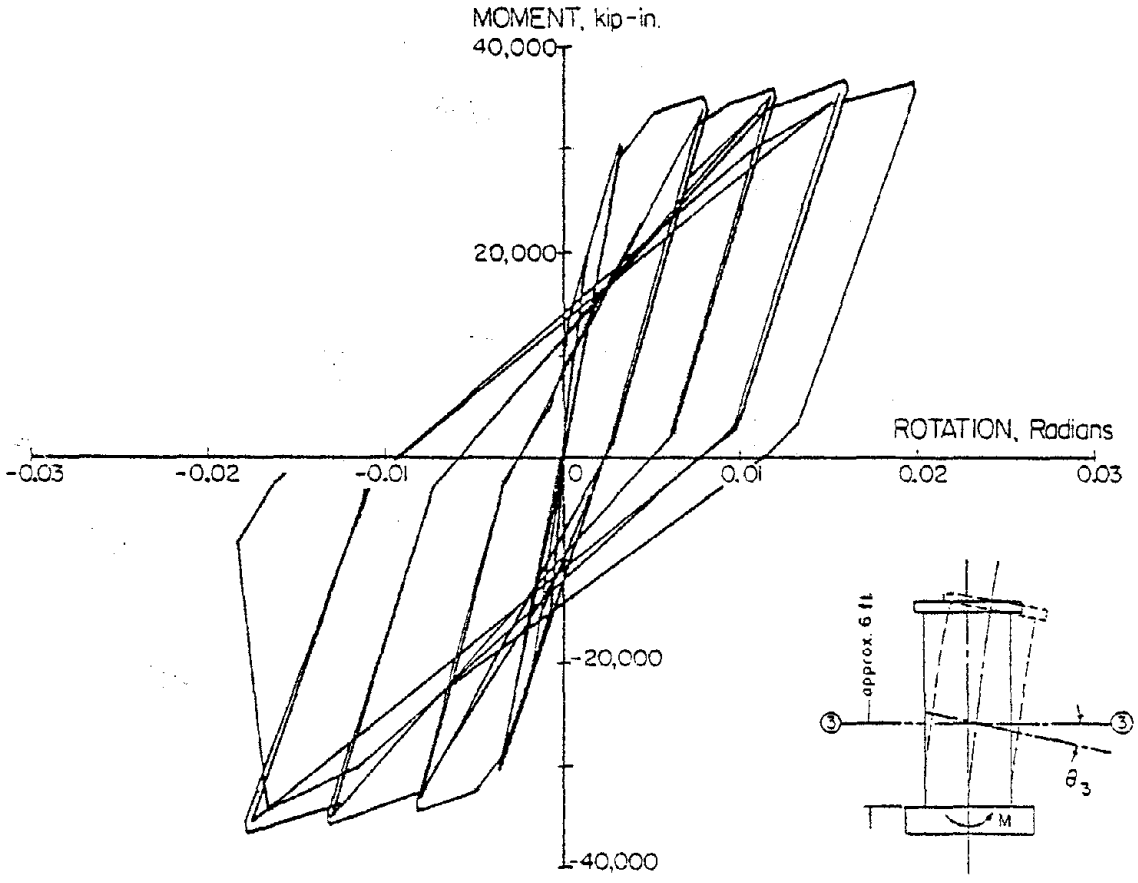

Fig. B3 Moment at Base Against Rotation Over Approximately 6Ft. Length from Base - Specimen F2

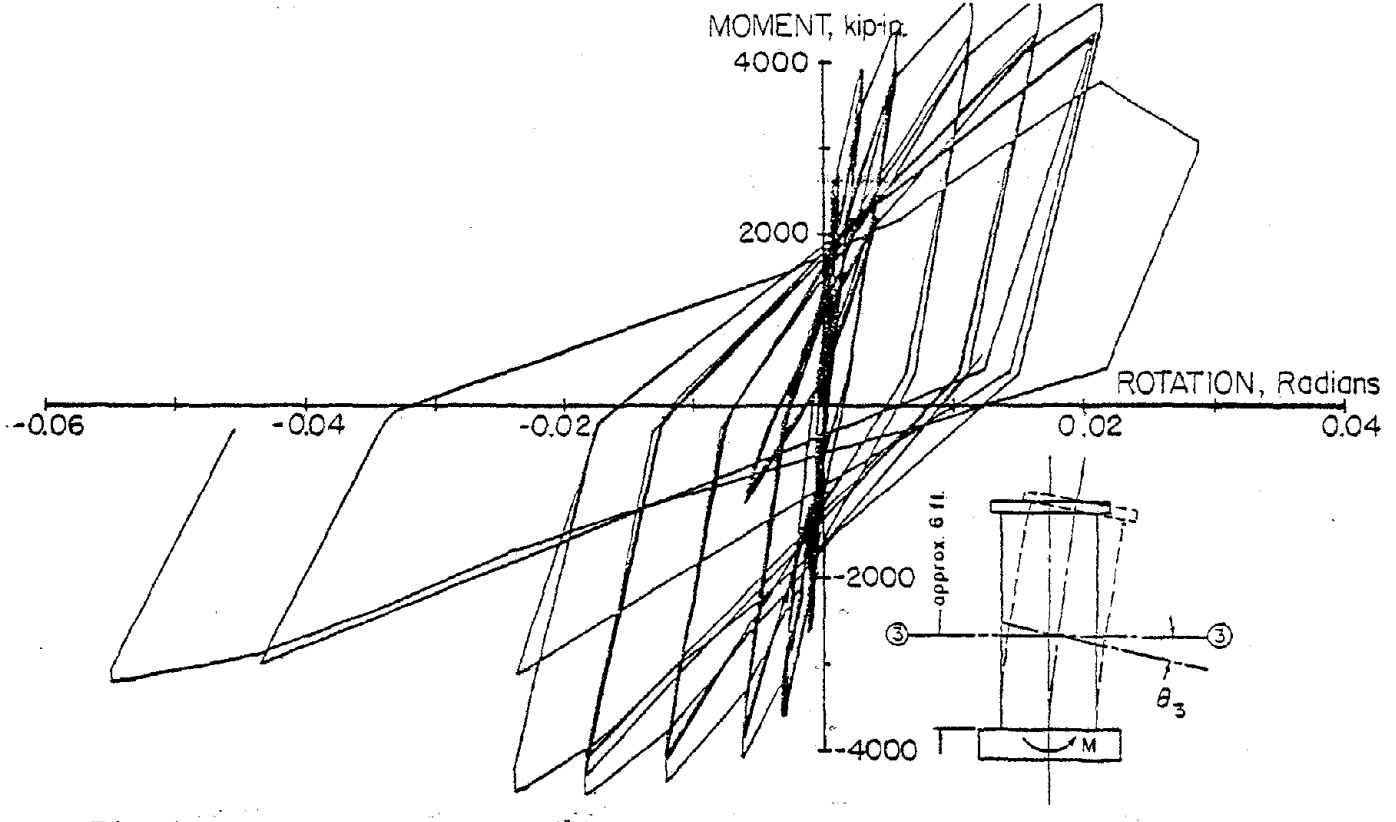

Fig. B4 Moment at Base Against Rotation Over Approximately 6 Ft. Length from Base - Specimen R1

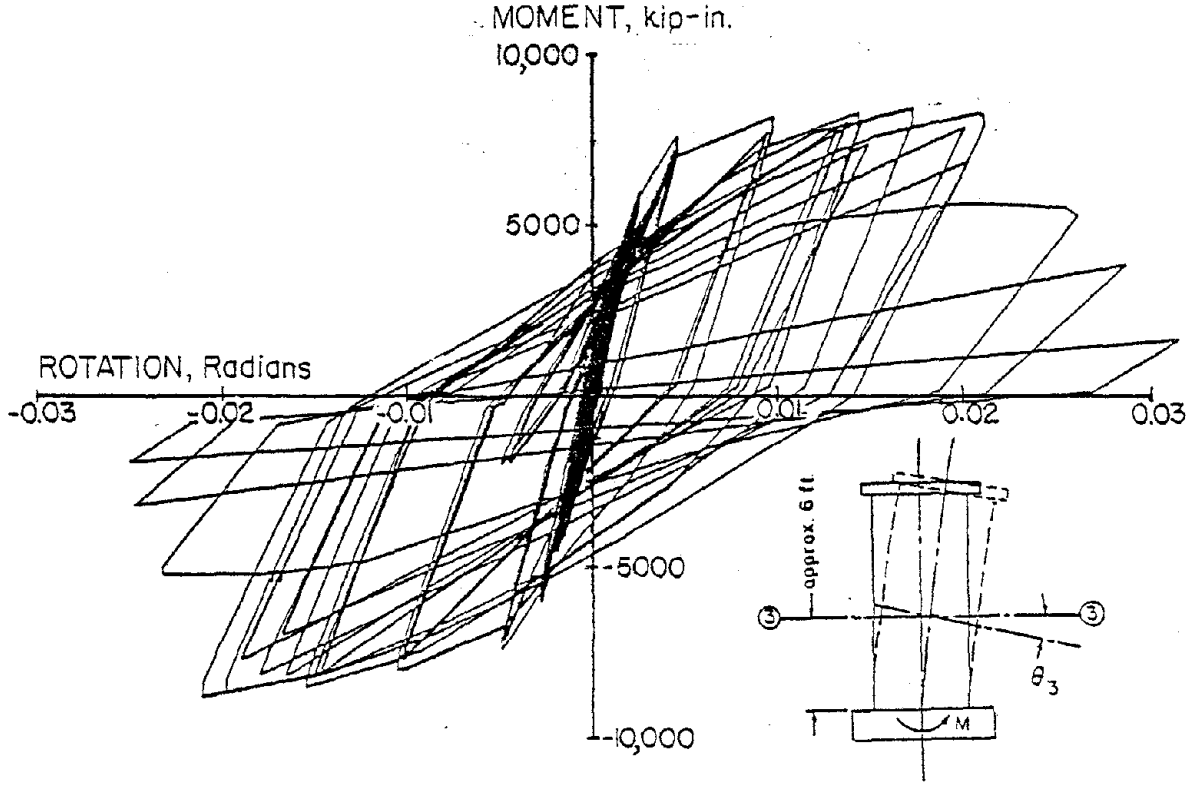

Fig. B5 Moment at Base Against Rotation Over Approximately 6 Ft. Length from Base - Specimen R2

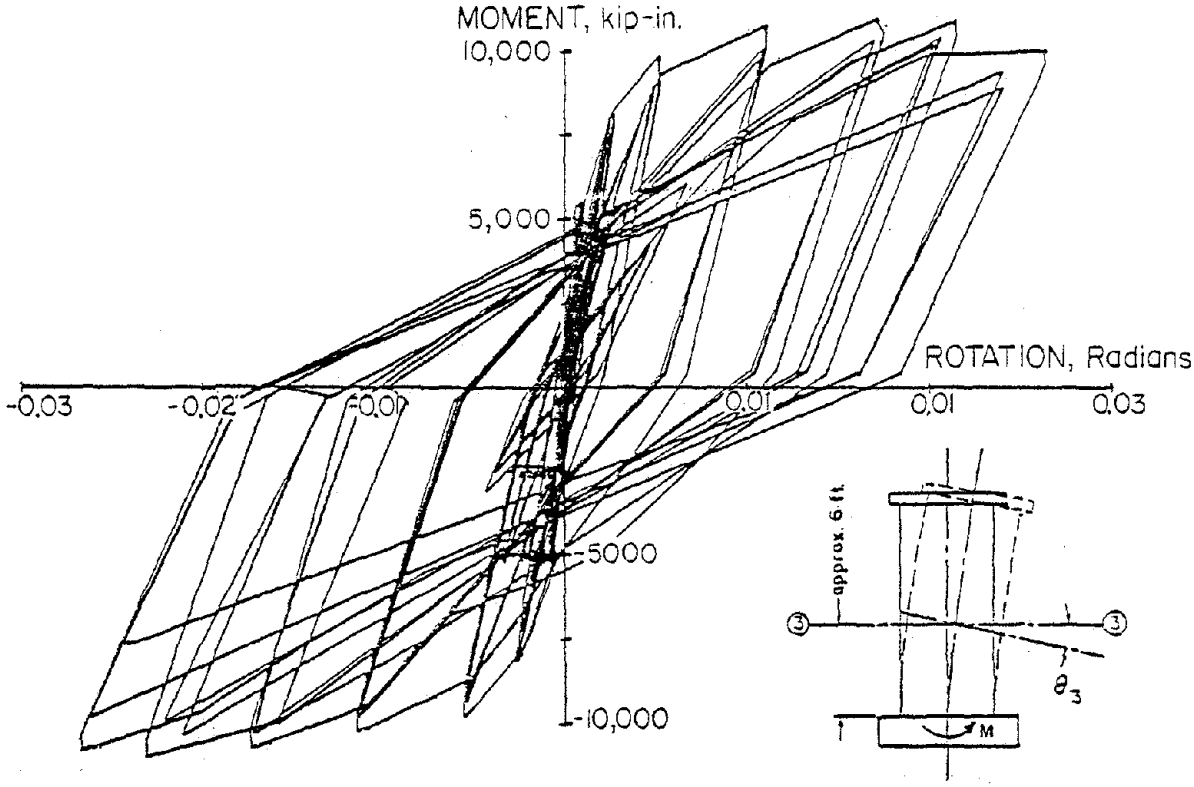

Fig. B6 Moment at Base Against Rotation Over Approximately 6 Ft. Length from Base - Specimen B1

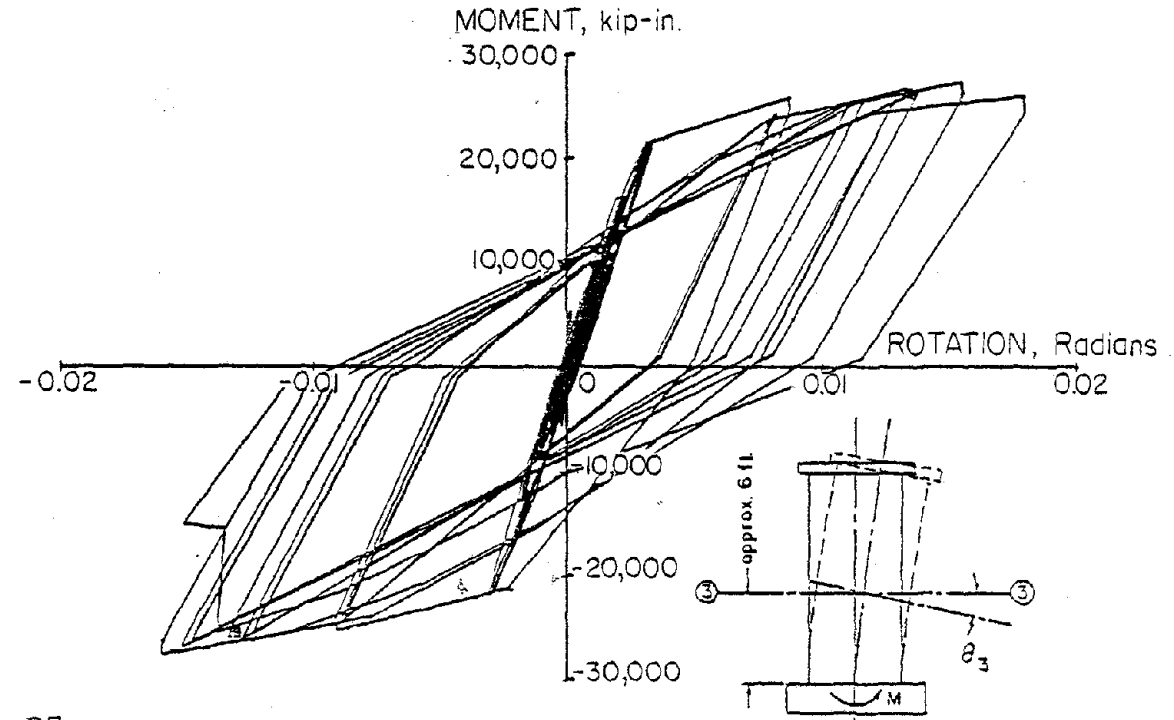

Fig. B7 Moment at Base Against Rotation Over Approximately 6 Ft. Length from Base - Specimen B2

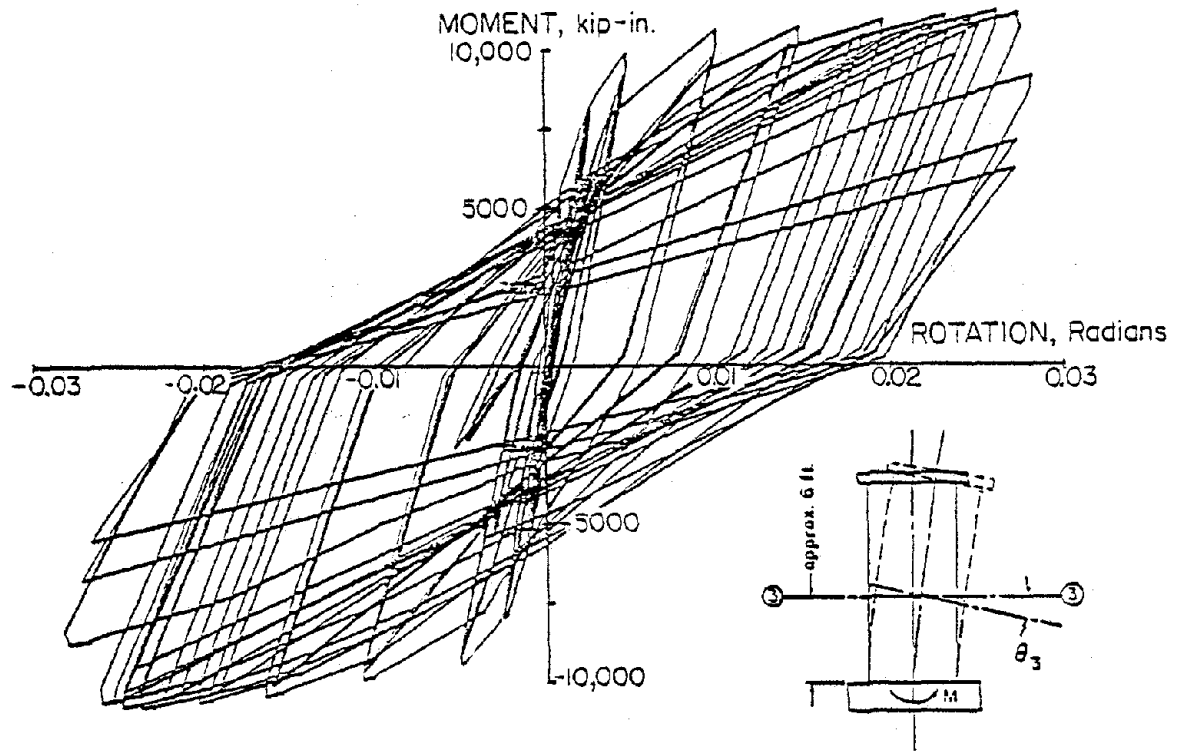

Fig. B8 Moment at Base Against Rotation Over Approximately 6 ft Length from Base - Specimen B3

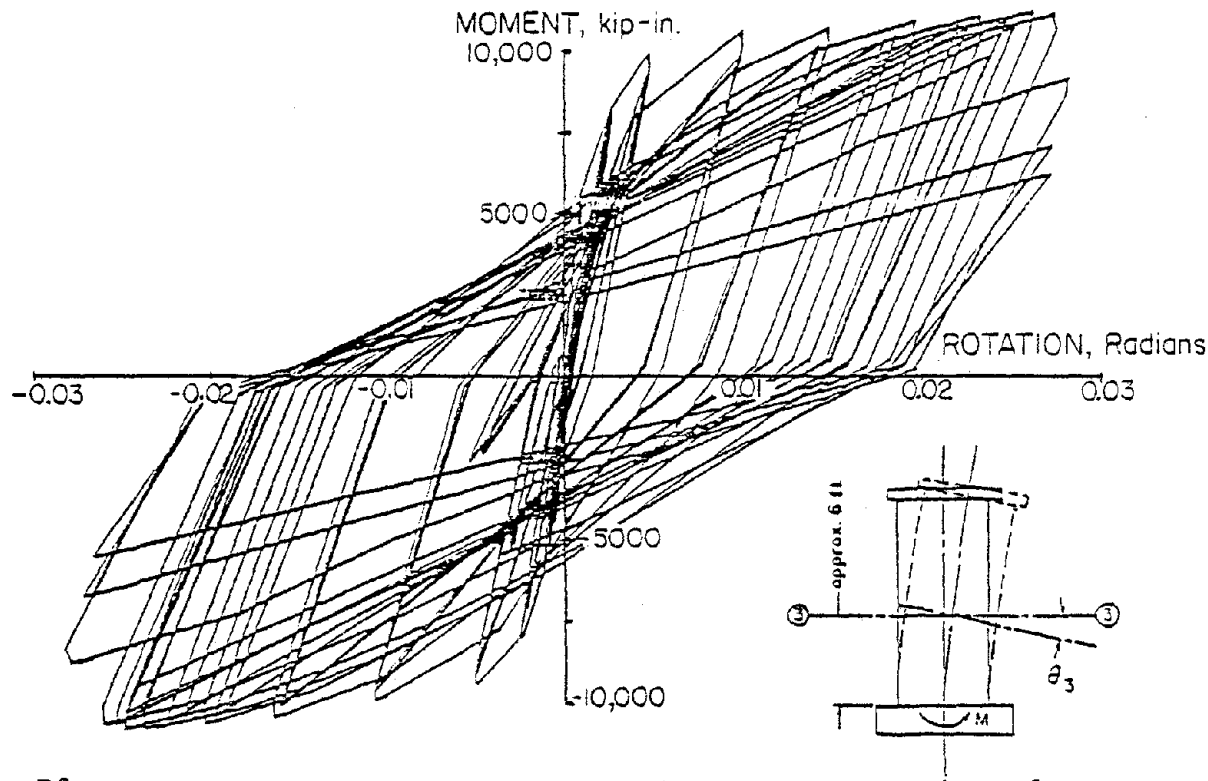

Fig. B9 Movement at Base Against Rotation Over Approximately 6 Ft. Length from Base - Specimen B4

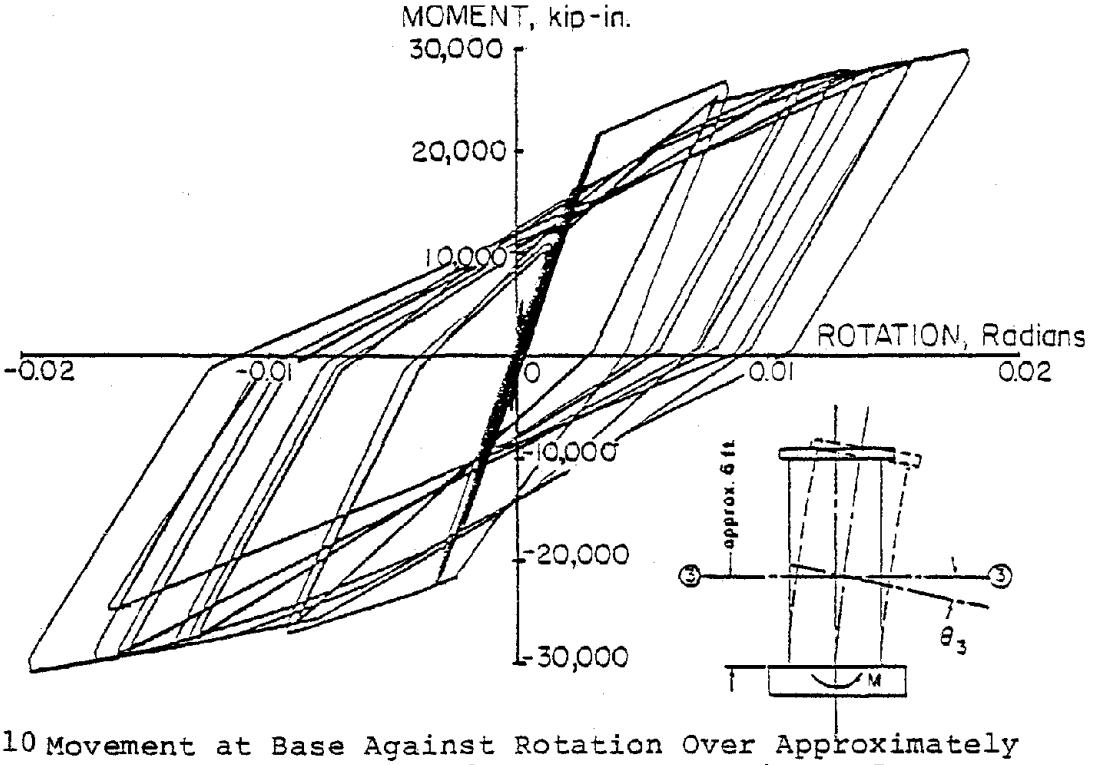

Fig. B10 Movement at Base Against Rotation Over Approximately 6 Ft. Length from Base - Specimen B5

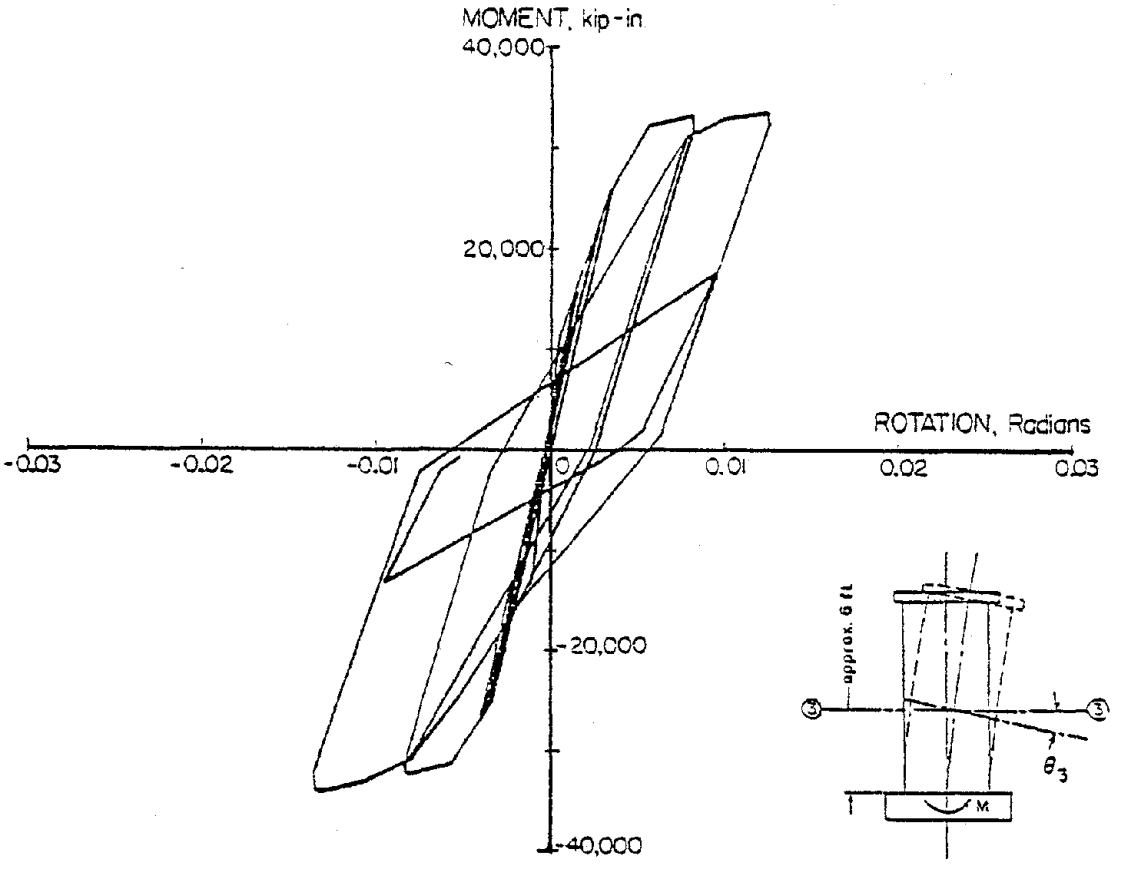

Fig. B11 Moment at Base Against Rotation Over Approximately 6 Ft. Length from Base - Specime B6

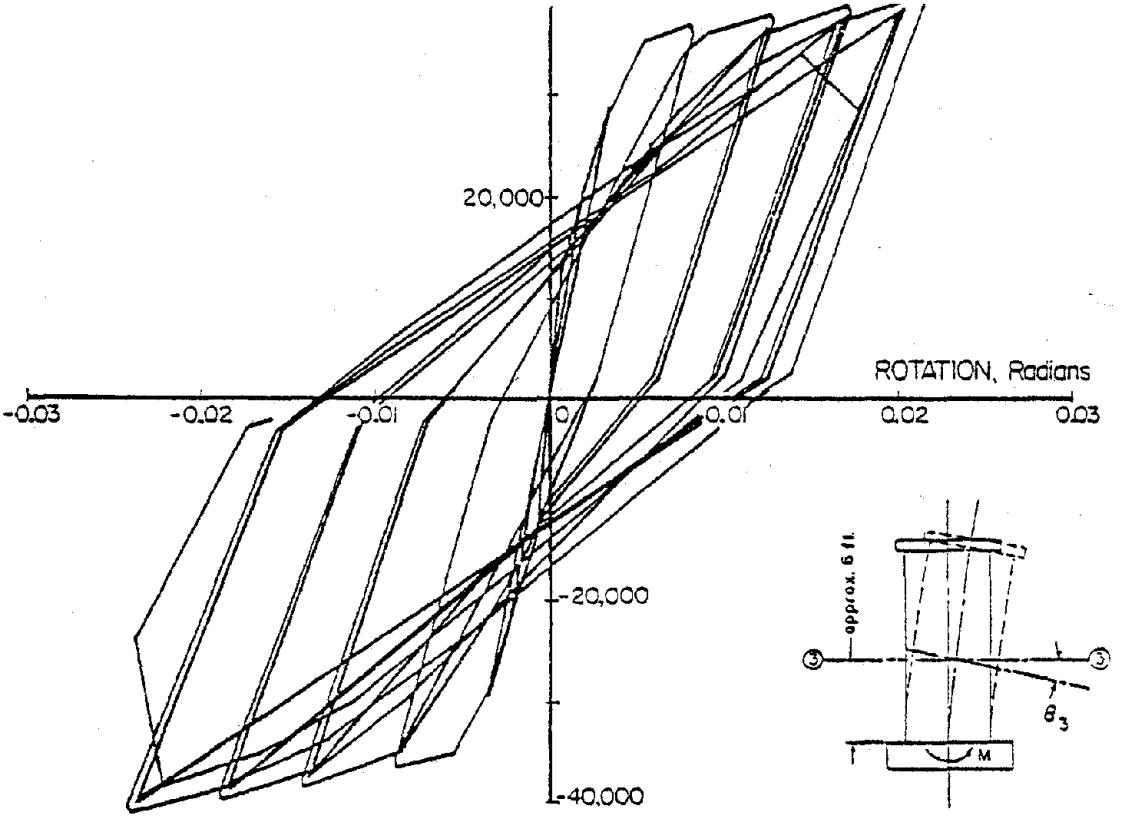

Fig. B12 Moment at Base Against Rotation Over Approximately 6 Ft. Length from Base - Specimen B7

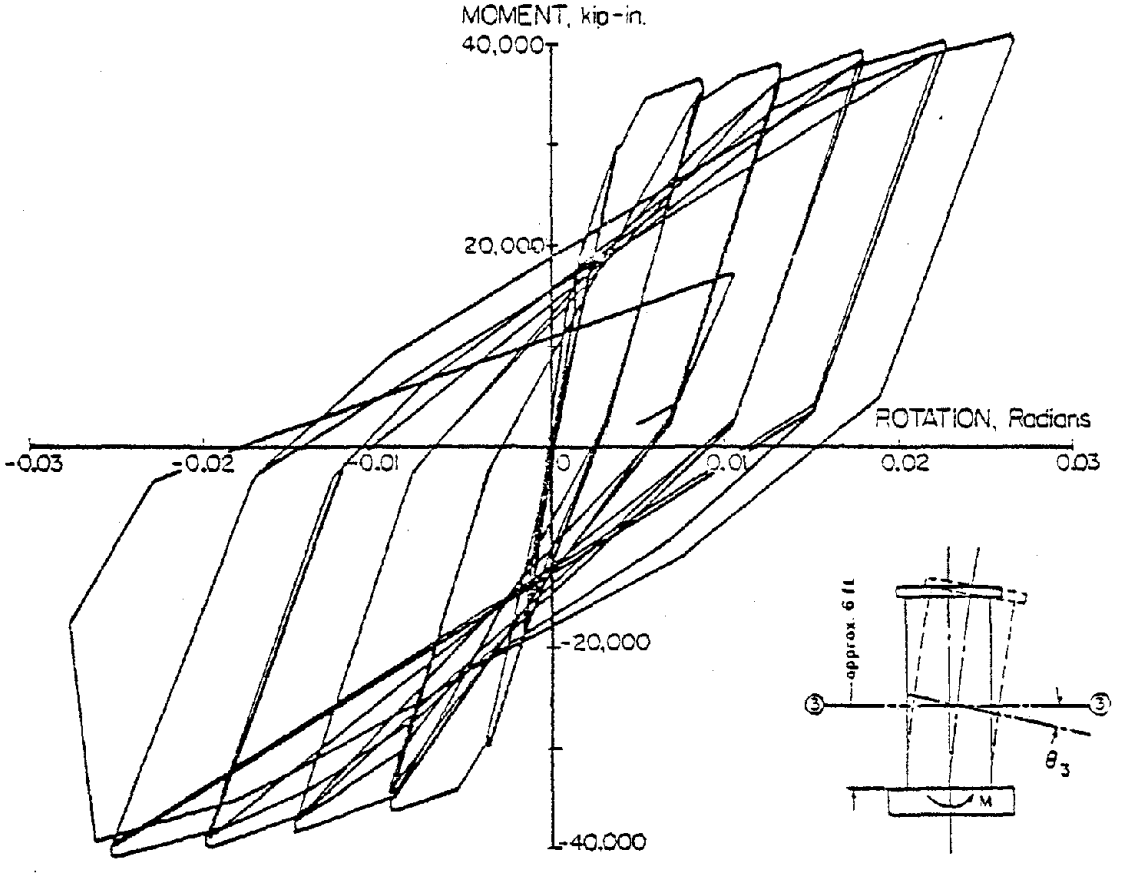

Fig. B13 Moment at Base Against Rotation Over Approximately 6 Ft. Length from Base - Specimen B8

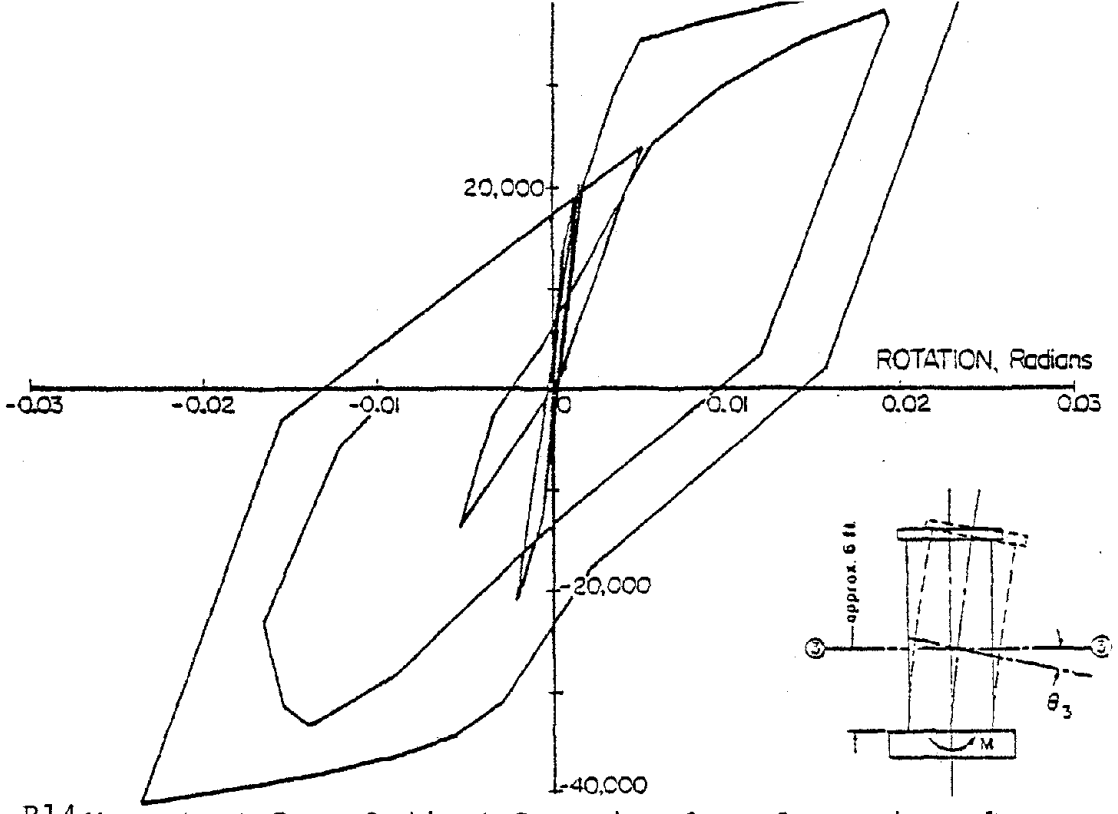

Fig. B14 Moment at Base Against Rotation Over Approximately 6 Ft. Length from Base - Specimen B9

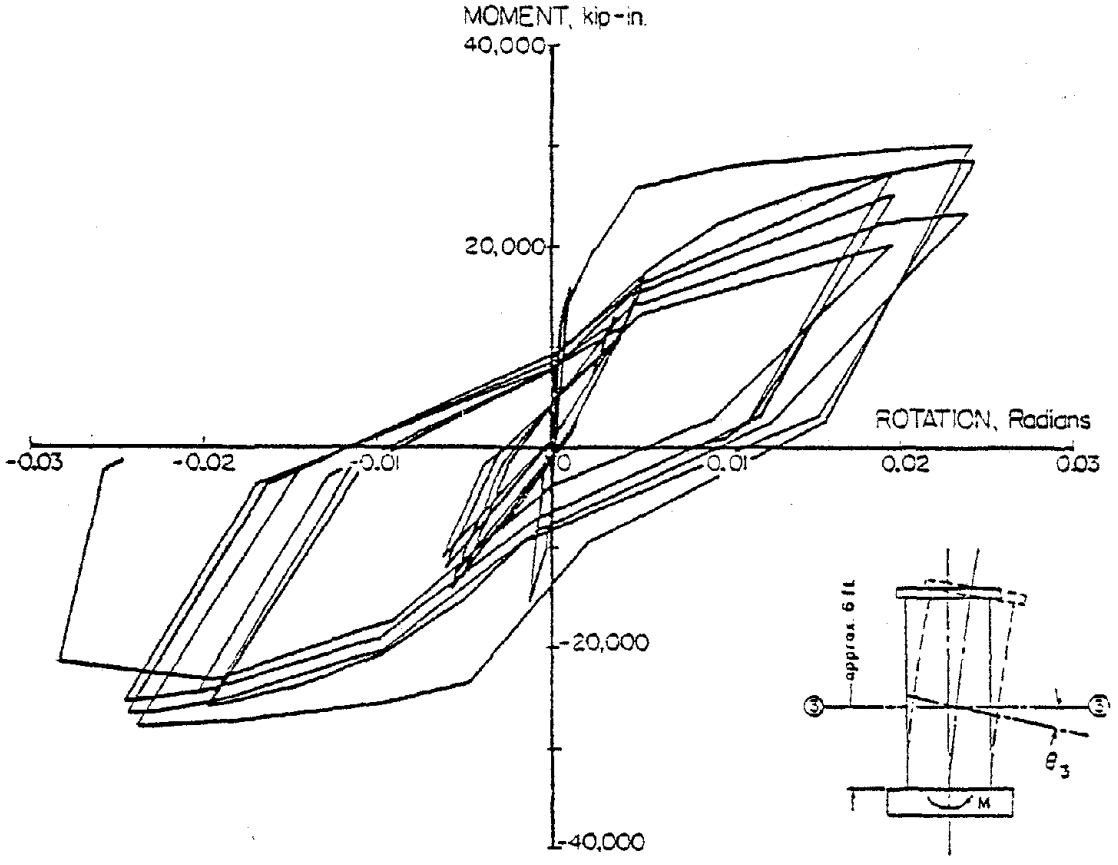

Fig. B15 Moment at Base Against Rotation Over Approximately 6 Ft. Length from Base - Specimen B10

APPENDIX C

EFFECT OF DEGREE OF BASE FIXITY

APPENDIX C

EFFECT OF DEGREE OF BASE FIXITY

Results presented in the main body of the report, are based on the assumption of full fixity at the base. An additional series of analyses was carried out to evaluate effects of rotation of the base.

The degree of base fixity is expressed in terms of a base fixity factor, F_B, defined as the ratio of the moment developed at the base of the wall due to a given lateral displacement to the moment that would be developed if the base were fully fixed. Thus, the fully fixed case corresponds to a fixity factor of 1.0. The rotational restraint at the base is represented in the analytical model by a linear spring as shown in Fig. C1.

Analyses were made using 20-story isolated walls only. Base fixity factors equal to 0.75 and 0.50 were considered. Results are summarized in Tables C1 through C6 and plotted in Figs. C2 through C4. These figures show the variation of different response quantities with fundamental period and degree of base fixity for different values of the yield level, M_y. In these figures, the fundamental period plotted along the horizontal axis corresponds to the fully-fixed-base structure. Thus, for a wall with a 50% base fixity, the fundamental period considered is that for the same wall when its base is fully fixed. Although in several cases the data do not exhibit clear trends, an attempt has been made to indicate what appear to be trends by drawing the smooth curves shown in the figures.

Figures C1 through C6 indicate that for a particular yield level and fundamental period, the rotational ductility, the maximum moment and the shear at the base decrease while the top displacement increases with a decrease in the degree of base fixity.

Figures C5 and C6 present the variation of the maximum top displacement, Δ_t, with fundamental period for different values of rotational ductility (reflecting the effect of flexural yield level). The dashed curves in these figures are meant to represent upper bounds on the plotted data. The increase in top displacement with increasing fundamental period is apparent in both curves, the rate of increase becoming less as the base fixity decreases.

Figures C7 and C9 show the flexural design factors corresponding to F_B = 0.50 and 0.75 respectively. It will be noted from a comparison of Figs. C5, C7, and Fig. 40 for the fully-fixed-base walls that the effect of μ_r^a (or the yield level, M_y) on αf diminishes as the base fixity factor decreases. This is reflected in the decrease in spacing between the curves for different μ_r^a as the base fixity factor decreases from 1.0 in Fig. 40 to 0.50 in Fig. C7. The same trend is noticeable, though less pronounced, in the curves for $\bar{\alpha}_v$ shown in Figs. C8 and C10, when compared to Fig. 43 for the fully-fixed-base condition.

Charts were developed for varying degrees of base fixity. The charts shown in Figs. C11 and C12 are similar to those for intensity factors developed in the main body of the report for adjusting the flexural and shear design factors of Figs. 51 and 52 (for SI = $1.5_{ref.}$). The figures were prepared by taking the ratio of the design factor for a particular F_b-value to that for the corresponding fully fixed 20-story wall. Figures C11 and C12 may be used with Figs. 51 and 52 to obtain design factors for different base fixity conditions. A similar chart that can be used in conjunction with Fig. 53b for maximum top displacements is given in Fig. C13.

APPENDIX C

List of Tables

List of Figures

Table C1

RESPONSE VALUES CORRESPONDING TO DIFFERENT EARTHQUAKE INPUT MOTIONS

$SI = 1.5\,(SI_{ref.})$, Duration = 10 sec.

20-Story Isolated Structural Walls

M_y = 750,000 in.-k

Base Fixity Factor = 50%

EARTHQUAKE INPUT	Yield Rotation, θ_y*x 10^{-3} Radian			
	T_1=0.8#	1.4	2.0	2.4
1 1971 Paciamo Dam S16E	1.68	4.83 (E)	8.89 (E)	11.72 (E)
2 Holiday Orion E-W	1.68	4.83	8.76 (E)	-
3 1952 Taft S69E	1.68	-	-	12.06 (E)
4 1940 El Centro E-W	-	4.83	8.89	12.21
5 1940 El Centro N-S	-	4.81	-	-
AVERAGE	1.68	4.83	8.85	12.00

*at second floor level
#Fundamental Period (Seconds)
^Difference between rotations at second floor level and base.

E.Q. Input No.	Fundamental Period, T_1 (sec.)			
	0.8	1.4	2.0	2.4
	MAX. TOP DISPL. (IN.)			
1	11.7*	14.6 (E)	17.0 (E)	17.5 (E)
2	10.9	13.8	13.7 (E)	-
3	10.3	-	-	19.0 (E)
4	-	12.3	19.2*	25.3*
5	-	18.3*	-	-
	MAX. INTERSTORY DISPL. (IN.)			
1	.65*	.85 (E)	1.04 (E)	1.13 (E)
2	.59	.82	.87 (E)	-
3	.57	-	-	1.29 (E)
4	-	1.33*	2.18*	2.22*
5	-	1.02	-	-
	MAX. BASE SHEAR (KIPS)			
1	1,328*	1,208 (E)	1,160*(E)	863 (E)
2	1,321	1,514*	944 (E)	-
3	1,154	-	-	844 (E)
4	-	1,070	1,087	1,273*
5	-	1,225	-	-
	MAX. BASE MOMENT (IN-KIPS)			
1	1,061,000*	767,000(E)	423,000(E)	349,000(E)
2	1,048,000	789,000	449,000(E)	-
3	1,015,000	-	-	444,000(E)
4	-	973,000*	869,000*	818,000*
5	-	859,000	-	-
	ROTATIONAL DUCTILITY #			
1	7.01	0.98 (E)	0.54 (E)	0.44 (E)
2	7.37*	1.01	0.57 (E)	-
3	6.05	-	-	0.57 (E)
4	-	4.74*	2.55*^	1.44*
5	-	2.51	-	-

*Critical (maximum) value for particular T_1
E = no yielding, i.e., linearly elastic response
#based on differential rotation between second floor level and base.

Table C 2

RESPONSE VALUES CORRESPONDING TO DIFFERENT EARTHQUAKE INPUT MOTIONS

SI = 1.5 ($SI_{ref.}$), Duration = 10 sec.

20-Story Isolated Structural Walls

M_y = 1,000,000 in.-k

Base Fixity Factor = 50 %

EARTHQUAKE INPUT	Yield Rotation, θ_y^* x 10^{-3} Radian			
	T_1=0.8♯	1.4	2.0	2.4
1 1971 Paciamo Dam S16E	3.36	9.56 (E)	-	23.23 (E)
2 Holiday Orion E-W	-	9.61 (E)	17.29 (E)	-
3 1952 Taft S69E	3.38	9.55 (E)	17.36 (E)	24.10 (E)
4 1940 El Centro E-W	-	9.63 (E)	17.43 (E)	23.98
5 1940 El Centro N-S	3.36 (E)	9.66 (E)	-	-
AVERAGE	3.37	9.60	17.36	23.77

*at second floor level
♯Fundamental Period (seconds)

*Difference between rotations at second floor level and base.

E.Q. Input No.	Fundamental Period, T_1 (sec.)			
	0.8	1.4	2.0	2.4
	MAX. TOP DISPL. (IN.)			
1	14.7*	14.6 (E)	-	17.5 (E)
2	-	13.8 (E)	13.7 (E)	-
3	10.6	15.0 (E)	19.4 (E)	19.0 (E)
4	-	20.4* (E)	27.4* (E)	26.7* (E)
5	7.9 (E)	17.5 (E)	-	-
	MAX. INTERSTORY DISPL. (IN.)			
1	.80*	.85 (E)	-	1.13 (E)
2	-	.82 (E)	.87 (E)	-
3	.59	.89 (E)	1.38 (E)	1.29 (E)
4	-	1.23* (E)	2.23* (E)	2.24* (E)
5	.44 (E)	1.19 (E)	-	-
	MAX. BASE SHEAR (KIPS)			
1	1,572	1,208 (E)	-	863 (E)
2	-	1,554* (E)	944 (E)	-
3	1,716*	1,185 (E)	1,454* (E)	844 (E)
4	-	1,355 (E)	1,111 (E)	1,273* (E)
5	1,116 (E)	1,231 (E)	-	-
	MAX. BASE MOMENT (IN-KIPS)			
1	1,852,000*	767,000(E)	-	349,000(E)
2	-	790,000(E)	449,000(E)	-
3	1,611,000	887,000(E)	674,000(E)	444,000(E)
4	-	1,278,000*(E)	1,069,000*(E)	877,000*(E)
5	1,284,000(E)	1,198,000(E)	-	-
	ROTATIONAL DUCTILITY ♯			
1	3.84*	0.49 (E)	-	0.22 (E)
2	-	0.51 (E)	0.29 (E)	-
3	1.25	0.57 (E)	0.43 (E)	0.29 (E)
4	-	0.82* (E)	0.70* (E)	0.57* (E)
5	0.81 (E)	0.77 (E)	-	-

*Critical (maximum value for particular T_1)
E = no yielding, i.e., linearly elastic response

♯based on differential rotation between second floor level and base.

Table C 3

RESPONSE VALUES CORRESPONDING TO DIFFERENT EARTHQUAKE INPUT MOTIONS

SI = 1.5 ($SI_{ref.}$), Duration = 10 sec.

20-Story Isolated Structural Walls

M_y = 1,500,000 in.-k

Base Fixity Factor = 50%

EARTHQUAKE INPUT	Yield Rotation, θ_y^* x 10^{-3} Radian			
	T_1=0.8#	1.4	2.0	2.4
1 1971 Paciamo Dam S16E	2.90	6.41 (E)	-	15.56 (E)
2 Holiday Orion E-W	2.24	6.44 (E)	11.59 (E)	-
3 1952 Taft S69E	2.25	6.39 (E)	11.67 (E)	16.07 (E)
4 1940 El Centro E-W	-	-	11.89	16.13
5 1940 El Centro N-S	-	6.47	-	-
AVERAGE	2.25	6.43	11.72	15.92

*at second floor level
#Fundamental Period (seconds)

*Difference between rotations at second floor level and base.

E.Q. Input No.	Fundamental Period, T_1 (sec.)			
	0.8	1.4	2.0	2.4
	MAX. TOP DISPL. (IN.)			
1	13.9*	14.6 (E)	-	17.5 (E)
2	10.5	13.8 (E)	13.7 (E)	-
3	8.5	14.9 (E)	19.4*(E)	19.0 (E)
4	-	-	26.9*	26.7*(E)
5	-	17.1	-	-
	MAX. INTERSTORY DISPL. (IN.)			
1	.76*	.85 (E)	-	1.13 (E)
2	.57	.82 (E)	.87 (E)	-
3	.48	.88 (E)	1.38 (E)	1.29 (E)
4	-	-	2.23*	2.24*(E)
5	-	1.19*	-	-
	MAX. BASE SHEAR (KIPS)			
1	1,335	1,208 (E)	-	863 (E)
2	1,772*	1,554*(E)	944 (E)	-
3	1,544	1,185 (E)	1,454*(E)	844 (E)
4	-	-	1,107	1,273*(E)
5	-	1,231	-	-
	MAX. BASE MOMENT (IN-KIPS)			
1	1,369,000*	767,000(E)	-	349,000(E)
2	1,261,000	790,000(E)	449,000(E)	-
3	1,188,000	888,000(E)	674,000(E)	444,000(E)
4	-	-	1,056,000*	877,000*(E)
5	-	1,108,000*	-	-
	ROTATIONAL DUCTILITY #			
1	6.65*	0.73 (E)	-	0.33 (E)
2	4.66	0.75 (E)	0.43 (E)	-
3	2.52	0.85 (E)	0.64 (E)	0.43 (E)
4	-	-	1.05*	0.85*(E)
5	-	1.59*	1.03	-

*Critical (maximum) value for particular T_1
E = no yielding, i.e., linearly elastic response
#based on differential rotation between second floor level and base.

Table C 4

RESPONSE VALUES CORRESPONDING TO DIFFERENT EARTHQUAKE INPUT MOTIONS

SI = 1.5 (SI$_{ref.}$), Duration = 10 sec.

20-Story Isolated Structural Walls

M_y = 750,000 in.-k

Base Fixity Factor = 75 %

EARTHQUAKE INPUT	Yield Rotation, θ_y^* x 10^{-3} Radian			
	T_1=0.8#	1.4	2.0	2.4
1 1971 Paciamo Dam S16E	0.88	2.59	4.59	6.33 (E)
2 Holiday Orion E-W	0.89	2.60	4.57 (E)	-
3 1952 Taft S69E	0.89	-	-	6.31
4 1940 El Centro E-W	-	2.57	4.71	6.36
5 1940 El Centro N-S	-	2.57	-	-
AVERAGE	0.89	2.58	4.62	6.33

*at second floor level
#Fundamental Period (seconds)
*Difference between rotations at second floor level and base.

E.Q. Input No.	Fundamental Period, T_1 (sec.)			
	0.8	1.4	2.0	2.4
	MAX. TOP DISPL. (IN.)			
1	10.6*	14.1	16.2*	17.6 (E)
2	7.9	15.0*	14.0 (E)	-
3	7.4	-	-	19.5* (E)
4	-	14.8	14.2	19.0
5	-	14.0	-	-
	MAX. INTERSTORY DISPL. (IN.)			
1	.59*	.82	1.18	1.19 (E)
2	.45	.90*	.94 (E)	-
3	.43	-	-	1.42
4	-	.84	1.88*	2.13*
5	-	.83	-	-
	MAX. BASE SHEAR (KIPS)			
1	1,225	1,121	1,566*	1,073 (E)
2	1,321*	1,455*	928 (E)	-
3	1,230	-	-	1,318 (E)
4	-	895	1,111	1,356*
5	-	1,127	-	-
	MAX. BASE MOMENT (IN-KIPS)			
1	1,083,000*	861,000	799,000	466,000(E)
2	998,000	876,000	638,000(E)	-
3	982,000	-	-	788,000(E)
4	-	907,000*	942,000*	869,000*
5	-	883,000	-	-
	ROTATIONAL DUCTILITY #			
1	8.73*	2.62	1.05	0.58 (E)
2	5.75	2.48	0.82(E)	-
3	5.00	-	-	0.98 (E)
4	-	3.50*	3.61*	2.79*
5	-	2.58	-	-

*Critical (maximum) value for particular T_1
E = no yielding, i.e., linearly elastic response
#based on differential rotation between second floor level and base.

Table C 5

RESPONSE VALUES CORRESPONDING TO DIFFERENT EARTHQUAKE INPUT MOTIONS

SI = 1.5 ($SI_{ref.}$), Duration = 10 sec.

20-Story Isolated Structural Walls

M_y = 1,000,000 in.-k

Base Fixity Factor = 75 %

EARTHQUAKE INPUT	Yield Rotation, θ_y^* x 10^{-3} Radian			
	T_1=0.8#	1.4	2.0	2.4
1 1971 Paciamo Dam S16E	1.18	3.44	-	8.49 (E)
2 Holiday Orion E-W	1.18	3.43	5.97 (E)	-
3 1952 Taft S69E	1.19	3.43	6.14 (E)	8.37 (E)
4 1940 El Centro E-W	-	-	6.25	8.57
5 1940 El Centro N-S	-	-	-	-
AVERAGE	1.18	3.43	6.12	8.48

*at second floor level
#Fundamental Period (seconds)
*Difference between rotations at second floor level and base.

E.Q. Input No.	Fundamental Period, T_1 (sec.)			
	0.8	1.4	2.0	2.4
	MAX. TOP DISPL. (IN.)			
1	11.9*	16.5	-	17.6 (E)
2	7.0	17.6*	14.0 (E)	-
3	7.6	14.1	16.2 (E)	19.8 (E)
4	-	-	22.0*	27.2*
5	-	-	-	-
	MAX. INTERSTORY DISPL. (IN.)			
1	.65*	.98	-	1.19 (E)
2	.40	1.06*	.94 (E)	-
3	.43	.91	1.19 (E)	1.42 (E)
4	-	-	1.79*	2.23*
5	-	-	-	-
	MAX. BASE SHEAR (KIPS)			
1	1,529*	1,070	-	1,073 (E)
2	1,315	1,626*	928 (E)	-
3	1,445	1,525	1,418*(E)	1,318 (E)
4	-	-	1,111	1,356*
5	-	-	-	-
	MAX. BASE MOMENT (IN-KIPS)			
1	1,387,000*	1,119,000	-	466,000(E)
2	1,236,000	1,134,000*	638,000(E)	-
3	1,231,000	1,077,000	892,000(E)	-
4	-	-	1,127,000*	1,066,000*
5	-	-	-	-
	ROTATIONAL DUCTILITY #			
1	7.31*	2.06	-	0.43 (E)
2	3.74	2.23*	0.62 (E)	-
3	3.57	1.33	0.86 (E)	0.74 (E)
4	-	-	1.89*	1.17*
5	-	-	-	-

*Critical (maximum) value for particular T_1
E = no yielding, i.e., linearly elastic response
#based on differential rotation between second floor level and base.

Table C 6

RESPONSE VALUES CORRESPONDING TO DIFFERENT EARTHQUAKE INPUT MOTIONS

SI = 1.5 ($SI_{ref.}$), Duration = 10 sec.

20-Story Isolated Structural Walls

M_y = 1,500,000 in.-k

Base Fixity Factor = 75%

EARTHQUAKE INPUT	Yield Rotation, θ_y^* x 10^{-3} Radian			
	T_1=0.8#	1.4	2.0	2.4
1 1971 Paciamo Dam S16E	1.77	5.21 (E)	-	12.82 (E)
2 Holiday Orion E-W	-	5.15	8.90 (E)	-
3 1952 Taft S69E	1.79	-	9.17 (E)	12.50 (E)
4 1940 El Centro E-W	2.15	5.17	9.36 (E)	12.79 (E)
5 1940 El Centro N-S	1.77	-	-	-
AVERAGE	1.78	5.18	9.14	12.70

*at second floor level
#Fundamental Period (seconds)
*Difference between rotations at second floor level and base.

E.Q. Input No.	Fundamental Period, T_1 (sec.)			
	0.8	1.4	2.0	2.4
	MAX. TOP DISPL. (IN.)			
1	12.7*	16.5 (E)	-	17.6 (E)
2	-	18.5	14.0 (E)	-
3	7.5	-	16.2 (E)	19.8 (E)
4	-	19.4*	27.6*(E)	29.3*(E)
5	9.0	-	-	-
	MAX. INTERSTORY DISPL. (IN.)			
1	.71*	1.01 (E)	-	1.19 (E)
2	-	1.17*	.94 (E)	-
3	.45	-	1.19 (E)	1.42 (E)
4	-	1.16	1.83*(E)	2.23*(E)
5	.50	-	-	-
	MAX. BASE SHEAR (KIPS)			
1	1,697	1,277 (E)	-	1,073 (E)
2	-	1,951*	928 (E)	-
3	1,718*	-	1,418*(E)	1,318 (E)
4	-	1,216	1,220 (E)	1,356*(E)
5	1,375	-	-	-
	MAX. BASE MOMENT (IN-KIPS)			
1	1,929,000*	1,293,000	-	466,000(E)
2	-	1,606,000*	638,000(E)	-
3	1,700,000	-	892,000(E)	787,000(E)
4	-	1,581,000	1,309,000*(E)	1,115,000*(E)
5	1,754,000	-	-	-
	ROTATIONAL DUCTILITY #			
1	4.92*	0.82 (E)	-	0.29 (E)
2	-	1.19*	0.41 (E)	-
3	1.89	-	0.57 (E)	0.50 (E)
4	-	1.03	0.85*(E)	0.71*(E)
5	2.70	-	-	-

*Critical (maximum) value for particular T_1
E = no yielding, i.e., linearly elastic response
#based on differential rotation between second floor level and base.

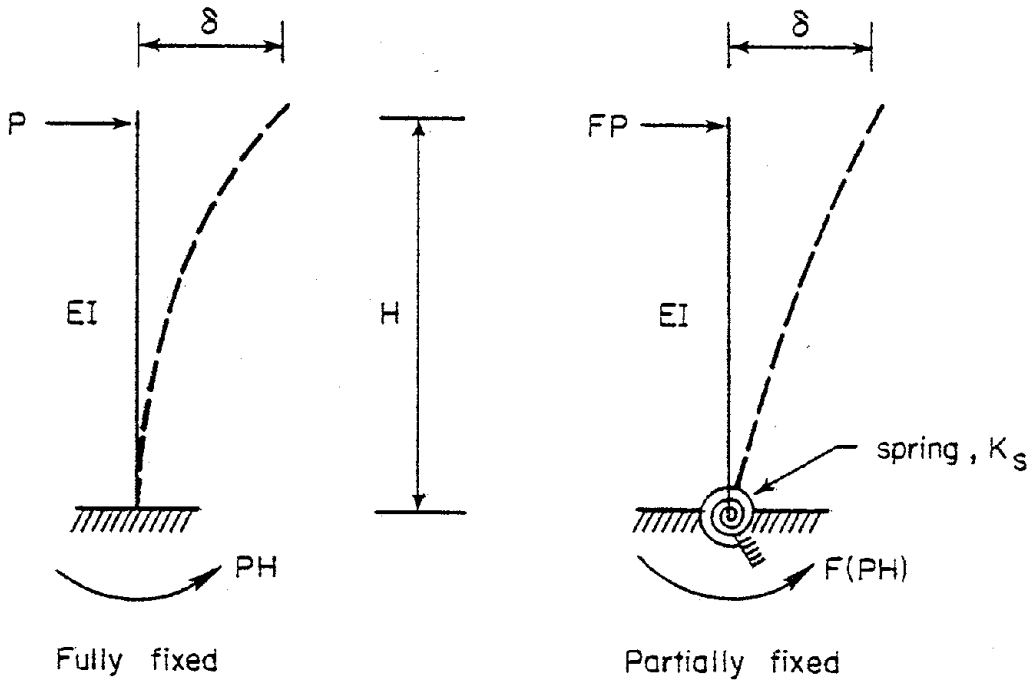

Fig. C1 Definition of Base Fixity Factor, F_B

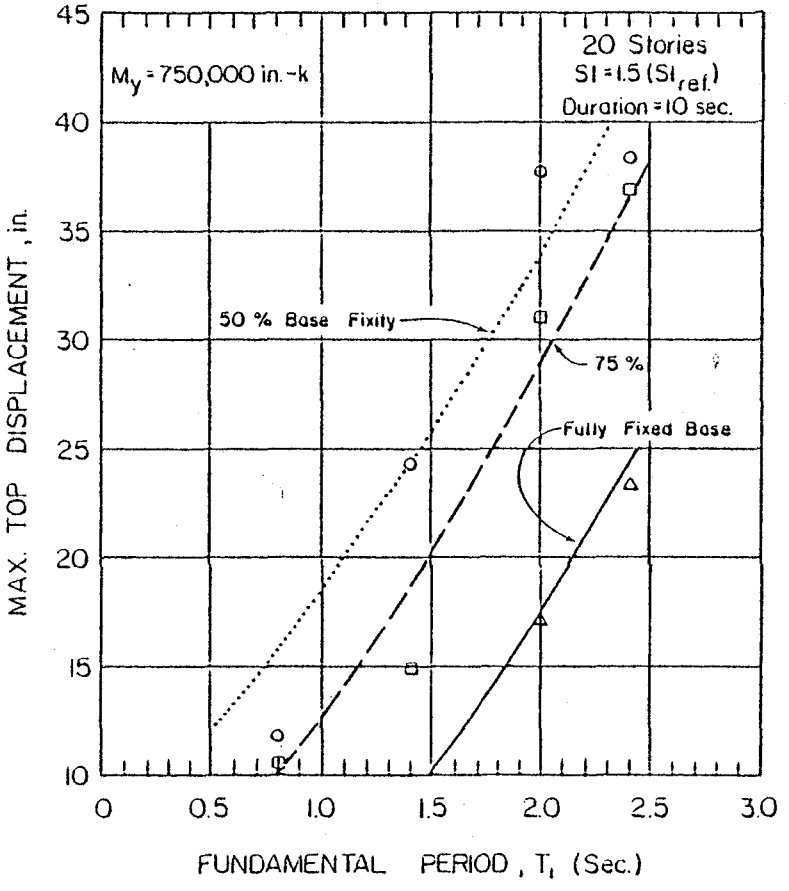

(a)

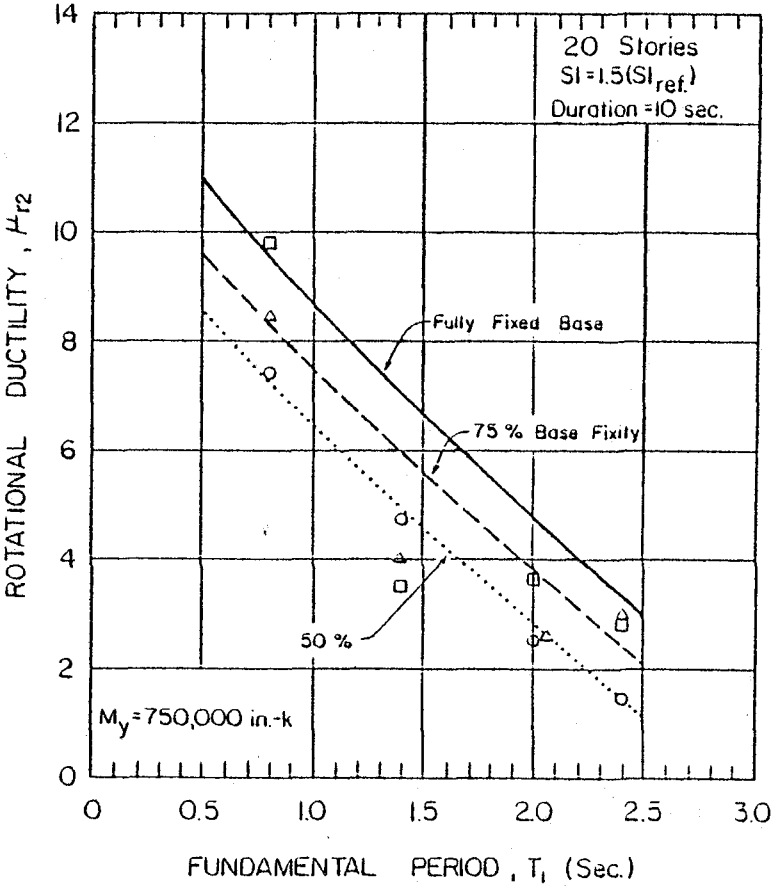

(b)

Fig. C2 Critical Response Values as Functions of Fundamental Period, T_1, and Degree of Base Fixity - 20 Story Isolated Walls, M_y = 750,000 in.-k

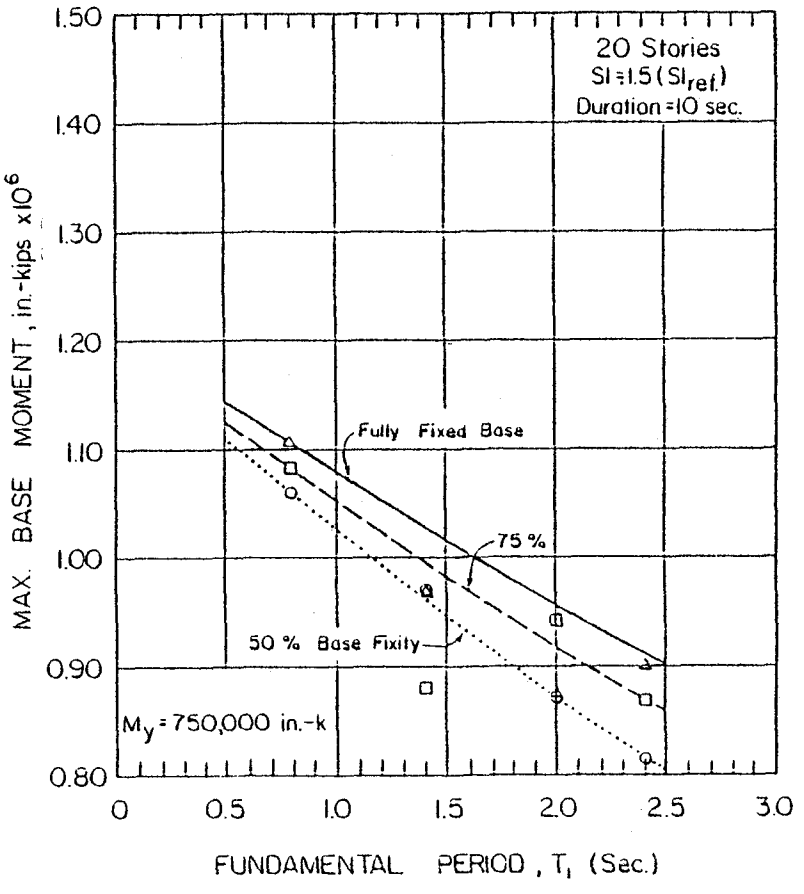

(c)

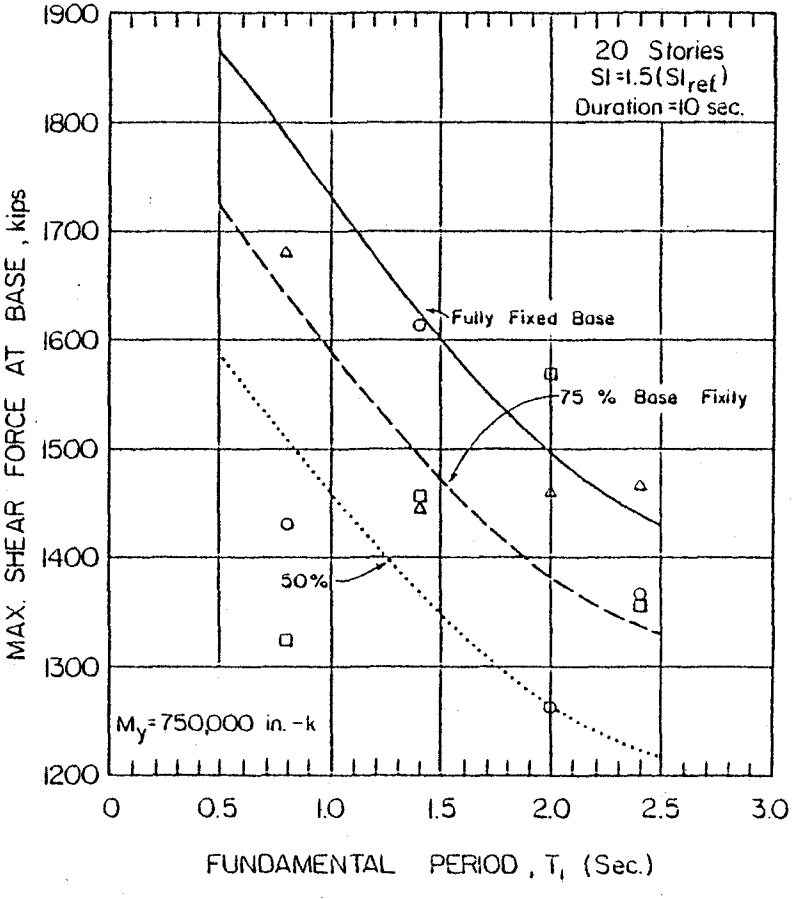

(d)

Fig. C2 (contd.) Critical Response Values as Functions of Fundamental Period, T_1 and Degree of Base Fixity - 20 Story Isolated Structural Walls, M_y = 750,000 in.-k

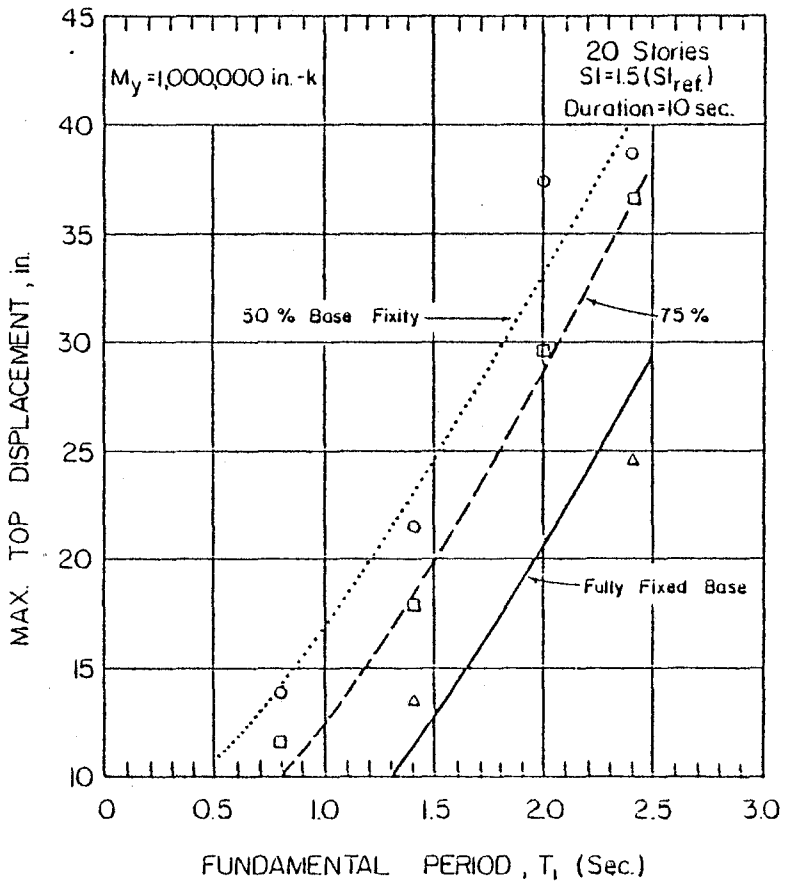

(a)

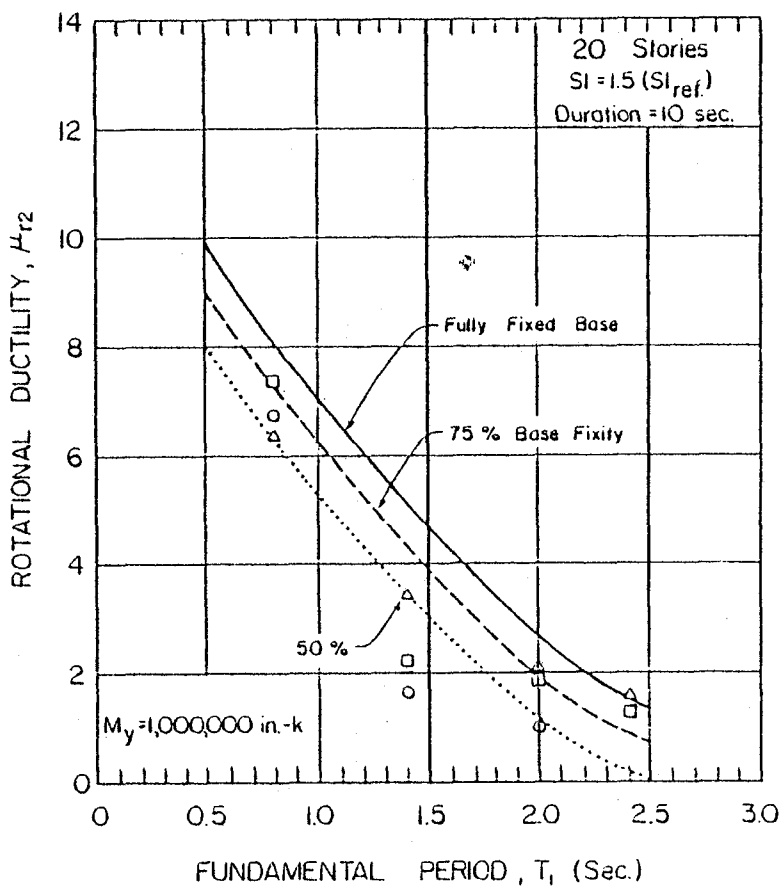

(b)

Fig. C3 Critical Response Values as Functions of Fundamental Period, T_1, and Degree of Base Fixity - 20 Story Isolated Structural Walls, M_y = 1,000,000 in.-k

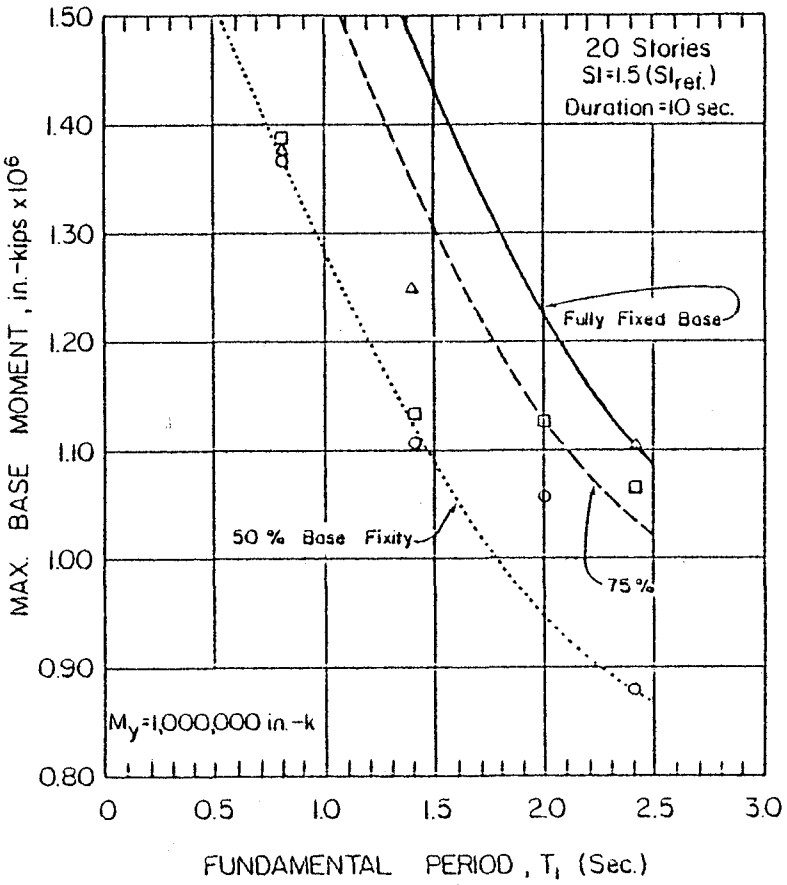

(c)

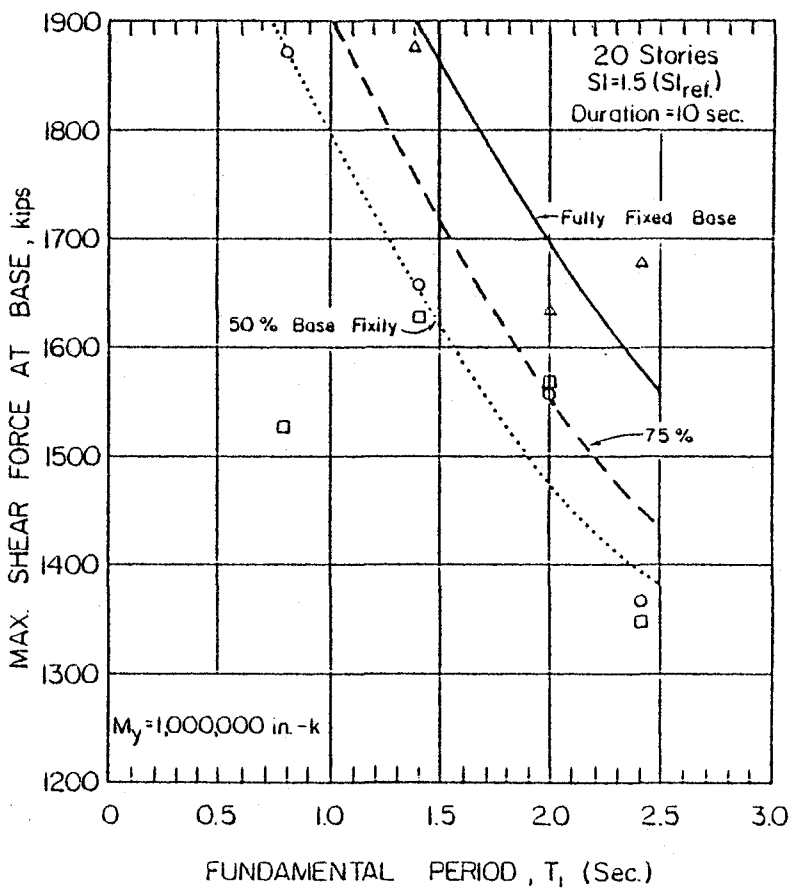

(d)

Fig. C3 (contd.) Critical Response Values as Functions of Fundamental Period, T_1 and Degree of Base Fixity - 20 Story Isolated Structural Walls, M_y = 1,000,000 in.-k

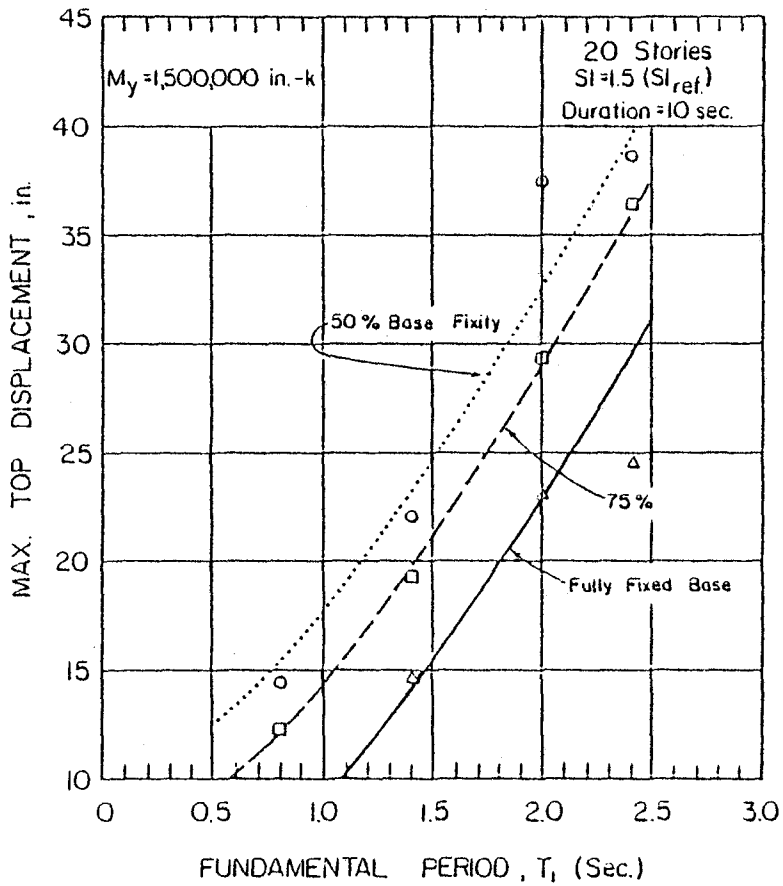

(a)

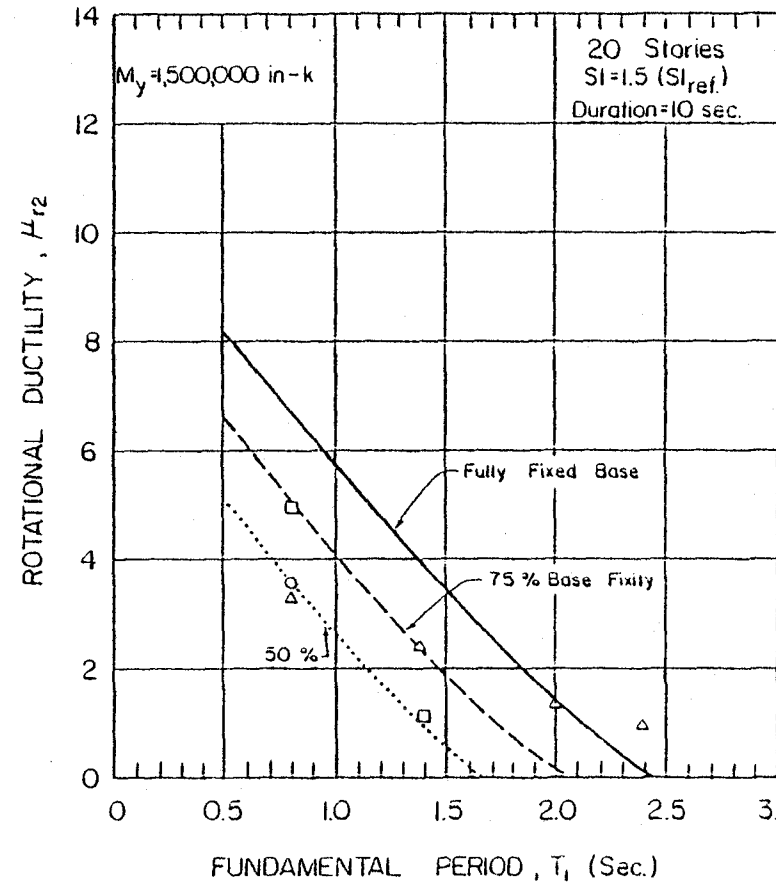

(b)

Fig. C4 Critical Response Values as Functions of Fundamental Period, T_1, and Degree of Base Fixity - 20 Story Isolated Structural Walls, M_y = 1,500,000 in.-k

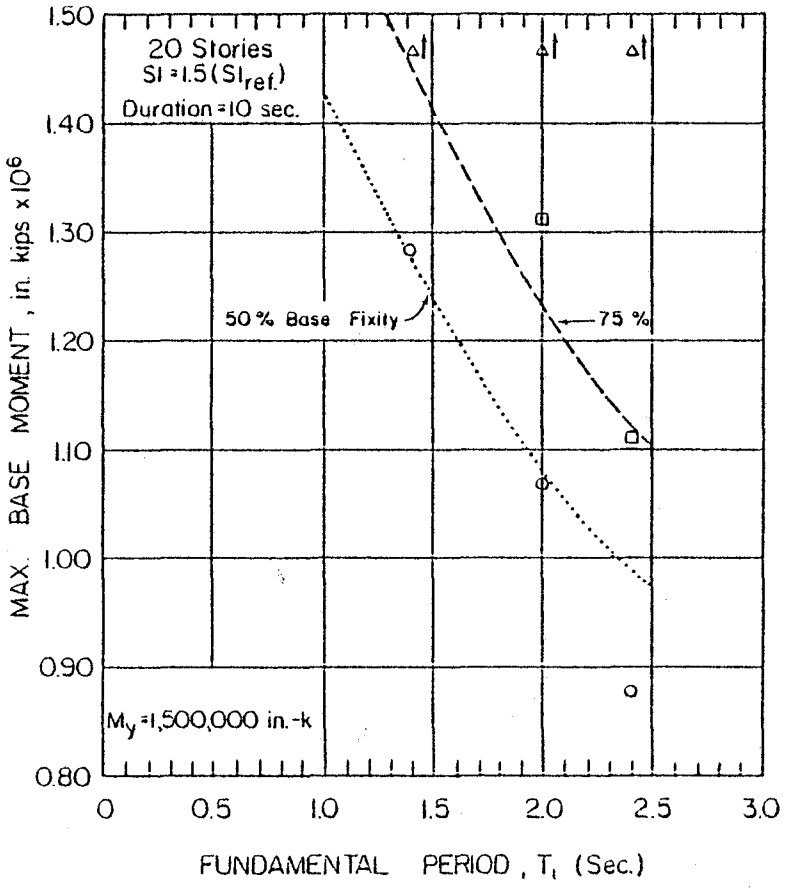

(c)

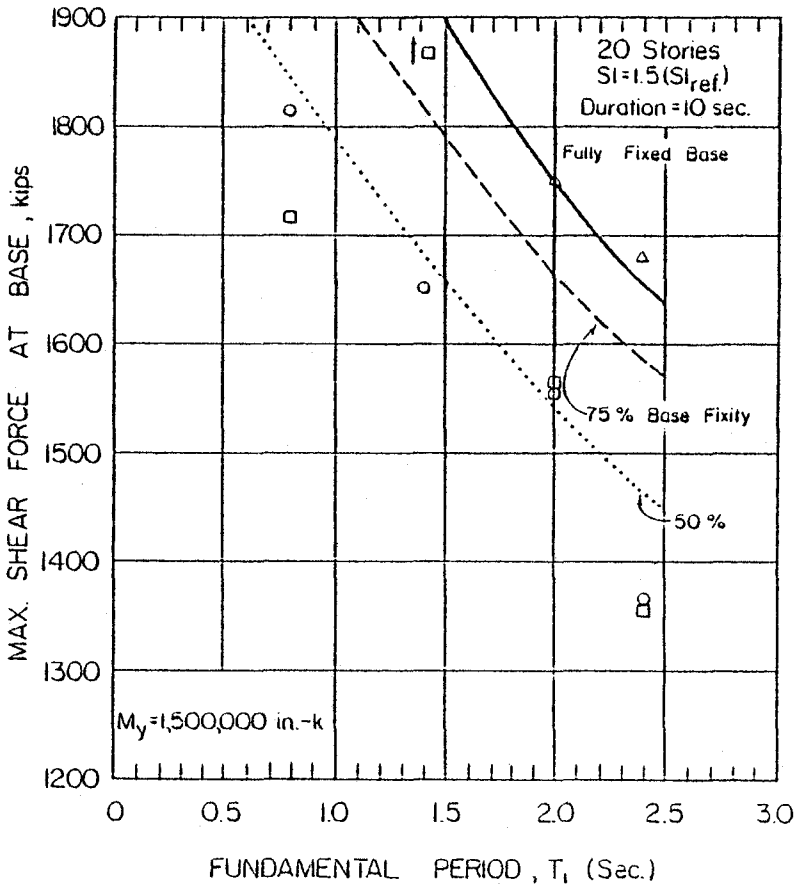

(d)

Fig. C4 (contd.) Critical Response Values as Functions of Fundamental Period, T_1, and Degree of Base Fixity - 20 Story Isolated Structural Walls, M_y = 1,500,000 in.-k

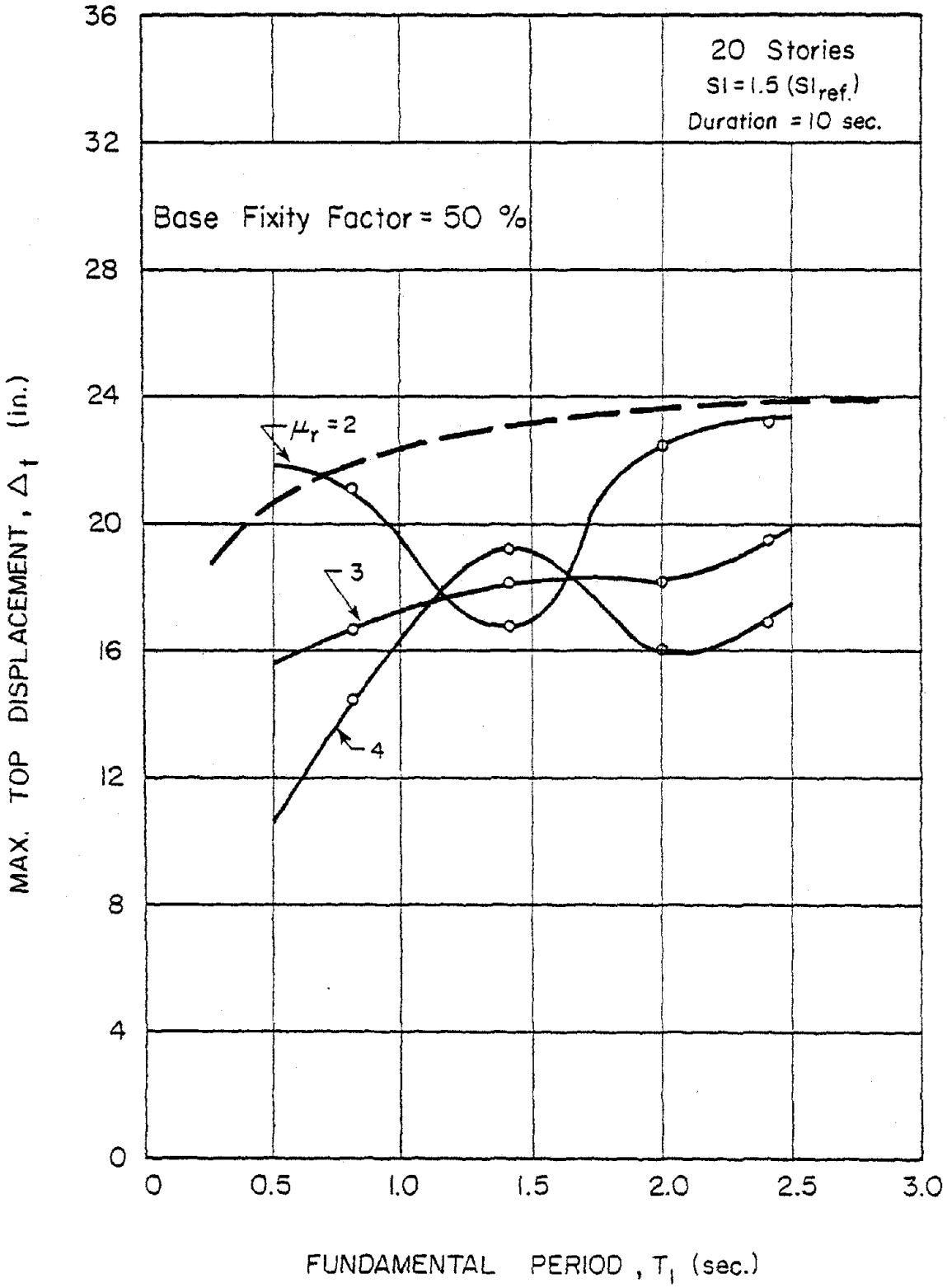

Fig. C5 Maximum Top Displacement as a Function of Fundamental Period, T_1, and Rotational Ductility at Base, μ_r - 20-Story Walls with Base Fixity Factor = 50%

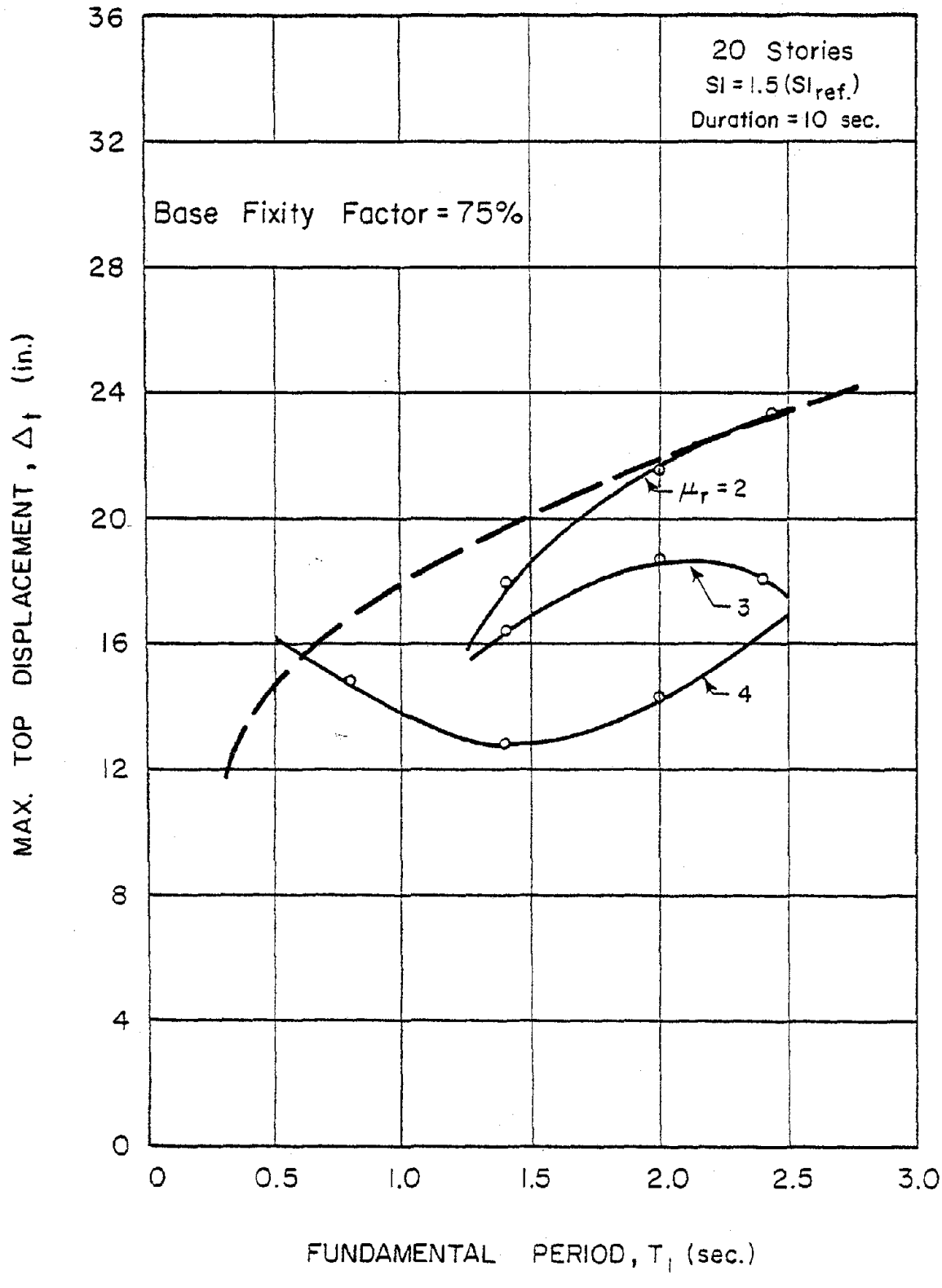

Fig. C6 Maximum Top Displacement as a Function of Fundamental Period, T_1, and Rotational Ductility at Base, μ_r - 20 Story Walls with Base Fixity Factor = 75%

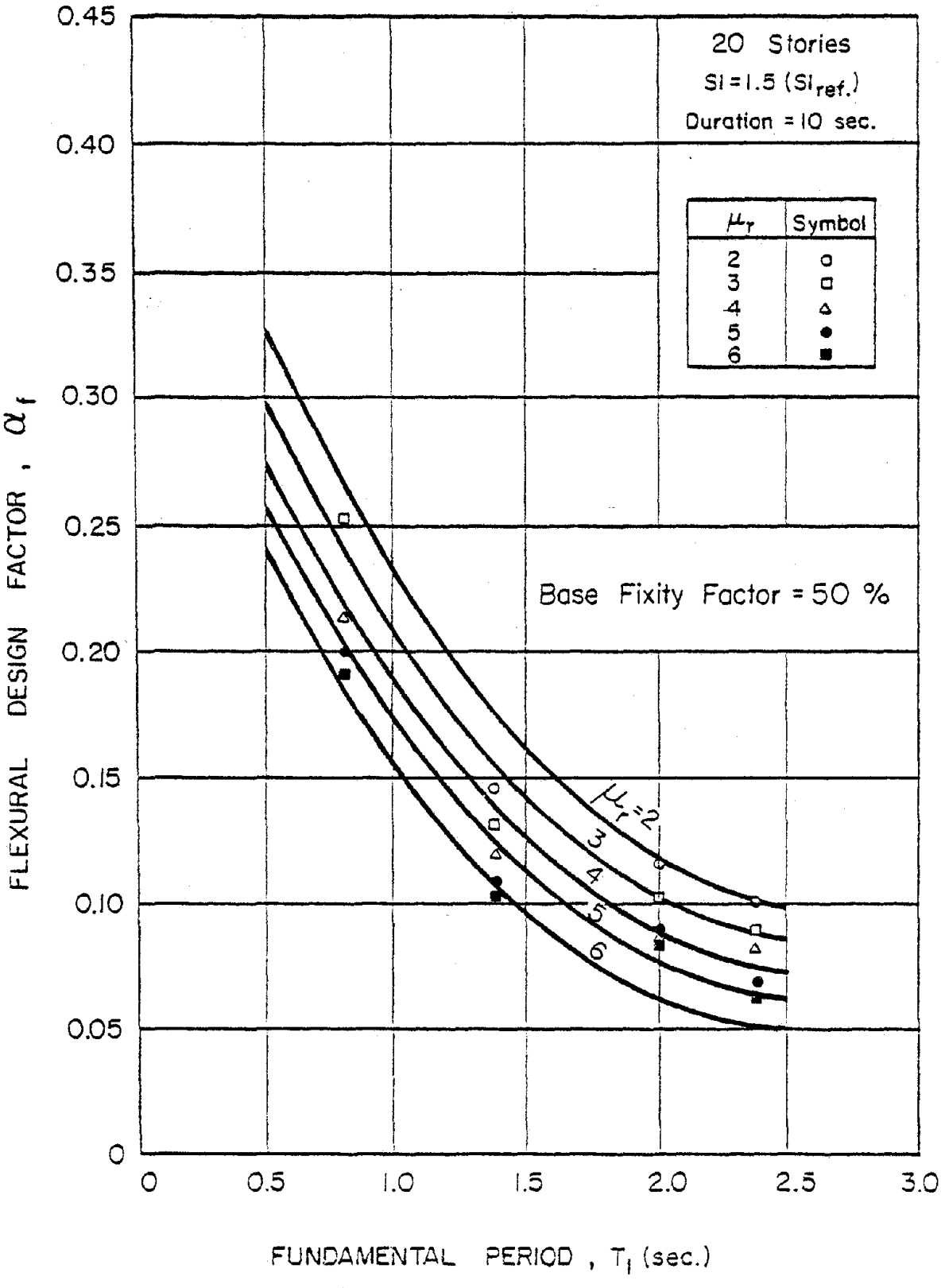

Fig. C7 Flexural Design Factor, α_f, as a Function of Fundamental Period, T_1 and Available Rotational Ductility, μ_r^a - 20-Story Walls with Base Fixity Factor = 50%

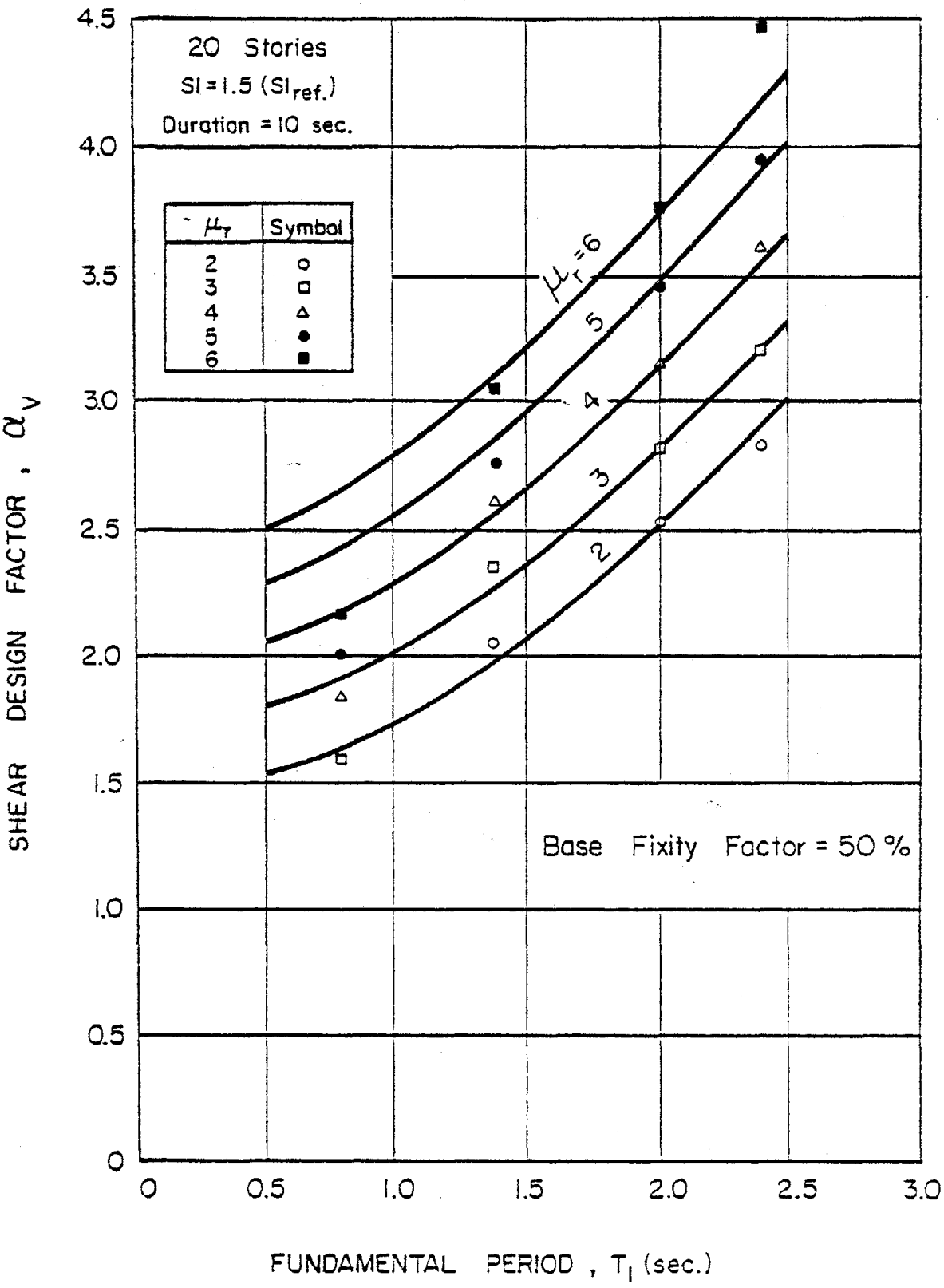

Fig. C8 Shear Design Factor, $\bar{\alpha}_v$, as a Function of Fundamental Period, T_1, and Available Rotational Ductility, μ_r^a - 20-Story Walls with Base Fixity Factor = 50%

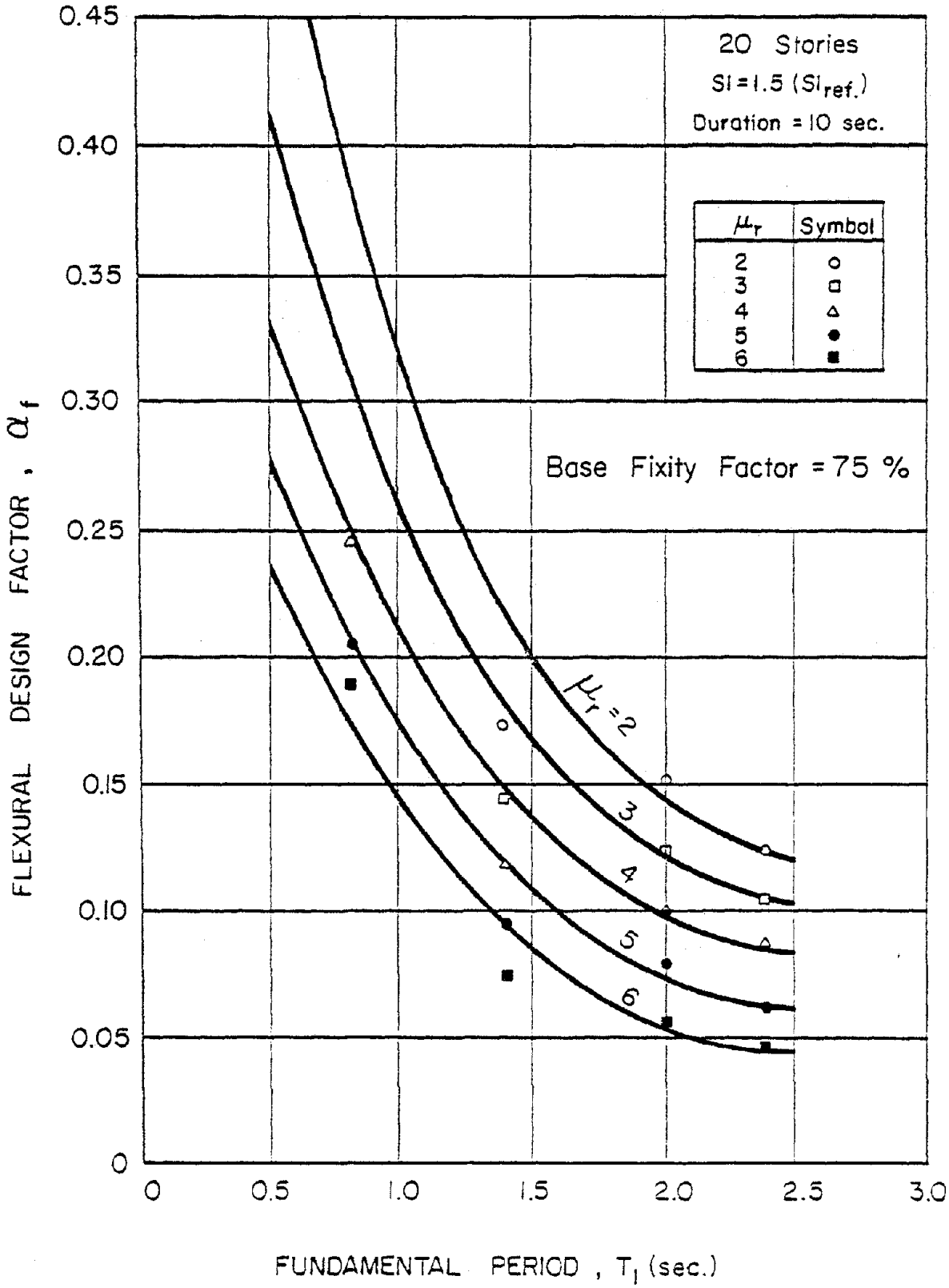

Fig. C9 Flexural Design Factor, α_f, as a Function of Fundamental Period, T_1 and Available Rotational Ductility, μ_r^a - 20-Story Walls with Base Fixity Factor = 75%

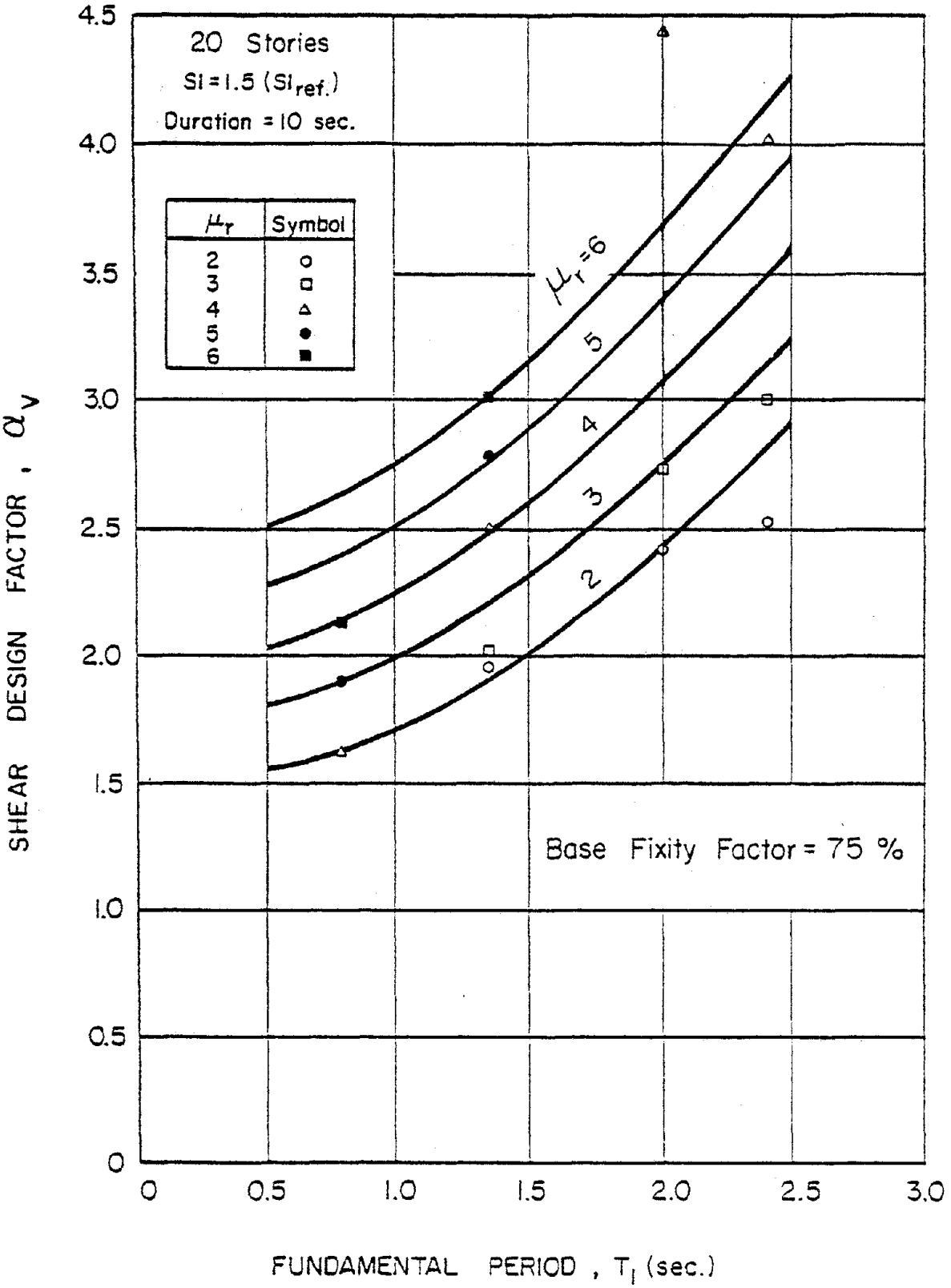

Fig. C10 Shear Design Factor, $\bar{\alpha}_v$, as a Function of Fundamental Period, T_1 and Available Rotational Ductility, μ_r^a - 20-Story Walls with Base Fixity Factor = 75%

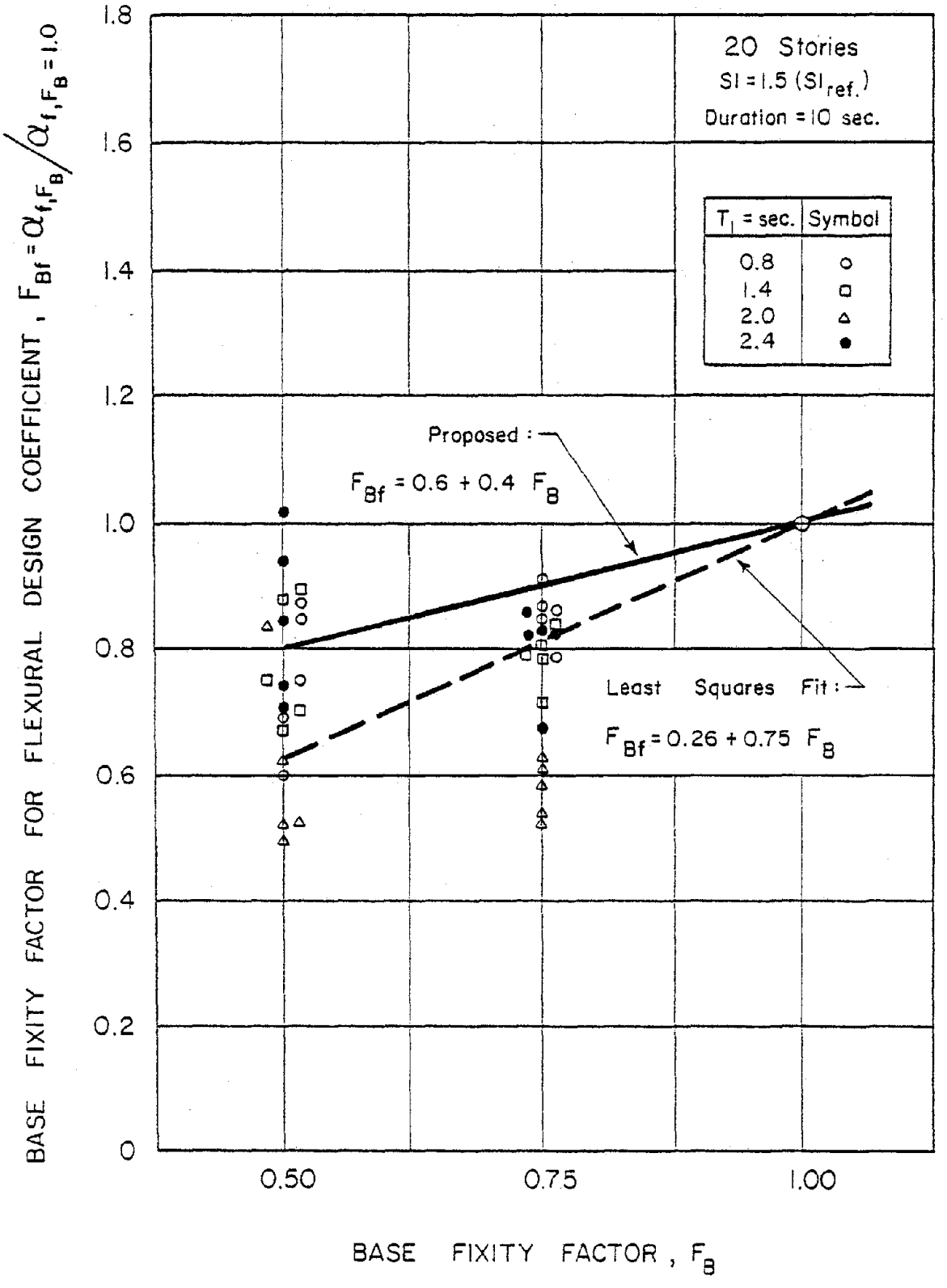

Fig. C11 Base Fixity Factor for Flexural Design Coefficient F_{Bf} - 20-Story Structural Walls

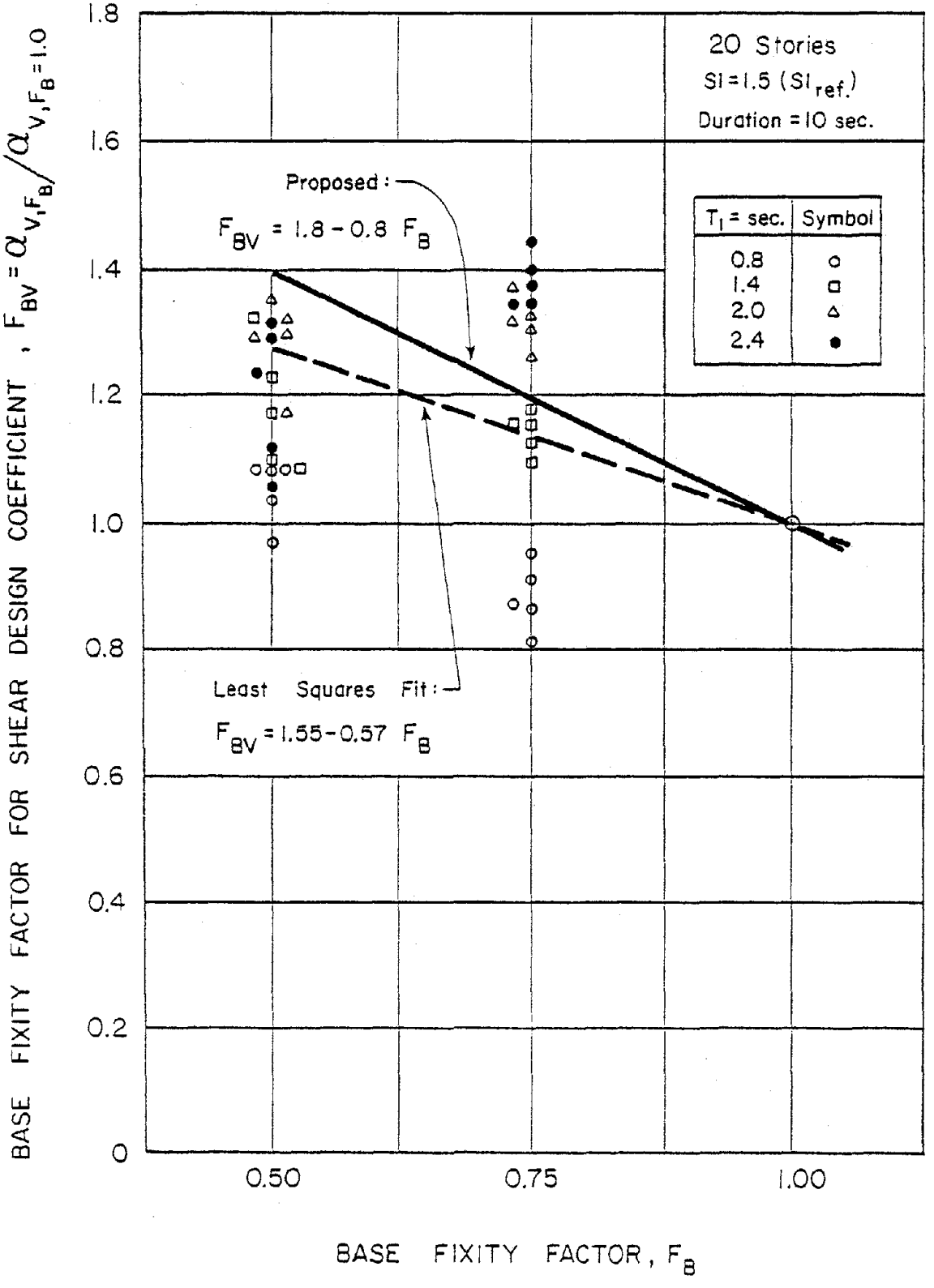

Fig. C12 Base Fixity Factor for Shear Design Coefficient, F_{Bv} - 20-Story Structural Walls

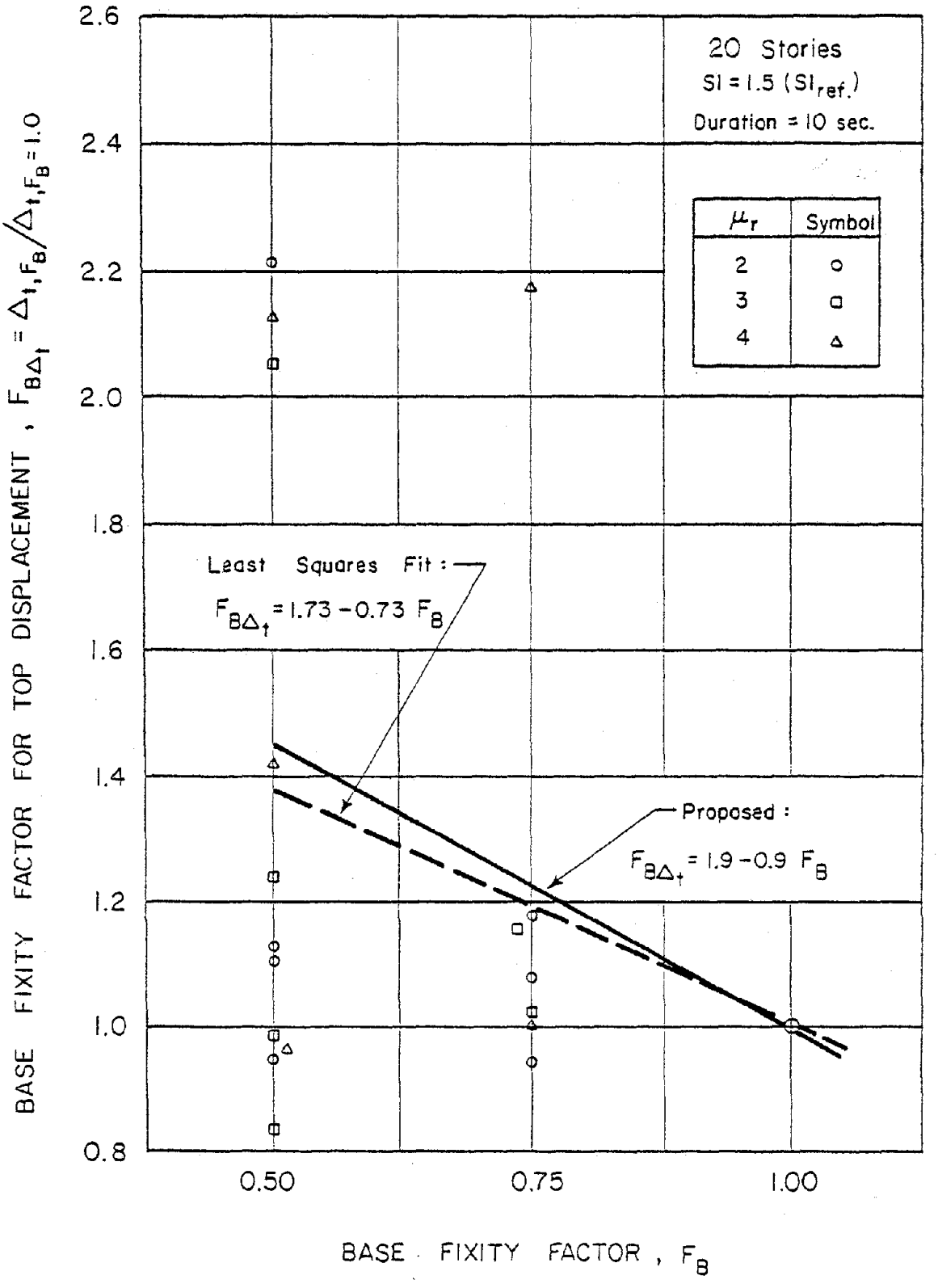

Fig. C13 Base Fixity Factor for Maximum Top Displacement, $F_{B\Delta_t}$ - 20-Story Structural Walls